haematologica
Journal of The Ferrata Storti Foundation

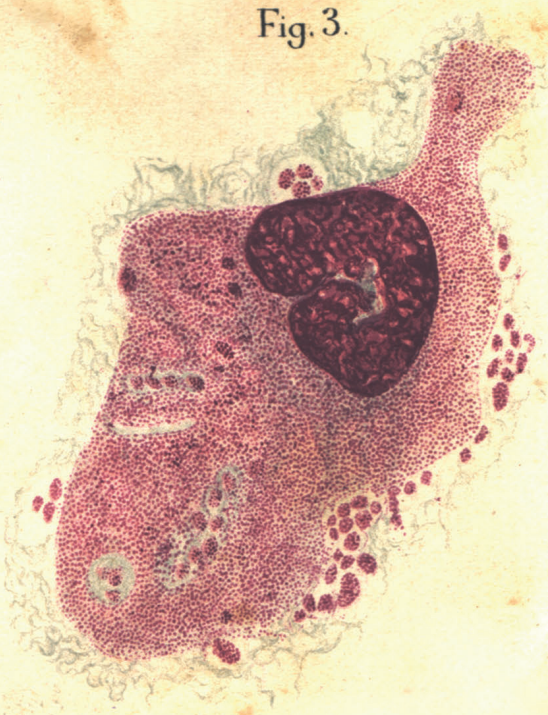

ISSN 0390-6078
Volume 105
JULY
2020 - 07

www.haematologica.org

haematologica
Journal of the Ferrata Storti Foundation

haematologica
Journal of the Ferrata Storti Foundation

Information for readers, authors and subscribers

Haematologica (print edition, pISSN 0390-6078, eISSN 1592-8721) publishes peer-reviewed papers on all areas of experimental and clinical hematology. The journal is owned by a non-profit organization, the Ferrata Storti Foundation, and serves the scientific community following the recommendations of the World Association of Medical Editors (www.wame.org) and the International Committee of Medical Journal Editors (www.icmje.org).

Haematologica publishes editorials, research articles, review articles, guideline articles and letters. Manuscripts should be prepared according to our guidelines (www.haematologica.org/information-for-authors), and the Uniform Requirements for Manuscripts Submitted to Biomedical Journals, prepared by the International Committee of Medical Journal Editors (www.icmje.org).

Manuscripts should be submitted online at http://www.haematologica.org/.

Conflict of interests. According to the International Committee of Medical Journal Editors (http://www.icmje.org/#conflicts), "Public trust in the peer review process and the credibility of published articles depend in part on how well conflict of interest is handled during writing, peer review, and editorial decision making". The ad hoc journal's policy is reported in detail online (www.haematologica.org/content/policies).

Transfer of Copyright and Permission to Reproduce Parts of Published Papers. Authors will grant copyright of their articles to the Ferrata Storti Foundation. No formal permission will be required to reproduce parts (tables or illustrations) of published papers, provided the source is quoted appropriately and reproduction has no commercial intent. Reproductions with commercial intent will require written permission and payment of royalties.

Detailed information about subscriptions is available online at www.haematologica.org. Haematologica is an open access journal. Access to the online journal is free. Use of the Haematologica App (available on the App Store and on Google Play) is free.
For subscriptions to the printed issue of the journal, please contact: Haematologica Office, via Giuseppe Belli 4, 27100 Pavia, Italy (phone +39.0382.27129, fax +39.0382.394705, E-mail: info@haematologica.org).

Rates of the International edition for the year 2019 are as following:

	Institutional	*Personal*
Print edition	*Euro 700*	*Euro 170*

Advertisements. Contact the Advertising Manager, Haematologica Office, via Giuseppe Belli 4, 27100 Pavia, Italy (phone +39.0382.27129, fax +39.0382.394705, e-mail: marketing@haematologica.org).

Direttore responsabile: Prof. Carlo Balduini; Autorizzazione del Tribunale di Pavia n. 63 del 5 marzo 1955.
Printing: Press Up, zona Via Cassia Km 36, 300 Zona Ind.le Settevene - 01036 Nepi (VT)

Associated with USPI, Unione Stampa Periodica Italiana.
Premiato per l'alto valore culturale dal Ministero dei Beni Culturali ed Ambientali

haematologica
Journal of the Ferrata Storti Foundation

Table of Contents

Volume 105, Issue 7: July 2020

About the cover

Editorials

Centenary Review Article

Review Article

Guideline Article

Articles

Hematopoiesis

Bone Marrow Failure

Red Cell Biology & its Disorders

haematologica
Journal of the Ferrata Storti Foundation

haematologica
Journal of the Ferrata Storti Foundation

Letters to the Editor

Letters are available online only at www.haematologica.org/content/105/7.toc

Case Reports

Case Reports are available online only at www.haematologica.org/content/105/7.toc

haematologica
Journal of the Ferrata Storti Foundation

Comments

Comments are available online only at www.haematologica.org/content/105/7.toc

100-year-old Haematologica images: the quarrel about the origin of platelets (III)

Carlo L. Balduini

Ferrata-Storti Foundation, Pavia, Italy

E-mail: CARLO L. BALDUINI - carlo.balduini@unipv.it

doi:10.3324/haematol.2020.256974

The fascinating story of platelets began in 1881 when Giulio Bizzozero identified these cells in peripheral blood and demonstrated that they play a key role in the hemostatic process.[1] He also observed that leukocytes are recruited into the platelet aggregates and offered the first images of platelet-leukocyte interaction. Bizzozero's successes in the study of platelets are not limited to these discoveries. In fact, twelve years earlier he had described for the first time megakaryocytes, which for a long time were called "Bizzozero's giant bone marrow cells".[2] However, he never recognized the close links between platelets and megakaryocytes. This was identified in 1916 by James Homer Wright, who noted the similarities in shape and color of the granules of megakaryocytes and platelets using his new polychrome staining technique: Wright's stain.[3] Moreover, by microscopy analysis of bone marrow sections, he showed platelets budding from megakaryocytes and entering the circulation.[4] However, despite this evidence, the origin of platelets was still under discussion at the time of the first issue of Haematologica in 1920.[5-7]

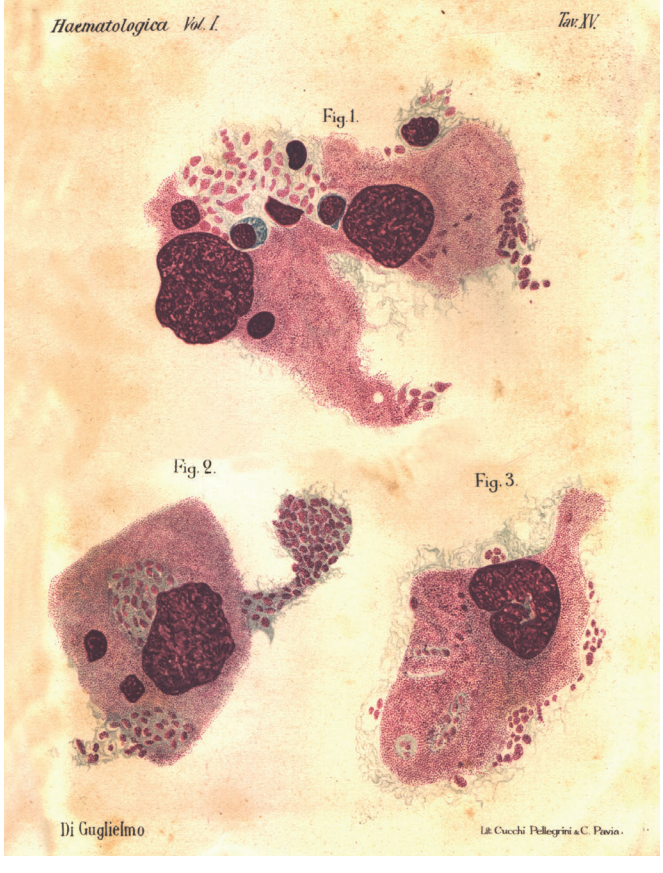

Figure 1. Hand-drawn color plate illustrating the Di Guglielmo paper entitled "Platelets and megakaryocytes" published in Haematologica in 1920. In this article, Di Guglielmo presented evidence to support the idea put forward by Wright that platelets are formed by megakaryocytes, a concept that was the subject of heated debate at the time.

Strong support for the derivation of platelets from megakaryocytes was given by an article published by Giovanni Di Guglielmo in the first issue of Haematologica.[8] At that time, Di Gugliemo was a young assistant to Adolfo Ferrata, the founder of Haematologica, at the Medical Clinic of Naples. (Interestingly, after the death of Ferrata in 1946, Di Guglielmo was the Editor of the journal until 1960.) This paper, entitled "Megakaryocytes and platelets", reported the presence of rare megakaryocytes in blood films of patients with chronic myeloid leukemia. Morphological evaluation of these cells revealed that megakaryocytes release platelets by two mechanisms (Figure 1): through the formation of long cytoplasmic extroflexions and by the direct fragmentation of cytoplasm (Figure 1). Both mechanisms have been confirmed in this new millennium.[9,10] The finding that circulating megakaryocytes are involved in platelet formation was also recently confirmed.[11]

References

1. Bizzozero, G. [Su di un nuovo elemento morfologico del sangue dei mammiferi e sulla sua importanza nella trombosi e nella coagulazione]. L'Osservatore Gazz Clin. 1881;17:785-787.
2. Bizzozero, G. [Sul midollo delle ossa]. Il Morgagni. 1869;11:617-646.
3. Wright JH. The origin and nature of blood platelets. Boston Med Surg J. 1906;154:643-645.
4. Wright JH. (1910) The histogenesis of the blood platelets. J Exp Med. 1910;21:263-278.
5. Mazzarello P. One hundred years of Haematologica. Haematologica. 2020;105(1):12-21.
6. Balduini CL. 100-year old Haematologica images: The quarrel about the origin of platelets (I). Haematologica. 2020;105(5):1169.
7. Balduini CL. 100-year old Haematologica images: The quarrel about the origin of platelets (II). Haematologica. 2020;105(6):1467.
8. Di Guglielmo G. [Megacariociti e piastrine]. Haematologica. 1920;1:303-332.
9. Nishimura S, Nagasaki M, Kunishima S, Sawaguchi A, Sakata A, et al. IL-1α induces thrombopoiesis through megakaryocyte rupture in response to acute platelet needs. J Cell Biol 2015;209(3):453-466.
10. Italiano JE Jr, Lecine P, Shivdasani RA, Hartwig JH. Blood platelets are assembled principally at the ends of proplatelet processes produced by differentiated megakaryocytes. J Cell Biol. 1999;147(6):1299-1312.
11. Lefrançais E, Ortiz-Muñoz G, Caudrillier A, et al. The lung is a site of platelet biogenesis and a reservoir for haematopoietic progenitors. Nature. 2017;544(7648):105-109.

Replacing the suppressed hormone: toward a better treatment for iron overload in β-thalassemia major?

Domenico Girelli and Fabiana Busti

Department of Medicine, Section of Internal Medicine, University of Verona, EuroBloodNet Referral Center for Iron Metabolism Disorders, Azienda Ospedaliera Universitaria Integrata of Verona, Verona, Italy

E-mail: DOMENICO GIRELLI - domenico.girelli@univr.it

doi:10.3324/haematol.2020.253393

The human body lacks a regulatory mechanism able to excrete excess iron. Therefore, any condition increasing iron entry into the body inevitably results in toxic iron overload.[1] The majority of iron overload disorders can be viewed as endocrine diseases[2] caused by insufficient production or activity of hepcidin, the key hormone that finely tunes systemic iron homeostasis.[3] Hepcidin controls body iron content by negatively modulating the absorption of dietary iron from the gut,[4] and also regulates iron fluxes among different cells and tissues, e.g. from iron-recycling splenic macrophages to erythroid progenitors in the bone marrow.[5]

Deficiency of this hormone, leading to intestinal iron hyperabsorption, is particularly relevant in the pathogenesis of hereditary hemochromatosis, due to gene mutations impairing hepcidin production, but it is also paramount in several inherited "iron-loading" anemias,[6] particularly in non-transfusion-dependent thalassemias (NTDT),[7] In these conditions, soluble factors produced by erythroid progenitors during expanded/ineffective erythropoiesis,[8] including erythroferrone,[9] directly suppress the synthesis of the hormone in the liver.

Things are more complicated in transfusion-dependent thalassemias (TDT), in which most of the abnormal iron accumulation derives from regular red blood cell transfusions, typically every 2-3 weeks.[10] Indeed, in TDT, hepcidin level fluctuates according to suppression of erythropoiesis by transfusions, with relatively high and low values immediately after and before red blood cell administration, respectively.[11] Thus, increased iron absorption can also contribute to iron overload in TDT, at least during intervals between transfusions.

As for many endocrine disorders, a logical therapeutic approach would be the replacement of the missing hor-

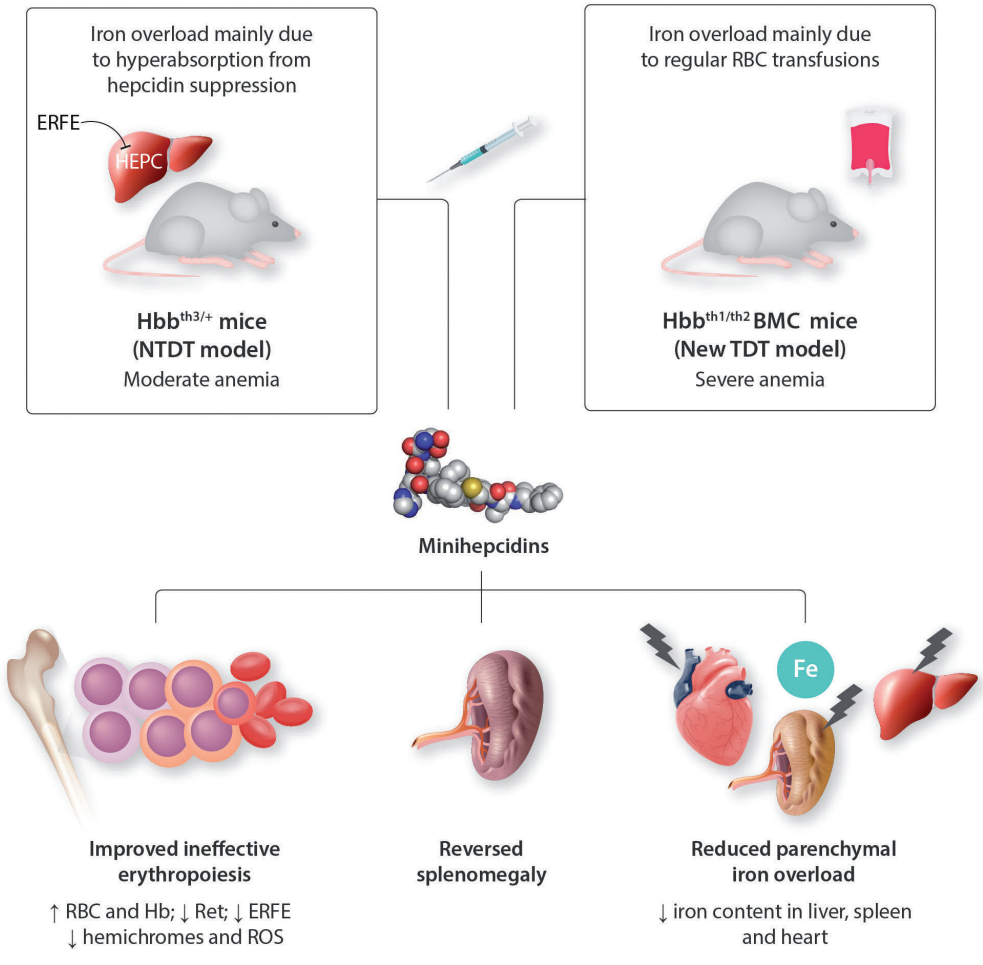

Figure 1. Effects of minihepcidins in non-transfusion-dependent and transfusion-dependent β-thalassemia mouse models. Treatment with minihepcidins has similar beneficial effects in both the non-transfusion-dependent β-thalassemia mouse model (*Hbb*$^{th3/+}$) and in the novel transfusion-dependent model (*Hbb*$^{th1/th2}$*BMC*) developed by Casu *et al.* In particular, in the transfused mice, minihepcidins improved ineffective erythropoiesis and splenomegaly, and reduced the severity of parenchymal iron overload. ERFE: erythroferrone; HEPC: hepcidin; NTDT: non-transfusion-dependent β-thalassemia; RBC: red blood cells; BMC: bone marrow chimera; TDT: transfusion-dependent β-thalassemia; Hb: hemoglobin; Ret: reticulocytes; ROS: reactive oxygen species.

mone through exogenous preparations. Unfortunately, replacing hepcidin is not as easy as in the case, for example, of levothyroxine in hypothyroidism, or different insulin preparations in type 1 diabetes mellitus. Hepcidin is a small peptide mainly produced by the liver, consisting of only 25 amino acids including eight cysteines which form four disulfide bonds determining a highly folded structure.[12] Attempts to synthesize a sufficient amount of the hormone in its natural conformation have proven exceedingly difficult.[13] Moreover, the natural hormone has a short plasma half-life, being rapidly eliminated by proteolysis and renal clearance.[14]

An alternative approach is represented by the production of long-acting molecules, collectively called "minihepcidins".[15] Minihepcidins are synthetic peptides containing the minimal N-terminal sequence (7 to 9 amino acids) of hepcidin still able to bind ferroportin and induce its degradation, further engineered to be resistant to proteolysis. Minihepcidins have been used previously in mouse models of severe hemochromatosis (with knockout of hepcidin anti-microbial peptide; *HAMP*$^{-/-}$),[16] and NTDT β-thalassemia.[17] In the latter model, minihepcidins proved useful in reducing iron overload and splenomegaly, but also improved anemia by either decreasing ineffective erythropoiesis or increasing red blood cell lifespan through reduced formation of hemichromes and reactive oxygen species[17] (Figure 1).

In this issue of *Haematologica*,[18] Casu and colleagues present the first mouse model of TDT β-thalassemia available so far. Previous attempts to model this disease were hampered by the early death of the animals. To resolve this problem, using an elegant approach the authors intercrossed two previous NTDT strains (*Hbb*$^{th1/th1}$ and *Hbb*$^{th2/+}$) and then transplanted *Hbb*$^{th1/th2}$ fetal liver cells into irradiated recipients to obtain *Hbb*$^{th1/th2}$ bone marrow chimera (*BMC*). These mice showed a severe phenotype resembling β-thalassemia major, requiring red blood cell transfusions for survival. As in the previous NTDT models, the administration of minihepcidins not only reduced splenomegaly and iron overload (especially in the heart, where it is particularly deadly), but also improved erythropoiesis and anemia (Figure 1). The latter effect is likely related to the apparent paradoxical benefit of iron restriction on thalassemic erythropoiesis, through a reduction in the synthesis of heme, which in turn decreases the production of α-globin chains and toxic hemichromes in a coordinated manner.[19]

The study by Casu and colleagues does, however, have several limitations. For example, minihepcidin treatment was started simultaneously with the first transfusion, i.e. before the massive iron accumulation that usually occurs in chronically transfused β-thalassemic patients. Thus, it remains to be demonstrated whether or not minihepcidins could also be beneficial in a setting more closely resembling clinical practice, in which typical TDT patients are kept on balance within acceptable iron overload by using iron chelators, which in turn are far from being optimal and easy to use.[20] Another limitation is that the *Hbb*$^{th1/th2}$ mice were treated with red blood cell transfusions only for a short period (6 weeks). Finally, these mice appear to maintain a particularly high level of iron absorption, which may not mirror what happens in chronically transfused β-thalassemic patients.

Anyway, the question is: are we ready for hepcidin replacement therapy in the clinic? Despite the promising results of Casu and colleagues, it is still too early to say. No human study on minihepcidins is currently underway. It is unknown whether technical or economic issues will hamper the translation of minihepcidins into the clinic. While, in principle, minihepcidins could be bioavailable after oral administration,[14] studies in animals used intraperitoneal or subcutaneous administration, which is not as convenient as the oral route. Interestingly, one study with a hepcidin analogue, LJPC-401, is ongoing in adult patients with genetic hemochromatosis (*https://clinicaltrials.gov/ct2/show/NCT03395704*), but results are not yet available. Despite extraordinary advances toward a definitive cure for β-thalassemia, by either allogeneic hematopoietic cell transplantation[21] or gene therapy,[22] much of the disease's burden occurs in low-income populations with limited access to such sophisticated resources, in which red blood cell transfusions and iron chelation remain the mainstay of therapy.[23] The research by Casu and colleagues provides a proof of concept that hepcidin replacement therapy or hepcidin agonists represent a fascinating and pathophysiologically sound approach[24] for treating iron overload in a variety of conditions, including iron-loading anemias.[25] In the near future, we will understand the place of such drugs in the rapidly evolving and exciting scenario of novel anti-anemic drugs, including activin type II receptor agonists[26] and others.[27]

References

1. Hentze MW, Muckenthaler MU, Galy B, Camaschella C. Two to tango: regulation of mammalian iron metabolism. Cell. 2010;142(1):24-38.
2. Pietrangelo A. Hemochromatosis: an endocrine liver disease. Hepatology. 2007;46(4):1291-1301.
3. Ganz T. Systemic iron homeostasis. Physiol Rev. 2013;93(4):1721-1741.
4. Gulec S, Anderson GJ, Collins JF. Mechanistic and regulatory aspects of intestinal iron absorption. Am J Physiol Gastrointest Liver Physiol. 2014;307(4):G397-409.
5. Girelli D, Nemeth E, Swinkels DW. Hepcidin in the diagnosis of iron disorders. Blood. 2016;127(23):2809-2813.
6. Camaschella C, Nai A, Silvestri L. Iron metabolism and iron disorders revisited in the hepcidin era. Haematologica. 2020;105(2):260-272.
7. Sleiman J, Tarhini A, Bou-Fakhredin R, Saliba AN, Cappellini MD, Taher AT. Non-transfusion-dependent thalassemia: an update on complications and management. Int J Mol Sci. 2018;19(1).
8. Ganz T. Erythropoietic regulators of iron metabolism. Free Radic Biol Med. 2019;133:69-74.
9. Coffey R, Ganz T. Erythroferrone: an erythroid regulator of hepcidin and iron metabolism. Hemasphere. 2018;2(2):e35.
10. Angelucci E, Barosi G, Camaschella C, et al. Italian Society of Hematology practice guidelines for the management of iron overload in thalassemia major and related disorders. Haematologica. 2008;93(5):741-752.
11. Pasricha SR, Frazer DM, Bowden DK, Anderson GJ. Transfusion suppresses erythropoiesis and increases hepcidin in adult patients with beta-thalassemia major: a longitudinal study. Blood. 2013;122(1):124-133.
12. Clark RJ, Tan CC, Preza GC, Nemeth E, Ganz T, Craik DJ. Understanding the structure/activity relationships of the iron regulatory peptide hepcidin. Chem Biol. 2011;18(3):336-343.
13. Jordan JB, Poppe L, Haniu M, Arvedson T, Syed R, Li V, et al. Hepcidin revisited, disulfide connectivity, dynamics, and structure. J Biol Chem. 2009;284(36):24155-24167.
14. Schmidt PJ, Fleming MD. Modulation of hepcidin as therapy for pri-

mary and secondary iron overload disorders: preclinical models and approaches. Hematol Oncol Clin North Am. 2014;28(2):387-401.
15. Preza GC, Ruchala P, Pinon R, et al. Minihepcidins are rationally designed small peptides that mimic hepcidin activity in mice and may be useful for the treatment of iron overload. J Clin Invest. 2011;121(12):4880-4888.
16. Ramos E, Ruchala P, Goodnough JB, et al. Minihepcidins prevent iron overload in a hepcidin-deficient mouse model of severe hemochromatosis. Blood. 2012;120(18):3829-3836.
17. Casu C, Oikonomidou PR, Chen H, et al. Minihepcidin peptides as disease modifiers in mice affected by beta-thalassemia and polycythemia vera. Blood. 2016;128(2):265-276.
18. Casu C, Chessa R, Liu A, et al. Minihepcidins improve ineffective erythropoiesis and splenomegaly in a new mouse model of adult β-thalassemia major. Haematologica. 2020;105(7):1835-1844.
19. Camaschella C. Treating iron overload. N Engl J Med. 2013;368(24):2325-2327.
20. Coates TD. Iron overload in transfusion-dependent patients. Hematology Am Soc Hematol Educ Program. 2019;2019(1):337-344.
21. Angelucci E. Hematopoietic stem cell transplantation in thalassemia. Hematology Am Soc Hematol Educ Program. 2010;2010:456-462.
22. Thompson AA, Walters MC, Kwiatkowski J, et al. Gene therapy in patients with transfusion-dependent beta-thalassemia. N Engl J Med. 2018;378(16):1479-1493.
23. Galanello R, Origa R. Beta-thalassemia. Orphanet J Rare Dis. 2010;5:11.
24. Casu C, Nemeth E, Rivella S. Hepcidin agonists as therapeutic tools. Blood. 2018;131(16):1790-1794.
25. Camaschella C, Nai A. Ineffective erythropoiesis and regulation of iron status in iron loading anaemias. Br J Haematol. 2016;172(4):512-523.
26. Cappellini MD, Viprakasit V, Taher AT, et al. A phase 3 trial of luspatercept in patients with transfusion-dependent beta-thalassemia. N Engl J Med. 2020;382(13):1219-1231.
27. Busti F, Marchi G, Lira Zidanes A, Castagna A, Girelli D. Treatment options for anemia in the elderly. Transfus Apher Sci. 2019;58(4):416-421.

ABL-class fusion positive acute lymphoblastic leukemia: can targeting ABL cure ALL?

Thai Hoa Tran[1] and Stephen P. Hunger[2]

[1]Division of Pediatric Hematology-Oncology, Charles-Bruneau Cancer Center, CHU Sainte-Justine, University of Montreal, Montreal, Quebec, Canada and [2]Department of Pediatrics, The Center for Childhood Cancer Research, Children's Hospital of Philadelphia, The Perelman School of Medicine, University of Pennsylvania, Philadelphia, PA, USA

E-mail: STEPHEN HUNGER - hungers@email.chop.edu

doi:10.3324/haematol.2020.252916

Five-year survival rates for pediatric acute lymphoblastic leukemia (ALL), a malignancy that was incurable in the 1950s, now exceed 90%.[1] However, 15-20% of National Cancer Institute (NCI) high-risk (HR) B-lineage ALL (B-ALL) patients relapse, and post-relapse outcomes remain poor, particularly following early marrow relapse [5-year overall survival (OS): 28%].[2] Genomic advances have identified a novel B-ALL subtype characterized by a heterogeneous spectrum of kinase-activating alterations, producing a gene expression signature similar to that of Philadelphia chromosome-positive (Ph^+) ALL, without the canonical BCR-ABL1 oncoprotein, referred to as BCR-ABL1-like ALL or Ph-like ALL, and now recognized as a provisional disease entity in the 2016 World Health Organization's classification of acute leukemias.[3,4] Ph-like ALL is associated with adverse clinical features and poor outcomes despite modern therapy.[4-6] It occurs in approximately 15% of children with NCI HR B-ALL and over 25% of adults with B-ALL, and contributes disproportionately to relapses.[4,6] Among Ph-like ALL patients, 10-14% of them harbor rearrangements of ABL-class genes (*ABL1, ABL2, CSF1R, LYN, PDGFRA, PDGFRB*) other than *BCR-ABL1*, collectively representing 2-3% of pediatric B-ALL cases.[4-6] While there are anecdotal reports of the short-term efficacy of adding the ABL tyrosine kinase inhibitors (TKI) imatinib or dasatinib to chemotherapy,[4,7,8] controlled data are lacking regarding the long-term efficacy of this approach. In this issue of Haematologica, Cario *et al.*[9] provide important new information on treatment of children with ALL and ABL-class fusions.

They report 46 ABL-class fusion positive B-ALL patients (15 involving *ABL1*, 5 *ABL2*, 3 *CSF1R*, and 23 *PDGFRB*) who were originally enrolled on the AIEOP-BFM ALL 2000 and 2009 trials, and identified retrospectively. ABL-class fusion-positive cases had a substantially worse early treatment response than other patients, as reflected by prednisone-poor response (50% *vs.* 5.6%, $P<0.0001$) or minimal residual disease (MRD) $\geq 5\times10^{-4}$ at end-induction (71.4% *vs.* 19.2%, $P<0.0001$) and end-protocol Ib (51.2% *vs.* 5.1%, $P<0.0001$). Thirty-six of 46 patients (78.3%) were classified as HR (*vs.* 11.1% of ALL-BFM 2000 B-ALL patients overall), and more than half (25 of 46, 54.3%) underwent hematopoietic stem cell transplantation (HSCT) in first complete remission (CR1). For the cohort of 46 patients with ABL-class fusions, the 5-year event-free survival (EFS) and OS were 49.1±8.9% and 69.6±7.8%, respectively. The 5-year cumulative incidence of relapse (CIR) and treatment-related mortality (TRM) were 25.6±8.2% and 20.8±6.8%, respectively. Thirteen patients (13 of 46, 28.3%) received TKI in combination with chemotherapy post-induction; their outcomes were not significantly different from those in the no-TKI group (n=33) (5-year EFS 62.9% *vs.* 47.7%, $P=0.98$; 5-year OS 75.5% *vs.* 70.9%, $P=0.64$). In parallel, ABL-class patients treated with or without HSCT had similar outcomes (5-year EFS 47.9% *vs.* 55.0%, $P=0.35$; 5-year OS 66.7% *vs.* 84.0%, $P=0.22$). Notably, in the 33 patients treated without TKI, there was a trend towards lower CIR rate among patients who underwent HSCT (n=16) compared to those who did not (n=17) (13.2% *vs.* 43.8%, $P=0.06$). The TRM rate was, nevertheless, exceedingly high in the HSCT group (32.3% *vs.* 0.0%, $P=0.034$). Furthermore, the majority of events in the HSCT group were non-relapse events, while relapses predominate in the no-HSCT group.

This article is valuable to clinicians as it confirms the adverse presenting features, poor early response and EFS/OS rates of a large cohort of ABL-class fusion positive B-ALL patients, similar to prior anecdotal reports[7] or smaller retrospective series.[8,10] Moreover, the authors highlight the striking clinical resemblance between ABL-class fusion positive B-ALL and Ph+ ALL. Both disease entities comprise approximately 3% of pediatric ALL, tend to be older patients with hyperleukocytosis, elevated MRD at the end of induction and consolidation, and the reported 5-year EFS of less than 50% for the ABL-class cohort mirrors that of Ph+ ALL in the pre-TKI era treated with the same chemotherapy backbone.[11,12] This has important therapeutic implications, suggesting that the addition of TKI to chemotherapy, which has transformed survival of Ph+ ALL, may similarly translate into improved outcomes for ABL-class patients.[13,14] In this series, six of the eight ABL-class patients who started TKI

A

	NCI SR[21]	Childhood NCI HR[5]	1-39 yo[4]	21-86 yo[6]
N = total # of B-ALL	1023	1389	1725	798
Ph-like ALL (%)	139 (13.6)	284 (20.4)	264 (15.3)	194 (24.3)
Ph+ ALL (%)	6 (0.6)	46 (3.3)	109 (6.3)	185 (23.2)
ABL-class fusions (%)	2 (0.2)	40 (2.9)	36 (2.0)	19 (2.4)

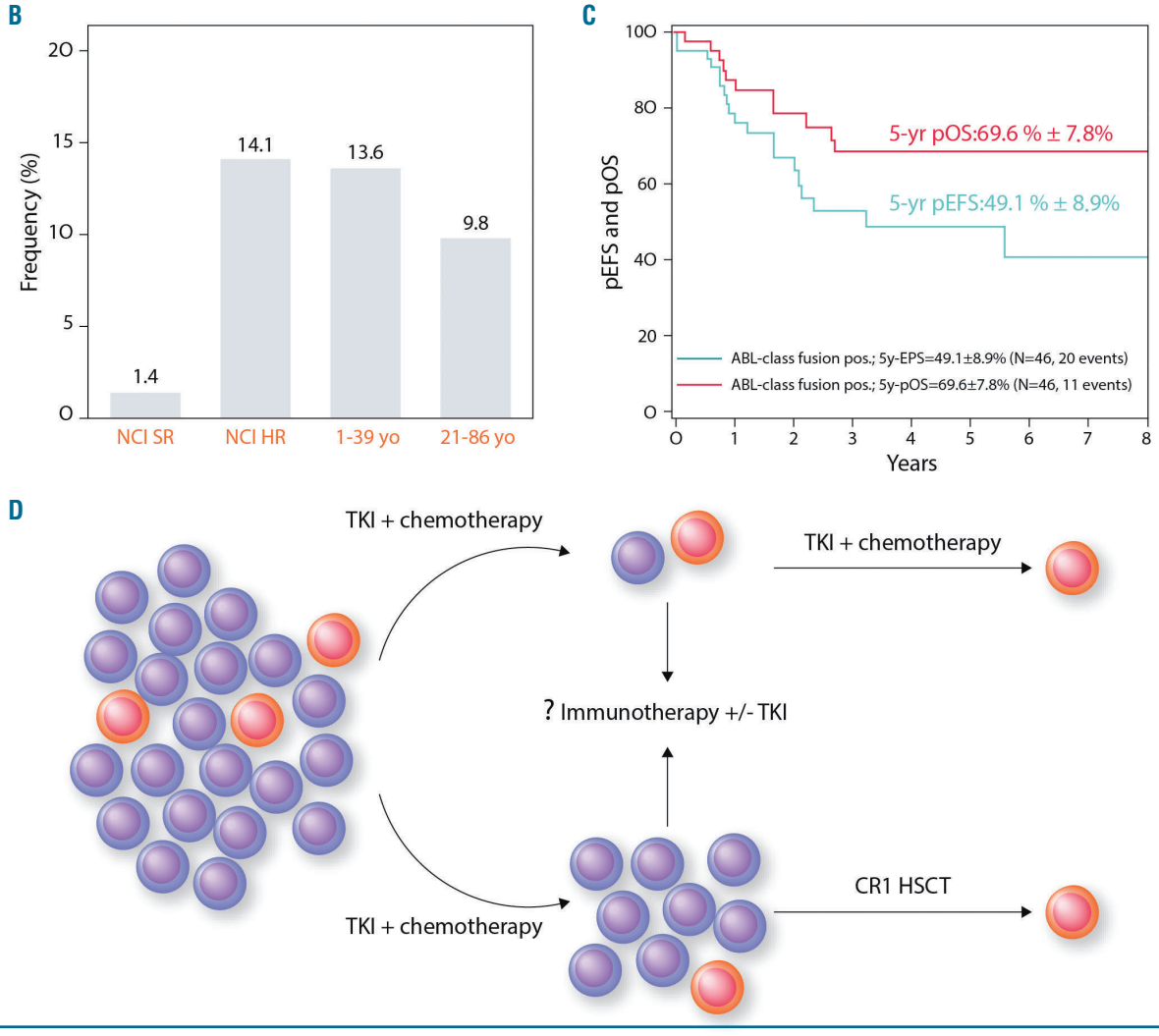

Figure 1. (A) Frequency of Philadelphia chromosome (Ph)-positive acute lymphoblastic leukemia (ALL), Ph-like ALL and ABL-class fusions in B-lineage ALL (B-ALL) according to National Cancer Institute (NCI) risk status and age group, based on the following studies: Roberts *et al.*,[21] Reshmi *et al.*,[5] Roberts *et al.*,[4] and Roberts *et al.*[6] NCI SR: National Cancer Institute Standard Risk; NCI HR: National Cancer Institute High Risk. (B) Frequency of ABL-class fusions in Ph-like ALL. (C) Outcomes of ABL-class fusion positive B-ALL patients treated on the AIEOP-BFM ALL 2000 and 2009 trials. pEFS: projected event-free survival; pOS: projected overall survival. (D) Proposed treatment paradigm for ABL-class fusion positive B-ALL. Early introduction of tyrosine kinase inhibitor (TKI) to induction chemotherapy to achieve remission. Good-responders may continue with TKI and post-induction chemotherapy. Poor-responders will undergo allogeneic hematopoietic stem cell transplantation in first remission (CR1). Incorporation of immunotherapy with or without TKI is being considered in future trials to improve outcomes. yr: year.

during consolidation had a low positive or negative end-Ib MRD, emphasizing the importance of early identification of ABL-class fusions and prompt TKI addition to achieve deep MRD response and, potentially, better outcomes. Despite the heterogeneity of ABL-class fusions, Cario *et al.* demonstrated that most ABL-class rearrangements could be detected by techniques such as fluorescence *in situ* hybridization (FISH) or polymerase chain reaction (PCR), which are standard techniques in clinical laboratories. Much effort in recent years has focused on screening for the kinase-activated signature that defines Ph-like ALL; however, ultimately, the clinically relevant goal is the prompt detection of the underlying therapeutically targetable genomic lesions. The Children's Oncology Group (COG) is now expanding their FISH panel to include *ABL1*, *ABL2* and *PDGFRB/CSF1R* dual-colored break-apart probes to screen for ABL-class gene rearrangements in order to introduce TKI by mid-induction. This strategy could perhaps overcome the high rates of induction failure and eradicate MRD levels early in the course of therapy for the majority of ABL-class patients, as early TKI introduction has done for Ph$^+$ ALL.[14,15] Prospective evaluation of the early addition of TKI to therapy of patients with ABL-class lesions is required; this can only be achieved by harnessing international collaborations to effectively design precision medicine trials for such rare disease entities as exemplified by the Ph$^+$ ALL experience (*clinicaltrials.gov identifers:* NCT0146016 and NCT03007147).

The article by Cario *et al.* also raises two fundamental questions which underlie the role of HSCT and the optimal chemotherapy backbone for ABL-class fusion positive B-ALL. HSCT appears to be an effective modality for disease control as fewer relapses occurred among ABL-class patients in the no-TKI group who underwent HSCT in CR1 (13.2% *vs*. 43.8%, *P*=0.06). A single-center study previously reported comparable outcomes between children with Ph-like ALL and non-Ph-like ALL (5-year EFS 90.0% *vs*. 88.4%, *P*=0.41, respectively), using MRD-directed therapy intensification for relevant patients.[16] Consequently, a significant higher proportion of Ph-like ALL patients underwent HSCT in CR1 due to end-induction MRD levels ≥1%.[16] Nevertheless, HSCT is associated with unacceptably high TRM rates, which account for a considerable proportion of events in this AIEOP-BFM retrospective cohort. Given that ABL-class fusion positive B-ALL biologically and clinically phenocopies Ph$^+$ ALL, one can speculate that early and continuous TKI administration in combination with chemotherapy may avoid HSCT in CR1 for a subset of ABL-class patients, allowing it to be reserved for patients at the highest risk of relapse.

With regards to the optimal chemotherapy backbone for pediatric ABL-class patients, three regimens are currently being investigated in clinical trials: 1) the Total Therapy-based chemotherapy backbone from St. Jude Children's Research Hospital (*clinicaltrials.gov identifer*: NCT03117751); 2) the multinational European EsPhALL regimen as utilized in EsPhALL2010 (*clinicaltrials.gov identifer*: NCT00287105) and AALL1122 (*clinicaltrials.gov identifer*: NCT01460160); and 3) the COG AALL1131 modified augmented BFM backbone (*clinicaltrials.gov identifer*: NCT02883049). The latter two regimens are being compared in a randomized fashion in the phase III international trial for Ph$^+$ ALL in a non-inferior design (COG AALL1631; *clinicaltrials.gov identifer*: NCT03007147), which investigators plan to amend to also include ABL-class fusion patients. While awaiting the AALL1631 results to determine the optimal chemotherapy backbone for ABL-class patients, Cario *et al.* alluded to the high TRM rates when treating with the EsPhALL-inspired regimen, contributing to the poor outcomes of ABL-class patients. Similar findings have been observed in a recent publication from the AIEOP-BFM consortia; older adolescents aged 15-17 years also experienced significantly higher treatment-related deaths compared to their younger counterparts when treated on the AEIOP-BFM ALL 2000 chemotherapy backbone (without TKI), particularly in the HR arm that is the chemotherapy backbone to the EsPhALL regimen.[17] Given that the prevalence of Ph-like ALL rises with increasing age, toxicity remains a primary concern when adding TKI to the EsPhALL post-induction chemotherapy backbone for ABL-class patients. While therapy intensification has been an effective strategy to better outcomes in the past, in the modern era, we might have reached a plateau where further intensification is more likely to result in excessive toxicities rather than improve survival. Fortunately, the landscape of relapsed/refractory ALL therapy has witnessed major paradigm shifts with the emergence of immunotherapy. The bispecific CD3/CD19 T-cell engager, blinatumomab, or the anti-CD22 antibody drug conjugate, inotuzumab ozogamicin, in monotherapy or in combination with TKI, have been used in Ph$^+$/Ph-like ALL with promising early results.[18-20] Therefore, incorporation of immunotherapy blocks intercalated within conventional chemotherapy backbone may represent an efficacious strategy to intensify therapy and reduce overlapping toxicities for ABL-class Ph-like ALL.

Cario *et al.* have provided an important dataset to fulfill the clinical portrait of the rare subset of ABL-class fusion positive B-ALL. The genomic landscape of Ph-like ALL and its associated poor prognosis have now been recognized for over a decade; thus, the time has come to act! The prospect of targeted therapy, immunotherapy and targeted use of CR1 HSCT, combined with lessons learned from previous Ph$^+$ ALL studies and international collaborations to conduct well-designed precision medicine trials, can establish pathways to increase cures for this high-risk ALL subset. One may dream that by improving outcomes of Ph-like ALL, we will be able to cure all ALL!

References

1. Hunger SP, Lu X, Devidas M, et al. Improved survival for children and adolescents with acute lymphoblastic leukemia between 1990 and 2005: a report from the children's oncology group. J Clin Oncol. 2012;30(14):1663-1669.
2. Rheingold SR, Ji L, Xu X, et al. Prognostic factors for survival after relapsed acute lymphoblastic leukemia (ALL): A Children's Oncology Group (COG) study. J Clin Oncol. 2019;37(15_suppl): 1008-1008.
3. Den Boer ML, van Slegtenhorst M, De Menezes RX, et al. A subtype of childhood acute lymphoblastic leukaemia with poor treatment outcome: a genome-wide classification study. Lancet Oncol. 2009;10(2):125-134.

4. Roberts KG, Li Y, Payne-Turner D, et al. Targetable kinase-activating lesions in Ph-like acute lymphoblastic leukemia. N Engl J Med. 2014;371(11):1005-1015.
5. Reshmi SC, Harvey RC, Roberts KG, et al. Targetable kinase gene fusions in high-risk B-ALL: a study from the Children's Oncology Group. Blood. 2017;129(25):3352-3361.
6. Roberts KG, Gu Z, Payne-Turner D, et al. High Frequency and Poor Outcome of Philadelphia Chromosome-Like Acute Lymphoblastic Leukemia in Adults. J Clin Oncol. 2017;35(4):394-401.
7. Weston BW, Hayden MA, Roberts KG, et al. Tyrosine kinase inhibitor therapy induces remission in a patient with refractory EBF1-PDGFRB-positive acute lymphoblastic leukemia. J Clin Oncol. 2013;31(25):e413-416.
8. Tanasi I, Ba I, Sirvent N, et al. Efficacy of tyrosine kinase inhibitors in Ph-like acute lymphoblastic leukemia harboring ABL-class rearrangements. Blood. 2019;134(16):1351-1355.
9. Cario G, Leoni V, Conter V, et al. Relapses and treatment-related events contributed equally to poor prognosis in children with ABL-class fusion positive B-cell acute lymphoblastic leukemia treated according to AIEOP-BFM protocols. Haematologica 2020;105(7):1887-1894.
10. Schwab C, Ryan SL, Chilton L, et al. EBF1-PDGFRB fusion in pediatric B-cell precursor acute lymphoblastic leukemia (BCP-ALL): genetic profile and clinical implications. Blood. 2016;127(18):2214-2218.
11. Conter V, Bartram CR, Valsecchi MG, et al. Molecular response to treatment redefines all prognostic factors in children and adolescents with B-cell precursor acute lymphoblastic leukemia: results in 3184 patients of the AIEOP-BFM ALL 2000 study. Blood. 2010;115(16):3206-3214.
12. Arico M, Valsecchi MG, Camitta B, et al. Outcome of treatment in children with Philadelphia chromosome-positive acute lymphoblastic leukemia. N Engl J Med. 2000;342(14):998-1006.
13. Schultz KR, Carroll A, Heerema NA, et al. Long-term follow-up of imatinib in pediatric Philadelphia chromosome-positive acute lymphoblastic leukemia: Children's Oncology Group study AALL0031. Leukemia. 2014;28(7):1467-1471.
14. Biondi A, Gandemer V, De Lorenzo P, et al. Imatinib treatment of paediatric Philadelphia chromosome-positive acute lymphoblastic leukaemia (EsPhALL2010): a prospective, intergroup, open-label, single-arm clinical trial. Lancet Haematol. 2018;5(12):e641-e652.
15. Slayton WB, Schultz KR, Kairalla JA, et al. Dasatinib Plus Intensive Chemotherapy in Children, Adolescents, and Young Adults With Philadelphia Chromosome-Positive Acute Lymphoblastic Leukemia: Results of Children's Oncology Group Trial AALL0622. J Clin Oncol. 2018;36(22):2306-2314.
16. Roberts KG, Pei D, Campana D, et al. Outcomes of children with BCR-ABL1-like acute lymphoblastic leukemia treated with risk-directed therapy based on the levels of minimal residual disease. J Clin Oncol. 2014;32(27):3012-3020.
17. Testi AM, Attarbaschi A, Valsecchi MG, et al. Outcome of adolescent patients with acute lymphoblastic leukaemia aged 10-14 years as compared with those aged 15-17 years: Long-term results of 1094 patients of the AIEOP-BFM ALL 2000 study. Eur J Cancer. 2019;122:61-71.
18. Martinelli G, Boissel N, Chevallier P, et al. Complete Hematologic and Molecular Response in Adult Patients With Relapsed/Refractory Philadelphia Chromosome-Positive B-Precursor Acute Lymphoblastic Leukemia Following Treatment With Blinatumomab: Results From a Phase II, Single-Arm, Multicenter Study. J Clin Oncol. 2017;35(16):1795-1802.
19. Chiaretti S, Bassan R, Vitale A, et al. Dasatinib-Blinatumomab Combination for the Front-Line Treatment of Adult Ph+ ALL Patients. Updated Results of the Gimema LAL2116 D-Alba Trial. Blood. 2019;134(Suppl 1):740.
20. Jabbour E, Roberts KG, Sasaki K, et al. Inotuzumab Ozogamicin May Overcome the Impact of Philadelphia Chromosome-like Phenotype in Adult Patients with Relapsed/Refractory Acute Lymphoblastic Leukemia. Blood. 2019;134(Suppl_1):1641.
21. Roberts KG, Reshmi SC, Harvey RC, et al. Genomic and Outcome Analyses of Ph-like ALL in NCI Standard-risk Patients: A Report from the Children's Oncology Group. Blood. 2018;132:815-824.

NUP98 and *KMT2A*: usually the bride rather than the bridesmaid

Alexandre Fagnan[1,2,3] and Thomas Mercher[1,2,3,4]

[1]INSERM U1170, Gustave Roussy Institute, Villejuif; [2]Université Paris Diderot, Paris; [3]Equipe labellisée Ligue Nationale Contre le Cancer, Paris and [4]Université Paris-Saclay, Villejuif, France

E-mail: THOMAS MERCHER - thomas.mercher@inserm.fr

doi:10.3324/haematol.2020.253476

In human hematopoietic malignancies, *KMT2A* and *NUP98* are each independently targeted by numerous chromosomal alterations leading to the expression of fusion oncogenes. In this issue of *Haematologica*, Fisher and colleagues from J. Schwaller's team report the functional study and creation of an *in vivo* model[1] for a unique fusion between these two genes[2] showing that leukemia development by NUP98-KMT2A is not associated with classical KMT2A fusion mechanisms.

KMT2A (a.k.a. MLL) is a large protein of almost 4,000 amino acids that is processed by the endopeptidase Taspase1. It interacts with numerous proteins and assembles into large protein complexes (Figure 1). The functions of KMT2A include writing the H3K4me3 chromatin mark characteristic of active promoter regions through its C-terminal SET domain. In both lymphoid and myeloid malignancies, KMT2A is targeted by numerous chromosomal alterations resulting in the expression of fusion oncogenes with over 80 different partners *in toto* (*https://mitelmandatabase.isb-cgc.org/*). Experimental models have demonstrated that several fusions containing the N-terminal portion of KMT2A and various partners [here termed KMT2A-X, where X is frequently AFF1, MLLT3, MLLT10 or MLLT1 in acute lymphoid leukemia patients, and MLLT3, MLLT10, MLLT1 or ELL in patients with acute myeloid leukemia (AML)] are important for disease development and maintenance.[3,4]

It has long been recognized that KMT2A-X fusions activate transcription of different *HOX* genes (e.g. *HOXC8*, *HOXA7*, *HOXA9*, and *HOXA10*) and are associated with high expression of the HOX cofactor *MEIS1*. At the molecular level, at least two distinct mechanisms have been involved in KMT2A-X leukemogenic properties and the deregulated expression of KMT2A-X target genes (Figure 1). On the one hand, the first 145 N-terminal amino acids of KMT2A interact with MEN1 and LEDGF to bind KMT2A target genes.[5] On the other hand, most fusion partners of KMT2A belong to the transcription elongation machinery leading to the active recruitment of various factors including (i) the P-TEFb complex (comprising CDK9), which phosphorylates RNA polymerase II; and (ii) the histone methyltransferases DOT1L and NSD1, which catalyze H3K79me3 and H3K36me2 marks deposited in the body of actively transcribed genes. This

creates an active gene transcription elongation environment at KMT2A-X target genes (e.g. *HOX* genes), which is reinforced by the recognition of acetylated lysines on histones at important oncogene loci (e.g. *MYC*) by the BET proteins including BRD4. Based on these dependencies, small molecule inhibitors of DOT1L, of BRD4 and of the interaction between KMT2A and MEN1 have been developed.[6-8]

Other alterations of KMT2A function are observed. In some instances reciprocal X-KMT2A fusions were shown to contribute to leukemogenesis in murine model (e.g. *AFF1-KMT2A* cooperation with *KMT2A-AFF1*[9]). *KMT2A* partial tandem duplications (*KMT2A*-PTD) are also found in AML and both murine modeling and human genetics indicate that *KMT2A*-PTD requires additional mutations to induce *bona fide* leukemia.[10,11]

Wildtype NUP98 is part of the nuclear pore complex, a large structure of ~30 proteins at the nuclear membrane which provides a bidirectional channel allowing small ions and peptides to diffuse and larger molecules (mRNA and proteins) to be actively transported by carriers. NUP98 is different from other nucleoporins as it contains multiple GLFG repeats allowing interaction with CREBBP/EP300 and it can be found throughout the nucleus. Nup98 was reported to be involved, together with Rae, in cell cycle progression and mitotic spindle regulation.[12] Notably, NUP98 is found at sites of actively transcribed genes presenting the H3K4me3 mark and is involved in cell cycle and development.[13] NUP98 is also involved with wildtype KMT2A and NSL in complexes regulating *HOX* gene expression.[14]

In leukemia, NUP98 is recurrently fused with over 30 different partners (including NSD1, KDM5A, but also homeodomain proteins such as HOXA9, HOXC11, HOXD11 or HOXD13). These fusions (termed NUP98-X here) result from chromosomal alterations that are frequently undetected by conventional cytogenetics due to the location of the *NUP98* gene close to the telomere of the short arm of chromosome 11 (11p15).[15,16] In the case of chimeras between NUP98 and homeodomain proteins, the GLFG repeats of NUP98 generally replace the transactivation domain. To date, all NUP98-X fusions have been

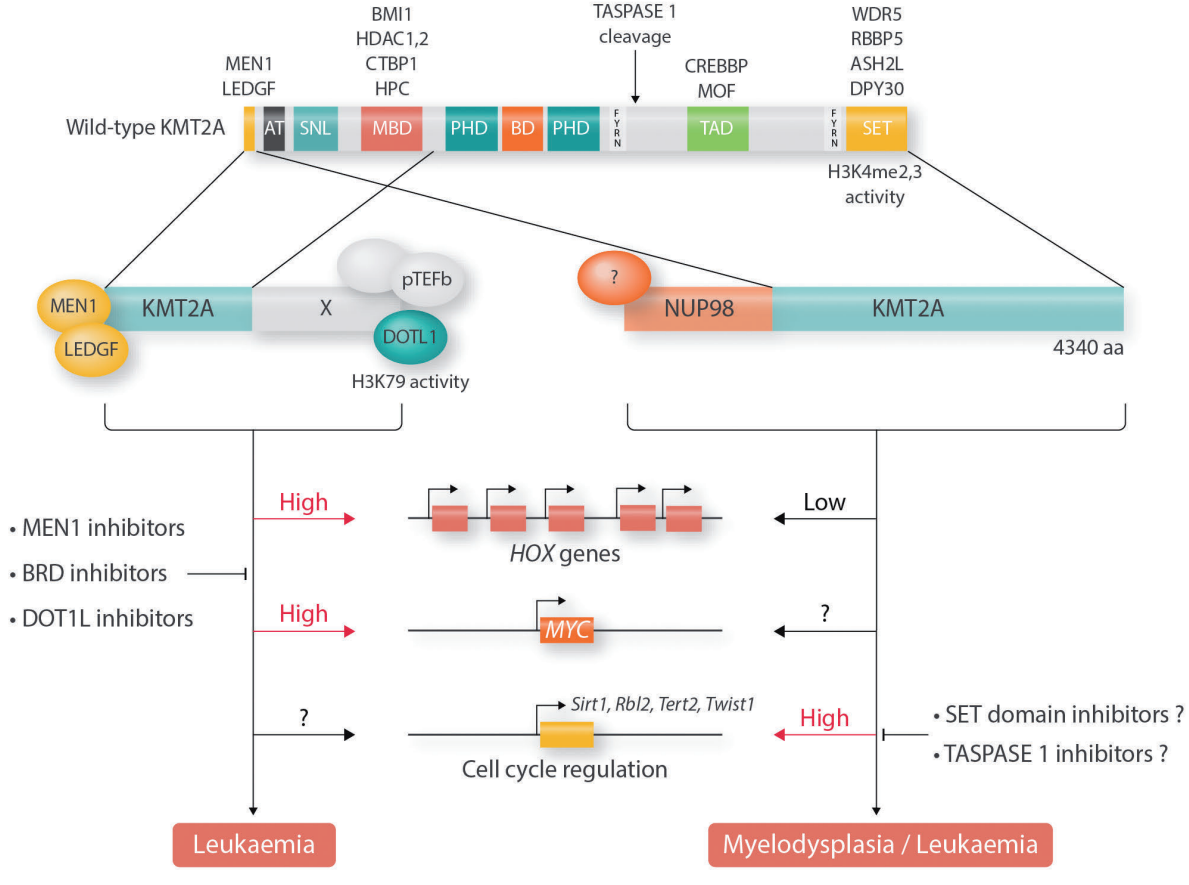

Figure 1. Molecular mechanisms associated with KMT2A-X and NUP98-KMT2A fusions. Schematic representation of the functional domains of wildtype KMT2A, KMT2A-X (where X corresponds to the fusion partners), and NUP98-KMT2A and the molecular mechanisms associated with leukemic transformation. While KMT2A-X fusions are associated with high expression (High) of *HOX* genes and *MYC*, NUP98-KMT2A is associated with low *HOX* genes (Low) and its regulation on *MYC* expression remains unknown (?). In mice, NUP98-KMT2A transformation is associated with high expression of cell cycle-associated genes (e.g. *Sirt1*, *Rbl2* and *Tert2*). Therapeutic targeting developed for KMT2A-X leukemia includes MEN1, DOT1L and BRD4 inhibitors. Whether small-molecule inhibitors of SET domain or TASPASE 1 activities would be efficient in NUP98-KMT2A leukemia is unknown. AT: AT-hook domain; SNL: speckled nuclear localization domains; MBD: MENIN 1-binding domain; PHD: plant homeodomain finger domain; BD: bromodomain; FYRN and FYRC: phenylalanine/tyrosine-rich-N- and C-terminal domains; TAD: transactivation domain; SET: SET methyltransferase activity domain.

associated with high *HOX* gene expression. Similarly to wildtype NUP98, the NUP98-HOXA9 fusion also interacts with wildtype KMT2A through the second GLFG repeat of NUP98 and KMT2A is important for the recruitment of NUP98-HOXA9 to the *HOXA* locus and NUP98-HOXA9-dependent *HOXA* genes expression.[17]

Fisher *et al.* performed functional modeling of a peculiar *NUP98-KMT2A* alteration, resulting from an inv(11)(p15;q23) characterized in two AML patients and leading to the fusion of *NUP98* exon 13 to *KMT2A* exon 2. The predicted *NUP98-KMT2A* fusion encodes a 4,340 amino acid protein lacking the MEN1-interacting domain but containing most of KMT2A including the H3K4 methylation SET domain, as opposed to KMT2A-X fusions (Figure 1). As the reciprocal *KMT2A-NUP98* fusion transcript (between exon 1 of *KMT2A* and exon 14 of *NUP98*) was detected in only one of the two original patients,[2] the hypothesis was that the *NUP98-KMT2A* fusion may represent the important disease driver. Fisher *et al.* achieved this *tour de force* through the development of a novel inducible NUP98-KMT2A transgenic mouse model.

The authors demonstrate the expansion and increased competitiveness of NUP98-KMT2A-expressing hematopoietic progenitor cells ($Lineage^{-}Sca1^{+}Kit^{+}$ cells) and concomitant cell cycle abnormalities without significant changes in the relative distribution between long-term hematopoietic stem cells and multi-potent progenitors. Upon long-term NUP98-KMT2A expression, mice succumbed to lethal myelodysplasia or AML. The median latency for development of a hematopoietic malignancy in inducible NUP98-KMT2A mice was rather long (>1 year) and sublethal irradiation to generate DNA damage accelerated disease. Together with the observation of additional mutations in other human *NUP98*-rearranged[15] or *KMT2A*-PTD,[11] this strongly suggests that cooperating mechanisms are required for induction of full-blown AML by NUP98-KMT2A. Interestingly, however, the co-expression of Flt3-ITD did not accelerate the disease in this inducible NUP98-KMT2A model, suggesting different cooperating networks as compared to the NUP98-NSD1 fusion.[18]

Inducible models allow elegant and formal testing of whether continuous expression of the driver oncogene is required for leukemia maintenance by removing doxycycline treatment in diseased animals. Previously, full dependence of AML on *KMT2A-MLLT3* expression was observed using a similar model.[19] Here, however, ceasing the doxycycline treatment in recipients of inducible NUP98-KMT2A cells did not abrogate the disease progression in all the mice. The authors suggest that this may result from a "leak" of residual NUP98-KMT2A expression inherent to this inducible system. In this regard, given that KMT2A-X and NUP98-KMT2A fusion transcript expression is controlled by different endogenous regulatory elements - KMT2A and NUP98 promoters, respectively - significantly different levels of fusion expression could be required for leukemia induction and maintenance. It remains to be formally tested whether NUP98-KMT2A expression is essential for the maintenance of already transformed leukemic cells in all cases.

At the molecular level, inducible NUP98-KMT2A murine leukemia cells, similarly to NUP98-KMT2A patient's leukemic cells,[2] do not show significant upregulation of *HOX* genes as compared to control cells or leukemia from two retroviral models of KMT2A fusions (KMT2A-ENL and KMT2A-MLLT3). Gene expression analyses in transgenic mouse embryonic fibroblasts confirmed cell cycle deregulation and further demonstrated a block in induction of senescence. Notably, a subset of cell cycle- and senescence-associated genes deregulated by transgene induction in mouse embryonic fibroblasts was also found to be deregulated in murine hematopoietic progenitor cells (e.g. *Sirt1*, *Rbl2*, *Tert2*). These data suggest that NUP98-KMT2A does not transform hematopoietic progenitor cells through aberrant expression of *HOX* genes and cofactors but through an alternative mechanism associated with a defective cell cycle checkpoint. Notably, this is further supported by the absence of significant cell cycle perturbation in inducible NUP98-KMT2A cells mediated by small MEN1 or BRD inhibitors, as opposed to their effects on KMT2A-MLLT3 cells.

Three NUP98 fusion partners (NSD1, NSD3, and KMT2A) have a SET domain and another partner is a known interactor of SET-containing proteins (SETBP1) with histone methyltransferase function. Although additional genome-wide chromatin analyses will be required to assess H3K4me3 profiles and NUP98-KMT2A DNA binding sites in NUP98-KMT2A cells, it could be hypothesized that aberrant deposition of H3K4me3 at NUP98 target genes enhances or ectopically creates promoter activities. More generally, it also remains to be determined: (i) whether the NUP98 or KMT2A moiety controls the identity of the target genes; (ii) whether dimerization is required for transformation as for other KMT2A-X fusions;[20] and (iii) whether the location of NUP98-KMT2A at the nuclear pore, reported to be in close proximity to the loci of actively transcribed cell cycle regulators, in part controls the identity of the target genes in a cell context-dependent manner.

Together, the identification of transcriptional targets of NUP98-KMT2A represents a first step toward the development of novel therapeutic strategies. Based on the protein structure, the NUP98-KMT2A transforming properties could depend on cleavage by TASPASE 1 and SET domain catalytic activity. As interference with these activities has been proposed,[21] future assessment of the efficacy and specificity of targeted therapies could be of interest in these human leukemias.

Acknowledgments

We thank Olivier A. Bernard and Brian J. Huntly for scientific discussions.

Funding

AF is supported by Fondation pour la Recherche Médicale. TM is supported by Institut National Du Cancer (PLBIO-2018-169), PAIR-Pédiatrie/CONECT-AML (Collaborative Network for Children and Teenagers with Acute Myeloblastic Leukemia: INCa-ARC-LIGUE_11905 and Association Laurette Fugain), Société Française des Cancers de l'Enfant, INCa-DGOS-INSERM_12551.

References

1. Fisher JN, Thanasopoulou A, Juge S. et al.Transforming activities of the NUP98-KMT2A fusion gene associated with myelodysplasia and acute myeloid leukemia. Haematologica 2020;105(7):1857-1867.
2. Kaltenbach S, Soler G, Barin C, et al. NUP98-MLL fusion in human acute myeloblastic leukemia. Blood. 2010;116(13):2332-2335.
3. Li BE, Ernst P. Two decades of leukemia oncoprotein epistasis: the MLL1 paradigm for epigenetic deregulation in leukemia. Exp Hematol. 2014;42(12):995-1012.
4. Slany RK. MLL fusion proteins and transcriptional control. Biochim Biophys Acta Gene Regul Mech. 2020;1863(3):194503.
5. Yokoyama A, Somervaille TCP, Smith KS, Rozenblatt-Rosen O, Meyerson M, Cleary ML. The menin tumor suppressor protein is an essential oncogenic cofactor for MLL-associated leukemogenesis. Cell. 2005;123(2):207-218.
6. Gilan O, Lam EYN, Becher I, et al. Functional interdependence of BRD4 and DOT1L in MLL leukemia. Nat Struct Mol Biol. 2016;23(7):673-681.
7. Daigle SR, Olhava EJ, Therkelsen CA, et al. Selective killing of mixed lineage leukemia cells by a potent small-molecule DOT1L inhibitor. Cancer Cell. 2011;20(1):53-65.
8. Krivtsov AV, Evans K, Gadrey JY, et al. A menin-MLL inhibitor induces specific chromatin changes and eradicates disease in models of MLL-rearranged leukemia. Cancer Cell. 2019;36(6):660-673.e11.
9. Gaussmann A, Wenger T, Eberle I, et al. Combined effects of the two reciprocal t(4;11) fusion proteins MLL.AF4 and AF4.MLL confer resistance to apoptosis, cell cycling capacity and growth transformation. Oncogene. 2007;26(23):3352-3363.
10. Zhang Y, Yan X, Sashida G, et al. Stress hematopoiesis reveals abnormal control of self-renewal, lineage bias, and myeloid differentiation in Mll partial tandem duplication (Mll-PTD) hematopoietic stem/progenitor cells. Blood. 2012;120(5):1118-1129.
11. Sun Q-Y, Ding L-W, Tan K-T, et al. Ordering of mutations in acute myeloid leukemia with partial tandem duplication of MLL (MLL-PTD). Leukemia 2017;31(1):1-10.
12. Jeganathan KB, Malureanu L, van Deursen JM. The Rae1-Nup98 complex prevents aneuploidy by inhibiting securin degradation. Nature. 2005;438(7070):1036-1039.
13. Kalverda B, Pickersgill H, Shloma VV, Fornerod M. Nucleoporins directly stimulate expression of developmental and cell-cycle genes inside the nucleoplasm. Cell. 2010;140(3):360-371.
14. Pascual-Garcia P, Jeong J, Capelson M. Nucleoporin Nup98 associates with Trx/MLL and NSL histone-modifying complexes and regulates Hox gene expression. Cell Rep. 2014;9(5):1981.
15. Struski S, Lagarde S, Bories P, et al. NUP98 is rearranged in 3.8% of pediatric AML forming a clinical and molecular homogenous group with a poor prognosis. Leukemia. 2017;31(3):565-572.
16. Gough SM, Slape CI, Aplan PD. NUP98 gene fusions and hematopoietic malignancies: common themes and new biologic insights. Blood. 2011;118(24):6247-6257.
17. Xu H, Valerio DG, Eisold ME, et al. NUP98 fusion proteins interact with the NSL and MLL1 complexes to drive leukemogenesis. Cancer Cell. 2016;30(6):863-878.
18. Thanasopoulou A, Tzankov A, Schwaller J. Potent co-operation between the NUP98-NSD1 fusion and the FLT3-ITD mutation in acute myeloid leukemia induction. Haematologica. 2014;99(9):1465-1471.
19. Stavropoulou V, Kaspar S, Brault L, et al. MLL-AF9 Expression in Hematopoietic stem cells drives a highly invasive AML expressing EMT-related genes linked to poor outcome. Cancer Cell. 2016;30(1):43-58.
20. So CW, Lin M, Ayton PM, Chen EH, Cleary ML. Dimerization contributes to oncogenic activation of MLL chimeras in acute leukemias. Cancer Cell. 2003;4(2):99-110.
21. Vedadi M, Blazer L, Eram MS, Barsyte-Lovejoy D, Arrowsmith CH, Hajian T. Targeting human SET1/MLL family of proteins. Protein Sci. 2017;26(4):662-676.

T-cell and NK-cell neoplasms of the gastrointestinal tract – recurrent themes, but clinical and biological distinctions exist

Elaine S. Jaffe

Hematopathology Section, Laboratory of Pathology, Center for Cancer Research, National Cancer Institute, National Institutes of Health, Bethesda, MD, USA.

E-mail: ELAINE S. JAFFE - ejaffe@mail.nih.gov

doi:10.3324/haematol.2020.252924

The history of intestinal T-cell lymphomas begins with the early work of Peter Isaacson and Dennis Wright who described cases of "malignant histiocytosis" of the intestine that they linked to malabsorption and ulcerative jejunitis.[1] Subsequent work showed that "malignant histiocytosis of the intestine" was a form of T-cell lymphoma, later named enteropathy-associated T-cell lymphoma (EATL).[2] Since then, we have come to understand the distinction between EATL, closely linked to celiac disease, and monomorphic epitheliotropic T-cell lymphoma (MEITL), formerly EATL type II (Figure 1).[3] The work of Isaacson and Wright shaped the modern classification of both T-cell and B-cell intestinal lymphomas, giving us not only EATL, but also mucosa-associated lymphoid tissue (MALT) lymphoma. Sadly Dennis Wright passed away on April 08, 2020 at the age of 88.

Most cases of intestinal T-cell lymphoma were highly aggressive, but in the 1990s there was a series of reports of low-grade intestinal T-cell neoplasms, some of which mimicked lymphomatous polyposis.[4-8] The nature of this rare form of T-cell lymphoma was better defined in subsequent reports,[9,10] and incorporated into the Revised 4th Edition of the World Health Organization (WHO) classification[3] as a provisional entity under the term indolent T-cell lymphoproliferative disorder of the gastrointestinal tract (ITLPD-GIT) (Figure 1). Most patients had a chronic, relapsing clinical course, although in both of the above series late instances of large-cell transformation were described.[10,11]

In the current issue of *Haematologica*, Soderquist *et al.* expand our knowledge regarding the immunophenotypic spectrum of ITLPD-GIT and provide new insights into its molecular pathogenesis.[12] As with prior reports, all cases were derived from αβ T cells with an equal proportion of cases expressing either CD4 or CD8. One case each had either a double-positive or double-negative phenotype. The authors also examined the expression of T-bet (TBX21) and GATA3, but any conclusions regarding the functional or clinical significance of these markers, which have been examined more extensively in nodal peripheral T-cell lymphomas,[13] remain premature.

This study confirms the importance of alterations in

JAK-STAT pathway genes in cases of ITLPD-GIT with a CD4+ phenotype. Five of six cases, either CD4+, or double-negative in one instance, had alterations with predicted activation of the pathway. Interestingly, functional evidence of activation of the pathway was less convincing. Cells with nuclear staining for p-STAT3 and p-STAT5 accounted for fewer than 10% of total cells in all nine cases studied. Activation of the JAK-STAT pathway is a very common finding in many forms of T-cell lymphoma, most of which have a cytotoxic phenotype. Initially reported in T-cell large granular lymphocyte leukemia,[14] activation of this pathway is a regular feature of hepatosplenic T-cell lymphoma,[15] intestinal T-cell lymphomas,[16,17] anaplastic large cell lymphoma (ALCL), ALK-positive and ALK-negative,[18,19] and breast-implant-associated ALCL.[20,21] Interestingly, similar alterations were not seen in the CD8+ cases, which share a cytotoxic phenotype with many of the above mentioned lesions. However, *JAK3* mutations have been reported in NK-cell enteropathy, an indolent NK-cell derived lymphoproliferative disease of the gastrointestinal tract that has a chronic relapsing and remitting clinical course similar to that of ITLPD-GIT.[22]

Prior reports have noted that ITLPD-GIT with a CD8+ phenotype has a similar immunophenotypic profile to that of primary cutaneous acral CD8+ T-cell lymphoma, another newly recognized provisional entity in the revised WHO classification.[3] This tumor presents with superficial, non-epidermotropic cutaneous lesions. Initially reported on the ear, it has subsequently been recognized presenting in other acral cutaneous sites. The neoplastic cells have a cytotoxic T-cell phenotype but, as in ITLPD-GIT, are positive for TIA-1 although negative for granzyme B and perforin. Acral CD8+ T-cell lymphoma has a similar indolent clinical course as ITLPD-GIT, with a low risk of disease beyond the skin. Given the current report by Soderquist *et al.*, which describes structural alterations of the *IL2* gene, extending these studies to other forms of indolent T-cell lymphoma is warranted. It is also notable both in this study, and in

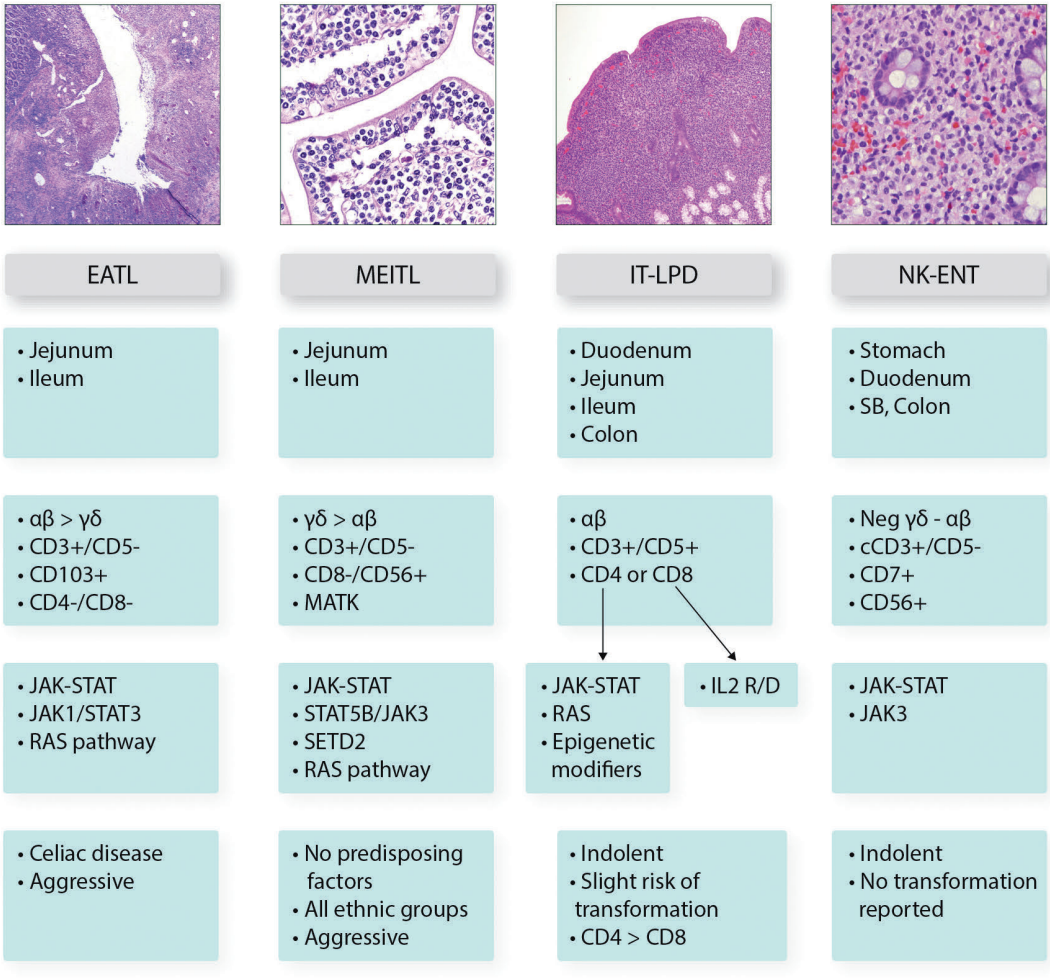

Figure 1. Distinguishing features of primary intestinal T-cell and NK-cell neoplasms. Major biological and clinical features of enteropathy-associated T-cell lymphoma (EATL), monomorphic epitheliotropic T-cell lymphoma (MEITL), indolent T-cell lymphoproliferative disorder of the gastrointestinal tract (IT-LPD) and natural killer-cell enteropathy (NK-ENT) are shown. EATL and MEITL are clinically aggressive, whereas IT-LPD and NK-ENT have a chronic relapsing clinical course, with a low risk of dissemination or transformation. Common recurrent features include a cytotoxic phenotype and activation of the JAK-STAT pathway in most of the entities. EATL: enteropathy associated T-cell lymphoma; MEITL: monomorphic epitheliotropic intestinal T-cell lymphoma; IT-LPD, indolent T-cell lymphoproliferative disorder of the gastrointestinal tract; NK-ENT, natural killer-cell enteropathy; SB; small bowel; R/D, rearrangement or deletion.

prior work, that the molecular pathogenesis of the CD4+ and CD8+ cases of ITLPD-GIT appears distinct.[10,23] Thus, more formal separation of these phenotypic variants may be warranted in the future.

The current series presents both similarities with and differences from prior clinical reports.[12] Endoscopic findings included multiple mucosal lesions, often with nodularity or polyps. Only one case was associated with mucosal ulceration. Most of the patients had a very protracted clinical course, with two patients being alive 19 and 21 years after diagnosis. There is a small but significant risk of transformation, with disease progressing in two patients after 11 and 27 years of follow-up. A variety of treatments were employed, with no patient stated to attain a complete remission.

In prior series, all patients had disease confined to the gastrointestinal tract, with extraintestinal dissemination seen only in patients with histological progression.[9,10] However, Soderquist *et al.* report bone marrow involvement in three cases, all of which were detected prior to transformation. In one case bone marrow involvement was detected only through an unidentified cytogenetic abnormality; the bone marrow was morphologically normal and lacked evidence of a monoclonal T-cell receptor gene rearrangement. This patient is alive with disease at 7 years after presentation, so the presence of bone marrow involvement, if real, has had little clinical impact. Two additional patients were reported to have inguinal lymph node involvement, one of whom also had positive bone marrow. This latter case is the only patient classified as having Ann Arbor Stage IV disease. This 41-year old male was asymptomatic at presentation, and is untreated, being alive with disease at 1 year. Curiously, the remaining three patients said to have "biopsy-proven" involvement of lymph node or bone marrow were classified as stage IE at diagnosis. Presumably, the stated bone marrow or lymph node involvement occurred at some later point during the clinical course. More data are needed to understand the clinical and biological significance of this extraintestinal dissemination, including molecular data to confirm involvement.

A remaining issue is the optimal therapy for ITLPD-GIT. Most of the data are anecdotal. A number of patients have been treated with a variety of chemotherapy regimens used in both B-cell and T-cell lymphomas.[9] Most patients have failed to achieve any long-term benefit from conventional chemotherapy. The JAK-STAT pathway appears to be an attractive target, especially in patients with CD4+ disease, and in recent years there has been interest in the use of targeted agents for a variety of mature T-cell and NK-cell malignancies.[24] Ruxolitinib is a JAK-inhibitor approved for use in myeloproliferative neoplasms, and has shown some activity in cutaneous T-cell lymphomas with activation of the JAK-STAT pathway.[24] Other agents under evaluation for T-cell and NK-cell lymphomas include tofacitinib, pacritinib, and the histone deacetylase inhibitor, chidamide. The use of targeted agents in combination with either chemotherapy or immunotherapy may offer promise in the future.

References

1. Isaacson P, Wright D. Malignant histiocytosis of the intestine: its relationship to malabsorption and ulcerative jejeunitis. Hum Pathol. 1978;9(6):661-677.
2. Isaacson P, Spencer J, Connolly C, et al. Malignant histiocytosis of the intestine: a T-cell lymphoma. Lancet. 1985;2(8457):688-691.
3. Swerdlow SH, Campo E, Pileri SA, et al. The 2016 revision of the World Health Organization classification of lymphoid neoplasms. Blood. 2016;127:2375-90.
4. Carbonnel F, Lavergne A, Messing B, et al. Extensive small intestinal T-cell lymphoma of low-grade malignancy associated with a new chromosomal translocation. Cancer. 1994;73(4):1286-1291.
5. Egawa N, Fukayama M, Kawaguchi K, et al. Relapsing oral and colonic ulcers with monoclonal T-cell infiltration. A low grade mucosal T-lymphoproliferative disease of the digestive tract. Cancer. 1995;75(7):1728-1733.
6. Hirakawa K, Fuchigami T, Nakamura S, et al. Primary gastrointestinal T-cell lymphoma resembling multiple lymphomatous polyposis. Gastroenterology. 1996;111(3):778-782.
7. Ranheim EA, Jones C, Zehnder JL, Warnke R, Yuen A. Spontaneously relapsing clonal, mucosal cytotoxic T-cell lymphoproliferative disorder: case report and review of the literature. Am J Surg Pathol. 2000;24(2):296-301.
8. Isomoto H, Maeda T, Akashi T, et al. Multiple lymphomatous polyposis of the colon originating from T-cells: a case report. Dig Liver Dis. 2004;36(3):218-221.
9. Perry AM, Warnke RA, Hu Q, et al. Indolent T-cell lymphoproliferative disease of the gastrointestinal tract. Blood. 2013;122(22):3599-3606.
10. Margolskee E, Jobanputra V, Lewis SK, Alobeid B, Green PH, Bhagat G. Indolent small intestinal CD4+ T-cell lymphoma is a distinct entity with unique biologic and clinical features. PLoS One. 2013;8:e68343.
11. Perry AM, Bailey NG, Bonnett M, Jaffe ES, Chan WC. Disease progression in a patient with indolent T-cell lymphoproliferative disease of the gastrointestinal tract. Int J Surg Pathol. 2019;27(1):102-107.
12. Soderquist CR, Patel N, Murty VV, et al. Genetic and phenotypic characterization of indolent T-cell lymphoproliferative disorders of the gastrointestinal tract. Haematologica. 2020;105(7):1895-1906.
13. Amador C, Greiner TC, Heavican TB, et al. Reproducing the molecular subclassification of peripheral T-cell lymphoma-NOS by immunohistochemistry. Blood. 2019;134(24):2159-2170.
14. Koskela HLM, Eldfors S, Ellonen P, et al. Somatic STAT3 mutations in large granular lymphocytic leukemia. N Engl J Med. 2012;366(20):1905-1913.
15. Nicolae A, Xi L, Pittaluga S, et al. Frequent STAT5B mutations in γδ hepatosplenic T-cell lymphomas. Leukemia. 2014;28 (11):2244-2248.
16. Nicolae A, Xi L, Pham TH, et al. Mutations in the JAK/STAT and RAS signaling pathways are common in intestinal T-cell lymphomas. Leukemia. 2016;30(11):2245-2247.
17. Roberti A, Dobay MP, Bisig B, et al. Type II enteropathy-associated T-cell lymphoma features a unique genomic profile with highly recurrent SETD2 alterations. Nat Commun. 2016;7:12602.
18. Chiarle R, Simmons WJ, Cai HY, et al. Stat3 is required for ALK-mediated lymphomagenesis and provides a possible therapeutic target. Nat Med. 2005;11(6):623-629.
19. Crescenzo R, Abate F, Lasorsa E, et al. Convergent mutations and kinase fusions lead to oncogenic STAT3 activation in anaplastic large cell lymphoma. Cancer Cell. 2015;27(4):516-532.
20. Blombery P, Thompson E, Jones K, et al. Whole exome sequencing reveals activating JAK1 and STAT3 mutations in breast-implant associated anaplastic large cell lymphoma. 2016;101(9):e387-e390.
21. Laurent C, Nicolae A, Laurent C, et al. Gene alterations in epigenetic modifiers and JAK-STAT signaling are frequent in breast implant-associated ALCL. Blood. 2020;135(5):360-370.
22. Xiao W, Gupta GK, Yao J, et al. Recurrent somatic JAK3 mutations in NK-cell enteropathy. Blood. 2019;134(12):986-991.
23. Sharma A, Oishi N, Boddicker RL, et al. Recurrent STAT3-JAK2 fusions in indolent T-cell lymphoproliferative disorder of the gastrointestinal tract. Blood. 2018;131(20):2262-2266.
24. Shouse G, Nikolaenko L. Targeting the JAK/STAT pathway in T cell lymphoproliferative disorders. Curr Hematol Malig Rep. 2019;14 (6):570-576.

Towards individualized radiation therapy in multiple myeloma

Felix Momm,[1] Christine Greil[2] and Henning Schäfer[3]

[1]Department of Radiation Oncology, Ortenau Klinikum Offenburg-Kehl, Teaching Hospital of Albert-Ludwigs University Freiburg, Offenburg; [2]Department of Hematology, Oncology and Stem Cell Transplantation, Medical Center, Faculty of Medicine, University of Freiburg, Freiburg and [3]Department of Radiation Oncology, Medical Center, Faculty of Medicine, University of Freiburg, German Cancer Consortium (DKTK) Partner Site Freiburg, German Cancer Research Center (DKFZ), Heidelberg, Germany

E-mail: FELIX MOMM - felix.momm@ortenau-klinikum.de

doi:10.3324/haematol.2019.243451

Fortunately, recent progress in systemic treatment has prolonged the median overall survival of myeloma patients.[1,2] However, this leads to increasing numbers of radiation cycles being administered for supportive reasons (e.g. pain, stability). Although radiation can result in hematopoietic insufficiency in a dose-dependent manner, leading to ineligibility for systemic treatment, the best radiation regimen providing optimal local control and minimized bone marrow toxicity is still under investigation. The current guidelines for radiotherapy in patients diagnosed with multiple myeloma were summarized in a critical review by the International Lymphoma Radiation Oncology Group in 2018.[3] In their letter published in this issue of *Haematologica*, Elhammali *et al*. contribute the large and high-value experience of the MD Andersson Cancer Center to this ongoing discussion.[4] After analysis of treatment, toxicities and tumor control in 772 myeloma patients with 1,513 irradiated lesions and a median follow-up of 65.6 months the authors claim that radiation doses as low as 20-25 Gy were sufficient to avoid reirradiation in more than 97% of all cases. However, in univariate analysis, a biologically effective dose assuming an α/β ratio of 10 Gy (BED_{10}) of <28 Gy was associated with an increased risk of reirradiation. As the authors state themselves, the study is limited by the well-known bias of retrospective data with a long observation period.[4] From our perspective, the most important problems seem to be the comparatively weak endpoint of reirradiation and the selection bias of how dose was determined in the individual patient.[4] Our own clinical experience shows that lower doses are preferentially given to elderly or frail patients, in order to save treatment time and reduce acute toxicity, or in cases of small lesions with low tumor burden. In fragile patients reirradiation is often not performed as these patients may die prior to local tumor recurrence because of systemic disease progression or relevant comorbidities and the reirradiation is therefore underestimated. In patients with small lesions, a lower irradiation dose may probably be sufficient to achieve local tumor control. Despite the reported data, we would therefore still recommend higher doses of 30-40 Gy to large lesions as stated by the International Lymphoma Radiation Oncology Group.[3] Especially when treating critical lesions of the spine or the skull base as well as lesions particularly prone to fractures, it is essential to reach stable local tumor control. In this context we suggest that toxicity should be avoided by shrinking the irradiation field rather than by reducing dose. Targeted dosage to bone lesions or extramedullary tumors will not compromise bone marrow function relevantly.

Nevertheless, the reported routine clinical records of a reference center with a high number of cases[4] still contribute valid arguments to the ongoing discussion: The authors could show that in this selected cohort comparatively low doses were sufficient for a high rate of tumor control, emphasizing that selected plasmacytoma sites with low tumor burden might definitely be effectively irradiated with doses as low as 20-25 Gy, and that in advanced disease stage, lower doses and therefore shorter time of treatment are still sufficient for local control.[4]

The best approach is probably to apply high doses precisely to sites with large tumor burden and to reduce doses in sites with less or disseminated tumor and if functional bone marrow may be affected. With modern inten-

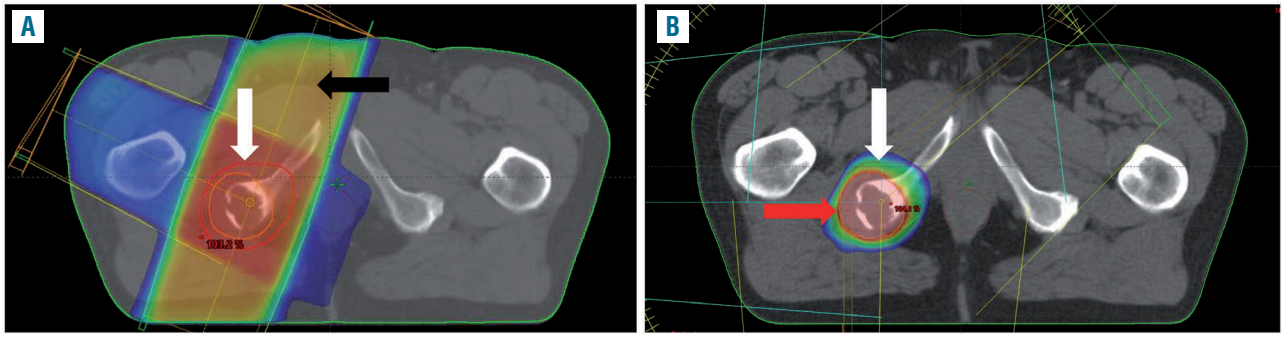

Figure 1. Planning computed tomography scanning of a myeloma lesion in the right ischium. The dose distribution is depicted by a color wash from red (= high dose) to dark blue (= low dose). (A) Conventional technique: 50 Gy in 20 fractions of 2.5 Gy to complete target volume. Black arrow: areas of high dose out of target volume (red line/white arrow). (B) Volume modulated arc therapy (VMAT) technique. Red line/white arrow: main target volume 40 Gy in 20 fractions of 2.0 Gy; orange line/red arrow: integrated boost target volume 50 Gy in 20 fractions of 2.5 Gy. The complete dose of each fraction is delivered simultaneously integrated to both target volumes.

sity-modulated radiotherapy or volume-modulated arc therapy such dose distributions can be routinely attained (Figure. 1). Considering possibilities of modern imaging, including magnetic resonance imaging and positron emission tomography/computed tomography, which are able to depict myeloma lesions very precisely, highly conformal radiotherapy techniques can be applied with a comparatively low risk of missing the target.[5] Thus, even high-precision stereotactic radiotherapy or radiosurgery can be considered for the treatment of critical multiple myeloma lesions in the spine.[6] Of course, using such radiation techniques, effective systemic therapy is an essential part of the interdisciplinary treatment concept.

Radiotherapy is the treatment of choice for multiple myeloma in two situations: as curative treatment for single plasmacytoma lesions and as palliation for local symptoms due to certain bone or extramedullary lesions. In both situations local tumor control is most important and, therefore, the radiation dose sought should not differ. In fact, the decision regarding each patient's or each lesion's dose should also be taken on the basis of that patient's general condition and life expectancy. In this context, specific help for dose decisions can be obtained by scores, such as the one developed by Rades *et al.*[7]

Furthermore, and probably most importantly, considering multiple myeloma and also solitary plasmacytoma as a systemic disease, radiation doses and volumes should not adversely affect the administration of essential systemic therapies by being toxic to the bone marrow. To ensure this, patients diagnosed with multiple myeloma should be treated in an interdisciplinary manner by oncologists and radiation oncologists together. In summary, the work by Elhammali *et al.* may not cause a paradigm shift, but it does contribute important data with regards to a concept of individualized radiation therapy.

References

1. Soekojo CY, Kumar SK. Stem-cell transplantation in multiple myeloma: how far have we come? Ther Adv Hematol. 2019;10: 2040620719888111.
2. Piechotta V, Jakob T, Langer P, et al. Multiple drug combinations of bortezomib, lenalidomide, and thalidomide for first-line treatment in adults with transplant-ineligible multiple myeloma: a network meta-analysis. Cochrane Database Syst Rev. 2019;2019(11).
3. Tsang RW, Campbell BA, Goda JS, et al. Radiation therapy for solitary plasmacytoma and multiple myeloma: guidelines from the International Lymphoma Radiation Oncology Group. Int J Radiat Oncol Biol Phys. 2018;101(4):794-808.
4. Elhammali A, Amini B, Ludmir EB, et al. New paradigm for radiation in multiple myeloma: lower yet effective dose to avoid radiation toxicity. Haematologica. 2020;105(7):e355-e357.
5. Zhu Q, Zou X, You R, et al. Establishment of an innovative staging system for extramedullary plasmacytoma. BMC Cancer. 2016; 16(1):777.
6. Miller JA, Balagamwala EH, Chao ST, et al. Spine stereotactic radiosurgery for the treatment of multiple myeloma. J Neurosurg Spine. 2017;26(3):282-290.
7. Rades D, Conde-Moreno AJ, Cacicedo J, et al. A predictive tool particularly designed for elderly myeloma patients presenting with spinal cord compression. BMC Cancer. 2016;16:292.

Myelodysplastic syndromes: moving towards personalized management

Ferrata Storti Foundation

Eva Hellström-Lindberg,[1] Magnus Tobiasson[1] and Peter Greenberg[2]

[1]Karolinska Institutet, Center for Hematology and Regenerative Medicine, Department of Medicine Huddinge, Karolinska University Hospital, Stockholm, Sweden and [2]Stanford Cancer Institute, Division of Hematology, Stanford University School of Medicine, Stanford, CA, USA

ABSTRACT

The myelodysplastic syndromes (MDS) share their origin in the hematopoietic stem cell but have otherwise very heterogeneous biological and genetic characteristics. Clinical features are dominated by cytopenia and a substantial risk for progression to acute myeloid leukemia. According to the World Health Organization, MDS is defined by cytopenia, bone marrow dysplasia and certain karyotypic abnormalities. The understanding of disease pathogenesis has undergone major development with the implementation of next-generation sequencing and a closer integration of morphology, cytogenetics and molecular genetics is currently paving the way for improved classification and prognostication. True precision medicine is still in the future for MDS and the development of novel therapeutic compounds with a propensity to markedly change patients' outcome lags behind that for many other blood cancers. Treatment of higher-risk MDS is dominated by monotherapy with hypomethylating agents but novel combinations are currently being evaluated in clinical trials. Agents that stimulate erythropoiesis continue to be first-line treatment for the anemia of lower-risk MDS but luspatercept has shown promise as second-line therapy for sideroblastic MDS and lenalidomide is an established second-line treatment for del(5q) lower-risk MDS. The only potentially curative option for MDS is hematopoietic stem cell transplantation, until recently associated with a relatively high risk of transplant-related mortality and relapse. However, recent studies show increased cure rates due to better tools to target the malignant clone with less toxicity. This review provides a comprehensive overview of the current status of the clinical evaluation, biology and therapeutic interventions for this spectrum of disorders.

Definition of myelodysplastic syndromes

The myelodysplastic syndromes (MDS) constitute a spectrum of disorders with variable degrees of cytopenias, morphological dysplasia and risk of progression to acute myeloid leukemia (AML). As such, they provide a clinical model of neoplastic disease capable of progressing from indolent to frankly aggressive. Thus, understanding the nature of MDS permits analysis of clinical and biological factors involved in maintaining clinical stability and those provoking active tumor progression.

Although MDS comprises heterogeneous subcategories these share a common origin in the hematopoietic stem and progenitor cell compartment.[1] The degree of cytopenia partly defines the World Health Organization (WHO) subcategories but certain MDS and subgroups of mixed MDS/myeloproliferative neoplasma (MPN) may present with increased white blood cell, monocyte and platelet counts. Moreover, a diagnosis of MDS can be made in patients with mild or borderline anemia if definite morphological or cytogenetic findings are present.[1]

Besides cytopenia, the main defining feature of MDS is the presence of morphological dysplasia of precursor and mature bone marrow blood cells. A number of dysplastic changes have been defined for each lineage of the bone marrow, as listed in Table 1.

Haematologica 2020
Volume 105(7):1765-1779

Correspondence:

MAGNUS TOBIASSON
magnus.tobiasson@ki.se

Received: March 23, 2020.

Accepted: April 24, 2020.

Pre-published: May 21, 2020.

doi:10.3324/haematol.2020.248955

Check the online version for the most updated information on this article, online supplements, and information on authorship & disclosures: www.haematologica.org/content/105/7/1765

Scope and limitations of this review

While definitions and classifications of MDS until 2001 included chronic myelomonocytic leukemia, in the 2008 WHO classification this former MDS subtype was transferred to a novel entity of mixed MDS/MPN.[2] MDS and MDS/MPN share several pathogenic features but also display important differences. Clinical trials that constitute the basis for therapeutic recommendations have often enrolled both MDS and MDS/MPN patients. In this review, we will focus on the current WHO diagnosis of MDS but discuss MDS/MPN when relevant for the context.

An area with relevance for MDS are variants of clonal hematopoiesis, defined as the presence of somatic myeloid mutations in the absence of diagnostic criteria for MDS or any other blood cancer.[3] Clonal hematopoiesis will be discussed herein as a differential diagnosis of MDS.

The review focuses on adult MDS. However, knowledge about germline conditions potentially predisposing to MDS has vastly increased over these past years, leading baseline investigation of patients with potential MDS to include evaluation of potential germline conditions.[4]

Classification systems

Historical perspective including the French-American-British classification

Morphological depiction of the disease spectrum has been difficult due to the somewhat subjective nature of defining marrow dysplasia and the patients' variable clinical courses. Since its initial description as 'preleukemia' in 1953 a multiplicity of terminologies have been used to describe this entity (Table 2). The French-American-British (FAB) morphological classification in 1982 helped to provide a consensus approach to grouping patients.[5] MDS emerged as a separate entity in the FAB classification, which recognized one group with an excess of blasts but not fulfilling the criteria for acute leukemia, and, as indicated above, another group with increased monocytosis termed chronic myelomonocytic leukemia, now characterized as an MDS/MPN.

Table 1. Morphological manifestations of dysplasias (WHO 5.01 and 6.02).*

Dyserythropoiesis
Nuclear
Nuclear budding
Internuclear bridging
Karyorrhexis
Multinuclearity
Megaloblastoid changes
Cytoplasmic
Ring sideroblasts
Vacuolization
Periodic acid-Schiff positivity
Dysgranulopoiesis
Small ***or*** unusually large size
Nuclear hyposegmentation (pseudo-Pelger-Huet)
Nuclear hypersegmentation
Decreased granules – agranularity
Pseudo-Chédiak-Higashi granules
Döhle bodies
Auer rods
Barr bodies
Dysmegakaryopoiesis
Micromegakaryocytes
Nuclear hypolobation
Multinucleation
Monocytosis
No specific morphology but persistent monocytosis ≥1 x 10^9/L with monocytes accounting for ≥10% of leukocytes

• Dysplasia may also be visible in peripheral blood films when dysplastic cells are released from the bone marrow

World Health Organization classification

In 2001, the WHO proposed an alternative classification for MDS which was subsequently updated in 2008 and in 2016[1] and currently identifies six MDS entities based on marrow morphology and cytogenetics (Table 3).[4,6] The denominator used for determining blast percentage was recently redefined to include all nucleated bone marrow cells as opposed to only non-erythroid cells. The division between MDS and AML is a continued area of debate. The clinical outcomes of MDS patients are not only related to the quantity of blasts, but also to a differing pace of disease related to distinctive biological and molecular features compared with those of *de novo* AML.[1,7,8] The National Comprehensive Cancer Network (NCCN) practice guidelines for MDS (also discussed by the WHO) allow for patients with 20% to 29% blasts AND a stable clinical course for at least 2 months to be considered as having either higher-risk MDS or AML.[9] Individuals with *FLT3* or *NPM1* mutations are more likely to have AML than MDS.[10] Future challenges will include methods to further stratify patients' clinical courses more effectively, using biological features (e.g., mutations) as adjuncts to morphology.

Demographics and clinical presentation

The incidence of MDS was previously based on large regional registries. The Düsseldorf Registry described 216 patients diagnosed between 1996 and 2005, corresponding to an incidence of 4.15 cases per 100,000 popula-

Table 2. Chronology of the terminology for myelodysplastic syndromes.

Term	Year	Author
Preleukemia	1953	Block *et al.*
Refractory anemia with ringed sideroblasts	1956	Bjorkman
Refractory normoblastic anemia	1959	Dacie *et al.*
Smoldering acute leukemia	1963	Rheingold *et al.*
Chronic erythremic myelosis	1969	Dameshek
Preleukemic syndrome	1973	Saarni and Linman
Subacute myelomonocytic leukemia	1974	Sexauer *et al.*
Chronic myelomonocytic leukemia	1974	Miescher and Farquet
Hypoplastic acute myelogenous leukemia	1975	Beard *et al.*
Refractory anemia with excess myeloblasts	1976	Dreyfus
Hematopoietic dysplasia	1978	Linman and Bagby
Subacute myeloid leukemia	1979	Cohen *et al.*
Dysmyelopoietic syndrome	1980	Streuli *et al.*
Myelodysplastic syndromes	1982	Bennett *et al.*

tion/year.[11] The median age, 71 years, was similar to that of the Revised International Prognostic Scoring System (IPSS-R) cohort.[12] More recent population-based reports show median ages of 75-76 years. A Swiss study showed an incidence of 3.6 cases per million.[13] A Swedish study described 1,329 patients with MDS or MDS-MPN, corresponding to a crude annual incidence of 2.9 cases per 100,000 population.[14] The lower incidence reflects that patients were double-reported from hematology and pathology departments, with non-MDS differential diagnoses most likely being excluded. In all registries the incidence sharply increases with age, making MDS one of the most common blood cancers in the elderly population.

The clinical presentation mainly consists of symptoms caused by cytopenia. According to the Swedish Registry 11% and 42% of newly diagnosed patients had hemoglobin levels <8 g/dL and 8-10 g/dL, respectively, and 50% needed erythrocyte transfusions, 40% had platelet counts below 100x10^9/L, 5% received platelet transfusions, and 20% had neutrophil counts <0.8x10^9/L.[14] Hence, symptoms of anemia, such as dyspnea and fatigue, dominate the clinical picture. Bleeding complications and infections become more pronounced during the course of disease. In a recent survey, 309 consecutive patients received a total of 11,350 red cell units and 1,956 platelet units over 777 person-years of follow-up, corresponding to an overall transfusion intensity of 14.6 and 2.5 units/person-year for red blood cells and platelets, respectively.[15]

Some MDS patients present with systemic inflammatory and autoimmune diagnoses before, in conjunction with, or after the diagnosis of MDS.[16] A recent French survey of 123 patients with MDS and systemic inflammatory and autoimmune diagnoses reported systemic vasculitis in 32%, connective tissue disease in 25%, inflammatory arthritis in 23%, and neutrophilic disorders in 10% of cases. A significant association was shown between chronic myelomonocytic leukemia and systemic vasculitis. Other symptoms and findings encompassed fever, skin abnormalities including Sweet syndrome, and bleeding due to disturbed coagulation, as recently reviewed.[17] It is important to recognize the MDS diagnosis in these patients, since intervention with corticosteroids and azacitidine may relieve symptoms.

Quality of life

MDS is a disease with a significant impact on every-day life due to cytopenia and the substantial risk of a fatal outcome. Recent studies provide important information about the quality of life in MDS. Troy *et al.* assessed the NCCN distress thermometer and problem list scores in 110 patients.[18] The three most frequently reported symptoms were fatigue, pain and worry. Stauder *et al.* used the prospective European LeukemiaNet Registry to compare health-related quality of life in 1,690 consecutive patients

Table 3. World Health Organization classification of myelodysplastic syndrome.

Name	Dysplastic lineages	Cytopenias*	Ring sideroblasts as % of marrow erythroid elements	BM and PB blasts	Cytogenetics by conventional karyotype analysis
MDS with single lineage dysplasia	1	1 or 2	<15%/ <5%†	BM <5%, PB <1%, no Auer rods	Any, unless fulfills all criteria for MDS with isolated del(5q)
MDS with multilineage dysplasia	2 or 3	1-3	<15%/ <5%†	BM <5%, PB <1%, no Auer rods	Any, unless fulfills all criteria for MDS with isolated del(5q)
MDS with ring sideroblasts (MDS-RS)					
MDS-RS with single lineage dysplasia	1	1 or 2	≥15%/≥5%†	BM <5%, PB <1%, no Auer rods	Any, unless fulfills all criteria for MDS with isolated del(5q)
MDS-RS with multilineage dysplasia	2 or 3	1-3	≥15%/≥5%†	BM <5%, PB <1%, no Auer rods	Any, unless fulfills all criteria for MDS with isolated del(5q)
MDS with isolated del(5q)	1-3	1-2	None or any	BM <5%, PB <1%, no Auer rods	del(5q) alone or with 1 additional abnormality except -7 or del(7q)
MDS with excess blasts (MDS-EB)					
MDS-EB-1	0-3	1-3	None or any	BM 5%-9% or PB 2%-4%, no Auer rods	Any
MDS-EB-2	0-3	1-3	None or any	BM 10%-19% or PB 5%-19% or Auer rods	Any
MDS, unclassifiable (MDS-U)					
MDS-U with 1% blood blasts	1-3	1-3	None or any	BM <5%, PB 1%,‡ no Auer rods	Any
MDS-U with single lineage dysplasia and pancytopenia	1	3	None or any	BM <5%, PB <1%, no Auer rods	Any
MDS-U based on defining cytogenetic abnormality		0	1-3	≥15%§	BM <5%, PB <1%, no Auer rods MDS-defining abnormality
Refractory cytopenia of childhood	1-3	1-3	None	BM <5%, PB <2%	Any

*Cytopenias defined as: hemoglobin <10 g/dL; platelet count <100 x10^9/L; and absolute neutrophil count <1.8 x 10^9/L. Rarely, myelodysplastic syndrome may present with mild anemia or thrombocytopenia above these levels. The peripheral blood monocyte count must be <1 x 10^9/L. †If *SF3B1* mutation is present. ‡One percent peripheral blood blasts must be recorded on at least two separate occasions. §Cases with ≥15% ring sideroblasts by definition have significant erythroid dysplasia, and are classified as myelodysplastic syndrome with ringed sideroblasts with single lineage dysplasia. BM: bone marrow; PB: peripheral blood.

with IPSS low/intermediate-1 risk MDS with an age- and sex-matched reference population.[19] MDS patients reported moderate/severe problems in the dimensions pain/discomfort (50%), mobility (41%), anxiety/depression (38%), and usual activities (36%). Limitations were more frequent in older patients, in females, and in those with a high comorbidity burden or needing red blood cell transfusions. Finally, Efficace and co-workers studied patients with higher-risk MDS and concluded that patient-reported outcomes provide important information regarding the prognosis of patients.[20]

Disease pathogenesis

A hallmark of MDS is the dysregulated hematopoietic differentiation resulting in impaired differentiation, morphological dysplasia, and cytopenia.[63] The cell of origin of MDS lies within the hematopoietic stem and progenitor cell compartment and can usually be tracked back to the pluripotent hematopoietic stem cell, implying that MDS is a malignancy for which cure usually cannot be reached with treatments other than allogeneic stem cell transplantation (SCT).[21] MDS cells accumulate in the bone marrow as a result of a complex interplay between genetic and epigenetic alterations, the bone marrow microenvironment, and the immune system, a process that can develop over several years (Figure 1).

The genetic landscape of MDS is quite well delineated. Early studies focused on structural cytogenetic abnormalities, identified by metaphase karyotyping in around 50% of MDS patients. Most of these abnormalities are unbalanced changes resulting in loss or gain of a large amount of chromosomal material e.g. deletion (del) 5q, monosomy 7, trisomy 8 and del 20q.[22] The advent of next-generation sequencing technology resulted in a comprehensive mapping of the MDS genome.[23-25] More than 50 genes have been identified as recurrently mutated in MDS. These genes are involved in biological processes such as DNA methylation, chromatin modification, RNA splicing, cohesion formation, regulation of transcription, signaling and DNA repair (Table 4). Some mutations result in specific phenotypes e.g. *SF3B1* and del5q which are described below. Interestingly, some of the recurrently mutated genes e.g., *DNMT3A*, *TET2* and *ASXL1*, are also found in healthy individuals (clonal hematopoiesis of indeterminate prognosis, CHIP), representing pre-leukemic clones with an age-associated incidence and a varying risk of subsequent development of MDS or other myeloid malignancies.[26,27]

Several of the recurrently mutated genes are epigenetic regulators.[28,29] The MDS epigenome exhibits distinct pathological patterns, which may be explained in part by such mutations but which can also be a consequence of stochastic epigenetic drift, seen with increasing age.[30] In analogy with the epigenetic profile, patients with MDS also demonstrate specific gene expression profiles.[31-33] Such clusters can be observed for morphological subgroups e.g. MDS with ringed sideroblasts (MDS-RS) and MDS with excess blasts, as well as for specific genetic lesions e.g., del(5q) and *SF3B1*.

Many studies have addressed the composition and function of the immune system in MDS and several immuno-

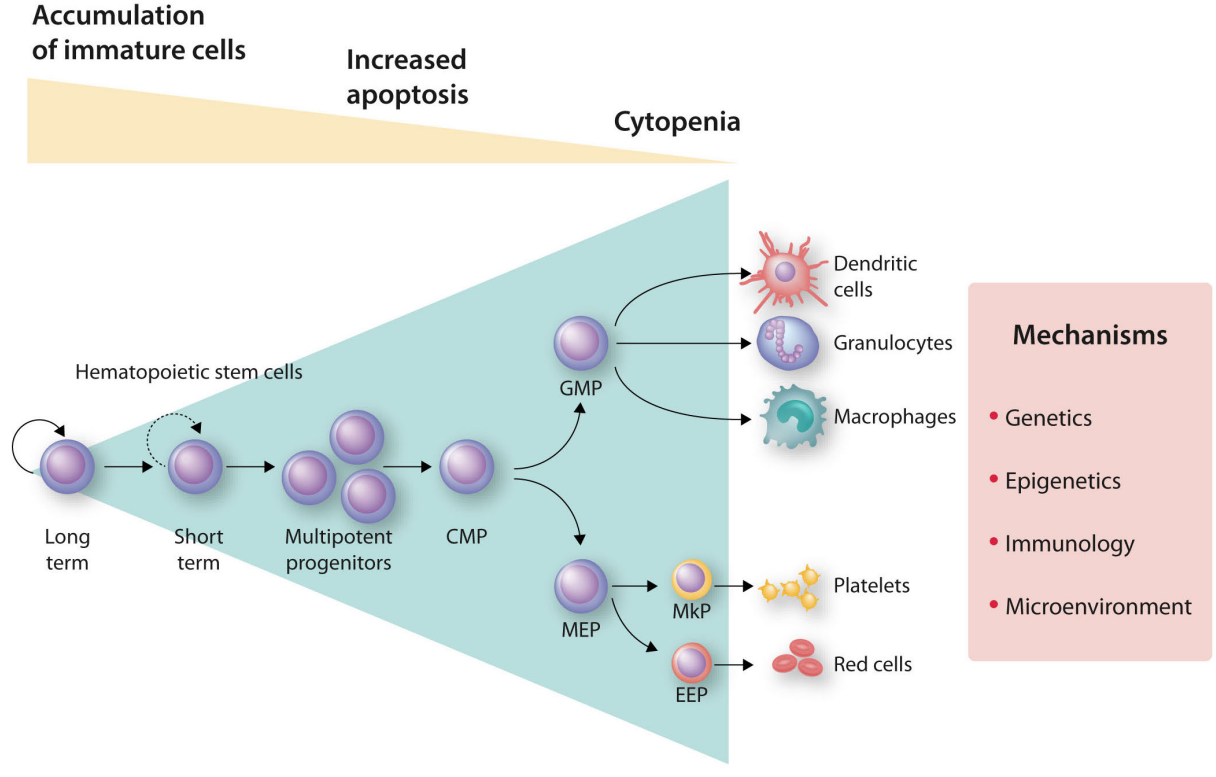

Figure 1. Pathogenesis of myelodyspastic syndromes: underlying mechanisms. CMP: common myeloid progenitors; GMP: granulocyte-monocyte progenitor; MEP: megakaryocyte-erythrocyte progenitor; MkP: megakaryocyte progenitor; EPP: early erythroid progenitor.

logical imbalances have been identified, in particular within the T-cell lineages. In lower-risk MDS, an upregulation of cytotoxic T cells has been observed, whereas higher-risk MDS is characterized by immune escape and upregulation of regulatory T cells.[34-36] Several studies have identified autonomous large granular lymphocyte T-cell clones in a large proportion of patients with MDS.[37,38] Similarly, the presence of plasma cell clones has been described.[39,40] Whether the MDS disease is evoking immune activation or whether an initial immune activation results in selection pressure giving mutated MDS cells a survival advantage is unclear.

The microenvironment in MDS shows abnormal morphological features. Molecular characterization of stromal niche cells has revealed various alterations, including disturbances in differentiation and in stem cell supporting functions.[41-46 47-49] Again, whether niche-alterations are initiating events or induced by the MDS clone is unknown. Murine models have suggested that manipulation of the niche can induce myeloid malignancies, but solid evidence from MDS patients remains to be presented.[50-52]

An important route to develop MDS is by exposure to cytostatic drugs or radiation-therapy, i.e., therapy-related MDS. The mechanisms involved are largely unknown. Case-control studies have demonstrated a higher frequency of underlying CHIP clones in patients developing therapy-related MDS.[53-55] Possibly, the survival pressure that is exerted on hematopoietic stem cells during treatment may give underlying CHIP clones a survival advantage resulting in emergence of the MDS. It has also been proposed that cytostatic/radiation therapy can cause direct DNA damage but evidence for this hypothesis is sparse.

5q- syndrome

Although the mechanisms underlying anemia in patients with del(5q) remain elusive, haploinsufficiency and dependence of erythroid cells on casein kinase (CK1α), encoded for by a gene within the common deleted region of del(5q), appear to be of central importance. The drug lenalidomide induces ubiquitination of CK1α through the E3 ubiquitin ligase cereblon, resulting in CK1α degradation.[56] Such degradation in the haploinsufficient del(5q) cells sensitizes these cells to lenalidomide, providing a basis for the therapeutic effects of the drug in these patients. Additionally, the E3 ubiquitin ligase RNF41 is a principal target responsible for erythropoietin receptor (EpoR) stabilization. Data suggest that lenalidomide also has E3 ubiquitin ligase inhibitory effects thus inhibiting RNF41 auto-ubiquitination and promoting membrane accumulation of signaling competent JAK2/EpoR complexes that augment responsiveness to erythropoietin.[57]

Myelodysplastic syndrome with ringed sideroblasts and *SF3B1* mutations

The characteristic mitochondrial ferritin accumulation in MDS-RS is associated with reduced expression of the iron transporter protein gene *ABCB7*.[58,59] In two pivotal papers, Papaemmanuil *et al.* and Yoshida *et al.* described recurrent mutations in splicing factor 3b subunit 1 (*SF3B1*) in more than 80% of patients with MDS-RS.[60,61] Subsequent studies identified aberrant splicing of genes involved in erythropoiesis and mitochondrial function, but the molecular and cellular links between the *SF3B1* mutation and ineffective erythropoiesis remain elusive.[62-64] Recent studies have tracked back the *SF3B1* mutations to multipotent hematopoietic stem cells and described how MDS-RS erythropoiesis can be confidently modeled *in vitro*, leading to new possibilities to assess the effects of novel compounds.[65,66] From a clinical perspective MDS-RS with *SF3B1* mutations appears as a clinically and morphologically distinct entity with affected patients having a favorable survival, a low risk of leukemic transformation but a high risk of developing refractory transfusion dependence.[6,67]

Genetic predisposition to myeloid neoplasms

Myeloid neoplasms with germline predisposition were recognized as a separate entity in the WHO 2016 classification.[1] Individuals with germline predisposition exhibit an increased risk of developing myeloid neoplasms, mainly AML and MDS. Estimates suggest that at least 5% to 15% of patients with MDS or AML carry germline pathogenic variants.[68,69]

Germline mutations are divided into those predisposing to myeloid neoplasms without a pre-existing disorder, mutations with pre-existing platelet dysfunction, and mutations associated with organ dysfunction. *GATA2* and *RUNX1* mutations are relatively common and mandate continuous surveillance of asymptomatic carriers, because of the high risk of such subjects developing a myeloid neoplasm.[21,68,70] Mutations in the telomerase complex usually lead to a complicated clinical presentation with multiorgan involvement, and mutations in the *SAMD9* and *SAMD9L* genes are associated with a high risk of progression to monosomy 7 MDS.[71,72] More recently identified

Table 4. Mutations in myelodysplastic syndromes.

Functional group	Included genes
DNA methylation	*DNMT3A, TET2, IDH1, IDH2*
Chromatin modification	*EZH2, SUZ12, EED, JARID2, ASXL1, KMT2, KDM6A, ARID2, PHF6, ATRX*
Cohesin complex formation	*STAG2, RAD21, SMC3, SMC1A*
RNA splicing	*SF3B1, SRSF2, U2AF1, U2AF2, ZRSR2, SF1, PRPF8, LUC7L2*
Transcription	*RUNX1,ETV6,GATA2,IRF1, CEBPA, BCOR, BCORL1, NCOR2, CUX1*
Cytokine receptor/tyrosine kinase	*FLT3, KIT, JAK2, MPL, CALR, CSF3R*
Other signaling	*GNAS, GNB1, FBWX7, PTEN*
Checkpoint/cell cycle	*TP53, CDKN2A*
DNA repair	*ATM, BRCC3, FANCL*
Other	*NPM1, SETBP1, DDX41*

homozygous mutations in *ERCC6L2* have been shown to predispose to the development of somatic *TP53* mutations and severe AML.[73] Mutations in *DDX41* predispose to myeloid neoplasms at higher ages than most other predisposing mutations, making this an important gene to analyze in potential adult sibling donors.[74]

Determining the diagnosis of myeloid neoplasms with germline predisposition is of crucial clinical significance since it may tailor therapy, dictate the selection of donors and conditioning regimens for allogeneic hematopoietic SCT, and enable relevant prophylactic measures and early intervention. The Nordic MDS group recently published a practical guideline program for diagnosis and management of such conditions.[4]

Risk assessment and prognostication

Clinical variables for risk-based classification

A number of disparate methods have been developed to clinically characterize MDS patients and evaluate their prognosis. These classification approaches incorporated a mixture of clinical features, including marrow blasts and cytogenetics, differing cytopenias, age, lactate dehydrogenase levels, and cytogenetic abnormalities. The International MDS Risk Analysis Workshop clarified these features and generated the consensus International Prognostic Scoring System for MDS (IPSS), dividing patients with MDS into four risk categories based on their cytopenias, marrow blast percentage and cytogenetic subgroup, with median survivals ranging from 0.4 to 5.7 years.[75] This classification method proved useful for prognostic evaluation and clinical trial design.

Over the ensuing 15 years, additional features were suggested to provide prognostic information in MDS, including ferritin and β_2-microglobulin levels, marrow fibrosis, the patient's comorbidities and performance status, and novel cytogenetic subgroups as well as refined morphological assessment of MDS.[2,76-81] To examine the prognostic impact of these variables, the coalescence of data from a new set of untreated primary MDS patients from multiple international institutions provided another global database of 7,012 patients via the International Working Group for Prognosis in MDS (IWG-PM) project. This database generated the Revised-IPSS (IPSS-R) allowing for a more comprehensive cytogenetic analysis, providing five cytogenetic subgroups based on an increased number of specific prognostic chromosomal categories (n=15)[12] compared to the six in the IPSS.[75] In addition and importantly, the revised system incorporated depth of cytopenias and differing marrow blast percentages. The revised model demonstrated five major prognostic categories (Figure 2). Some patients in the IWG-PM project were also assessed by the WHO classification-based Prognostic Scoring System (WPSS) parameters, including red cell transfusion dependence and WHO-defined clinical subgroups, with similar prognostic efficacy.[82]

Since 2012, the IPSS-R has been a standard for evaluation of risk-based clinical outcomes, and design of therapeutic strategies and clinical trials based on prognostic risk-based features. The European LeukemiaNet and the American NCCN MDS practice guidelines recommend treatment based on the IPSS-R, age and performance status.[9,83] The IPSS-R has been confirmed to be a valuable method for risk-classifying MDS patients, albeit with some degree of variablity.[84-88]

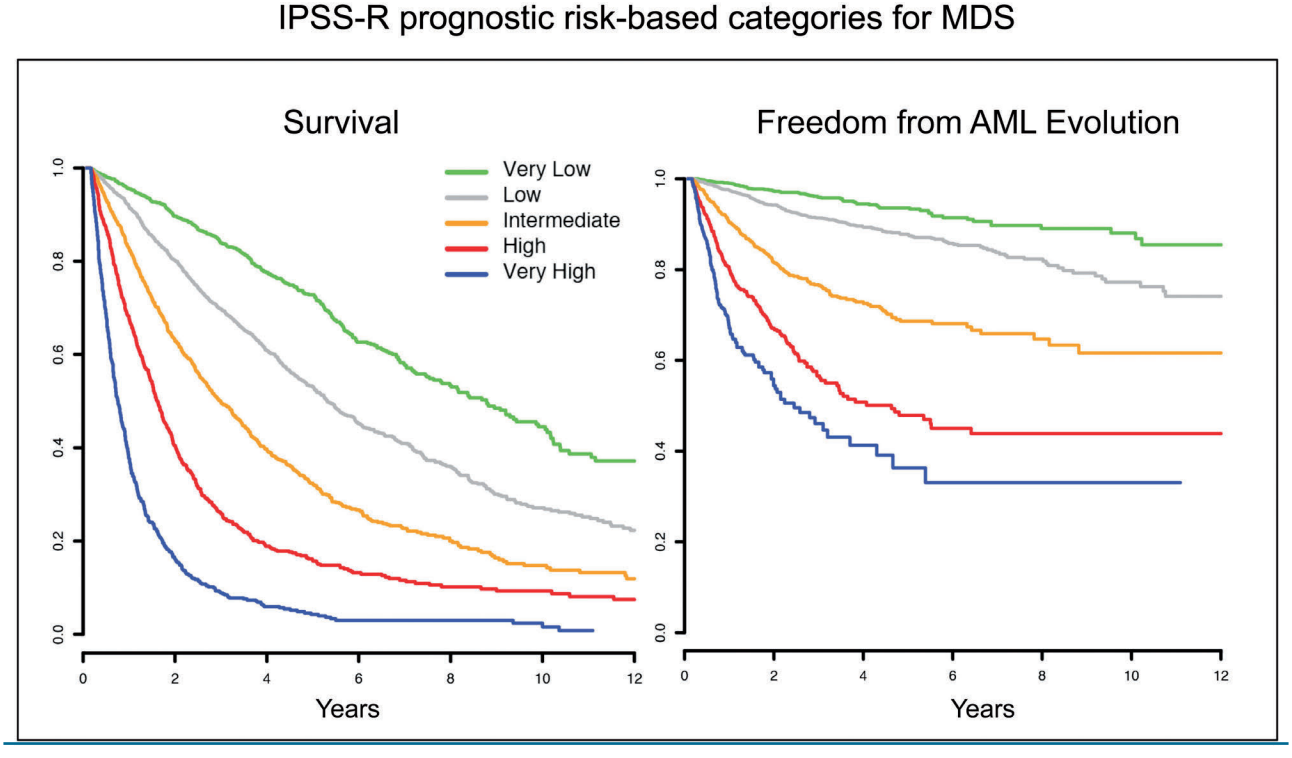

Figure 2. Clinical outcomes of patients with myelodysplastic syndrome in relation to Revised International Prognostic Scoring System prognostic risk-based categories. Survival, n = 7012, *P*<0.001. Evolution to acute myeloid leukemia, n = 6485, *P*<0.001.[12] IPSS-R: Revised International Prognostic Scoring System; AML: acute myeloid leukemia.

Genomics in the International Prognostic Scoring System risk assessment

Recent molecular studies have demonstrated the major impact on survival and disease progression of specific somatic mutations, including those that are additive to the IPSS-R clinical characterization.[23-25,89-91] At least five genes - *TP53*, *ASXL1*, *EZH2*, *ETV6*, and *RUNX1* - have an adverse prognostic impact whereas *SF3B1* has a positive impact. Additionally, a group of approximately 60 genes have been recurrently demonstrated to be involved in the various subtypes of MDS, with varying incidence levels (Table 4). Bone marrow samples from a representative cohort of over 3,000 MDS patients were sequenced using a next-generation sequencing panel optimized for myeloid disease. Analysis of *TP53* mutations in 380 patients enabled segregation of patients according to two *TP53* states: a mono-allelic state in which one wildtype allele remained and a multi-hit/bi-allelic state in which *TP53* was altered multiple times by either mutations, deletions or copy neutral loss of heterozygosity (67% of *TP53*-mutated patients).[92] *TP53* state rather than mutation alone was found to be an independent diagnostic and prognostic biomarker in MDS. Mono-allelic *TP53* patients had more favorable disease than multi-hit *TP53* patients and were enriched in low-risk WHO subtypes. Critically, multi-hit *TP53* was associated with a worse overall survival as compared to mono-allelic *TP53*, and with more pronounced AML transformation.[92]

Patients' management

MDS is a complex disease displaying marked inter-individual differences with regard to disease mechanisms and potential therapeutic options. Compared to many other blood cancers, the diagnostic process is more challenging and effective targeted treatments less abundant. In Europe, the MDS-Europe platform offers comprehensive consensus-based MDS guidelines for diagnosis, prognosis and treatment derived from two consecutive European Union research projects (*www.mds-europe.eu*).[83] Moreover, many Western countries have local web-based guidelines with links from *mds-europe.org*. In the USA the NCCN guidelines (*www.nccn.org/professionals/physician_gls/PDF/mds.pdf*)[9] offer the same service.

Diagnostic work-up

The diagnostic work-up follows the recommendations in the WHO 2016 classification.[1] Cornerstones are bone marrow morphology and histopathology, and cytogenetic analysis. Flow cytometry immune-phenotyping is recommended but not mandatory.[93] It is a necessary tool to exclude certain differential diagnoses, such as paroxysmal nocturnal hemoglobinuria and large granular lymphocytic leukemia. Molecular genetics, mainly targeted DNA sequencing, is strongly recommended, in particular in patients who are candidates for active treatment.[25,60] Differential diagnoses of MDS encompass a long list of both benign and malignant diagnoses, as summarized in Table 5. Since management depends on a correct diagnosis, many national cancer programs mandate that diagnosis and prognosis are established in multi-professional conferences.

Clonal cytopenia of unknown significance

Clonal hematopoiesis becomes more prevalent with increasing age and may be present in the absence of cytopenias [CHIP/aging-related clonal hematopoiesis (ARCH)]. Interestingly, a recent study based on the Danish twin registry failed to show a clear relation between CHIP

Table 5. Causes of cytopenia and/or dysplasia other than myelodysplastic syndromes.

Differential diagnosis	Diagnostic tests
Aplastic anemia, pure red cell aplasia	Histology, cytology, parvovirus B19
Metastatic carcinoma	Histology, immunohistochemistry
Toxic bone marrow injury (alcohol, lead, zinc, copper deficiency, nonsteroidal anti-rheumatic drugs, etc.)	History, laboratory tests
Reactive bone marrow changes (infections e.g. sepsis, HIV, hepatitis, tuberculosis and other chronic infections, autoimmune diseases, thyroid disease, etc.), copper deficiency	Cytology, history, laboratory tests
Paroxysmal nocturnal hemoglobinuria	Immunophenotyping
Immune thrombocytopenia	History, course
Megaloblastic anemia	Vitamin B12/folic acid concentration
Hypersplenic syndromes	History/clinical features (splenomegaly)
Acute leukemia (especially erythroleukemia, FAB-M6)	Cytology, histology, immunophenotyping, genetic and molecular genetic testing
Myeloproliferative diseases (especially CMML, aCML, PMF)	Histology, cytogenetic and molecular genetic testing
Hairy cell leukemia, large granular lymphocytic leukemia	Cytology, immunophenotyping, molecular genetic testing (*BRAF*, *STAT3*), T-cell receptor
Congenital dyserythropoietic anemia (rare)	Molecular genetic testing
Idiopathic cytopenia of undetermined significance	ICUS minimal diagnostic criteria
Clonal cytopenia of undetermined significance	CCUS diagnostic criteria

HIV: human immunodeficiency virus; FAB: French-American-British; CMML: chronic myelomonocytic leukemia; aCML: atypical chronic myeloid leukemia; PMF: primary myelofibrosis; ICUS: idiopathic cytopenia of undetermined significance; CCUS: clonal cytopenia of undetermined significance.

and survival and did not point towards a common genetic basis.[94] The term clonal cytopenia of unknown significance defines individuals with myeloid mutations and some degree of cytopenia, but without fulfilling criteria for MDS or other hematologic diagnoses. The type and number of mutations, and variant allele frequencies are potential predictors of risk of progression and are currently being evaluated and reviewed in large cohorts.[95,96] Single mutations in *TET2* or *DNMT3A* with limited variant allele frequencies are observed in a relatively large fraction of individuals above 60 years and could thus be considered normal, while the presence of more than one mutation and any splice factor mutation may predict a high risk of developing MDS. Patients with clonal cytopenia of unknown significance, in particular if they are potential candidates for curative treatment, should be followed up, but results are presently too divergent to allow for precise recommendations.

Risk-based therapeutic decision-making

In addition to disease-specific variables, patient-related factors are also essential for risk estimation. Age and comorbidities, naturally, influence the spectrum of available therapies. A number of comorbidity and so-called frailty scores have been developed both for MDS and blood cancers in general and, accounting for both disease- and patient-related factors, considerably improve risk stratification. Several comorbidity scores have been tested in the general MDS patient population, including the MDS-Specific Comorbidity Index and the Charlson comorbidity index.[97,98]

Therapeutic options

Therapeutic options for patients with MDS vary from supportive care to allogeneic SCT, depending on disease- and patient-related risk factors. Table 6 provides an overview of therapeutic options and is divided into treatments which either are formally approved by the FDA and/or EMA or are part of long-standing routine treatment used for MDS, albeit having been approved for other diagnosis, or are in the process of being approved. As the MDS-Europe and NCCN guidelines are relatively specific about indications and dosing, these will not be detailed in the present review.

Supportive care

Supportive care is a cornerstone of the management of all MDS and MDS/MPN patients.[91] Recent studies show reduced progression-free survival and quality of life in patients with a higher density of transfusions.[15,19,99] A Nordic study showed that quality of life improved in patients responding to growth factors, but also in non-responders transfused to a target hemoglobin of >12 g/dL.[100] A British study showed that higher transfusion targets were associated with improved quality of life.[101] Indeed, increasing evidence suggests that transfusion therapy should be tailored according to the patient's subjective symptoms and not to specific hemoglobin trigger levels.[83]

Severe thrombocytopenia with the need for transfusions becomes increasingly frequent with time.[14] Consensus-based guidelines agree that platelet transfusions should be governed by trigger platelet count levels during active treatment with chemotherapy and hypomethylating agents (HMA), but mainly based on bleeding symptoms during untreated chronic thrombocytopenia. Eltrombopag and romiplostim are licensed (the latter only in the USA) for the treatment of severe chronic immune thrombocytopenia. The results from the pivotal studies in lower-risk and higher-risk MDS did not generate licensing in any region, even though some positive responses were observed.[102,103] Eltrombopag did not improve the outcome of patients treated with azacytidine in a randomized phase III study.[103] These compounds may relieve bleeding symptoms in patients with lower-risk hypoplastic MDS with severe thrombocytopenia, and are sometimes used for such individuals. Granulocyte colony-stimulating factor (G-CSF) is not indicated for low neutrophil counts, but can be used as supportive care in the case of neutropenia caused by HMA treatment, in particular after recurrent infectious events.[9,83]

Iron chelation

Close to 50% of MDS patients need red blood cell transfusions as supportive care.[21,30,50] Transfusion dependence leading to iron overload has a negative impact on organ function as well as infectious complications in some analyses.[104-106] In cases of iron overload, the transferrin binding of iron is overwhelmed and free non-transferrin bound iron, a redox active component in the plasma, appears to be an important mediator of tissue damage.[107-110]

Prior observational studies have indicated that iron overload may contribute to poorer clinical outcomes in patients with low/intermediate-1-risk MDS.[111,112] Although studies have shown that iron chelation therapy may improve patients' outcomes, most studies had limitations, such as

Table 6. Therapeutic options for myelodysplastic syndrome.

Approved by EMA *or* FDA or part of standard care

- Transfusion therapy
- Iron chelation[1]
- Erythropoiesis-stimulating factors
- Immunosuppressive treatment
- Lenalidomide for lower-risk del(5q) MDS
- Azacytidine[2]
- Decitabine[3]
- Induction chemotherapy
- Stem cell transplantation

Available therapeutic options, but not approved for MDS by EMA or FDA

- Venetoclax (+ HMA hypomethylating agents or low-dose cytarabine)[4]
- Luspatercept[5]
- Eltrombopag, romiplostim6
- Ivosidenib (*IDH1*) and enasidenib (*IDH2*)[7]

[1]Desferrioxamine, deferasirox and deferiprone available in Europe. 1Desferrioxamine and deferasirox available in the USA. [2]Approved for International Prognostic Scoring System (IPSS) intermediate-2 and high-risk myelodysplastic syndrome (MDS), and acute myeloid leukemia (AML) with 20-29% myeloblasts by the European Medicines Agency (EMA). Approved for all MDS and AML with 20-29% myeloblasts by the Food and Drug Administration (FDA). [3]Approved for IPSS intermediate-2 and high-risk MDS by the FDA. Approved for AML by the FDA and EMA [4]Approved for AML (in combination with hypomethylating agents, low-dose ara-C) by the FDA. Approved for chronic lymphocytic leukemia by the EMA. [5]Expected FDA approval in April 2020. [6]Eltrombopag and romiplostim approved for immune thrombocytopenic purpura, thrombocytopenia associated with hepatitis C, and aplastic anemia by the FDA. Only eltrombopag approved by the EMA. [7]Approved for AML by the FDA. Not approved by the EMA.

being retrospective analyses or registry studies.[113-117] Currently, the drugs used for iron chelation are deferasirox (oral), deferioxamine (intravenous via an infusion pump) and deferiprone (oral). A prospective randomized, double-blind study was performed, which assessed event-free survival and safety of deferasirox compared with placebo.[118] Although not demonstrating an improvement in overall survival, the median event-free survival was prolonged by approximately 1 year with deferasirox treatment. Clinical guidelines include recommendations for the use of iron chelation therapy in some populations of MDS patients. However, debate regarding the clinical utility of iron chelation therapy remains.[9,82,119-122]

Erythropoiesis-stimulating agents

Erythropoiesis-stimulating agents (ESA) constitute standard treatment for the anemia of lower-risk MDS.[9,83] Both the EMA and FDA have evaluated numerous studies on the effects of ESA in the treatment of anemia in MDS, although both agencies formally approved erythropoietin and darbepoetin only recently, based on placebo-controlled trials.[123,124] Erythropoietin α and β and later darbepoetin have been extensively evaluated for MDS and were shown to improve hemoglobin levels and reduce transfusion needs in 40% to over 60% of patients with an overall duration of 18-24 months.[125] Higher doses (60,000 to 80,000 U per week) may give a slightly better response rate in transfusion-dependent patients.[126] Lower serum erythropoietin levels are associated with higher response rates. There is no evidence from any trial or registry that treatment with ESA is associated with an increased risk of disease progression or leukemic transformation.[125]

A study of a large cohort of patients included in the European Union MDS Registry recently added significant novel information. Patients with symptomatic anemia who did not require transfusions and were treated with ESA had a significantly better response rate and longer time to a permanent transfusion need than those treated after the onset of regular transfusions.[127] This led to an important change in the European guidelines, which now recommend treatment at the onset of symptomatic anemia. Relapse of anemia is usually not associated with disease progression and the biological reasons for treatment failure are yet to be explored. Several randomized phase II studies and epidemiological investigations also showed that the addition of low-dose G-CSF to erythropoeitin may improve the response rate to ESA, and improve overall survival.[128-130] The synergistic effect is seen particularly in MDS-RS and is related to the anti-apoptotic effects of G-CSF on mitochondria-mediated apoptosis.

Lenalidomide for del(5q)

An initial clinical trial showed that MDS patients with the del(5q31) chromosomal abnormality were particularly responsive to lenalidomide, demonstrating a major reduction in transfusion requirements and reversal of cytogenetic abnormalities.[131] These effects were confirmed and extended in a larger phase II trial and a subsequent phase III, randomized, placebo-controlled trial which demonstrated erythroid response rates of ~50-60%, including a transfusion independence rate of ~28% together with concomitant cytogenetic responses.[132] A phase III randomized trial in lower-risk, ESA-refractory, non-del(5q) patients comparing lenalidomide alone with lenalidomide in conjunction with recombinant human erythropoietin suggested that lenalidomide may restore sensitivity of MDS erythroid precursors to erythropoietin.[133] These data led to the recommendation in the NCCN and MDS-Europe guidelines on the symptomatic treatment of anemic del(5q) MDS patients with lenalidomide.[9,83] The negative impact of *TP53* mutations (present in ~30% of these patients) on responsiveness and outcome after lenalidomide is notable.[134]

Immunosuppressive treatment

Treatment with immunosuppressive agents such as antithymocyte globulin and cyclosporine A may improve cytopenias in certain patients with MDS.[135-138] As recently described in a well-performed meta-analysis there are few large prospective studies, follow-up times in many studies are short, and each study has used different immunosuppressive regimens.[139] In an analysis of 570 patients with a median age of 62 years, 80% of patients had low or intermediate-1 IPSS scores, the complete response and red cell transfusion independence rates were 12.5% and 33%, respectively, and the rate of progression to AML was 8.6% per patient-year. Immunosuppressive therapy has not been confidently evaluated in relation to mutational profiles. Both European and USA guidelines identify a group of younger, lower-risk MDS patients with hypo- or normoplastic bone marrow and normal karyotype, with the exception of trisomy 8, who may respond to immunosuppressive therapy. Some responders may experience durable and possibly permanent responses, indicating that immunosuppressive therapy may be considered prior to SCT in patients with these features.

Hypomethylating agents

Azacitidine

Based on early phase I/II studies, two large randomized phase III studies were designed to evaluate the effects of azacitidine in MDS.[140-142] The CALGB9221 trial included patients with all subtypes of MDS, and showed improved overall response rate and progression-free survival in the azacitidine arm. The second randomized study, AZA-001, was designed to demonstrate a possible difference in overall survival.[143] The median overall survival for the azacitidine-treated patients was 24.5 months *vs.* 15 months for patients assigned to the control arm. Both studies showed that responses are often delayed until the patient has received ≥3 treatment cycles.[142,143] Azacitidine is approved in Europe for the treatment of higher-risk MDS and in the USA for the treatment of all MDS subgroups.

Some phase II studies have also shown effects in lower-risk MDS although the clinical benefits and risks in this population are still unclear and no studies have provided evidence for prolonged survival in this group of patients.[141,144-146] A large randomized study (NCT01566695) is assessing the effect of oral azacitidine in lower-risk MDS and will perhaps bring more clarity on its role in the treatment of these patients.

Much effort has been given to identifying factors that could predict response. Predictive models based on basic clinical data have not generated clinically meaningful tools.[147-149] Neither have studies on mutational profiles resulted in robust response prediction. Better responses have been reported for patients with *TET2*, *ASXL1* and *EZH2* mutations but the data are conflicting.[149-152]

Decitabine

Decitabine has been evaluated in two phase II studies assessing higher-risk MDS patients.[153,154] Both studies showed similar efficacy, with overall response rates of 32-39% and median survivals of ~20 months. The safety and efficacy data were similar to those for azacytidine, although phase III data, available for azacitidine, are lacking for decitabine. Both HMA are recommended by the NCCN for treating higher-risk patients, with a special focus also as a bridge to allogeneic SCT for eligible patients. High response rates have been reported for *TP53*-mutated AML patients treated with a 10-day decitabine regimen, although the durations of the responses were short.[155]

Intensive chemotherapy

Since the advent of HMA and other disease-modifying drugs, the use of intensive chemotherapy has decreased substantially but it may be considered after failure to benefit from HMA in younger fit patients, particularly as bridging-therapy to SCT. The rate of complete responses achieved with intensive chemotherapy is around 50%, which is lower than that for *de novo* AML patients, and time to relapse is often short.[156-158] The clinical benefit of this approach for non-SCT candidates in whom azacitidine therapy has failed has not been established.

Allogeneic stem cell transplantation

SCT is the only potentially curative treatment for patients with MDS. Due to potential severe complications, SCT is generally offered only to fit patients up to around 70-75 years of age. Historical data document long-term survival rates of between 25% and 45% with non-relapse mortality and relapse occurring in approximately a third of the patients.[159-161] A more recent prospective study found a higher 2-year relapse-free survival of 60%.[162] Since the median age (50 years) in that study was relatively low, the outcome does not represent a real-world population.

Optimal timing of SCT is essential, considering that patients with high-risk MDS have a high risk of both relapse and mortality after SCT.[163] A general recommendation is to transplant higher-risk patients as part of an upfront process, while lower-risk MDS patients should be monitored and transplanted upon disease progression. Defining which patients should be considered low- and high-risk is therefore crucial for a correct transplantation plan. All three prognostic scoring systems (IPSS, IPSS-R and WPSS) are predictive of survival after allogeneic SCT.[160,161,164,165] Genetic aberrations have a large impact on relapse risk. Relapse-free survival at 5 years in the five IPSS-R cytogenetic risk groups ranges between 10% and 42%.[160,166] In addition, mutations in *TP53* and the *RAS*-pathway genes have been reported to be risk factors for relapse.[167-169]

Disease status is also important for SCT outcome.[161,168,170] Disease-modifying treatment is usually given to patients with a more proliferative disease, aiming for the best possible remission before SCT. The usefulness of such treatment has, however, not been tested in prospective clinical trials. Retrospective studies have demonstrated similar outcomes for treated and untreated patients although selection bias is an obvious potential pitfall in these studies.[171-173] Similarly, retrospective studies have not shown any advantage for either HMA or intensive chemotherapy as disease-modifying treatment before SCT.[174]

Retrospective studies have shown higher relapse rates but lower non-relapse mortality for reduced intensity conditioning, generating similar overall survival rates.[159,161,162] Good results have been reported for the fludarabine plus treosulfan regimen which is often used in younger patients.[175-177]

The prognosis after a post-SCT relapse is dismal although donor lymphocyte infusions and HMA may reverse the relapse in some cases.[178] No validated minimal residual disease markers are yet available for MDS. The Nordic MDS group is presently conducting a clinical trial (NCT02872662) in which patient-specific mutations are tracked in serial post-SCT samples using digital droplet PCR. Preliminary data indicate that these markers may predict relapse and can be used for initiation of pre-emptive treatment.

Investigational therapies for myelodysplastic syndromes

There are limited therapeutic options available to exploit our increasing understanding of the molecular pathophysiology of MDS. As indicated above, only one therapy, lenalidomide, targets a specific clinical subset [patients with del(5q) cytogenetics], and two epigenetic modulators (azacytidine and decitabine) have been approved for the treatment of patients with presumed hypermethylation. Recurrently mutated intracellular functional pathways are frequently implicated in MDS and a number of novel therapies targeting these molecular defects have recently shown potential utility for treating MDS patients. In addition, drugs capable of modifying the toxic marrow microenvironmental influences for erythropoiesis have been developed.

IDH1 and *IDH2* mutation inhibitors

Understanding of the pathophysiology of *IDH1/2* mutations in MDS and AML has led to development of clinical *IDH1* and *IDH2* mutation inhibitors. *IDH1* and *IDH2* mutations occur in approximately 5-12% of MDS patients (P51). Recent data have shown encouraging results from the use of ivosidenib or enasidenib for patients with *IDH1* or *IDH2* mutations, respectively.[179,180]

BCL2 inhibitor

The anti-apoptotic protein B-cell leukemia/lymphoma-2 (BCL2) is overexpressed in hematologic malignancies including some cases of MDS, in which it has been implicated in the maintenance and survival of myeloid cells, resistance to therapy, and poor clinical outcomes.[181] In recent studies in higher-risk MDS patients either previously untreated or resistant to HMA, initial data suggest potential clinical efficacy of the BCL2 inhibitor, venetoclax, when combined with azacytidine.[182,183]

Drugs acting on p53

In hematologic malignancies, including MDS, *TP53* mutations confer a poor prognosis. These mutations are particularly common in therapy-related MDS and a portion of patients with del(5q) cytogenetics.[184] The drug APR-246 restores wildtype conformation to the mutant p53 and has recently shown beneficial clinical activity in MDS.[185,186] Another approach to reactivate p53-mediated tumor suppression is to inhibit the frequently overexpressed p53 suppressor proteins MDMX and MDM2 in tumors. ALRN-6924, a cell-penetrating stapled α-helical peptide disrupts

the interaction between p53 and endogenous inhibitors thereby reactivating p53-mediated tumor suppression in AML cells.[187] Phase I/II clinical testing with these drugs is ongoing.

Telomerase inhibition

Defective maintenance of telomere integrity is a hallmark of cancer and is implicated in the pathogenesis of MDS. In MDS, telomere erosion and dysfunction potentiate persistent DNA damage and accumulation of molecular alterations.[188,189] Evidence suggests that telomere erosion can suppress hematopoietic stem cell self-renewal, repopulating capacity, and differentiation. Imetelstat is a telomerase inhibitor that targets cells with short telomeres and highly active telomerase, and has been shown in early clinical studies to have activity in myeloid malignancies.[190] Initial data on the use of imetelstat in lower-risk MDS patients resistant to ESA has shown encouraging erythroid responses.[191]

Luspatercept

Increased levels of the transforming growth factor β (TGFβ) superfamily inhibitors of erythropoiesis (predominantly growth and differentiation factor-11) occur within MDS erythroid cells.[192] Luspatercept, a recombinant fusion protein, is considered to bind TGFβ superfamily ligands and reduce SMAD2 and SMAD3 signaling, reduce erythroid hyperplasia, and enhance erythroid maturation and hemoglobin levels in MDS.[193,194] In a recent phase III trial, luspatercept was shown to reduce the severity of anemia in transfusion-dependent patients with MDS-RS who had disease refractory to or were unlikely to respond to ESA (38% of patients achieved transfusion independence).[195] This drug is currently undergoing USA FDA review for therapeutic use in MDS-RS.

Future considerations

Given the stem cell origin and the multiplicity of molecular abnormalities in MDS, it is difficult to identify potentially effective drugs that can be used to treat a high proportion of patients. Recent studies have demonstrated the feasibility of *ex vivo* drug cytotoxicity platforms to screen effectively for multiple, potentially useful and novel drugs in myeloid neoplasms, including MDS, to provide functional data to guide personalized therapy for treatment-refractory patients with myeloid malignancies and to accurately predict clinical responses *in vivo*.[196-198] Such studies will likely synergize with molecular data and emerging genomics- and cellular-based precision medicine approaches such as *in silico* computational biology modeling.[199,200] Ultimately, combining both genomics-based and *ex vivo* functional data may further refine precision therapy in myeloid neoplasms such as MDS and translate into improved patients' outcomes.

Acknowledgment

This work is part of the MDS-RIGHT activities, which has received funding from the European Union's Horizon 2020 research and innovation programme under grant agreement No 634789 - "Providing the right care to the right patient with MyeloDysplastic Syndrome at the right time".

References

1. Arber DA, Orazi A, Hasserjian R, et al. The 2016 revision to the World Health Organization classification of myeloid neoplasms and acute leukemia. Blood. 2016;127(20):2391-2405.
2. Vardiman JW, Thiele J, Arber DA, et al. The 2008 revision of the World Health Organization (WHO) classification of myeloid neoplasms and acute leukemia: rationale and important changes. Blood. 2009;114(5):937-951.
3. Jaiswal S, Ebert BL. Clonal hematopoiesis in human aging and disease. Science. 2019;366 (6465):eaan4673.
4. Baliakas P, Tesi B, Wartiovaara-Kautto U, et al. Nordic guidelines for germline predisposition to myeloid neoplasms in adults: recommendations for genetic diagnosis, clinical management and follow-up. HemaSphere. 2019;3(6):e321.
5. Bennett JM, Catovsky D, Daniel M, et al. Proposals for the classification of the myelodysplastic syndromes. Br J Haematol. 1982;51(2):189-199.
6. Malcovati L, Karimi M, Papaemmanuil E, et al. SF3B1 mutation identifies a distinct subset of myelodysplastic syndrome with ring sideroblasts. Blood. 2015;126(2):233-241.
7. Greenberg P, Anderson J, De Witte T, et al. Problematic WHO reclassification of myelodysplastic syndromes. Members of the International MDS Study Group. J Clin Oncol. 2000;18(19):3447-3452.
8. Hasserjian RP, Campigotto F, Klepeis V, et al. De novo acute myeloid leukemia with 20–29% blasts is less aggressive than acute myeloid leukemia with ≥30% blasts in older adults: a Bone Marrow Pathology Group study. Am J Hematol. 2014;89(11):E193-E199.
9. Greenberg PL, Stone RM, Al-Kali A, et al. Myelodysplastic syndromes, version 2.2017, NCCN clinical practice guidelines in oncology. J Natl Compr Canc Netw. 2017;15(1):60-87.
10. Bains A, Luthra R, Medeiros LJ, et al. FLT3 and NPM1 mutations in myelodysplastic syndromes: frequency and potential value for predicting progression to acute myeloid leukemia. Am J Clin Pathol. 2011;135(1):62-69.
11. Neukirchen J, Schoonen WM, Strupp C, et al. Incidence and prevalence of myelodysplastic syndromes: data from the Dusseldorf MDS-registry. Leuk Res. 2011;35(12):1591-1596.
12. Greenberg PL, Tuechler H, Schanz J, et al. Revised international prognostic scoring system for myelodysplastic syndromes. Blood. 2012;120(12):2454-2465.
13. Bonadies N, Feller A, Rovo A, et al. Trends of classification, incidence, mortality, and survival of MDS patients in Switzerland between 2001 and 2012. Cancer Epidemiol. 2017;46:85-92.
14. Moreno Berggren D, Folkvaljon Y, Engvall M, et al. Prognostic scoring systems for myelodysplastic syndromes (MDS) in a population–based setting: a report from the Swedish MDS register. Br J Haematol. 2018;181(5):614-627.
15. Ryden J, Edgren G, Karimi M, et al. Male sex and the pattern of recurrent myeloid mutations are strong independent predictors of blood transfusion intensity in patients with myelodysplastic syndromes. Leukemia. 2019;33(2):522-527.
16. Mekinian A, Grignano E, Braun T, et al. Systemic inflammatory and autoimmune manifestations associated with myelodysplastic syndromes and chronic myelomonocytic leukaemia: a French multicentre retrospective study. Rheumatology. 2016;55(2): 291-300.
17. Wolach O, Stone R. Autoimmunity and Inflammation in myelodysplastic syndromes. Acta Haematol. 2016;136(2):108-117.
18. Troy JD, de Castro CM, Pupa MR, et al. Patient-reported distress in myelodysplastic syndromes and its association with clinical outcomes: a retrospective cohort study. J Natl Compr Canc Netw. 2018;16(3):267-273.
19. Stauder R, Yu G, Koinig KA, et al. Health-related quality of life in lower-risk MDS patients compared with age- and sex-matched reference populations: a European LeukemiaNet study. Leukemia. 2018;32(6): 1380-1392.
20. Efficace F, Cottone F, Abel G, et al. Patient-reported outcomes enhance the survival prediction of traditional disease risk classifications: an international study in patients with myelodysplastic syndromes. Cancer. 2018; 124(6):1251-1259.
21. Kroger N. Induction, Bridging, or straight ahead: the ongoing dilemma of allografting in advanced myelodysplastic syndrome. Biol Blood Marrow Transplant. 2019;25(8):e247-e249.
22. Haase D, Germing U, Schanz J, et al. New insights into the prognostic impact of the karyotype in MDS and correlation with sub-

types: evidence from a core dataset of 2124 patients. Blood. 2007;110(13):4385-4395.
23. Bejar R, Stevenson K, Abdel-Wahab O, et al. Clinical effect of point mutations in myelodysplastic syndromes. N Engl J Med. 2011;364(26):2496-2506.
24. Papaemmanuil E, Gerstung M, Malcovati L, et al. Clinical and biological implications of driver mutations in myelodysplastic syndromes. Blood. 2013;122(22):3616-3627; quiz 99.
25. Haferlach T, Nagata Y, Grossmann V, et al. Landscape of genetic lesions in 944 patients with myelodysplastic syndromes. Leukemia. 2014;28(2):241-247.
26. Jaiswal S, Fontanillas P, Flannick J, et al. Age-related clonal hematopoiesis associated with adverse outcomes. N Engl J Med. 2014;371(26):2488-2498.
27. Genovese G, Kahler AK, Handsaker RE, et al. Clonal hematopoiesis and blood-cancer risk inferred from blood DNA sequence. N Engl J Med. 2014;371(26):2477-2487.
28. Figueroa ME, Abdel-Wahab O, Lu C, et al. Leukemic IDH1 and IDH2 mutations result in a hypermethylation phenotype, disrupt TET2 function, and impair hematopoietic differentiation. Cancer Cell. 2010;18(6):553-567.
29. Abdel-Wahab O, Gao J, Adli M, et al. Deletion of Asxl1 results in myelodysplasia and severe developmental defects in vivo. J Exp Med. 2013;210(12):2641-2659.
30. Feinberg AP, Irizarry RA. Evolution in health and medicine Sackler colloquium: stochastic epigenetic variation as a driving force of development, evolutionary adaptation, and disease. Proc Natl Acad Sci U S A. 2010;107(Suppl 1):1757-1764.
31. Pellagatti A, Benner A, Mills KI, et al. Identification of gene expression-based prognostic markers in the hematopoietic stem cells of patients with myelodysplastic syndromes. J Clin Oncol. 2013;31(28):3557-3564.
32. Shiozawa Y, Malcovati L, Gallì A, et al. Gene expression and risk of leukemic transformation in myelodysplasia. Blood. 2017;130(24):2642-2653.
33. Im H, Rao V, Sridhar K, et al. Distinct transcriptomic and exomic abnormalities within myelodysplastic syndrome marrow cells. Leuk Lymphoma. 2018;59(12):2952-2962.
34. Chamuleau ME, Westers TM, van Dreunen L, et al. Immune mediated autologous cytotoxicity against hematopoietic precursor cells in patients with myelodysplastic syndrome. Haematologica. 2009;94(4):496-506.
35. Kordasti SY, Ingram W, Hayden J, et al. CD4+CD25high Foxp3+ regulatory T cells in myelodysplastic syndrome (MDS). Blood. 2007;110(3):847-850.
36. Kotsianidis I, Bouchliou I, Nakou E, et al. Kinetics, function and bone marrow trafficking of CD4+CD25+FOXP3+ regulatory T cells in myelodysplastic syndromes (MDS). Leukemia. 2009;23(3):510-518.
37. Roe C, Ali N, Epling-Burnette PK, et al. T-cell large granular lymphocyte proliferation (LGL) in patients with myelodysplastic syndromes (MDS): not an Innocent bystander? Clin Lymphoma Myeloma Leuk. 2016;16:S89.
38. Durrani J, Awada H, Kishtagari A, et al. Large granular lymphocytic leukemia coexists with myeloid clones and myelodysplastic syndrome. Leukemia. 2020;34(3):957-962.
39. Yoshida Y, Oguma S, Ohno H, et al. Co-occurrence of monoclonal gammopathy and myelodysplasia: a retrospective study of fourteen cases. Int J Hematol. 2014;99(6):721-725.
40. Mailankody S, Pfeiffer RM, Kristinsson SY, et al. Risk of acute myeloid leukemia and myelodysplastic syndromes after multiple myeloma and its precursor disease (MGUS). Blood. 2011;118(15):4086-4092.
41. Blau O, Baldus CD, Hofmann WK, et al. Mesenchymal stromal cells of myelodysplastic syndrome and acute myeloid leukemia patients have distinct genetic abnormalities compared with leukemic blasts. Blood. 2011;118(20):5583-5592.
42. von der Heide EK, Neumann M, Vosberg S, et al. Molecular alterations in bone marrow mesenchymal stromal cells derived from acute myeloid leukemia patients. Leukemia. 2017;31(5):1069-1078.
43. Kim Y, Jekarl DW, Kim J, et al. Genetic and epigenetic alterations of bone marrow stromal cells in myelodysplastic syndrome and acute myeloid leukemia patients. Stem Cell Res. 2015;14(2):177-184.
44. Santamaria C, Muntion S, Roson B, et al. Impaired expression of DICER, DROSHA, SBDS and some microRNAs in mesenchymal stromal cells from myelodysplastic syndrome patients. Haematologica. 2012;97(8):1218-1224.
45. Lopez-Villar O, Garcia JL, Sanchez-Guijo FM, et al. Both expanded and uncultured mesenchymal stem cells from MDS patients are genomically abnormal, showing a specific genetic profile for the 5q- syndrome. Leukemia. 2009;23(4):664-672.
46. Zambetti NA, Ping Z, Chen S, et al. Mesenchymal inflammation drives genotoxic stress in hematopoietic stem cells and predicts disease evolution in human pre-leukemia. Cell Stem Cell. 2016;19(5):613-627.
47. Geyh S, Oz S, Cadeddu RP, et al. Insufficient stromal support in MDS results from molecular and functional deficits of mesenchymal stromal cells. Leukemia. 2013;27(9):1841-1851.
48. Geyh S, Rodriguez-Paredes M, Jager P, et al. Functional inhibition of mesenchymal stromal cells in acute myeloid leukemia. Leukemia. 2016;30(3):683-691.
49. Medyouf H, Mossner M, Jann JC, et al. Myelodysplastic cells in patients reprogram mesenchymal stromal cells to establish a transplantable stem cell niche disease unit. Cell Stem Cell. 2014;14(6):824-837.
50. Walkley CR, Olsen GH, Dworkin S, et al. A microenvironment-induced myeloproliferative syndrome caused by retinoic acid receptor gamma deficiency. Cell. 2007;129(6):1097-1110.
51. Dong L, Yu WM, Zheng H, et al. Leukaemogenic effects of Ptpn11 activating mutations in the stem cell microenvironment. Nature. 2016;539(7628):304-308.
52. Kim YW, Koo BK, Jeong HW, et al. Defective Notch activation in microenvironment leads to myeloproliferative disease. Blood. 2008;112(12):4628-4638.
53. Takahashi K, Wang F, Kantarjian H, et al. Preleukaemic clonal haemopoiesis and risk of therapy-related myeloid neoplasms: a case-control study. Lancet Oncol. 2017;18(1):100-111.
54. Coombs CC, Zehir A, Devlin SM, et al. Therapy-related clonal hematopoiesis in patients with non-hematologic cancers is common and associated with adverse clinical outcomes. Cell Stem Cell. 2017;21(3):374-382.e4.
55. Wong TN, Ramsingh G, Young AL, et al. Role of TP53 mutations in the origin and evolution of therapy-related acute myeloid leukaemia. Nature. 2015;518(7540):552-555.
56. Krönke J, Fink EC, Hollenbach PW, et al. Lenalidomide induces ubiquitination and degradation of CK1a in del (5q) MDS. Nature. 2015;523(7559):183-188.
57. Basiorka AA, McGraw KL, De Ceuninck L, et al. Lenalidomide stabilizes the erythropoietin receptor by inhibiting the E3 ubiquitin ligase RNF41. Cancer Res. 2016;76(12):3531-3540.
58. Cazzola M, Invernizzi R, Bergamaschi G, et al. Mitochondrial ferritin expression in erythroid cells from patients with sideroblastic anemia. Blood. 2003;101(5):1996-2000.
59. Nikpour M, Scharenberg C, Liu A, et al. The transporter ABCB7 is a mediator of the phenotype of acquired refractory anemia with ring sideroblasts. Leukemia. 2013;27(4):889-896.
60. Papaemmanuil E, Cazzola M, Boultwood J, et al. Somatic SF3B1 mutation in myelodysplasia with ring sideroblasts. N Engl J Med. 2011;365(15):1384-1395.
61. Yoshida K, Sanada M, Shiraishi Y, et al. Frequent pathway mutations of splicing machinery in myelodysplasia. Nature. 2011;478(7367):64-69.
62. Shiozawa Y, Malcovati L, Galli A, et al. Aberrant splicing and defective mRNA production induced by somatic spliceosome mutations in myelodysplasia. Nat Commun. 2018;9(1):3649.
63. Obeng EA, Chappell RJ, Seiler M, et al. Physiologic expression of Sf3b1(K700E) causes impaired erythropoiesis, aberrant splicing, and sensitivity to therapeutic spliceosome modulation. Cancer Cell. 2016;30(3):404-417.
64. Mupo A, Seiler M, Sathiaseelan V, et al. Hemopoietic-specific Sf3b1-K700E knock-in mice display the splicing defect seen in human MDS but develop anemia without ring sideroblasts. Leukemia. 2017;31(3):720-727.
65. Mortera-Blanco T, Dimitriou M, Woll PS, et al. SF3B1-initiating mutations in MDS-RSs target lymphomyeloid hematopoietic stem cells. Blood. 2017;130(7):881-890.
66. Elvarsdottir EM, Mortera-Blanco T, Dimitriou M, et al. A three-dimensional in vitro model of erythropoiesis recapitulates erythroid failure in myelodysplastic syndromes. Leukemia. 2020;34(1):271-282.
67. Malcovati L, Stevenson K, Papaemmanuil E, et al. SF3B1-mutant myelodysplastic syndrome as a distinct disease subtype - a proposal of the International Working Group for the Prognosis of Myelodysplastic Syndromes (IWG-PM). Blood, in press. 2020.
68. Churpek JE. Familial myelodysplastic syndrome/acute myeloid leukemia. Best Pract Res Clin Haematol. 2017;30(4):287-289.
69. Godley LA, Shimamura A. Genetic predisposition to hematologic malignancies: management and surveillance. Blood. 2017;130(4):424-432.
70. Wlodarski MW, Collin M, Horwitz MS. GATA2 deficiency and related myeloid neoplasms. Semin Hematol. 2017;54(2):81-86.
71. Calado RT, Young NS. Telomere diseases. N Engl J Med. 2009;361(24):2353-2365.
72. Tesi B, Davidsson J, Voss M, et al. Gain-of-function SAMD9L mutations cause a syndrome of cytopenia, immunodeficiency, MDS, and neurological symptoms. Blood. 2017;129(16):2266-2279.
73. Douglas SPM, Siipola P, Kovanen PE, et al. ERCC6L2 defines a novel entity within inherited acute myeloid leukemia. Blood.

2019;133(25):2724-2728.
74. Sebert M, Passet M, Raimbault A, et al. Germline DDX41 mutations define a significant entity within adult MDS/AML patients. Blood. 2019;134(17):1441-1444.
75. Greenberg P, Cox C, LeBeau MM, et al. International scoring system for evaluating prognosis in myelodysplastic syndromes. Blood. 1997;89(6):2079-2088.
76. Germing U, Hildebrandt B, Pfeilstöcker M, et al. Refinement of the international prognostic scoring system (IPSS) by including LDH as an additional prognostic variable to improve risk assessment in patients with primary myelodysplastic syndromes (MDS). Leukemia. 2005;19(12):2223-2231.
77. Sanz G, Nomdedeu B, Such E, et al. Independent impact of iron overload and transfusion dependency on survival and leukemic evolution in patients with myelodysplastic syndrome. Blood. 2008; 112(11):640.
78. Della Porta MG, Malcovati L, Boveri E, et al. Clinical relevance of bone marrow fibrosis and CD34-positive cell clusters in primary myelodysplastic syndromes. J Clin Oncol. 2009;27(5):754-762.
79. Naqvi K, Garcia-Manero G, Sardesai S, et al. Association of comorbidities with overall survival in myelodysplastic syndrome: development of a prognostic model. J Clin Oncol. 2011;29(16):2240-2246.
80. Stauder R, Nösslinger T, Pfeilstöcker M, et al. Impact of age and comorbidity in myelodysplastic syndromes. J Natl Compr Cancer Netw. 2008;6(9):927-934.
81. Schanz J, Tüchler H, Solé F, et al. New comprehensive cytogenetic scoring system for primary myelodysplastic syndromes (MDS) and oligoblastic acute myeloid leukemia after MDS derived from an international database merge. J Clin Oncol. 2012;30(8): 820-829.
82. Della Porta M, Tuechler H, Malcovati L, et al. Validation of WHO classification-based Prognostic Scoring System (WPSS) for myelodysplastic syndromes and comparison with the revised International Prognostic Scoring System (IPSS-R). A study of the International Working Group for Prognosis in Myelodysplasia (IWG-PM). Leukemia. 2015;29(7):1502-1513.
83. https://mds-europe.eu/management.
84. Mishra A, Corrales–Yepez M, Ali NA, et al. Validation of the revised International Prognostic Scoring System in treated patients with myelodysplastic syndromes. Am J Hematol. 2013;88(7):566-570.
85. Lamarque M, Raynaud S, Itzykson R, et al. The revised IPSS is a powerful tool to evaluate the outcome of MDS patients treated with azacitidine: the GFM experience. Blood. 2012;120(25):5084-5085.
86. Pfeilstöcker M, Tüchler H, Schönmetzler A, et al. Time changes in predictive power of established and recently proposed clinical, cytogenetical and comorbidity scores for myelodysplastic syndromes. Leuk Res. 2012;36(2):132-139.
87. Voso MT, Fenu S, Latagliata R, et al. Revised International Prognostic Scoring System (IPSS) predicts survival and leukemic evolution of myelodysplastic syndromes significantly better than IPSS and WHO Prognostic Scoring System: validation by the Gruppo Romano Mielodisplasie Italian Regional Database. J Clin Oncol. 2013;31(21):2671-2677.
88. Neukirchen J, Lauseker M, Blum S, et al. Validation of the revised international prognostic scoring system (IPSS-R) in patients with myelodysplastic syndrome: a multicenter study. Leuk Res. 2014;38(1):57-64.
89. Bejar R, Papaemmanuil E, Haferlach T, et al. Somatic mutations in MDS patients are associated with clinical features and predict prognosis independent of the IPSS-R: analysis of combined datasets from the International Working Group for Prognosis in MDS-Molecular Committee. Blood. 2015;126(23):907.
90. Nazha A, Al-Issa K, Hamilton B, et al. Adding molecular data to prognostic models can improve predictive power in treated patients with myelodysplastic syndromes. Leukemia. 2017;31(12):2848-2850.
91. Tefferi A, Gangat N, Mudireddy M, et al. Mayo alliance prognostic model for myelodysplastic syndromes: integration of genetic and clinical information. Mayo Clin Proc. 2018;93(10):1363-1374.
92. Bernard E, Nannya Y, Yoshizato T, et al. TP53 state dictates genome stability, clinical presentation and outcomes in myelodysplastic syndromes. Blood. 2019;134 (Suppl_1):675.
93. Duetz C, Bachas C, Westers TM, et al. Computational analysis of flow cytometry data in hematological malignancies: future clinical practice? Curr Opin Oncol. 2020;32(2):162-169.
94. Hansen JW, Pedersen DA, Larsen LA, et al. Clonal hematopoiesis in elderly twins: concordance, discordance, and mortality. Blood. 2020;135(4):261-268.
95. Malcovati L, Galli A, Travaglino E, et al. Clinical significance of somatic mutation in unexplained blood cytopenia. Blood. 2017;129(25):3371-3378.
96. Luis TC, Wilkinson AC, Beerman I, et al. Biological implications of clonal hematopoiesis. Exp Hematol. 2019;77:1-5.
97. Breccia M, Federico V, Latagliata R, et al. Evaluation of comorbidities at diagnosis predicts outcome in myelodysplastic syndrome patients. Leuk Res. 2011;35(2):159-162.
98. Sorror ML, Sandmaier BM, Storer BE, et al. Comorbidity and disease status based risk stratification of outcomes among patients with acute myeloid leukemia or myelodysplasia receiving allogeneic hematopoietic cell transplantation. J Clin Oncol. 2007; 25(27):4246-4254.
99. de Swart L, Crouch S, Hoeks M, et al. Impact of red blood cell transfusion dose density on progression-free survival in lower-risk myelodysplastic syndromes patients. Haematologica. 2020;105(3):632-639.
100. Nilsson-Ehle H, Birgegard G, Samuelsson J, et al. Quality of life, physical function and MRI T2* in elderly low-risk MDS patients treated to a haemoglobin level of >/=120 g/L with darbepoetin alfa +/- filgrastim or erythrocyte transfusions. Eur J Haematol. 2011;87(3):244-252.
101. Stanworth SJ, Killick S, McQuilten ZK, et al. Red cell transfusion in outpatients with myelodysplastic syndromes: a feasibility and exploratory randomised trial. Br J Haematol. 2020;189(2):279-290.
102. Mittelman M, Platzbecker U, Afanasyev B, et al. Eltrombopag for advanced myelodysplastic syndromes or acute myeloid leukaemia and severe thrombocytopenia (ASPIRE): a randomised, placebo-controlled, phase 2 trial. Lancet Haematol. 2018; 5(1):e34-e43.
103. Dickinson M, Cherif H, Fenaux P, et al. Azacitidine with or without eltrombopag for first-line treatment of intermediate- or high-risk MDS with thrombocytopenia. Blood. 2018;132(25):2629-2638.
104. Goldberg SL, Chen E, Corral M, et al. Incidence and clinical complications of myelodysplastic syndromes among United States Medicare beneficiaries. J Clin Oncol. 2010;28(17):2847-2852.
105. Malcovati L, Porta MGD, Pascutto C, et al. Prognostic factors and life expectancy in myelodysplastic syndromes classified according to WHO criteria: a basis for clinical decision making. J Clin Oncol. 2005;23(30):7594-7603.
106. Schafer AI, Cheron RG, Dluhy R, et al. Clinical consequences of acquired transfusional iron overload in adults. N Engl J Med. 1981;304(6):319-324.
107. Hershko C, Link G, Cabantchik I. Pathophysiology of iron overload. Ann N Y Acad Sci. 1998;850:191-201.
108. Cabantchik ZI, Breuer W, Zanninelli G, et al. LPI-labile plasma iron in iron overload. Best Pract Res Clin Haematol. 2005;18(2):277-287.
109. Cortelezzi A, Cattaneo C, Cristiani S, et al. Non-transferrin-bound iron in myelodysplastic syndromes: a marker of ineffective erythropoiesis? Hematol J. 2000;1(3):153-158.
110. Greenberg PL, Rigsby CK, Stone RM, et al. NCCN Task Force: transfusion and iron overload in patients with myelodysplastic syndromes. J Natl Compr Cancer Netw. 2009;7(Suppl_9):S-1-S-16.
111. De Swart L, Smith A, Fenaux P, et al. Transfusion-dependency is the most important prognostic factor for survival in 1000 newly diagnosed MDS patients with low- and intermediate-1 risk MDS in the European LeukemiaNet MDS registry. Blood. 2011;118(21):2775.
112. Malcovati L, Della Porta MG, Strupp C, et al. Impact of the degree of anemia on the outcome of patients with myelodysplastic syndrome and its integration into the WHO classification-based Prognostic Scoring System (WPSS). Haematologica. 2011;96 (10):1433-1440.
113. Lyons RM, Marek BJ, Paley C, et al. Relation between chelation and clinical outcomes in lower-risk patients with myelodysplastic syndromes:registry analysis at 5 years. Leuk Res. 2017;56:88-95.
114. Leitch HA, Parmar A, Wells RA, et al. Overall survival in lower IPSS risk MDS by receipt of iron chelation therapy, adjusting for patient–related factors and measuring from time of first red blood cell transfusion dependence: an MDS–CAN analysis. Br J Haematol. 2017;179(1):83-97.
115. Mainous AG 3rd, Tanner RJ, Hulihan MM, et al. The impact of chelation therapy on survival in transfusional iron overload: a meta–analysis of myelodysplastic syndrome. Br J Haematol. 2014;167(5):720-723.
116. Zeidan AM, Giri S, DeVeaux M, et al. Systematic review and meta-analysis of the effect of iron chelation therapy on overall survival and disease progression in patients with lower-risk myelodysplastic syndromes. Ann Hematol. 2019;98(2):339-350.
117. Hoeks M, Yu G, Langemeijer S, et al. Impact of treatment with iron chelation therapy in patients with lower-risk myelodysplastic syndromes participating in the European MDS registry. Haematologica. 2020;105 (3):640-651.
118. Angelucci E, Li J, Greenberg P, et al. Iron chelation in transfusion-dependent low/intermediate-1-risk myelodysplastic syndromes patients: a randomized trial. Ann Intern Med. 2020;172(8):513-522.

119. Leitch HA, Buckstein R, Zhu N, et al. Iron overload in myelodysplastic syndromes: evidence based guidelines from the Canadian consortium on MDS. Leuk Res. 2018;74:21-41.
120. Killick SB. Iron chelation therapy in low risk myelodysplastic syndrome. Br J Haematol. 2017;177(3):375-387.
121. Meerpohl JJ, Antes G, Ruecker G, et al. Deferasirox for managing iron overload in people with myelodysplastic syndrome. Cochrane Database Syst Rev. 2010;(11): CD007461.
122. Steensma DP, Gattermann N. When is iron overload deleterious, and when and how should iron chelation therapy be administered in myelodysplastic syndromes? Best Pract Res Clin Haematol. 2013;26(4):431-444.
123. Fenaux P, Santini V, Spiriti MAA, et al. A phase 3 randomized, placebo-controlled study assessing the efficacy and safety of epoetin-alpha in anemic patients with low-risk MDS. Leukemia. 2018;32(12):2648-2658.
124. Platzbecker U, Symeonidis A, Oliva EN, et al. A phase 3 randomized placebo-controlled trial of darbepoetin alfa in patients with anemia and lower-risk myelodysplastic syndromes. Leukemia. 2017;31(9):1944-1950.
125. Park S, Kelaidi C, Meunier M, et al. The prognostic value of serum erythropoietin in patients with lower-risk myelodysplastic syndromes: a review of the literature and expert opinion. Ann Hematol. 2020;99(1):7-19.
126. Balleari E, Filiberti RA, Salvetti C, et al. Effects of different doses of erythropoietin in patients with myelodysplastic syndromes: a propensity score-matched analysis. Cancer Med. 2019;8(18):7567-7576.
127. Garelius HK, Johnston WT, Smith AG, et al. Erythropoiesis-stimulating agents significantly delay the onset of a regular transfusion need in nontransfused patients with lower-risk myelodysplastic syndrome. J Intern Med. 2017;281(3):284-299.
128. Negrin RS, Stein R, Doherty K, et al. Maintenance treatment of the anemia of myelodysplastic syndromes with recombinant human granulocyte colony-stimulating factor and erythropoietin: evidence for in vivo synergy. Blood. 1996;87(10):4076-4081.
129. Hellstrom-Lindberg E, Ahlgren T, Beguin Y, et al. Treatment of anemia in myelodysplastic syndromes with granulocyte colony-stimulating factor plus erythropoietin: results from a randomized phase II study and long-term follow-up of 71 patients. Blood. 1998;92(1):68-75.
130. Jadersten M, Malcovati L, Dybedal I, et al. Erythropoietin and granulocyte-colony stimulating factor treatment associated with improved survival in myelodysplastic syndrome. J Clin Oncol. 2008;26(21):3607-3613.
131. List A, Dewald G, Bennett J, et al. Lenalidomide in the myelodysplastic syndrome with chromosome 5q deletion. N Engl J Med. 2006;355(14):1456-1465.
132. Raza A, Reeves JA, Feldman EJ, et al. Phase 2 study of lenalidomide in transfusion-dependent, low-risk, and intermediate-1–risk myelodysplastic syndromes with karyotypes other than deletion 5q. Blood. 2008;111(1):86-93.
133. Toma A, Kosmider O, Chevret S, et al. Lenalidomide with or without erythropoietin in transfusion-dependent erythropoiesis-stimulating agent-refractory lower-risk MDS without 5q deletion. Leukemia. 2016;30(4):897-905.
134. Mossner M, Jann J-C, Nowak D, et al. Prevalence, clonal dynamics and clinical impact of TP53 mutations in patients with myelodysplastic syndrome with isolated deletion (5q) treated with lenalidomide: results from a prospective multicenter study of the german MDS study group (GMDS). Leukemia. 2016;30(9):1956-1959.
135. Sloand EM, Wu CO, Greenberg P, et al. Factors affecting response and survival in patients with myelodysplasia treated with immunosuppressive therapy. J Clin Oncol. 2008;26(15):2505-2511.
136. Kadia TM, Borthakur G, Garcia-Manero G, et al. Final results of the phase II study of rabbit anti-thymocyte globulin, ciclosporin, methylprednisone, and granulocyte colony-stimulating factor in patients with aplastic anaemia and myelodysplastic syndrome. Br J Haematol. 2012;157(3):312-320.
137. Passweg JR, Giagounidis AA, Simcock M, et al. Immunosuppressive therapy for patients with myelodysplastic syndrome: a prospective randomized multicenter phase III trial comparing antithymocyte globulin plus cyclosporine with best supportive care--SAKK 33/99. J Clin Oncol. 2011;29(3):303-309.
138. Stahl M, DeVeaux M, de Witte T, et al. The use of immunosuppressive therapy in MDS: clinical outcomes and their predictors in a large international patient cohort. Blood Adv. 2018;2(14):1765-1772.
139. Stahl M, Bewersdorf JP, Giri S, et al. Use of immunosuppressive therapy for management of myelodysplastic syndromes: a systematic review and meta-analysis. Haematologica. 2020;105(1):102-111.
140. Silverman LR, Holland JF, Weinberg RS, et al. Effects of treatment with 5-azacytidine on the in vivo and in vitro hematopoiesis in patients with myelodysplastic syndromes. Leukemia. 1993;7(Suppl 1):21-29.
141. Silverman LR, Demakos EP, Peterson BL, et al. Randomized controlled trial of azacitidine in patients with the myelodysplastic syndrome: a study of the Cancer and Leukemia Group B. J Clin Oncol. 2002;20 (10):2429-2440.
142. Silverman LR, McKenzie DR, Peterson BL, et al. Further analysis of trials with azacitidine in patients with myelodysplastic syndrome: studies 8421, 8921, and 9221 by the Cancer and Leukemia Group B. J Clin Oncol. 2006;24(24):3895-3903.
143. Fenaux P, Mufti GJ, Hellstrom-Lindberg E, et al. Efficacy of azacitidine compared with that of conventional care regimens in the treatment of higher-risk myelodysplastic syndromes: a randomised, open-label, phase III study. Lancet Oncol. 2009;10(3):223-232.
144. Komrokji R, Swern AS, Grinblatt D, et al. Azacitidine in lower-risk myelodysplastic syndromes: a meta-analysis of data from prospective studies. Oncologist. 2018;23 (2):159-70.
145. Tobiasson M, Dybedahl I, Holm MS, et al. Limited clinical efficacy of azacitidine in transfusion-dependent, growth factor-resistant, low- and Int-1-risk MDS: results from the Nordic NMDSG08A phase II trial. Blood Cancer J. 2014;4:e189.
146. Garcia-Manero G, Jabbour E, Borthakur G, et al. Randomized open-label phase II study of decitabine in patients with low- or intermediate-risk myelodysplastic syndromes. J Clin Oncol. 2013;31(20):2548-2553.
147. Itzykson R, Thepot S, Quesnel B, et al. Prognostic factors for response and overall survival in 282 patients with higher-risk myelodysplastic syndromes treated with azacitidine. Blood. 2011;117(2):403-411.
148. Hwang KL, Song MK, Shin HJ, et al. Monosomal and complex karyotypes as prognostic parameters in patients with International Prognostic Scoring System higher risk myelodysplastic syndrome treated with azacitidine. Blood Res. 2014;49 (4):234-240.
149. Bejar R, Lord A, Stevenson K, et al. TET2 mutations predict response to hypomethylating agents in myelodysplastic syndrome patients. Blood. 2014;124(17):2705-2712.
150. Traina F, Visconte V, Elson P, et al. Impact of molecular mutations on treatment response to DNMT inhibitors in myelodysplasia and related neoplasms. Leukemia. 2014;28(1):78-87.
151. Itzykson R, Kosmider O, Cluzeau T, et al. Impact of TET2 mutations on response rate to azacitidine in myelodysplastic syndromes and low blast count acute myeloid leukemias. Leukemia. 2011;25(7):1147-1152.
152. Jin J, Hu C, Yu M, et al. Prognostic value of isocitrate dehydrogenase mutations in myelodysplastic syndromes: a retrospective cohort study and meta-analysis. PLoS One. 2014;9(6):e100206.
153. Steensma DP, Baer MR, Slack JL, et al. Multicenter study of decitabine administered daily for 5 days every 4 weeks to adults with myelodysplastic syndromes: the alternative dosing for outpatient treatment (ADOPT) trial. J Clin Oncol. 2009;27 (23):3842-3848.
154. Kantarjian HM, O'Brien S, Shan J, et al. Update of the decitabine experience in higher risk myelodysplastic syndrome and analysis of prognostic factors associated with outcome. Cancer. 2007;109(2):265-273.
155. Welch JS, Petti AA, Miller CA, et al. TP53 and decitabine in acute myeloid leukemia and myelodysplastic syndromes. N Engl J Med. 2016;375(21):2023-2036.
156. de Witte T, Suciu S, Peetermans M, et al. Intensive chemotherapy for poor prognosis myelodysplasia (MDS) and secondary acute myeloid leukemia (sAML) following MDS of more than 6 months duration. A pilot study by the Leukemia Cooperative Group of the European Organisation for Research and Treatment in Cancer (EORTC-LCG). Leukemia. 1995;9(11):1805-1811.
157. Ganser A, Heil G, Seipelt G, et al. Intensive chemotherapy with idarubicin, ara-C, etoposide, and m-AMSA followed by immunotherapy with interleukin-2 for myelodysplastic syndromes and high-risk acute myeloid leukemia (AML). Ann Hematol. 2000;79(1):30-35.
158. Kantarjian H, O'Brien S, Cortes J, et al. Results of intensive chemotherapy in 998 patients age 65 years or older with acute myeloid leukemia or high-risk myelodysplastic syndrome: predictive prognostic models for outcome. Cancer. 2006;106(5): 1090-1098.
159. Martino R, Iacobelli S, Brand R, et al. Retrospective comparison of reduced-intensity conditioning and conventional high-dose conditioning for allogeneic hematopoietic stem cell transplantation using HLA-identical sibling donors in myelodysplastic syndromes. Blood. 2006;108(3):836-846.
160. Koenecke C, Gohring G, de Wreede LC, et al. Impact of the revised International Prognostic Scoring System, cytogenetics and monosomal karyotype on outcome after allogeneic stem cell transplantation for myelodysplastic syndromes and secondary acute myeloid leukemia evolving from myelodysplastic syndromes: a retrospective

multicenter study of the European Society of Blood and Marrow Transplantation. Haematologica. 2015;100(3):400-408.
161. Deeg HJ, Scott BL, Fang M, et al. Five-group cytogenetic risk classification, monosomal karyotype, and outcome after hematopoietic cell transplantation for MDS or acute leukemia evolving from MDS. Blood. 2012;120(7):1398-1408.
162. Kroger N, Iacobelli S, Franke GN, et al. Dose-reduced versus standard conditioning followed by allogeneic stem-cell transplantation for patients with myelodysplastic syndrome: a prospective randomized phase III study of the EBMT (RICMAC Trial). J Clin Oncol. 2017;35(19):2157-2164.
163. Cutler CS, Lee SJ, Greenberg P, et al. A decision analysis of allogeneic bone marrow transplantation for the myelodysplastic syndromes: delayed transplantation for low-risk myelodysplasia is associated with improved outcome. Blood. 2004;104(2):579-585.
164. Della Porta MG, Alessandrino EP, Bacigalupo A, et al. Predictive factors for the outcome of allogeneic transplantation in patients with MDS stratified according to the revised IPSS-R. Blood. 2014;123(15): 2333-2342.
165. Alessandrino EP, Della Porta MG, Bacigalupo A, et al. WHO classification and WPSS predict posttransplantation outcome in patients with myelodysplastic syndrome: a study from the Gruppo Italiano Trapianto di Midollo Osseo (GITMO). Blood. 2008;112(3):895-902.
166. Della Porta MG, Galli A, Bacigalupo A, et al. Clinical effects of driver somatic mutations on the outcomes of patients with myelodysplastic syndromes treated with allogeneic hematopoietic stem-cell transplantation. J Clin Oncol. 2016;34(30):3627-3637.
167. Bejar R, Stevenson KE, Caughey B, et al. Somatic mutations predict poor outcome in patients with myelodysplastic syndrome after hematopoietic stem-cell transplantation. J Clin Oncol. 2014;32(25):2691-2698.
168. Yoshizato T, Nannya Y, Atsuta Y, et al. Genetic abnormalities in myelodysplasia and secondary acute myeloid leukemia: impact on outcome of stem cell transplantation. Blood. 2017;129(17):2347-2358.
169. Lindsley RC, Saber W, Mar BG, et al. Prognostic mutations in myelodysplastic syndrome after stem-cell transplantation. N Engl J Med. 2017;376(6):536-547.
170. Yahng SA, Kim M, Kim TM, et al. Better transplant outcome with pre-transplant marrow response after hypomethylating treatment in higher-risk MDS with excess blasts. Oncotarget. 2017;8(7):12342-12354.
171. Damaj G, Mohty M, Robin M, et al. Upfront allogeneic stem cell transplantation after reduced-intensity/nonmyeloablative conditioning for patients with myelodysplastic syndrome: a study by the Societe Francaise de Greffe de Moelle et de Therapie Cellulaire. Biol Blood Marrow Transplant. 2014;20(9):1349-1355.
172. Oran B, Kongtim P, Popat U, et al. Cytogenetics, donor type, and use of hypomethylating agents in myelodysplastic syndrome with allogeneic stem cell transplantation. Biol Blood Marrow Transplant. 2014;20(10):1618-1625.
173. Schroeder T, Wegener N, Lauseker M, et al. Comparison between upfront transplantation and different pretransplant cytoreductive treatment approaches in patients with high-risk myelodysplastic syndrome and secondary acute myelogenous leukemia. Biol Blood Marrow Transplant. 2019;25(8):1550-1559.
174. Damaj G, Duhamel A, Robin M, et al. Impact of azacitidine before allogeneic stem-cell transplantation for myelodysplastic syndromes: a study by the Société Française de Greffe de Moelle et de Thérapie-Cellulaire and the Groupe-Francophone des Myélodysplasies. J Clin Oncol. 2012;30(36):4533-4540.
175. Beelen DW, Trenschel R, Stelljes M, et al. Treosulfan or busulfan plus fludarabine as conditioning treatment before allogeneic haemopoietic stem cell transplantation for older patients with acute myeloid leukaemia or myelodysplastic syndrome (MC-FludT.14/L): a randomised, non-inferiority, phase 3 trial. Lancet Haematol. 2020;7(1):e28-e39.
176. Casper J, Knauf W, Kiefer T, et al. Treosulfan and fludarabine: a new toxicity-reduced conditioning regimen for allogeneic hematopoietic stem cell transplantation. Blood. 2004;103(2):725-731.
177. Ruutu T, Volin L, Beelen DW, et al. Reduced-toxicity conditioning with treosulfan and fludarabine in allogeneic hematopoietic stem cell transplantation for myelodysplastic syndromes: final results of an international prospective phase II trial. Haematologica. 2011;96(9):1344-1350.
178. Schroeder T, Rachlis E, Bug G, et al. Treatment of acute myeloid leukemia or myelodysplastic syndrome relapse after allogeneic stem cell transplantation with azacitidine and donor lymphocyte infusions--a retrospective multicenter analysis from the German Cooperative Transplant Study Group. Biol Blood Marrow Transplant. 2015;21(4):653-660.
179. DiNardo CD, Stein EM, de Botton S, et al. Durable remissions with ivosidenib in IDH1-mutated relapsed or refractory AML. N Engl J Med. 2018;378(25):2386-2398.
180. Stein EM, Fathi AT, DiNardo CD, et al. Enasidenib in patients with mutant IDH2 myelodysplastic syndromes: a phase 1 subgroup analysis of the multicentre, AG221-C-001 trial. Lancet Haematol. 2020;7(4):e309-e319.
181. Vousden KH, Lu X. Live or let die: the cell's response to p53. Nat Rev Cancer. 2002;2(8):594-604.
182. Wei AH, Garcia JS, Borate U, et al. A phase 1b study evaluating the safety and efficacy of venetoclax in combination with azacitidine in treatment-naïve patients with higher-risk myelodysplastic syndrome. Blood. 2019;134(Suppl_1):568.
183. Zeidan AM, Pollyea DA, Garcia JS, et al. A phase 1b study evaluating the safety and efficacy of venetoclax as monotherapy or in combination with azacitidine for the treatment of relapsed/refractory myelodysplastic syndrome. Bood. 2019;134(Suppl_1):565.
184. Kulasekararaj AG, Smith AE, Mian SA, et al. TP 53 mutations in myelodysplastic syndrome are strongly correlated with aberrations of chromosome 5, and correlate with adverse prognosis. Br J Haemat. 2013;160(5):660-672.
185. Deneberg S, Cherif H, Lazarevic V, et al. An open-label phase I dose-finding study of APR-246 in hematological malignancies. Blood Cancer J. 2016;6(7):e447.
186. Sallman DA, DeZern AE, Garcia-Manero G, et al. Phase 2 results of APR-246 and azacitidine (AZA) in patients with TP53 mutant myelodysplastic syndromes (MDS) and oligoblastic acute myeloid leukemia (AML). Blood. 2019;134(Suppl_1):676.
187. Carvajal LA, Ben-Neriah D, Senecal A, et al. Dual inhibition of Mdmx and Mdm2 using an alpha-helical P53 stapled peptide (ALRN-6924) as a novel therapeutic strategy in acute myeloid leukemia. Blood. 2017;130 (Suppl_1):795.
188. Rudolph KL, Chang S, Lee H-W, et al. Longevity, stress response, and cancer in aging telomerase-deficient mice. Cell. 1999;96(5):701-712.
189. di Fagagna FdA, Reaper PM, Clay-Farrace L, et al. A DNA damage checkpoint response in telomere-initiated senescence. Nature. 2003;426(6963):194-198.
190. Tefferi A, Lasho TL, Begna KH, et al. A pilot study of the telomerase inhibitor imetelstat for myelofibrosis. N Engl J Med. 2015;373(10):908-919.
191. Platzbecker U, Steensma DP, Van Eygen K, et al. Imerge: a study to evaluate imetelstat (GRN163L) in transfusion-dependent subjects with IPSS low or intermediate-1 risk myelodysplastic syndromes (MDS) that is relapsed/refractory to erythropoiesis-stimulating agent (ESA) treatment. Blood. 2019;134(Suppl_1):4248.
192. Bataller A, Montalban-Bravo G, Soltysiak KA, et al. The role of TGFβ in hematopoiesis and myeloid disorders. Leukemia. 2019;33(5):1076-1089.
193. Zhou L, Nguyen AN, Sohal D, et al. Inhibition of the TGF-β receptor I kinase promotes hematopoiesis in MDS. Blood. 2008;112(8):3434-3443.
194. Suragani RN, Cadena SM, Cawley SM, et al. Transforming growth factor-β superfamily ligand trap ACE-536 corrects anemia by promoting late-stage erythropoiesis. Nat Med. 2014;20(4):408-414.
195. Fenaux P, Platzbecker U, Mufti GJ, et al. Luspatercept in patients with lower-risk myelodysplastic syndromes. N Engl J Med. 2020;382(2):140-151.
196. Kurtz SE, Eide CA, Kaempf A, et al. Molecularly targeted drug combinations demonstrate selective effectiveness for myeloid-and lymphoid-derived hematologic malignancies. Proc Natl Acad Sci U S A. 2017;114(36):E7554-E7563.
197. Swords RT, Azzam D, Al-Ali H, et al. Ex-vivo sensitivity profiling to guide clinical decision making in acute myeloid leukemia: a pilot study. Leuk Res. 2018;64:34-41.
198. Spinner MA, Aleshin A, Santaguida MA, et al. A feasibility study of biologically focused therapy for myelodysplastic syndrome patients refractory to hypomethylating agents. Blood (2019):134: (Suppl 1):4239.
199. Drusbosky LM, Cogle CR. Computational modeling and treatment identification in the myelodysplastic syndromes. Curr Hematol Malig Rep. 2017;12(5):478-483.
200. Drusbosky LM, Singh NK, Hawkins KE, et al. A genomics-informed computational biology platform prospectively predicts treatment responses in AML and MDS patients. Blood Adv. 2019;3(12):1837-1847.

REVIEW ARTICLE

Ferrata Storti Foundation

Multiple myeloma with central nervous system relapse

Philip A. Egan,[1] Patrick T Elder,[2] W. Ian Deighan,[3] Sheila J.M. O'Connor[4] and H. Denis Alexander[1]

[1]Northern Ireland Centre for Stratified Medicine, Ulster University, Derry/Londonderry, Northern Ireland; [2]Department of Haematology, North West Cancer Centre, Altnagelvin Area Hospital, Derry/Londonderry, Northern Ireland; [3]Department of Clinical Chemistry, Altnagelvin Area Hospital, Derry/Londonderry, Northern Ireland and [4]Haematological Malignancy Diagnostic Service, St James's Institute of Oncology, Leeds, England, UK

Haematologica 2020
Volume 105(7):1780-1790

ABSTRACT

Central nervous system involvement in multiple myeloma is a rare complication but carries a very poor prognosis. We provide a review of current literature, including presentation, treatment and survival data, and describe our experience in a regional hematologic malignancy diagnosis center where, over a 15-year period, ten cases were identified. Although the median age of onset, frequently between 50-60 years, is comparatively young, those diagnosed usually have a preceding diagnosis of multiple myeloma and often have had several lines of treatment. We discuss putative underlying factors such as prior treatment and associations including possible risk factors and features suggestive of a distinct biology. Central nervous system involvement may be challenging to diagnose in myeloma, displaying heterogeneous symptoms that can be confounded by neurological symptoms caused by the typical features of myeloma or treatment side-effects. We discuss the clinical features, imaging and laboratory methods used in diagnosis, and highlight the importance of considering this rare complication when neurological symptoms occur at presentation or, more commonly, during the disease pathway. In the absence of clinical trial data to inform an evidence-based approach to treatment, we discuss current and novel treatment options. Finally, we propose the establishment of an International Registry of such cases as the best way to collect and subsequently disseminate presentation, diagnostic and treatment outcome data on this rare complication of multiple myeloma.

Correspondence:

H DENIS ALEXANDER
d.alexander@ulster.ac.uk

Received: February 3, 2020.

Accepted: April 14, 2020.

Pre-published: May 15, 2020.

doi:10.3324/haematol.2020.248518

Check the online version for the most updated information on this article, online supplements, and information on authorship & disclosures: www.haematologica.org/content/105/7/1780

Introduction

Extramedullary disease (EMD) occurs in up to 5% of multiple myeloma (MM) patients, arising *via* hematogenous spread or through the bone cortex into contiguous tissues.[1,2] It can occur in the skin, lymph nodes, abdominal organs, upper airway and the central nervous system (CNS).[3] Plasma cell leukemia (PCL) and extramedullary solitary plasmacytomas are biologically and prognostically distinct conditions and therefore not referred to as EMD.[2,4] The reported incidence of EMD has increased, possibly in part due to improved survival in MM patients through the use of enhanced treatment modalities, in particular stem cell transplantation (SCT), proteasome inhibitors (PI), and immunomodulatory drugs (IMiD).[2] According to one study, there has been an increase in EMD detected at the time of MM diagnosis from 4% to 12% between 1971-93 and 2000-2007 patient cohorts, suggesting improved detection by modern imaging techniques.[5] Since it represents a minority of MM cases, clinical trials have not focused on EMD or any of its subtypes such as MM with CNS involvement (CNS-MM), and thus available data come from single cases and small retrospective studies.[6]

Multiple myeloma with CNS involvement is a rare form of EMD characterized by plasma cell infiltration of the CNS, meninges or cerebrospinal fluid (CSF). It is observed in a small number of MM cases at diagnosis and around a fifth of extramedullary relapses, typically two or three years after the initial MM

diagnosis.[7-10] Infiltration of the CNS or meninges is rarer in myeloma than in most other hematologic malignancies, affecting well under 1% of patients, and carries a very poor prognosis with reported median overall survival (OS) of seven months or less following its diagnosis.[8-13] However, intracerebral plasmacytomas that develop from osseous lesions of the cranium can be treated successfully with radiation, unlike the more serious myelomatous meningitis.[14]

Incidence and prevalence

The reported median age of onset of CNS-MM is often younger (50-60-year old age group) than the usual median age of approximately 70 years for MM diagnosis, with up to 20-25% of cases discovered at the initial myeloma diagnosis.[8,15] However, age at presentation varies between studies, including that of our own data (Table 1), suggesting CNS-MM may be underdiagnosed in older patients. CNS-MM can arise at any stage of MM, and although previous studies suggest a bias towards later stage disease,[1] a recent large-scale retrospective study did not find an association with MM clinical stage.[8] The improved OS of MM patients is expected to lead to an increased incidence of EMD and CNS-MM, possibly due to the extra time available for mutations in residual, drug-resistant tumor cells following treatments, that alter expression of adhesion molecules, oncogenes and tumor suppressor genes.[14] Furthermore, there may also be an increase in the time from MM diagnosis to CNS involvement due to the effectiveness of high-dose chemotherapy and treatment using novel agents.[10] Indeed, patients have often had several lines of treatment by the time CNS-MM is diagnosed.[8,16]

In our own experience in a regional hematologic malignancy diagnosis center (HMDS, Leeds, UK) over a 15-year period (December 2003-March 2019), ten cases (6 female, 4 male) of CNS-MM were identified (*SO'C, 2019, unpublished data*). Two of these were at MM presentation, whilst the remainder occurred 6-108 months following MM diagnosis (Table 1). The incidence was well under 1% overall (5,238 cases of MM were investigated at HMDS during this period). A higher incidence of female (F) to male (M), and lambda (λ)-restricted to kappa (κ)-restricted, patients, to that found in newly diagnosed MM (ND-MM), was noted. Although absence of CD56 expression was more frequent (4 out of 10 cases) than seen in ND-MM, and one case showed rearranged immunoglobulin heavy chain (IGH), and one loss of 1p with gain of 1q, none of these parameters, including immunophenotypic or acquired cytogenetic aberrations, was seen in adequate numbers to be suggestive of significant association with CNS involvement. Furthermore, bone marrow (BM) interphase fluorescence *in situ* hybridization (iFISH) was not available in the earlier cases, so association of CNS-MM with cytogenetic aberrations predisposing to its development cannot be reported due to small sample size. In all cases, the immunophenotype of the CNS plasma cells was identical

Table 1. Regional hematologic malignancy diagnostic service data (*SO'C, 2019, unpublished data*).

Case n.	Gender	Age at CNS-MM	MM to CNS-MM (months)	CNS CD56 status	BM FISH	CNS FISH	Additional comments
1	F	76	20	$CD56^{+/-}$	*	No	
2	F	89	18	$CD56^{-}$	*	No	
3	M	71	15	$CD56^{-}$	*	*IGH* rearranged	Insufficient CSF sample for full FISH panel
4	F	90	0	$CD56^{-}$	*	No	Patient presented with CSN disease (limb weakness and cranial nerve palsy). BM aspirate not received
5	M	55	0	$CD56^{++}$	*	No	Patient presented with CNS disease (cranial nerve palsy), BM requested after CSF sample report
6	F	77	6	$CD56^{+/-}$	Deletion *TP53*, monosomy 13, *IGH-MAF* translocation	No	Bone plasmacytoma, myeloma diagnosed on BM; plasma cell leukemia 2 months prior to CNS disease
7	M	76	41	$CD56^{++}$	Insufficient sample	No	
8	F	57	28	$CD56^{+}$	*IGH-FGFR3* translocation, 1q21 gain, 13q loss	No	Multiple plasmacytomas, myeloma diagnosed on BM
9	M	70	28	$CD56^{-}$	Hyperdiploid (Chr 5, 9, 15)	No	Concurrent plasma cell leukemia and CNS disease
10	F	65	108	$CD56^{+}$	1q21.3 gain, 1p32.3 loss	1q21.3 gain, 1p32.3 loss	Identical iFISH cytogenetic abnormalities as at presentation despite 108-month separation
Mean	F:M ratio 1.5:1	73	26	4/10 $CD56^{-}$ 2/10 CD56wk	n/a	n/a	n/a

Ten multiple myeloma with CNS involvement (CNS-MM) cases were identified over a 15-year period during which 5,238 myeloma cases were assessed. Recent audit shows samples from 20% of cases are too poor to proceed to $CD138^{+}$ plasma cell selection (short sample, hemodiluted, etc.). A neoplastic plasma cell phenotype was identified in all cases by flow cytometry; six cases were $CD56^{+}$ and four were $CD56^{-}$; in all cases the neoplastic phenotype of the CNS-MM plasma cells was identical to the bone marrow (BM) plasma cells. Cytogenetic testing of the central nervous system (CNS) plasma cells was limited by the low volume of cerebrospinal fluid (CSF) sample received for diagnostic workup. As these non-clinical trial samples were diagnosed in a regional diagnostic laboratory, treatment and follow-up information is not available. iFISH: interphase fluorescence *in situ* hybridization; FDG-PET: fluorodeoxyglucose positron-emission tomography; IGH: immunoglobulin heavy chain; Chr: chromosome; n/a: not available; M: male; F: female.

to the BM plasma cells. Overall, the ability to carry out iFISH or molecular testing was compromized in most instances by inadequate sample and/or myeloma cell numbers.

A summary of presentation, treatment and survival data from all papers reviewed is presented in Table 2. Although limited by variations in both the approach and incomplete data in the original manuscripts, this analysis confirms the bias towards a lower M:F ratio, and more frequent λ light chain restriction than in ND-MM without CNS involvement. Furthermore, CNS relapse 26 months following MM diagnosis is in keeping with the duration generally quoted. Because of incomplete data, definitive treatment analysis preceding and following CNS-MM relapse could not be ascertained. However, within these limitations, summary treatment data are annotated in Table 2.

Cause

Multiple myeloma with CNS involvement develops *via* hematogenous dissemination of malignant cells or contiguous spread of the tumor, often associated with PCL and cranial plasmacytoma, respectively.[1,15] Although it has been suggested that invasion of the CNS is enabled by treatment of MM with immunomodulatory drugs (IMiD), with a report of an MM patient receiving lenalidomide prior to CNS-MM progression,[17] this is not robust evidence. Data for EMD in general suggest that escape from the BM is enabled by mutations to tumor suppressor genes such as *TP53*, oncogenes such as *RAS*, and altered expression of adhesion molecules, as outlined above.[18-21] These genetic changes may enable proliferation independent of stimuli provided by the BM environment. Furthermore, recent studies do not support a causal link between modern MM treatment and subsequent EMD which may rather be a consequence of longer survival of patients treated with novel agents.[2,21-23] Additionally, recent increases in EMD prevalence have been seen at MM diagnosis as well as post treatment, and therefore may be due to improved detection.[2] In another study, the only risk factor for an extramedullary relapse following autologous stem cell transplant (SCT) was EMD at MM diagnosis.[5] Further weak evidence for a causal relationship between loss of neural cell adhesion molecule (NCAM) (CD56) and CNS-MM, which has a role in cell-cell adhesion, is presented in our own data (Table 1).

Prognosis

The majority of CNS-MM cases are in patients who have received MM therapy prior to CNS involvement (Table 2) and whose survival is generally short and may depend on subsequent treatment.[6,8,15,24] In a recent retrospective study of 172 CNS-MM patients, Jurczyszyn *et al.* found the median overall survival (OS) from the onset of CNS involvement to be seven months; multivariate analysis revealed that receiving MM therapy before CNS involvement, and having >1 cytogenetic marker of poor prognosis, were risk factors that reduced median OS from 25 months to 5.5 months when either was present, and to two months with both present.[8] Jurczyszyn *et al.* also showed a median OS of 12 months in patients who received systemic therapy following CNS-MM diagnosis.[8] Similarly, Chen *et al.* analyzed records for 37 patients treated between 1999-2010 and found a group of nine longer survivors with a median OS of 17.1 months from CNS-MM diagnosis, who were typically treated with radiotherapy, intrathecal chemotherapy, and IMiD.[15] Majd *et al.* studied nine CNS-MM patients treated between 2008-2013 and observed that the three longest survivors received stem cell transplant after CNS involvement was detected.[25] Interestingly, none of these nine patients was receiving maintenance therapy before CNS involvement was detected.[25]

Table 2. Analysis of data from studies referenced.

Parameter				Mean of all studies (range)
% detected at MM diagnosis				16
Months from MM diagnosis to CNS-MM				26 (0 - 216)
% male				57
Age				57
% IgG				38
% IgA				26
% IgD				4
% biclonal				5
% light chain only				21
% lambda				50
iFISH on CSF (compared BM at MM Dx)				
13q loss 33% (38%)				
17p loss 14% (9%)				
1q gain 10% (17%)				
t(4;14) 14% (9%)				
t(11;14)14% (5%)				
Courses of MM treatment before CNS-MM				2.2
OS from CNS-MM diagnosis (Months)				4.5
MM treatment				**CNS-MM median OS**
IMiD	PI	SCT	XRT	
√	√			2.6
√		√		6.0
√	√	√		3.5
	√			10.9
		√		3.0
			√	4.0
None of the above				1.6
CNS-MM treatment				**CNS-MM median OS**
IMiD	PI	SCT	XRT	
√	√			5.1
√			√	4.7
√	√		√	7.3
		√		5.8
			√	2.0
	√		√	6.0
		√	√	9.0
None of the above				1.0

Summary, where data are available. Means and medians were weighted according to study size and used to calculate an overall mean. MM: multiple myeloma; CNS-MM: multiple myeloma with central nervous system (CNS) involvement; OS: overall survival. Cerebrospinal fluid (CSF) interphase fluorescence *in situ* hybridization (iFISH) data from 21 cases (3 studies) compared to that from 64 cases (12 studies) at diagnosis (Dx) of multiple myeloma (MM Dx). Treatment data obtained from 123 cases of CNS-MM. Prior to CNS-MM diagnosis, 36% of patients received one or more stem cell transplants (SCT); 27% were treated with one or more immunomodulatory drugs (IMiD); 24% received a proteasome inhibitor (PI); and 9% received radiotherapy (XRT). BM: bone marrow.

The recent study of 50 patients with intracranial myeloma by Gozzetti *et al.* illustrates the distinction of osteodural myeloma from CNS-MM, with osteodural myeloma patients showing a median OS more than three times that of patients whose CNS-MM was defined by the presence of plasma cells in CSF.[26] Dias *et al.* studied 20 patients with CNS infiltration, 17 of whom had only osteodural myeloma without leptomeningeal involvement and median OS of 40.3 months from the start of CNS involvement, compared to 5.8 months with leptomeningeal involvement.[27] Our overall analysis of CNS-MM survival data from studies cited in this review (4.5 months) (Table 2) is in accordance with these figures.

Cytogenetics

The cytogenetic risk factors of MM have been established as prognostic indicators of poor OS in CNS-MM patients. Jurczyszyn *et al.* found del(13q) (39%) and del(17p) (23%) to be the most common.[8] del(13q) is detected at a similar frequency in CNS-MM to MM, and therefore this study concurs with an older review by Nieuwenhuizen and Biesma which found no association between CNS-MM and del(13q).[1,8] Jurczyszyn *et al.* also observed the frequency of del(17p) in CNS-MM to be similar to that in MM.[8] Smaller studies, however, have shown higher rates of del(13q)[24] and del(17p) in CNS-MM.[18] A similar pattern of cytogenetic abnormalities is seen in EMD and BM-MM, apart from the t(4;14) *FGFR3/IgH* translocation and del(17p), which showed a higher frequency in EMD.[7] A small study using immunostaining to compare EMD with BM-MM showed higher aberrant expression of p53 in EMD.[20] We advocate caution in the interpretation of some data providing apparently convincing evidence of association between specific acquired cytogenetic aberrations such as del17p,[18] published well over a decade ago when methodologies and iFISH probe quality were questionable. In our own experience, we have failed to detect any significant association between BM iFISH results at diagnosis and co-existing or subsequent development of CNS-MM. Also, we have refined our iFISH technique during the past 15 years, including preselection of CD138 positive plasma cells, and switched to alternative iFISH probes giving clearer signals, so would include our own earlier results in this 'questionable' category.

Other associations

Associations between CNS-MM and several further parameters have been suggested, although some evidence comes from small studies. IgA myeloma represented 27% of CNS-MM cases in the multi-center study by Jurczyszyn *et al.* compared to 21% of the 1,027 newly-diagnosed MM (ND-MM) cases studied by Kyle *et al.*[8,28] The figure of 27% is very similar to that of 26% in the summary analysis of data referenced in this review (Table 2). The review by Nieuwenhuizen and Biesma shows a higher proportion of cases of λ than κ light chain expression in CNS-MM patients, to that observed in MM.[1] Jurczyszyn *et al.* report 52% of cases expressing κ, 42% λ and 5% both κ and λ, also suggesting a higher frequency of λ-expressing myeloma in CNS-MM than in MM.[8] Nieuwenhuizen and Biesma also observed 8.3% of CNS-MM cases expressing IgD and 7.3% showing biclonal immunoglobulin expression,[1] both of which are around 2% in ND-MM.[28] Other studies suggest a higher likelihood of IgD and light chain myeloma in CNS-MM.[25,29] According to Jurczyszyn *et al.*, however, 2% of CNS-MM cases were IgD and 1% had biclonal immunoglobulins; the proportions of cases with light chain myeloma and IgG myeloma were also similar to those seen in ND-MM.[8,28] Data from studies of EMD in general show a higher prevalence of IgD myeloma among EMD at relapse than in MM;[21] and cases with EMD at MM diagnosis are more likely to be IgD, λ or non-secretory myeloma.[5] Our summary analysis of studies referenced in this review identified 4% of cases expressed IgD, and 5% showed biclonal immunoglobulin expression. Overall, however, there is no consensus for associations between light chain restriction, or Ig class, and CNS-MM.

The phenomenon that CNS-MM might be seen more often in autologous SCT (ASCT)-receiving patients might be: a) by chance; b) because specifically those patients may show longer survival and may, with prolonged survival, develop extramedullary site (EM)-MM; and/or c) because EM/CNS-MM specifically homes to sites other than the BM, as has been observed after intensive therapies, such as ASCT and allogeneic-SCT.[30,31]

Other associations seen in CNS-MM suggest features of late disease or, alternatively, distinct biology. In Nieuwenhuizen and Biesma's 2008 review, 41.3% of CNS-MM were stage 3 disease by the Durie-Salmon staging system.[1] The later study by Jurczystyn *et al. f*ound only 27% to be stage 3, using the International Staging System (ISS), although 47% showed elevation of lactate dehydrogenase (LDH), one of the parameters of late-stage MM used in the ISS.[8] The 18 cases studied by Fassas *et al.* suggest an association between CNS-MM and tumor mass, other EMD, PCL and plasmablastic morphology.[32] Nieuwenhuizen and Biesma observed circulating plasma cells (cPC) in 20% of CNS-MM and postulated an association, although the Kyle *et al.* study reported cPC in the majority of ND-MM.[28] Some groups propose loss of the cellular adhesion molecule CD56 from the surface of malignant plasma cells as a mechanism of extramedullary spread and, hence, CNS infiltration.[33] Although our own data suggested a higher incidence of CD56 loss in CNS-MM than in ND-MM, data from some other studies do not support this or the presence of a CNS-specific immunophenotype.[29,34-37] Studies of EMD in general have revealed a putative biological signature which includes increased LDH,[7,38] along with evidence of a reduction in CD56 expression.[20,39] We found no difference in features such as cytogenetics, cytology and histopathology between CNS-MM diagnosed at the time of MM diagnosis and those diagnosed at relapse. A summary of studies considered in this review is given in Table 3.

Diagnosis

Multiple myeloma with CNS involvement is difficult to diagnose as it can produce heterogeneous symptoms related to either spinal, cranial or meningeal infiltration, which can be confounded by neurological symptoms caused by the hypercalcemia, uremia, paraproteinemia and bone damage typical in MM,[8] as well as side-effects of drug therapy and, in some cases, amyloid protein.[32] In addition, clinical and laboratory findings of CNS-MM are not always MM-specific; for example, they can be similar to those of leptomeningeal metastases from other hematologic malignancies.[40] CNS-MM patients can present with impairments to sight, speech, motor and sensory functions, radicular pain, headache, confusion, dizziness and,

less frequently, seizures, vomiting, cranial nerve palsy, lethargy, fever, convulsion, vertigo, hearing loss and incontinence.[1,8] When such symptoms are seen in MM patients, the ensuing investigations employ imaging, cytological and/or cytometric techniques. The suggested approach to diagnosis of CNS-MM is shown in Figure 1.

Cytological techniques can detect atypical plasma cells and flow cytometry can detect monoclonal CD38/CD138 expressing cells in CSF in approximately 90% of CNS-MM cases, thus confirming the disease.[8,41] CSF cytology and flow cytometry are both particularly useful since the former can employ immunocytochemistry to identify unknown tumors,[42] and the latter can be used to distinguish the clonal plasma cells found in MM from polyclonal plasma cells present in CSF in other conditions.[43] Furthermore, the presence of a paraprotein, including clonal free light chains (FLC), in CSF obtained from a clean lumbar puncture, can be diagnostic. Minute or undetectable concentrations of paraprotein in the parallel analysis of serum is strong evidence that monoclonal immunoprotein detected in CSF originates from plasma cells in the CNS rather than BM.

In the study of 172 CNS-MM patients by Jurczyszyn *et al.*, magnetic resonance imaging (MRI) of the brain and/or spine showed evidence of CNS involvement in 93% of cases, while computed tomography (CT) scans showed evidence in 81%.[8] In the patients who underwent imaging, leptomeningeal involvement was found in over half, intracranial mass in approximately half, and both in approximately 20%.[8] Fluorescence *in situ* hybridization can reveal EMD and is therefore potentially useful for detection of CNS-MM.[44,45] Diagnosis of CNS-MM is confirmed using imaging and by detection of monoclonal immunoprotein and/or clonal plasma cells in CSF (Figure 2), with the last of these especially useful for leptomeningeal involvement.[25,35] Imaging techniques are effective in most cases, although studies estimate a 10% false negative rate.[8] Detection of plasma cells in CSF provides strong evidence of CNS-MM, although these can be absent when infiltration of parenchymal CNS has occurred.[8,46]

Treatment of multiple myeloma with CNS involvement: current approaches and future directions

The optimal approach to treatment of CNS-MM is not currently known. The relatively small numbers of patients presenting with this complication means that there is no high quality, prospective clinical trial data to inform an evidence-based approach to therapy. The current approach mirrors those treatment modalities used in lymphoproliferative disease infiltrating the CNS, namely, systemic therapy, intrathecal (IT) therapy, and CNS irradiation, often in combination.

Systemic therapy

Drug therapies successfully employed in MM might be ineffective in CNS-MM due to: tumor resistance after previous therapy,[8] because they require interaction with the

Table 3. Studies considered in this review.

Reference	Study dates	CNS-MM	Topic of study	Reference	Study dates	CNS-MM	Topic of study
Nieuwenhuizen L and Biesma DH. 2008[1]	1968-2007	109*	Literature review – diagnosis and treatment	Fassas AB *et al.* 2002[32]	1990-2002	18*	Features associated with CNS-MM including cytogenetic
Varga G *et al.* 2018[6]	2007-2017	13	Imaging, CSF analysis, treatment, survival	Chang H *et al.* 2005[33]	2005	8	CSF plasma cell, CD56
Jurczyszyn A *et al.* 2016[8]	1995-2014	172	Multicenter study of pathology, imaging and survival	Liu XJ *et al.* 2015[34]	2015	1	Case description
Paludo J *et al.* 2016[9]	1998-2014	29	Plasma cell detection in CSF	Marini A *et al.* 2014[35]	2014	1	Flow cytometry for rapid diagnosis, CD56
Gangatharan SA *et al.* 2012[10]	2001-2010	7	CNS-MM and novel agents	Lopes AC *et al.* 2017[36]	2017	1	$CD56^+$ CNS infiltration
Fassas AB *et al.* 2004[11]	1990-2004	25**	Risk markers including cytogenetic	Kaplan JG *et al.* 1990[40]	1990	63	Presentation and cytology
Lee D *et al.* 2013[12]	2000-2011	17	CSF protein, intrathecal therapy	Mendez CE *et al.* 2010[46]	2010	1	Case study with dural involvement
Abdallah AO *et al.* 2014[13]	1996-2012	35	Diagnosis and treatment	Fukunaga H *et al.* 2017[44]	2017	1	FDG-PET
Chen CI *et al.* 2013[15]	1999-2010	37	Treatment and survival	Bommer M *et al.* 2018[41]	2017	16	Cytology, flow cytometry and iFISH for diagnosis
Ruiz-Heredia Y *et al.* 2018[17]	2018	1	CNS-MM concurrent with PML	Ren H *et al.* 2017[42]	2017	2	CSF cytology for diagnosis
Chang H *et al.* 2004[18]	2000-2003	9	Cytogenetics	Riley JM *et al.* 2011[58]	2011	1	Radiotherapy
Chang WJ *et al.* 2014[24]	2006-2010	8	Cytogenetics	Katodritou E *et al.* 2015[52]	2000-2013	31	Treatment with novel agents
Majd N *et al.* 2016[25]	1998-2012	9	Characterization	Vicari P *et al.* 2003[51]	2003*	54	Thalidomide
Gozzetti A *et al.* 2012[26]	2000-2010	0	Intracranial EMD and novel therapies	Mussetti A *et al.* 2013[54]	2009-2013	1	Pomalidomide
Dias A *et al.* 2018[27]	2008-2016	3	Brazilian center	Badros A *et al.* 2017[55]	2008-2016	2	Marizomib
Kyle RA *et al.* 2003[28]	1985-1998	0***	Large-scale MM study	Kauffmann G *et al.* 2017[59]	2017	1	Proton therapy
Marchesi F *et al.* 2016[29]	2016	4	Flow cytometry	Marron TU *et al.* 2015[82]	2011-2013	9	FLC measurement in CSF

*Nieuwenhuizen *et al.* (2008)[1] included 18 cases from Fassas *et al.* (2002)[32] and 54 cases from Vicari *et al.* (2003).[51] **Fassas *et al.* (2004)[11] includes 18 cases from Fassas *et al.* (2002).[32] ***Multiple myeloma cases only. CNS: central nervous system; MM: multiple myeloma; CNS-MM: multiple myeloma with CNS involvement; CSF: cerebrospinal fluid; PML: progressive multifocal leukoencephalopathy; FDG-PET: fluorodeoxyglucose positron-emission tomography; FLC: serum free light chain; iFISH: interphase fluorescence *in situ* hybridization.

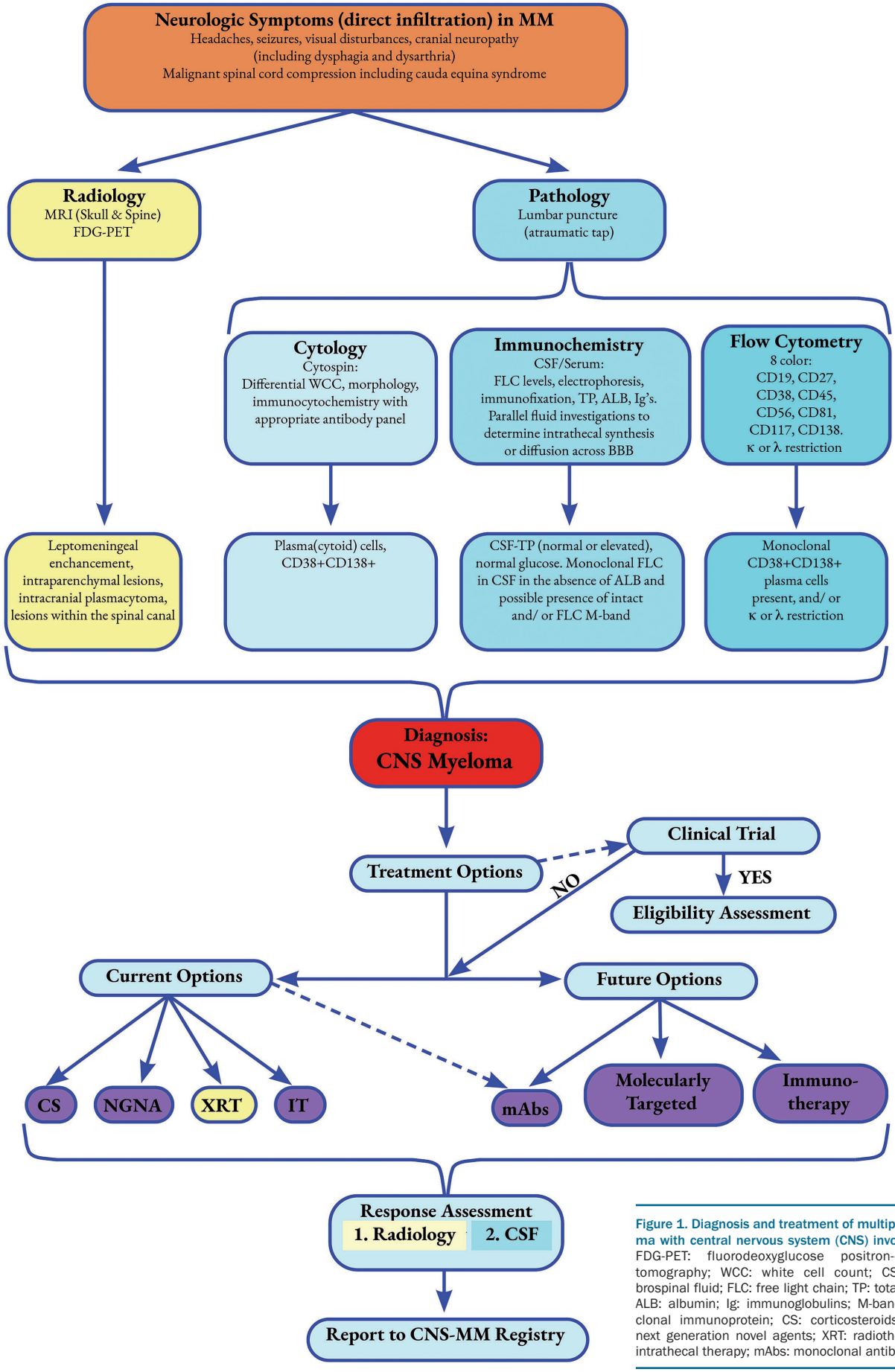

Figure 1. Diagnosis and treatment of multiple myeloma with central nervous system (CNS) involvement. FDG-PET: fluorodeoxyglucose positron-emission tomography; WCC: white cell count; CSF: cerebrospinal fluid; FLC: free light chain; TP: total protein; ALB: albumin; Ig: immunoglobulins; M-band: monoclonal immunoprotein; CS: corticosteroids; NGNA: next generation novel agents; XRT: radiotherapy; IT: intrathecal therapy; mAbs: monoclonal antibodies.

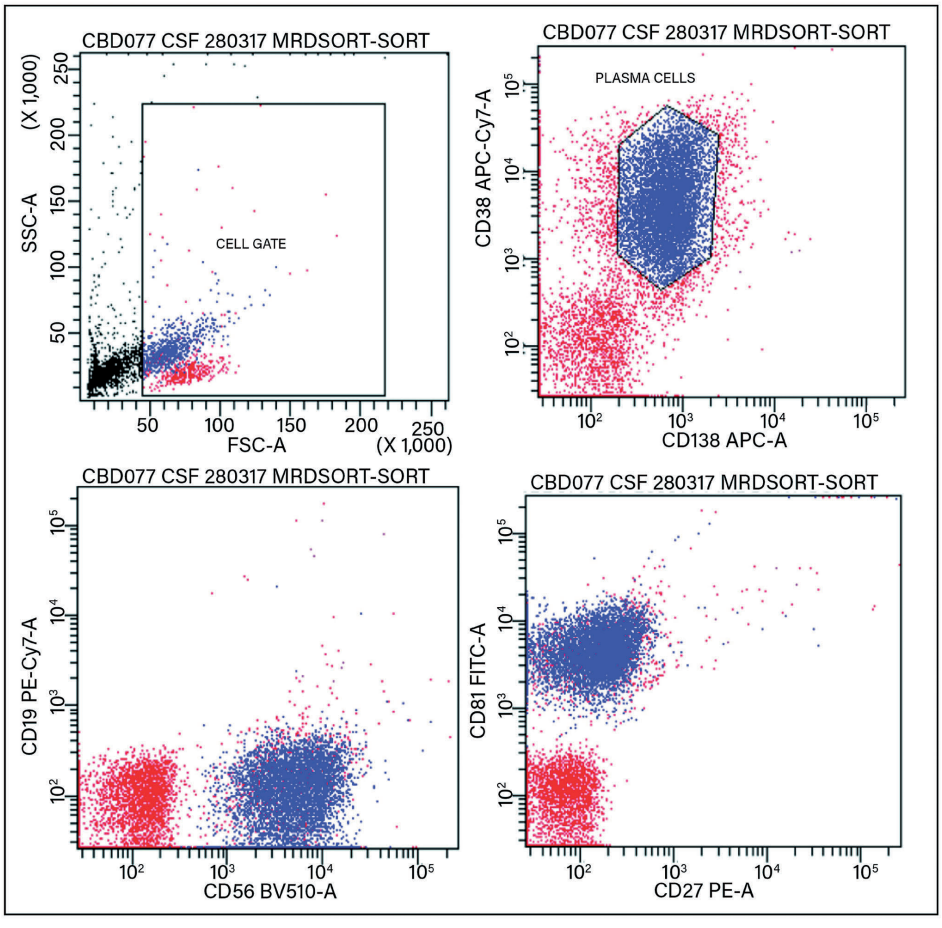

Figure 2. Detection and characterization of myeloma cells in cerebrospinal fluid by flow cytometry. Clonal plasma cells (blue) distinguished from other lymphocyte populations (red) and debris (black).

BM microenvironment,[47] or the inability to cross the blood-brain barrier (BBB).[1] It has been suggested that, by preventing access of drugs to the brain, the BBB provides a safe haven for the tumor that only radiotherapy or IT administration can overcome.[14] Therefore, when considering systemic therapy, a prerequisite is that the chosen agent(s) have the potential to cross the BBB. Standard cytotoxic regimens lack efficacy in CNS-MM as they are either poor at penetrating the BBB (alkylating agents including melphalan and cyclophosphamide) or ineffective against myeloma cells (high-dose methotrexate or cytarabine). Bendamustine is capable of permeating the BBB and has shown some efficacy in two cases of leptomeningeal relapse of myeloma in combination with thalidomide, dexamethasone and craniospinal irradiation.[48] High-dose steroids are known to cross the BBB, although they are of limited benefit when used in isolation.

The retrospective analysis of 172 patients with CNS-MM published by Jurczyszyn *et al.* in 2016 highlighted the importance of incorporating systemic therapy into any planned treatment strategy.[8] Ninety-seven percent of patients were treated, receiving systemic therapy (76%), radiotherapy (36%), and IT therapy (32%). The only group to have a significantly longer median OS than the untreated group received systemic treatment (OS 12 *vs.* 3 months), although the number of patients not given systemic therapy was small. Furthermore, these data need to be interpreted with caution as it appears fair to assume that patients in whom systemic treatment could be considered were in better condition to tolerate that treatment when CNS-MM was diagnosed. Hence, this is a potential source of bias in the interpretation of the OS data.

The IMiD thalidomide and lenalidomide have been reported to penetrate the BBB in non-human primates.[49] In patients, thalidomide has been shown to cross the BBB in leptomeningeal CNS-MM;[50] however, it is not certain whether it is sufficiently fast-acting to stabilize CNS-MM disease.[8,51] A 2015 review of 31 Greek patients with CNS-MM showed no survival benefit from the use of novel agents (including thalidomide and lenalidomide) or radiotherapy, although it should be noted that they received no high-dose systemic therapy or SCT.[52] Chen *et al.*'s 2013 study observed 6 of 9 long-term CNS-MM survivors when treated with IMiD-based therapy (5 thalidomide; 1 lenalidomide), with concomitant multi–dosing IT therapy and cranial/spinal irradiation.[15] The third-generation IMiD pomalidomide has demonstrated activity in EMD[22] and good penetrance of the BBB in a murine model.[53] Notably, a durable CSF emission has been reported using pomalidomide-dexamethasone treatment.[54]

The current PI in regular clinical use (bortezomib, carfilzomib and ixazomib) are not thought to cross the BBB. However, bortezomib has shown some efficacy when

used in combination with other agents and treatment modalities in CNS-MM.[26] This benefit may be due to pathological changes such as inflammation and angiogenesis increasing the permeability of the BBB, thus allowing passage of the drug. Marizomib, a newer PI which can cross the BBB, can be detected in the CNS upon systemic therapy, and has shown potential efficacy in relapsed refractory MM (RRMM), malignant glioma, and a small number of CNS-MM patients.[16,55]

Intrathecal therapy

The typical intrathecal therapy (IT) therapy regimen administered in CNS-MM is the triplet of IT hydrocortisone, methotrexate and/or cytarabine. This is repeated until clearance of plasma cells and free light chains from the CSF. Its use is controversial as myeloma cells are not thought to be particularly susceptible to methotrexate or cytarabine and it is unlikely to penetrate parenchymal CNS lesions. In two 2013 studies, one of 17 CNS-MM cases showed longer median OS in patients given IT therapy (methotrexate and/or dexamethasone) compared to those who had not,[12] and a study of 37 patients identified a subgroup treated with radiotherapy, IMiD and IT therapy (hydrocortisone, methotrexate and/or cytarabine) who had longer median OS.[15] Since patients were not randomly grouped, the effect of bias cannot be ruled out in these studies. No such positive effect was observed in a 2014 study of eight patients where IT therapy was associated with a median OS of 0.9 months,[24] consistent with other studies that have only shown a modest benefit of IT therapy.[25] Intrathecal use of rituximab [a humanized anti-CD20 monoclonal antibody (mAb)] has been shown to be safe for this method of administration in the setting of CNS lymphoma[56] which might suggest a future role for other mAb with anti-myeloma activity being administered by this route.

Cranial or cranial-spinal irradiation

Malignant plasma cells are known to be sensitive to radiotherapy and this treatment modality is the cornerstone of treatment for solitary plasmacytomas of bone and EM plasmacytomas.[57] Cranial irradiation was reported in one review to show statistically significant benefit in improving survival (median 3 *vs*. 0.81 months) compared to those not receiving this treatment modality.[1] Targeted radiotherapy can alleviate focal symptoms such as muscle weakness caused by intramedullary spinal cord lesions.[58] There is evidence that modern radiotherapy techniques can deliver impressive responses in parenchymal CNS-MM lesions without significant myelotoxic sequelae.[59]

Stem cell transplantation

Stem cell transplantation can overcome the poor prognosis of EMD when detected at MM diagnosis,[60,61] and can have a similar effect in extramedullary relapse as in BM relapse, contradicting the theory that EMD has its own immunological environment that will not support a graft-*versus*-myeloma response.[2] In a study of 18 CNS-MM patients, the longest survivor (25 months) had received an allo-SCT after the diagnosis of CNS-MM and had no evidence of CNS-MM relapse at the time of death, suggesting a graft-*versus*-myeloma effect in the CNS.[32] However, unlike in EMD, SCT is not currently considered a standard salvage treatment option in most cases of CNS-MM due to their short survival time.

Current approach

Important factors in the approach to treatment of CNS-MM include the following.

- Accurate diagnosis with a clear understanding of which part of the CNS is involved in order to help target therapy and penetrate site of disease.
- Patient factors, including: a) current BM function and likelihood of being able to tolerate further systemic therapy; b) practicalities of delivering frequent IT therapy; c) potential toxicities of CNS irradiation.
- Acknowledgment of prior lines of systemic therapy, to avoid use of likely disease-resistant agent(s). However, drug resistance in the primary site of the tumor (BM) may not necessarily be replicated in the CNS due to the absence of BM mesenchymal stromal cells which may provide protection to the tumor cells in the BM environment.
- Constraints of treatment options in resource-poor countries.
- Choice of agents known to cross the BBB and with evidence of efficacy in CNS-MM.

Given the limited therapeutic evidence-base described, our current approach to patients with suspected CNS-MM is as follows: accurate diagnosis (as summarized in Figure 1) employing MRI of brain and whole spine, analysis of CSF including serum free light chain (FLC) analysis and multi-color flow cytometry to demonstrate presence of MM cells, and, less commonly, stereotactic brain biopsy as indicated; a backbone of systemic therapy incorporating IMiD and high-dose steroid, and anti-CD38 mAb (see below) depending on local funding directives; and appropriate site-directed CNS irradiation. We would acknowledge that, whilst IT therapy is controversial, it remains part of the standard of care in most centers.

Future direction

Several newer agents have demonstrated activity in B-cell neoplasms including CNS-MM. Monoclonal antibodies are of considerable interest and may play an important part in improving outcomes in CNS-MM. Daratumumab is a humanized mAb specific for CD38 and there is evidence it can cross the intact BBB, being measurable in CSF.[62] It has shown significant activity in parenchymal CNS-MM in combination with IT therapy and radiotherapy (XRT).[63] Also, in a study of relapsed / refractory MM (RRMM) with CNS involvement, a patient treated systemically with daratumumab achieved a response, clearing the CSF of plasma cells, although there was concomitant use of IT therapy.[6] Isatuximab, another anti-CD38 mAb, has shown efficacy in heavily pre-treated MM patients[64] and is currently being evaluated in phase III studies in combination with steroid and novel agents.[65] Elotuzumab is a humanized mAb directed against SLAMF7, also called CS1. SLAMF7 is expressed on most myeloma and natural killer cells, but not on normal tissues. More than 95% of BM myeloma cells have been demonstrated to express SLAMF7. Elotuzumab has been shown to have activity in RRMM in combination with IMiD and steroid.[66,67] However, there are no current data on its use in CNS-MM.

Translocations involving chromosome 14 are a recurrent finding in MM and approximately 15% of patients demonstrate a t(11;14) (q13;q32) involving the *CCND1/IGH* genes. This juxtaposition results in *CCND1* being overexpressed, leading to kinase activation and tumor cell pro-

liferation. t(11;14) cases in MM are predicted to be BCL-2-dependent resulting in upregulation of anti-apoptotic proteins and thereby making BCL-2 a potential target in this subtype of myeloma.[68] Venetoclax is a BCL-2 inhibitor and promotes apoptosis *via* a *TP53* mutation-independent pathway and is of proven efficacy in patients with chronic lymphocytic leukemia (CLL) with del(17p) and/or *TP53* mutation.[69] It has also been demonstrated to cross the BBB in CLL and is therefore of potential efficacy in CNS-MM.[70] Several phase III trials are currently underway using venetoclax in patients with RRMM.

The *BRAF* gene encodes protein kinases which regulate the intracellular MAP/ERK signaling pathway involved in cell proliferation and survival. Somatic mutations arising in this gene can lead to oncogenesis. The *BRAF*^{V600E} mutation is seen in up to 10% of MM patients at diagnosis and up to 20% at relapse.[71,72] Inhibition of this pathway using selective inhibitors of *BRAF*^{V600E} kinase such as vemurafenib, has shown some efficacy in RRMM.[73] Other agents targeting this pathway are currently the subject of prospective clinical trials in Europe (*clinicaltrials.gov identifier: NCT02834364*) and in the United States (*clinicaltrials.gov identifier: NCT03091257)*. There is evidence such agents may cross the BBB[74] and at least one case report of a patient with BRAF^{V600E} positive CNS-MM relapse responding clinically and radiologically to BRAF-MEK inhibitors.[75]

Chimeric antigen receptor-modified T-cell (CAR-T) therapy is in preclinical stages of development for patients with RRMM. The CAR-T construct targets the B-cell maturation antigen (BCMA) which is highly expressed on malignant plasma cells. Soluble BCMA levels are significantly increased in CSF in primary CNS lymphoma.[76] There is an assumption that CAR-T products cross the BBB given that neurotoxicity is a frequent but generally temporary side effect of this therapy. Its use in treating patients diagnosed with CNS-MM might be impeded by the fact that currently the time from patient leukapheresis to re-infusion with the CAR-T product is approximately four weeks. However, development of 'off-the-shelf' CAR-T products may overcome this obstacle in the future.[77] Other immunotherapy modalities that target the BCMA include bispecific antibody constructs, including BiTE® (bispecific T-cell engager) immuno-oncology therapies, and antibody-drug conjugates (ADC). These products, like CAR-T, have shown efficacy in RRMM.[78] However, unlike CAR-T, they have the advantage of not requiring *ex vivo* manipulation of patients' cells, therefore conferring a significantly faster time-to-treatment following diagnosis. Studies have suggested sBCMA is not just a suitable target for drug therapy but that it may also have an important role in MM as a biomarker at diagnosis for its prognostic value, in assessment of response to therapy, and in minimal residual disease monitoring.[78-81]

Conclusions

Prevention of CNS-MM and improved outcomes face significant challenges due to the rarity of the condition, and its rapid progression. Sensitive detection of monoclonal immunoprotein and plasma cells in CSF enables efficient diagnosis and monitoring of treatment response.[13,82] This, together with new drugs, such as the next generation of PI, mAb and molecularly targeted and immune-oncological therapies, potentially offers improved risk stratification and treatment options. However, there remains a paucity of data to provide a clear evidence base on whether novel agents offer improved therapy for these patients, especially at relapse.[52,83,84] Furthermore, myelosuppression is a side-effect of myeloma drug treatment, including some of the most recent novel agents such as pomalidomide,[85] although modern radiotherapy may allow targeting of CNS-MM to avoid the BM and resultant damage to hematopoiesis.[59]

The difficulties in recruiting adequate numbers of patients with CNS-MM to clinical trials is acknowledged. Thus, these innovative treatment approaches may best be achieved through worldwide group efforts to determine optimum diagnostics and treatments, and offer the best evidence-based potential to improve outcomes. We therefore recommend the establishment of an International Registry of such cases as the best way to produce a database to underpin best practice recommendations for both diagnosis and treatment. The design of a 'proforma' to be submitted with each dataset registered will be of paramount importance to enable capture of this information. This approach has been used successfully in, for example, light chain (AL) amyloidosis and POEMS syndrome.

Finally, in EMD, there is evidence that poor prognosis is not linked to advanced disease alone, or to treatment received, but to tumor biology.[2] Therefore, an improved understanding of this would enable identification of MM cases at risk of CNS relapse. This, in turn, would allow consideration of prophylaxis in patients thus identified, as, for example, in high grade B-cell lymphoma.[16] However, at present, CNS-MM confers a bleak outlook and urgently requires an innovative approach to treatment.

References

1. Nieuwenhuizen L, Biesma DH. Central nervous system myelomatosis: review of the literature. Eur J Haematol. 2008;80(1):1-9.
2. Wirk B, Wingard JR, Moreb JS. Extramedullary disease in plasma cell myeloma: the iceberg phenomenon. Bone Marrow Transplant. 2013;48(1):10-18.
3. Tirumani SH, Shinagare AB, Jagannathan JP, Krajewski KM, Munshi NC, Ramaiya NH. MRI features of extramedullary myeloma. AJR Am J Roentgenol. 2014;202 (4):803-810.
4. Weberpals J, Pulte D, Jansen L, et al. Survival of patients with lymphoplasmacytic lymphoma and solitary plasmacytoma in Germany and the United States of America in the early 21(st) century. Haematologica. 2017;102(6):e229-e232.
5. Varettoni M, Corso A, Pica G, Mangiacavalli S, Pascutto C, Lazzarino M. Incidence, presenting features and outcome of extramedullary disease in multiple myeloma: a longitudinal study on 1003 consecutive patients. Ann Oncol. 2010;21 (2):325-330.
6. Varga G, Mikala G, Gopcsa L, et al. Multiple Myeloma of the Central Nervous System: 13 Cases and Review of the Literature. J Oncol. 2018;2018:3970169.
7. Rasche L, Bernard C, Topp MS, et al. Features of extramedullary myeloma relapse: high proliferation, minimal marrow involvement, adverse cytogenetics: a retrospective single-center study of 24 cases. Ann Hematol. 2012;91(7):1031-1037.
8. Jurczyszyn A, Grzasko N, Gozzetti A, et al. Central nervous system involvement by multiple myeloma: A multi-institutional retrospective study of 172 patients in daily clinical practice. Am J Hematol. 2016;91(6):575-580.

9. Paludo J, Painuly U, Kumar S, et al. Myelomatous Involvement of the Central Nervous System. Clin Lymphoma Myeloma Leuk. 2016;16(11):644-654.
10. Gangatharan SA, Carney DA, Prince HM, et al. Emergence of central nervous system myeloma in the era of novel agents. Hematol Oncol. 2012;30(4):170-174.
11. Fassas AB, Ward S, Muwalla F, et al. Myeloma of the central nervous system: strong association with unfavorable chromosomal abnormalities and other high-risk disease features. Leuk Lymphoma. 2004;45(2):291-300.
12. Lee D, Kalff A, Low M, et al. Central nervous system multiple myeloma--potential roles for intrathecal therapy and measurement of cerebrospinal fluid light chains. Br J Haematol. 2013;162(3):371-375.
13. Abdallah AO, Atrash S, Shahid Z, et al. Patterns of central nervous system involvement in relapsed and refractory multiple myeloma. Clin Lymphoma Myeloma Leuk. 2014;14(3):211-214.
14. Gertz MA. Pomalidomide and myeloma meningitis. Leuk Lymphoma. 2013;54(4):681-682.
15. Chen CI, Masih-Khan E, Jiang H, et al. Central nervous system involvement with multiple myeloma: long term survival can be achieved with radiation, intrathecal chemotherapy, and immunomodulatory agents. Br J Haematol. 2013;162(4):483-488.
16. Harrison SJ, Spencer A, Quach H. Myeloma of the central nervous system - an ongoing conundrum! Leuk Lymphoma. 2016;57(7):1505-1506.
17. Ruiz-Heredia Y, Sanchez-Vega B, Barrio S, et al. Concurrent progressive multifocal leukoencephalopathy and central nervous system infiltration by multiple myeloma: A case report. J Oncol Pharm Pract. 2019;25(4):998-1002.
18. Chang H, Sloan S, Li D, Keith Stewart A. Multiple myeloma involving central nervous system: high frequency of chromosome 17p13.1 (p53) deletions. Br J Haematol. 2004;127(3):280-284.
19. Rasmussen T, Kuehl M, Lodahl M, Johnsen HE, Dahl IM. Possible roles for activating RAS mutations in the MGUS to MM transition and in the intramedullary to extramedullary transition in some plasma cell tumors. Blood. 2005;105(1):317-323.
20. Sheth N, Yeung J, Chang H. p53 nuclear accumulation is associated with extramedullary progression of multiple myeloma. Leuk Res. 2009;33(10):1357-1360.
21. Deng S, Xu Y, An G, et al. Features of extramedullary disease of multiple myeloma: high frequency of p53 deletion and poor survival: a retrospective single-center study of 834 cases. Clin Lymphoma Myeloma Leuk. 2015;15(5):286-291.
22. Short KD, Rajkumar SV, Larson D, et al. Incidence of extramedullary disease in patients with multiple myeloma in the era of novel therapy, and the activity of pomalidomide on extramedullary myeloma. Leukemia. 2011;25(6):906-908.
23. Varga C, Xie W, Laubach J, et al. Development of extramedullary myeloma in the era of novel agents: no evidence of increased risk with lenalidomide-bortezomib combinations. Br J Haematol. 2015;169(6):843-850.
24. Chang WJ, Kim SJ, Kim K. Central nervous system multiple myeloma: a different cytogenetic profile? Br J Haematol. 2014;164(5):745-748.
25. Majd N, Wei X, Demopoulos A, Hormigo A, Chari A. Characterization of central nervous system multiple myeloma in the era of novel therapies. Leuk Lymphoma. 2016;57(7):1709-1713.
26. Gozzetti A, Cerase A, Lotti F, et al. Extramedullary intracranial localization of multiple myeloma and treatment with novel agents: a retrospective survey of 50 patients. Cancer. 2012;118(6):1574-1584.
27. Dias A, Higashi F, Peres ALM, Cury P, Crusoe EQ, Hungria VTM. Multiple myeloma and central nervous system involvement: experience of a Brazilian center. Rev Bras Hematol Hemoter. 2018;40(1):30-36.
28. Kyle RA, Gertz MA, Witzig TE, et al. Review of 1027 patients with newly diagnosed multiple myeloma. Mayo Clin Proc. 2003;78(1):21-33.
29. Marchesi F, Masi S, Summa V, et al. Flow cytometry characterization in central nervous system and pleural effusion multiple myeloma infiltration: an Italian national cancer institute experience. Br J Haematol. 2016;172(6):980-982.
30. Greil C, Engelhardt M, Ihorst G, et al. Allogeneic transplantation of multiple myeloma patients may allow long-term survival in carefully selected patients with acceptable toxicity and preserved quality of life. Haematologica. 2019;104(2):370-379.
31. Zeiser R, Deschler B, Bertz H, Finke J, Engelhardt M. Extramedullary vs medullary relapse after autologous or allogeneic hematopoietic stem cell transplantation (HSCT) in multiple myeloma (MM) and its correlation to clinical outcome. Bone Marrow Transplant. 2004;34(12):1057-1065.
32. Fassas AB, Muwalla F, Berryman T, et al. Myeloma of the central nervous system: association with high-risk chromosomal abnormalities, plasmablastic morphology and extramedullary manifestations. Br J Haematol. 2002;117(1):103-108.
33. Chang H, Bartlett ES, Patterson B, Chen CI, Yi QL. The absence of CD56 on malignant plasma cells in the cerebrospinal fluid is the hallmark of multiple myeloma involving central nervous system. Br J Haematol. 2005;129(4):539-541.
34. Liu XJ, Wang FX, Yang L, et al. One Case of Multiple Myeloma with Central Nervous System Infiltration. Zhongguo Shi Yan Xue Ye Xue Za Zhi. 2015;23(3):742-745.
35. Marini A, Carulli G, Lari T, et al. Myelomatous meningitis evaluated by multiparameter flow cytometry : report of a case and review of the literature. J Clin Exp Hematop. 2014;54(2):129-136.
36. Lopes AC, Xavier FD, de Souza Barroso R, Gomes HR, Sales MM. Massive central nervous system infiltration by CD56-positive plasma cells in multiple myeloma. Cytopathology. 2017;28(2):172-174.
37. Flores-Montero J, de Tute R, Paiva B, et al. Immunophenotype of normal vs. myeloma plasma cells: Toward antibody panel specifications for MRD detection in multiple myeloma. Cytometry B Clin Cytom. 2016;90(1):61-72.
38. Barlogie B, Smallwood L, Smith T, Alexanian R. High serum levels of lactic dehydrogenase identify a high-grade lymphoma-like myeloma. Ann Intern Med. 1989;110(7):521-525.
39. Dahl IM, Rasmussen T, Kauric G, Husebekk A. Differential expression of CD56 and CD44 in the evolution of extramedullary myeloma. Br J Haematol. 2002;116(2):273-277.
40. Kaplan JG, DeSouza TG, Farkash A, et al. Leptomeningeal metastases: comparison of clinical features and laboratory data of solid tumors, lymphomas and leukemias. J Neurooncol. 1990;9(3):225-229.
41. Bommer M, Kull M, Teleanu V, et al. Leptomeningeal Myelomatosis: A Rare but Devastating Manifestation of Multiple Myeloma Diagnosed Using Cytology, Flow Cytometry, and Fluorescent in situ Hybridization. Acta Haematol. 2018;139(4):247-254.
42. Ren H, Zou Y, Zhao Y, et al. Cerebrospinal Fluid Cytological Diagnosis in Multiple Myeloma With Leptomeningeal Involvement: A Report of Two Cases. Diagn Cytopathol. 2017;45(1):66-68.
43. Peter A. The plasma cells of the cerebrospinal fluid. J Neurol Sci. 1967;4(2):227-239.
44. Fukunaga H, Mutoh T, Tatewaki Y, et al. Neuro-Myelomatosis of the Brachial Plexus - An Unusual Site of Disease Visualized by FDG-PET/CT: A Case Report. Am J Case Rep. 2017;18:478-481.
45. Durie BG, Waxman AD, D'Agnolo A, Williams CM. Whole-body (18)F-FDG PET identifies high-risk myeloma. J Nucl Med. 2002;43(11):1457-1463.
46. Mendez CE, Hwang BJ, Destian S, Mazumder A, Jagannath S, Vesole DH. Intracranial multifocal dural involvement in multiple myeloma: case report and review of the literature. Clin Lymphoma Myeloma Leuk. 2010;10(3):220-223.
47. Anderson KC. Lenalidomide and thalidomide: mechanisms of action--similarities and differences. Semin Hematol. 2005;42(4 Suppl 4):S3-8.
48. Nahi H, Svedmyr E, Lerner R. Bendamustine in combination with high-dose radiotherapy and thalidomide is effective in treatment of multiple myeloma with central nervous system involvement. Eur J Haematol. 2014;92(5):454-455.
49. Muscal JA, Sun Y, Nuchtern JG, et al. Plasma and cerebrospinal fluid pharmacokinetics of thalidomide and lenalidomide in nonhuman primates. Cancer Chemother Pharmacol. 2012;69(4):943-947.
50. Hattori Y, Yabe M, Okamoto S, Morita K, Tanigawara Y, Ikeda Y. Thalidomide for the treatment of leptomeningeal multiple myeloma. Eur J Haematol. 2006;76(4):358-359.
51. Vicari P, Ribas C, Sampaio M, et al. Can thalidomide be effective to treat plasma cell leptomeningeal infiltration? Eur J Haematol. 2003;70(3):198-199.
52. Katodritou E, Terpos E, Kastritis E, et al. Lack of survival improvement with novel antimyeloma agents for patients with multiple myeloma and central nervous system involvement: the Greek Myeloma Study Group experience. Ann Hematol. 2015;94(12):2033-2042.
53. Li Z, Qiu Y, Personett D, et al. Pomalidomide shows significant therapeutic activity against CNS lymphoma with a major impact on the tumor microenvironment in murine models. PLoS One. 2013;8(8):e71754.
54. Mussetti A, Dalto S, Montefusco V. Effective treatment of pomalidomide in central nervous system myelomatosis. Leuk Lymphoma. 2013;54(4):864-866.
55. Badros A, Singh Z, Dhakal B, et al. Marizomib for central nervous system-multiple myeloma. Br J Haematol. 2017;177(2):221-225.
56. Villela L, Garcia M, Caballero R, Borbolla-

Escoboza JR, Bolanos-Meade J. Rapid complete response using intrathecal rituximab in a patient with leptomeningeal lymphomatosis due to mantle cell lymphoma. Anticancer Drugs. 2008;19(9):917-920.
57. Tsang RW, Campbell BA, Goda JS, et al. Radiation Therapy for Solitary Plasmacytoma and Multiple Myeloma: Guidelines From the International Lymphoma Radiation Oncology Group. Int J Radiat Oncol Biol Phys. 2018;101(4):794-808.
58. Riley JM, Russo JK, Shipp A, Alsharif M, Jenrette JM. Central nervous system myelomatosis with optic neuropathy and intramedullary spinal cord compression responding to radiation therapy. Jpn J Radiol. 2011;29(7):513-516.
59. Kauffmann G, Buerki RA, Lukas RV, Gondi V, Chmura SJ. Case Report of Bone Marrow-Sparing Proton Therapy Craniospinal Irradiation for Central Nervous System Myelomatosis. Cureus. 2017;9(11):e1885.
60. Lee SE, Kim JH, Jeon YW, et al. Impact of extramedullary plasmacytomas on outcomes according to treatment approach in newly diagnosed symptomatic multiple myeloma. Ann Hematol. 2015;94(3):445-452.
61. Wu P, Davies FE, Boyd K, et al. The impact of extramedullary disease at presentation on the outcome of myeloma. Leuk Lymphoma. 2009;50(2):230-235.
62. Vercruyssen M, El Hachem G, Maerevoet M. The Daratumumab crosses the blood brain barrier. Clin Lymphoma Myeloma Leuk. 2018;18:S289.
63. Elhassadi E, Murphy M, Hacking D, Farrell M. Durable treatment response of relapsing CNS plasmacytoma using intrathecal chemotherapy, radiotherapy, and Daratumumab. Clin Case Rep. 2018;6(4):723-728.
64. Martin T, Strickland S, Glenn M, et al. Phase I trial of isatuximab monotherapy in the treatment of refractory multiple myeloma. Blood Cancer J. 2019;9(4):41.
65. Attal M, Richardson PG, Rajkumar SV, et al. Isatuximab plus pomalidomide and low-dose dexamethasone versus pomalidomide and low-dose dexamethasone in patients with relapsed and refractory multiple myeloma (ICARIA-MM): a randomised, multicentre, open-label, phase 3 study. Lancet. 2019;394(10214):2096-2107.
66. Dimopoulos MA, Dytfeld D, Grosicki S, et al. Elotuzumab plus Pomalidomide and Dexamethasone for Multiple Myeloma. N Engl J Med. 2018;379(19):1811-1822.
67. Lonial S, Dimopoulos M, Palumbo A, et al. Elotuzumab Therapy for Relapsed or Refractory Multiple Myeloma. N Engl J Med. 2015;373(7):621-631.
68. Pistofidis R, Ghobrial I. Targeting a Myeloma Translocation for the First Time: The t(11;14) Journey. The Hematologist. 2018;15(4).
69. Campo E, Cymbalista F, Ghia P, et al. TP53 aberrations in chronic lymphocytic leukemia: an overview of the clinical implications of improved diagnostics. Haematologica. 2018;103(12):1956-1968.
70. Reda G, Cassin R, Dovrtelova G, et al. Venetoclax penetrates in cerebrospinal fluid and may be effective in chronic lymphocytic leukemia with central nervous system involvement. Haematologica. 2019;104(5):e222-e223.
71. Ruiz-Heredia Y, Sanchez-Vega B, Onecha E, et al. Mutational screening of newly diagnosed multiple myeloma patients by deep targeted sequencing. Haematologica. 2018;103(11):e544-e548.
72. Kortum KM, Mai EK, Hanafiah NH, et al. Targeted sequencing of refractory myeloma reveals a high incidence of mutations in CRBN and Ras pathway genes. Blood. 2016;128(9):1226-1233.
73. Hyman DM, Puzanov I, Subbiah V, et al. Vemurafenib in Multiple Nonmelanoma Cancers with BRAF V600 Mutations. N Engl J Med. 2015;373(8):726-736.
74. Davies MA, Saiag P, Robert C, et al. Dabrafenib plus trametinib in patients with BRAF(V600)-mutant melanoma brain metastases (COMBI-MB): a multicentre, multicohort, open-label, phase 2 trial. Lancet Oncol. 2017;18(7):863-873.
75. Da Via MC, Solimando AG, Garitano-Trojaola A, et al. CIC Mutation as a Molecular Mechanism of Acquired Resistance to Combined BRAF-MEK Inhibition in Extramedullary Multiple Myeloma with Central Nervous System Involvement. Oncologist. 2020;25(2):112-118.
76. Thaler FS, Laurent SA, Huber M, et al. Soluble TACI and soluble BCMA as biomarkers in primary central nervous system lymphoma. Neuro Oncol. 2017;19(12):1618-1627.
77. Benjamin R. Advances in off-the-shelf CAR T-cell therapy. Clin Adv Hematol Oncol. 2019;17(3):155-157.
78. Shah N, Chari A, Scott E, Mezzi K, Usmani SZ. B-cell maturation antigen (BCMA) in multiple myeloma: rationale for targeting and current therapeutic approaches. Leukemia. 2020;34(4):985-1005.
79. Sanchez E, Li M, Kitto A, et al. Serum B-cell maturation antigen is elevated in multiple myeloma and correlates with disease status and survival. Br J Haematol. 2012;158(6):727-738.
80. Ghermezi M, Li M, Vardanyan S, et al. Serum B-cell maturation antigen: a novel biomarker to predict outcomes for multiple myeloma patients. Haematologica. 2017;102(4):785-795.
81. Bujarski S, Soof C, Li M, et al. Baseline and Early Changes in Serum B-Cell Maturation Antigen Levels Predict Progression Free Survival and Response Status for Multiple Myeloma Patients in a Phase 1 Trial Evaluating Ruxolitinib, Lenalidomide and Methylprednisolone. Blood. 2018;132:1894.
82. Marron TU, Ramanathan L, Chari A. Diagnostic utility of measuring free light chains in the cerebrospinal fluid of patients with multiple myeloma. Clin Lymphoma Myeloma Leuk. 2015;15(6):e127-131.
83. Qu X, Chen L, Qiu H, et al. Extramedullary manifestation in multiple myeloma bears high incidence of poor cytogenetic aberration and novel agents resistance. Biomed Res Int. 2015;2015:787809.
84. Gozzetti A, Cerase A, Bocchia M. Central nervous system multiple myeloma. Ann Hematol. 2016;95(3):519-520.
85. Lacy MQ, Allred JB, Gertz MA, et al. Pomalidomide plus low-dose dexamethasone in myeloma refractory to both bortezomib and lenalidomide: comparison of 2 dosing strategies in dual-refractory disease. Blood. 2011;118(11):2970-2975.

International recommendations on the diagnosis and treatment of acquired hemophilia A

Andreas Tiede,[1] Peter Collins,[2] Paul Knoebl,[3] Jerome Teitel,[4] Craig Kessler,[5] Midori Shima,[6] Giovanni Di Minno,[7] Roseline d'Oiron,[8] Peter Salaj,[9] Victor Jiménez-Yuste,[10] Angela Huth-Kühne[11] and Paul Giangrande[12]

[1]Hannover Medical School, Department of Hematology, Hemostasis, Oncology and Stem Cell Transplantation, Hannover, Germany; [2]Arthur Bloom Haemophilia Centre, University Hospital of Wales School of Medicine, Cardiff University, Cardiff, UK; [3]Department of Medicine 1, Division of Hematology and Hemostasis, Medical University of Vienna, Vienna, Austria; [4]Division of Hematology and Oncology, St. Michael's Hospital, Toronto, and Department of Medicine, University of Toronto, Toronto, Canada; [5]Georgetown University Hospital, Lombardi Cancer Center, Division of Hematology/Oncology, Washington, DC, USA; [6]Department of Pediatrics, Nara Medical University, Nara, Japan; [7]Regional Reference Center for Coagulation Disorders, Federico II University Hospital, Naples, Italy; [8]Centre de Référence de l'Hémophilie et des Maladies Hémorragiques Constitutionnelles Rares, Hôpitaux Universitaires Paris Sud, Hôpital Bicêtre APHP, Le Kremlin-Bicêtre, France; [9]Institute of Hematology and Blood Transfusion, Prague, Czech Republic; [10]Hematology Department, La Paz University Hospital, Autonoma University, Madrid, Spain; [11]SRH Kurpfalzkrankenhaus Heidelberg GmbH and Hemophilia Center, Heidelberg, Germany and [12]Green Templeton College, University of Oxford, Oxford, UK

Ferrata Storti Foundation

Haematologica 2020
Volume 105(7):1791-1801

ABSTRACT

Acquired hemophilia A (AHA), a rare bleeding disorder caused by neutralizing autoantibodies against coagulation factor VIII (FVIII), occurs in both men and women without a previous history of bleeding. Patients typically present with an isolated prolonged activated partial thromboplastin time due to FVIII deficiency. Neutralizing antibodies (inhibitors) are detected using the Nijmegen-modified Bethesda assay. Approximately 10% of patients do not present with bleeding and, therefore, a prolonged activated partial thromboplastin time should never be ignored prior to invasive procedures. Control of acute bleeding and prevention of injuries that may provoke bleeding are top priorities in patients with AHA. We recommend treatment with bypassing agents, including recombinant activated factor VII, activated prothrombin complex concentrate, or recombinant porcine FVIII in bleeding patients. Autoantibody eradication can be achieved with immunosuppressive therapy, including corticosteroids, cyclophosphamide and rituximab, or combinations thereof. The median time to remission is 5 weeks, with considerable interindividual variation. FVIII activity at presentation, inhibitor titer and autoantibody isotype are prognostic markers for remission and survival. Comparative clinical studies to support treatment recommendations for AHA do not exist; therefore, we provide practical consensus guidance based on recent registry findings and the authors' clinical experience in treating patients with AHA.

Introduction

Acquired hemophilia A (AHA) is characterized by neutralizing autoantibodies, called inhibitors, against factor VIII (FVIII).[1] AHA is a rare disorder, affecting men and women of all ages.[2] Two peaks in AHA incidence are typically observed; one associated with pregnancy, and another with older age (>60 years old). Approximately half of patients with AHA have concomitant disorders, most often other autoimmune disorders or malignancy.[3,4] In approximately 1–5% of cases, AHA is diagnosed during pregnancy or within 1 year following childbirth.[5] The bleeding phenotype of AHA is variable, ranging from life-threatening bleeds to

Correspondence:

ANDREAS TIEDE
tiede.andreas@mh-hannover.de

Received: June 27, 2019.

Accepted: April 7, 2020.

Pre-published: May 7, 2020.

doi:10.3324/haematol.2019.230771

Check the online version for the most updated information on this article, online supplements, and information on authorship & disclosures: www.haematologica.org/content/105/7/1791

mild or no bleeding. Subcutaneous hematomas are characteristic of AHA and can be the first indication of the disease.

Patients with AHA are often elderly; comorbidities and medications, such as antiplatelet agents and anticoagulants, may influence the clinical picture and require an individualized therapeutic approach. In contrast to congenital hemophilia, comparative clinical studies are not available in AHA, largely because of the rarity of the disorder and the severe clinical condition of patients at presentation. Treatment decisions are often based on the expertise and clinical experience of treating physicians, and referral to expert centers is often recommended to provide the best possible care.

In 2009, Huth-Kühne *et al.* published international recommendations for AHA.[1] Since then, other guidance has also been published.[6] These documents are recognized as important sources of guidance for hematologists and other specialists. The 2009 recommendations were mainly based on the authors' collective experience in treating a large number of patients with AHA. Data from several AHA registries have since been published, including the EACH2 (European ACquired Haemophilia),[3,5,7,8] SACHA (*Surveillance des Auto-antiCorps au cours de l'Hémophilie Acquise*)[9] and GTH (*Gesellschaft für Thrombose- und Hämostaseforschung*) registries[10-13] in Europe, as well as the HTRS (Hemostasis and Thrombosis Research Society) registry in the USA.[14] Moreover, a clinical trial investigating the use of a recently introduced treatment for AHA, recombinant porcine FVIII (rpFVIII), has been reported.[15] Here, we provide an updated set of recommendations based on this higher level of recent evidence, which has influenced clinical practices in AHA.

Methods

First, each author independently reviewed the 2009 international AHA recommendations,[1] identifying areas in which an update was required based on their personal experience and knowledge of current literature. Feedback was consolidated in a single document, and the latest available published evidence was assessed to ascertain the extent to which each proposed statement was justified, with particular emphasis on the results of the AHA registries summarized in Table 1. A PubMed literature search was conducted to identify additional relevant publications published since 2009. The search strategy and a PRISMA diagram are provided in the *Online Supplementary Material*.

Recommendations were formulated according to Guyatt *et al.*,[16] as detailed in *Online Supplementary Table S1*. We used GRADE 1 for recommendations ("we recommend") whenever a clear impact on patients' safety or benefit would outweigh risks and burden. More specifically, GRADE 1B was used when the statement was supported by data from at least one observational or interventional study, and when the recommendation seemed to apply to most patients in most circumstances without reservation; GRADE 1C was used for recommendations that lacked support from such evidence, but still appeared to be important for patients' safety or benefit. GRADE 2 ("we suggest") was used for weaker suggestions (2B for those with support from registries or studies, and 2C without) that may change when new data become available. Table 2 lists our main recommendations in the order in which they are discussed.

Diagnosis

AHA is rare, usually occurring unexpectedly, with physicians of different specialties potentially seeing patients initially. Therefore, a simplified diagnostic algorithm to assist physicians who may not have direct experience of AHA is required (Figure 1).

Typically, patients with AHA present with acute or recent bleeding symptoms, without a previous history of bleeding, with laboratory investigations showing an isolated prolonged activated partial thromboplastin time (APTT), reduced FVIII activity (FVIII:C) (<1% in 50% of cases; <5%

Table 1. Recent studies and registries in acquired hemophilia A.

Study name	Study type	Design	Collection period	Total n. of patients	Treatment/outcome data available information				Survival information (pts)	Reference
					Hemostatic therapy (n. of pts)*	Bleeding resolved (n. of pts or episodes)	IST (n. of pts)**	Remission (n. of pts)		
UK surveillance study	Registry	Prospective, consecutive	2001–2003	172	97	-	151	105	113	(2)
EACH2	Registry	Retrospective (3 years); prospective (3 years)	2003–2009	501	307	288 patients (1st episodes)	331	331	331	(3, 5, 7, 8)
SACHA	Registry	Prospective	2001–2006	82	38	38 patients	77	77	82	(9)
GTH-AH 01/2010	Registry	Prospective	2010–2013	102	70	162 episodes	101	101	102	(10-12, 37)
HTRS	Registry	Prospective	2004–2011	166	68 (rFVIIa only)	139 episodes	-	-		(14)
OBI-1	Clinical trial	Prospective, single-arm	-	29	28 (rpFVIII only)	28 patients	-	-	29	(15)

*Number of patients reported to have received recombinant activated factor VII (rFVIIa), activated prothrombin concentrate complex (APCC), factor VIII (FVIII) and/or recombinant porcine factor VIII (rpFVIII). Differences in the numbers reported vs. the total number of patients may be due to no treatment or lack of reporting. **Number of patients reported to have received immunosuppressive therapy. N: number; IST: immunosuppressive therapy; UK: United Kingdom; EACH2: European ACquired Haemophilia; SACHA: *Surveillance des Auto-antiCorps au cours de l'Hémophilie Acquise*; GTH: *Gesellschaft für Thrombose- und Hämostaseforschung*; HTRS: Hemostasis and Thrombosis Research Society; OBI-1: susoctocog alfa.

in 75% of cases; <40% in 100% of cases), and the presence of autoantibodies, detected by the Bethesda assay or by enzyme-linked immunosorbent assay (ELISA).[10] If the prothrombin time (PT) is prolonged, it must be attributed to other reasons, e.g., anticoagulant treatment. The bleeding pattern in AHA is characteristic of the disease, with subcutaneous bleeds being most common (observed in 80% of patients), followed by muscle, gastrointestinal, genitourinary, and retroperitoneal bleeds (in 45%, 21%, 9% and 9% of patients, respectively).[2] Joint bleeds, the hallmark of congenital hemophilia, are much less common in AHA.[2,8] In some cases, patients with AHA have not yet started to bleed at the time of diagnosis.[2] In these patients, a prolonged APTT may be the only sign of AHA.

Table 2. Summary of recommendations on the diagnosis and treatment of patients with acquired hemophilia A.

Recommendation	Grade according to Guyatt *et al.*[16]
Diagnosis	
• We recommend that the diagnosis of AHA should be considered whenever an acute or recent onset of bleeding is accompanied by an unexplained prolonged APTT.	1B
• We recommend that an unexplained APTT prolongation prior to surgery should be investigated and not ignored.	1C
• We recommend confirming a diagnosis of AHA by testing FVIII activity and inhibitor concentration using the Bethesda assay and/or an anti-FVIII ELISA.	1B
• We recommend testing for anti-porcine inhibitors using a modified Bethesda assay, if treatment with rpFVIII is an option.	1B
Hemostatic treatment	
• We recommend that hemostatic treatment be initiated in patients with AHA and clinically relevant bleeding irrespective of inhibitor titer and residual FVIII activity.	1B
• We recommend the use of rFVIIa, APCC or rpFVIII instead of human FVIII concentrates or desmopressin for the treatment of clinically relevant bleeding in patients with AHA.	1B
• We recommend that alternative treatment strategies from among the first-line agents be used if appropriate initial treatment fails.	1C
• For initial treatment with rFVIIa, we recommend bolus injection of 90 μg/kg every 2–3 h until hemostasis is achieved.	1B
• For initial treatment with APCC, we recommend bolus injections of between 50–100 U/kg every 8–12 h, up to a maximum of 200 U/kg/day.	1B
• For initial treatment with rpFVIII, we recommend the approved dose of 200 U/kg, followed by further doses to maintain trough levels >50%.	1B
• We recommend close monitoring of FVIII activity during therapy with rpFVIII.	1B
• We suggest the use of recombinant or plasma-derived human FVIII concentrates only if bypassing agents or rpFVIII are unavailable or ineffective and the inhibitor titer is low. We recommend against the use of desmopressin.	1B
• We recommend the prophylactic use of bypassing agents or rpFVIII to cover minor or major invasive procedures.	1B
Inhibitor eradication	
• We recommend IST in all patients with AHA. However, particular caution should be exercised in frail patients.	1B
• We suggest using prognostic markers (FVIII activity, inhibitor titer, if available) to individualize IST.	2B
• We suggest that patients with FVIII ≥1 IU/dL and inhibitor titer ≤20 BU at baseline receive first-line treatment with corticosteroids alone for 3–4 weeks.	2B
• We suggest combining corticosteroids with rituximab or a cytotoxic agent for first-line therapy in patients with FVIII <1 IU/dL or inhibitor titer >20 BU.	2B
• We suggest extending observation in patients who do not achieve remission with first-line IST but have continued improvement of FVIII activity and inhibitor titer.	2B
• We suggest second-line therapy with rituximab or a cytotoxic agent, whichever was not used during first-line therapy.	1B
• For corticosteroid therapy, we suggest prednisolone or prednisone at a dose of 1 mg/kg/day PO for a maximum of 4–6 weeks (followed by a tapered withdrawal).	2B
• We suggest rituximab at a dose of 375 mg/m^2 weekly for a maximum of 4 cycles.	2B
• As cytotoxic therapy, we suggest cyclophosphamide at a dose of 1.5–2 mg/kg/day PO for a maximum of 6 weeks, or MMF at a dose of 1 g/day for 1 week, followed by 2 g/day.	2B
• We do not recommend the use of high-dose human FVIII for immune tolerance induction in AHA.	2C
• We do not recommend the use of high-dose intravenous immunoglobulins for inhibitor eradication in patients with AHA.	1B
• We recommend follow-up after complete remission, using FVIII:C monitoring monthly during the first 6 months, every 2–3 months up to 12 months, and every 6 months during the second year and beyond, if possible.	1B
• In women with pregnancy-associated AHA, we suggest the same approach for IST as in other patients, but with a more careful consideration regarding the use of cytotoxic agents.	2C
• We recommend thromboprophylaxis according to ASH guidelines if FVIII:C has returned to normal levels. If indicated, therapy with anti-platelet drugs or oral anticoagulants should be initiated after normal FVIII:C levels have been achieved.	1C

AHA: acquired hemophilia A; APTT: activated partial thromboplastin time; FVIII: factor VIII; ELISA: enzyme-linked immunosorbent assay; rpFVIII: recombinant porcine FVIII; rFVIIa: recombinant activated factor VII; APCC: activated prothrombin complex concentrate; IST: immunosuppressive therapy; BU: Bethesda unit; PO: orally; MMF: mycophenolate mofetil; IVIG: intravenous immunoglobulins; FVIII:C: factor VIII activity; ASH: American Society of Hematology.

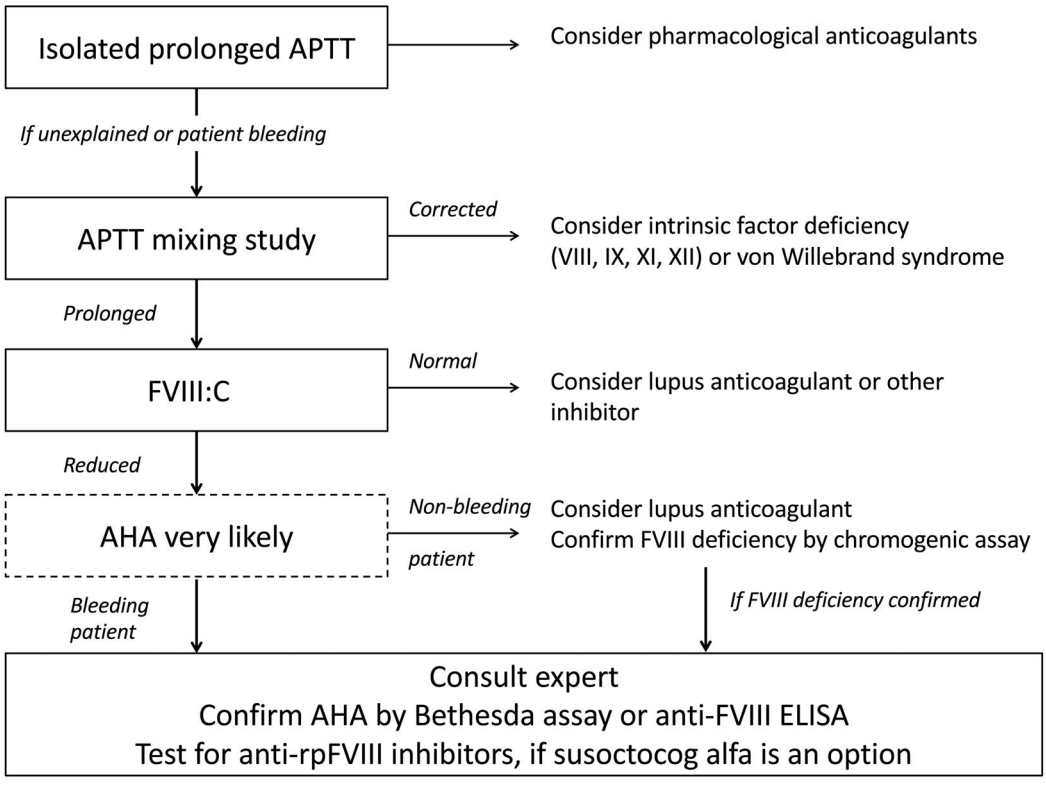

Figure 1. Diagnostic pathway for acquired hemophilia A. The activated partial thromboplastin time (APTT) mixing study will not be needed in an environment in which factor VIII (FVIII) activity is immediately available. Note that the presence of lupus anticoagulant does not exclude acquired hemophilia A. See the 'Diagnosis' section for more details. FVIII:C: factor VIII activity; AHA: acquired hemophilia A; ELISA: enzyme-linked immunosorbent assay; rpFVIII: recombinant porcine factor VIII.

A prolonged APTT is not specific to FVIII deficiency; other causes of APTT prolongation are much more common. Therefore, a prolonged APTT does not constitute a good predictive biomarker for bleeding, as evidenced by UK guidelines recommending against routine testing in unselected patients.[17] However, we recommend that an unexplained APTT prolongation should not be ignored if it is encountered before surgery or in bleeding patients. Measuring normal FVIII, factor IX (FIX) or factor XI (FXI) levels will exclude a bleeding diathesis in such cases and testing for conditions that prolong the APTT but do not pose a bleeding risk, such as lupus anticoagulant (LA) and factor XII deficiency, may be performed.

We recommend that the diagnosis of AHA should be considered whenever an acute or recent onset of bleeding is accompanied by an unexplained prolonged APTT (GRADE 1B).

We recommend that unexplained APTT prolongation prior to surgery should be investigated and not ignored (GRADE 1C).

Mixing tests

Coagulation factor deficiencies or coagulation factor inhibitors, including autoantibodies, LA, or pharmacological anticoagulants, may result in a prolonged APTT. To distinguish a factor deficiency from the presence of an inhibitory substance, mixing tests may be conducted if FVIII:C is not immediately available. AHA FVIII inhibitors are time- and temperature-dependent, so APTT results obtained immediately following the mixture of normal and patient plasma and after a 2 h incubation should be compared.[18] These tests are poorly standardized and cannot be used to establish or exclude AHA.[19] Further investigation is always required, and specific factor activity assays should be performed in parallel to facilitate early diagnosis.

Coagulation factor measurements

An isolated low FVIII level suggests a diagnosis of AHA. However, differential diagnoses of low FVIII:C include von Willebrand disease, congenital hemophilia A and the acquired von Willebrand syndrome.[19] A decrease in all intrinsic coagulation factors may be an *in vitro* false result arising from inhibitor-induced FVIII depletion in the substrate plasma.[20] LA-induced inhibition of phospholipid in the factor activity assay can also result in reduced factor levels. LA can be excluded by a negative diluted Russell viper venom test, which is typically not affected by FVIII inhibitors.[21] *Vice versa*, interference of LA on FVIII activity and the Bethesda assay can be excluded by using chromogenic substrate assays that are usually insensitive to LA.[22,23] Alternatively, a normal chromogenic assay FVIII:C excludes AHA in cases in which LA decreases one-stage FVIII assay results. However, it should be noted that AHA and LA are both autoimmune disorders that can co-exist in the same patient.[24,25]

Bethesda assay and modifications

The Bethesda assay was developed to detect and quantify FVIII alloantibodies in congenital hemophilia A that display linear type 1 kinetics.[26] It is also useful in detecting FVIII inhibitors in AHA, but these often display complex

and non-linear type 2 kinetics and so the assay may not be able to estimate the true potency of the autoantibody.[27] By consensus, the dilution closest to a 50% inhibition of FVIII in normal plasma is selected to estimate the inhibitor titer:[28] 1 Bethesda unit (BU) = the amount of inhibitor that neutralizes 50% of FVIII:C in normal plasma after incubation for 2 h at 37°C. Sometimes several dilutions are close to 50%, introducing some uncertainty in assigning the inhibitor titer. LA may interfere with the Bethesda assay and cause low-positive results. Immunoassays to detect anti-FVIII antibodies may help to distinguish LA from FVIII inhibitors in such cases.[13,29] The Nijmegen modification has been developed to improve specificity in the detection of low-titer inhibitors.[30] Pre-analytical heat inactivation of test plasma may improve assay accuracy/sensitivity.[31,32]

Anti-porcine inhibitor titer

The porcine FVIII inhibitor titer should be quantified if rpFVIII is considered as a treatment option. The assay is performed in the same way as the Bethesda assay, but with rpFVIII as the substrate instead of normal human plasma. In the rpFVIII OBI-1 pivotal clinical trial, patients with an anti-porcine titer of >20 BU were excluded.[15] Lower, albeit detectable, anti-porcine titers had implications for dosing of rpFVIII (see the 'Recombinant porcine FVIII' section for more details).

Anti-factor VIII enzyme-linked immunosorbent assay

A commercial anti-FVIII ELISA was shown to be sensitive and specific for diagnosing AHA.[13] It may be particularly helpful when interference with LA is suspected in a positive Bethesda assay, or if the Bethesda assay cannot be performed because rpFVIII has already been given. In addition, determining the anti-FVIII isotype may have prognostic implications, as shown for anti-FVIII IgA.[11]

We recommend confirming a diagnosis of AHA by testing FVIII activity and inhibitor concentration using the Bethesda assay and/or an anti-FVIII ELISA (GRADE 1B).

We recommend testing for anti-porcine inhibitors using a modified Bethesda assay, if treatment with rpFVIII is an option (GRADE 1B).

Hemostatic treatment

Treatment of bleeds in patients with AHA should be carried out in a specialist center; if immediate referral is not possible, expert advice should be sought. The first priority is to control acute bleeds and to prevent injury, including iatrogenic, that may provoke further bleeding. Surgical interventions and other invasive procedures should be performed only at specialist centers, or with expert advice. If a central venous line is required, it may be preferable to use the femoral vein. Venipuncture should be performed by experienced staff, and blood pressure measured only as often as deemed clinically relevant. Fasciotomy for intramuscular bleeds should be avoided because this can result in uncontrolled bleeding.[33,34] Early hemostatic therapy may prevent compartment syndrome in most patients or even reverse symptoms of developing compartment syndrome.[35] In the EACH2 registry, the only parameter that differed between patients who responded to treatment and those who did not was a delay in time to treatment.[8]

The decision to initiate treatment is guided by the clinical relevance of acute bleeds. Overall, approximately 70% of patients with AHA need hemostatic treatment. According to data from the UK and the EACH2 registry, approximately 30% of patients were untreated,[2,8] apparently because they had no bleeds or only non-severe subcutaneous bleeds. However, close observation may be warranted because even fatal bleeding can occur up to 5 months after first presentation in patients with persistent inhibitors.[2]

A lack of correlation between FVIII:C or inhibitor titer and bleeding phenotype in AHA has been described in many studies.[2,3,36] Inhibitor titer and FVIII:C should not therefore influence the decision to initiate treatment for clinically relevant bleeding.

Any hemostatic treatment is associated with a risk of arterial and thrombotic events, particularly in elderly patients and those with risk factors or recent thromboembolic events. Acute illness and immobility in bleeding patients with AHA is a risk factor for thromboembolism; however, controlling acute bleeds should usually be prioritized.

We recommend that hemostatic treatment be initiated in patients with AHA and clinically relevant bleeding irrespective of inhibitor titer and residual FVIII activity (GRADE 1B).

Choice of first- and second-line treatment for acute bleeds

Parallel-group, comparative-treatment studies are not available in AHA. Propensity score-matched analysis of registry data on bypassing agents, including recombinant activated factor VII (rFVIIa; NovoSeven®) and activated prothrombin concentrate complex (APCC; FEIBA®), as well as a single-arm clinical trial on rpFVIII did not show a clear efficacy or safety benefit of one drug over the others.[8,15,37] A similar analysis showed that the efficacy of human FVIII concentrates and desmopressin was clearly lower than that of bypassing agents in EACH2.[8] Therefore, APCC, rFVIIa and rpFVIII can all be considered appropriate first-line treatments (Figure 2). The final choice will be influenced mostly by the anti-porcine titer, as well as availability, cost and ability to monitor rpFVIII.

We recommend the use of rFVIIa, APCC or rpFVIII instead of human FVIII concentrates or desmopressin for the treatment of clinically relevant bleeding in patients with AHA (GRADE 1B).

Patients should be closely monitored for treatment efficacy. Such monitoring is based mainly on clinical judgment. Depending on the bleeding site, serial blood count measurements, inspection and palpation of bleeding sites, patient-reported changes in pain or mobility, as well as imaging studies should be taken into consideration.[38] When using rpFVIII treatment, monitoring of FVIII:C can also help to guide subsequent dosing, although clinical efficacy may not always correlate with FVIII:C.[15] Depending on the severity of the condition, failure to improve bleeding symptoms or the appearance of new symptoms may indicate the need for treatment intensification or switching to one of the alternative therapies.

We recommend that alternative treatment strategies from among the first-line agents be used if appropriate initial treatment fails (GRADE 1C).

Recombinant activated factor VII

The efficacy of rFVIIa [eptacog alfa (activated)] in AHA was recently addressed in a systematic literature review.[37] A total of 12 studies, reporting on 671 patients and 1,063

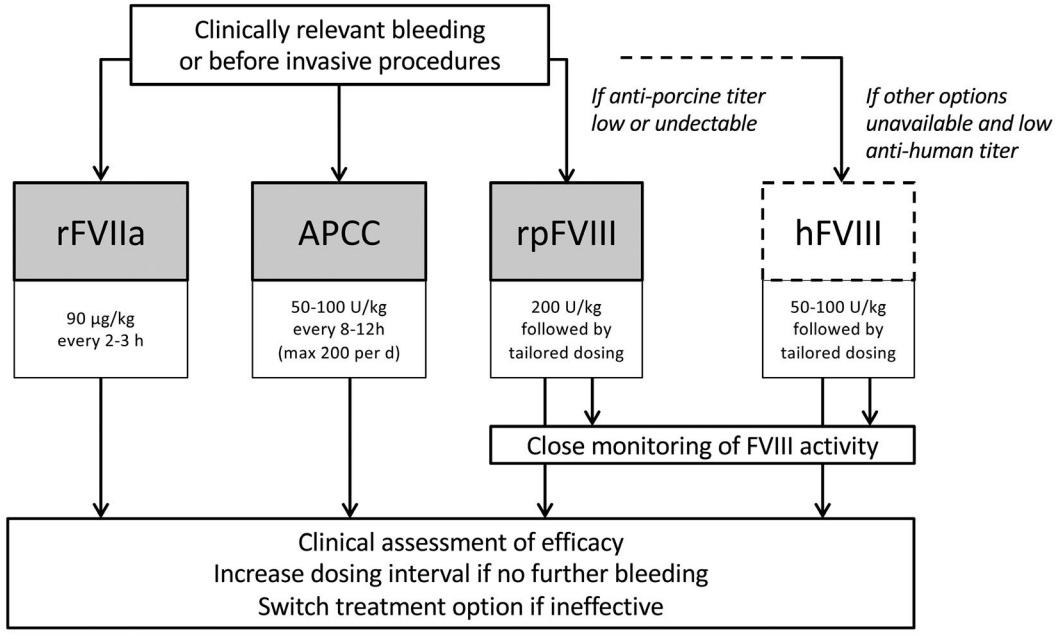

Figure 2. Choice and monitoring of hemostatic therapy in acquired hemophilia A. rFVIIa, recombinant activated factor VII (eptacog alfa); APCC, activated prothrombin complex concentrate; rpFVIII: recombinant porcine factor VIII (susoctocog alfa), hFVIII, human (plasma-derived or recombinant) factor VIII; h: hour; d: day.

bleeds treated with rFVIIa, were analyzed. The reported median initial rFVIIa dose was 90–105 µg/kg body weight, with ranges between 25–181 µg/kg in individual studies. Doses were repeated mostly every 2–3 h, with the median total number of doses being 10–28. rFVIIa was used as first-line treatment in the majority of cases, and 39–90% of treated bleeds were severe. There was considerable variability across the 12 studies in terms of how hemostatic effectiveness was defined. The only effectiveness outcome that provided sufficient data was defined as 'complete' or 'partial response', available for six studies. In five of these six studies, treatment efficacy was >90%, at both patient and bleed levels.

The safety of rFVIIa in AHA was also addressed in the same systematic review.[37] Thromboembolic and cardiovascular events were assessed in eight of the 12 studies and reported in 0–5% of patients. Mortality was included in ten of the studies, with eight reporting no mortality related to rFVIIa. The two studies that reported deaths from thromboembolic events potentially related to rFVIIa were a Japanese surveillance study (2 deaths in 132 rFVIIa-treated patients)[39] and the GTH study (3 deaths in 61 rFVIIa-treated patients).[10] One patient in the GTH study died from portal vein thrombosis on day 6 while on rFVIIa for 3 days. The other two patients died of ischemic stroke on days 5 and 35 of rFVIIa treatment; these two patients received rFVIIa together with tranexamic acid. In EACH2, thrombotic events were reported in 5/174 (2.9%) patients in association with rFVIIa treatment.[8]

For initial treatment with rFVIIa, we recommend bolus injections of 90 µg/kg every 2–3 h until hemostasis is achieved (GRADE 1B).

Activated prothrombin complex concentrate

APCC is used for the treatment and prevention of bleeds in patients with congenital hemophilia with inhibitors,[40-42] and is widely used for AHA, although no systematic reviews are available. The recommended dose is 50–100 U/kg every 8–12 h, up to a maximum of 200 U/kg/day.[1] In the EACH2 registry, propensity score-matched analysis indicated indistinguishable efficacy for APCC compared with rFVIIa, with >90% bleed control rates when used as first-line treatment.[8] An earlier study collected data from 34 cases in three centers in the USA over 10 years.[43] A total of 55 bleeding events were observed and the response rate was 76% and 100% for patients with severe and moderate bleeds, respectively.[43] APCC has also been used for secondary prophylaxis.[44,45]

In a retrospective study, APCC exhibited a favorable safety profile indicating that it is well-tolerated with few adverse events.[46] Thrombotic events, including myocardial infarction and venous thrombosis, were mostly reported in patients with additional risk factors.[46,47] In EACH2, thrombotic events with APCC were reported in 3/63 (4.8%) patients.[8] Disseminated intravascular coagulation has been observed following APCC administration in some patients receiving doses higher than 200 U/kg/day.[47] APCC is contraindicated in patients with signs of disseminated intravascular coagulation.

For initial treatment with APCC, we recommend bolus injections of between 50–100 U/kg every 8–12 h, up to a maximum of 200 U/kg/day (GRADE 1B).

Recombinant porcine factor VIII

Although animal-derived concentrates are no longer available, porcine plasma-derived FVIII concentrate was used extensively in the past for the treatment of AHA because anti-FVIII autoantibodies often exhibited low cross-reactivity with porcine FVIII.[48] rpFVIII (susoctocog alfa) was assessed in a prospective, single-arm clinical study.[15] Patients with AHA and a serious bleed were eligible, but were excluded if they had an anti-rpFVIII inhibitor

titer >20 BU. rpFVII was administered at an initial dose of 200 U/kg. Subsequent doses and dosing intervals were assigned by the treating physician based on the clinical response and FVIII:C measured, with the aim of maintaining FVIII:C >80% for severe bleeds of particular concern" (e.g. severe mucous, intracranial, retro- or intra-abdominal, genitourinary, neck, traumatic or postoperative bleeds), and >50% for all other bleeds. Clinical assessment after 24 h indicated an effective response in 24/28 patients and a partial response in 4/28 patients. The bleeding was controlled at the time of the final dose in 24/28 (86%) patients. FVIII levels measured immediately after the first dose and 24 h later were 22–540% and 2–369% of normal, respectively. The presence of cross-reacting antibodies did not appear to affect the clinical response after 24 h, but patients with cross-reactivity needed higher doses in the first 24 h than patients without cross-reactivity (median 1,400 and 300 U/kg, respectively). Cross-reacting anti-rpFVIII inhibitors were found in 44% of patients in a recent study.[49] A retrospective study used a lower starting dose of 100 U/kg in six of seven patients given rpFVIII as second-line therapy, with five of these six patients achieving FVIII:C >100% after infusion (one patient had unmeasurable FVIII:C).[50] Overall, treatment was effective in five of the seven patients. These data suggest that, although the approved initial dose for rpFVIII is 200 U/kg, an initial dose of 100 U/kg appears to be sufficient for most patients, and FVIII:C should be closely monitored to prevent excess FVIII:C. The baseline anti-rpFVIII titer may help to identify those patients for whom rpFVIII is unlikely to be efficacious.

In the pivotal trial, rpFVIII was well-tolerated in all patients.[15] A total of 5/18 patients who did not have anti-rpFVIII inhibitors at baseline developed *de novo* anti-rpFVIII antibodies after 8–85 days, prompting discontinuation of the drug in two patients. No patient developed thromboembolic events.

For initial treatment with rpFVIII, we recommend the approved dose of 200 U/kg, followed by further doses to maintain trough levels >50% (GRADE 1B).

We recommend close monitoring of FVIII activity during therapy with rpFVIII (GRADE 1B).

Human factor VIII concentrates and desmopressin

The 2009 international AHA recommendations suggested the use of human FVIII concentrates or desmopressin only if therapy with bypassing agents was not available.[1] In the EACH2 registry, an efficacy assessment of the treatment of first bleeding episodes could be performed in 288 patients, of whom 219 (76%) received bypassing agents and 69 (24%) received human FVIII or desmopressin.[8] Patients administered human FVIII concentrates or desmopressin had higher initial FVIII levels, lower inhibitor titers, less severe bleeds and received tranexamic acid more often. When comparing propensity score-matched groups (n=60 per group), significantly lower efficacy rates were observed for treatment with FVIII or desmopressin (68%) compared with bypassing agents (93%). Of note, there was no matching for tranexamic acid use in this comparison. There may be a risk of fluid overload, heart failure and severe hyponatremia with desmopressin and it should not, therefore, be used in elderly patients.[51]

We suggest the use of recombinant or plasma-derived human FVIII concentrates only if bypassing agents or rpFVIII are unavailable or ineffective and the inhibitor titer is low. We recommend against the use of desmopressin (GRADE 1B).

Anti-fibrinolytics and other treatments

Some controversy persists regarding the use of anti-fibrinolytic agents in conjunction with bypassing agents. Anti-fibrinolytic agents should be used with caution in patients treated with APCC.[52] However, in a small case series of combination therapy of tranexamic acid with APCC, which included one patient with AHA, no thromboembolic events or disseminated intravascular coagulation were reported.[53] Combining tranexamic acid with rFVIIa has been of less concern traditionally.[54] In the EACH2 registry, 17% of rFVIIa patients received ancillary anti-fibrinolytic therapy compared with only 5% of patients treated with APCC.[8] In the GTH study, 32/102 (31%) patients received tranexamic acid, 63/102 (62%) received rFVIIa, and 21 (21%) received both concomitantly.[10] Of the three fatal thromboembolic events observed in relation to rFVIIa, two occurred in the 21 patients receiving concomitant tranexamic acid and rFVIIa.[10] We, therefore, suggest caution when combining tranexamic acid with bypassing agents. Topical tranexamic acid may be used as an alternative for some types of bleeding.

A plasma-derived, purified FVIIa/factor X concentrate (MC710, Byclot) is approved in Japan for the treatment of acute bleeds in patients with inhibitors against FVIII or FIX.[55] Studies in AHA are not available.

Emicizumab is a recombinant, humanized, bispecific monoclonal antibody with FVIII-mimetic activity. It was recently licensed for prophylaxis in patients with hemophilia A with or without inhibitors.[56] The drug has been used in a few patients with AHA with severe bleeding.[57,58] However, the safety and efficacy of emicizumab in AHA is unknown and so this antibody should not be used in this group of patients outside of clinical trials. This is particularly relevant for elderly patients, in whom cardiovascular events are more common, and in women who are considering use of hormonal therapy or future pregnancy, as emicizumab is an IgG4 antibody and may therefore be transferred across the placenta. Given its long half-life of approximately 1 month, patients treated with emicizumab are exposed for up to 6 months after their last dose.

Invasive procedures

In patients with AHA, even minor invasive procedures can result in significant bleeding;[36,59] therefore, particular caution should be exercised during all procedures and surgery and, if possible, they should be delayed until after the inhibitor has been eradicated. Use of a bypassing agent or rpFVIII is usually required for central venous access, taking biopsies or performing other invasive procedures.

We recommend the prophylactic use of bypassing agents or rpFVIII to cover minor or major invasive procedures (GRADE 1B).

Immunosuppressive therapy

Goals of immunosuppressive therapy and definition of remission

The goal of immunosuppressive therapy (IST) is to reduce the risk of bleeding by shortening the time to achieve remission of AHA. Spontaneous remissions have been observed in patients not treated with IST, but this outcome is unpredictable.[60] Definitions of remission vary across studies and registries. The UK surveillance study defined complete remission as: FVIII normal, inhibitor undetectable, and immunosuppression stopped or

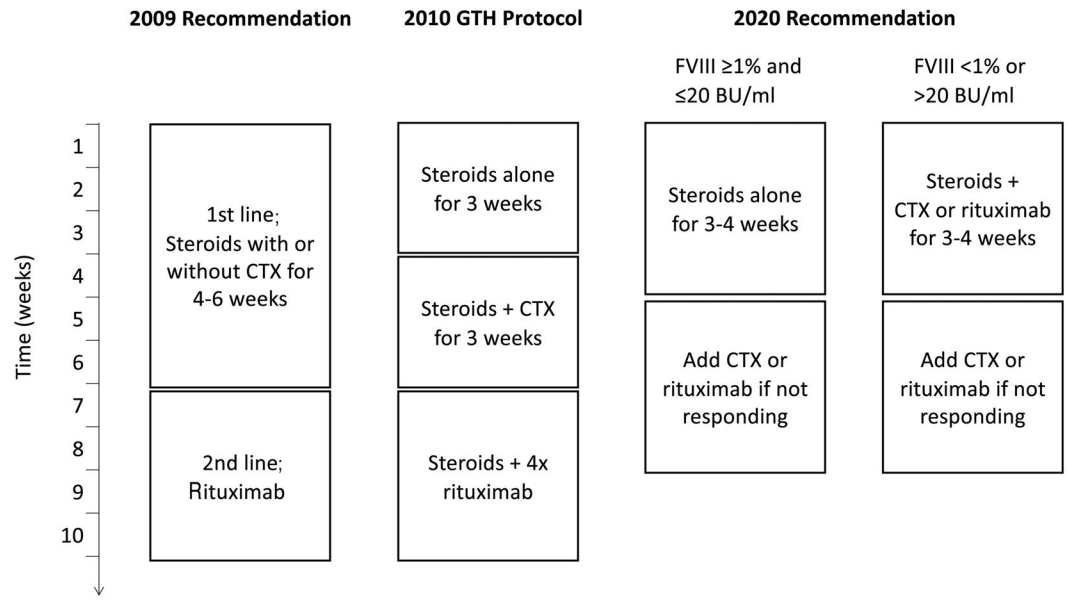

Figure 3. Recommendations regarding Immunosuppressive therapy in patients with acquired hemophilia A. Comparison of immunosuppressive therapy regimens recommended in the 2009 international recommendations by Huth-Kühne *et al.*[1] the GTH study[10] and the current paper. FVIII; factor VIII activity; BU: Bethseda unit; CTX, cyclophosphamide.

reduced to doses used before AHA developed without relapse.[2] The GTH study also included a definition for partial remission: FVIII restored to >50% and no bleeding after stopping any hemostatic treatment for at least 24 h.[10]

General strategy and prognostic factors

The 2009 international AHA guidelines recommended starting IST in all patients with AHA immediately following diagnosis.[1] This recommendation was mainly based on the high bleed-related mortality in earlier studies and the observation that the initial bleeding tendency was not predictive of later major or even fatal bleeding.[61] Initial treatment with corticosteroids alone or in combination with cyclophosphamide was recommended for up to 6 weeks, while second-line therapy with rituximab was suggested if first-line IST failed or was contraindicated (Figure 3).

The GTH-AH 01/2010 study protocol was designed as a variant of this recommendation and was the first IST protocol investigated prospectively.[10] Patients were enrolled ≤7 days after starting any IST, and follow-up data were collected weekly until complete remission was achieved. The 1-year survival rate was 68%. The most frequent cause of death among the 34 patients who died was infection (n=16), followed by cardiovascular disorders (n=6), underlying disorders (n=3), and bleeding (n=3). Fourteen deaths were considered to be directly related to IST. These results established that IST-related mortality, in particular infection, exceeds the current risk of fatal bleeding in AHA. Patients with a poor World Health Organization (WHO) performance status (>2) at presentation had a 4-fold increased risk of mortality. Therefore, careful individual consideration of the requirement for and contraindications against IST, its intensity and timing is warranted in frail patients with AHA and should be a priority for future research. IST should be stopped if severe side effects to treatment develop.

We recommend IST in all patients with AHA. However, particular caution should be exercised in frail patients (GRADE 1B).

The success of IST, in particular the time to achieve remission, varies largely among patients. In the GTH study, 85/102 (83%) patients achieved a partial remission after a median time of 5 weeks (range, 1–52 weeks).[10] FVIII:C at presentation was the most important prognostic factor; patients with FVIII <1% achieved partial remission less often compared with other patients (77 *vs*. 89%, respectively) and after a significantly longer time on IST (43 *vs*. 24 days, respectively). Anti-FVIII IgA autoantibodies were predictors of relapse as observed in 45% of patients with anti-FVIII IgA titers >1:80. These data suggest that IST should be individualized in patients with AHA according to baseline characteristics, although interventional studies with stratified protocols have not been performed.

We suggest using prognostic markers (FVIII activity, inhibitor titer, if available) to individualize IST (GRADE 2B).

The benefit of combining corticosteroids with other immunosuppressants for first-line therapy is uncertain and cannot be concluded from the published observational studies. Combination therapy shortened the time to remission in the EACH2 registry[7] but not in the UK surveillance study.[2] GTH data indicated that achieving partial remission within 21 days of steroid therapy was unlikely (negative predictive value, 84%) if patients had FVIII <1% or an inhibitor titer >20 BU.[10] We, therefore, suggest combination therapy in these patients. In all other patients (i.e., those with FVIII ≥1% and inhibitor ≤20 BU), we suggest using steroids alone, because the benefit of more intense regimens is uncertain, and the risk of infectious complications currently exceeds the risk of bleeding.

We suggest that patients with FVIII ≥1 IU/dL and inhibitor titer ≤20 BU at baseline receive first-line treatment with corticosteroids alone for 3–4 weeks (GRADE 2B).

We suggest combining corticosteroids with rituximab or a cyto-

toxic agent for first-line therapy in patients with FVIII <1 IU/dL or inhibitor titer >20 BU (GRADE 2B).

In the GTH study, 23 patients had a continuous improvement of their FVIII:C and/or inhibitor titer while not achieving partial remission during the first 3 weeks on steroids.[10] These patients were not escalated to second-line IST and all achieved partial remission after a median of 29 days.

We suggest extending observation in patients who do not achieve remission with first-line IST but have continued improvement of FVIII activity and inhibitor titer (GRADE 2B).

Patients not responding to steroids after 3 weeks were escalated to second-line therapy with cyclophosphamide, and later rituximab, in the GTH study. Eighty-three percent of these patients achieved remission.

We suggest second-line therapy with rituximab or a cytotoxic agent, whichever was not used during first-line therapy (GRADE 1B).

Corticosteroids

Corticosteroid therapy with prednisolone or prednisone 1 mg/kg/day PO for 4–6 weeks was suggested in the 2009 international AHA recommendations.[1] This regimen was also used in the GTH study.[10]

For corticosteroid therapy, we suggest prednisolone or prednisone at a dose of 1 mg/kg/day PO for a maximum of 4–6 weeks (followed by tapered withdrawal) (GRADE 2B).

Rituximab

Second-line therapy with rituximab for inhibitor eradication was recommended in the 2009 international AHA recommendations.[1] Rituximab is often used at the licensed dose for the treatment of non-Hodgkin lymphoma (i.e., 375 mg/m^2/week), but has also been used in lower doses of 100 mg/week in some reported cases.[62-65] The drug is licensed for the treatment of rheumatoid arthritis at a fixed dose of 1,000 mg on days 1 and 15.[66] This regimen has also been used in immune thrombocytopenia.[67,68] Although not licensed for the treatment of AHA, we suggest adding rituximab to first-line IST in patients with poor prognostic markers, in those with contraindications against corticosteroids, or as second-line therapy.

We suggest rituximab at a dose of 375 mg/m^2 weekly for a maximum of four cycles (GRADE 2B).

Cytotoxic agents

Cyclophosphamide therapy was recommended at a dose of 1.5–2 mg/kg/day PO in the 2009 international AHA recommendations.[1] Intravenous pulse therapy of cyclophosphamide 500–1,000 mg/m^2 is licensed for the treatment of severe lupus nephritis and Wegener granulomatosis, although there is no experience in AHA.[69] Recently, the use of mycophenolate mofetil (MMF) was reported in a retrospective collection of 11 AHA patients.[70] MMF was started at 1 g/day and increased to 2 g/day after 1 week. Among seven patients given MMF together with prednisolone as first-line IST, one complete and five partial remissions were achieved after 4 to 77 weeks; among four patients receiving MMF for second-line IST after a median of 14 weeks of other treatments, three complete remissions and one parital remission were observed. Close monitoring for leukopenia, thrombocytopenia, and infections is required during treatment with any cytotoxic agent. These agents should not be used in pregnancy or in women who are breastfeeding.

As cytotoxic therapy, we suggest cyclophosphamide at a dose of 1.5–2 mg/kg/day PO for a maximum of 6 weeks, or MMF at a dose of 1 g/day for 1 week, followed by 2 g/day (GRADE 2B).

Immunoadsorption, immune tolerance regimens and immunoglobulins

Immunoadsorption protocols have been used successfully to deplete inhibitors in patients with AHA. The modified Bonn-Malmö protocol combined immunoadsorption with high-dose FVIII, intravenous immunoglobulins and immunosuppression.[71] Inhibitors were eliminated after a median of 3 days. Whether the overall response rate is superior to that achieved with IST alone remains unclear, as does the relative contribution of FVIII and immunoglobulins in this regimen. We, therefore, suggest that this protocol is used only in patients with particularly severe bleeding or those who are resistant to other therapy.

Similarly to immune tolerance in hemophilia A with inhibitors, high-dose FVIII has been combined with IST by several investigators in AHA.[71-74] However, a conclusion as to whether FVIII increased the efficacy of IST cannot be reached based on these studies due to the lack of a control group for comparison. We, therefore, suggest this treatment only in patients with life-threatening bleeding in whom the available hemostatic therapies have failed.

We do not recommend the use of high-dose human FVIII for immune tolerance induction in AHA (GRADE 2C).

High-dose intravenous immunoglobulins are known to be effective in idiopathic thrombocytopenic purpura; however, they had little or no effect in patients with AHA in the one currently available study on this therapeutic strategy.[75]

We do not recommend use of high-dose intravenous immunoglobulins for inhibitor eradication in patients with AHA (GRADE 1B).

Follow-up

Adverse events occurred in 66% of patients in the GTH registry (including IST-related events in 50%): 25% of the events occurred after more than 100 days.[10] Relapse occurred in 12–18% of EACH2 patients after a median time of 138 days.[7] Given the risks of adverse events and of recurrence, patients should be closely monitored until they achieve complete remission and for several months thereafter. Monitoring of FVIII:C is more sensitive than APTT for detecting recurrence.

We recommend follow-up after complete remission, using FVIII:C monitoring monthly during the first 6 months, every 2–3 months up to 12 months, and every 6 months during the second year and beyond, if possible (GRADE 1B).

Pregnancy-associated acquired hemophilia A

Hemostatic therapy and the response to it were similar in 42 women with pregnancy-associated AHA as compared with other patients in the EACH2 registry.[5] A total of 70% of the women received steroids alone for IST, while the rest received steroids and rituximab, cytotoxic agents, or intravenous immunoglobulins. The success rates and times to remission were similar in these women compared with those in other AHA patients in the registry. The mortality rate was lower than in the other patients, possibly because of the younger age of women with pregnancy-associated AHA, and the risk of relapse

appeared to be low (2 patients). We do not, therefore, recommend a different approach for IST in pregnancy-associated AHA, except for more careful consideration regarding the use of cytotoxic agents in women of childbearing age because of the potential of these drugs to reduce fertility and cause embryotoxicity.

In women with pregnancy-associated AHA, we suggest the same approach for IST as in other patients, but with more careful consideration regarding the use of cytotoxic agents (GRADE 2C).

Thromboprophylaxis

Cardiovascular events, including thrombosis, myocardial infarction and stroke, were recorded as the cause of death in 6–7% of patients with AHA in the GTH and SACHA registries.[9,10] It therefore appears justified to recommend thromboprophylaxis according to the 2018 American Society of Hematology (ASH) guidelines in non-bleeding patients whose FVIII:C has returned to normal.[76] If an indication for antiplatelet drugs (e.g., history of myocardial infarction or stroke) or oral anticoagulants (e.g., atrial fibrillation, artificial heart valves or recurrent venous thromboembolism) exists, the use of these drugs should be initiated after FVIII has returned to normal levels.

We recommend thromboprophylaxis according to ASH guidelines if FVIII:C has returned to normal levels. If indicated, therapy with anti-platelet drugs or oral anticoagulants should be initiated, after normal FVIII:C levels have been achieved (GRADE 1C).

Acknowledgments

Editorial support was provided by Physicians World GmbH, Mannheim, Germany, supported by Novo Nordisk Health Care AG, Zürich, Switzerland.

References

1. Huth-Kuhne A, Baudo F, Collins P, et al. International recommendations on the diagnosis and treatment of patients with acquired hemophilia A. Haematologica. 2009;94(4):566-575.
2. Collins PW, Hirsch S, Baglin TP, et al. Acquired hemophilia A in the United Kingdom: a 2-year national surveillance study by the United Kingdom Haemophilia Centre Doctors' Organisation. Blood. 2007;109(5):1870-1877.
3. Knoebl P, Marco P, Baudo F, et al. Demographic and clinical data in acquired hemophilia A: results from the European Acquired Haemophilia Registry (EACH2). J Thromb Haemost. 2012;10(4):622-631.
4. Napolitano M, Siragusa S, Mancuso S, Kessler CM. Acquired haemophilia in cancer: a systematic and critical literature review. Haemophilia. 2018;24(1):43-56.
5. Tengborn L, Baudo F, Huth-Kuhne A, et al. Pregnancy-associated acquired haemophilia A: results from the European Acquired Haemophilia (EACH2) registry. BJOG. 2012;119(12):1529-1537.
6. Collins P, Chalmers E, Hart D, et al. Diagnosis and management of acquired coagulation inhibitors: a guideline from UKHCDO. Br J Haematol. 2013;162(6):758-773.
7. Collins P, Baudo F, Knoebl P, et al. Immunosuppression for acquired hemophilia A: results from the European Acquired Haemophilia Registry (EACH2). Blood. 2012;120(1):47-55.
8. Baudo F, Collins P, Huth-Kuhne A, et al. Management of bleeding in acquired hemophilia A: results from the European Acquired Haemophilia (EACH2) Registry. Blood. 2012;120(1):39-46.
9. Borg JY, Guillet B, Le Cam-Duchez V, Goudemand J, Levesque H, Group SS. Outcome of acquired haemophilia in France: the prospective SACHA (Surveillance des Auto antiCorps au cours de l'Hemophilie Acquise) registry. Haemophilia. 2013;19(4):564-570.
10. Tiede A, Klamroth R, Scharf RE, et al. Prognostic factors for remission of and survival in acquired hemophilia A (AHA): results from the GTH-AH 01/2010 study. Blood. 2015;125(7):1091-1097.
11. Tiede A, Hofbauer CJ, Werwitzke S, et al. Anti-factor VIII IgA as a potential marker of poor prognosis in acquired hemophilia A: results from the GTH-AH 01/2010 study. Blood. 2016;127(19):2289-2297.
12. Holstein K, Liu X, Smith A, et al. Factor VIII activity and risk of bleeding in acquired hemophilia A: results from the GTH-AH 01/2010 study. Blood. 2020 Feb 20. [Epub ahead of print]
13. Werwitzke S, Geisen U, Nowak-Gottl U, et al. Diagnostic and prognostic value of factor VIII binding antibodies in acquired hemophilia A: data from the GTH-AH 01/2010 study. J Thromb Haemost. 2016;14(5):940-947.
14. Ma AD, Kessler CM, Al-Mondhiry HA, Gut RZ, Cooper DL. Use of recombinant activated factor VII for acute bleeding episodes in acquired hemophilia: final analysis from the Hemostasis and Thrombosis Research Society Registry acquired hemophilia study. Blood Coagul Fibrinolysis. 2016;27(7):753-760.
15. Kruse-Jarres R, St-Louis J, Greist A, et al. Efficacy and safety of OBI-1, an antihaemophilic factor VIII (recombinant), porcine sequence, in subjects with acquired haemophilia A. Haemophilia. 2015;21(2):162-170.
16. Guyatt G, Oxman AD, Akl EA, et al. GRADE guidelines: 1. Introduction-GRADE evidence profiles and summary of findings tables. J Clin Epidemiol. 2011;64(4):383-394.
17. Chee YL, Crawford JC, Watson HG, Greaves M. Guidelines on the assessment of bleeding risk prior to surgery or invasive procedures. Br J Haematol. 2008;140(5):496-504.
18. Lossing TS, Kasper CK, Feinstein DI. Detection of factor VIII inhibitors with the partial thromboplastin time. Blood. 1977;49(5):793-797.
19. Tiede A, Werwitzke S, Scharf RE. Laboratory diagnosis of acquired hemophilia A: limitations, consequences, and challenges. Semin Thromb Hemost. 2014;40(7):803-811.
20. Kasper CK. Laboratory tests for factor VIII inhibitors, their variation, significance and interpretation. Blood Coagul Fibrinolysis. 1991;2(Suppl 1):7-10.
21. Blanco AN, Cardozo MA, Candela M, Santarelli MT, Perez Bianco R, Lazzari MA. Anti-factor VIII inhibitors and lupus anticoagulants in haemophilia A patients. Thromb Haemost. 1997;77(4):656-659.
22. Chandler WL, Ferrell C, Lee J, Tun T, Kha H. Comparison of three methods for measuring factor VIII levels in plasma. Am J Clin Pathol. 2003;120(1):34-39.
23. de Maistre E, Wahl D, Perret-Guillaume C, et al. A chromogenic assay allows reliable measurement of factor VIII levels in the presence of strong lupus anticoagulants. Thromb Haemost. 1998;79(1):237-238.
24. Taher A, Abiad R, Uthman I. Coexistence of lupus anticoagulant and acquired haemophilia in a patient with monoclonal gammopathy of unknown significance. Lupus. 2003;12(11):854-856.
25. Seethala S, Collins NP Jr, Comerci G Jr. An unusual etiology for elevation of activated partial thromboplastin time (aPTT) in SLE: acquired hemophilia and lupus anticoagulant. Case Report Hematol. 2013;2013:521785.
26. Kasper CK, Aledort L, Aronson D, et al. Proceedings: a more uniform measurement of factor VIII inhibitors. Thromb Diath Haemorrh. 1975;34(2):612.
27. Gawryl MS, Hoyer LW. Inactivation of factor VIII coagulant activity by two different types of human antibodies. Blood. 1982;60(5):1103-1109.
28. Kitchen S, McCraw A, Echenagucia M. Diagnosis of Haemophilia and Other Bleeding Disorders (second edition). World Federation of Hemophilia, 2010.
29. Rampersad AG, Boylan B, Miller CH, Shapiro A. Distinguishing lupus anticoagulants from factor VIII inhibitors in haemophilic and non-haemophilic patients. Haemophilia. 2018;24(5):807-814.
30. Verbruggen B, Novakova I, Wessels H, Boezeman J, van den Berg M, Mauser-Bunschoten E. The Nijmegen modification of the Bethesda assay for factor VIII:C inhibitors: improved specificity and reliability. Thromb Haemost. 1995;73(2):247-251.
31. Batty P, Platton S, Bowles L, Pasi KJ, Hart DP. Pre-analytical heat treatment and a FVIII ELISA improve factor VIII antibody detection in acquired haemophilia A. Br J Haematol. 2014;166(6):953-956.
32. Boylan B, Miller CH. Effects of pre-analytical heat treatment in factor VIII (FVIII) inhibitor assays on FVIII antibody levels. Haemophilia. 2018;24(3):487-491.
33. Pham TV, Sorenson CA, Nable JV. Acquired

factor VIII deficiency presenting with compartment syndrome. Am J Emerg Med. 2014;32(2):195.
34. Dachman AF, Margolis H, Aboulafia E. Does Sjogren's syndrome predispose surgical patients to acquired hemophilia? J Am Osteopath Assoc. 1995;95(2):115-118, 121.
35. Lusher JM. Early treatment with recombinant factor VIIa results in greater efficacy with less product. Eur J Haematol Suppl. 1998;63:7-10.
36. Delgado J, Jimenez-Yuste V, Hernandez-Navarro F, Villar A. Acquired haemophilia: review and meta-analysis focused on therapy and prognostic factors. Br J Haematol. 2003;121(1):21-35.
37. Tiede A, Worster A. Lessons from a systematic literature review of the effectiveness of recombinant factor VIIa in acquired haemophilia. Ann Hematol. 2018;97(10):1889-1901.
38. Tiede A, Giangrande P, Teitel J, et al. Clinical evaluation of bleeds and response to haemostatic treatment in patients with acquired haemophilia: a global expert consensus statement. Haemophilia. 2019;25(6):969-978.
39. Seita I, Amano K, Higasa S, Sawada A, Kuwahara M, Shima M. Treatment of acute bleeding episodes in acquired haemophilia with recombinant activated factor VII (rFVIIa): analysis from 10-year Japanese postmarketing surveillance. J Thromb Haemost. 2013;11(Suppl. 2):119.
40. Dimichele D, Negrier C. A retrospective postlicensure survey of FEIBA efficacy and safety. Haemophilia. 2006;12(4):352-362.
41. Leissinger CA, Becton DL, Ewing NP, Valentino LA. Prophylactic treatment with activated prothrombin complex concentrate (FEIBA) reduces the frequency of bleeding episodes in paediatric patients with haemophilia A and inhibitors. Haemophilia. 2007;13(3):249-255.
42. Tjonnfjord GE, Holme PA. Factor eight inhibitor bypass activity (FEIBA) in the management of bleeds in hemophilia patients with high-titer inhibitors. Vasc Health Risk Manag. 2007;3(4):527-531.
43. Sallah S. Treatment of acquired haemophilia with factor eight inhibitor bypassing activity. Haemophilia. 2004;10(2):169-173.
44. Zanon E, Milan M, Gamba G, et al. Activated prothrombin complex concentrate (FEIBA®) for the treatment and prevention of bleeding in patients with acquired haemophilia: a sequential study. Thromb Res. 2015;136(6):1299-1302.
45. Arokszallasi A, Razso K, Ilonczai P, et al. A decade-long clinical experience on the prophylactic use of activated prothrombin complex concentrate in acquired haemophilia A: a case series from a tertiary care centre. Blood Coagul Fibrinolysis. 2018;29(3):282-287.
46. Aledort LM. Comparative thrombotic event incidence after infusion of recombinant factor VIIa versus factor VIII inhibitor bypass activity. J Thromb Haemost. 2004;2(10):1700-1708.
47. Ehrlich HJ, Henzl MJ, Gomperts ED. Safety of factor VIII inhibitor bypass activity (FEIBA): 10-year compilation of thrombotic adverse events. Haemophilia. 2002;8(2):83-90.
48. Giangrande PL. Porcine factor VIII. Haemophilia. 2012;18(3):305-309.
49. Turkantoz H, Konigs C, Knobl P, et al. Cross-reacting inhibitors against recombinant porcine factor VIII in acquired hemophilia A: data from the GTH-AH 01/2010 study. J Thromb Haemost. 2020;18(1):36-43.
50. Tarantino MD, Cuker A, Hardesty B, Roberts JC, Sholzberg M. Recombinant porcine sequence factor VIII (rpFVIII) for acquired haemophilia A: practical clinical experience of its use in seven patients. Haemophilia. 2017;23(1):25-32.
51. EMC. Summary of Product Characteristics - DDAVP/Desmopressin Injection 2019. Available from: https://www.medicines.org.uk/emc/product/5447/smpc [Accessed 13 Apr 2020].
52. Baxter Corp. FEIBA VH, Anti-inhibitor coagulant complex, Vapor-Heated. Summary of Product Characteristics 2005; Available from: https://www.rxlist.com/feiba-vh-drug.htm [Accessed 13 Apr 2020].
53. Holmstrom M, Tran HT, Holme PA. Combined treatment with APCC (FEIBA®) and tranexamic acid in patients with haemophilia A with inhibitors and in patients with acquired haemophilia A--a two-centre experience. Haemophilia. 2012;18(4):544-549.
54. Baudo F, de Cataldo F. Acquired hemophilia: a critical bleeding syndrome. Haematologica. 2004;89(1):96-100.
55. Pharmaceuticals and Medical Devices Agency Japan. Annual Report FY 2014. Available from: http://www.pmda.go.jp/files/000208305.pdf [Accessed 13 Apr 2020]
56. EMA. Summary of Product Characteristics - Hemlibra 2018; Available at https://www.ema.europa.eu/en/documents/product-information/hemlibra-epar-product-information_en.pdf ; Accessed 13 Apr 2020.
57. Knoebl P, Sperr WR, Schellongowski P, et al. Emicizumab for the treatment of acquired hemophilia A: lessons learned from 4 very different cases. Blood. 2018;132(Suppl 1):2476.
58. Mohnle P, Pekrul I, Spannagl M, Sturm A, Singh D, Dechant C. Emicizumab in the treatment of acquired haemophilia: a case report. Transfus Med Hemother. 2019;46(2):121-123.
59. Hay CR. Acquired haemophilia. Baillieres Clin Haematol. 1998;11(2):287-303.
60. Lottenberg R, Kentro TB, Kitchens CS. Acquired hemophilia. A natural history study of 16 patients with factor VIII inhibitors receiving little or no therapy. Arch Intern Med. 1987;147(6):1077-1081.
61. Hay CR, Brown S, Collins PW, Keeling DM, Liesner R. The diagnosis and management of factor VIII and IX inhibitors: a guideline from the United Kingdom Haemophilia Centre Doctors Organisation. Br J Haematol. 2006;133(6):591-605.
62. Mumoli N, Giorgi-Pierfranceschi M, Ferretti A, Vitale J, Cei M. Acquired hemophilia treated using low-dose of rituximab. J Am Geriatr Soc. 2016;64(8):1744-1745.
63. Wermke M, von Bonin M, Gehrisch S, Siegert G, Ehninger G, Platzbecker U. Successful eradication of acquired factor-VIII-inhibitor using single low-dose rituximab. Haematologica. 2010;95(3):521-522.
64. Xu Y, Zhang X, Zhao Y, Zhao L, Qiu H, Wu D. Successful treatment of a patient with acquired haemophilia A with a combination of a low-dose rituximab and recombinant human FVIIa. Haemophilia. 2013;19(2):e95-96.
65. Yao Q, Zhu X, Liu Y, et al. Low-dose rituximab in the treatment of acquired haemophilia. Hematology. 2014;19(8):483-486.
66. EMA. Summary of Product Characteristics - MabThera 2018. Available at: https://www.ema.europa.eu/documents/product-information/mabthera-epar-product-information_en.pdf [Accessed 13 Apr 2020].
67. Tran H, Brighton T, Grigg A, et al. A multicentre, single-arm, open-label study evaluating the safety and efficacy of fixed dose rituximab in patients with refractory, relapsed or chronic idiopathic thrombocytopenic purpura (R-ITP1000 study). Br J Haematol. 2014;167(2):243-251.
68. Gudbrandsdottir S, Birgens HS, Frederiksen H, et al. Rituximab and dexamethasone vs dexamethasone monotherapy in newly diagnosed patients with primary immune thrombocytopenia. Blood. 2013;121(11):1976-1981.
69. EMA. Summary of Product Characteristics - Cyclophosphamide 500 mg Powder for Solution for Injection or Infusion 2017. Available at: https://www.medicines.org.uk/emc/product/3526/smpc [Accessed 13 Apr 2020].
70. Obaji S, Rayment R, Collins PW. Mycophenolate mofetil as adjunctive therapy in acquired haemophilia A. Haemophilia. 2019;25(1):e59-e65.
71. Zeitler H, Ulrich-Merzenich G, Hess L, et al. Treatment of acquired hemophilia by the Bonn-Malmo protocol: documentation of an in vivo immunomodulating concept. Blood. 2005;105(6):2287-2293.
72. Nemes L, Pitlik E. New protocol for immune tolerance induction in acquired hemophilia. Haematologica. 2000;85(10 Suppl):64-68.
73. Lian EC, Villar MJ, Noy LI, Ruiz-Dayao Z. Acquired factor VIII inhibitor treated with cyclophosphamide, vincristine, and prednisone. Am J Hematol. 2002;69(4):294-295.
74. Huth-Kuhne A, Lages P, Hampel H, Zimmermann R. Management of severe hemorrhage and inhibitor elimination in acquired hemophilia: the modified Heidelberg-Malmö protocol. Haematologica. 2003;88(S12):86-92.
75. Schwartz RS, Gabriel DA, Aledort LM, Green D, Kessler CM. A prospective study of treatment of acquired (autoimmune) factor VIII inhibitors with high-dose intravenous gammaglobulin. Blood. 1995;86(2):797-804.
76. Schunemann HJ, Cushman M, Burnett AE, et al. American Society of Hematology 2018 guidelines for management of venous thromboembolism: prophylaxis for hospitalized and nonhospitalized medical patients. Blood Adv. 2018;2(22):3198-3225.

Ferrata Storti Foundation

Haematologica 2020
Volume 105(7):1802-1812

The dynamic emergence of GATA1 complexes identified in *in vitro* embryonic stem cell differentiation and *in vivo* mouse fetal liver

Xiao Yu,[1,2] Andrea Martella,[1,3] Petros Kolovos,[1,4] Mary Stevens,[1] Ralph Stadhouders,[1,5] Frank G. Grosveld[1] and Charlotte Andrieu-Soler[1,6,7]

[1]Department of Cell Biology, ErasmusMC, Rotterdam, the Netherlands; [2]Current address: Department of Medical Microbiology, Amsterdam University Medical Center, Amsterdam, the Netherlands; [3]AstraZeneca, R&D Innovative Medicines, Cambridge Science Park, Milton Road, Cambridge, UK; [4]Biotech Research & Innovation Centre, University of Copenhagen, Copenhagen, Denmark; [5]Department of Pulmonary Medicine, Erasmus MC, Rotterdam, the Netherlands; [6]Institut de Génétique Moléculaire Montpellier, Université de Montpellier, CNRS, Montpellier, France and [7]Université de Paris, Laboratoire d'excellence (LabEx) du globule rouge GR-Ex, Paris, France

ABSTRACT

GATA1 is an essential transcriptional regulator of myeloid hematopoietic differentiation towards red blood cells. During erythroid differentiation, GATA1 forms different complexes with other transcription factors such as LDB1, TAL1, E2A and LMO2 ("the LDB1 complex") or with FOG1. The functions of GATA1 complexes have been studied extensively in definitive erythroid differentiation; however, the temporal and spatial formation of these complexes during erythroid development is unknown. We applied proximity ligation assay (PLA) to detect, localize and quantify individual interactions during embryonic stem cell differentiation and in mouse fetal liver (FL) tissue. We show that GATA1/LDB1 interactions appear before the proerythroblast stage and increase in a subset of the CD71^{+}/TER119^{-} cells to activate the terminal erythroid differentiation program in 12.5 day FL. Using *Ldb1* and *Gata1* knockdown FL cells, we studied the functional contribution of the GATA1/LDB1 complex during differentiation. This shows that the active LDB1 complex appears quite late at the proerythroblast stage of differentiation and confirms the power of PLA in studying the dynamic interaction of proteins in cell differentiation at the single cell level. We provide dynamic insight into the temporal and spatial formation of the GATA1 and LDB1 transcription factor complexes during hematopoietic development and differentiation.

Correspondence:

CHARLOTTE ANDRIEU-SOLER
charlotte.andrieu-soler@igmm.cnrs.fr

Received: January 7, 2019.

Accepted: October 3, 2019.

Pre-published: October 3, 2019.

doi:10.3324/haematol.2019.216010

Check the online version for the most updated information on this article, online supplements, and information on authorship & disclosures: www.haematologica.org/content/105/7/1802

Introduction

The first hematopoietic cells appear in yolk sac blood islands on embryonic day 6.5 (E6.5) during mouse development. On E10.5 to E11, definitive hematopoietic stem cells (HSC) appear in the aorta-gonad-mesonephros (AGM) region within the embryo (and the vitelline and umbilical arteries). They migrate to the fetal liver (FL), mature from pre-HSC to HSC, and after moving, reside in the adult bone marrow.[1,2] One of the lineages originating from HSC generates erythroid cells.

GATA1 is one of the essential transcription factors for the erythroid (and megakaryocytic) program. *Gata1* knockouts (KO) (*Gata1*$^{-/-}$) die between E9.5 to E10 due to a block of differentiation at the proerythroblast stage, leading to the absence of mature red blood cells.[3,4] GATA1 can form several complexes to regulate erythroid gene expression.[5] Two proteins of particular interest bind directly to GATA1. The first, FOG1 (Friend of GATA1), binds to the N-terminal zinc finger (ZnF) of GATA1 and recruits the chromatin remodeling complex NuRD/MeCP1 and/or the C-terminal binding protein (CTBP) corepressor-containing complex to regulate GATA1 target genes.[6] The second is LMO2, which is part of a larger complex[7-9] containing the LIM-domain-binding protein 1 (LDB1). LDB1 functions as a scaffold

protein to form multiprotein transcription complexes that regulate the differentiation of various cell types. *Ldb1* KO (*Ldb1*$^{-/-}$) mice die between E9.5 and E10 due to severe defects in a number of developing tissues, including abnormal hematopoietic development.[10] This abnormal hematopoiesis is also observed in knockout mouse embryos lacking the LDB1 binding-partners TAL1[11] or LMO2.[12]

Despite the knowledge on GATA1 binding partners, it is not known when and where GATA1 complexes form. In order to identify the temporal and spatial appearance of GATA1/FOG1 and GATA1/LDB1 complexes during differentiation, we applied proximity ligation assays (PLA)[13] in differentiated mouse embryonic stem (ES) cells and FL cells. We detect the first significant GATA1/LDB1 interaction in CD71^{+} FL cells. Knockdown (KD) of LDB1 *in vitro* led to fetal cell death and decreased the CD71^{+} cell populations, providing functional evidence for its essential role at that stage of erythroid differentiation in normal FL.

Methods

Cell culture and mouse FL collection

Wild-type (WT) and *Ldb1*$^{-/-}$ mouse ES cells were cultured in DMEM-15% FCS-1% non-essential amino acids-100 units/mL penicillin-100 mg/mL streptomycin-6.3e-4% 2-mercaptoethanol-100 units/mL Esgro. Day 12.5 (D12.5) or D13.5 FL were used for cell sorting, nuclear extraction, or directly embedded in OCT Tissue-Tek (Sakura) for tissue slicing. All animal experiments were performed according to guidelines and protocols that had been approved by an independent committee on the ethical use of experimental animals (DEC).

ES cell differentiation by the hanging drop method

Mouse WT and *Ldb1*$^{-/-}$ ES cells were differentiated as described.[14] On D4, D5 or D9 of ES cell differentiation, embryoid bodies (EB) were collected by flushing with PBS in 50 mL falcon tubes then embedded in the OCT Tissue-Tek.

Flow cytometry analysis and cell sorting

Mouse E12.5 or E13.5 FL cells (infected or not by LDB1 or GATA1 small hairpin RNA [shRNA]) were labeled with CD71-FITC and TER119-PE antibodies and sorted on a FACSAria III (BD Biosciences) into four populations: P1 (CD71^{-}/TER119^{-}), P2 (CD71^{+}/TER119^{-}), P3 (CD71^{+}/TER119^{+}) and P4 (CD71^{-}/TER119^{+}).

Real-time quantitative PCR (RT-qPCR)

Total RNA was isolated from sorted FL cells or trypsin-dissociated EB up to D6 of differentiation with Trizol (Invitrogen). RT-qPCR was performed using SybrGreen (Applied Biosystem) on Bio-Rad CFX96. *Rnh1* (ribonuclease inhibitor 1) gene was used as internal control for normalization. Primers are indicated in the *Online Supplementary Table S1*.

Gene expression profiling by RNA sequencing (RNA-seq)

RNA samples from sorted mouse E12.5 FL cells, P1 to P4, were sequenced and analyzed as described[10] using independent biological replicates. Significant (at least ±0.6 log two-fold change and *P*-value ≤0.05) up- and down-regulated genes were selected. Data are deposited in the Sequence Read Archive (SRA) (Accession Number: SRP158286).

Antibodies

Antibodies are indicated in the *Online Supplementary Table S2*.

RNA interference

Lentiviral particles for LDB1 were produced as described by Stadhouders R[15] using *Ldb1* shRNA (shRNA#1: 5'-GGACCAAA-GAGATATACCA-3', shRNA#2: 5'-GACTCTGTGTGATACTA-GA-3') and *Gata1* shRNA (5'-GTTTGGATGCAGCATCTTCTT-3') with non-targeting shRNA as controls. Lentiviral infected cells were harvested 72 hours after transduction and processed for nuclear extraction.

Protein analysis

Murine erythroleukemia (MEL) cells or EB nuclear extract and immunoprecipitation (IP) were prepared as described[16] and size-exclusion chromatography was performed on an AKTA-FPLC apparatus with a Superose-6 10/30 column (Amersham Biosciences). Fractions were precipitated with trichloroacetic acid and analyzed by Western blotting using Odyssey system (LI-COR).

Immunofluorescent staining

MEL or FL cells were stained as described[8] and analyzed by confocal microscopy (Leica SP5).

PLA on EB and mouse embryo tissue

10 μm sliced E4, 5, 9 EB or E12.5 mouse fetal tissues were fixed and processed for PLA following the manufacturer's protocol (Duolink, OLINK) using antibodies indicated in the *Online Supplemntary Table S2*. PLA signals were visualized by Leica SP5 confocal microscopy and were analyzed using BlobFinder software (Uppsala University, Sweden). Signals contained in or adjacent to nuclei were compared between different groups (n=3). The Kruskal–Wallis test for variance between groups was performed and the Tukey method to counteract multiple comparison errors was applied. Deconvolution of PLA signals and volume analysis was performed using Huygens Suite as published.[17]

Results

LDB1 complexes start to form at D4 of *in vitro* ES cell differentiation

We applied PLA[18] on sliced *in vitro* differentiated EB to identify when GATA1 complexes form. This enables low level detection of endogenous protein-protein interaction *in situ*.

First, we characterized gene expression dynamic for genes of interest during ES cell differentiation (Figure 1A). As expected, the stem cell marker *Rex1* is expressed early (day 0 to 2 [D0-D2]) and decreases during differentiation, while *β-globin* increases at later stages at D5-D6. Thus *Ldb1* is expressed both in early and late stages of ES differentiation, and in the erythroid cell lineage at D5-D6. Following differentiation *Gata1, Fog1, Gata2, Flk1, Tal1* and *Lmo2* expression gradually increases. Of note *Gata2* gene induction starts at D4 whereas *Gata1* expression is delayed for 24 hours (h) (Kolovos *et al.* submitted), *i.e.* the GATA-switch occurs in early embryogenesis.[19]

PLA representing combinations of transcription factor (TF) interactions (GATA1/LDB1, GATA1/FOG1 and LDB1/E2A) was performed in undifferentiated cells D0, D4, D5 and D9 differentiated WT or *Ldb1*-KO EB (Figure 1B). Quantification of PLA signals showed that these interactions are absent in ESC, while GATA1/LDB1 and LDB1/E2A interactions already occur at D4 of ES cell differentiation. The GATA1/FOG1 interaction appeared 24 h later at D5. No red blood cells emerged in *Ldb1*-KO EB at

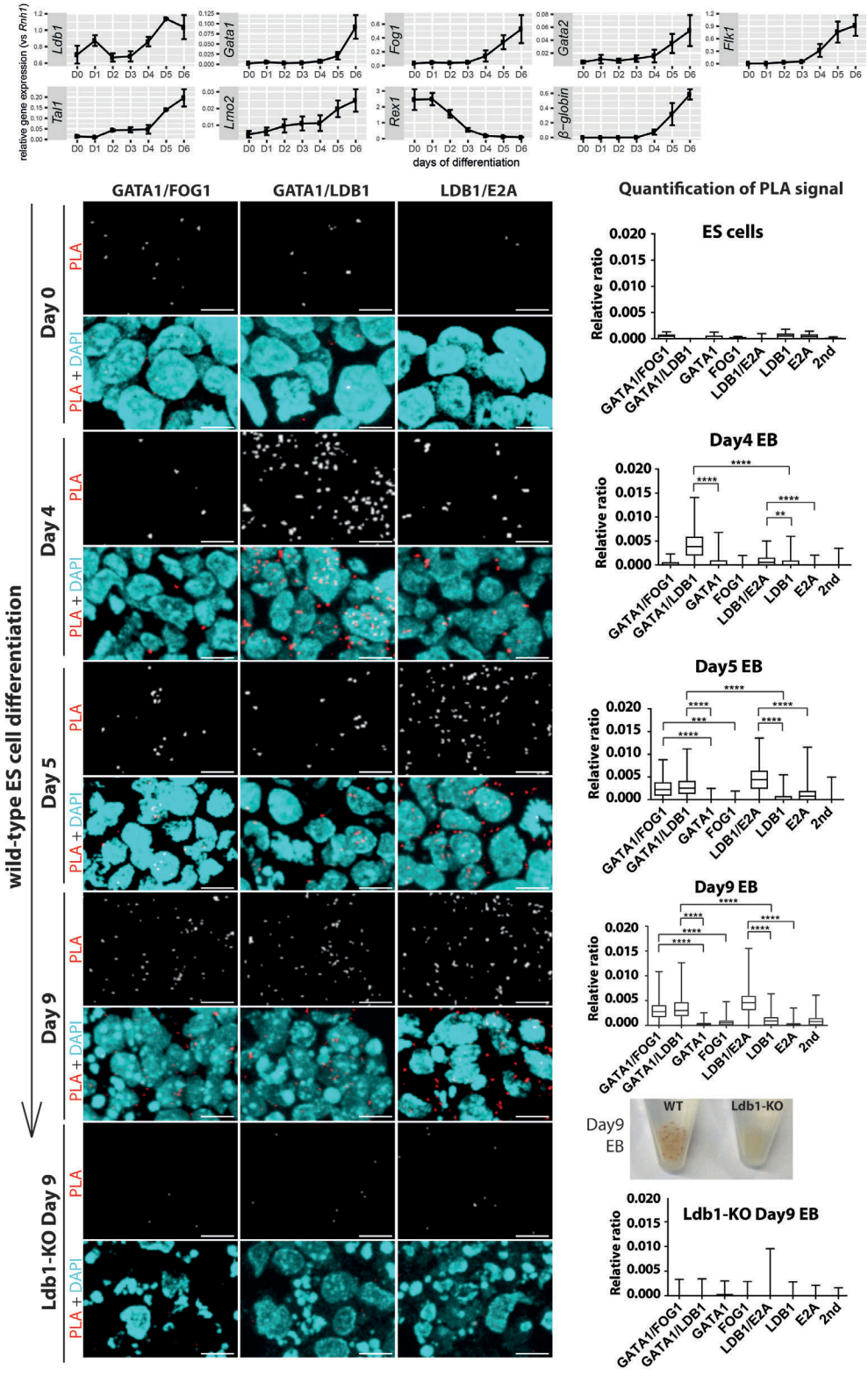

Figure 1. Gene expression and proximity ligation assay on embryonic stem cell differentiation. (AcGene expression during embryonic stem (ES) cell differentiation from day 0 until day 6 (D0-D6) of genes of interest. Standard error of the mean (SEM) from three biological replicates is shown as error bar. (B) Proximity ligation assay (PLA) detection of GATA1/FOG1, GATA1/LDB1 and LDB1/E2A complexes was performed on wild-type ES cell differentiation at D0 (ES cells), D4, D5 and D9, and *Ldb1*-KO ES cell differentiation at D9. On D9, EB from wild-type (WT) or *Ldb1*-KO are collected and pictured as shown. PLA signal representing protein-protein interaction was in white on a black background and in Texas-Red in merged pictures together with DAPI in blue. Each red dot represents a fluorescent signal of GATA1 complex formation. The images were analyzed using BlobFinder software[38] which quantifies the number of PLA-positive dots in cells. The boxplot (Figure 1B, right panel) shows the density of the dots related to its nuclear area (from three biological replicates). Comparisons of the PLA signals obtained with two primary antibodies *versus* those obtained in the negative controls were tested in ANOVA and the significance is shown in asterisks. All scale bars represent 10 μm. PLA signals have been quantified on each day and compared with negative controls including GATA1, FOG1, or E2A single-antibody or secondary antibodies alone. Asterisk shows the significant interactions between the two primary antibodies PLA signal and single primary antibody controls. The significance was analyzed with Kruskal-Wallis test as follows, ****: $P \leq 0.0001$, ***: $P \leq 0.001$, **: $P \leq 0.01$, *: $P \leq 0.05$. The Tukey method to counteract multiple comparison errors was applied.

D9 as shown by the lack of red coloration. This correlates with absence of interaction detection by PLA constituting an important control for PLA specificity, in addition to the single probes and secondary antibodies alone used a negative control.

We next characterized the dynamic expression of hematopoietic TF proteins during the time course of ES cell differentiation at D4-5 using *Ldb1*-KO cells as the control (*Online Supplementary Figure S1A*). This showed that the different factors already form a complex as determined by immunoprecipitation at D4 and D5 (*Online Supplementary Figure S1C-D*) using *Ldb1*-KO cells as the control (*Online Supplementary Figure S1E*). *Online Supplementary Figure S1C* shows that LDB1 and FOG1 fail to pull down GATA1 (and *vice versa*) in D4 differentiated cells, which is likely due to very low amounts of the bridging factor LMO2. Day 5 (*Online Supplementary Figure S1D*) shows more GATA1, but LMO2 is still undetectable and LDB1 and GATA1 appear to fail pulling down each other. The same is seen for GATA1 and FOG1. Interestingly FOG1 appears to be regulated by (the) LDB1 (complex) as it is present in D5 WT cells, but not in *Ldb1*-KO cells. This agrees with our observation that LDB1 binds to the *Fog1* gene in *Flk1* positive cells sorted four days after ES cell differentiation and the reduction of *Fog1* expression in *Ldb1*-KO cells analysed by RNA-Seq.[10] The amounts of the proteins involved (directly or indirectly) were too low to allow their detection by immunoprecipitation or mass spectrometry (*data not shown*), because D4 and D5 differentiated ES cells are a mixture of few hematopoietic cells in the presence of many non-hematopoietic cells. For example, many cells express *Oct4* (*Online Supplementary Figure S1A*) or cardiac genes in cardiac progenitors.[20] The complexes are barely detectable by size-exclusion chromatography (*Online Supplementary Figure S1B*). By contrast, the clear PLA signals (Figure 1B) show the power of PLA to analyze complexes in individual cells. The few PLA signals in undifferentiated ES cells are background since such signals are also detected with single antibody controls.

In summary, PLA monitors the dynamic changes of different protein complexes even of low amounts present in a subset of cells. The PLA signals in D5 EB appear to distinguish a subpopulation of cells, suggesting that some specification is already in progress towards hematopoietic cells in the mixed three-dimensional cell aggregates.

The GATA1 complexes (GATA1/LDB1 and GATA1/FOG1) are observed in mouse E12.5 FL cells

(Pre-)HSC move to the FL at embryonic day E10.5 to 11.5. We applied PLA on FL sections at E12.5 to understand the temporal appearance of the two GATA1 complexes in definitive blood cells. Figure 2 shows the comparison of the GATA1/LDB1 and GATA1/FOG1 complexes, together with negative controls of GATA1, FOG1 or LDB1 single-primary antibody. Although FL tissue is compact and single cells can be difficult to distinguish, clearly some cells contained very dense GATA1/LDB1 PLA signals when compared to surrounding cells (Figure 2A). Close up images show that the signal co-localizes with the DAPI staining (of note, those cells have little cytoplasm relative to the size of the nucleus) and that cells with no signal (next to strong positive ones) include FL endothelial cells which are expected to be negative for GATA1. A similar result was found in fetal aorta (*not shown*). Specific PLA signals were also detected for LDB1/LMO2, which is part of the same GATA1/LDB1 complex (Figure 2B) suggesting GATA1/LDB1 and LDB1/LMO2 and by inference the GATA1/LDB1/LMO2 complex are present at a high level in a subpopulation of cells. This is in accordance with our previous co-immunoprecipitation and ChIP-sequencing co-localisation data of these factors in MEL and in Flk1$^+$ cells sorted four days after ES cell differentiation.[5,8,10] In contrast, GATA1/FOG1 signals appear in similar numbers of cells but are less abundant/weaker and more evenly distributed (Figure 2, upper panel A). In agreement with the PLA results, immunofluorescent staining for individual LDB1, GATA1 and FOG1 proteins in FL sections showed higher co-expression of GATA1 and LDB1 in a subpopulation of cells than GATA1 and FOG1 (*Online Supplementary Figure S2*), although it should be noted these are signals from different antibodies (see *Methods*).

FL contains erythroid cells at different stages of differentiation and the PLA results suggest that the LDB1 complex, is more important at particular stages of erythroid cells in agreement with data showing that GATA1 increases before the end stage of erythroid differentiation[8] primarily in the LDB1 complex.

GATA1/LDB1 complex is highly localized in early erythroid differentiating cells in sorted FL

In order to identify the cells containing high PLA signals, E12.5 or E13.5 FL cells were sorted using glycophorin (TER119) and transferrin receptor (CD71) antibodies into four populations: P1 (CD71$^-$/TER119$^-$), P2 (CD71$^+$/TER119$^-$), P3 (CD71$^+$/TER119$^+$) and P4 (CD71$^-$/TER119$^+$) in order to separate different stages from proerythroblasts to orthochromatic erythroblasts[21,22] (Figure 3A).

First, gene expression was measured in the four populations (Figure 3B). At early stages (P1 and P2), expression of *Ldb1, Gata1* and *Fog1* starts increasing followed by a decrease at P3 for *Ldb1* and at P4 for *Gata1* and *Fog1*, which follow each other. *Gata2, c-Kit* and *c-Myb* genes are expressed highly in P1 which contains precursor cells (and other cell types), their expression decreases during differentiation, whereas the *β-globin* gene increased dramatically from P3 to P4. The CD71/TER119 sorted cells were used for RNA-seq analysis in two independent biological replicates for each P1 to P4 population of E12.5 FL cells. Principal component analysis (Figure 3C) shows that biological replicates of each population cluster and can be separated from each other. As expected, the RNA-seq result in those populations (*Online Supplementary Figure S3*) is very similar to the genes analysed by qPCR (Figure 3B and *Online Supplementary Figure S3*). There is an increase of expression of the transcription factors *Ldb1, Gata1* and *Fog1* from P1 to P2 (together with *E2A*) and continuing to P3 for *Gata1* and *Fog1* (together with *Klf1*). *Gata2, c-myb* and *c-kit* expression is inversely correlated and follows the same trend as *Eto2* and *Irf2bp2*, with a decrease peaking at P3 followed by erythroid specific markers such as *β-globin, Alas2* and *Gypa* and the transcription factor *Lmo2*. The result shows that the sorting method clearly separates the different stages of the erythroid cells. The significantly differentially expressed genes (±0.6 log log two-fold change and *P*-value ≤0.05) between the populations is shown in the *Online Supplementary Table S3*. Of note *Ldb1* expression presents a two-fold increase between P1 and P2, but is not included in the *Online Supplementary Table S3* due to

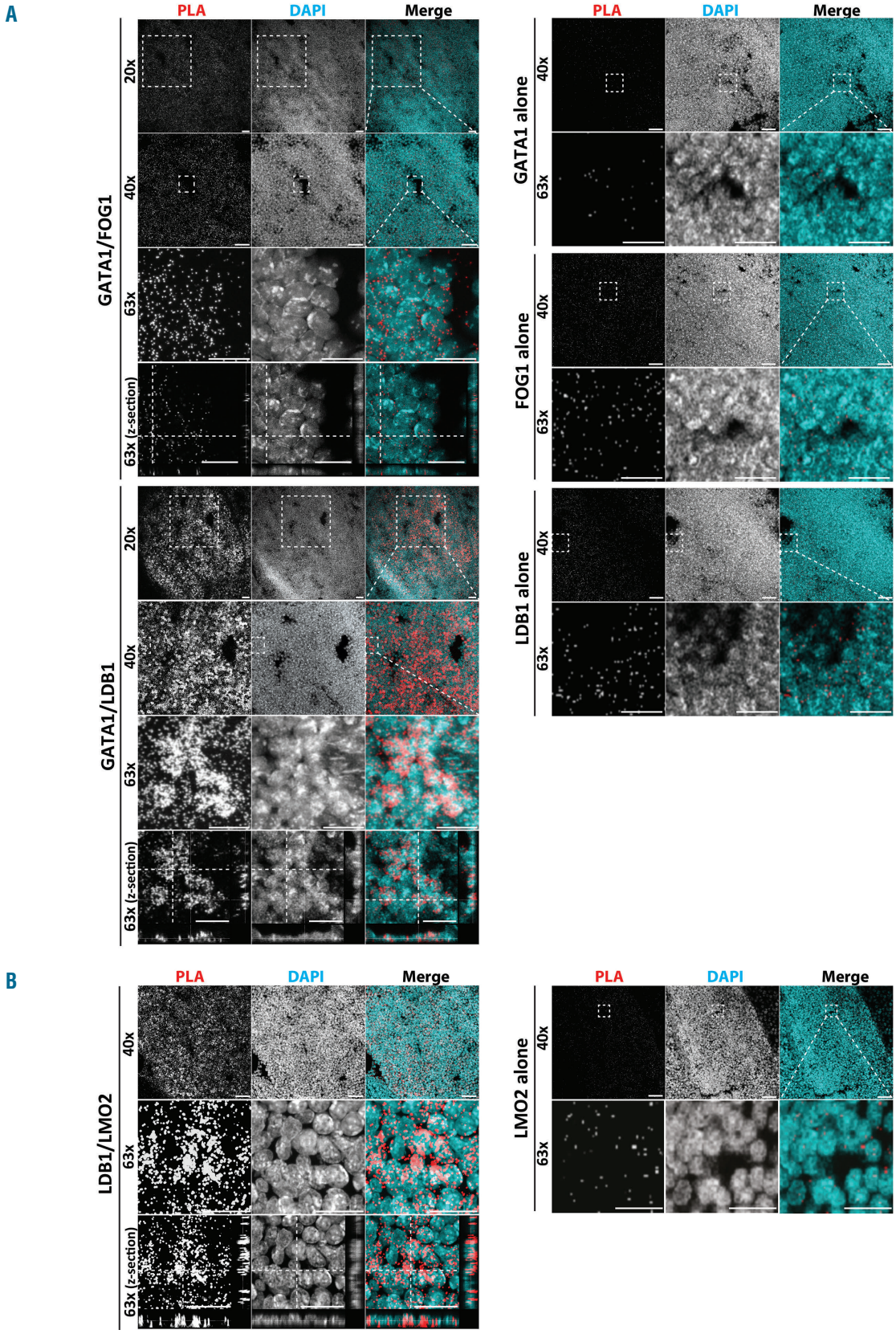

Figure 2. Proximity ligation assay of GATA1 complexes in E12.5 fetal liver tissue. (A) Proximity ligation assay (PLA) for GATA1/FOG1 and GATA1/LDB1 interactions was performed on sections of mouse fetal liver (FL) tissue at embryonic day 12.5 (E12.5), together with GATA1, FOG1 or LDB1 single-primary antibody negative controls. PLA protein interactions were visualized in red, and DAPI staining in blue was used to visualize the nucleus (scale bars, 50 μm in 20x and 40x). For each interaction zoom-in pictures corresponding to the white square area are also shown (scale bars, 20 μm in 63x). Z-stack images of each protein combination and fluorescent channels were projected by Maxi-Projection algorithm. (B) PLA for GATA1/LMO2 was performed as in Panel A using LMO2 antibodies replacing FOG1 antibodies. Scale bars represent 50 μm apart fromscale bars in zoom in picures bars which represent 10 μm.

the threshold parameters used in our study to detect the strongest differentially expressed genes. In P1 and P2, 65% of the downregulated genes are enriched for *e.g.* neutrophil degranulation, cytokine production and hemostasis, *i.e.* genes crucial for other cell types (Figure 3D). The up-regulated genes (35%) represent essential functions for erythroid genes, *e.g.* erythrocyte homeostasis, porphyrin-synthesis and cell cycle genes as cells at this stage are still replicating. During mid- (P2 to P3) or late (P3 to P4) differentiation, the majority (76% and 67%) of upregulated genes have erythroid differentiation bio-functions. Down-regulated genes, (24% and 33%) show functions like lymphocyte differentiation, B-cell differentiation and lymphocyte migration. At these stages (P3 to P4), cell cycle functions are suppressed as erythroid cells enter the terminal differentiation and proceed to enucleation. Next GATA1/LDB1 PLA was applied on the four sorted populations (Figure 4A), showing high signals in P2 and P3. Quantification confirmed that P2 had the highest density of GATA1/LDB1 interaction signals per nuclear area

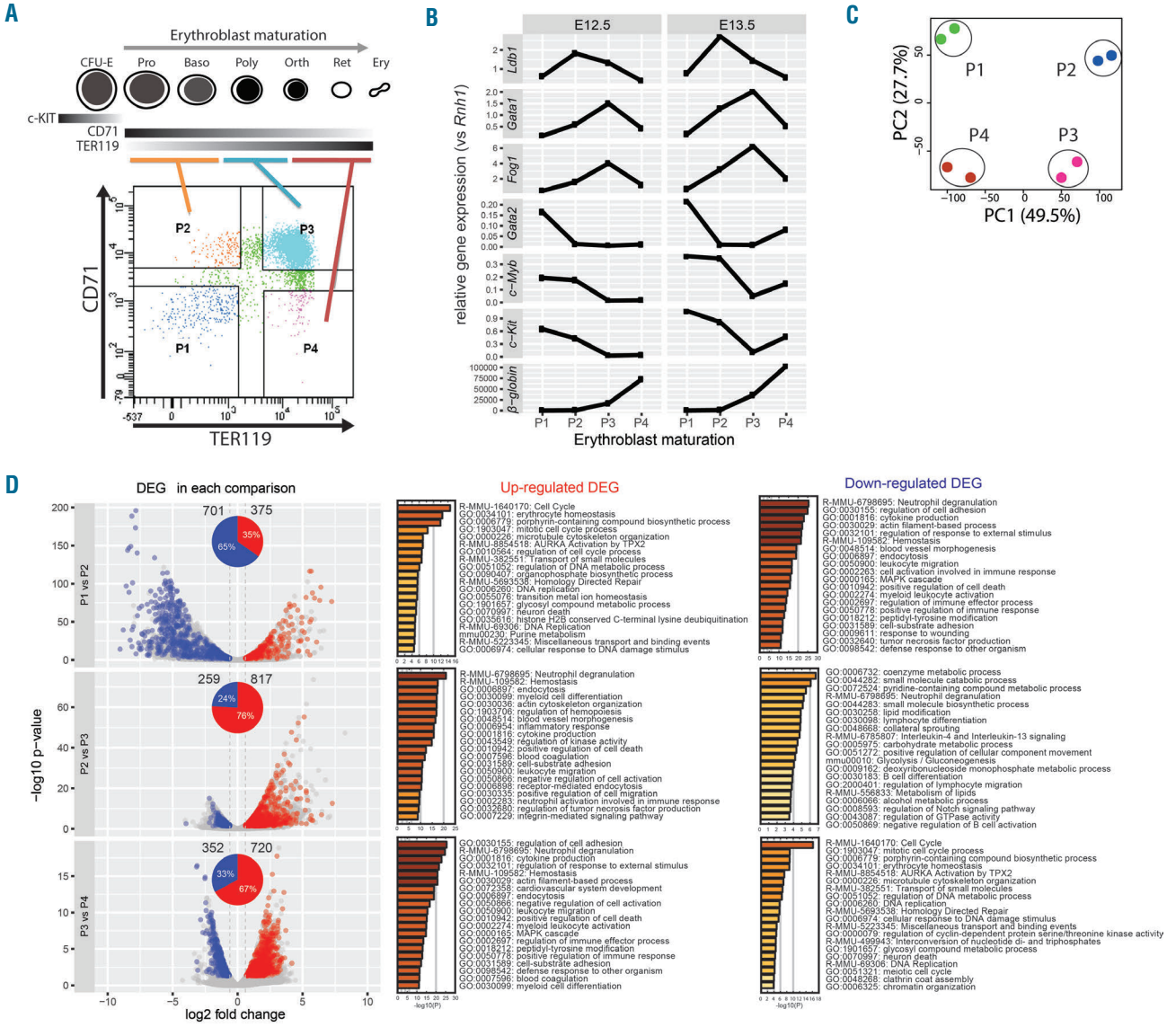

Figure 3. Fetal liver cell sorting and RNA-sequencing data analysis. (A) Schematic description of erythroblast development. Fetal liver (FL) cells are sorted into four populations based on membrane markers TER119 and CD71. Different stages of erythroblasts are indicated into P2 to P4 populations. The C-KIT positive cell population (P1, CD71$^-$/TER119$^-$) represents precursors or other lineage cell types present before the initiation of erythroblast maturation. Proerythroblasts/colony forming unit-erythroid [CFU-E] cells) express high level of CD71 and low level of TER119 (P2, CD71$^+$/TER119$^-$). Following erythroblast maturation, TER119 expression increases (P3, CD71$^+$/TER119$^+$). When the differentiation reaches the orthochromatic stage, they loose CD71 expression (P4, CD71$^-$/TER119$^+$). Pro: immature proerythroblast; Baso: basophilic erythroblast; Poly: polychromatic erythroblast; Orth: orthochromatic erythroblast; Ret: reticulocytes; Ery: erythrocyte. Gray bars represent the changes of *c-Kit, Cd71* and *Ter119* gene expression. The darker color of the bar represents higher expression for the indicated gene. (B) Quantitative PCR on indicated genes in E12.5 or E13.5 sorted FL cells (E12.5 and E13.5 were used as duplicates) as described in Panel A. Relative expression values are calculated by comparing to control gene *Rnh1*. (C) Principle component analysis of RNA-sequencing data from two replicates of each P1 to P4 sorted FL cells as described in (A) (D) The total number of down-regulated or up-regulated differentially expressed genes (DEG) are shown for each comparison in a Volcanoplot, in which x-axis represents log two-fold change and y-axis represents log 10 adjusted *P*-value. Significant DEG are shown in blue for down-regulated and red for up-regulated. Gray dots represent the non-significant genes. The ratio of down- or up-regulated DEG in each comparison is shown in pie-chart inserted in the Volcanoplot. Top 20 gene ontology terms for down- or up-regulated DEG in each comparison are shown.

(Figure 4B). Interaction between the LDB1 and GATA1 proteins appears already shortly before the proerythroblast stage. It is most abundant in the P2 population (most likely colony forming unit-erythroid [CFU-E] cells) and basophilic erythroblasts but decreases during the final stages of differentiation *in vivo*. We applied PLA to detect the interaction between GATA1/FOG1, GATA1/LDB1, GATA1/TAL1, LDB1/LMO2 and LDB1/ETO2 in MEL cells, which mimic FL cells. Uninduced MEL cells represent proerythroblasts, *i.e.* part of the P1 and P2 population, while induced MEL cells represent P3 and further differentiated populations.[9, 28,29] Figure 5A shows the detection of the GATA1/FOG1 interaction by PLA using single-primary antibody and secondary antibody alone as controls. Quantification of the PLA signals in nuclei show a significant increase of GATA1/FOG1 interaction after MEL cell differentiation. An additional negative control experiment to further demonstrate the specificity of the PLA assay was a TAL1/FOG1 interaction which is known not to be formed.[5] Quantification of the different PLA signals confirmed the absence of TAL1/FOG1 interaction detection in MEL cells and is comparable to the one of the single probe GATA1 only control, thereby supporting the specificity of positive PLA signals (Figure 5B). This control on non-interacting highly expressed proteins (TAL1 and FOG1 in MEL cells)[5] also ruled out a potential threshold effect of PLA *i.e.* where ligations may be more likely when the relevant TF partners are expressed highly. Similar quantification of PLA signals was performed in the cytoplasm (Figure 5B). It was much lower than that observed in the nucleus and does not increase upon differentiation as seen in the nuclei. Of note the increase of signal was not due to an increase of signal volume between the differentiated and undifferentiated states (Figure 5C). In MEL cells, the LDB1 complex binds its target genes during erythroid differentiation,[23] *e.g.* the *α-* and *β-globin* locus bind the LDB1 complex in differentiated cells resulting in upregulation,[24-27] due to the loss of the repressor ETO2 (encoding by *Cbfa2t3*) from the complex.[9] We quantified the PLA signals for GATA1/LDB1, LDB1/LMO2 and LDB1/ETO2 interactions (Figure 5D-F) and confirmed not only an increase of both GATA1/LDB1, and LDB1/LMO2 interactions upon differentiation but further confirmed that the LDB1/ETO2 interaction is lost during differentiation in MEL[9] (Figure 5F), supporting its role as a negative regulator during erythroid differentiation where ETO2 and IRF2BP2 with the NCOR1/SMRT co-repressor complex suppress the expression of typical erythroid genes such as *Klf1* which is needed to express *β-globin* and *Gypa* genes.[8,26]

In conclusion, the GATA1/LDB1 complex starts to be formed just before the proerythroblast stage and activates erythroid specific genes of erythroid differentiation *in vivo*, when it looses ETO2.

LDB1 KD results in loss of the erythroid cell population

We examined the importance of the GATA1/LDB1 complex in fetal erythropoiesis at E12.5 by three independent (partial) KD rather than a (lethal) KO using anti-LDB1 shRNA (shLDB1_1 and shLDB1_2) and an anti-GATA1 shRNA (shGATA1). Treatment with an empty vector pLL3.7 shRNA or scrambled shRNA (Scr) was used as the controls. The level of LDB1 or GATA1 protein relative to valosin containing protein (VCP) decreased in the FL cells from D1 to D3 in the KD (*Online Supplementary Figure S4*). On D3, the cells were sorted by fluorescence-activated cell

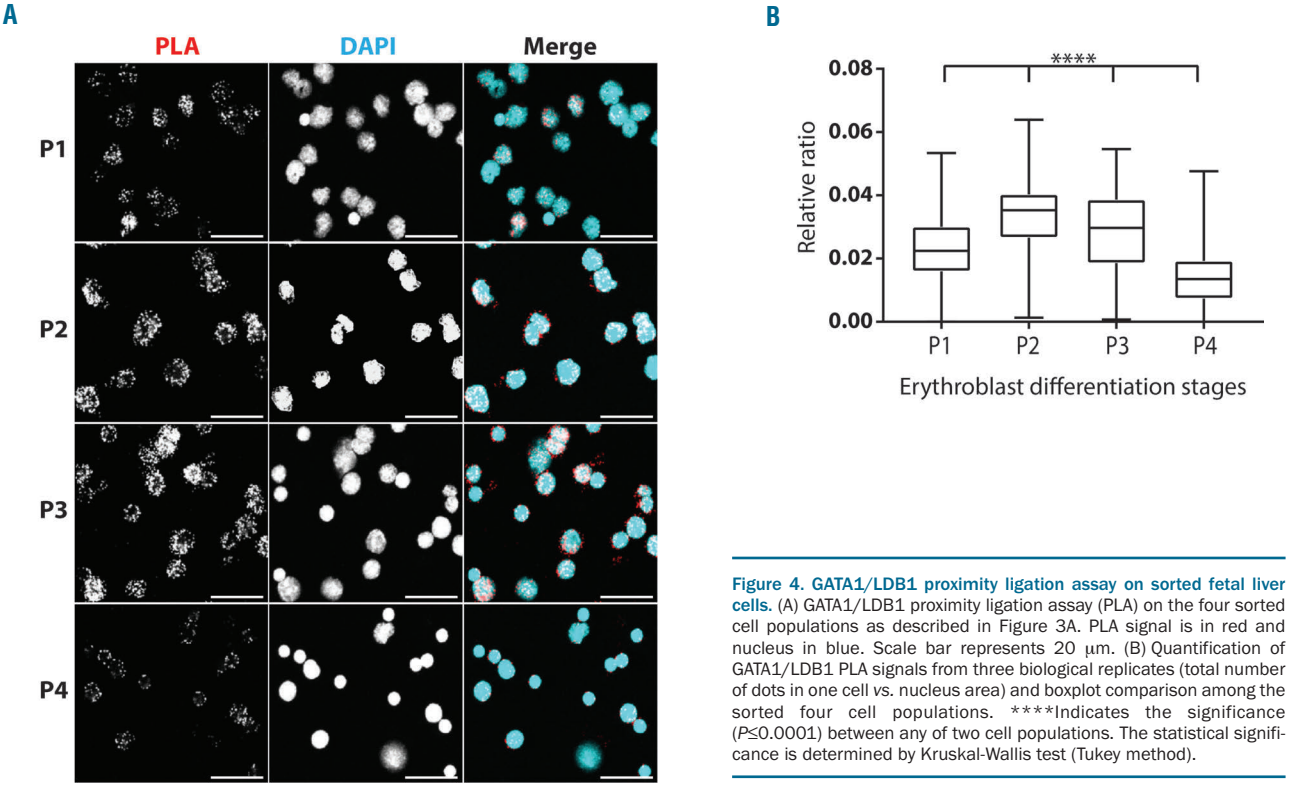

Figure 4. GATA1/LDB1 proximity ligation assay on sorted fetal liver cells. (A) GATA1/LDB1 proximity ligation assay (PLA) on the four sorted cell populations as described in Figure 3A. PLA signal is in red and nucleus in blue. Scale bar represents 20 μm. (B) Quantification of GATA1/LDB1 PLA signals from three biological replicates (total number of dots in one cell *vs.* nucleus area) and boxplot comparison among the sorted four cell populations. ****Indicates the significance ($P \leq 0.0001$) between any of two cell populations. The statistical significance is determined by Kruskal-Wallis test (Tukey method).

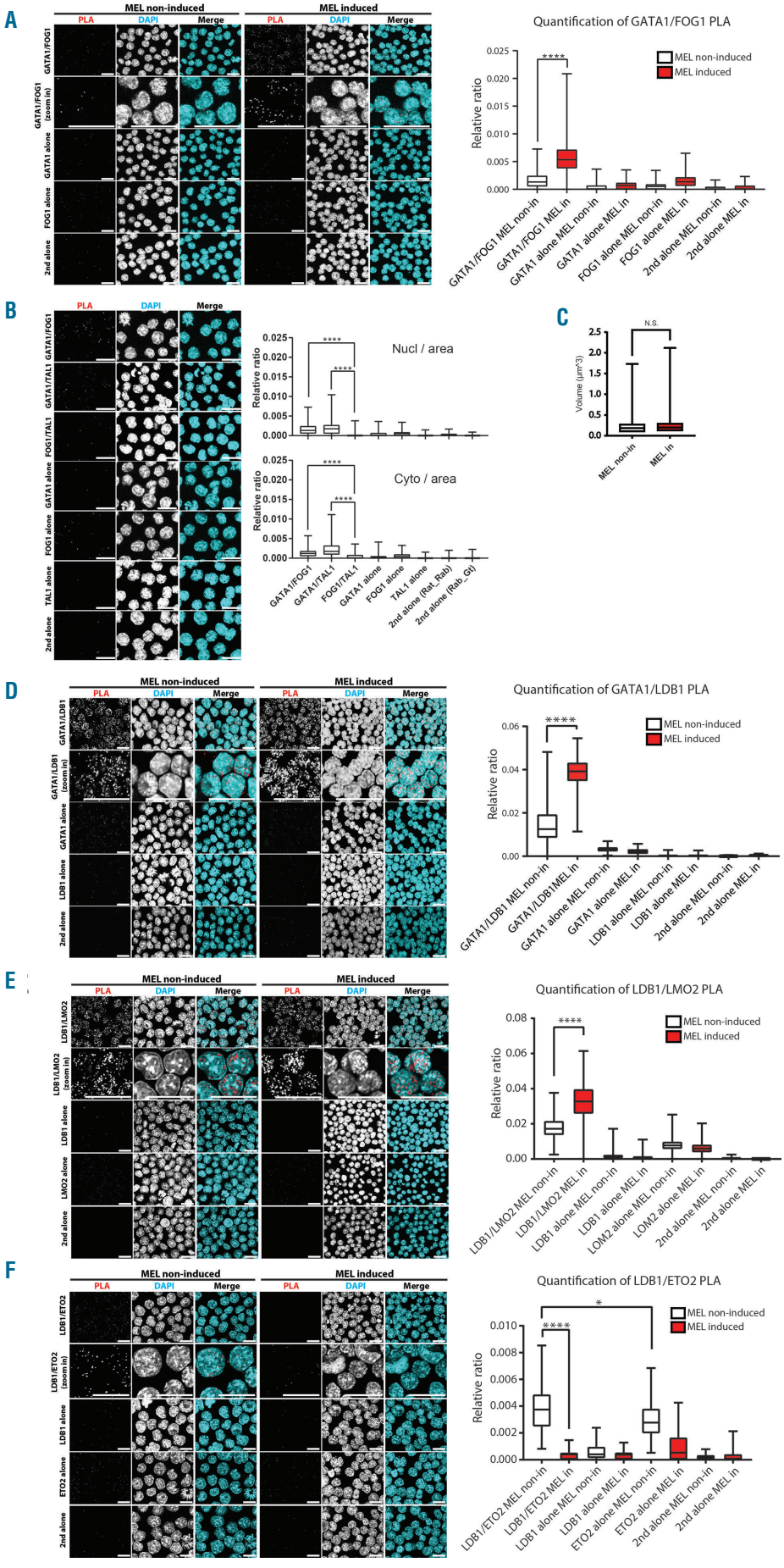

Figure 5. Proximity ligation assay on GATA1 complexes in MEL cells. (A) GATA1/FOG1 proximity ligation assay (PLA) on non-induced and induced MEL cells. PLA signal representing protein-protein interaction in white in a black background and in red in merged pictures together with DAPI in blue. GATA1 or LDB1 antibody alone was also performed as negative controls. All scale bars represent 20 µm. The significance from three biological replicates was analyzed with Kruskal-Wallis test as ****: $P \leq 0.0001$ and *: $P \leq 0.05$. The statistical significance is determined by Kruskal-Wallis test (Tukey method). (B) PLA detection of GATA1/FOG1 and GATA1/TAL1 interaction compared to non-existing interaction FOG1/TAL1 in MEL non-induced cells. The PLA signal is separated into relative ratio in nucleus or cytoplasm. ****Indicates the significance ($P \leq 0.0001$) between indicated interactions and is determined by Kruskal-Wallis test (Tukey method). (C) The volume of individual GATA1/LDB1 PLA signals from 53 MEL non-induced and 56 induced cells is calculated following deconvolution and shown in boxplot. *P*-values of both statistical analysis of parametric (*t*-test) and non-parametric (Mann-Whitney) are 0.827 and 0.674, respectively. (D) GATA1/LDB1 PLA on MEL cells as in (A) (E) LDB1/LMO2 PLA on MEL cells as in Panel A. Panel F: LDB1/ETO2 PLA on MEL cells as in Panel A.

sorting (FACS) using TER119 and CD71 expression and the relative ratio normalized *versus* pLL3.7 control (ctrl), in each population is shown in the *Online Supplementary Figure S4B*. LDB1 protein decreased by ~60% at D3 (54.3%, for shRNA#1 and 64.3% for shRNA#2 compared to ctrl) which resulted in a ±50% decrease in the P2, P3 and P4 population of cells (see above). In three additional LDB1 KD, a pLL3.7 plasmid containing EGFP was used to determine the RNA levels in GFP$^+$ cells *versus* the total cells ("All cells"). As expected, the "All cells" result shows a similar ratio in each population as was observed in Figure 3A. The GFP$^+$ cells representing the really infected cells, showed a strong KD effect in P2 to P3 compared to pLL3.7 control, when the level of LDB1 appears highest (Figure 3A). The GATA1 KD showed a decrease of GATA1 protein of ~43.5% at D3 (relative to Scr ctrl) resulting in a ±40% decrease in the P3 population while majority of cells are P1. This result is consistent with the phenotype observed in inducible *Gata1* KO mice showing an over-representation of cells in P1 and an under-representation of cells in P3 and P4).[28] The difference of the KD effect in LDB1 and GATA1 therefore correlates with their expression in those populations (Figure 3B). It is impossible to conclude whether the decrease in the LDB1 complex has an effect before the proerythroblast stage, because the number of progenitors committed to the erythroid lineage in the P1 is not known, but the 40-50% decrease in P2 to P4 suggests that there is a decrease in the number of proerythroblasts that is propagated to the later cell compartments. Of note, the cells (P2 to P4) were strongly affected by the KD of LDB1 or GATA1 and were dying.

Discussion

Our study shows a modulation of the levels of the protein complexes from the early stages of erythroid differentiation of the systems that we used (erythroid differentiation from embryonic stem cells, MEL cells, primary erythroid cell populations from mouse FL and FL tissue sections). These diverse systems represent different stages and therefore heterogeneous systems of hematopoietic development and differentiation. They show that the same complex is formed at these quite different stages, although these experiments do not directly show that the formation of the complex is essential at all these stages and one system might not directly extrapolate to the other. However previous data using KO or KD experiments of individual components of the complex lead to defective hematopoiesis/erythropoiesis.[9,10,29] We therefore conclude that GATA1/LDB1 complex formation is essential in these diverse systems and provide novel insight in GATA1 complexes. The result describes the sequential emergence of GATA1/LDB1, GATA1/FOG1 and LDB1/E2A complexes in early stage ES cell differentiation, suggesting dynamic changes of the complexes and their function taking place during the blast colony-forming cell (BL-CFC) stage similar to the hemangioblast stage *in vivo*. GATA1 as part of the LDB1 complex is absent in undifferentiated ES cells and only appears after a few days of differentiation, while GATA2 is expressed and is part of the LDB1 complex in the very early stages of differentiation where it activates GATA1[19] in a feed forward type system (Kolovos *et al.*, in revision), which is in agreement with the data on the function of GATA1 and GATA2 in mice or differentiating ES cells.[4,30]

GATA2 is present during early erythropoiesis and binds to the *Gata1* gene to activate its expression.[19] *Gata1* expression in turn represses *Gata2* expression *via* the FOG1/MeCP1 complex, while activating its own expression. This "GATA switch" represents a forward drive towards late stage erythroid differentiation through changes in gene expression.[19,31] GATA2 regulates important proliferation genes of stem or progenitor cells whereas GATA1 also regulates the final erythroid fate through the expression of erythroid specific genes. A similar process operates early during embryonic development. GATA2 is present before GATA1 during ES cells differentiation to the hematopoietic lineage. The GATA2/LDB1 complex is present in very low concentration binding a small set of hematopoietic specific transcription factors in a co-factor dependent manner (PK, CA-S and FG, manuscript in revision). Unfortunately, the low level of GATA2 and poor quality of its antibodies prevent a PLA signal although the GATA switch must start early as we identified the GATA1/LDB1 and LDB1/E2A complexes already in D4 EB. PLA does not show which cell population contains the GATA1/LDB1 and LDB1/E2A complexes in D4 EB, but it is known that LDB1 is expressed in BL-CFC.[10] The cells expressing GATA1 and LDB1 in D4 EB are differentiating hematopoietic cells. We know from ChIP-seq data that the two factors already form a complex at this stage targeting a core set of genes enriched for categories related to differentiation/quantity of blood/hematopoietic progenitor cells (Kolovos *et al.*, manuscript in preparation). Moreover, we described in Mylona *et al.* 2013[10] that blast colony-forming cells deficient for *Ldb1* (*i.e.* Flk1$^+$ cells sorted four days after ES cell differentiation) are unable to differentiate to the hematopoietic lineages with a severe reduction in the number of blast colony forming cells and their failure to give rise to blast colonies.

These cells appear between ES cell differentiation D3.75 to D4.25 expressing vascular endothelial growth factor receptor-2 (VEGFR2, *i.e.* FLK1). The absence of LDB1 results in less BL-CFC and failure to generate hematopoietic and endothelial lineages.[10] Of its targets *Gata2, Scl/Tal1, Runx1* and *Gif1b* are down-regulated showing that the complex is essential for activation of early embryonic hematopoiesis in agreement with our observation here that the GATA1/LDB1 interaction already takes place at this early stage. It has been shown that a KO of *Gata1* in ES cells did not affect the formation of clonogenic progenitors in chimeric *in vitro* differentiation, and *Gata1* KO colonies contained phenotypically normal macrophages, neutrophils and megakaryocytes,[3,4] suggesting that GATA1 is not yet essential at this early stage. Importantly GATA2 is essential for the generation of FLK1$^+$ BL-CFC during *in vitro* ES cell differentiation[32] and *Gata2*$^{-/-}$ embryos die at E11.5 with severe anemia.[30]

LDB1 IP experiments in undifferentiated ES cells show that a GATA1/LDB1 complex is absent, but appears at low levels in nuclear extracts (NE) from D4 and D5 ES cell EB (*Online Supplementary Figure S1C-D*). The expression of FOG1, LDB1 and GATA1 increases from D4 to D5, but is still very low and the binding partner LDB1 could not detected by IP in a GATA1 pulldown (*Online Supplementary Figure S1*). The E2A protein was detected in the LDB1 IP only at D5, but again the band is very weak. We also applied size-exclusion chromatography to distinguish the different GATA1 complexes. The expression of LMO2 protein increases at D4 (*Online Supplementary Figure*

S1B), most of it is in the fractions of 37-39, but some is present in fractions 22-24 indicating that some complex has formed. In MEL cells, *i.e.* a much later stage of development and differentiation, most LMO2 is in the fractions overlapping with LDB1 (*Online Supplementary Figure S1B*), showing they are in the same complex consistent with previous results.[8] Although the expression of GATA1 and partners is low at D4-5 ES cell differentiation, we could detect the formation of the different complexes by PLA due to its ability to detect 10^2-fold or 10^6-fold lower protein concentrations than ELISA or WB, respectively.[33]

GATA1/FOG1 regulates genes that are less important for erythroid specific functions in the undifferentiated stage, *e.g.* pro-erythroblasts. We originally postulated a switch from GATA1/FOG1, repressing alternative lineage genes to GATA1/GFI1B repressing proliferation related genes during differentiation.[5] In MEL non-induced cells, GFI1B and LDB1 can also be detected in an ETO2 pull-down, indicating that LDB1 complexes containing ETO2 and/or GFI1B proteins suppress archetypical erythroid genes primed for the onset of terminal erythroid differentiation.[26] Indeed, RNA-seq data shows that *Cbfa2t3* (encoding ETO2) and *Irf2bp2* expression decreased from P1 to P2 suggesting these genes mainly function in P1 to P2, similar to the stage of non-induced MEL cells. Meanwhile, *Klf1* increased its expression and reached the peak at P3, together with the increase of typical erythroid specific genes (*Online Supplementary Figure S3*). This result indicates that clear erythroid differentiation starts at P2. Our PLA result on sorted FL cells show that the GATA1/LDB1 interaction peaks in $CD71^+/TER119^-$ cells at a relatively early stage of erythropoietic differentiation, like undifferentiated MEL cells, when many erythroid genes are still suppressed, until ETO2 disappears from the complex turning on typical erythroid genes. Other LDB1 complex regulated genes such as *c-myb* remain suppressed, because they no longer bind the (activating) LDB1 complex through an as yet unresolved mechanism (Giraud *et al.*, unpublished data).

We show that PLA can detect endogenous level of GATA1/LDB1 and GATA1/FOG1 interactions in FL tissues and we located the GATA1/LDB1 interaction in a specific cell type *in situ*. Whether it corresponds to E7.5 yolk-sac derived primitive cells, E8.5/E9 yolk sac and placenta derived intermediate erythroid-myeloid,[34,35] or HSC derived definitive progenitors is still an open question.

From PLA images a number of transcription factor complexes seem to be located outside the nuclei. The studied factors are certainly formed in the cytoplasm and travel to the nuclei; whether a fraction of interacting factors remains in the cytoplasm is a possibility. The extensive set of complementary experiments that would aim at studying the existence of interactions in the cytoplasm, such as cellular compartment fractionation followed by IP would be similarly questionable, as (like for PLA) it would be difficult to exclude the possibility of the nuclear extract fractions leaking out in the cytoplasmic fractions. We performed an additional control by quantifying the PLA signals in the cytoplasmic area of MEL cells for the positive GATA1/FOG1 and the non-existing TAL1/FOG1 interactions and associated negative controls (single probes and secondary antibodies only), and observed that non-existing TAL1/FOG1 interaction detection presents a lower level to the existing GATA1/FOG1 and GATA1/TAL1 in the cytoplasm (Figure 5B). These differences suggest the existence of a certain level of transcription factor interaction in the cytoplasmic fraction and the amount of signal in TAL1/FOG1 sets the level of background of the PLA technique. It should also be noted that the level of PLA signals from different interactions cannot be compared directly, since PLA is dependent on antibody quality. Therefore, like other immuno-based technic PLA present a certain level of background, easily quantifiable by using single probe, secondary antibodies only, protein mutant and/or non-existing interaction detection. PLA can detect an interaction up to a 40 nm distance[36] and enables super high resolution immunofluorescence microscopy, which can distinguish molecules at a similar distance[37]. Although PLA cannot detect real-time protein-protein interaction, quantification of PLA signals of different GATA1 complexes in sequential stages of ES cell differentiation improves our understanding on the temporal changes of these complexes.

This study therefore reveals that PLA is a powerful tool to examine dynamic protein/protein interactions and their dynamics in differentiating erythroid cells and demonstrates that it provides an excellent alternative for cells in which the abundance of proteins is too low to perform standard co-IP experiments. Our study revealed that PLA can be used to detect very low amount of essential GATA1 complexes emerging at early time point of ES cell differentiation and later on FL tissue, the site of definitive erythropoiesis. In addition we show that the increase followed by a decrease of expression of GATA1 and LDB1 affects a number of genes differentially, for example the expression of the *c-myb* gene which is regulated by the LDB1 complex[15] decreases during differentiation, while the expression of the *β-globin* genes, which are also dependent on the LDB1 complex increases. Further studies will be needed to understand how these differences are regulated.

References

1. Dzierzak E, Speck NA. Of lineage and legacy: the development of mammalian hematopoietic stem cells. Nat Immunol. 2008;9(2):129-136.
2. Medvinsky A, Rybtsov S, Taoudi S. Embryonic origin of the adult hematopoietic system: advances and questions. Development. 2011;138(6):1017-1031.
3. Takahashi S, Onodera K, Motohashi H, et al. Arrest in primitive erythroid cell development caused by promoter-specific disruption of the GATA-1 gene. J Biol Chem. 1997;272(19):12611-12615.
4. Pevny L, Lin CS, D'Agati V, Simon MC, Orkin SH, Costantini F. Development of hematopoietic cells lacking transcription factor GATA-1. Development. 1995; 121(1):163-172.
5. Rodriguez P, Bonte E, Krijgsveld J, et al. GATA-1 forms distinct activating and repressive complexes in erythroid cells. EMBO J. 2005;24(13):2354-2366.
6. Snow JW, Orkin SH. Translational isoforms of FOG1 regulate GATA1-interacting complexes. J Biol Chem. 2009;284(43):29310-29319.
7. Wadman I, Li J, Bash RO, et al. Specific in vivo association between the bHLH and LIM proteins implicated in human T cell leukemia. EMBO J. 1994;13(20):4831-4839.
8. Meier N, Krpic S, Rodriguez P, et al. Novel binding partners of Ldb1 are required for haematopoietic development.

Development. 2006;133(24):4913-4923.
9. Soler E, Andrieu-Soler C, de Boer E, et al. The genome-wide dynamics of the binding of Ldb1 complexes during erythroid differentiation. Genes Dev. 2010;24(3):277-289.
10. Mylona A, Andrieu-Soler C, Thongjuea S, et al. Genome-wide analysis shows that Ldb1 controls essential hematopoietic genes/pathways in mouse early development and reveals novel players in hematopoiesis. Blood. 2013;121(15):2902-2913.
11. Shivdasani RA, Mayer EL, Orkin SH. Absence of blood formation in mice lacking the T-cell leukaemia oncoprotein tal-1/SCL. Nature. 1995;373(6513):432-434.
12. Warren AJ, Colledge WH, Carlton MB, Evans MJ, Smith AJ, Rabbitts TH. The oncogenic cysteine-rich LIM domain protein rbtn2 is essential for erythroid development. Cell. 1994;78(1):45-57.
13. Fredriksson S, Gullberg M, Jarvius J, et al. Protein detection using proximity-dependent DNA ligation assays. Nat Biotechnol. 2002;20(5):473-477.
14. Gutierrez L, Lindeboom F, Ferreira R, et al. A hanging drop culture method to study terminal erythroid differentiation. Exp Hematol. 2005;33(10):1083-1091.
15. Stadhouders R, Thongjuea S, Andrieu-Soler C, et al. Dynamic long-range chromatin interactions control Myb proto-oncogene transcription during erythroid development. EMBO J. 2012;31(4):986-999.
16. de Boer E, Rodriguez P, Bonte E, et al. Efficient biotinylation and single-step purification of tagged transcription factors in mammalian cells and transgenic mice. Proc Natl Acad Sci U S A. 2003;100(13):7480-7485.
17. van de Corput MP, de Boer E, Knoch TA, et al. Super-resolution imaging reveals three-dimensional folding dynamics of the beta-globin locus upon gene activation. J Cell Sci. 2012;125(Pt 19):4630-4639.
18. Soderberg O, Gullberg M, Jarvius M, et al. Direct observation of individual endogenous protein complexes in situ by proximity ligation. Nat Methods. 2006;3(12):995-1000.
19. Grass JA, Boyer ME, Pal S, Wu J, Weiss MJ, Bresnick EH. GATA-1-dependent transcriptional repression of GATA-2 via disruption of positive autoregulation and domain-wide chromatin remodeling. Proc Natl Acad Sci U S A. 2003;100(15):8811-8816.
20. Caputo L, Witzel HR, Kolovos P, et al. The Isl1/Ldb1 complex orchestrates genome-wide chromatin organization to instruct differentiation of multipotent cardiac progenitors. Cell Stem Cell. 2015;17(3):287-299.
21. Socolovsky M, Nam H, Fleming MD, Haase VH, Brugnara C, Lodish HF. Ineffective erythropoiesis in Stat5a(-/-)5b(-/-) mice due to decreased survival of early erythroblasts. Blood. 2001;98(12):3261-3273.
22. Liu Y, Pop R, Sadegh C, Brugnara C, Haase VH, Socolovsky M. Suppression of Fas-FasL coexpression by erythropoietin mediates erythroblast expansion during the erythropoietic stress response in vivo. Blood. 2006;108(1):123-133.
23. Brand M, Ranish JA, Kummer NT, et al. Dynamic changes in transcription factor complexes during erythroid differentiation revealed by quantitative proteomics. Nat Struct Mol Biol. 2004;11(1):73-80.
24. Song SH, Hou C, Dean A. A positive role for NLI/Ldb1 in long-range beta-globin locus control region function. Mol Cell. 2007;28(5):810-822.
25. Anguita E, Hughes J, Heyworth C, Blobel GA, Wood WG, Higgs DR. Globin gene activation during haemopoiesis is driven by protein complexes nucleated by GATA-1 and GATA-2. EMBO J. 2004;23(14):2841-2852.
26. Stadhouders R, Cico A, Stephen T, et al. Control of developmentally primed erythroid genes by combinatorial co-repressor actions. Nat Commun. 2015;6:8893.
27. Goardon N, Lambert JA, Rodriguez P, et al. ETO2 coordinates cellular proliferation and differentiation during erythropoiesis. EMBO J. 2006;25(2):357-366.
28. Gutierrez L, Tsukamoto S, Suzuki M, et al. Ablation of Gata1 in adult mice results in aplastic crisis, revealing its essential role in steady-state and stress erythropoiesis. Blood. 2008;111(8):4375-4385.
29. Li L, Jothi R, Cui K, et al. Nuclear adaptor Ldb1 regulates a transcriptional program essential for the maintenance of hematopoietic stem cells. Nat Immunol. 2011;12(2):129-136.
30. Tsai FY, Keller G, Kuo FC, et al. An early haematopoietic defect in mice lacking the transcription factor GATA-2. Nature. 1994;371(6494):221-226.
31. Kaneko H, Shimizu R, Yamamoto M. GATA factor switching during erythroid differentiation. Curr Opin Hematol. 2010;17(3):163-168.
32. Lugus JJ, Chung YS, Mills JC, et al. GATA2 functions at multiple steps in hemangioblast development and differentiation. Development. 2007;134(2):393-405.
33. Gustafsdottir SM, Schallmeiner E, Fredriksson S, et al. Proximity ligation assays for sensitive and specific protein analyses. Anal Biochem. 2005;345(1):2-9.
34. Alvarez-Silva M, Belo-Diabangouaya P, Salaun J, Dieterlen-Lievre F. Mouse placenta is a major hematopoietic organ. Development. 2003;130(22):5437-5444.
35. McGrath KE, Palis J. Hematopoiesis in the yolk sac: more than meets the eye. Exp Hematol. 2005;33(9):1021-1028.
36. Zatloukal B, Kufferath I, Thueringer A, Landegren U, Zatloukal K, Haybaeck J. Sensitivity and specificity of in situ proximity ligation for protein interaction analysis in a model of steatohepatitis with Mallory-Denk bodies. PLoS One. 2014;9(5):e96690.
37. Zeng Z, Ma J, Xi P, Xu C. Joint tagging assisted fluctuation nanoscopy enables fast high-density super-resolution imaging. J Biophotonics. 2018;11(9):e201800020.
38. Allalou A, Wahlby C. BlobFinder, a tool for fluorescence microscopy image cytometry. Comput Methods Programs Biomed. 2009;94(1):58-65.

ARTICLE

Clonal tracking of erythropoiesis in rhesus macaques

Xing Fan,[1] Chuanfeng Wu,[1] Lauren L. Truitt,[1] Diego A. Espinoza,[1,2] Stephanie Sellers,[1] Aylin Bonifacino,[1] Yifan Zhou,[1,3] Stefan F. Cordes,[1] Allen Krouse,[1] Mark Metzger,[1] Robert E. Donahue,[1] Rong Lu[4] and Cynthia E. Dunbar[1]

[1]Translational Stem Cell Biology Branch, National Heart, Lung, and Blood Institute, National Institute of Health, Bethesda, MA, USA; [2]Perelman School of Medicine, University of Pennsylvania, Philadelphia, PA, USA; [3]Wellcome Trust Sanger Institute, Wellcome Trust Genome Campus, Hinxton, UK and [4]Eli and Edythe Broad Center for Regenerative Medicine and Stem Cell Research, University of Southern California, Los Angeles, CA, USA

Ferrata Storti Foundation

Haematologica 2020
Volume 105(7):1813-1824

ABSTRACT

The classical model of hematopoietic hierarchies is being reconsidered on the basis of data from *in vitro* assays and single cell expression profiling. Recent experiments suggested that the erythroid lineage might differentiate directly from multipotent hematopoietic stem cells / progenitors or from a highly biased subpopulation of stem cells, rather than transiting through common myeloid progenitors or megakaryocyte-erythrocyte progenitors. We genetically barcoded autologous rhesus macaque stem and progenitor cells, allowing quantitative tracking of the *in vivo* clonal output of thousands of individual cells over time following transplantation. $CD34^+$ cells were lentiviral-transduced with a high diversity barcode library, with the barcode in an expressed region of the provirus, allowing barcode retrieval from DNA or RNA, with each barcode representing an individual stem or progenitor cell clone. Barcode profiles from bone marrow $CD45^-CD71^+$ maturing nucleated red blood cells were compared with other lineages purified from the same bone marrow sample. There was very high correlation of barcode contributions between marrow nucleated red blood cells and other lineages, with the highest correlation between nucleated red blood cells and myeloid lineages, whether at earlier or later time points post transplantation, without obvious clonal contributions from highly erythroid-biased or restricted clones. A similar profile occurred even under stressors such as aging or erythropoietin stimulation. RNA barcode analysis on circulating mature red blood cells followed over long time periods demonstrated stable erythroid clonal contributions. Overall, in this non-human primate model with great relevance to human hematopoiesis, we documented continuous production of erythroid cells from multipotent, non-biased hematopoietic stem cell clones at steady-state or under stress.

Introduction

In the classical model of hematopoiesis, initially constructed from data obtained *via in vitro* colony assays and transplantation of populations of flow-sorted phenotypically-defined murine bone marrow (BM) cells, the top of the hematopoietic hierarchy is comprised of a pool of homogenous, self-renewing and always multipotent long-term hematopoietic stem cells (LT-HSC), producing downstream stem and progenitor cells *via* branching pathways passing through discrete intermediate stages. These processes were characterized by stepwise restriction of self-renewal and lineage potential, passing through short-term multipotent HSC (ST-HSC), multipotent progenitors (MPP), and lineage-restricted progenitors, bifurcating first into lymphoid *versus* myeloid progenitors, followed by common myeloid progenitors (CMP) branching towards granulocyte-monocyte progenitors (GMP) and megakaryocyte-erythrocyte progenitors (MEP) in both murine and human studies.[1-3] Optimized *in vitro* clonal assays, large-scale single cell murine transplantation assays, *in vivo* clonal tracking *via* genetic tags and single cell gene

Correspondence:

CYNTHIA DUNBAR
dunbarc@nhlbi.nih.gov

Received: July 8, 2019.

Accepted: October 3, 2019.

Pre-published: October 3, 2019.

doi:10.3324/haematol.2019.231811

Check the online version for the most updated information on this article, online supplements, and information on authorship & disclosures: www.haematologica.org/content/105/7/1813

expression profiling analyzed by computation algorithms predicting differentiation trajectories have challenged the classical branching hematopoietic model in both rodents and humans. Adolffson and co-workers reported direct differentiation of murine megakaryocytic-erythroid lineages from HSC/ MPP.[4] Notta and co-workers analyzed human MPP subpopulations and demonstrated almost exclusively uni-lineage potential of single cells *in vitro*, suggesting that both erythroid and megakaryocytic lineages differentiate directly and separately from HSC/MPP.[5] *In vitro* assays and single cell gene expression mapping of classical human MEP populations also suggested distinct erythroid and megakaryocytic pathways immediately downstream of multipotent progenitors, although other groups were able to purify rare bipotent progenitor cells.[6,7] Both murine and human single-cell RNA-seq profiling of hematopoietic stem and progenitor cells (HSPC) uncovered very early transcriptional lineage priming immediately downstream of HSC, imputing early branching towards individual hematopoietic lineages, and in some models the earliest branch being erythroid.[8-13]

In addition, large-scale optimized single cell murine transplantation assays have suggested that all long-term and self-renewing engrafting cells are not necessarily homogeneous or multipotent, with evidence for lineage-bias or even lineage-restriction. Dykstra and co-workers reported different classes of such cells with myeloid, or multipotent engraftment patterns long-term, maintained in secondary transplants, but did not examine erythroid or megakaryocytic lineages, given lack of expression of standard congenic markers on these lineages.[14] More recently, groups have devised strategies to allow tracking in all murine lineages, and uncovered megakaryocytic-restricted or highly-biased intermediate[15] or long-term engrafting/self-renewing single cells.[16] Use of an inducible transposon to create clonal tags in non-transplanted mice also uncovered a megakaryocyte-restricted differentiation pathway, and both clonal label propagation through various progenitor populations and gene expression profiling suggested that megakaryocyte-primed HSC are located at the top of the hematopoietic hierarchy.[17] These powerful *in vivo* approaches are dependent on methodologies such as single cell transplantation, transposon activation or lineage tracing that are not feasible in humans or large animals.

We have employed rhesus macaque (RM) HSPC autologous transplantation combined with lentiviral genetic barcoding to quantitatively track the *in vivo* clonal output of thousands of individual HSPC over time, in a model with great relevance to human hematopoiesis.[18] Macaques and humans have prolonged lifespans and similar HSPC cycling and dynamics.[19] We previously demonstrated early lineage-restricted engraftment of short-term progenitors for several months, followed by stable very long-term output from engrafted multipotent HSPC, analyzing DNA barcodes from nucleated neutrophils and lymphoid lineages, in the peripheral blood (PB) and BM.[20,21] Persistent myeloid or B-cell lineage bias, although not complete lineage restriction, could be appreciated,[20] and was increased in aged macaques.[22] Peripheral maintenance and expansion of T-cell and mature natural killer (NK) clones was documented.[23] We now apply this macaque model to examine the clonal ontogeny of the erythroid lineage at steady state post transplantation and under erythropoietic stimulation, employing both DNA and expressed RNA barcode analysis. Results in both young and aged macaques revealed closely shared clonal landscapes for erythropoiesis compared to myeloid and lymphoid lineages at both steady states following transplantation and under erythropoietic stress, and clonally-stable erythropoiesis over time.

Methods

Autologous rhesus macaque transplantation

All experiments were carried out on protocols approved by the National Heart, Lung and Blood Institute (NHLBI) Animal Care and Use Committee, following institutional and Department of Health and Human Services guidelines. Details of peripheral blood HSPC mobilization, CD34$^+$ purification, lentiviral transduction, and autologous transplantation following myeloablative (500 rads x2) total body irradiation have been published[24] including details for the specific animals included in the current paper.[20,21,23] Table 1 summarizes transplanted cell doses and length of follow up. Details of transplantation and the clonal patterns in non-erythroid lineages from animals ZH33, ZG66, ZJ31, ZK22, ZL40 and ZH19 have been previously reported.[20,23,25,26]

Barcoded library preparation, validation, transduction, and retrieval

The barcoded lentiviral vector consists of the backbone pCDH (Systems Biosciences) expressing the CopGFP marker gene followed by a 6 base pair (bp) library identifier and a 27 or 35bp highly diverse DNA barcode, flanked by polymerase chain reaction (PCR) amplification sites.[27] Lentiviral vectors were produced using the χHIV packaging system optimized for RM HSPC transduction.[28] CD34$^+$ HSPC were transduced with high-diversity barcoded libraries ensuring that the majority of transduced HSPC contain only one barcode per cell and that each barcode uniquely defines a single HSPC, as described and validated.[20,29] DNA from target cell

Table 1. Transplantation and follow-up characteristics of animals included in this study.

	ZH33	ZG66	ZJ31	ZH19	ZK22	ZL40	JD76	JM82	RQ3600
CD34$^+$ transplant dose (millions)	32	48	23	48	82	57	44.4	91	58.4
CD34$^+$ transplant dose/kg (millions)	6.9	8.5	4.1	7.1	7.2	8.1	4.1	7.2	15.9
% GFP$^+$ infused cells	35%	35%	35%	23%	31%	22.5%	27.1%	34%	35%
Infused GFP$^+$cells (millions)	11.1	16.7	8.0	11.0	25.2	12.8	12.0	30.6	20.4
Follow-up time points (months)	46, 54.5, 60, 61	48, 53, 55.5	3.5, 28, 31, 32, 33, 35	41, 44.5, 45.5, 48.5, 49	9, 11.5, 12.5, 15.5, 17.5	10.5, 12, 15.5	3.5	3.5	46, 48, 49

Details of transplantation and the clonal patterns in non-erythroid lineages from animals ZH33, ZG66, ZJ31, ZH19, ZK22, ZL40 and RQ3600 been previously reported.[20,23,25,26]

populations or cDNA reverse-transcribed from cellular RNA underwent low cycle PCR with primers bracketing the barcode followed by multiplex Illumina sequencing; see the *Online Supplementary Appendix* for details. Sequencing output was processed using custom Python and R code to retrieve and quantitate barcode contributions (available at: *www.github.com/dunbarlabNIH/*), previously validated to closely reflect fractional contributions of each clone within polyclonal cellular populations.[21]

Hematopoietic cell purification and phenotypic analyses

0-15 mL BM aspirates were obtained from the posterior iliac crests or ischial tuberosities. BM and PB samples were separated into mononuclear cell (MNC) and granulocyte (Gr) fractions via centrifugation over a Ficoll gradient (MP Biomedicals). Red blood cells (RBC) were removed from the Gr pellet via red cell lysis with ACK buffer (Quality Biological). BM MNC were passed over an immunoselection column to purify $CD34^+$ HSPC as described.[24] $CD34^-$ MNC flowing through the column or PB MNC were stained with lineage-specific antibodies and sorted for $CD45^-CD71^+$ nucleated red blood cells (NRBC) as described,[30] $CD3^+$ T cells, $CD20^+$ B cells, and $CD3^-CD20^-CD14^+$ monocytes (Mono) as reported previously,[23] using gating strategies shown in *Online Supplementary Figure S1*. The purity of sorted erythroid cells was validated by morphologic scoring of at least 500 cells on Wright's stained and benzidine-stained cytospins. Erythroid cells constituted at least 95% of sorted preparations. Monoclonal antibodies utilized are given in *Online Supplementary Table S1*.

Leukocyte depletion of peripheral blood was performed by filtration through a 10 mL syringe packed with 5 mL of cellulose fibers (Sigma-Aldrich) and fitted with two layers of Whatman™ lens paper (GE Healthcare Life Sciences) covering the outlet.[31] Before use, columns were rinsed with phosphate buffered saline (PBS) and then 5 mL whole blood was added and gently pressed to run through in droplets. Each product was checked for extent of $CD45^+$ cell depletion by flow cytometry, and by morphologic scoring of at least 500 cells on a Wright's stained smear. Each blood sample was >99%-depleted of non-erythroid cells.

Colony-forming unit assays

$CD34^+$ cells were plated for colony-forming unit (CFU) assays according to the manufacturer's (STEMCELL Technologies) instructions in two different methylcellulose formulations: one is MethoCult GF$^+$H4435 complete methylcellulose medium containing human IL-3, IL-6, SCF, G-CSF and GM-CSF to support formation of myeloid CFU, the other is MethoCult H4230 methylcellulose medium supplemented with 3 IU/mL human erythropoietin (EPO) (PeproTech), 5 ng/mL rhesus IL-3 (R&D) and 100 ng/mL human SCF (Miltenyi Biotec), to support erythroid colony formation.[32] Cells were plated at 1000 cells/mL in H4435 medium or at 10,000 cells/ mL in EPO-supplemented H4230 medium, incubated at 37°C and 5% CO_2. At day 12-14, colonies were enumerated and well-separated CFU were plucked individually for molecular analyses.

Erythropoietin treatment

Purified recombinant human EPO (PeproTech) was injected subcutaneously at 3000 U/kg for two doses 12 hours apart to stimulate macaque erythropoiesis[33-35] in barcoded animal ZL40 at 12 months post transplantation. Baseline BM and PB samples were collected five weeks before EPO stimulation, and reticulocyte concentrations in the PB were monitored every other day post EPO administration. When the reticulocytes rose to ≥8%, BM and PB samples were collected. Recovery samples were collected three months post EPO stimulation.

Results

Approaches for erythroid lineage tracking in the rhesus macaque model

In order to track clonal contributions to erythropoiesis in comparison to other lineages, $CD34^+$ HSPC from seven young RM and one aged RM were transduced with high diversity barcoded lentiviral libraries under conditions favoring a single unique barcode marking individual HSPC and reinfused into the autologous RM following ablative total body irradiation (TBI); see Table 1 for a summary of transplantation and transduction parameters. Following engraftment, samples were obtained from BM and PB (Figure 1). As reported previously, short-lived, lineage-restricted progenitors contributed for the first 1-2 months, followed by stable highly polyclonal contributions to Gr, monocytes, B cells, T cells and $CD56^{bright}$ NK cells from long-lived, stable, multipotent long-term repopulating HSPC clones.[21,23] In the current study, we designed assays to study clonal contributions to the erythroid lineage (Figure 1), with the anucleate state of mature circulating erythrocytes requiring design of alternative approaches for mapping of clonal contributions.

Clonal contributions to nucleated erythroid cells are shared with myeloid lineages

Nucleated RBC represent the final stage in marrow erythroid differentiation, before nuclear extrusion and exit from the BM into the PB. NRBC can be identified and sorted to high purity based on absent/low expression of the pan leukocyte marker CD45, and high expression of the transferrin receptor CD71[30,36] (Figure 2A). Unfortunately, RM-reactive antibodies recognizing other erythroid markers, such as glycophorin, do not currently exist. We sorted NRBC from BM MNC based on a $CD45^-CD71^+$ phenotype, with a starting population of 0.2-4.7%, and generated NRBC preparations with high purity (>95%) as confirmed by fluorescence-activated cell sorting (FACS), Wright-Giemsa staining and benzidine staining (Figure 2A and *Online Supplementary Figure S4*). Concurrent purified populations of NRBC, $CD34^+$ HSPC, T cells, B cells, monocytes and Gr were isolated from 10-15 mL BM aspirates from four young adult rhesus monkeys (JD76, ZK22, ZH19 and ZH33, 7-10 years of age) 3.5-46 months post transplantation, and one aged rhesus monkey (RQ3600, 23 years of age), 48 months post transplantation and DNA was obtained for barcode retrieval. Obtaining enough BM prior to three months post transplantation was not feasible due to low marrow cellularity during recovery from TBI.

As we reported recently,[23] there is marked clonal geographic segregation of the output from HSPC in the BM for at least six months post transplantation, followed by very gradual clonal mixing at different BM sites over subsequent months to years. Therefore, we analyzed the barcode clonal pattern of all lineages from the same BM sample, rather than comparing NRBC from one or a few BM sites to circulating myeloid and lymphoid cells. We visualized the contributions of the largest clones to each lineage mapped across all lineages in heat maps (Figure 2B) and analyzed Pearson correlations between all contributing clones (Figure 2C). At both early (3.5 months) and later time points up to several years post transplantation, clonal contributions were closely correlated between NRBC, monocytes and Gr (r values ranged from 0.68 to 0.95;

$P<0.05$) in both young and aged monkeys. Correlations were also high with B cells, known to be produced from HSPC locally in the BM, but clonal contributions to T cells were very distinct and poorly correlated, given that the final stages of T-cell development occur primarily in the thymus, thus T cells in the BM have returned back from the blood and represent the total body clonal T-cell landscape.[23] Figure 2D groups clonal contributions by degree of lineage bias for the young and aged macaques and demonstrates no appreciable contributions from HSPC clones contributing solely or in a highly biased way to NRBC but not to other hematopoietic lineages. The bias and relative size of barcoded clones in other lineages are shown in *Online Supplementary Figure S2*.

Erythroid and myeloid colony-forming units share clonal contributions

Colony-forming unit assays are widely used to study HSPC output and differentiation at a single cell level. Previous publications reported erythroid-biased output

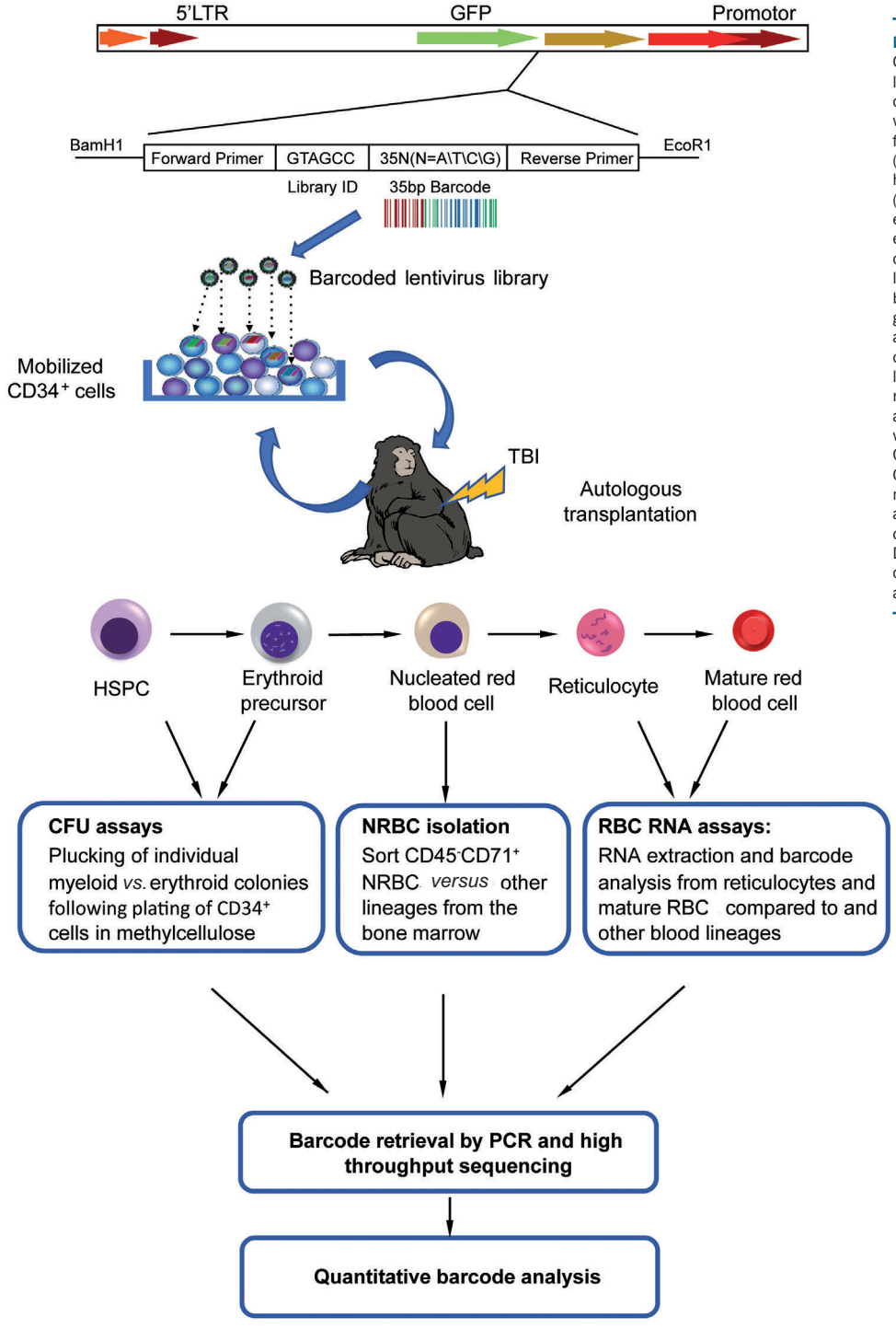

Figure 1. Experimental design. Oligonucleotides consisting of a 6bp library ID followed by a 27-35bp high diversity random sequence barcode were inserted into a lentiviral vector flanked by polymerase chain reaction (PCR) primer sites. RM CD34+ hematopoietic stem and progenitor cell (HSPC) were mobilized into the peripheral blood (PB), collected by apheresis, enriched *via* immunoselection, transduced with the barcoded lentiviral library, and infused back into the total body irradiation (TBI) irradiated autologous macaque. After engraftment, PB and bone marrow (BM) samples were obtained, and various hematopoietic lineages were purified for barcode retrieval and analyses. Lineage cells and nucleated red blood cell (NRBC) were purified from the BM and/or PB. Colony-forming unit (CFU) derived from CD34+ BM cells cultured in semi-solid media, and mature red blood cell (RBC) and reticulocytes were enriched *via* depleting nucleated cells from the PB. DNA and/or RNA were extracted for barcode PCR, high-throughput sequencing, and custom data analysis.

from individual HSPC based on CFU assays.[5,6] We conducted barcode analysis on CFU to investigate clonal output in this progenitor population. CD34+ cells were purified from BM samples post transplantation and cultured at low density under erythroid or myeloid cytokine conditions (Figure 3A). Individual CFU-E or CFU-GM were plucked and 450-600 of each type were pooled together for DNA extraction and barcode recovery. Cell populations of NRBC, T cells, B cells, monocytes and Gr were also purified from the remaining CD34- BM cells after CD34+ cell selection.

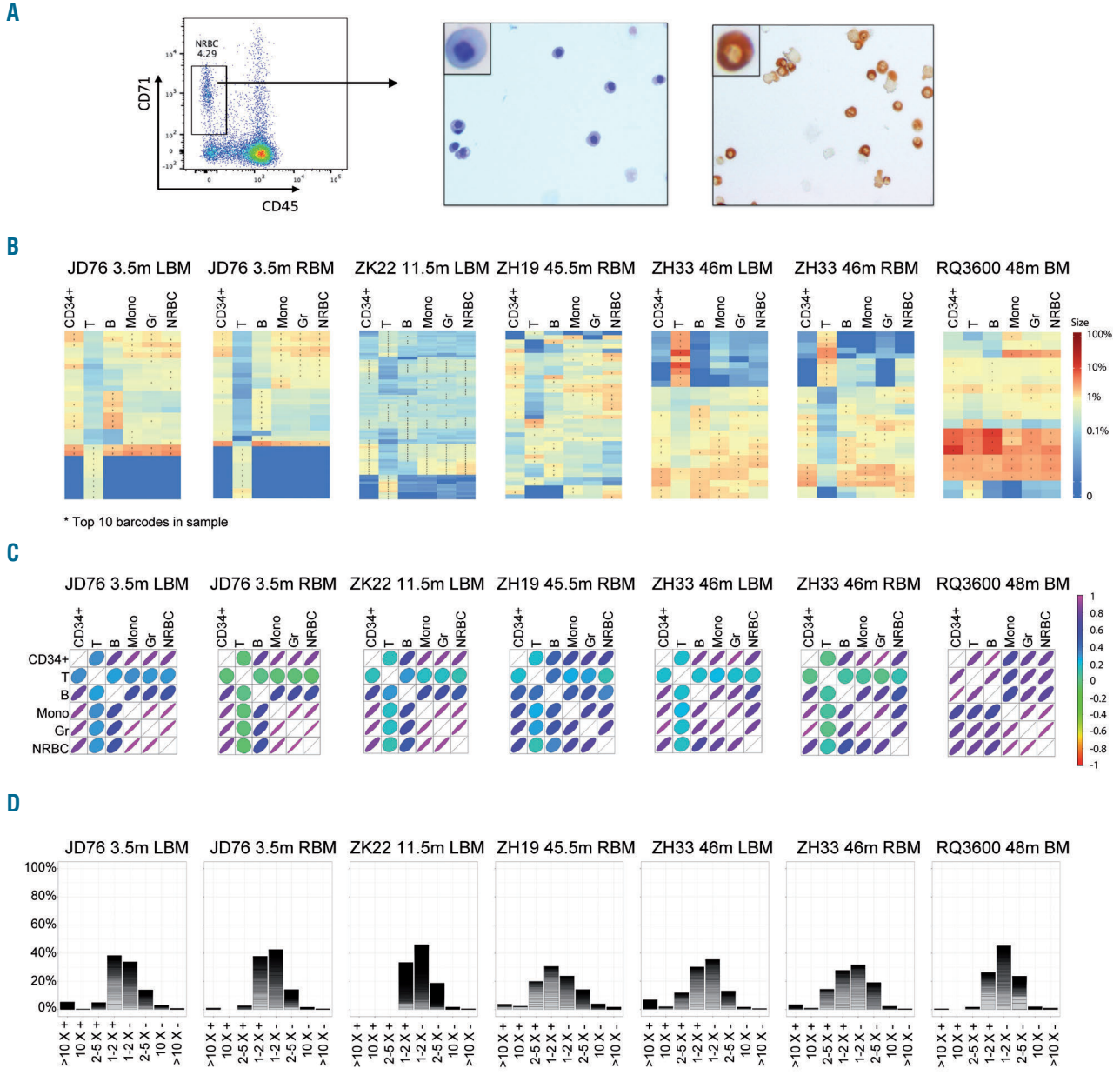

Figure 2. Clonal relationships between erythroid and other hematopoietic lineages. (A) CD45-CD71+ nucleated red blood cell (NRBC) were FACS-purified from six bone marrow (BM) mononuclear cell (MNC) samples obtained from four macaques post transplantation. A representative flow plot and corresponding cytospins of Wright-Giemsa staining and Benzidine staining of purified NRBC are shown. The percentage of NRBC was 94.3±0.8% by Wright-Giemsa staining, and 95.2% by Benzidine staining, counting at least 500 cells. (B) Heat maps representing the log fractional contributions of the top ten most abundant contributing clones retrieved from each different bone marrow (BM) cell lineage population plotted over all BM cell populations. Each individual row represents the fractional contributions from an individual barcode (clone), and each individual column represents a sample. *A barcode is one of the top ten contributing clones in that cell sample (column). Since the top ten barcoded clones in each sample are plotted across all samples, each row in the heat map has at least one*, and each column has exactly ten*. The rows are ordered by unsupervised hierarchical clustering using Euclidean distances to group barcoded clones together that manifest similar patterns of clonal contributions. The color scale on the right depicts the log fractional contribution size. Samples include CD34+ hematopoietic stem and progenitor cell (HSPC), T cells, B cells, monocytes (Mono), granulocytes (Gr), and NRBC. (C) Pearson correlation coefficients comparing all barcoded clonal contributions between different lineages in the same six BM samples shown in (A). The color scale bar for r values is on the right, the shape and the color signify the strength of the correlation. (D) Stacked histograms displaying the degree of erythroid lineage bias and relative size of barcoded clonal contributions (largest to smallest, with smallest clonal contributions appearing only as overlapping lines). Erythroid lineage bias is calculated *via* a ratio of the fractional contribution of a barcode to NRBC *versus* the fractional contribution of the barcode to another lineage (Gr, Mono, CD34+, T, or B), using the largest fractional contribution among the other lineages for each barcode to calculate the ratio. The positive sign (+) indicates bias towards the NRBC lineage and the negative sign (-) indicates bias away from the NRBC lineage.

We analyzed CFU from two animals at 3.5 months post-transplantation (ZJ31 and JD76). The clone heatmaps from these two monkeys documented that the majority of barcodes retrieved from pooled CFU-E were also detected in pooled CFU-GM, along with purified monocytes and Gr, suggesting a shared unbiased myeloid-erythroid HSPC pool (Figure 3B). In addition, we observed unique groups of clones contributing to either CFU-E or CFU-GM but not to both, and those unique clones were also detected as low-contributing clones in circulating blood lineages (Figure 3B), suggesting that the apparent lineage restriction may be due to sampling limitations of the pooled CFU approach.

RNA barcoding tracing of reticulocytes and mature red blood cells from peripheral blood

In an attempt to analyze contributions to the erythroid lineage more comprehensively, sampling the entire blood compartment instead of localized marrow sites, we designed an approach to barcode retrieval from circulating erythroid cells. During the process of erythropoiesis, maturing erythroid cells excluded their nuclei and exited the marrow as reticulocytes containing ample RNA, with loss of RNA over time during the approximately 100-day lifespan of circulating erythrocytes, given lack of ongoing transcription in anucleate cells. Since the lentiviral vectors utilized located the barcodes in a transcribed region of the integrated provirus, we asked whether barcode retrieval from cellular RNA could be used to quantitatively study clonal contributions to various lineages, allowing comparisons between circulating RBC and other blood lineages (Figure 4A). We purified RBC depleted of >99% of nucleated leukocytes as confirmed *via* flow cytometry for CD45 expression and by morphologic scoring (Figure 4B). Polychromatophilic reticulocytes containing ample RNA could be identified by larger size and a grayish color on Wright's-stained blood smears (Figure 4B).

To ask whether RNA barcode contributions match DNA clonal contributions for nucleated blood lineages, we first compared both DNA and RNA barcodes retrieved from the same blood or marrow samples of Gr, monocytes, B cells, T cells and marrow NRBC, specifically from animal ZK22 15.5 months post transplantation; a time point late enough to reach clonal equilibration and homogeneity between different BM sites and PB. In these nucleated cells, the fractional contributions of barcoded clones to DNA *versus* RNA from the same sample were overall well-correlated, with Pearson correlation coefficients (r values) of 0.76±0.04 (Figure 4C), although it is apparent and not surprising that some clones in all lineages contribute primarily at a DNA but not an RNA level, likely due to insertions in chromatin at sites inhospitable to pro-viral gene expression.

However, in comparing major barcode contributions in RNA from circulating RBC *versus* BM NRBC (Figure 4D), most of the barcodes found in NRBC and myeloid samples were also present in the RBC RNA barcodes. But quantitatively the relative levels of individual barcode contributions could vary markedly between immature NRBC and more mature anucleate circulating cells,

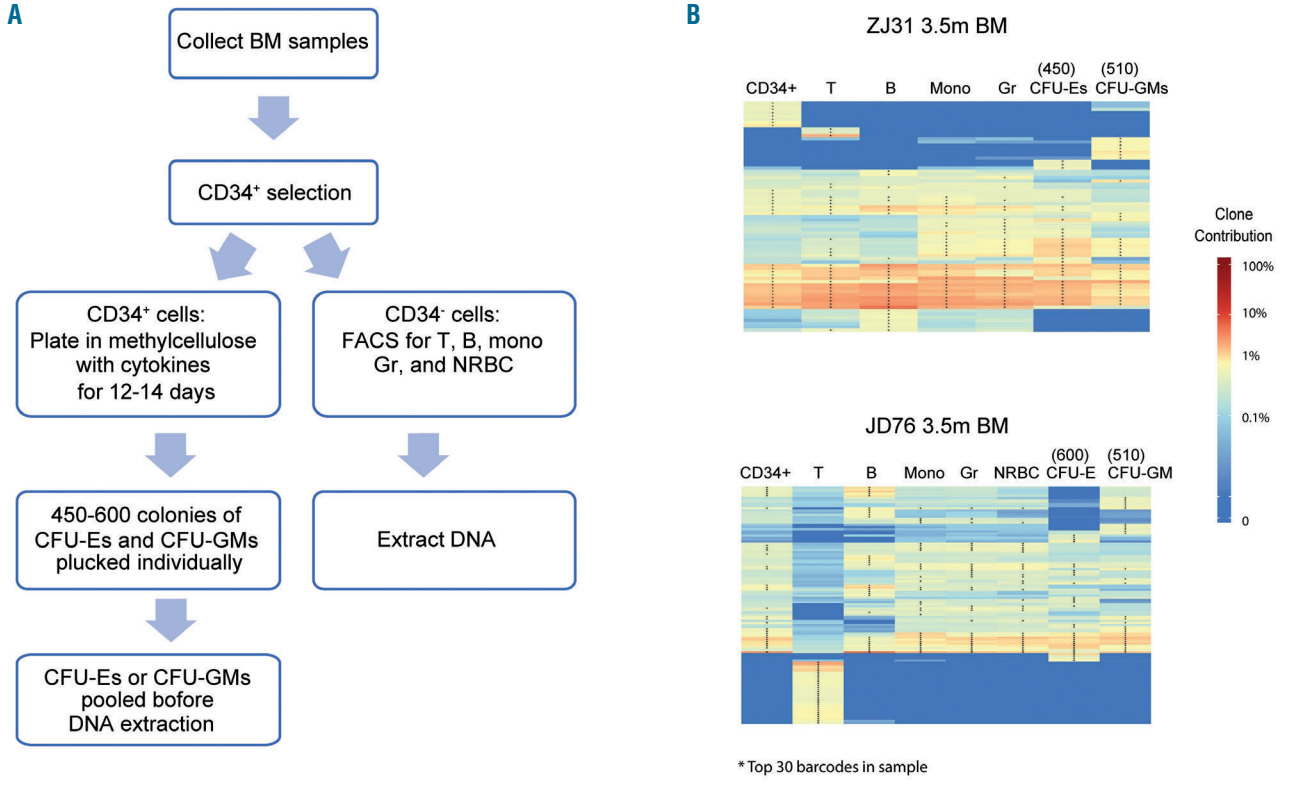

Figure 3. Barcode analysis of bone marrow (BM) colony-forming units (CFU). (A) Flowchart for CFU collection and barcode retrieval. (B) Heatmap of top 30 clones in BM CD34+ cells, T, B, Mono, Gr and nucleated red blood cell (NRBC), and pooled myeloid and erythroid CFU samples from ZJ31 (3.5m) and JD76 (3.5m). The colony number of CFU-E and CFU-GM pooled for DNA extraction and analysis are given on top of each CFU column. Heatmaps were constructed as described in Figure 2B.

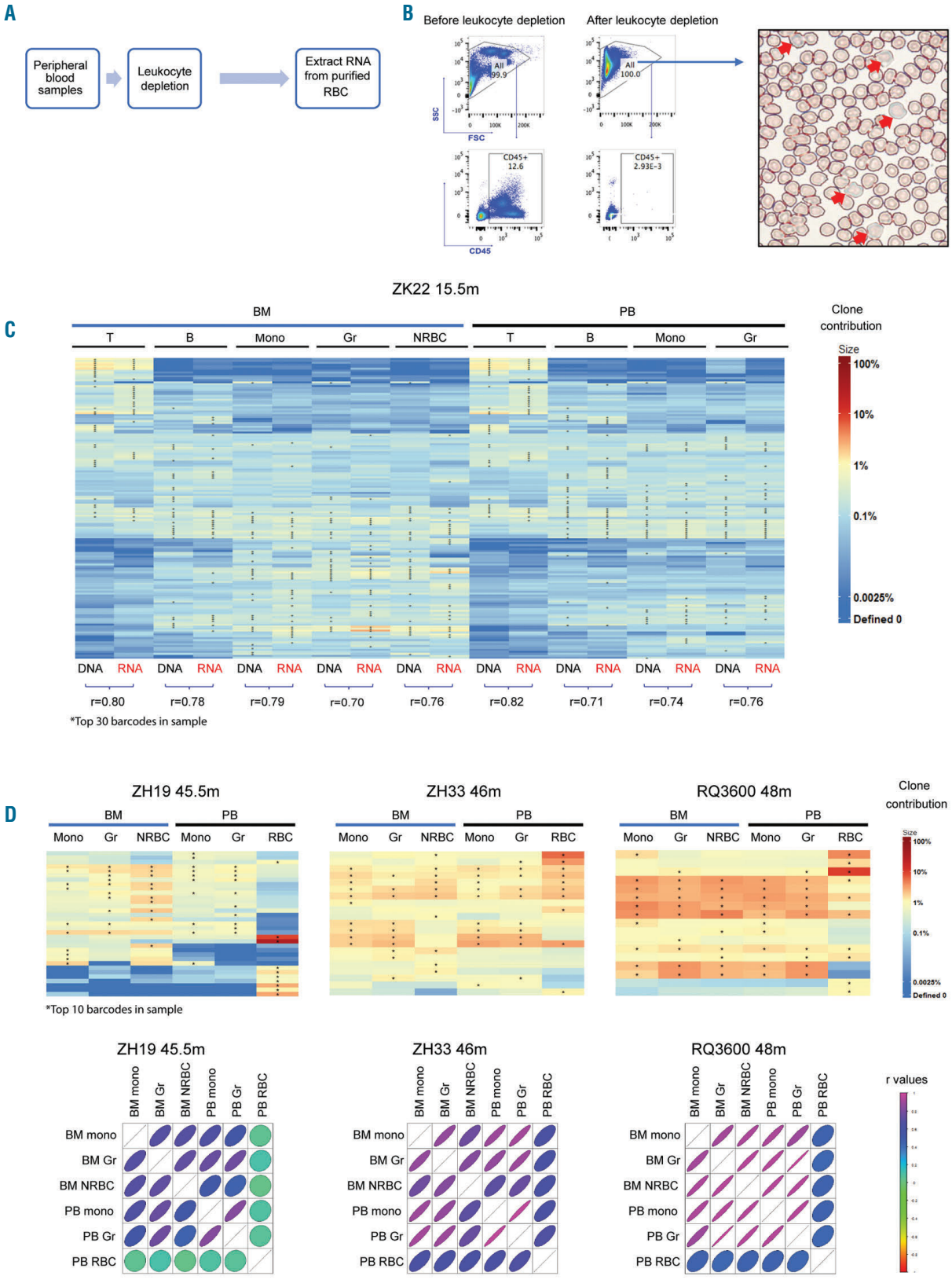

Figure 4. Clonal contributions to circulating erythrocytes. (A) Flowchart for RNA barcode retrieval from circulating anucleate mature red blood cells (RBC) and reticulocytes. (B) FACS plots (left panel) showing CD45 expression on whole blood cells before and after leukocyte depletion, and a Wright's stained blood smear post leukocyte depletion (right panel). The red arrows indicate polychromatophilic reticulocytes with a blue-gray color due to increased RNA content. (C) Heatmap plotting contributions from the top 30 clones in each sample of DNA or RNA obtained from ZK22 15.5m post transplantation, plotted across all samples; heatmap was made as explained in Figure 2B. The paired Pearson correlations between DNA and RNA global barcode contributions to the same sample are given on the bottom of the heatmap. (D) The heatmaps (upper panel) and Pearson correlation plots (lower panel) show peripheral blood (PB) RBC RNA barcodes and the DNA barcode from PB Mono and granulocyte (Gr) and BM Mono, Gr, nucleated red blood cell (NRBC) at the same time point from three rhesus macaque (RM). The color scale is on the right of each panel.

including some barcodes found contributing at high relative levels to RBC compared to NRBC or to other lineages. Conversely, many clones found contributing to NRBC as well as BM or circulating myeloid cells (Gr and Mono) were undetectable or contributing at a fractionally much lower level in RBC. Overall, the Pearson correlations between RNA barcodes contributing to RBC *versus* myeloid cells were much lower than between the other lineages, including between NRBC and myeloid cells, and low even between NRBC and RBC (Figure 4D). These findings may result from legitimate HSPC clonal bias, i.e. HSPC clones that contribute in a highly-biased manner to the erythroid *versus* other lineages. But this seems unlikely, given the discrepancy in clonal patterns between NRBC and anucleate RBC. Instead, we suspect this reflects the marked transcriptional restriction and differential RNA stability occurring in maturing RBC as they transition towards producing massive amounts of only a few proteins, most notably hemoglobin.[37] A large fraction of vector insertion sites may be silenced transcriptionally or translationally during the final stages of RBC enucleation and release, making extrapolating clonal contributions from RNA barcode expression problematic.

We were, however, able to use RNA barcode retrieval to track the stability of clonal contributions to circulating RBC over time, studying six macaques for intervals of up to 15 months. PB RBC RNA barcode analysis showed very stable barcode RBC contribution patterns over time in both young and old animals (Figure 5).

Erythropoietin stimulation does not alter erythroid clonal patterns

We investigated the impact of erythropoietic stress on erythroid clonal patterns. EPO is the key lineage-specific humoral regulator of mammalian erythropoiesis, and in the setting of anemia, levels increase to expand the erythroid compartment. To assess whether lineage-biased clones could be recruited *via* lineage-specific stimulation, we administered a short course of high-dose EPO to achieve significant erythroid proliferation[33-35] in barcoded monkey ZL40. BM and PB samples were collected from animal ZL40 at baseline 10.5 months following transplantation, at the peak of reticulocytosis on day 6 of EPO administration, and at recovery several months later, once blood counts and reticulocyte numbers had returned to baseline (Figure 6A and B).

The clonal patterns in BM NRBC were stable over time whether at baseline, peak or recovery following EPO, and matched those of BM monocytes and Gr (Figure 6C). The RNA barcode analysis of PB RBC RNA also showed an unchanged clonal pattern in response to EPO (Figure 6C). The results indicated that the EPO administration did not change the erythroid clonal output, it only stimulated the existing erythroid progenitor pool to produce more RBC, but without recruiting previously-quiescent HSPC clones to generate new erythroid cells.

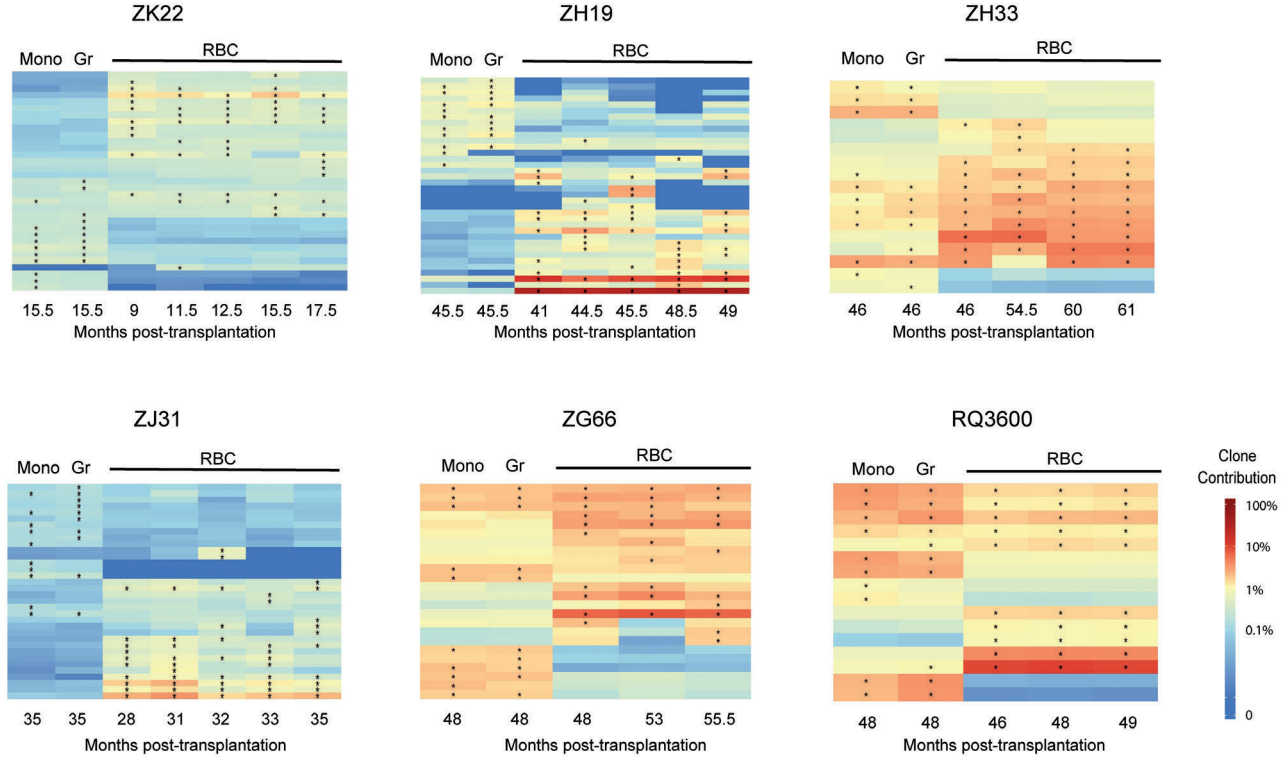

*Top 10 barcodes in sample

Figure 5. Stability of erythroid clonal contributions over time. Heatmaps plotting barcode contributions to peripheral blood (PB) red blood cell (RBC) RNA over time in five young macaques and one aged (RQ3600) macaque, compared to DNA barcode from PB monocytes (Mono) and granulocytes (Gr). Each heatmap plots the top ten contributing clones in each sample across all samples, heatmaps were made as explained in Figure 2B. The color scale is on the right.

Discussion

The cellular differentiation pathways supporting ongoing adult erythropoiesis from primitive marrow HSPC are still not completely clear, with some contradictory findings in murine and human studies, particularly regarding whether erythroid production is supported by multipotent then bipotent intermediate steps downstream from the most primitive HSC, as in the classical model.[1-3] Recent findings in murine model human cells studied in robust single cell *in vitro* assays, and pseudotemporal ordering of single cell RNA-Seq gene expression patterns have raised the possibility that the erythroid and megakaryocytic lineages, along with eosinophils and basophils in some studies, may represent the earliest branch point during hematopoiesis from self-renewing LT-HSC.[5,8-10,12,13,17,38,39] The RNA-Seq study most relevant to erythropoiesis came from Tusi and co-workers, enriching for cell populations previously linked to erythropoiesis to study differentiation trajectories, reporting that HSC/MPP first bifurcate towards erythroid-basophil-megakaryocytes *versus* myeloid-lymphoid pathways before constricting to erythroid or towards myeloid and lymphoid fates. Murine lineage tracing studies using platelet lineage-specific promoters have uncovered evidence for long-lasting and self-renewing megakaryocyte-restricted HSC, but to date, erythroid-restricted engrafting HSPC have not been uncovered, despite the suggestion, based on gene expression studies, that they may exist.[15-17,40] These observations led us to ask whether we could detect long-lived erythroid-restricted or highly erythroid-biased HSPC in our RM barcoded clonal tracking model.

Techniques allowing long-term tracking of hematopoiesis *in vivo* at a single cell level *via* fate mapping or clonal tags are powerful tools to provide answers to these questions and have been utilized primarily in murine models over the past decade. Yamamoto *et al.*[15] used single cell murine HSPC transplants along with lineage-specific markers and demonstrated lineage-restricted engrafting progenitors producing platelets, platelets and red cells, or all myeloid/erythroid lineages, and single cells able to produce both megakaryocyte and multipotent engrafting daughter cells, but no other uni-lineage daughter HSC. Using a non-transplant "naïve hematopoiesis" murine transposon-tagging model, Rodriguez *et al.* came to similar conclusions regarding LT-HSPC heterogeneity, showing megakaryocytic-restricted long-term contributing HSPC clones, but did not examine erythroid output at a clonal level.[17] The Jacobsen laboratory also reported lineage-restricted long-term self-renewing potential initially only for the platelet lineage in mice,[40] more recently adding an erythroid-specific tracer that did not reveal long-term erythroid-restricted HSPC, but did uncover very rare platelet-erythroid

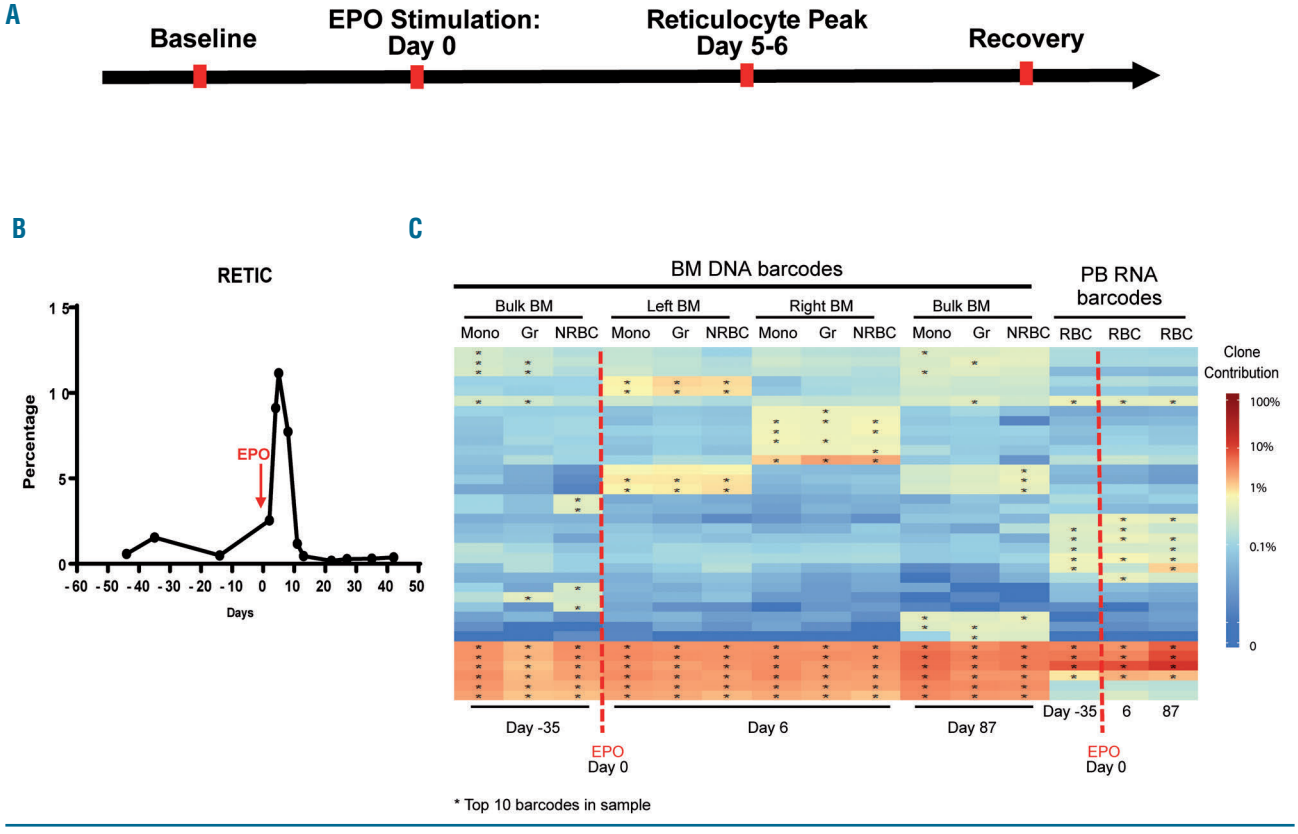

Figure 6. Impact of erythropoietin (EPO) administration on erythroid clonal patterns. (A) Timeline of EPO stimulation and sampling in ZL40, EPO was administrated at 11.5m post transplantation. (B) The reticulocyte (RETIC) percentage during EPO stimulation. (C) Heatmap of the top ten contributing clones from bone marrow (BM) monocytes (Mono), granulocytes (Gr) and nucleated red blood cell (NRBC) DNA barcodes and peripheral blood (PB) red blood cell (RBC) RNA barcodes samples before and post EPO stimulation. Heatmap was constructed as described in Figure 2B. day -35: baseline, day 6: reticulocyte peak, and day 87: recovery after EPO stimulation are shown.

restricted LT-HSPC.[16] However, the majority of single HSPC were multipotent.

Similar *in vivo* studies of human LT-HSPC properties *via* single cell transplantation or naïve hematopoietic tagging are not feasible, but the significant differences between human and rodent hematopoiesis make extrapolation difficult.[41] *In vitro* single cell CFU assays are the classic approach to study lineage relationships and search for intermediate progenitors in hematopoiesis.[1,3] Notta *et al.*[5] found that populations of human CD34$^+$ HSPC sorted by previously-described erythroid and megakaryocytic lineage markers and grown in single cell culture did not reveal single progenitors with both erythroid and megakaryocytic or erythroid and myeloid potential, in contrast to the presence of such progenitors in fetal liver and cord blood, thereby supporting the concept that both erythroid and megakaryocytic lineages emerge directly from multipotent HSC, at least postnatally. In contrast, several other groups did find appreciable numbers of single human progenitors with both erythroid and myeloid potential using a different culture system and lineage-defining antibodies.[6,7]

Our macaque barcoding approach provides a robust platform to quantitatively track the output of thousands of individual HPSC clones long-term over multiple lineages *in vivo*. The clonal landscape in NRBC closely matched that of other hematopoietic lineages sampled from the same BM locus at same time point, with a particularly close relationship between NRBC and Gr and monocytes, which are continuously produced from HSPC, in contrast to T cells that can clonally expand and renew peripherally. Our analysis of thousands of individual clones contributing to purified nucleated erythroid precursors *versus* other lineages at the same time point and at the same marrow location did not uncover a measurable population of markedly erythroid-biased LT-HSPC in this post-transplantation model. Likewise, analysis of barcodes from hundreds of pooled myeloid and erythroid CFU grown from marrow post transplantation led to similar conclusions, although a small fraction of clones unique to CFU-E were identified; however, CFU-GM analyses also revealed unique clones. Given that engraftment in macaques results from many thousands of individual LT-HSPC,[20] the apparent presence of lineage-restricted CFU was likely due to sampling bias or potentially differential clonal *in vivo versus* in CFU *in vitro*. However, we cannot rule out that these lineage-restricted clones detected only *via* CFU analysis represent true myeloid or erythroid-restricted clones not detected in our NRBC analyses.

Our findings were confirmed at various time points from months to years post transplantation. Even in an aged macaque, previously shown to have long-term persistence of highly myeloid and lymphoid biased clones,[22] we found no evidence for erythroid-biased clones not also biased towards myeloid output. A recent human lentiviral gene therapy study in patients with an immunodeficiency disorder used insertion site retrieval to map clonal relationships between lineages, and also reported primarily shared clones contributing to erythroid and myeloid lineages.[42] Of note, our findings do not contradict the concept, derived from recent single cell gene expression studies, that erythroid pathways diverge very early from myeloid and lymphoid lineages, representing one of the first branches from differentiating LT-HSC. A multipotent LT-HSC marked by a barcode could produce daughters going down both erythroid and non-erythroid pathways. Our results do suggest that no significant contributions from self-renewing or engrafting erythroid-restricted or highly biased progenitors could be detected, at least in this transplantation model. However, in several murine studies, the stress of transplantation or *in vitro* culture was shown to drive megakaryocytic-biased HSC to contribute to additional lineages,[16,17] thus our transplantation model may not reflect physiologic naïve hematopoiesis.

Since we have discovered that clonal output from individual HSPC can remain highly geographically restricted within the BM for up to years post transplantation,[23] it may be difficult to study the entire clonal composition of NRBC or erythroid progenitors *via* marrow sampling alone. Thus we also analyzed the barcodes in circulating mature RBC and reticulocytes *via* retrieval of RNA barcodes, given the lack of DNA in enucleated cells. Fractional contributions of DNA and RNA barcodes retrieved from the same nucleated sample of each lineage were compared and showed high correlation, suggesting the differentiation pathway for these lineages does not impact significantly on expression level of barcodes from our vector regardless of insertion site, due to expression of the marker gene and the barcode RNA from a strong constitutive viral promoter. However, RNA barcodes in circulating reticulocytes/mature RBC revealed a less diverse clonal pattern and major differences from clonal contribution patterns revealed in RNA of circulating myeloid and lymphoid cells, and even from NRBC concurrently sampled from the BM in animals many years post transplantation. Rather than implying erythroid lineage bias, we suspect these findings resulted from a major constriction of gene expression in anucleate erythroid cells, with marked silencing of many endogenous genes other than hemoglobin and red cell structural proteins. Bonafoux *et al.*[43] reported globally skewed transcriptional activity follow erythroid differentiation, with major differences in gene expression between end stage anucleate erythroid cells and leukocytes, and even in comparison with earlier stage erythroid progenitors. More than 50% of transcripts in these end stage erythroid cells encoded globin. The fact that many viral integrations were likely also silenced and thus did not express the barcode is supported by the observation that the GFP percentage in RBC was much lower than in Gr in all our macaques (*Online Supplementary Figure S3*). Despite the difficulties in comparing clonal contributions in RBC RNA to other lineages, sampling of PB RBC over prolonged periods of time allowed us to establish the long-term clonal stability of contributing HSPC to erythropoiesis for as long as four years post transplantation.

Given the advantage of our experimental models, we sought to answer some additional questions, including whether erythropoiesis at a clonal level will be stable under lineage-specific stimulation, or if lineage-specific clones might be recruited under this proliferative stress, as has been suggested for lineage-restricted megakaryocytopoiesis.[44] Thus, we tracked the clonal characteristics of hematopoiesis under stimulation by EPO, a key lineage-specific humoral regulator responsible for erythroid progenitor proliferation and accelerated maturation. We found no detectable impact on clonal contributions under EPO stimulation, suggesting that the pool of HSPC contributing to erythropoiesis does not shift between steady state and proliferative stress resulting from EPO stimula-

tion. It would be of interest to examine megakaryocytes/platelet output in our model, at steady state or under stress, but the size and lack of nucleus in platelets present challenges, as does the rarity of megakaryocytes in the BM. We are developing an optimized vector allowing concurrent single cell RNA-Seq and barcode retrieval to further investigate platelet and other lineage relationships.[17]

In conclusion, this study is the first to quantitatively track erythropoiesis at a clonal level *in vivo* in a translationally-relevant model. Overall, our analyses indicate long-term shared ontogeny with other lineages, particularly myeloid cells, without measurable contributions from highly erythroid-biased or restricted long-term engrafting HSPC, even under stressors such as aging or erythroid lineage-specific cytokine stimulation. A better understanding of erythropoiesis at this level has relevance for further development of new therapies targeting erythroid disorders.

Funding

This research was supported by the NHLBI Division of Intramural Research.

Acknowledgments

We thank Naoya Uchida for the χHIV plasmid, and Keyvan Keyvanfar for cell sorting. We acknowledge the support of the NHLBI FACS Core, the NHLBI DNA Sequencing and Genomics Core, the NHLBI animal care and veterinary staff, and the NIH Biowulf High-Performance Computing Resource.

References

1. Akashi K, Traver D, Miyamoto T, Weissman IL. A clonogenic common myeloid progenitor that gives rise to all myeloid lineages. Nature. 2000; 404(6774):193-197.
2. Vannucchi AM, Paoletti F, Linari S, et al. Identification and characterization of a bipotent (erythroid and megakaryocytic) cell precursor from the spleen of phenylhydrazine-treated mice. Blood. 2000; 95(8):2559-2568.
3. Manz MG, Miyamoto T, Akashi K, Weissman IL. Prospective isolation of human clonogenic common myeloid progenitors. Proc Natl Acad Sci U S A. 2002; 99(18):11872-11877.
4. Adolfsson J, Mansson R, Buza-Vidas N, et al. Identification of Flt3+ lympho-myeloid stem cells lacking erythro-megakaryocytic potential a revised road map for adult blood lineage commitment. Cell. 2005;121(2):295-306.
5. Notta F, Zandi S, Takayama N, et al. Distinct routes of lineage development reshape the human blood hierarchy across ontogeny. Science. 2016;351(6269): aab2116.
6. Psaila B, Barkas N, Iskander D, et al. Single-cell profiling of human megakaryocyte-erythroid progenitors identifies distinct megakaryocyte and erythroid differentiation pathways. Genome Biol. 2016;17:83.
7. Sanada C, Xavier-Ferrucio J, Lu YC, et al. Adult human megakaryocyte-erythroid progenitors are in the CD34+CD38mid fraction. Blood. 2016;128(7):923-933.
8. Athanasiadis EI, Botthof JG, Andres H, Ferreira L, Lio P, Cvejic A. Single-cell RNA-sequencing uncovers transcriptional states and fate decisions in haematopoiesis. Nat Commun. 2017;8(1):2045.
9. Tusi BK, Wolock SL, Weinreb C, et al. Population snapshots predict early haematopoietic and erythroid hierarchies. Nature. 2018;555(7694):54-60.
10. de Graaf CA, Choi J, Baldwin TM, et al. Haemopedia: An Expression Atlas of Murine Hematopoietic Cells. Stem Cell Reports. 2016;7(3):571-582.
11. Hamey FK, Nestorowa S, Kinston SJ, Kent DG, Wilson NK, Gottgens B. Reconstructing blood stem cell regulatory network models from single-cell molecular profiles. Proc Natl Acad Sci U S A. 2017;114(23):5822-5829.
12. Paul F, Arkin Y, Giladi A, et al. Transcriptional Heterogeneity and Lineage Commitment in Myeloid Progenitors. Cell. 2015;163(7):1663-1677.
13. Velten L, Haas SF, Raffel S, et al. Human haematopoietic stem cell lineage commitment is a continuous process. Nat Cell Biol. 2017;19(4):271-281.
14. Dykstra B, Kent D, Bowie M, et al. Long-term propagation of distinct hematopoietic differentiation programs in vivo. Cell Stem Cell. 2007;1(2):218-229.
15. Yamamoto R, Morita Y, Ooehara J, et al. Clonal analysis unveils self-renewing lineage-restricted progenitors generated directly from hematopoietic stem cells. Cell. 2013; 154(5):1112-1126.
16. Carrelha J, Meng Y, Kettyle LM, et al. Hierarchically related lineage-restricted fates of multipotent haematopoietic stem cells. Nature. 2018;554(7690):106-111.
17. Rodriguez-Fraticelli AE, Wolock SL, Weinreb CS, et al. Clonal analysis of lineage fate in native haematopoiesis. Nature. 2018; 553(7687):212-216.
18. Donahue RE, Dunbar CE. Update on the use of nonhuman primate models for preclinical testing of gene therapy approaches targeting hematopoietic cells. Hum Gene Ther. 2001; 12(6):607-617.
19. Shepherd BE, Kiem HP, Lansdorp PM, et al. Hematopoietic stem-cell behavior in nonhuman primates. Blood. 2007;110(6):1806-1813.
20. Koelle SJ, Espinoza DA, Wu C, et al. Quantitative stability of hematopoietic stem and progenitor cell clonal output in rhesus macaques receiving transplants. Blood. 2017;129(11):1448-1457.
21. Wu C, Li B, Lu R, et al. Clonal tracking of rhesus macaque hematopoiesis highlights a distinct lineage origin for natural killer cells. Cell Stem Cell. 2014;14(4):486-499.
22. Yu KR, Espinoza DA, Wu C, et al. The impact of aging on primate hematopoiesis as interrogated by clonal tracking. Blood. 2018;131(11):1195-1205.
23. Wu C, Espinoza DA, Koelle SJ, et al. Geographic clonal tracking in macaques provides insights into HSPC migration and differentiation. J Exp Med. 2018;215(1):217-232.
24. Donahue RE, Kuramoto K, Dunbar CE. Large animal models for stem and progenitor cell analysis. Curr Protoc Immunol. 2005;Chapter 22:Unit 22A.1.
25. Wu C, Li B, Lu R, et al. Clonal tracking of rhesus macaque hematopoiesis highlights a distinct lineage origin for natural killer cells. Cell Stem Cell. 2014;14(4):486-499.
26. Yu KR, Espinoza DA, Wu C, et al. The impact of aging on primate hematopoiesis as interrogated by clonal tracking. Blood. 2018;131(11):1195-1205.
27. Lu R, Neff NF, Quake SR, Weissman IL. Tracking single hematopoietic stem cells in vivo using high-throughput sequencing in conjunction with viral genetic barcoding. Nat Biotechnol. 2011;29(10):928-933.
28. Uchida N, Washington KN, Hayakawa J, et al. Development of a human immunodeficiency virus type 1-based lentiviral vector that allows efficient transduction of both human and rhesus blood cells. J Virol. 2009; 83(19):9854-9862.
29. Lu R, Neff NF, Quake SR, Weissman IL. Tracking single hematopoietic stem cells in vivo using high-throughput sequencing in conjunction with viral genetic barcoding. Nat Biotechnol. 2011;29(10):928-933.
30. Fornas O, Domingo JC, Marin P, Petriz J. Flow cytometric-based isolation of nucleated erythroid cells during maturation: an approach to cell surface antigen studies. Cytometry. 2002;50(6):305-312.
31. Sriprawat K, Kaewpongsri S, Suwanarusk R, et al. Effective and cheap removal of leukocytes and platelets from Plasmodium vivax infected blood. Malar J. 2009;8:115.
32. Wong S, Keyvanfar K, Wan Z, Kajigaya S, Young NS, Zhi N. Establishment of an erythroid cell line from primary CD36+ erythroid progenitor cells. Exp Hematol. 2010;38(11):994-1005.e1-2.
33. Ramakrishnan R, Cheung WK, Farrell F, Joffee L, Jusko WJ. Pharmacokinetic and pharmacodynamic modeling of recombinant human erythropoietin after intravenous and subcutaneous dose administration in cynomolgus monkeys. J Pharmacol Exp Ther. 2003;306(1):324-331.
34. Lavelle D, Molokie R, Ducksworth J, DeSimone J. Effects of hydroxurea, stem cell factor, and erythropoietin in combination on fetal hemoglobin in the baboon. Exp Hematol. 2001;29(2):156-162.
35. Umemura T, al-Khatti A, Donahue RE, Papayannopoulou T, Stamatoyannopoulos G. Effects of interleukin-3 and erythropoi-

etin on in vivo erythropoiesis and F-cell formation in primates. Blood. 1989;74(5):1571-1576.
36. Dzierzak E, Philipsen S. Erythropoiesis: development and differentiation. Cold Spring Harb Perspect Med. 2013; 3(4):a011601.
37. Thiadens KA, von Lindern M. Selective mRNA translation in erythropoiesis. Biochem Soc Trans. 2015;43(3):343-347.
38. Wilson NK, Kent DG, Buettner F, et al. Combined Single-Cell Functional and Gene Expression Analysis Resolves Heterogeneity within Stem Cell Populations. Cell Stem Cell. 2015;16(6):712-724.
39. Pellin D, Loperfido M, Baricordi C, et al. A comprehensive single cell transcriptional landscape of human hematopoietic progenitors. Nat Commun. 2019;10(1):2395.
40. Sanjuan-Pla A, Macaulay IC, Jensen CT, et al. Platelet-biased stem cells reside at the apex of the haematopoietic stem-cell hierarchy. Nature. 2013;502(7470):232-236.
41. Doulatov S, Notta F, Laurenti E, Dick JE. Hematopoiesis: a human perspective. Cell Stem Cell. 2012;10(2):120-136.
42. Biasco L, Pellin D, Scala S, et al. In vivo tracking of human hematopoiesis reveals patterns of clonal dynamics during early and steady-state reconstitution phases. Cell Stem Cell. 2016;19(1):107-119.
43. Bonafoux B, Lejeune M, Piquemal D, et al. Analysis of remnant reticulocyte mRNA reveals new genes and antisense transcripts expressed in the human erythroid lineage. Haematologica. 2004;89(12):1434-1438.
44. Haas S, Hansson J, Klimmeck D, et al. Inflammation-induced emergency megakaryopoiesis driven by hematopoietic stem cell-like megakaryocyte progenitors. Cell Stem Cell. 2015;17(4):422-434.

ARTICLE

Characterization and genotype-phenotype correlation of patients with Fanconi anemia in a multi-ethnic population

Orna Steinberg-Shemer,[1,2,3*] Tracie A. Goldberg,[1*] Joanne Yacobovich,[1,2] Carina Levin,[4,5] Ariel Koren,[4,5] Shoshana Revel-Vilk,[6] Tal Ben-Ami,[7] Amir A. Kuperman,[8,9] Vered Shkalim Zemer,[1,2] Amos Toren,[2,10] Joseph Kapelushnik,[11] Ayelet Ben-Barak,[12] Hagit Miskin,[6] Tanya Krasnov,[3] Sharon Noy-Lotan,[3] Orly Dgany[3] and Hannah Tamary[1,2,3]

[1]Department of Hematology-Oncology, Schneider Children's Medical Center of Israel, Petach Tikva; [2]Sackler Faculty of Medicine, Tel Aviv University, Tel Aviv; [3]Pediatric Hematology Laboratory, Felsenstein Medical Research Center, Petach Tikva; [4]Pediatric Hematology Unit, Emek Medical Center, Afula; [5]The Ruth and Bruce Rappaport Faculty of Medicine, Technion-Israel Institute of Technology, Haifa; [6]Pediatric Hematology/Oncology Unit, Shaare Zedek Medical Center, Jerusalem, affiliated with Hadassah- Hebrew University Medical School, Jerusalem; [7]Pediatric Hematology Unit, Kaplan Medical Center, Rehovot; [8]Blood Coagulation Service and Pediatric Hematology Clinic, Galilee Medical Center, Nahariya; [9]Azrieli Faculty of Medicine, Bar-Ilan University, Safed; [10]Department of Pediatric Hemato-Oncology, Children's Hospital (Edmond and Lily), Sheba Medical Center, Tel-Hashomer; [11]Pediatric Hematology, Soroka University Medical Center, Ben-Gurion University, Beer Sheva and [12]Pediatric Hematology-Oncology Department, Rambam Medical Center, Haifa, Israel

OS-S and TAG contributed equally as co-first authors.

Ferrata Storti Foundation

Haematologica 2020
Volume 105(7):1825-1834

ABSTRACT

Fanconi anemia (FA), an inherited bone marrow failure (BMF) syndrome, caused by mutations in DNA repair genes, is characterized by congenital anomalies, aplastic anemia, high risk of malignancies and extreme sensitivity to alkylating agents. We aimed to study the clinical presentation, molecular diagnosis and genotype-phenotype correlation among patients with FA from the Israeli inherited BMF registry. Overall, 111 patients of Arab (57%) and Jewish (43%) descent were followed for a median of 15 years (range: 0.1-49); 63% were offspring of consanguineous parents. One-hundred patients (90%) had at least one congenital anomaly; over 80% of the patients developed bone marrow failure; 53% underwent hematopoietic stem-cell transplantation; 33% of the patients developed cancer; no significant association was found between hematopoietic stem-cell transplant and solid tumor development. Nearly 95% of the patients tested had confirmed mutations in the Fanconi genes *FANCA* (67%), *FANCC* (13%), *FANCG* (14%), *FANCJ* (3%) and *FANCD1* (2%), including twenty novel mutations. Patients with *FANCA* mutations developed cancer at a significantly older age compared to patients with mutations in other Fanconi genes (mean 18.5 and 5.2 years, respectively, P=0.001); however, the overall survival did not depend on the causative gene. We hereby describe a large national cohort of patients with FA, the vast majority genetically diagnosed. Our results suggest an older age for cancer development in patients with *FANCA* mutations and no increased incidence of solid tumors following hematopoietic stem-cell transplant. Further studies are needed to guide individual treatment and follow-up programs.

Introduction

Fanconi Anemia (FA), an inherited bone marrow failure (BMF) syndrome, results from defects in the DNA repair pathway, leading to chromosomal instability. The disease is rare with an estimated prevalence of 1:130,000[1] but tends to be higher in certain communities due to founder mutations, especially those with a high rate of

Correspondence:

HANNAH TAMARY
htamary@post.tau.ac.il

ORNA STEINBERG-SHEMER
orna.steinberg@gmail.com

Received: March 27, 2019.

Accepted: September 25, 2019.

Pre-published: September 26, 2019.

doi:10.3324/haematol.2019.222877

Check the online version for the most updated information on this article, online supplements, and information on authorship & disclosures: www.haematologica.org/content/105/7/1825

consanguinity.[1-5] The clinical phenotype includes congenital anomalies, aplastic anemia, a high risk of malignancies, and extreme sensitivity to cross-linking agents. Patients with FA classically present with multiple congenital anomalies and cytopenias, although several patients have no physical defects and normal blood counts, complicating the diagnosis, which is based on the chromosomal breakage test. Genotyping confirms the diagnosis and allows for proper genetic counseling. Some patients exhibit mosaicism, requiring testing by chromosomal breakage and genetic analysis in non-hematopoietic tissue.[6]

FA is usually inherited in an autosomal recessive fashion, with the exception of the X-linked *FANCB* and the dominantly inherited *FANCR*. To date, mutations in more than 20 genes have been detected. Detecting genotype-phenotype correlations is important for prognostic predictions, treatment decisions and establishment of directed follow-up programs. However, to date, a clear correlation between the affected gene and the patient's phenotype has not been found. One exception is the more pronounced cancer predisposition in patients with *FANCD1/BRCA2* and *FANCN/PALB2* mutations, in which early onset of malignancy is almost invariably present. Some evidence suggests that the type of mutation correlates better with the phenotype than the specific gene. For example, one report found that patients with null mutations in *FANCA* present with a more severe phenotype than those with mutations leading to altered FANCA protein production.[7] Conversely, in a separate report, no functional or clinical difference was found between patients with absent FANCA protein or those with altered FANCA protein.[8] It is possible that specific mutations, as opposed to affected gene or type of mutation, best correlate with the phenotype.[9] However, even for a specific mutation, there is a variable phenotypic severity among different ethnicities and among siblings, even twins, suggesting a role for genetic or epigenetic modifiers and/or environmental factors.

Here, we present data regarding 111 patients with FA in Israel. This large cohort is unique due to Israel's ethnic diversity, a high degree of consanguinity and a very high percentage of genetically diagnosed patients.

Methods

FA was defined by an abnormal chromosomal breakage test and/or a genetic diagnosis of biallelic mutations in one of the known FA genes. Patients with FA were registered by their treating hematologist as part of the Israeli inherited bone marrow failure registry (I-IBMFR). The I-IBMFR is approved by each local Institutional Review Board. Data was collected at entry to the registry and annually. Data were extracted by the treating physician or by the research team from the patients' charts including demographics, clinical characteristics, laboratory data (including chromosomal breakage tests results), molecular diagnosis, and data regarding treatment.

BMF was defined by one of these criteria: a patient who underwent hematopoietic stem cell transplantation (HSCT) for a non-malignant indication, transfusion dependence or at least one cytopenia defined as: absolute neutrophil count (ANC) <1000/μL, platelet count <100,000/μL or hemoglobin <10 g/dL. Severe BMF was further defined as ANC <500/μL and platelet count <20,000/μL.

A five-item congenital abnormality score (CABS) was calculated for each patient by adding up the total number of phenotypic abnormalities in a set consisting of developmental delay, heart or lung abnormalities, renal anomalies, hearing loss and head abnormalities.[10] Whenever possible, genetic analysis was performed as part of the routine work-up. Patients were included in this study if they were clinically suspected as having FA and had either a confirmed genetic diagnosis of FA or an abnormal chromosomal breakage test, or both.

Genetic analysis was performed by Sanger sequencing, as previously described.[11] Sequencing was performed on an ABIPrism 3130xl Genetic Analyzer (Applied Biosystems, Foster City, CA, USA). Chromatograms were visualized with CHROMAS (v.2.6.4; www.thechnelysium.com.au). Variant pathogenicity was determined based on the American College of Medical Genetics and Genomics (ACMG) criteria. Multiplex ligation dependent probe amplification (MLPA) was performed using the commercially available kit SALSA MLPA probemix P031-B2/P032-B2 FANCA (MRC-Holland) following the manufacturer's instruction.

Data organization was performed with Microsoft Excel (Windows, Version 16.11.1). The data were analyzed using BMDP software (1993, University of California Press, USA). Pearson's chi-square test or Fisher's exact test (two-tailed) was used for analysis of between-group differences in discrete variables, and analysis of variance (ANOVA) was used for continuous variables. Those variables which did not have Gaussian distributions or when the sample size was very small were compared using the non-parametric Mann-Whitney test. The Kaplan-Meier estimate was used to show survival for the cohort and various sub-groups. Calculations and graphic representation of survival curves were performed on Prism 7 (Graph Pad Software) and on MedCalc software (Belgium). A *P*-value of ≤0.05 was considered significant.

Table 1. Characteristics of Fanconi anemia patients in Israel.

N= 108 patients		Ethnicities	
46	26	Sephardic	Jewish
	10	Ashkenazi	
	9	Mixed	
62	1	Ethiopian	Arab
	54	Muslim	
	6	Druze	
	2	Christian	

Results

Patient demographics

One hundred and eleven patients (53% male) with FA diagnosed between 1980 and 2016 were registered in the I-IBMFR and followed for a median of 15 (range: 0.1-49) years. (Table 1). The median survival time was 27.9 years Brookmayer-Crowley 95% Confidence interval [CI]: 24-35) (Figure 1A).

Ethnic Origin

Over half of the patients with FA in our cohort were of Arab descent, while the rest were Jewish, mostly of Sephardic origin (Table 1). 63% of the patients were offspring of consanguineous parents. Consanguinity was reported in 93% of Arab patients and in 21% of Jewish patients. Notably all of the Druze patients were offspring of consanguineous parents.

Clinical Features

The median age at the time of diagnosis of FA was 6 years (range: 0-26.5); 20% were born small for the gestational age, and 57% fit criteria for short stature. The majority of patients (90%) had at least one congenital anomaly. More than half had café-au-lait spots (52.3%) followed by renal anomalies (39.6%). Of the 18% of the patients with hearing loss, all had a conductive component (Table 2).

Previous publications have reported an association between the presence or absence of radial ray anomalies and a five-item CABS on disease prognosis.[10,12] Five-item CABS were calculated for each patient,[10] resulting in 41 patients with CABS 0, an additional 41 patients with CABS 1, 22 patients with CABS 2, five patients with CABS 3 and one patient each with CABS 4 and CABS 5. There was no correlation between the CAB score and survival (Figure 1B). In our cohort, 82% of the patients developed BMF, of which 18% fit criteria for severe BMF. All patients with higher CABS (3-5) exhibited BMF with the exception of one patient who developed infant AML and was transplanted at the age of five months. No association was found between radial ray anomalies and BMF development.

Malignancy

During the follow-up period of this patient cohort, 30% developed myelodysplastic syndrome (MDS), leukemia and/or solid tumors (Table 3). The mean age for the first event of MDS was 13.3 years (standard deviation [SD] 8.6), for leukemia 10.8 years (SD 6.2) and for solid tumors 26.6 years (SD 4.9). No significant difference was detected

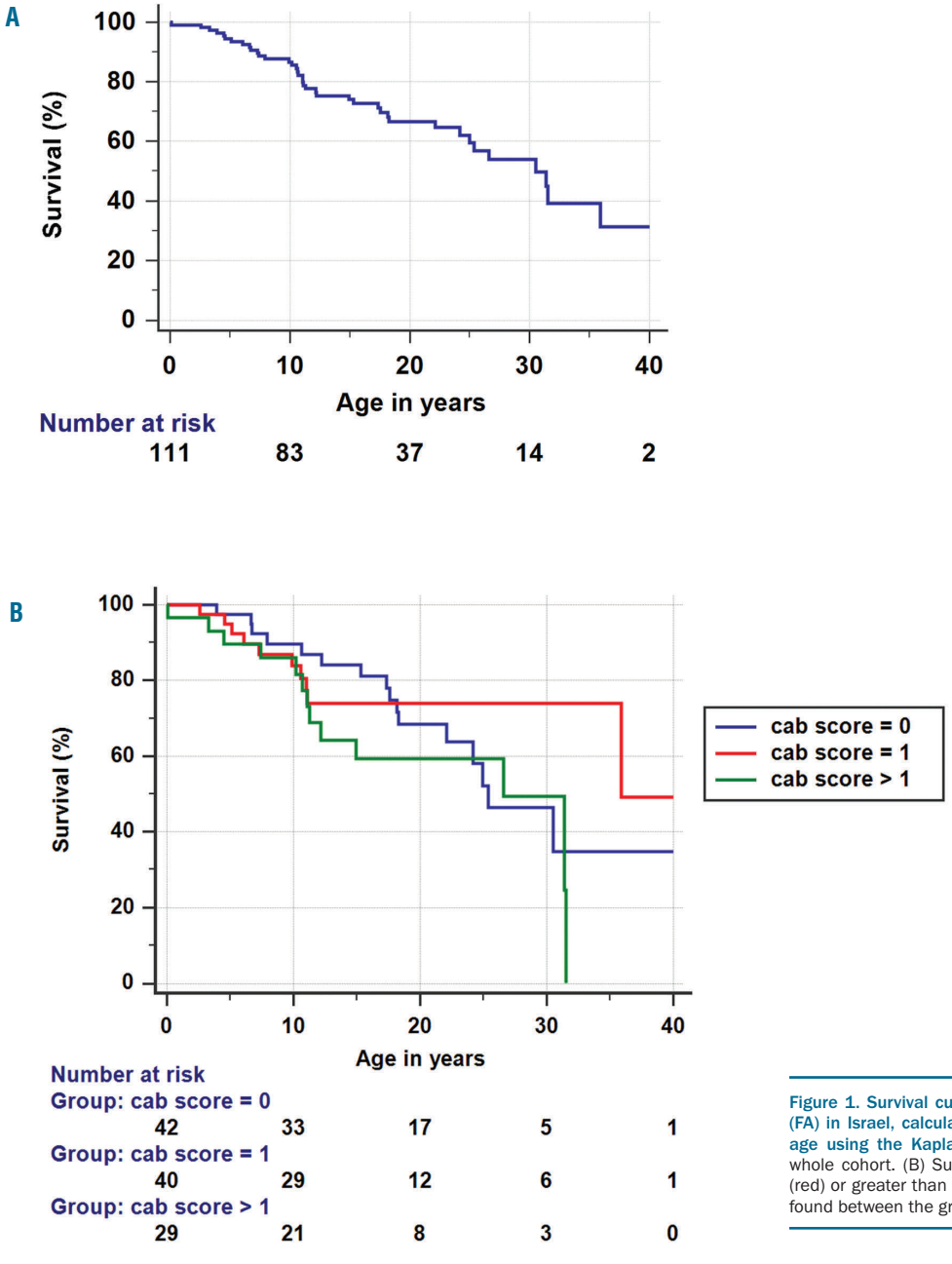

Figure 1. Survival curves for patients with Fanconi anemia (FA) in Israel, calculating the proportion of live patients by age using the Kaplan-Meier methods. (A) Survival for the whole cohort. (B) Survival divided by cab score 0 (blue), 1 (red) or greater than 1 (green). No significant difference was found between the groups.

between the age of the first event of MDS and the age of the first event of leukemia; however, both MDS and leukemia were diagnosed significantly earlier relative to solid tumors (P=0.001 and P<0.001, respectively) (Figure 2A). Seven patients developed two cancers, three patients developed three cancers, and two patients developed four cancers.

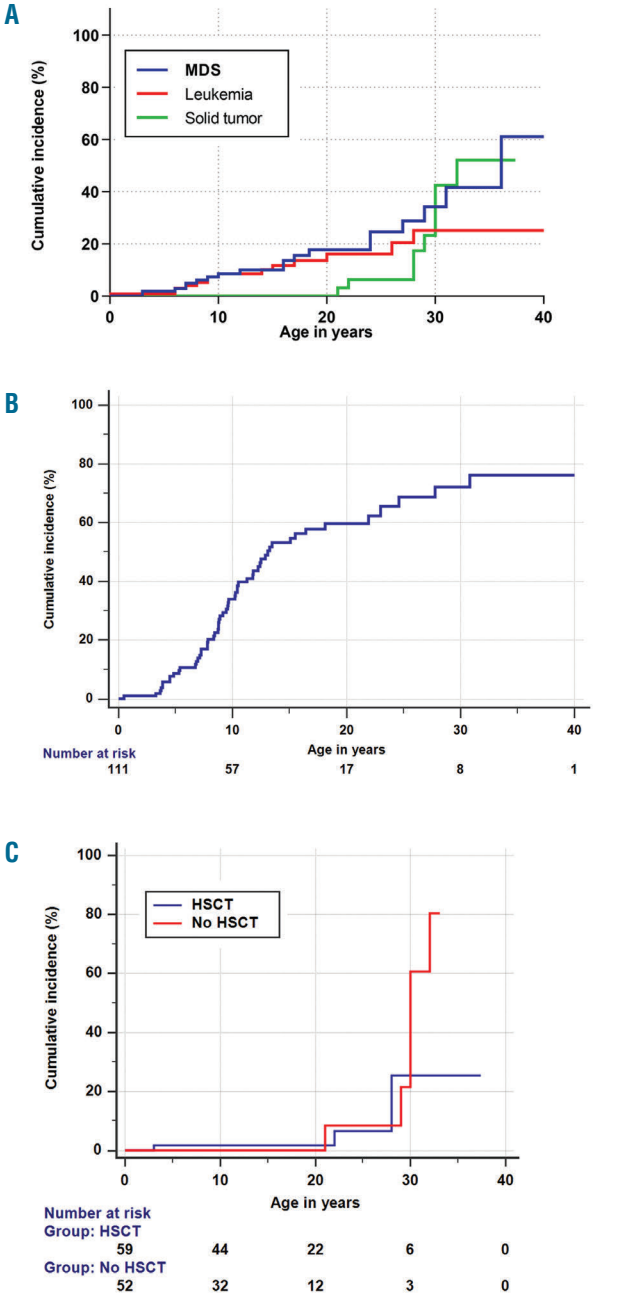

Figure 2. Cumulative incidence (CI) by age for adverse events in patient with Fanconi anemia (FA). (A) CI by age of first cancer. Myelodysplastic syndrome (MDS) – blue; leukemia – red; solid tumors – green. MDS and leukemia events both appeared significantly earlier than solid tumors (P=0.001 and P<0.001, respectively). No significant difference was found between the age of first event of MDS *versus* leukemia; (B) CI of HSCT. (C) CI of solid tumors for patient who underwent hematopoietic stem cell transplantation (HSCT) (blue) or did not have a transplant (red). No significant difference was found between the groups.

Hematopoietic stem cell transplantation

Approximately half of the patients with FA in the registry (n=59) underwent a HSCT; seven of the patients underwent a second transplant. The median age for the first transplant was 9.3 years (range: 0.45-30.8) (Figure 2B). Indication for HSCT was MDS/leukemia in 15 patients; the rest (n=44) were transplanted due to BMF. 25% were transplanted in the 1990s, 39% in the years 2000-2009, and 36% between 2010-2017. No association was found between a history of HSCT and incidence of solid tumor or age of first cancer (Figure 2C). Solid tumors were reported in six non-transplanted patients and in four transplanted patients, of which two were transplanted due to MDS/leukemia and the other two due to BMF. Among the four transplanted patients, the median time from transplant until solid tumor diagnosis was 10 years (range: 2.5-18). The five patients with at least three events of cancer had no previous HSCT.

Survival

Currently 65 of the 111 patients (59%) in the cohort are alive with a median age of 16.5 years (range: 0.8-37). Forty-three patients have died, and three were lost to follow-up. The median age of death was 11 years (range: 0.1-49). Causes of death were mostly cancer related (23 patients; 53%) or transplant-related (11 patients; 25%). 64% of transplanted patients are alive, and 56% of non-transplanted patients are alive and no significant (NS) difference was found in the age of death between transplanted and non-transplanted patients. The 5-year survival of the post-HSCT cohort was 44%, and 10-year post-HSCT survival was 27%. Among the transplanted patients, 78% of those transplanted due to BMF are alive, while only 27% of those transplanted for MDS/leukemia are alive.

Genotype

Genetic analysis was performed on 94 patients (85% of the cohort), of which 88 patients (94% tested) reached a genetic diagnosis. The majority were found to have mutations in the *FANCA* gene, followed by mutations in *FANCG, FANCC, FANCJ,* and *FANCD1* (Figure 3). The six undiagnosed patients had an incomplete genetic analysis performed. Of these, two siblings were found to have a heterozygous mutation in *FANCC* (Table 4).

Table 2. Congenital anomalies of patients with Fanconi anemia in Israel.

Anomaly	N=111
Any anomaly	100 (90.1%)
Café-au-lait spots	58 (52.3%)
Renal structure	44 (39.6%)
CNS structure	21 (18.9%)
Hearing loss	20 (18%)
Congenital heart disease	18 (16.2%)
Male genitourinary	18 (16.2%)
Radial ray	18 (16.2%)
Gastrointestinal structure	9 (8.1%)
Spine	6 (5.4%)
Cleft lip/palate	2 (1.8%)

Anomalies as reported in patient charts. CNS: central nervous system.

34 different mutations were found, including 21 in *FANCA* and three each in *FANCC, FANCD1, FANCG* and *FANCJ* (Table 4); 76 patients were homozygous for mutations in Fanconi genes, and 12 patients were compound heterozygous; 33 different combinations of mutations were found (Table 4); 20 novel mutations were detected in the cohort, as detailed in the *Online Supplementary Table S1*; 7 of these were previously reported by our group.[13-15] The type of mutation varied, as detailed in Table 4. 26 patients had frameshift mutations, 19 patients had splice site mutations, 15 patients had deletions, 13 patients had nonsense mutations, nine patients had missense muta-

Table 3. Number of events of myelodysplastic syndrome, leukemia and solid tumors.

Cancer type	Total	FANCA	FANCC	FANCD1	FANCG	FANCJ	Undiagnosed
MDS	19	8	3	0	1	1	6
Leukemia							
AML	14	3	1	1	2	1	6
ALL	1	1	0	0	0	0	0
Head and Neck	6	3	0	0	0	0	3
GU	3	3	0	0	0	0	0
GI	3	1	0	0	0	0	2
Skin	3	2	0	0	0	0	1
Breast	1	0	0	0	0	0	1
MB	1	0	0	1	0	0	0

ALL: acute lymphoblastic leukemia; AML: acute myeloid leukemia; GI: gastrointestinal; GU: genitourinary; MB: medulloblastoma; MDS: myelodysplastic syndrome.

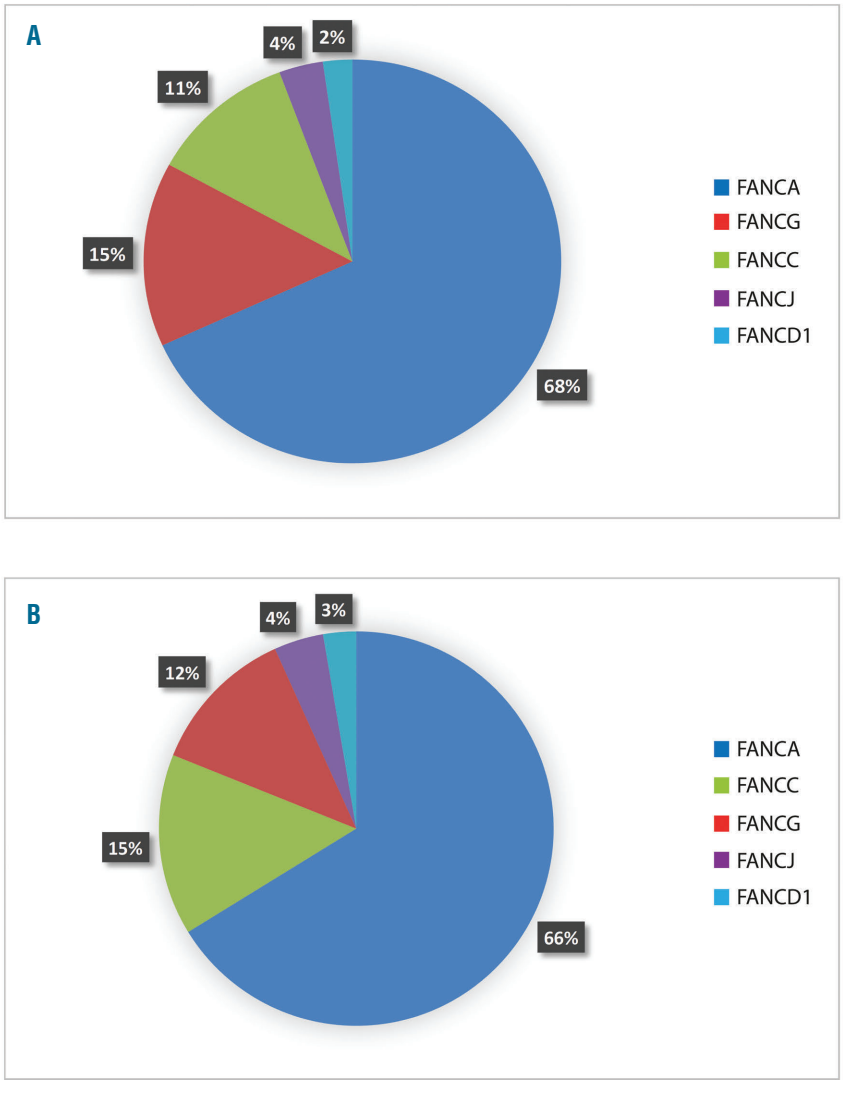

Figure 3. The distribution of the Fanconi anemia (FA) genes in Israel: (A) including siblings and (B) excluding siblings.

Table 4. Genetics of Fanconi anemia in Israel.

#	Gene	Mutation 1	Mutation 2	Effect 1	Effect 2	Ethnicities
11	*FANCA*	c.2172-2173 insG (p. S725Vfs*69) (13)	c.2172-2173 insG (p. S725Vfs*69) (13)	frame shift	frame shift	Sephardic Jewish
8	*FANCA*	c.4261-2A>C (IVS43-2a>c) (14)	c.4261-2A>C (IVS43-2a>c) (14)	splice site	splice site	Arab Muslim Arab Christian
8	*FANCA*	c.3788-3790delTCT (25) 6-31	c.3788-3790delTCT(25)	frame shift	frame shift	Arab Druze Sephardic Jewish
5	*FANCA*	ex6-31 del (14)	ex6-31 del(14)	large deletion	large deletion	Arab Muslim
5	*FANCA*	ex21 del(26, 27)	ex21 del(26, 27)	large deletion	large deletion	Arab Muslim
3	*FANCA*	c.4069-4070insT^	c.4069-4070insT^	frame shift	frame shift	Arab Muslim
3	*FANCA*	p.Gln1128Ter(15)	p.Gln1128T(15)	nonsense	nonsense	Arab Muslim
2	*FANCA*	ex31-37del(15)	4275delT (p.Asp1427Thr fsX6) (13)	large deletion	deletion	Sephardic Jewish
2	*FANCA*	p.Pro1164Ser^	p.Pro1164Ser^	missense	missense	Arab Muslim
1	*FANCA*	c.2172-2173 insG (p.S725Vfs*69) (13)	deletion exons 4-7(8)	frame shift	large deletion	mixed Jewish
1	*FANCA*	c.4275delT (p.Asp1427Thr fsX6) (13)	c.2172-2173 insG (p.S725Vfs*69) (13)	frame shift	frame shift	Sephardic Jewish
1	*FANCA*	c.4275delT (p.Asp1427Thr fsX6) (13)	4275delT (p.Asp1427Thr fsX6) (13)	frame shift	frame shift	Sephardic Jewish
1	*FANCA*	c.65G>A (p.Trp22Ter) (25)	c.65G>A (p.Trp22Ter) (25)	missense	missense	Ashkenazi Jewish
1	*FANCA*	c.65G>A (p.Trp22Ter) (25)	ex1-24del^	missense	large deletion	mixed Jewish
1	*FANCA*	c.891-893 delGCTG (13)	c.2172-2173 insG (p.S725Vfs*69) (13)	frame shift	frame shift	Sephardic Jewish
1	*FANCA*	c.2172-2173 insG (p.S725Vfs*69) (13)	ex1,2,4,5del^	frame shift	large deletion	Sephardic Jewish
1	FANCA	c.891-893 delGCTG (13)	c.65G>A (p.Trp22Ter) (25)	frame shift	nonsense	mixed Jewish
1	*FANCA*	ex15-21 del(28)	ex15-21 del(28)	large deletion	large deletion	Arab Muslim
1	*FANCA*	ex1-6 del (29)	ex1-6 del (29)	large deletion	large deletion	Arab Christian
1	*FANCA*	c.189+1G>A (IVS2+1 g>a) ^	c.2778+2T>C (IVS28+2 T>C) ^	splice site	splice site	Arab Muslim
1	*FANCA*	p.Arg880Ter (30)	p.Arg880Ter (30)	nonsense	nonsense	Ashkenazi Jewish
1	*FANCA*	c.3520-3522 delTGG (25)	c.1471-401_1626+395del ^	deletion	large deletion	mixed Jewish
7	*FANCC*	c. 456+4a>t (IVS4+4 a>t) (5)	c. 456+4a>t (IVS4+4 a>t) (5)	splice site	splice site	Ashkenazi Jewish
2	*FANCC*	p. Gln3Ter^	p. Gln3Ter^	nonsense	nonsense	Arab Muslim
1	FANCC	c. 456+4a>t (IVS4+4 a>t) (5)	del 97116249-97124749 (31)	splice site	deletion	mixed Jewish
1	*FANCD1*	c.6174delT(24)	c.6174delT(24)	frame shift	frame shift	mixed Jewish
1	*FANCD1*	c.7579delG (p.V2527X)^	c.9693delA (p.S3231fs16*)^	nonsense	frame shift	Ethiopian Jewish
6	*FANCG*	c.1742C<G (p.Ser581Ter)^	c.1742C<G (p.Ser581Ter)^	nonsense	nonsense	Arab Muslim
4	*FANCG*	c.212T>C (p. Leu71Pro)(32)	c.212T>C (p. Leu71Pro)(32)	missense	missense	Arab Muslim
3	*FANCG*	c.510+3A>G (IVS4+3 A>G) ^	c.510+3A>G (IVS4+3 A>G) ^	splice site	splice site	Arab Muslim
1	*FANCJ*	p.Arg251Cys(33)	p.Arg251Cys(33)	missense	missense	Arab Muslim
1	*FANCJ*	p.Arg848His(34)	p.Arg848His(34)	missense	missense	Arab Muslim
1	*FANCJ*	p.Gln376Ter^	p.Gln376Ter^	nonsense	nonsense	Arab Muslim
2	@ *FANCC*	c. 456+4a>t (IVS4+4 a>t) (5)	Unknown	splice site	Unknown	mixed Jewish
4	@	Unknown	Unknown			

#: number of patients; ^: mutations not previously described; @: not included in the analyses.

tions and six patients had a combination of mutation types.

In our cohort, the most common mutations in *FANCA* were c.2172-2173 insG (p.S725Vfs*69), most frequent in the Sephardic Jewish population, c.4261-2A>C (IVS43-2a>c) in Arab Muslims and Christians and c.3788-3790delTCT, detected in both Arab Druze and Sephardic Jews. The most common mutation in *FANCC* was c.456+4a>t (IVS4+4 a>t) in the Ashkenazi Jewish population. The mutation most commonly found in *FANCG* was the novel mutation c.1742C<G (p.Ser581Ter) in the Arab Muslim population.

Genotype-phenotype correlations

Genotype-phenotype correlations were first analyzed by the specific affected gene. In addition, patients were grouped by function of altered genes into those encoding proteins of the core complex (*FANCA, FANCC, FANCG*) versus those downstream (*FANCD1, FANCJ*). Finally, analysis was done according to the type of mutation (deletion, frame shift, missense, nonsense, splice site).

No association was found between the affected gene and survival (Figure 4). Survival was not significantly different between patients with core complex mutations and those with mutations in downstream genes. Neither the specific FA gene nor function were associated with the development of BMF. Of note, neither of the patients with *FANCD1* mutations developed BMF. One underwent HSCT for AML before the age of six months, while the other had no complications by the age of 17 years.

Looking at congenital anomalies, no association was found between the CAB score and the affected FA gene. Rib abnormalities were observed only in patients with *FANCC* mutations. Cleft lip was more common in patients with *FANCD1* mutations, compared with other FA genes (P<0.001). Patients with mutations in the downstream genes *FANCD1* and *FANCJ* were significantly shorter compared with the others (P=0.003). Patients with downstream mutations were found to have significantly more skull anomalies (P<0.001), central nervous system (CNS) abnormalities (P=0.005) and genitourinary anomalies (P=0.03), compared with patients with core complex mutations.

All the solid tumors in our cohort were reported in patients with *FANCA* mutations or in undiagnosed patients, except for one case of medulloblastoma in a patient with *FANCD1* mutation (Table 3). Due to the relatively small numbers of reported cancers in patients with non-*FANCA* mutations (Table 3), we compared the age of the first cancer (including MDS) between patients with

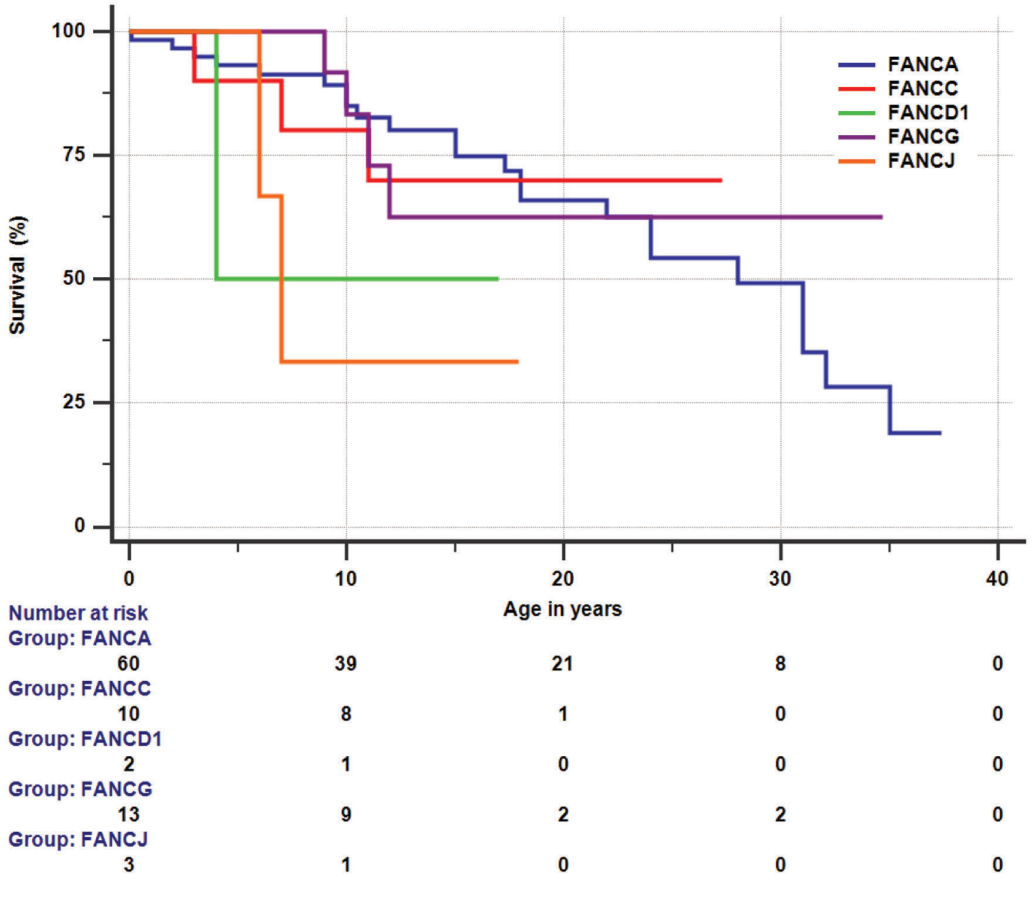

Figure 4. Survival according to the Fanconi anemia (FA) gene. Survival curves for patients with FA in Israel, calculating the proportion of live patients by age using the Kaplan-Meier methods according to the mutated gene: *FANCA* (blue), *FANCC* (red), *FANCD1* (green), *FANCG* (purple) and *FANCJ* (orange). No significant difference was found between the groups.

FANCA mutations and patients with non-*FANCA* mutations. The mean age of the first cancer was 18.5 years (SD 6.3 years) for patients with *FANCA*, relative to 5.2 years (SD 3.7 years) for patients with *FANCC, FANCD1, FANCG* and *FANCJ* mutations, with a statistically significant difference (P=0.001). This difference remains statistically significant upon exclusion of solid tumors; patients with *FANCA* mutations developed MDS/leukemia at a significantly older age as compared to patients with *FANCA* mutations (P=0.002). All patients with mutations in *FANCA* developed cancer after the age of 10 years, while all other genetically diagnosed patients developed their first cancer by the age of 10 years. There was a trend towards more MDS in patients with *FANCC* mutations and less MDS and cancer in patients with *FANCG* mutations, compared with patients with mutations in other genes (NS).

No association was found between the mutation type and survival. In addition, no association was found between the mutation type and the development of MDS, leukemia or solid tumors, although patients with nonsense and splice site mutations developed the first cancer at a significantly lower age than patients with deletions (P=0.011 and P=0.012, respectively). No association was found between the CAB score and mutation type. However, some significant correlations were found between the mutation type and specific congenital anomalies. Patients with deletions were shorter than patients with nonsense mutations (P=0.018). Patients with splice site mutations had significantly more CNS anomalies and developmental delay, compared with the other patients (P=0.03 and P=0.038, respectively). Patients with missense mutations had significantly less congenital heart disease (P=0.022).

Discussion

We hereby present a large cohort of 111 patients with FA in Israel. In a previous report of Israeli patients with BMF syndromes, 66 of these patients were included.[15] Our cohort is unique in a few aspects. First, the vast majority of the patients included in this cohort are genetically diagnosed. Second, the ethnic diversity in this population is distinct with a larger representation of patients from Arab descent compared to those of Jewish descent; this is in contrast to the general population of Israel comprised of 74% Jews and 21% Arabs. In addition, the patient population exhibited a high degree of consanguinity, especially in the Arab population, most likely the cause of their skewed representation in this cohort.

The large majority of our patients (90%) had at least one congenital malformation. In an Italian registry, including 97 patients, only 76% had at least one somatic malformation, although abnormal facial features were not included.[16] We calculated a CAB score for all the patients in our cohort as described in a previous publication.[10] In the German cohort, including 181 patients, this score predicted BMF.[12] In agreement, in our cohort, all patients with higher CAB scores (CABS 3-5) developed BMF. In addition, the two patients in our cohort with the highest CAB scores (CABS 4-5) did not develop cancer. This low number of patients does not allow statistical analysis; however it is consistent with previous publications finding an inverse correlation between congenital anomalies and malignancy in patients with FA.[10,12]

Of the patients in this FA cohort, 82% developed BMF. This is similar to the 80% described by the International Fanconi Anemia Registry.[17] In contrast, in the German cohort, only 36% developed BMF.[12] Neither of the patients with *FANCD1* mutations in our cohort developed BMF, in agreement with previous publications.[7] However, it should be noted that one of the patients with a *FANCD1* mutation was transplanted at a very young age for the treatment of leukemia, essentially eliminating the risk of BMF development.

Nearly one third of this cohort of patients with FA in Israel developed MDS, leukemia and/or solid tumors. Twelve of the 111 patients had more than one cancer event. The median age at initial diagnosis of cancer was 16 years in our cohort. Hematological malignancies appeared at a significantly earlier age relative to solid tumors. Of note, one patient with a *FANCD1* mutation developed medulloblastoma at the age of 3 years. Patients with *FANCD1* mutations have been previously described as uniquely developing solid tumors early in life,[18] requiring screening for childhood cancer from a very young age. Excluding this particular patient with FANCD1 mutation, initial diagnosis of solid tumors in this cohort ranged from 21-32 years of age. These data support the need to start early cancer surveillance for patients with FA.

Approximately half of the patients in this cohort underwent HSCT, similar to the Italian FA registry report.[19] There was no difference in survival between patients who did or did not undergo a HSCT. In the International Fanconi Anemia Registry, HSCT was found to be a predictor of poor prognosis.[17] The patients from our cohort were transplanted over a three-decade time frame. Therefore, differences in donor selection and conditioning treatment plus patient selection bias may explain the discrepancy. The indication for HSCT had a large impact on survival in our cohort, with patients transplanted due to BMF having a much better survival relative to those transplanted due to MDS/leukemia. These results, if confirmed in future studies, may influence the decision on choosing the right timing for HSCT.

In this cohort, HSCT did not appear to hasten the onset of solid tumors. Similar findings were reported in the International Fanconi Anemia Registry as well as in the Italian Fanconi Anemia Registry, including 754 and 180 patients, respectively.[17,19] In contrast, the German registry reported a hazard ratio of 3.8 for developing solid tumors in patients with FA post-transplant, compared to those not transplanted.[12] The National Cancer Institute also detected an increased incidence of cancer in FA patients and a younger age at cancer detection post-transplant in their cohorts of patients with FA.[20,21] Indeed, reconciling this discrepancy holds paramount importance in clinical decision-making regarding optimal timing for initiation of cancer surveillance. More up-to-date studies will be needed to identify if any association exists.

We aimed to perform a genetic diagnosis for all Israeli patients with FA for whom DNA was available. By conventional Sanger sequencing and MLPA, we arrived at a genetic diagnosis in almost 95% of those tested. Of the six patients for whom genetic diagnosis was not achieved, only a partial work-up was performed due to the lack of remaining DNA samples. Two of these were found to be heterozygous for a *FANCC* mutation. In our cohort, 34 different mutations were found, with 20 of

them either not previously published or reported only by our group (Table 4).

In this Israeli cohort of FA patients, two-thirds of genetically diagnosed patients had biallelic *FANCA* mutations. These numbers are similar to the International Fanconi Anemia Registry, in which 60% of the diagnosed patients had FANCA mutations,[17] and the European cohort, in which 70% had *FANCA* mutations[7] but in contrast to the Italian cohort, in which 90% of the patients diagnosed were found to have *FANCA* mutations.[16] The other FA genes were represented in our cohort similar to previous publications.[22,23] We did not find a significant correlation between survival and the affected gene. This is in contrast to the International Fanconi Anemia Registry, in which patients with *FANCC* mutations had a poorer survival.[17]

Some mutations were exclusively or more commonly found in specific ethnic populations in our cohort. For example, in the Ashkenazi Jewish population, the most common mutation was c. 456+4a>t (IVS4+4 a>t) in *FANCC*, as previously described.[24] In contrast, in the Sephardic Jewish population, the most common mutations was in c.2172-2173 insG (p.S725Vfs*69) in *FANCA*. Both these mutations were exclusive to Ashkenazi Jewish and Sephardic Jewish patients with FA, respectively. Patients with *FANCG* and *FANCJ* mutations were all from Arab Muslim descent.

A number of correlations were found between the genotype and development of cancer in our cohort. Patients with *FANCA* mutations developed cancer at a significantly older age, compared with patients with non-*FANCA* mutations. In addition, there was a trend towards a higher prevalence of MDS in patients with *FANCC* mutations and less MDS and cancer in patients with *FANCG* mutations in our cohort. In contrast, in a larger cohort recently published from the National Cancer Institute,[20] there was no clear association between the genotype and malignancy. Patients with *FANCG* mutations were even reported previously to have a higher incidence of leukemia.[7] These data may reflect the unique population in our cohort, as most of the patients with *FANCG* mutations were of Arab Muslim origin, and all 13 patients were homozygous for 1 of 3 mutations: c.1742C>G (p.Ser581Ter), c.212T>C (p.Leu71Pro) and c.510+3A>G (IVS4+3 A>G). Further studies will be needed to elucidate the specific characteristics of these mutations.

Regarding the type of mutation in our cohort, no association was found between the mutation type and survival, the risk of development of cancer or the CAB score. However, we found a few correlations between specific congenital anomalies and the type of mutation. A few previous publications looked at correlations between specific mutation types of *FANCA* and phenotype. One study reported a higher incidence of leukemia in patients with null mutations of *FANCA*, compared to those with other types of mutations.[7] In contrast, in the Spanish cohort, no association was found between the type of *FANCA* mutations and hematologic disease or somatic malformations.[8] The discrepancies between these studies may reflect specific population characteristics, making it difficult to rely on the Fanconi group or the type of mutation in defining the risk for disease complications.

This cohort includes patients treated in various medical centers in Israel. The biggest limitation of this report is that not all patients were seen by the same medical team. We overcame this by using a standardized and elaborate medical form for each patient included in the I-IBMFR, followed by an annual update. In addition, genetic analysis was uniformly performed in our centralized hematology molecular laboratory.

This study includes a relatively large cohort of patients with FA in a nation with a unique ethnic diversity and a high degree of consanguinity. Our high success rate of genetic diagnosis has enabled the detection of several novel mutations and unreported genotype-phenotype correlations. We found that patients with *FANCA* mutations developed cancer at a later age; however the causative gene was not found to affect the overall survival of patients. In our cohort, HSCT did not increase the risk of solid tumor development. Continuation of this registry and establishment of similar registries worldwide are paramount for further advancement of our understanding of this rare disease.

Acknowledgments

The authors are grateful to Dr. Blanche Alter, from the Division of Cancer Epidemiology and Genetics, National Cancer Institute, for her helpful suggestions with writing this manuscript. The authors would like to thank Ms. Pearl Lilos for her help with the statistical analyses. The I-IBMF registry was supported by the Hayim association for children with cancer in Israel.

References

1. Rosenberg PS, Tamary H, Alter BP. How high are carrier frequencies of rare recessive syndromes? Contemporary estimates for Fanconi Anemia in the United States and Israel. Am J Med Genet A. 2011; 155A(8):1877-1883.
2. Callen E, Casado JA, Tischkowitz MD, et al. A common founder mutation in FANCA underlies the world's highest prevalence of Fanconi anemia in Gypsy families from Spain. Blood. 2005;105(5):1946-1949.
3. Morgan NV, Essop F, Demuth I, et al. A common Fanconi anemia mutation in black populations of sub-Saharan Africa. Blood. 2005;105(9):3542-3544.
4. Rosendorff J, Bernstein R, Macdougall L, Jenkins T. Fanconi anemia: another disease of unusually high prevalence in the Afrikaans population of South Africa. Am J Med Genet. 1987;27(4):793-797.
5. Whitney MA, Jakobs P, Kaback M, Moses RE, Grompe M. The Ashkenazi Jewish Fanconi anemia mutation: incidence among patients and carrier frequency in the at-risk population. Hum Mutat. 1994;3(4):339-341.
6. Fargo JH, Rochowski A, Giri N, Savage SA, Olson SB, Alter BP. Comparison of chromosome breakage in non-mosaic and mosaic patients with Fanconi anemia, relatives, and patients with other inherited bone marrow failure syndromes. Cytogenet Genome Res. 2014;144(1):15-27.
7. Faivre L, Guardiola P, Lewis C, et al. Association of complementation group and mutation type with clinical outcome in fanconi anemia. European Fanconi Anemia Research Group. Blood. 2000;96(13):4064-4070.
8. Castella M, Pujol R, Callen E, et al. Origin, functional role, and clinical impact of Fanconi anemia FANCA mutations. Blood. 2011;117(14):3759-3769.
9. Neveling K, Endt D, Hoehn H, Schindler D. Genotype-phenotype correlations in Fanconi anemia. Mutat Res. 2009 ;668(1-2):73-91.
10. Rosenberg PS, Huang Y, Alter BP. Individualized risks of first adverse events in patients with Fanconi anemia. Blood. 2004;104(2):350-355.
11. Sanger F, Coulson AR. A rapid method for determining sequences in DNA by primed synthesis with DNA polymerase. J Mol Biol. 1975;94(3):441-448.

12. Rosenberg PS, Alter BP, Ebell W. Cancer risks in Fanconi anemia: findings from the German Fanconi Anemia Registry. Haematologica. 2008;93(4):511-517.
13. Tamary H, Bar-Yam R, Shalmon L, et al. Fanconi anaemia group A (FANCA) mutations in Israeli non-Ashkenazi Jewish patients. Br J Haematol. 2000;111(1):338-343.
14. Tamary H, Dgany O, Toledano H, et al. Molecular characterization of three novel Fanconi anemia mutations in Israeli Arabs. Eur J Haematol. 2004;72(5):330-335.
15. Tamary H, Nishri D, Yacobovich J, et al. Frequency and natural history of inherited bone marrow failure syndromes: the Israeli Inherited Bone Marrow Failure Registry. Haematologica. 2010;95(8):1300-1307.
16. Svahn J, Bagnasco F, Cappelli E, et al. Somatic, hematologic phenotype, long-term outcome, and effect of hematopoietic stem cell transplantation. An analysis of 97 Fanconi anemia patients from the Italian national database on behalf of the Marrow Failure Study Group of the AIEOP (Italian Association of Pediatric Hematology-Oncology). Am Journal Hematol. 2016;91(7):666-671.
17. Kutler DI, Singh B, Satagopan J, et al. A 20-year perspective on the International Fanconi Anemia Registry (IFAR). Blood. 2003;101(4):1249-1256.
18. Malric A, Defachelles AS, Leblanc T, et al. Fanconi anemia and solid malignancies in childhood: a national retrospective study. Pediatr Blood Cancer. 2015;62(3):463-470.
19. Risitano AM, Marotta S, Calzone R, Grimaldi F, Zatterale A. Twenty years of the Italian Fanconi Anemia Registry: where we stand and what remains to be learned. Haematologica. 2016;101(3):319-327.
20. Alter BP, Giri N, Savage SA, Rosenberg PS. Cancer in the National Cancer Institute inherited bone marrow failure syndrome cohort after fifteen years of follow-up. Haematologica. 2018;103(1):30-39.
21. Rosenberg PS, Socie G, Alter BP, Gluckman E. Risk of head and neck squamous cell cancer and death in patients with Fanconi anemia who did and did not receive transplants. Blood. 2005;105(1):67-73.
22. Kee Y, D'Andrea AD. Molecular pathogenesis and clinical management of Fanconi anemia. J Clin Invest. 2012;122(11):3799-3806.
23. Wegman-Ostrosky T, Savage SA. The genomics of inherited bone marrow failure: from mechanism to the clinic. Br J Haematol. 2017;177(4):526-542.
24. Kutler DI, Auerbach AD. Fanconi anemia in Ashkenazi Jews. Fam Cancer. 2004;3(3-4):241-248.
25. Levran O, Erlich T, Magdalena N, et al. Sequence variation in the Fanconi anemia gene FAA. Proc Natl Acad Sci U S A . 1997;94(24):13051-13056.
26. Chen F, Peng GJ, Zhang K, Hu Q, Zhang LQ, Liu AG. [FANCA gene mutation analysis in Fanconi anemia patients]. Zhonghua Xue Ye Xue Za Zhi. 2005;26(10):616-618.
27. Tsangaris E, Klaassen R, Fernandez CV, et al. Genetic analysis of inherited bone marrow failure syndromes from one prospective, comprehensive and population-based cohort and identification of novel mutations. J Med Genet. 2011;48(9):618-628.
28. Yagasaki H, Hamanoue S, Oda T, Nakahata T, Asano S, Yamashita T. Identification and characterization of novel mutations of the major Fanconi anemia gene FANCA in the Japanese population. Hum Mutat. 2004;24(6):481-490.
29. Levran O, Diotti R, Pujara K, Batish SD, Hanenberg H, Auerbach AD. Spectrum of sequence variations in the FANCA gene: an International Fanconi Anemia Registry (IFAR) study. Hum Mutat. 2005;25(2):142-149.
30. Ameziane N, Errami A, Leveille F, et al. Genetic subtyping of Fanconi anemia by comprehensive mutation screening. Hum Mutat. 2008;29(1):159-166.
31. Chandrasekharappa SC, Lach FP, Kimble DC, et al. Massively parallel sequencing, aCGH, and RNA-Seq technologies provide a comprehensive molecular diagnosis of Fanconi anemia. Blood. 2013;121(22):e138-148.
32. Demuth I, Wlodarski M, Tipping AJ, et al. Spectrum of mutations in the Fanconi anaemia group G gene, FANCG/XRCC9. Eur J Hum Genet. 2000;8(11):861-868.
33. Guo M, Vidhyasagar V, Ding H, Wu Y. Insight into the roles of helicase motif Ia by characterizing Fanconi anemia group J protein (FANCJ) patient mutations. J Biol Chem. 2014;289(15):10551-10565.
34. Kim H, Cho DY, Choi DH, et al. Analysis of BRIP1 variants among Korean patients with BRCA1/2 mutation-negative high-risk breast cancer. Cancer Res Treat. 2016;48(3):955-961.

ARTICLE

Minihepcidins improve ineffective erythropoiesis and splenomegaly in a new mouse model of adult β-thalassemia major

Carla Casu,[1*] Roberta Chessa,[1*] Alison Liu,[1] Ritama Gupta,[1] Hal Drakesmith,[2] Robert Fleming,[3] Yelena Z. Ginzburg,[4] Brian MacDonald[5] and Stefano Rivella[1]

[1]Department of Pediatrics, Division of Hematology, The Children's Hospital of Philadelphia (CHOP), Philadelphia, PA, USA; [2]MRC Human Immunology Unit, MRC Weatherall Institute of Molecular Medicine, University of Oxford, John Radcliffe Hospital, Oxford, UK; [3]Department of Pediatrics, Saint Louis University School of Medicine, St. Louis, MO, USA; [4]Division of Hematology and Medical Oncology, Tisch Cancer Center, Icahn School of Medicine at Mount Sinai, New York, NY, USA and [5]Merganser Biotech Inc. King of Prussia, PA, USA

**CC and RC contributed equally as co-first authors.*

Ferrata Storti Foundation

Haematologica 2020
Volume 105(7):1835-1844

ABSTRACT

Minihepcidins are hepcidin agonists that have been previously shown to reverse iron overload and improve erythropoiesis in mice affected by non-transfusion-dependent thalassemia. Given the extreme anemia that occurred with the previous model of transfusion-dependent thalassemia, that model was inadequate for investigating whether minihepcidins can improve red blood cell quality, lifespan and ineffective erythropoiesis. To overcome this limitation, we generated a new murine model of transfusion-dependent thalassemia with severe anemia and splenomegaly, but sufficient red cells and hemoglobin production to test the effect of minihepcidins. Furthermore, this new model demonstrates cardiac iron overload for the first time. In the absence of transfusions, minihepcidins improved red blood cell morphology and lifespan as well as ineffective erythropoiesis. Administration of a minihepcidin in combination with chronic red blood cell transfusion further improved the ineffective erythropoiesis and splenomegaly and reversed cardiac iron overload. These studies indicate that drugs such as minihepcidins have therapeutic potential for patients with transfusion-dependent thalassemia.

Introduction

Non-transfusion and transfusion-dependent thalassemia (NTDT and TDT, respectively) are characterized by imbalanced synthesis of α- and β-globin chains, leading to the formation of unstable α-globin chain/heme aggregates (hemichromes) in erythroid cells. Hemichromes impair the differentiation and survival of erythroid progenitors as well as the lifespan of enucleated red blood cells (RBC).[1-6]

Both NTDT and TDT patients suffer from iron overload and require chronic iron chelation therapy to prevent major complications, such as liver and heart failure.[5-9] The mechanism leading to iron accumulation in organs is different in NTDT *vs.* TDT.[5,6,10,11] In NTDT, iron overload is likely mediated by a variety of factors, including increased erythropoiesis, hypoxia and the contribution of factors such as erythroferrone, which suppresses hepcidin synthesis in the liver.[12-16] Because hepcidin functionally inhibits iron egress from cells by binding and internalizing the iron transporter ferroportin in enterocytes, iron absorption is increased under conditions of reduced hepcidin synthesis.[3,16-18] Additionally, in hypoxic conditions, synthesis of molecules responsible for mediating iron absorption (including ferroportin) are increased in the duodenum, further contributing to the iron overload in NTDT.[4,19,20] In contrast to NTDT patients, TDT patients require chronic RBC transfusion for survival.[9,18,21] Because transfused RBC ultimately undergo senescence and require removal by splenic and liver macrophages and because there is no physio-

Correspondence:

STEFANO RIVELLA
rivellas@email.chop.edu

Received: November 19, 2018.
Accepted: September 26, 2019.
Pre-published: October 3, 2019.

doi:10.3324/haematol.2018.212589

Check the online version for the most updated information on this article, online supplements, and information on authorship & disclosures: www.haematologica.org/content/105/7/1835

logical way of excreting the iron recycled from these cells, continuous infusion of RBC is the primary reason for iron overload in TDT patients.[18,21,22]

Mouse models of β-thalassemia intermedia (e.g. *Hbb*$^{th3/+}$ mice) exhibit ineffective erythropoiesis, anemia and reduced or inappropriately normal hepcidin synthesis, but do not require RBC transfusion for survival, similarly to NTDT patients. Minihepcidins function as hepcidin agonists, target ferroportin, and reduce iron absorption and transferrin saturation.[23,24] We and others showed that administration of minihepcidins or agents that induce hepcidin expression in *Hbb*$^{th3/+}$ mice decreased transferrin saturation, heme synthesis, hemichrome formation, and improved RBC lifespan, anemia, and splenomegaly.[17,25-29] Taken together, these experiments demonstrated the potential benefits of minihepcidins in NTDT. However, it is unclear whether minihepcidins would improve anemia, transfusion requirements, and iron overload in TDT.

Based on the pathophysiology of TDT and the effect of minihepcidins on iron metabolism and erythropoiesis in NTDT, we speculate that minihepcidins may: (i) improve ineffective erythropoiesis; (ii) increase RBC lifespan and reverse anemia; (iii) decrease RBC transfusion requirements (decrease frequency of transfusion); (iv) reverse splenomegaly and extramedullary erythropoiesis; (v) decrease indications for splenectomy; and (vi) reverse iron overload in TDT patients.

Multiple existing mouse models of β-thalassemia intermedia harbor different mutations leading to decreased mouse β-globin genes synthesis, triggering ineffective erythropoiesis and anemia (Figure 1A-C). However, some animals do not require RBC transfusion for survival, while others produce very few RBC.[30-33] For example, *Hbb*$^{th1/th1}$ mice carry a homozygous spontaneous deletion of 3.7 Kb containing the β-major gene and 2 Kb of the 5' flanking region, including the promoter (Figure 1A).[34] *Hbb*$^{th2/+}$ mice were created by inserting a neomycin-resistant cassette into exon 2 of the β-major gene such that heterozygotes are mildly anemic while homozygotes die perinatally due to severe anemia (Figure 1B).[35] *Hbb*$^{th3/+}$ mice have one copy of the normal β-globin cluster and an allele with a deletion of both the β-major and β-minor genes (Figure 1C), resulting in moderate anemia that is not severe enough to require transfusion, a phenotype similar to that of *Hbb*$^{th1/th1}$ mice.[36,37] Homozygous *Hbb*$^{th3/th3}$ mice die perinatally, preventing their use as an adult model of TDT.[36]

We previously used a transplant model in which fetal liver cells from E13.5-15.5 day *Hbb*$^{th3/th3}$ embryos are transplanted into irradiated wildtype (WT) syngeneic mice.[36-38] Successful engraftment of *Hbb*$^{th3/th3}$ fetal liver cells led to ineffective erythropoiesis and severe anemia resulting in death 3 months after transplantation if the animals were not transfused.[16,38,39] This and other models were utilized to study dysregulated iron metabolism in β-thalassemia major.[16,35-39] However, *Hbb*$^{th3/th3}$ mice are characterized by such low hemoglobin and RBC production that they make testing drugs, such as minihepcidins that have the potential to modify RBC quality and lifespan and improve ineffective erythropoiesis, complex if not impossible.

To assess the efficacy of minihepcidins in TDT, we generated a new mouse model (*Hbb*$^{th1/th2}$) that closely resembles the human TDT phenotype (Figure 1D). Our aim was to use combinations of already existing mutations in order to generate a model intermediate in severity to those already in use, in which some RBC are produced although their synthesis is insufficient to support long-

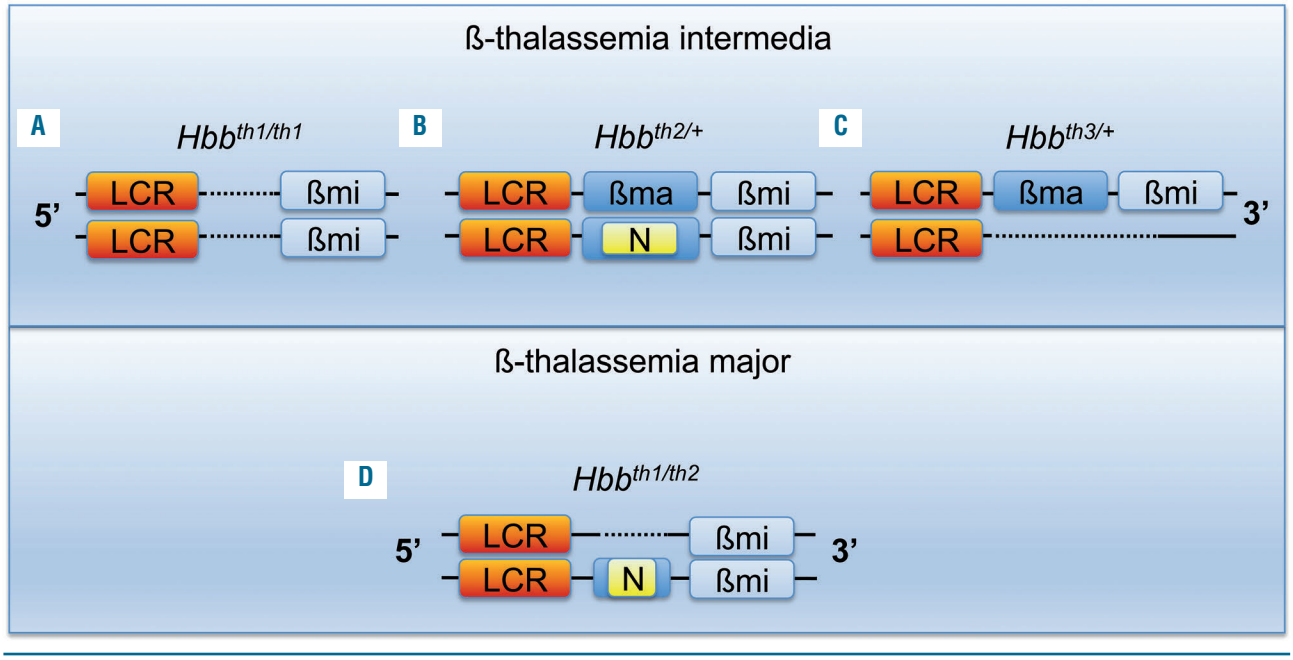

Figure 1. Genetic makeup of established mouse models of β-thalassemia intermedia and a new model of ß-thalassemia major. (A-C) Mouse models of β-thalassemia Intermedia: (A) *Hbb*$^{th1/th1}$, (B) *Hbb*$^{th2/+}$, (C) *Hbb*$^{th3/+}$ and (D) a new mouse model of β-thalassemia major: *Hbb*$^{th1/th2}$. The mouse β-globin locus is represented in the 5' to 3' orientation; for simplicity, only the β-globin genes are indicated; not in scale. LCR: β-globin locus control region; βma: β-globin major gene; βmi: β-globin minor gene; N: neomycin gene. Dotted lines represent DNA deletions.

term survival in the absence of transfusion. Using these mice, we demonstrate the potential beneficial effect of minihepcidins in mice affected by TDT which were or were not given transfusions.

Methods

Animal models

Hbb$^{th1/th1}$ mice (B6.D2-Hbb^{d3th}/BrkJ stock n. 000996) were crossed with *Hbb*$^{th2/+}$ animals (B6.129P2-Hbb^{tm1Unc}/J stock n. 002204).[34-36] All recipient mice were 8- to 12-week old females transgenic for either green fluorescent protein (C57BL/6-Tg(UBC-GFP)30Scha/J)[40] or B6.SJL-*Ptprc*^{a} *Pepc*^{b}/BoyJ (known as Pep Boy). The Pep Boy mice allow us to discriminate between endogenous cells [which carry the differential *Ptprc*^{a} pan-leukocyte marker (commonly known as CD45.1 or Ly5.1)] from the donor fetal liver cells (which carry the CD45.2 or Ly5. variant); similarly, GFP^{+} donors can be distinguished from GFP- recipient source RBC. Blood samples were analyzed as previously described.[3,41]

Hematopoietic chimeras and genotyping

Donor fetal liver cells were harvested from embryos (E13.5-15.5 days) obtained by intercrossing *Hbb*$^{th1/th1}$, *Hbb*$^{th2/+}$, or WT mice. Embryonic genotypes were screened by DNA extraction (KAPA Biosystems, Kapa Mouse Genotyping Kit hotstart, KK7352) and polymerase chain reaction analysis (see *Online Supplementary Tables S1* and *S2*). Fetal liver cells were kept on ice and resuspended in sterile phosphate-buffered saline (ThermoFisher PBS, Ph 7.4, CAT 10010023). To establish bone marrow chimeras, 2.0-5.0x10^{6} cells were injected retro-orbitally into each of the irradiated female recipients. Recipient mice were irradiated with 10 Gy (split dose of 2×5 Gy) on the day of transplantation (ISOVOLT Titan E Series X-Ray Generators).

Blood transfusion

Transfusion was performed as previously described.[16] Starting 2 months after transplantation, mice were transfused weekly via retro-orbital venous plexus with 300 µL freshly harvested blood from normal healthy C57BL/6 mice or GFP. The first transfusion was delivered at the same time as the first minihepcidin administration. The last transfusion was delivered 1 week before the last minihepcidin injection.

Mouse serum erythroferrone measurement

The immunoaffinity liquid chromatography-tandem mass spectrometry assay to quantify total erythroferrone protein levels in mouse serum was developed in-house using surrogate peptide analysis. Briefly, total erythroferrone from 25 µL serum was enriched using a biotinylated mouse anti-erythroferrone antibody (Drakesmith Lab) by diluting serum into 75 µL of phosphate-buffered saline-Tween and incubating with antibody at 30°C for 4 h with interval mixing at 600 rpm. Magnetic streptavidin beads were added and incubated for an additional 30 min with interval mixing at 1200 rpm. The bound erythroferrone protein was then eluted from the beads using hydrochloric acid and processed for digestion using Promega trypsin-LysC enzyme at 37°C overnight. The liquid chromatography-tandem mass spectrometry quantification was carried out by monitoring two unique erythroferrone-specific surrogate peptides (EFQLLLK and SGSHFSAILLGL) using a standard curve generated with a recombinant mouse erythroferrone-Fc protein construct. Levels were measured with a lower limit of quantification (LLOQ) of 0.25 ng/mL.[42-44]

Statistics

Bars represent standard deviation (SD). When multiple comparisons were needed, statistical analysis was performed using ordinary one-way or two-way analysis of variance (ANOVA) with the Tukey or Sidak adjustment for multiple comparisons. An unpaired two-tailed Student *t*-test was used for comparisons between two groups. *P* values <0.05 are considered statistically significant. All data were analyzed using GraphPad Prism version 7 (Microsoft GraphPad Software, La Jolla, CA, USA). Data for WT fetal liver cells are presented as a reference.

Animal study approval

All animal studies were conducted under protocols approved by the Institutional Animal Care and Use Committee of The Children's Hospital of Philadelphia.

Results

Generation of a new mouse model of β-thalassemia major or transfusion-dependent thalassemia

We hypothesized that intercrossing *Hbb*$^{th1/th1}$ and *Hbb*$^{th2/+}$ mice (Figure 1A, B) could generate animals that are able to produce RBC, but with insufficient levels of adult hemoglobin for long-term survival (Figure 1D). At birth *Hbb*$^{th1/th2}$ pups were extremely pale but alive (for up to 8 h) and died despite transfusion (*Online Supplementary Figure S1A*) likely due to irreversible damage associated with the severe hypoxia in late gestation. We then focused on generating mice through transplantation of *Hbb*$^{th1/th2}$ fetal liver cells into recipient transgenic animals expressing GFP or Pep Boy mice [*Hbb*$^{th1/th2}$ bone marrow chimeras (*Hbb*$^{th1/th2}$BMC)] (*Online Supplementary Figures S1B* and *S2A*, B; *Online Supplementary Table S1* and *S2*). The GFP^{+} and the Pep Boy (CD45.1) mice were utilized to monitor the chimerism of circulating RBC over time (GFP^{-} *vs*. GFP^{+} RBC) or bone marrow leukocytes (CD45.2 *vs*. CD45.1) and assess engraftment of donor cells. The resulting models demonstrate the desired phenotype 2 months after transplantation, including production of GFP^{-} RBC or CD45.2 bone marrow leukocytes and anemia (*Online Supplementary Figure S3A*, B, Figure 2).

Hbb$^{th1/th2}$BMC animals showed features of β-thalassemia major, requiring transfusion for long-term survival

Two months after transplantation, analysis of the hematologic parameters indicated that *Hbb*$^{th1/th2}$BMC mice produce few RBC, low hemoglobin levels, but high reticulocyte counts (Figure 2A-C). *Hbb*$^{th1/th2}$BMC mice showed the largest increase in spleen weight (Figure 2D). Peripheral blood smears confirmed more severe anisocytosis, poikilocytosis and hypochromasia (Figure 2E) than in models of NTDT. Because *Hbb*$^{th1/th2}$BMC mice do not require transfusion for survival for up to 4 months after transplantation, we analyzed the effect of minihepcidins in the absence of transfusion. After this period, *Hbb*$^{th1/th2}$BMC mice showed exacerbation of their anemia, incompatible with survival.

Administration of minihepcidins ameliorated red blood cell lifespan, ineffective erythropoiesis, anemia and splenomegaly in untransfused *Hbb*$^{th1/th2}$BMC mice

Hbb$^{th1/th2}$BMC were treated with two doses of minihepcidins, 2.625 mg/kg [(low dose (MH_L)] or 5.25 mg/kg

[high dose (MH_H)] 2 months after transplantation. The experimental design is shown in *Online Supplementary Figure 4A, B*. The duration of the treatment was selected based on the findings of our previous pharmacokinetic studies.[28] Compared to controls (V- vehicle), administration of minihepcidins improved hematologic parameters in a dose-dependent manner. Using the lowest dose, we observed a trend of improved parameters, with the improvement reaching statistical significance with the highest dose. RBC count and hemoglobin concentration were statistically significantly improved in animals treated with the high dose (Figure 3A, B). Similarly, reticulocyte count and splenomegaly decreased more in MH_H-treated *Hbb*$^{th1/th2}$BMC mice (Figure 3C, D). We then focused only on the highest dose. Minihepcidin administration also decreased hemichrome formation (Figure 3E) and reactive oxygen species production (Figure 3F). Accordingly, RBC morphology (Figure 4A) and lifespan (Figure 4B) improved in MH_H-treated mice, relative to vehicle-treated *Hbb*$^{th1/th2}$BMC mice. Flow cytometric analysis of bone marrow and spleen samples (Figure 4C) demonstrated improved ineffective erythropoiesis in minihepcidin-treated *Hbb*$^{th1/th2}$BMC mice as the percentage (Figure 4D, E) of erythroid progenitor cells decreased compared to that of mature RBC.

Administration of minihepcidins ameliorated iron overload in untransfused *Hbb*$^{th1/th2}$BMC mice

As erythropoiesis improved in *Hbb*$^{th1/th2}$BMC MH_H-treated mice, we investigated whether minihepcidins had a beneficial effect on endogenous hepcidin synthesis and iron metabolism. *Hbb*$^{th1/th2}$BMC mice treated with vehicle demonstrated a significant increase in serum erythroferrone levels compared to WT animals, but a reduction in these values when treated with MH_H (Table 1, Figure 5A). Endogenous serum hepcidin concentrations were different between untreated and treated animals (Figure 5B), but no significant differences were observed in transferrin saturation levels (Figure 5C). However, serum iron levels decreased significantly in MH_H-treated *Hbb*$^{th1/th2}$BMC mice (Figure 5D). Moreover, *Hbb*$^{th1/th2}$BMC MH_H-treated mice showed significant reductions of iron by ~33% and ~77% in the liver and spleen, respectively, but not in the kidney (tissue iron content in the kidney not shown). (Figure 5E, F and *Online Supplementary Figure S5*).

Minihepcidin treatment ameliorated ineffective erythropoiesis, reversed splenomegaly, and reduced serum iron and heart iron concentration in transfused *Hbb*$^{th1/th2}$*BMC* mice

Compared to *Hbb*$^{th1/th2}$BMC mice treated with vehicle,

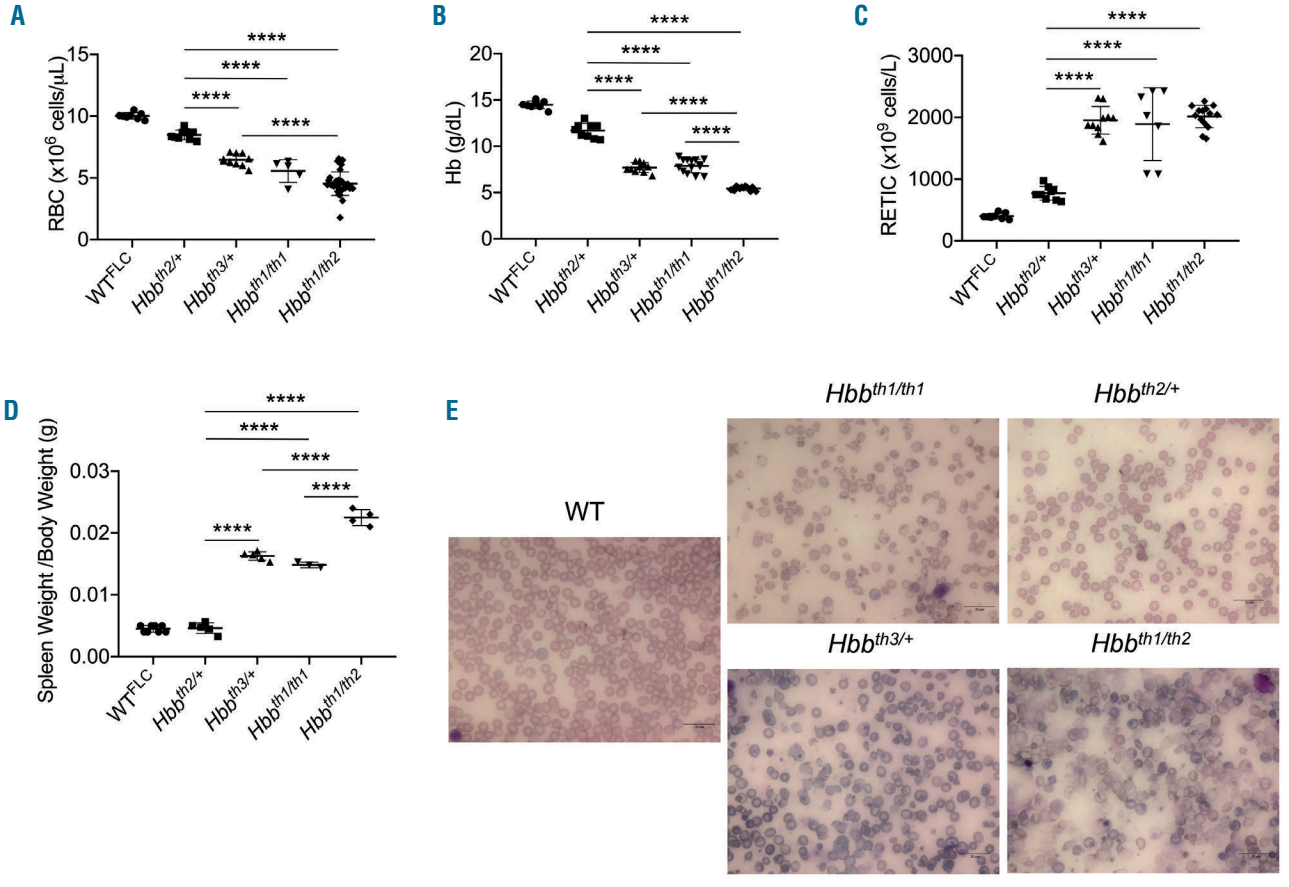

Figure 2. Complete blood count analysis of animals affected by β-thalassemia intermedia or major. (A) Red blood cell (RBC) number, (B) hemoglobin (Hb) levels, (C) reticulocytes (RETIC) count and (D) spleen weight. Bars represent standard deviation. ****P≤0.001. (E) RBC morphology (shown by Giemsa staining of peripheral blood smears) of wildtype (WT), β-thalassemia intermedia and *Hbb*$^{th1/th2}$*-BMC* mice.

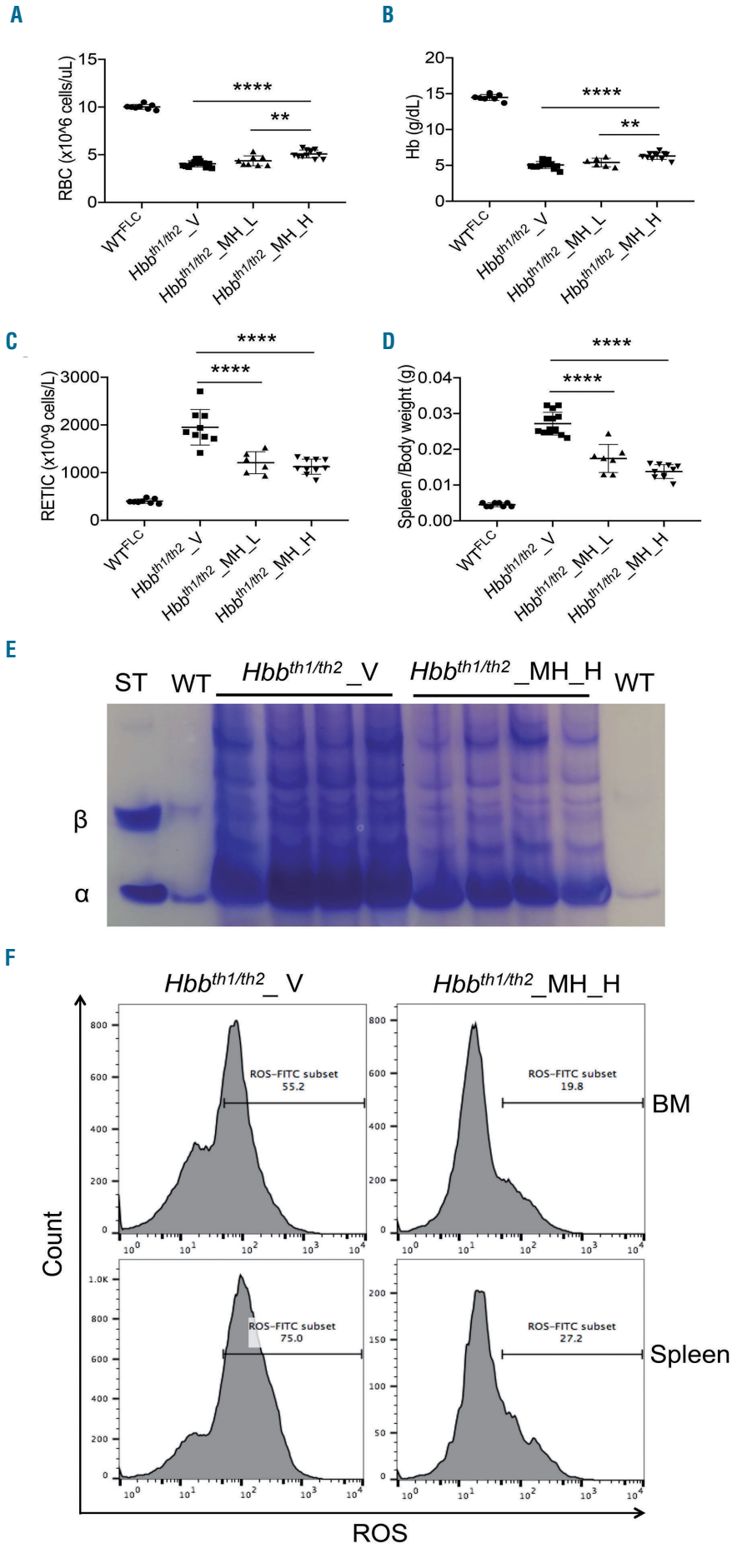

Figure 3. The effect of minihepcidin on complete blood count and splenomegaly in *Hbb*$^{th1/th2}$-BMC mice. Administration of a low dose of minihepcidin (MH_L) (2.625 mg/kg) or a high-dose (MH_H) (5.25 mg/kg) to *Hbb*$^{th1/th2}$-BMC mice resulted in dose-dependent increases in (A) red blood cell (RBC) count and (B) hemoglobin (Hb) concentration and decreases in (C) reticulocyte (RETIC) count and (D) spleen weight. Bars represent the standard deviation. ****$P \leq 0.001$, **$P \leq 0.01$. (E) Minihepcidin administration also decreased hemichrome formation. (F) Flow cytometry studies of bone marrow and spleen erythroid populations of *Hbb*$^{th1/th2}$-BMC mice treated with MH_H showed reduced levels of reactive oxygen species. BM: bone marrow; ROS: reactive oxygen species.

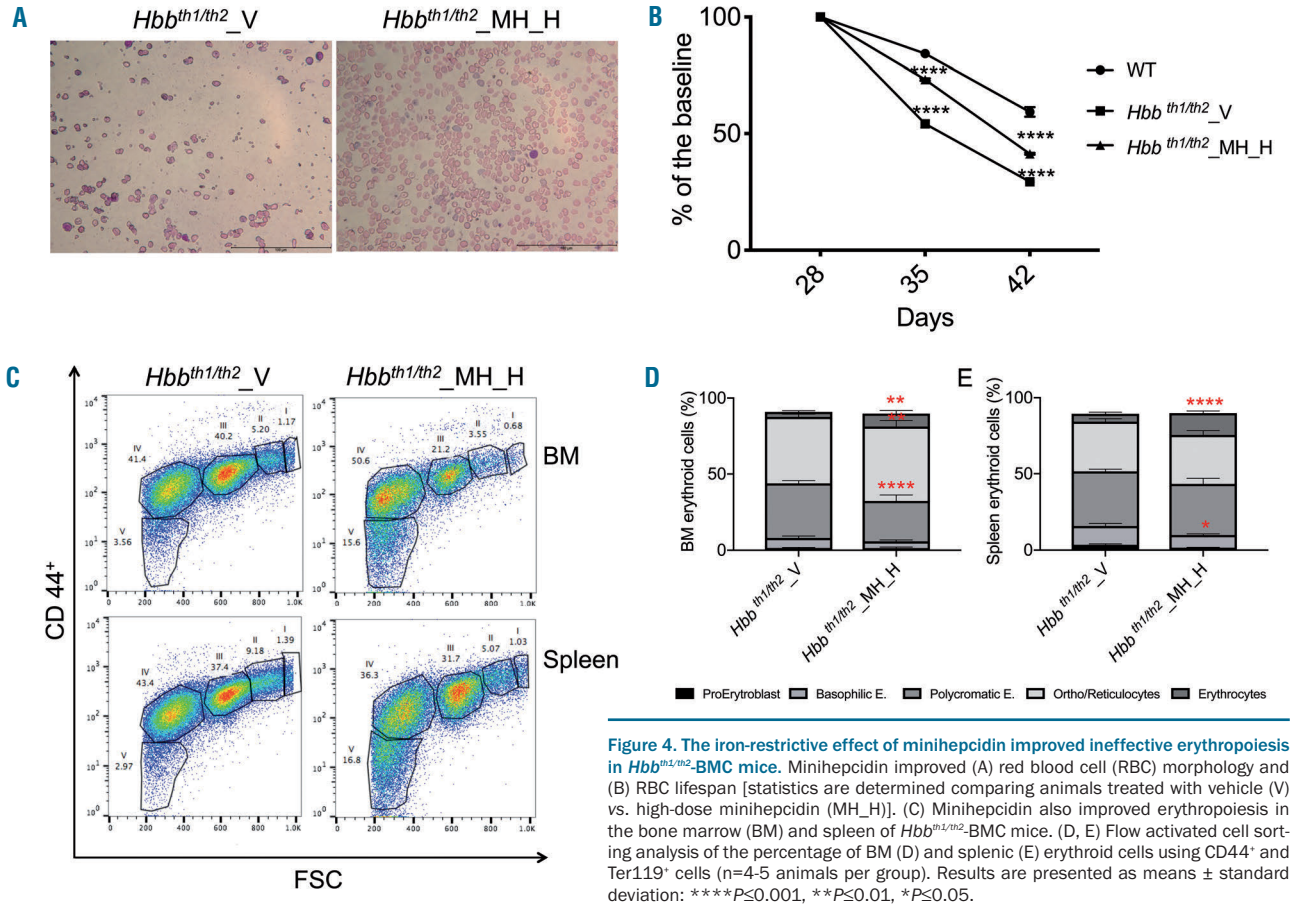

Figure 4. The iron-restrictive effect of minihepcidin improved ineffective erythropoiesis in *Hbb*$^{th1/th2}$-BMC mice. Minihepcidin improved (A) red blood cell (RBC) morphology and (B) RBC lifespan [statistics are determined comparing animals treated with vehicle (V) *vs.* high-dose minihepcidin (MH_H)]. (C) Minihepcidin also improved erythropoiesis in the bone marrow (BM) and spleen of *Hbb*$^{th1/th2}$-BMC mice. (D, E) Flow activated cell sorting analysis of the percentage of BM (D) and splenic (E) erythroid cells using CD44$^+$ and Ter119$^+$ cells (n=4-5 animals per group). Results are presented as means ± standard deviation: ****P≤0.001, **P≤0.01, *P≤0.05.

blood transfusion in animals treated or not with MH_H (see experimental design in *Online Supplementary Figure S4B*) resulted in increased RBC count and hemoglobin concentration, and decreased reticulocyte count and serum erythropoietin concentration (Figure 6A-D). Furthermore, flow cytometric analysis of bone marrow and splenic erythroid cells demonstrated that the combination of MH_H and blood transfusion further reduced the total number of erythroid progenitors compared to blood transfusion alone, indicating an improvement of ineffective erythropoiesis (*Online Supplementary Figure S6A-C*).

Transfusion alone in *Hbb*$^{th1/th2}$BMC mice resulted in significantly increased serum hepcidin (Figure 7A), likely due to suppression of both serum erythropoietin concentration (Figure 6D) and endogenous erythropoiesis (*Online Supplementary Figure S6*). Administration of MH_H (with and without blood transfusion) had little effect on transferrin saturation (Figure 7B), but improved serum iron levels (Figure 7C) in non-transfused *Hbb*$^{th1/th2}$BMC mice. Compared to *Hbb*$^{th1/th2}$BMC mice treated with vehicle alone, transfusion significantly decreased liver iron concentration (Figure 7D, *Online Supplementary Figure S7*), likely due to the increased levels in serum hepcidin (Figure 7A), but no further decrease was observed in MH_H-treated transfused *Hbb*$^{th1/th2}$BMC mice.

Appreciable iron deposition in the heart makes our model helpful to study a pathological feature extremely relevant in patients affected by thalassemia major. In particular, when we looked at the iron concentration in the heart, we observed that minihepcidins in combination with a transfusion regimen significantly reduced iron content (Figure 7E). Furthermore, as minihepicidins enable iron sequestration and reduce ineffective erythropoiesis, we postulate that the decreased erythroid mass also reduces the amount of iron utilized, leading to a relative normalization of transferrin saturation and parenchymal iron deposition. Furthermore, MH_H treatment in transfused *Hbb*$^{th1/th2}$BMC mice decreased total spleen iron

Table 1. Serum erythroferrone measurements.

Erythroferrone ng/mL WT	*Hbb*$^{th1/th2}$-V	*Hbb*$^{th1/th2}$_MH_H****
1.0	9.6	4.3
LLOQ	17.1	8.5
LLOQ	13.0	7.0
2.2	14.3	6.8
LLOQ	15.2	7.7
LLOQ	9.6	4.3
2.4	17.1	8.5

Serum erythroferrone levels in wildtype (WT) and thalassemic animals, treated with vehicle (V) or a high dose of minihepcidin (MH_H). A statistically significant difference was observed comparing *Hbb*$^{th1/th2}$ BMC vehicle-treated *vs.* *Hbb*$^{th1/th2}$ BMC MH_H-treated animals (****P≤0.001). The lower limit of quantification (LLOQ) in wildtype animals was 0.25 ng/mL.

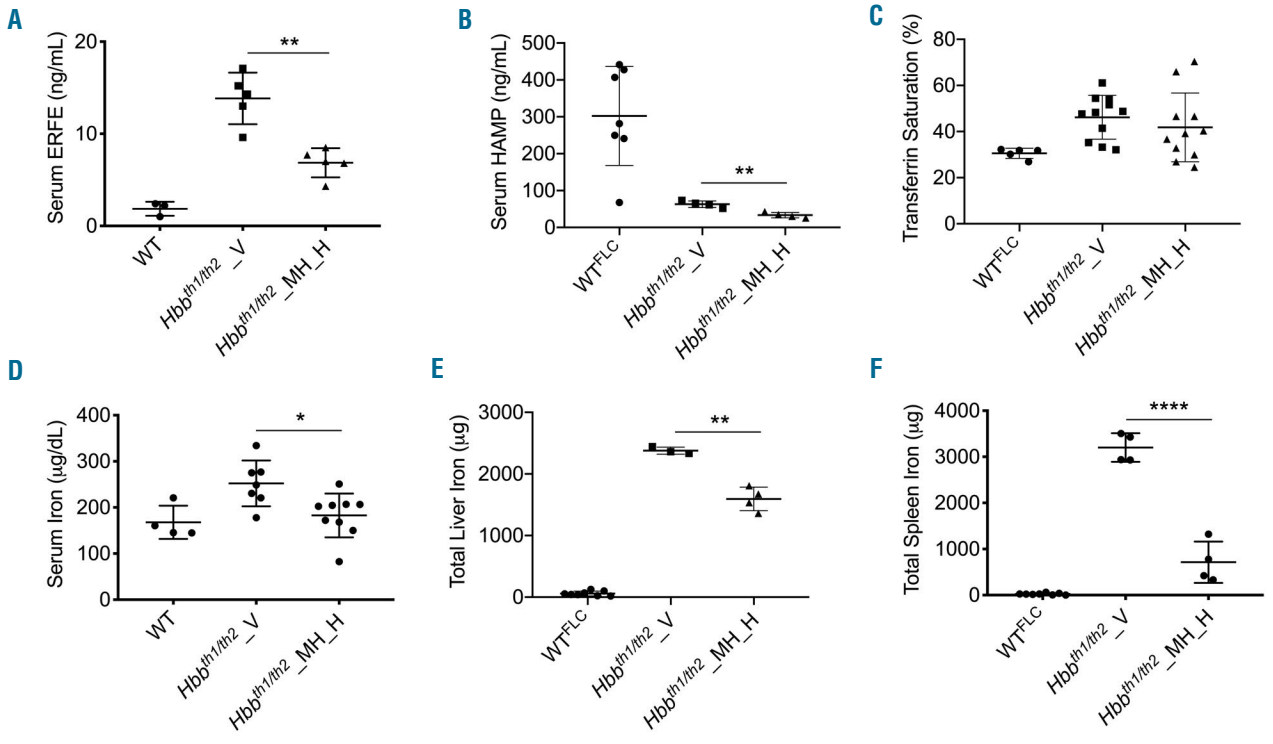

Figure 5. Serum and tissues iron analysis showed improvements in *Hbb*$^{th1/th2}$-BMC mice after treatment with minihepcidin. In a comparison of animals treated with vehicle (V) or high-dose hepcidin (MH_H), (A) serum erythroferrone (ERFE) levels were significantly different, (B) serum hepcidin (HAMP) was decreased, (C) while transferrin saturation did not show significant differences. (D) Serum iron was significantly reduced after MH_H administration. As a result of a decreased erythroid iron uptake, total organ iron content was reduced in the (E) liver and (F) spleen, but not in the kidney (*not shown*). Bars represent the standard deviation. ****P≤0.001, **P≤0.01; *P≤0.05.

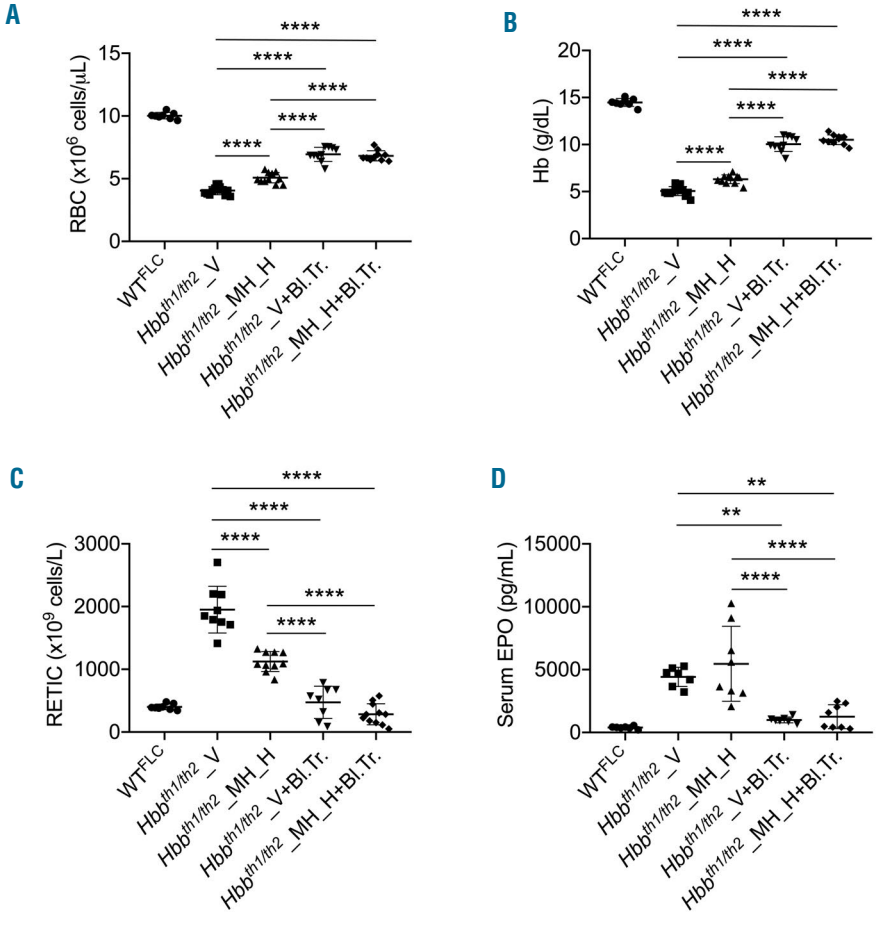

Figure 6. Minihepcidin and blood transfusion improved hematologic parameters and reduced serum erythropoietin in *Hbb*$^{th1/th2}$-BMC mice. Administration of minihepcidin resulted in (A) increased red blood cell (RBC) count and (B) hemoglobin (Hb) levels, while (C) reticulocytes (RETIC) numbers were reduced. (D) Serum erythropoietin (EPO) concentration did not show statistical differences. Bars represent standard deviation. ****P≤0.001, **P≤0.01. WT: wildtype; FLC: fetal liver cells; V: vehicle; MH_H: high-dose minihepcidin; Bl.Tr: blood transfusion.

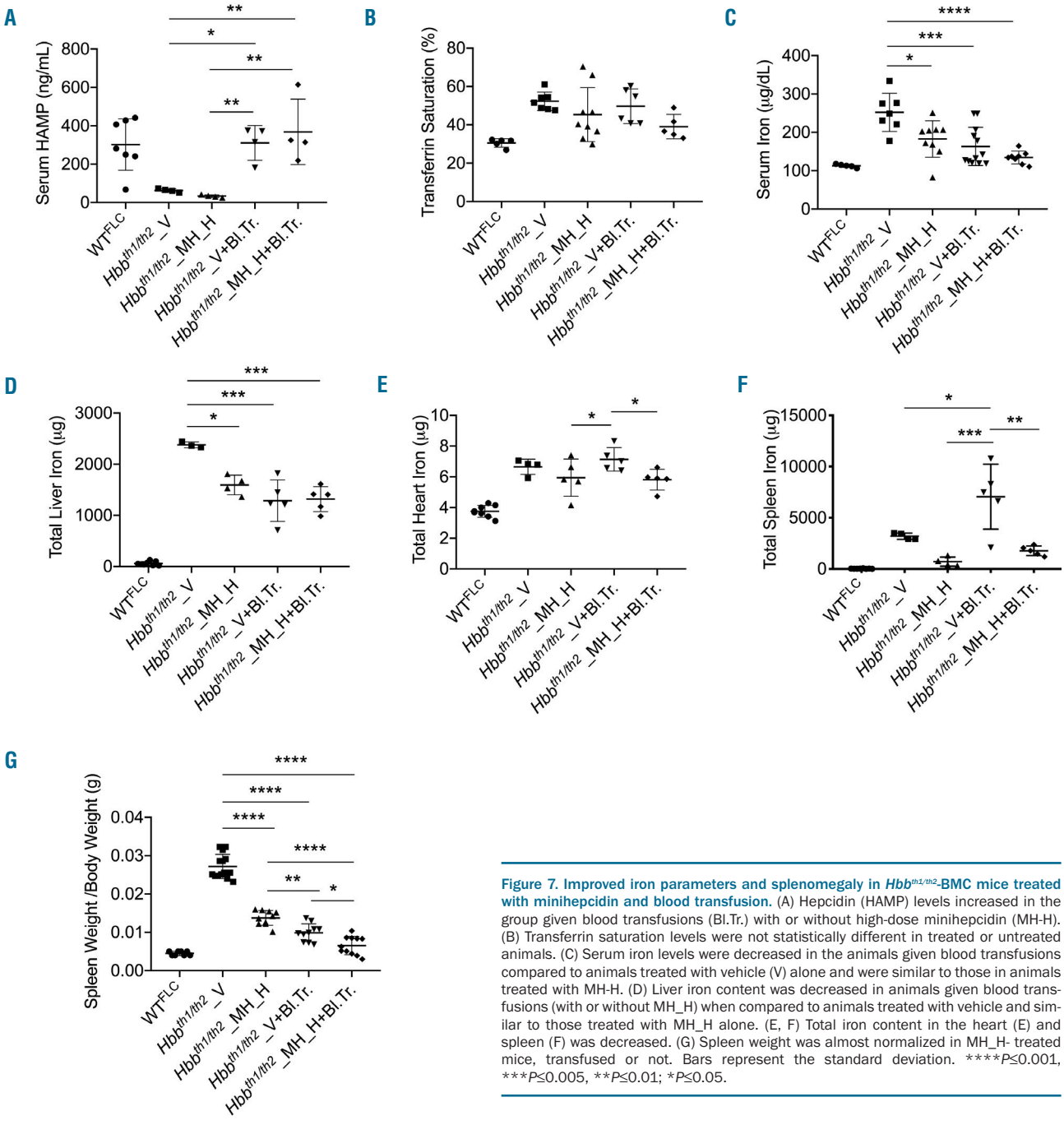

Figure 7. Improved iron parameters and splenomegaly in *Hbb*$^{th1/th2}$-BMC mice treated with minihepcidin and blood transfusion. (A) Hepcidin (HAMP) levels increased in the group given blood transfusions (Bl.Tr.) with or without high-dose minihepcidin (MH-H). (B) Transferrin saturation levels were not statistically different in treated or untreated animals. (C) Serum iron levels were decreased in the animals given blood transfusions compared to animals treated with vehicle (V) alone and were similar to those in animals treated with MH-H. (D) Liver iron content was decreased in animals given blood transfusions (with or without MH_H) when compared to animals treated with vehicle and similar to those treated with MH_H alone. (E, F) Total iron content in the heart (E) and spleen (F) was decreased. (G) Spleen weight was almost normalized in MH_H- treated mice, transfused or not. Bars represent the standard deviation. ****P≤0.001, ***P≤0.005, **P≤0.01; *P≤0.05.

(Figure 7F, *Online Supplementary Figure S7*) and splenomegaly (Figure 7G), reaching levels similar to those in WT mice. Therefore, administration of minihepcidins may also be beneficial in reducing or preventing splenomegaly and organ-associated iron overload in the presence of blood transfusion.

Discussion

We crossed models of NTDT *Hbb*$^{th1/th1}$ with *Hbb*$^{th2/+}$ to generate a combination of mutations that decreased synthesis of mouse β-globin genes to mimic TDT. These models exhibit severe anemia, high erythroferrone and low hepcidin levels in the serum, iron overload and succumbed to death due to anemia 4 months after transplantation, mimicking the most severe form of thalassemia in humans. This relatively slow progression to fatal anemia enables this model to be used to study drugs, such as minihepcidins, with the potential to modulate ineffective erythropoiesis in the presence and absence of transfusions.

The administration of a minihepcidin improved RBC morphology, hemichrome formation, and thus the quality of RBC, and reversed splenomegaly, ineffective erythropoiesis, and anemia in *Hbb*$^{th1/th2}$BMC mice, our new model of TDT. Furthermore, iron parameters, such as serum, liver, and spleen iron concentration, were

decreased in the minihepcidin-treated *Hbb*$^{th1/th2}$BMC mice. Interestingly, serum erythroferrone levels were decreased, as expected by a reduction in the number of erythroid progenitor cells, while hepcidin level was reduced in comparison to that in untreated mice. This could be explained by the reduction in liver iron concentration, which may prevail over reduced erythroferrone levels on regulating hepcidin expression. When a minihepcidin was combined with transfusion, it further improved splenomegaly, with animals treated in this way showing an average spleen weight similar to that of WT mice. This suggests that, in TDT patients, this approach could further prevent or decrease splenomegaly, thereby reducing the requirement for splenectomy.

Interestingly, in this setting (6 weeks of weekly blood transfusions), we did not observe any effect of the minihepcidin on anemia (seen 6 days after the last blood transfusion). It is possible that our transfusion regimen (rate of administration, 6-week treatment and volume of blood transfused) may have been insufficient to show potential differences associated with the administration of minihepcidins. Alternatively, administration of the minihepcidin may have slightly reduced the life-span of transfused RBC (*Online Supplementary Figure S8*). Future studies will address whether this phenomenon is associated only with this compound or with any drug that activates or mimics hepcidin activity. Looking at the characteristics of this mouse model, different endpoints may be observed in ß-thalassemic patients treated with a similar drug. For instance these animals appear to absorb more iron and produce more reticulocytes compared to humans. In addition, the amount of transfusion was limited (only 6 weeks compared to lifelong treatment in humans) and the regimen of drug administration will likely be different in young and old patients. Nevertheless, our data indicate that minihepcidin administration provides several beneficial effects in combination with transfusion, such as reducing serum and heart iron concentration, while improving ineffective erythropoiesis, and splenomegaly. Based on previous data from thalassemia intermedia mice and now from this new TDT model, we speculate that administration of minihepcidins may reduce or eliminate the requirement for transfusions by enhancing the efficiency of endogenous, more iron-restricted, erythropoiesis in several scenarios: (i) for those NTDT patients who become progressively more transfusion-dependent due to disease progression and (ii) in patients with intermittent transfusion requirements, stabilizing endogenous hemoglobin synthesis sufficiently to avoid transfusion.[4,5,45,46] These potentially beneficial effects of minihepicidins may be further enhanced by combination with drugs that increase RBC synthesis, such as luspatercept or sotatercept.[47-50]

In conclusion, we generated a new model of TDT that can be utilized to test drugs with the potential to improve ineffective erythropoiesis and anemia. Furthermore, we demonstrate that a minihepicidin has the potential to improve erythropoiesis and iron metabolism in this model, providing pre-clinical proof-of-concept for its use also in β-thalassemic patients affected by forms of anemias more severe than those observed in NTDT.

Acknowledgments

This work was supported by Merganser Biotech and grants from the National Institute of Diabetes and Digestive and Kidney Diseases and National Heart, Lung, and Blood Institute of the National Institutes of Health: R01 DK090554 (to SR), R01 DK095112 (to RF, SR, and YZG), R01 DK107670 (to YZG). Complete blood count were analyzed by the Translational Core Laboratory of the CHOP Research Institute and the Institutional Clinical and Translational Science Award Research Center, National Center for Advancing Translational Sciences (NIH/NCATS) grant UL1TR000003.

References

1. Rachmilewitz EA, Thorell B. Hemichromes in single inclusion bodies in red cells of beta thalassemia. Blood. 1972;39(6):794-800.
2. Shinar E, Rachmilewitz EA. Oxidative denaturation of red blood cells in thalassemia. Semin Hematol. 1990;27(1):70-82.
3. Gardenghi S, Ramos P, Marongiu MF, et al. Hepcidin as a therapeutic tool to limit iron overload and improve anemia in β-thalassemic mice. J Clin Invest. 2010;120(12):4466-4477.
4. Rivella S. β-thalassemias: paradigmatic diseases for scientific discoveries and development of innovative therapies. Haematologica. 2015;100(4):418-430.
5. Porter JB, Cappellini MD, Kattamis A, et al. Iron overload across the spectrum of non-transfusion-dependent thalassaemias: role of erythropoiesis, splenectomy and transfusions. Br J Haematol. 2017;176(2):288-299.
6. Taher AT, Weatherall DJ, Cappellini MD. Thalassaemia. Lancet. 2018;391(10116):155-167.
7. Danjou F, Origa R, Anni Fet al. Longitudinal analysis of heart and liver iron in thalassemia major patients according to chelation treatment. Blood Cells Mol Dis. 2013;51(3):142-145.
8. Taher AT, Cappellini MD. How I manage medical complications of β-thalassemia in adults. Blood. 2018;132(17):1781-1791.
9. Lal A, Wong TE, Andrews J, et al. Transfusion practices and complications in thalassemia. Transfusion. 2018;58(12):2826-2835.
10. Musallam KM, Rivella S, Vichinsky E, et al. Non-transfusion-dependent thalassemias. Haematologica. 2013;98(6):833-844.
11. Moukhadder HM, Halawi R, Cappellini MD, et al. Hepatocellular carcinoma as an emerging morbidity in the thalassemia syndromes: a comprehensive review. Cancer. 2017;123(5):751-758.
12. Kautz L, Jung G, Valore EV, et al. Identification of erythroferrone as an erythroid regulator of iron metabolism. Nat Genet. 2014;46(7):678-684.
13. Ganz T, Jung G, Naeim A, et al. Immunoassay for human serum erythroferrone. Blood. 2017;130(10):1243-1246.
14. Arezes J, Foy N, McHugh K, et al. Erythroferrone inhibits the induction of hepcidin by BMP6. Blood. 2018;132(14):1473-1477.
15. Kautz L, Jung G, Du X, et al. Erythroferrone contributes to hepcidin suppression and iron overload in a mouse model of β-thalassemia. Blood. 2015;126(17):2031-2037.
16. Gardenghi S, Marongiu MF, Ramos P, et al. Ineffective erythropoiesis in beta-thalassemia is characterized by increased iron absorption mediated by down-regulation of hepcidin and up-regulation of ferroportin. Blood. 2007;109(11):5027-5035.
17. Guo S, Casu C, Gardenghi S, et al. Reducing TMPRSS6 ameliorates hemochromatosis and β-thalassemia in mice. J Clin Invest. 2013;123(4):1531-1541.
18. Aydinok Y. Iron Chelation therapy as a modality of management. Hematol Oncol Clin North Am. 2018;32(2):261-275.
19. Ginzburg Y, Rivella S. β-thalassemia: a model for elucidating the dynamic regulation of ineffective erythropoiesis and iron metabolism. Blood. 2011;118(16):4321-4330.
20. Anderson ER, Taylor M, Xue X, et al. Intestinal HIF2α promotes tissue-iron accumulation in disorders of iron overload with anemia. Proc Natl Acad Sci U S A. 2013;110(50):E4922-4930.
21. Cappellini MD, Porter JB, Viprakasit V, et al. A paradigm shift on beta-thalassaemia treatment: how will we manage this old disease

with new therapies? Blood Rev. 2018;32(4):300-311.
22. Cohen AR, Glimm E, Porter JB. Effect of transfusional iron intake on response to chelation therapy in beta-thalassemia major. Blood. 2008;111(2):583-587.
23. Preza GC, Ruchala P, Pinon R, et al. Minihepcidins are rationally designed small peptides that mimic hepcidin activity in mice and may be useful for the treatment of iron overload. J Clin Invest. 2011;121(12):4880-4888.
24. Ramos E, Ruchala P, Goodnough JB, et al. Minihepcidins prevent iron overload in a hepcidin-deficient mouse model of severe hemochromatosis. Blood. 2012;120(18):3829-3836.
25. Schmidt PJ, Toudjarska I, Sendamarai AK, et al. An RNAi therapeutic targeting Tmprss6 decreases iron overload in Hfe-/- mice and ameliorates anemia and iron overload in murine β-thalassemia intermedia. Blood. 2013;121(7):1200-1208.
26. Schmidt PJ, Racie T, Westerman M, et al. Combination therapy with a Tmprss6 RNAi-therapeutic and the oral iron chelator deferiprone additively diminishes secondary iron overload in a mouse model of β-thalassemia intermedia. Am J Hematol. 2015;90(4):310-313.
27. Casu C, Aghajan M, Oikonomidou PR, et al. Combination of Tmprss6- ASO and the iron chelator deferiprone improves erythropoiesis and reduces iron overload in a mouse model of beta-thalassemia intermedia. Haematologica. 2016;101(1):e8-e11.
28. Casu C, Oikonomidou PR, Chen H, et al. Minihepcidin peptides as disease modifiers in mice affected by β-thalassemia and polycythemia vera. Blood. 2016;128(2):265-276.
29. Chen H, Choesang T, Li H, et al. Increased hepcidin in transferrin-treated thalassemic mice correlates with increased liver BMP2 expression and decreased hepatocyte ERK activation. Haematologica. 2016;101(3):297-308.
30. Huo Y, McConnell SC, Ryan TM. Preclinical transfusion-dependent humanized mouse model of beta thalassemia major. Blood. 2009;113(19):4763-4770.
31. Huo Y, McConnell SC, Liu SR, et al. Humanized mouse model of Cooley's anemia. J Biol Chem. 2009;284(8):4889-4896.
32. Huo Y, McConnell SC, Liu S, et al. Humanized mouse models of Cooley's anemia: correct fetal-to-adult hemoglobin switching, disease onset, and disease pathology. Ann N Y Acad Sci. 2010;1202:45-51.
33. McColl B, Vadolas J. Animal models of β-hemoglobinopathies: utility and limitations. J Blood Med. 2016;7:263-274.
34. Skow LC, Burkhart BA, Johnson FM, et al. A mouse model for beta-thalassemia. Cell. 1983;34(3):1043-1052.
35. Shehee WR, Oliver P, Smithies O. Lethal thalassemia after insertional disruption of the mouse major adult beta-globin gene. Proc Natl Acad Sci U S A. 1993;90(8):3177-3181.
36. Yang B, Kirby S, Lewis J, et al. A mouse model for beta 0-thalassemia. Proc Natl Acad Sci U S A. 1995;92(25):11608-11612.
37. Ciavatta DJ, Ryan TM, Farmer SC, et al. Mouse model of human beta zero thalassemia: targeted deletion of the mouse beta maj- and beta min-globin genes in embryonic stem cells. Proc Natl Acad Sci U S A. 1995;92(20):9259-9263.
38. Rivella S, May C, Chadburn A, et al. A novel murine model of Cooley anemia and its rescue by lentiviral-mediated human beta-globin gene transfer. Blood. 2003;101(8):2932-2939.
39. Libani IV, Guy EC, Melchiori L, et al. Decreased differentiation of erythroid cells exacerbates ineffective erythropoiesis in beta-thalassemia. Blood. 2008;112(3):875-885.
40. Schaefer BC, Schaefer ML, Kappler JW, et al. Observation of antigen-dependent CD8+ T-cell/ dendritic cell interactions in vivo. Cell Immunol. 2001;214(2):110-122.
41. Mercier FE, Sykes DB, Scadden DT. Single targeted exon mutation creates a true congenic mouse for competitive Hematopoietic stem cell transplantation: the C57BL/6-CD45.1(STEM) mouse. Stem Cell Reports. 2016;6(6):985-992.
42. Ocana MF, Neubert H. An immunoaffinity liquid chromatography-tandem mass spectrometry assay for the quantitation of matrix metalloproteinase 9 in mouse serum. Anal Biochem. 2010;399(2):202-210.
43. McAvoy T, Lassman ME, Spellman DS, et al. Quantification of tau in cerebrospinal fluid by immunoaffinity enrichment and tandem mass spectrometry. Clin Chem. 2014;60(4):683-689.
44. Palandra J, Finelli A, Zhu M, et al. Highly specific and sensitive measurements of human and monkey interleukin 21 using sequential protein and tryptic peptide immunoaffinity LC-MS/MS. Anal Chem. 2013;85(11):5522-5529.
45. Kohne E. Hemoglobinopathies: clinical manifestations, diagnosis, and treatment. Dtsch Arztebl Int. 2011;108(31-32):532-540.
46. Oikonomidou PR, Rivella S. What can we learn from ineffective erythropoiesis in thalassemia? Blood Rev. 2018;32(2):130-143.
47. Suragani RN, Cadena SM, Cawley SM, et al. Transforming growth factor-β superfamily ligand trap ACE-536 corrects anemia by promoting late-stage erythropoiesis. Nat Med. 2014;20(4):408-414.
48. Suragani RN, Cawley SM, Li R, et al. Modified activin receptor IIB ligand trap mitigates ineffective erythropoiesis and disease complications in murine β-thalassemia. Blood. 2014;123(25):3864-3872.
49. Dussiot M, Maciel TT, Fricot A, et al. An activin receptor IIA ligand trap corrects ineffective erythropoiesis in β-thalassemia. Nat Med. 2014;20(4):398-407.
50. Cappellini MD, Porter J, Origa R, et al. Sotatercept, a novel transforming growth factor β ligand trap, improves anemia in β-thalassemia: a phase 2, open-label, dose-finding study. Haematologica. 2019;104(3):477-484.

ARTICLE

Src family kinase-mediated vesicle trafficking is critical for neutrophil basement membrane penetration

Ina Rohwedder,[1] Angela R.M. Kurz,[1] Monika Pruenster,[1] Roland Immler,[1] Robert Pick,[1] Tanja Eggersmann,[1] Sarah Klapproth,[1] Jennifer L. Johnson,[2] Sergi Masgrau Alsina,[1] Clifford A. Lowell,[3] Attila Mócsai,[4] Sergio D. Catz[2] and Markus Sperandio[1]

[1]Walter-Brendel-Center of Experimental Medicine, Institute of Cardiovascular Physiology and Pathophysiology, Klinikum der Universität, Ludwig-Maximilians-University Munich, Planegg-Martinsried, Germany; [2]Department of Molecular Medicine, The Scripps Research Institute, La Jolla, CA, USA; [3]Department of Laboratory Medicine, University of California, San Francisco, CA, USA and [4]Department of Physiology, Semmelweis University School of Medicine, Budapest, Hungary

Ferrata Storti Foundation

Haematologica 2020
Volume 105(7):1845-1856

ABSTRACT

Leukocyte recruitment into inflamed tissue is highly dependent on the activation and binding of integrins to their respective ligands, followed by the induction of various signaling events within the cell referred to as outside-in signaling. Src family kinases (SFK) are the central players in the outside-in signaling process, assigning them a critical role for proper immune cell function. Our study investigated the role of SFK on neutrophil recruitment *in vivo* using *Hck*$^{-/-}$ *Fgr*$^{-/-}$ *Lyn*$^{-/-}$ mice, which lack SFK expressed in neutrophils. We show that loss of SFK strongly reduces neutrophil adhesion and post-arrest modifications in a shear force dependent manner. Additionally, we found that in the absence of SFK, neutrophils display impaired Rab27a-dependent surface mobilization of neutrophil elastase, VLA3 and VLA6 containing vesicles. This results in a defect in neutrophil vascular basement membrane penetration and thus strongly impaired extravasation. Taken together, we demonstrate that SFK play a role in neutrophil post-arrest modifications and extravasation during acute inflammation. These findings may support the current efforts to use SFK-inhibitors in inflammatory diseases with unwanted neutrophil recruitment.

Introduction

Chronic inflammatory diseases are an increasing problem in western industrialized countries. A hallmark of these disorders is the recruitment of leukocytes from the circulation into affected tissues. This process follows a well-defined cascade of activation and adhesion events starting with the initial capture of leukocytes from the blood stream, followed by rolling along inflamed endothelium.[1] Both steps are mediated by selectins interacting with glycosylated ligands on leukocytes.[2] Through binding of the leukocyte specific integrin LFA1 (αLβ2) to ICAM-1 on endothelial cells, leukocytes slow down their rolling velocity, and in combination with chemokine stimulation, firmly arrest on the endothelial surface. This is followed by post-arrest modifications, a process characterized by cell spreading, cytoskeleton rearrangements and crawling along the endothelium, that is critical for tight adhesion to the substrate and allows an appropriate spot for extravasation into tissue. Transmigration involves the crossing of the venular wall and the underlying vascular basement membrane (BM), two steps which are still incompletely understood. Several reports suggest a role for the integrins VLA3 (α3β1) and VLA6 (α6β1) along with neutrophil elastase (NE) in this process.[3-5] Recently, our group has shown that neutrophils translocate VLA3, VLA6 and NE from internally stored vesicles to the cell surface, to subsequently cross the vascular BM.[6] The release of these vesicles is initiated by interactions of neutrophils with the inflamed endothelium in a PECAM-1/ICAM-1- and CXCL1-dependent manner. Vesicle transport is

Correspondence:

MARKUS SPERANDIO
markus.sperandio@lmu.de

Received: April 29, 2019.

Accepted: November 5, 2019.

Pre-published: November 7, 2019.

doi:10.3324/haematol.2019.225722

Check the online version for the most updated information on this article, online supplements, and information on authorship & disclosures: www.haematologica.org/content/105/7/1845

mainly regulated by Rab GTPases and their effector proteins with Rab27a being the main Rab molecule involved in the secretory machinery of neutrophils.[7] Rab27a function is mediated by the two effector molecules synaptotagmin-like protein 1 (JFC1, encoded by Sytl1 in mice) and Munc13-4 (Unc13d).[8] Although most of these processes rely on integrin signaling, integrins themselves lack enzymatic activity. Therefore, numerous proteins are recruited to their intracellular tails, among those Src family kinases (SFK). Their early recruitment during integrin activation assigns SFK a critical role in the so-called outside-in signaling process and thus regulation of central signaling pathways downstream of integrin-receptor ligation.[9] Neutrophils express three members of this family, namely Hck, Fgr and Lyn.[10] Their function has been intensively studied in SFK single, double (*Hck*$^{-/-}$*Fgr*$^{-/-}$), and triple knockout (ko) (*Hck*$^{-/-}$*Fg*$^{-/-}$*Lyn*$^{-/-}$) mice,[11] demonstrating a role for SFK in integrin activation[12] and their downstream signaling. Neutrophils isolated from *Hck*$^{-/-}$*Fgr*$^{-/-}$ mice showed poor spreading, indicating that integrin outside-in signaling is impaired.[13] Additionally, neutrophil migration into the liver of *Hck*$^{-/-}$*Fgr*$^{-/-}$ mice in an *in vivo* endotoxemia model is severely reduced.[14] Furthermore, Kovács *et al.* recently showed that neutrophils exhibit reduced capability to create a microinflammatory environment, resulting in diminished neutrophil extravasation in a model of autoantibody-induced arthritis and inflammatory blistering skin disease.[15]

Our study aimed to investigate the effect of SFK on leukocyte recruitment in an *in vivo* setting of acute inflammation, focusing on post-arrest modifications and the molecular mechanism of vascular BM penetration. We show that, in the genetic absence of SFK, these two steps are strongly impaired. Adherent *Hck*$^{-/-}$*Fgr*$^{-/-}$*Lyn*$^{-/-}$ neutrophils are unable to withstand shear forces and display diminished LFA1 clustering with reduced phosphorylation levels of Paxillin, Cortactin and Syk, suggesting that SFK depletion results in severely impaired adhesion strengthening. In addition, we show that SFK are critical for crossing the vascular BM during neutrophil extravasation by facilitating translocation of VLA3-, VLA6- and NE-containing vesicles to the cell surface. Therefore, SFK are not only important mediators of neutrophil post-arrest modifications, but are also required to breach the vascular BM.

Methods

Animals

Lyz2^{GFP}, SFK-ko (*Hck*$^{-/-}$*Fgr*$^{-/-}$*Lyn*$^{-/-}$) and SFK-ko *Lyz2*^{GFP} mice were generated as described earlier.[16-18] C57BL/6 wildtype mice were purchased from Janvier Labs (Saint Berthevin, France). All animal experiments were approved by the Regierung von Oberbayern, Germany (AZ 55.2-1-54-2531-80-76/12 and 55.2-1-54-2532-102-2017).

Live cell imaging of *in vitro* laminin digestion

Transmigration of neutrophils was analyzed in µ-Slide membrane ibiPore flow chambers (Ibidi, Planegg, Germany) equipped with a 300-nm thick membrane with 5-µm pores, and a subjacent rat-tail collagen gel (1.5 mg/mL) containing 10 µM N-formylmethionyl-leucyl-phenylalanine (fMLP) as chemoattractant. The upper compartment was coated with Laminin (LN), PECAM-1 and ICAM-1, and, in addition, LN was visualized using an anti-LN antibody conjugated to Alexa Fluor-647 (novusbio, Littleton, CO, USA). Isolated neutrophils from wildtype and SFK-ko animals were labeled with CellTracker™ Green CMFDA Dye and CellTracker™ Red CMTPX Dye (Thermo Fisher, Waltham, MA, USA), respectively, and distributed into the upper chamber compartment in a 1:1 ratio. Time-lapse microscopy with an interval of 50 seconds was performed using an upright spinning-disk confocal microscope (Examiner; Zeiss) equipped with a confocal scanner unit CSU-X1 (Yokogawa Electric Corporation, Japan), an EMCCD camera (Evolve; Photometrics), and a x20/1.0 NA water immersion objective (Plan Apochromat; Zeiss). 3D images (70 z-stacks with a step size of 2µm) were acquired per time point and analyzed by generating maximum z-projections over time using Slidebook 6.0.8 software (3i) and ImageJ. Interaction strength was analyzed with the MosaicIA interaction plugin of Fiji.

Functional *in vitro* and *in vivo* experiments, including intravital microscopy,[19] peritonitis experiments, flow chamber experiments, vesicle trafficking, flow cytometry, western blot analysis and statistics are described in detail in the *Online Supplementary Methods.*

Data sharing statement

Original data are available on request.

Results

Src family kinase depletion reduces neutrophil adhesion and extravasation in inflamed postcapillary venules *in vivo*

We first investigated how loss of neutrophil-expressed SFK influences neutrophil adhesion in TNFα-stimulated cremaster muscle postcapillary venules using intravital microscopy. Interestingly, the absolute number of adherent neutrophils was strongly increased compared to wildtype control mice (*Online Supplementary Figure S1A*). However, after adjusting the number of adherent neutrophils to the circulating neutrophil count, which was significantly higher in SFK-ko mice compared to wildtype mice (*Online Supplementary Figure S1B and C*), the neutrophil adhesion efficiency calculated as number of adherent cells/mm^2 divided by the systemic neutrophil count was significantly reduced in SFK-ko mice (0.48±0.04) compared to wildtype mice (1.04±0.08) (Figure 1A). This was not due to altered surface expression of rolling and adhesion relevant surface proteins including CD18, CD11a, CD11b, CD62L, PSGL1, CXCR2, and CD44 as their surface expression was equal between wildtype and SFK-ko neutrophils (*Online Supplementary Figure S1D*). We therefore conclude that SFK are critical for neutrophil adhesion *in vivo*.

Efficient neutrophil extravasation into tissue is required for proper host defense. Recently, Kovács *et al.* demonstrated in the K/B×N serum-transfer arthritis model that SFK deficiency resulted in lower levels of cytokine production and release leading to impaired leukocyte extravasation.[15] To investigate a cell intrinsic adhesion defect in SFK-ko mice, we injected TNFα into the mouse scrotum. This approach circumvents possible effects of a reduced inflammatory environment and enables us to focus on neutrophil recruitment itself. Performing Giemsa staining of TNFα stimulated cremaster muscle whole mounts revealed strongly reduced numbers of extravasated neutrophils in SFK-ko mice compared to wildtype mice (306.51±43.7 *vs.* 578.6±72.9, respectively) (Figure 1B and *Online Supplementary Figure S1E*). Moreover, we calculated the extravasation efficiency as total number of extravasat-

ed leukocytes divided by the total number of adherent leukocytes to differentiate between reduced extravasation due to decreased adhesion *versus* a specific extravasation defect. Surprisingly, we observed a strongly reduced extravasation efficiency in SFK-ko mice (0.21 in SFK-ko mice *vs.* 0.77 in wildtype mice) (Figure 1C), indicating that SFK depletion does not only affect neutrophil adhesion, but also interferes with extravasation itself. Finally, we also compared neutrophil cell numbers in the peritoneal cavity 2 hours (h) after TNFα-induced peritonitis (Figure 1D). In SFK-ko animals, peritoneal neutrophil numbers were reduced to 50% compared to wildtype mice ($0.42x10^6$ *vs.* 10^6, respectively). Taken together, these experiments demonstrate an important role for SFK in neutrophil extravasation.

Adhesion strengthening is severely impaired in Src family kinase-knockout neutrophils *in vitro*

Our experiments suggest that SFK-deletion in neutrophils results in an extravasation defect in the presence of the proinflammatory cytokine TNFα. After firm adhesion to the inflamed endothelium, neutrophils start to polarize and crawl along the endothelium to find a suitable spot for extravasation. These changes are highly dependent on β2 integrins LFA1 (αLβ2) and Mac1 (αMβ2) and integrin outside-in signaling.[20] We analyzed neutrophil crawling using time-lapse microscopy in TNFα-stimulated cremaster muscle venules of SFK-ko and wildtype mice. We observed no differences in crawling direction (Figure 2A), but, interestingly, crawling velocity was significantly increased in SFK-ko mice (12.3 μm/min) compared to wildtype mice (10.7 μm/min) (Figure 2B), suggesting defective adhesion strengthening. Subsequently, we performed *ex vivo* flow chamber assays using glass capillaries coated with E-Selectin/ICAM-1/CXCL1 to mimic the inflamed endothelium. Plots of single cell tracks displayed more SFK-ko neutrophils crawling in flow direction compared to wildtype neutrophils (Figure 2C). Crawling velocity was increased in SFK-ko leukocytes (Figure 2D), verifying our *in vivo* results. Interestingly, only 20% of SFK-ko neutrophils were able to crawl under flow (Figure 2E and *Online Supplementary Mov1*), compared to 80% of wildtype cells, suggesting that SFK-ko neutrophils are unable to maintain stable adhesion to the substrate. Together, these findings demonstrate a decreased capability of SFK-ko neutrophils to withstand shear forces, indicating that SFK are necessary for adhesion strengthening during post-arrest modifications. To further investigate a shear stress dependent adhesion defect in the absence of neutrophil SFK, we conducted detachment assays in the

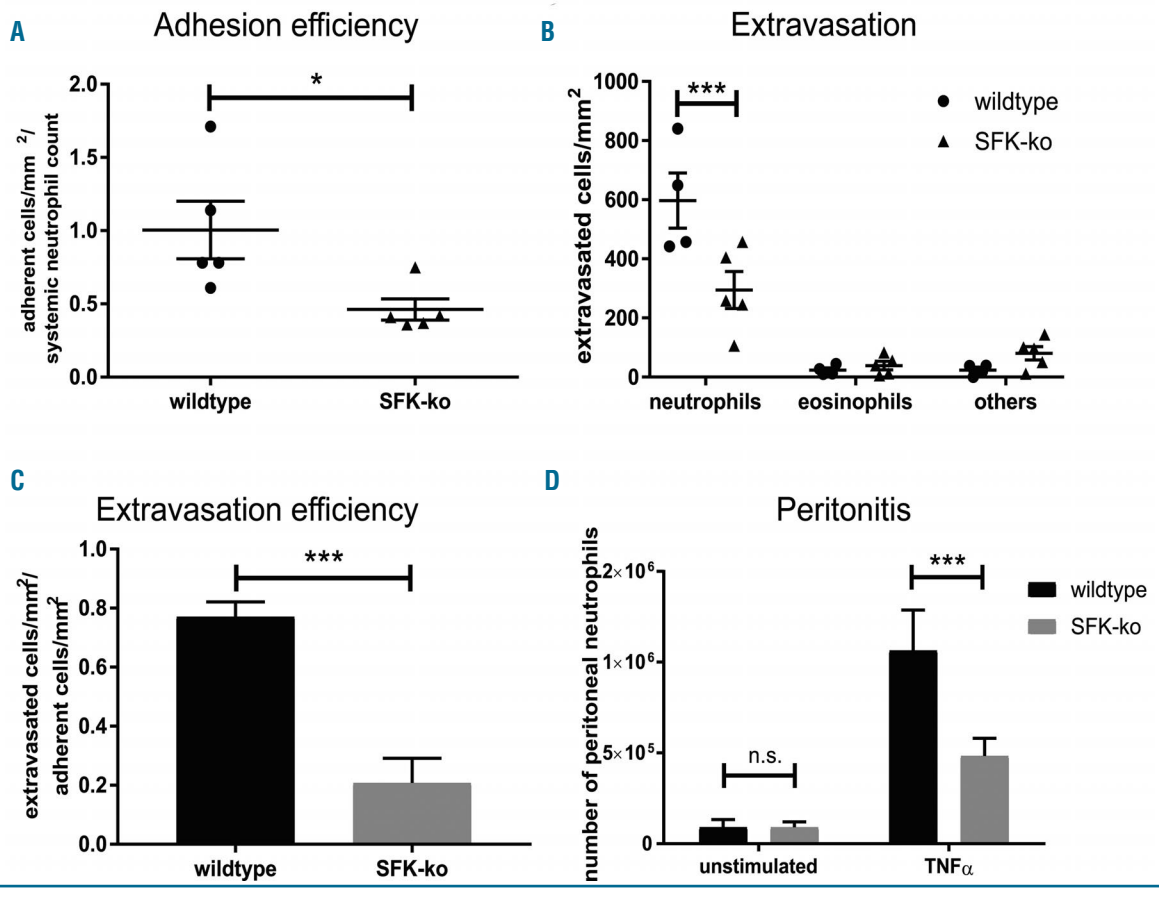

Figure 1. Src family kinases (SFK) are required for slow rolling, neutrophil adhesion and extravasation. All data are presented as mean± standard error of the mean (SEM). *P<0.05; ***P<0.001; n.s. : not significant (unpaired Student *t*-test or two-way ANOVA, Sidak multiple comparison test). (A) Adhesion efficiency from wildtype or SFK-knockout (ko) mice: n= 5 wildtype; n=5 SFK-ko mice. (B) *In vivo* leukocyte extravasation in TNFα-stimulated venules of mouse cremaster muscle. Differential total cell counts of neutrophils, eosinophils and other cells: n= 4 wildtype; n=5 SFK-ko mice. (C) Extravasation efficiency was calculated by the number of extravasated cells/mm^2 divided by number of adherent cells/mm^2. (D) Total neutrophil numbers after peritoneal lavage of the unstimulated or TNFα–stimulated peritoneal cavity of wildtype and SFK-ko mice: n=7 wildtype and n=6 SFK-ko mice for unstimulated controls and n=6 wild-type and n=6 SFK-ko mice for TNFα.

flow chamber using increasing shear forces. Adherent neutrophils were assessed for each shear stress level and related to the number of adherent neutrophils under low flow conditions (Figure 2F). Loss of SFK resulted in a decrease in shear stress resistant adhesion compared to wildtype cells. At wall shear stress levels of 140 dyn/cm^2, only 36% of SFK-ko leukocytes could adhere to the flow chamber, while 84% of wildtype leukocytes were still attached. To analyze if these findings also apply under *in vivo* conditions, we correlated *in vivo* shear rates to

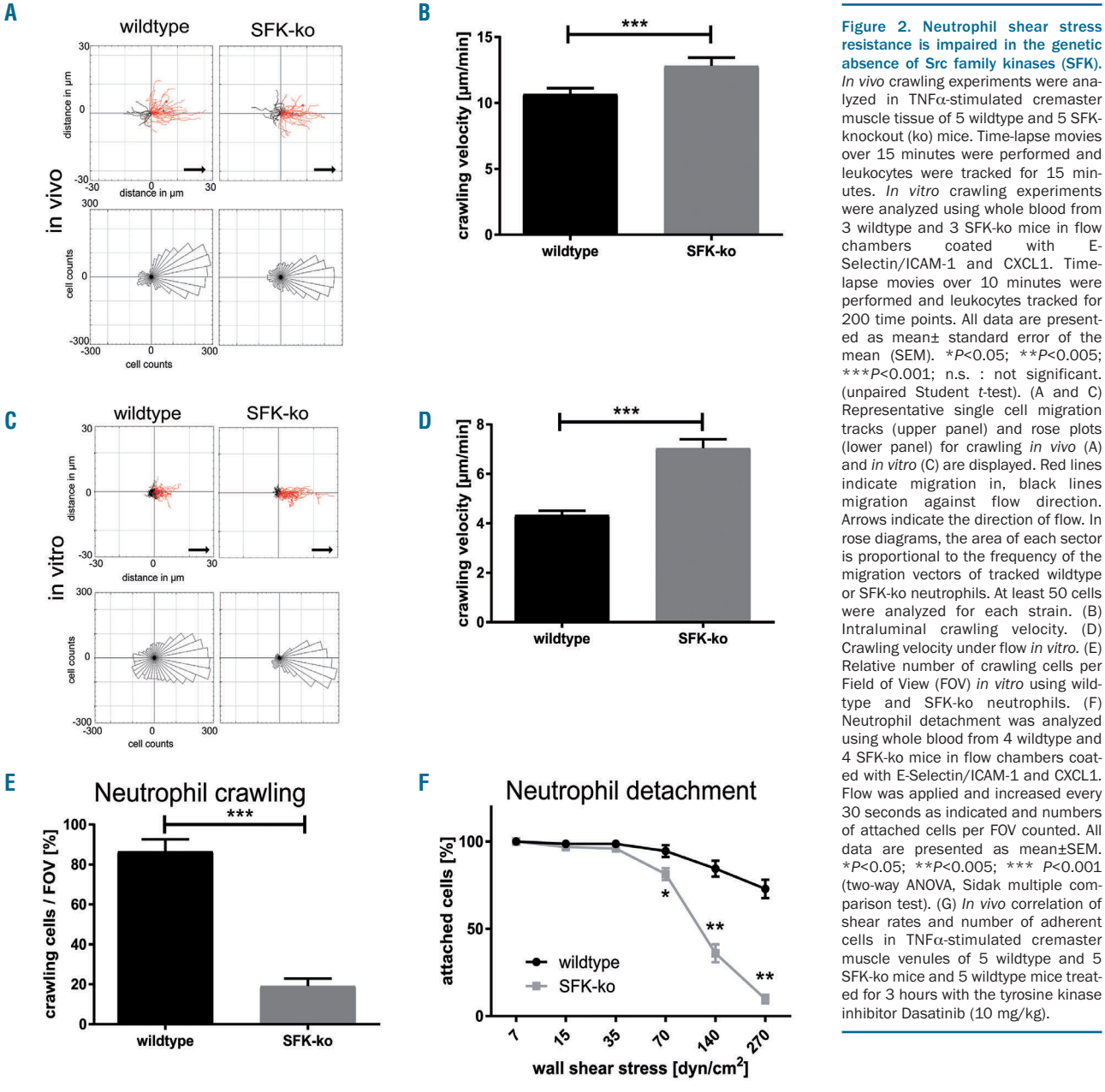

Figure 2. Neutrophil shear stress resistance is impaired in the genetic absence of Src family kinases (SFK). *In vivo* crawling experiments were analyzed in TNFα-stimulated cremaster muscle tissue of 5 wildtype and 5 SFK-knockout (ko) mice. Time-lapse movies over 15 minutes were performed and leukocytes were tracked for 15 minutes. *In vitro* crawling experiments were analyzed using whole blood from 3 wildtype and 3 SFK-ko mice in flow chambers coated with E-Selectin/ICAM-1 and CXCL1. Time-lapse movies over 10 minutes were performed and leukocytes tracked for 200 time points. All data are presented as mean± standard error of the mean (SEM). *P<0.05; **P<0.005; ***P<0.001; n.s. : not significant. (unpaired Student *t*-test). (A and C) Representative single cell migration tracks (upper panel) and rose plots (lower panel) for crawling *in vivo* (A) and *in vitro* (C) are displayed. Red lines indicate migration in, black lines migration against flow direction. Arrows indicate the direction of flow. In rose diagrams, the area of each sector is proportional to the frequency of the migration vectors of tracked wildtype or SFK-ko neutrophils. At least 50 cells were analyzed for each strain. (B) Intraluminal crawling velocity. (D) Crawling velocity under flow *in vitro*. (E) Relative number of crawling cells per Field of View (FOV) *in vitro* using wildtype and SFK-ko neutrophils. (F) Neutrophil detachment was analyzed using whole blood from 4 wildtype and 4 SFK-ko mice in flow chambers coated with E-Selectin/ICAM-1 and CXCL1. Flow was applied and increased every 30 seconds as indicated and numbers of attached cells per FOV counted. All data are presented as mean±SEM. *P<0.05; **P<0.005; *** P<0.001 (two-way ANOVA, Sidak multiple comparison test). (G) *In vivo* correlation of shear rates and number of adherent cells in TNFα-stimulated cremaster muscle venules of 5 wildtype and 5 SFK-ko mice and 5 wildtype mice treated for 3 hours with the tyrosine kinase inhibitor Dasatinib (10 mg/kg).

absolute numbers of adherent cells/mm^2 in TNFα-stimulated post-capillary cremaster muscle venules of SFK-ko and wildtype mice (Figure 2G). We found a similar shear rate dependent decrease in the number of adherent cells/mm^2 in SFK-ko mice *in vivo* compared to wildtype mice. Additionally, we used a pharmacological approach and administered the broad-spectrum tyrosine kinase inhibitor Dasatinib before TNFα-stimulation. Dasatinib has been used in various studies as a SFK inhibitor and led to promising results as an immune modulator.[21] Similar to the results in SFK-ko mice, we found a decrease in adherent cells with increasing shear rates. Importantly, SKF-ko mice receiving Dasatinib did not show any further decrease in adherent cells at high shear stress levels, indicating that Dasatinib exerts its observed effects on adhesion *via* inhibition of SFK (*Online Supplementary Figure S1F*). Taken together, these *in vivo* and *in vitro* findings indicate that loss of SFK in neutrophils leads to a shear force dependent inability to firmly adhere to the inflamed endothelium, a prerequisite for subsequent extravasation.

Reduced phosphorylation of cytoskeleton-associated proteins in Src family kinase-deficient neutrophils

To further elucidate the molecular mechanisms of SFK dependent neutrophil extravasation, we analyzed different steps of integrin outside-in signaling that occur after integrins bind to their receptor. This includes integrin clustering and cytoskeletal rearrangements.[22] To analyze integrin clustering, we performed time-lapse confocal microscopy and studied LFA1 clustering in SFK-ko and wildtype neutrophils in flow chambers coated with E-selectin/ICAM-1/CXCL1 (Figure 3A and *Online Supplementary Mov2*). We observed spreading and polarizing wild-type neutrophils which showed an accumulating LFA1 signal (clustering) over time at the neutrophil uropod (Figure 3B). In contrast, SFK-deficient neutrophils appeared round and unpolarized with no obvious LFA1 clustering. Several cytoskeleton-associated proteins and signaling molecules are known to be tyrosine phosphorylated upon integrin ligation.[23] We investigated the phosphorylation and activation of the direct SFK target[24,25] Syk in SFK-ko and wildtype neutrophils plated on ICAM-1 and then stimulated with CXCL1 or PMA. Western blot analysis of phospho-Syk (Tyr519/520) revealed a strong upregulation of phosphorylation following stimulation of wildtype cells. In contrast, SFK deficiency prevented the upregulation of phosphorylation following stimulation with CXCL1 or PMA (Figure 3C), indicating that Syk activation is defective in the absence of SFK. Moreover, we tested the phosphorylation of the adaptor protein Paxillin, one of the critical proteins for cell adhesion, migration and podosome formation, that is known to be tyrosine phosphorylated upon β_2 integrin activation.[26,27] Western blot analysis showed significant upregulation of Paxillin phosphorylation when stimulated with CXCL1 or PMA in wildtype cells, while no upregulation was detectable in SFK-ko neutrophils (Figure 3D). In addition, we also investigated the tyrosine phosphorylation of Cortactin, which regulates actin branching and therefore cell migration. Likewise, we observed no significant upregulation of Cortactin Tyr421 phosphorylation upon CXCL1 or PMA stimulation in SFK-ko cell, in contrast to wildtype neutrophils (Figure 3E). Because during neutrophil adhesion and migration SFK do not selectively signal *via* LFA1, but also *via* Mac1, we additionally analyzed Paxillin phosphorylation after plating the cells on Fibrinogen (*Online Supplementary Figure S1G*). Similar to ICAM1 we observed a stimulus dependent phosphorylation of Paxillin in wildtype neutrophils, which was absent in SFK-ko neutrophils. Taken together, these experiments show that β_2-integrin clustering and subsequent outside-in signaling is severely impaired in SFK-ko neutrophils.

Src family kinase are indispensable to pass the vascular basement membrane

For successful extravasation into inflamed tissue, neutrophils need to cross the endothelial cell layer and the underlying vascular basement membrane. We aimed to investigate whether SFK are required to perform this last step of extravasation. First, we analyzed transmigration capacity of SFK-ko neutrophils in a transwell assay using CXCL1 as chemoattractant (*Online Supplementary Figure S2A*). In line with previous results,[15] we observed no difference in transmigration between SFK-ko neutrophils and wildtype neutrophils. Both groups displayed a proportional increase in transmigration with rising CXCL1 concentrations. As a next step, we coated transwells with laminin-111 (LN1) or a combination of LN1 and PECAM-1/ICAM-1 and stimulated them with CXCL1 in order to mimic the situation at the vascular BM, as reported previously.[6] No difference in transmigration through LN alone was detected between wildtype and SFK-ko neutrophils (Figure 4A). Coating with LN1/PECAM-1/ICAM-1 (LN/P/I) together with CXCL1 stimulation induced a strong increase in transmigration of wildtype cells. However, SFK-ko cells failed to cross the artificial BM. How exactly neutrophils cross the vascular BM is still a matter of debate, especially, whether the BM is permanently modified by extravasating neutrophils. To further address this, we conducted transwell assays as described above, coated with a combination of LN1 and PECAM-1/ICAM-1 and stimulated with CXCL1. We also used the same total cell number (2x10^5), but this time mixed SFK-ko x *Lyz2GFP* neutrophils and wildtype neutrophils in a 1:1 ratio (1x10^5 wildtype and 1x10^5 SFK-ko x *Lyz2GFP* neutrophils). In this manner, transmigrated SFK-ko neutrophils were identified by their GFP signal. Interestingly, in combination with wildtype neutrophils, SFK-ko neutrophils were able to overcome the BM to the same extent as wildtype cells, suggesting that wildtype neutrophils facilitate BM penetration by providing exit points for SFK-ko neutrophils (Figure 4A). To confirm these findings *in vivo*, we performed whole mount staining of TNFα-stimulated cremaster muscles for LN (green) to visualize the BM, and MRP14 (red) to visualize neutrophils, then analyzed the localization of neutrophils by confocal microscopy. In wildtype tissue, we were able to detect local areas of increased extravasation, which is in accordance with published literature, describing transmigration hotspots[28] (Figure 4B). In contrast, none of these spots could be found in cremaster muscle tissue of SFK-ko mice. MPR14-positive cells remained located within the vascular compartment and only few extravasated neutrophils could be detected, mainly remaining in close vicinity to the vessel (white arrows). Overall, SFK-ko neutrophils covered less distance away from the vessel wall when compared to wildtype neutrophils (8.0 μm *vs.* 17.3 μm, respectively) (*Online Supplementary Figure S2B*). These *in vivo* findings support our earlier *in vitro* findings that SFK are critical for neutrophils to cross the BM.

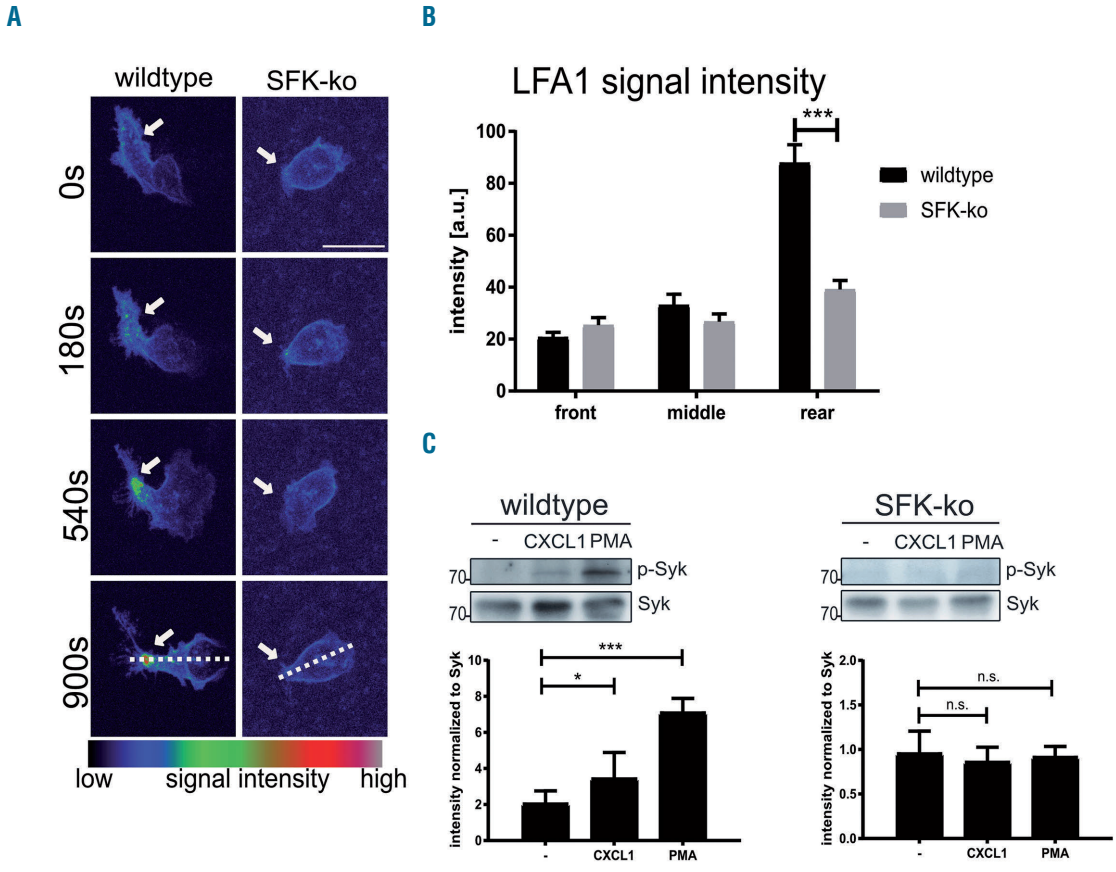

Figure 3. Defective LFA1 clustering and adhesion strengthening in Src family kinases (SFK)-knockout (ko) mice. Integrin downstream signaling was analyzed in isolated wildtype and SFK-knockout (ko) neutrophils. (A) *In vitro* integrin clustering experiments were performed using whole blood from wildtype and SFK-ko mice in flow chambers coated with E-Selectin/ICAM-1 and CXCL1. Blood samples were incubated with anti-LFA1-Alexa547 (2D7) to visualize LFA1 and crawling cells were analyzed for 15 minutes by confocal microscopy. LFA1 intensity is displayed at different time points. White arrows point to the uropod. Color code indicates signal intensity. Dashed lines are exemplary for drawn intensity profiles analyzed in (B) n=3 wildtype and 3 SFK-ko mice. Scale bar: 5 μm. (B) Mean signal intensities of an intensity profile of LFA1 signal, grouped into 3 regions: front, middle and rear of the neutrophil. (C-E) Western blot and respective quantitative analysis of Syk (Tyr519/520) (72kDa), Paxillin (Tyr118) (68kDa) and Cortactin (Tyr421) (80kDa) phosphorylation after CXCL1 and PMA stimulation in wildtype and SFK-ko neutrophils plated on ICAM1. Band intensity was normalized to respective total protein. All data are presented as mean± standard error of the mean (SEM). *P<0.05; ***P<0.001; n.s. : not significant (one-way ANOVA, Dunnett's multiple comparisons test). N=3 wildtype and 3 SFK-ko mice.

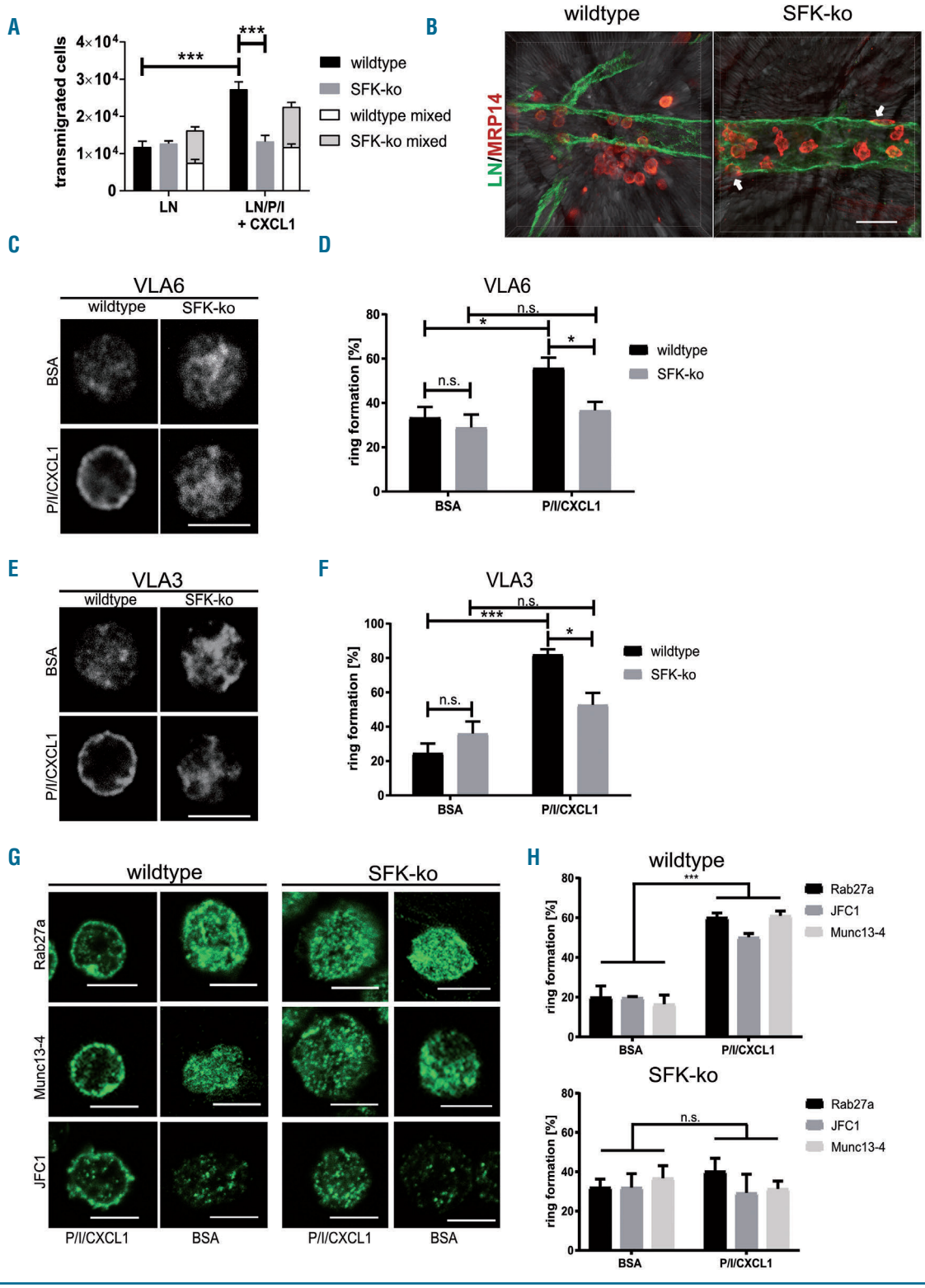

Figure 4. Rab27a dependent vesicle transfer is impaired in Src family kinases (SFK)-knockout (ko) neutrophils, leading to an impaired basement membrane penetration. (A) Neutrophil transmigration in a transwell assay with or without CXCL1 through filters coated with laminin (LN), or LN, PECAM-1, and ICAM-1 (LN/P/I). All data are presented as mean± standard error of the mean (SEM). *P<0.05; ***P<0.001; n.s. : not significant (two-way ANOVA, Sidak multiple comparison test). N=3 wildtype and 3 SFK-ko x *Lyz2GFP* mice, transwell assays were performed in duplicates. (B) Maximum projections of confocal microscopic images of venules in TNFα–stimulated cremaster muscle whole mounts from wildtype and SFK-ko mice. Basement membrane was visualized by anti-LN5 (green), neutrophils by anti-MRP14 (red). Surrounding muscle tissue was visualized by bright field microscopy. White arrows point at extravasated, but still attached neutrophils in SFK-ko tissue. Scale bar: 20 μm. (C) and (E) immunostaining of representative wildtype and SFK-ko neutrophils on BSA- or PECAM-1/ICAM-1/CXCL1–coated (P/I/CXCL1) coverslips for (C) VLA6 and (E) VLA3 analyzed by confocal microscopy. Scale bar: 10 μm. (D) and (F) Quantification of ring formation for VLA6 (D) and VLA3 (F). At least 80 cells from 3 wildtype and 3 SFK-ko mice were analyzed for each condition. (G) Immunostaining of representative wildtype and SFK-ko neutrophils on BSA- or PECAM-1/ICAM-1/CXCL1–coated coverslips for Rab27a (upper panel), Munc13-4 (middle panel), and JFC1 (lower panel). Scale bar is 5μm. (H) Quantification of ring formation for Rab27a, Munc13-4 and JFC1. At least 80 cells from 3 wildtype and 3 SFK-ko mice were analyzed for each condition. All data are presented as mean±SEM. *P<0.05; P<0.005; ***P<0.001; n.s. : not significant (two-way ANOVA, Sidak multiple comparison test).

Impaired vesicle transport in the absence of Src family kinase in neutrophils

We and others have previously shown that mobilization of vesicles containing VLA3 and VLA6 to the plasma membrane is an important process during vascular BM penetration.[3,4,6] To investigate whether SFK have a role in this process, we analyzed the SFK-dependent translocation of VLA6 and VLA3 to the plasma membrane of SFK-ko and wildtype neutrophils. Bone marrow derived neutrophils of SFK-ko and wildtype mice were plated on BSA or, again, on a combination of PECAM-1/ICAM-1 and CXCL1 and subsequently stained for VLA6 or VLA3. Plasma membrane translocation was visualized by confocal microscopy as "ring formation" (Figure 4C and E). We observed fewer SFK-ko cells (37%) displaying a ring of VLA6, when plated on PECAM-1/ICAM-1/CXCL1 compared to wildtype (55%) (Figure 4D). This observation was also true for VLA3, where only 52% of SFK-deficient neutrophils showed vesicle translocation, compared to 82% of wildtype cells (Figure 4F). To test whether ring formation can also be observed *in vivo*, whole mount cremaster muscle stainings were conducted for VLA6, which revealed a similar trend as *in vitro*. In wildtype whole mounts, extravasated neutrophils displayed a ring-like staining for VLA6, while intravascular neutrophils showed only a diffuse signal. In SFK-ko whole mounts, intravascular and extravasated cells showed no clear peripheral staining (*Online Supplementary Figure S2C*). Next, we plated wildtype neutrophils on BSA or PECAM-1/ICAM-1/CXCL1 and stained for SFK. Confocal micrographs revealed diffuse intracellular SFK staining when cells were plated on BSA (*Online Supplementary Figure S2D*). Upon stimulation with PECAM-1/ICAM-1/CXCL1, we observed a clear SFK signal at the cell border. Again, we quantified SFK distribution and observed a pronounced SFK translocation to the cell periphery when neutrophils were plated on PECAM-1/ICAM-1/CXCL1 (*Online Supplementary Figure S2E*). These experiments support a critical role for SFK by strongly interfering in vesicle trafficking of neutrophils *in vitro* and *in vivo*.

Src family kinase regulate Rab27a-dependent vesicle translocation

Vesicle trafficking in neutrophils is mainly regulated by Rab27a GTPases and their corresponding effector proteins. In neutrophils, Rab27a works in collaboration with two of its known effectors, JFC1 and Munc13-4, on vesicle trafficking and exocytosis of secretory vesicles and azurophilic granules.[8] We analyzed the translocation of Rab27a, JFC1 and Munc13-4 to the cell periphery upon PECAM-1/ICAM-1/CXCL1 stimulation as described above. In wildtype neutrophils, stimulation resulted in translocation of Rab27a and its effectors (Figure 4G). While 60% of wildtype neutrophils displayed a ring-like structure, only 40.1% showed Rab27a translocation in SFK-ko neutrophils (Figure 4H). Similarly, staining for JFC1 (50.1% *vs.* 29.2%) and Munc13-4 (60.9% *vs.* 31.3%) revealed an equal trend for wildtype *vs.* SFK-ko neutrophils, respectively. Taken together, these experiments show a clear SFK-dependent activation of the secretory machinery in neutrophils.

NE-dependent laminin degradation is defective in Src family kinase-ko neutrophils

Neutrophil extravasation is not only dependent on the translocation of LN binding β1 integrins, but also on the serine proteinase neutrophil elastase (NE).[5,29] We first analyzed the localization of NE in neutrophils plated on either BSA or PECAM-1/ICAM-1/CXCL1 as described above (Figure 5A). Similar to VLA3 and VLA6, we observed an increase in ring formation from 21.9% in BSA stimulated wildtype neutrophils to 59.1% of wildtype neutrophils stimulated on PECAM-1/ICAM-1/CXCL1 (Figure 5B). This upregulation of vesicle translocation was absent in SFK-ko neutrophils (20.0% for BSA *vs.* 31.2% for PECAM-1/ICAM-1/CXCL1 coating). In neutrophils, NE is stored in azurophilic granules together with a variety of other proteinases and antimicrobial proteins such as myeloperoxidase (MPO). Neutrophils release MPO after stimulation with TNFα.[30,31] Thus, we additionally quantified MPO release in the serum of SFK-ko and wildtype mice by ELISA 2 h after TNFα stimulation. While we did not observe upregulation of MPO in the serum of SFK-ko mice 2 h after TNFα stimulation (158.4 ng/mL before *vs.* 184.0 ng/mL after TNFα stimulation) (Figure 5C), MPO levels were markedly increased in the serum of TNFα stimulated wildtype mice (113.0 ng/mL before *vs.* 473.5 ng/mL after TNFα stimulation). This indicates that SFK are required for the release of azurophilic granule content including NE and MPO. Earlier studies revealed that NE is able to proteolytically cleave laminins. In addition, NE activates different matrix metalloproteinases (MMP) that are involved in matrix degradation.[32-34] However, the relevance of these NE functions for neutrophil transmigration are still not completely understood. By applying a NE-fluorescent activatable substrate (NE680FAST) in postcapillary venules with or without TNFα stimulation we were able to investigate NE activity in wildtype and SFK-ko cremaster whole mounts. Compared to unstimulated controls, TNFα stimulation led to a robust NE activity signal in wildtype mice (Figure 5D). As expected, this activity was reduced in SFK-ko venules, indicating that there is reduced NE dependent substrate cleavage in the absence of SFK (Figure 5D).

Next, we investigated whether wildtype neutrophils are able to degrade BM constituents under *in vitro* conditions. To this end, we performed transwell experiments in a system that allows us to image neutrophil crawling and extravasation by spinning disc confocal microscopy. Neutrophils from wildtype and SFK-ko mice were isolated and stained with different cell trackers (CellTracker™ Red CMTPX Dye and CellTracker™ Green CMFDA Dye,) to image both neutrophil populations in one transmigration chamber. In addition, laminin was visualized with an Alexa-647 coupled antibody. We observed intensive degradation of LN by wildtype neutrophils only, which could be identified by the disappearance of fluorescently labeled LN over time (Figure 5E, *Online Supplementary Figure S3A and Online Supplementary Mov3*). When we used SFK-ko neutrophils only, no degradation of LN was observed (*Online Supplementary Figure S3B*). Interestingly we found that SFK-ko neutrophils, which were unable to digest the LN layer, migrated strongly towards wildtype neutrophils during the observation period (Figure 5F and G and *Online Supplementary Mov4*). We quantified this association of SFK-ko neutrophils around wildtype cells in a randomization approach. Here, the interaction strength is a measure of the degree of dependence of spatial distribution between wildtype and SFK-ko neutrophils. We observed an interaction strength of 5.1 after 1,000 seconds

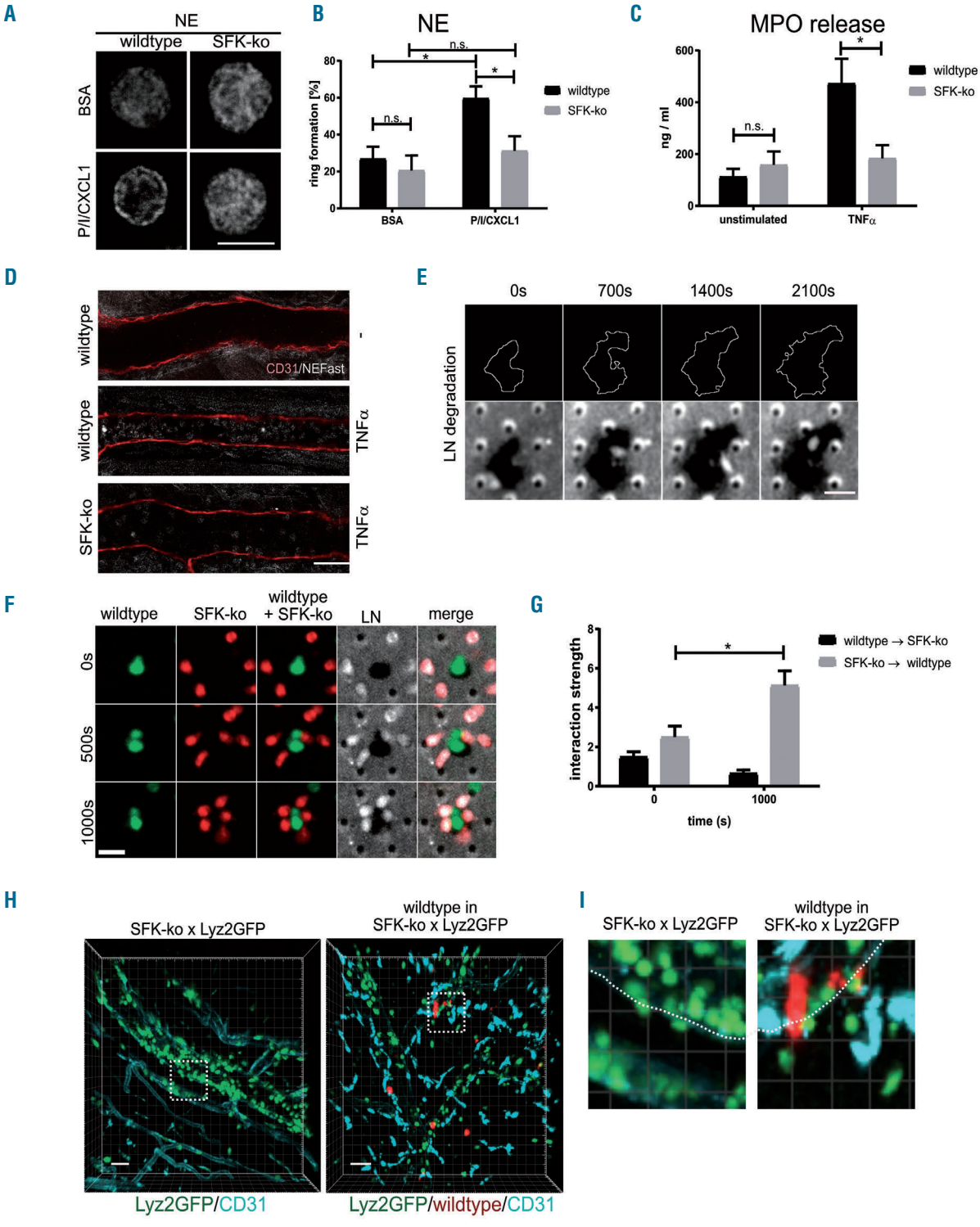

Figure 5. Src family kinases (SFK)-dependent neutrophil elastase (NE) translocation is critical for degradation of the basement membrane. (A) Immunostaining of representative wildtype and SFK-knockout (ko) neutrophils on BSA- or PECAM-1/ICAM-1/CXCL1–coated (P/I/CXCL1) coverslips for NE analyzed by confocal microscopy. Scale bar: 10 μm. N=3 wildtype and 3 SFK-ko mice. (B) Quantification of ring formation for NE. At least 80 cells from 3 wildtype and 3 SFK-ko mice were analyzed. All data are presented as mean± standard error of the mean (SEM). *P<0.05; ***P<0.001; n.s. : not significant (two-way ANOVA, Sidak multiple comparison test). (C) Quantitative analysis for myeloidperoxidase (MPO) release in blood plasma samples from wildtype and SFK-ko mice 2 hours after TNFα injection by quantitative ELISA assay; 3 wildtype and 3 SFK-ko mice were analyzed. All data are presented as mean±SEM. *P<0.05; **P<0.005; ***P<0.001; n.s. : not significant. (D) NE activity (white) within cremaster muscle venules without (upper image) or with TNFα middle and lower image) stimulation from wildtype and SFK-ko mice imaged by confocal microscopy. Venules were visualized using a CD31 antibody (red) (n=3 mice per group). Scale bar: 40 μm (E) Spinning disk confocal micrographs of LN degradation (indicated by black areas compared to white LN staining) by wildtype neutrophils at indicated time points (Lower panels). White lines outline the increase in degradation area over time (Upper panels). Scale bar: 10 μm. (F) Spinning disk confocal micrographs of wildtype (green) and SFK-ko (red) neutrophils plated on antibody-labeled LN (white) at indicated time points. Scale bar: 10 μm. (G) Randomization approach to test for wildtype/SFK-ko interaction strength during migration using the nearest-neighbor analysis. (H) Multi photon microscopy of TNFα-stimulated SFK-ko x *Lyz2GFP* or SFK-ko x *Lyz2GFP* mice with 1x10^7 injected deep red labeled wildtype neutrophils. Venules were visualized using a CD31 antibody (turquoise). Dotted squares indicate areas of interest (see panel I) (n=4 mice per group). Scale bar: 30 μm. (I) Close-up of vessel wall of SFK-ko x Lyz2^{GFP} or SFK-ko x Lyz2^{GFP} mice with 1x10^7 injected deep red labeled wildtype neutrophils.

of observation (*Online Supplementary Figure S3C and D*), indicating that this accumulation is not random, but highly dependent. These experiments strongly support the concept of SFK-dependent BM degradation by extravasating wildtype neutrophils. In addition, our results indicate that LN degradation fragments might exert chemotactic activity.

To finally show that these *in vitro* findings are also relevant under *in vivo* conditions, we injected labeled (CellTracker™ Deep Red Dye) SFK-ko or wildtype neutrophils into Lyz2^{GFP} or SFK-ko x Lyz2^{GFP} mice, respectively, and observed neutrophil behavior using multi-photon microscopy of the mouse cremaster muscle vasculature. Compared to SFK-ko x Lyz2^{GFP} mice, where neutrophils accumulated in the vessel or were stuck to the abluminal side, we observed strongly elevated numbers of extravasated neutrophils in the periphery, when wildtype neutrophils were present (Figure 5H and *Online Supplementary Mov5 and 6*). Additionally, we were able to visualize SFK-ko x Lyz2^{GFP} neutrophils accumulating around adherent wildtype cells, confirming the observed behavior of SFK-ko neutrophils in the *in vitro* setting (Figure 5I). Also, in the experiment in which we inverted the procedure, by injecting fluorescently labeled SFK-ko neutrophils into Lyz2^{GFP} mice, we could observe extravasated SFK-ko neutrophils (*Online Supplementary Figure S3E and Online Supplementary Mov7 and 8*). These experiments strengthen the concept of wildtype neutrophils creating a path through the BM which enables SFK-ko neutrophils to extravasate into inflamed tissue *in vivo*.

Discussion

Integrin outside-in signaling is critical for neutrophil firm adhesion to and extravasation through the vessel wall into inflamed tissue. The short intracellular integrin tail has no enzymatic activity and acts exclusively as a binding site for recruited proteins, which, in turn, activate a broad range of pathways, spanning from cytoskeletal rearrangements and integrin clustering to vesicle trafficking. It has been widely accepted that tyrosine phosphorylation of ITAM motives by members of the Src family kinases is one way of integrin outside-in signaling.[35] Therefore, SFK triple knockout mice (*Hck$^{-/-}$Fgr$^{-/-}$Lyn$^{-/-}$*, here named SFK-ko) have been used to study the function of these kinases in neutrophils in an *in vivo* model of acute inflammation. Interestingly, *Hck$^{-/-}$Fgr$^{-/-}$* neutrophils displayed no adhesion defect in earlier static adhesion experiments on ICAM-1,[13,36] while our findings show a dramatic decrease in neutrophil adhesion efficiency in inflamed cremaster muscle venules *in vivo* implying that SFK-dependent neutrophil adhesion is sensitive to shear stress. We also found that neutrophil extravasation in SFK-deficient mice was dramatically decreased when compared to wildtype mice, which was caused by an SFK-dependent intrinsic extravasation defect. This observation is in line with various reports in different inflammation models with SFK-ko mice[14,15,21] where decreased numbers of neutrophils were observed. Lowell *et al*. linked low PMN numbers in the liver during endotoxemia to a failure of *Hck$^{-/-}$Fgr$^{-/-}$* neutrophils to rearrange their actin cytoskeleton, while cytokine production was unchanged. We clearly demonstrate that in the absence of SFK, neutrophils are unable to strongly adhere to the substrate under flow and detach *in vitro* and *in vivo*, due to defective LFA1 clustering and poor adhesion strengthening. The application of the tyrosine inhibitor Dasatinib led to a comparable shear rate dependent decrease in adherent neutrophils in inflamed venules *in vivo*. This strengthens previous findings of an improved outcome during sepsis after Dasatinib application, where leukocyte infiltration into the inflamed peritoneum was reduced in a dose-dependent manner.[21] Interestingly, most *in vitro* studies were performed under steady state conditions, where integrin clustering and crawling were unaffected in SFK deficient leukocytes,[15,37] neglecting the impact of shear stress on neutrophil adhesion. This phenomenon was previously observed in WASP- and mAbp1-deficient mice, where integrin clustering and migration defects only arose when neutrophils were analyzed under shear stress.[38,39] Our study demonstrates that neutrophil adhesion strengthening under flow conditions is dependent on SFK which mediate clustering of integrins, the rearrangement of the actin cytoskeleton along with polarization of the cell.[40] Several cytoskeleton associated proteins required for adhesion are reported phosphorylation targets of SFK (directly or indirectly via Syk) like Paxillin and Cortactin.[41-43] Here we clearly show reduced phosphorylation of these adhesion-relevant proteins.

We also aimed to answer the question as to whether SFK are required for the extravasation process beyond the endothelial layer. It was suggested that leukocytes predominantly cross the vascular BM at LN low expression regions (LER),[44] and recent publications, including those from our lab, showed that neutrophils need to translocate vesicles containing VLA3, VLA6 and NE to their surface in a MST1-Rab27a dependent manner in order to overcome the BM.[3-6,45,46] Our results identify for the first time SFK to be an additional critical component of this process. We show that SFK-ko neutrophils fail to pass an artificial LN barrier, and even when stimulated with PECAM-1 and ICAM-1, SFK-ko neutrophils are unable to release azurophilic granules and translocate integrin containing secretory vesicles. Exocytosis and vesicle transfer in neutrophils is strongly regulated by the GTPase Rab27a and its two effectors JFC1 and Munc13-4.[8,47] We demonstrate that PECAM-1/ICAM-1 and CXCL1 stimulation facilitates the translocation of all three proteins to the membrane of wildtype neutrophils, suggesting that SFK regulate vesicle transport in a Rab27a-dependent manner. How MST1 and SFK co-operate in this process is still unclear and needs further investigation. Of note, MPO release was not defective in MST1 deficient neutrophils (*M Sperandio, 2019, unpublished data/personal communication*) compared to SFK-ko neutrophils, where a marked impairment in MPO release could be observed, suggesting that SFK are involved in neutrophil vesicle trafficking independently of MST1.

The role of NE during neutrophil extravasation is still controversial, as is the role of BM degradation by elastases or MMP.[5,48-52] However, recent findings suggest that this might, at least in part, be related to the experimental model used. Reichel *et al*. could clearly demonstrate decreased extravasation into inflamed cremaster muscle tissue after blockage of gelatinases by the specific inhibitor MMP-2/-9 inhibitor III.[53] Furthermore, Young *et al*. were able to show NE-dependent extravasation using the same model.[29] It was also suggested that NE/MMP-

dependent LN degradation creates peptides that are chemoattractant for neutrophils.[33] In line with these findings, we were able to show diminished LN degradation by SFK-ko neutrophils *in vitro* using spinning disk confocal microscopy. Surprisingly, we observed that SFK-ko neutrophils, which are unable to degrade the LN barrier themselves, arrange around wildtype neutrophils, strongly supporting the hypothesis of the chemoattractant function of LN-fragments. Although our data seem to partly contrast with the study by Kovács *et al.*, in which no intrinsic neutrophil migration defect was observed in the genetic absence of SFK,[15] we propose that this is due to the different models used. It is also likely that the rescued extravasation into the synovial joint in their mixed chimeric mice (50% SFK-ko, 50% wildtype neutrophils) is in part due to restored NE or protease secretion and subsequent BM degradation by wildtype neutrophils.

Taken together, we have demonstrated a critical role for SFK in various steps along the neutrophil adhesion cascade during acute inflammation. While its effect on adhesion strengthening is the direct consequence of its prominent role directly downstream of integrin ligation and signaling, the regulation of vesicle trafficking during neutrophil extravasation is unexpected and provides new insights on the extravasation process through the vascular BM, supporting the concept of neutrophil-mediated vascular BM digestion along this route.

Acknowledgments

The authors would like to thank Susanne Bierschenk and Nadine Schmidt for their excellent technical assistance, as well as Andreas Thomae and Steffen Dietzel (Core Facility BioImaging, BioMedical Center, Ludwig-Maximilians-Universität München) for their help with confocal and multi-photon microscopy. The authors thank Thomas Graf for providing the Lyz2^{GFP} mice.

Funding

This work was supported by grants from the European Community's Seventh Framework Programme (FP7-2007-2013) under grant agreement HEALTH-F4-2011-282095 (TARKINAID to MS and AM), Deutsche Forschungsgemeinschaft (SFB 914, project B01 [MS], Z03 [MS]) and the Else Kröner-Fresenius-Stiftung (grant 2015_A68 [IR]).

References

1. Ley K, Laudanna C, Cybulsky MI, Nourshargh S. Getting to the site of inflammation: the leukocyte adhesion cascade updated. Nat Rev Immunol. 2007;7(9):678-689.
2. Sperandio M, Gleissner CA, Ley K. Glycosylation in immune cell trafficking. Immunol Rev. 2009;230(1):97-113.
3. Hyun Y-M, Sumagin R, Sarangi PP, et al. Uropod elongation is a common final step in leukocyte extravasation through inflamed vessels. J Exp Med. 2012;209(7):1349-1362.
4. Dangerfield JP, Wang S, Nourshargh S. Blockade of α6 integrin inhibits IL-1-β but not TNF-α-induced neutrophil transmigration in vivo. J Leukoc Biol. 2005;77:159-165.
5. Wang S, Dangerfield JP, Young RE, Nourshargh S. PECAM-1, alpha6 integrins and neutrophil elastase cooperate in mediating neutrophil transmigration. J Cell Sci. 2005;118(Pt 9):2067-2076.
6. Kurz ARM, Pruenster M, Rohwedder I, et al. MST1-dependent vesicle trafficking regulates neutrophil transmigration through the vascular basement membrane. J Clin Invest. 2016;126(11):4125-4139.
7. Catz SD. The role of Rab27a in the regulation of neutrophil function. Cell Microbiol. 2014;16(9):1301-1310.
8. Brzezinska AA, Johnson JL, Munafo DB, et al. The Rab27a effectors JFC1/Slp1 and munc13-4 regulate exocytosis of neutrophil granules. Traffic. 2008;9(12):2151-2164.
9. Thomas SM, Brugge JS. Cellular Functions Regulated By Src Family Kinases. Annu Rev Cell Dev Biol. 1997;13(1):513-609.
10. Lowell CA. Inhibitory Pathways in Innate Immune Cells : Signaling Cross Talk. Cold Spring Harb Perspect Biol. 2011;1-16.
11. Futosi K, Mócsai A. Tyrosine kinase signaling pathways in neutrophils. Immunol Rev. 2016;273(1):121-139.
12. Zarbock A, Abram CL, Hundt M, Altman A, Lowell CA, Ley K. PSGL-1 engagement by E-selectin signals through Src kinase Fgr and ITAM adapters DAP12 and FcR gamma to induce slow leukocyte rolling. J Exp Med. 2008;205(10):2339-2347.
13. Lowell CA, Fumagalli L, Berton G. Deficiency of src family kinases p59/61hck and p58c-fgr results in defective adhesion-dependent neutrophil functions. J Cell Biol. 1996;133(4):895-910.
14. Lowell CA, Berton G. Resistance to endotoxic shock and reduced neutrophil migration in mice deficient for the Src-family kinases Hck and Fgr. Proc Natl Acad Sci U S A. 1998;95(13):7580-7584.
15. Kovács M, Németh T, Jakus Z, et al. The Src family kinases Hck, Fgr, and Lyn are critical for the generation of the in vivo inflammatory environment without a direct role in leukocyte recruitment. J Exp Med. 2014;211(10):1993-2011.
16. Faust N, Varas F, Kelly LM, Heck S, Graf T. Insertion of enhanced green fluorescent protein into the lysozyme gene creates mice with green fluorescent granulocytes and macrophages. Blood. 2000;96(2):719-726.
17. Lowell CA, Soriano P, Varmus HE. Functional overlap in the src gene family: Inactivation of hck and fgr impairs natural immunity. Genes Dev. 1994;8(4):387-398.
18. Chan VWF, Meng F, Soriano P, DeFranco AL, Lowell CA. Characterization of the B lymphocyte populations in lyn-deficient mice and the role of lyn in signal initiation and down-regulation. Immunity. 1997;7(1):69-81.
19. Pruenster M, Kurz ARM, Chung K-J, et al. Extracellular MRP8/14 is a regulator of β2 integrin-dependent neutrophil slow rolling and adhesion. Nat Commun. 2015;6:6915.
20. Ley K, Zarbock A. Hold on to Your Endothelium: Postarrest Steps of the Leukocyte Adhesion Cascade. Immunity. 2006;25(2):185-187.
21. Gonçalves-de-Albuquerque CF, Rohwedder I, Silva AR, et al. The Yin and Yang of tyrosine kinase inhibition during experimental polymicrobial sepsis. Front Immunol. 2018;9:901.
22. Abram CL, Lowell CA. The ins and outs of leukocyte integrin signaling. Annu Rev Immunol. 2011;27339-27362.
23. Yamada KM GB. Molecular interactions in cell adhesion complexes. Curr Opin Cell Biol. 1997;9(1):76-85.
24. Fernandez R, Suchard SJ. Syk activation is required for spreading and H2O2 release in adherent human neutrophils. J Immunol. 1998;160(10):5154-5162.
25. Gallet C, Rosa JP, Habib A, Lebret M, Lévy-Tolédano S, Maclouf J. Tyrosine phosphorylation of cortactin associated with Syk accompanies thromboxane analogue-induced platelet shape change. J Biol Chem. 1999;274(33):23610-23616.
26. Deakin NO, Turner CE. Paxillin comes of age. J Cell Sci. 2008;121(15):2435-2444.
27. Fuortes M, Jin WW, Nathan C. β2 Integrin-dependent tyrosine phosphorylation of paxillin in human neutrophils treated with tumor necrosis factor. J Cell Biol. 1994;127(5):1477-1483.
28. Wang S, Voisin M-B, Larbi KY, et al. Venular basement membranes contain specific matrix protein low expression regions that act as exit points for emigrating neutrophils. J Exp Med. 2006;203(6):1519-1532.
29. Young RE, Voisin MB, Wang S, Dangerfield J, Nourshargh S. Role of neutrophil elastase in LTB 4-induced neutrophil transmigration in vivo assessed with a specific inhibitor and neutrophil elastase deficient mice. Br J Pharmacol. 2007;151(5):628-637.
30. Burt HM, Jackson JK. The priming action of tumour necrosis factor-alpha (TNF-α) and granulocyte-macrophage colony-stimulating factor (GM-CSF) on neutrophils activated by inflammatory microcrystals. Clin Exp Immunol. 1997;108(3):432-437.
31. Brandt E, Petersen F, Flad HD. Recombinant tumor necrosis factor-alpha potentiates neutrophil degranulation in response to host defense cytokines neutrophil-activating peptide 2 and IL-8 by modulating intracellular cyclic AMP levels. J Immunol. 1992;149(4):1356-1364.
32. Okada Y and Nakanishi I. Activation of matrix metallorproteinase 3 (stromelysin)

and matrix metalloproteinase 2 (gelatinase) by human neutrophil elastase and cathepsin G. FEBS Lett. 1989;249(2):353-356.
33. Mydel P, Shipley JM, Adair-Kirk TL, et al. Neutrophil elastase cleaves laminin-332 (laminin-5) generating peptides that are chemotactic for neutrophils. J Biol Chem. 2008;283(15):9513-9522.
34. Ferry G, Lonchampt M, Pennel L, De Nanteuil G, Canet E, Tucker GC. Activation of MMP-9 by neutrophil elastase in an in vivo model of acute lung injury. FEBS Lett. 1997;402(2-3):111-115.
35. Zarbock A, Lowell CA, Ley K. Syk signaling is necessary for E-selectin-induced LFA-1-ICAM-1 association and rolling but not arrest. Immunity. 2007;26(6):773-783.
36. Mócsai A, Ligeti E, Lowell CA, Berton G. Adhesion-dependent degranulation of neutrophils requires the Src family kinases Fgr and Hck. J Immunol. 1999;162(2):1120-1126.
37. Giagulli C, Ottoboni L, Caveggion E, et al. The Src family Kinases Hck and Fgr are dispensable for inside-out, chemoattractant-induced signaling Regulating β2 Integrin affinity and valency in neutrophils, but are required for β2 integrin-mediated outside-in signaling involved in sustained adhesion. J Immunol. 2006;177(1):604-611.
38. Zhang H, Schaff UY, Green CE, et al. Impaired integrin-dependent Function in Wiskott-Aldrich syndrome protein-deficient murine and human neutrophils. Immunity. 2006;25(2):285-295.
39. Schymeinsky J, Gerstl R, Mannigel I, et al. A fundamental role of mAbp1 in neutrophils : impact on β2 integrin – mediated phagocytosis and adhesion in vivo. Blood. 2009; 114(19):4209-4221.
40. Begandt D, Thome S, Sperandio M, Walzog B. How neutrophils resist shear stress at blood vessel walls: molecular mechanisms, subcellular structures, and cell–cell interactions. J Leukoc Biol. 2017;102(3):699-709.
41. Suen PW, Ilic D, Caveggion E, Berton G, Damsky CH, Lowell CA. Impaired integrin-mediated signal transduction, altered cytoskeletal structure and reduced motility in Hck/Fgr deficient macrophages. J Cell Sci. 1999;112:4067-4078.
42. Mócsai A, Zhou M, Meng F, Tybulewicz VL, Lowell CA. Syk is required for integrin signaling in neutrophils. Immunity. 2002; 16(4):547-558.
43. Fumagalli L, Zhang H, Baruzzi A, Lowell CA, Berton G. The Src family kinases Hck and Fgr regulate neutrophil responses to N-formyl-methionyl-leucyl-phenylalanine. J Immunol. 2007;178(6):3874-3885.
44. Voisin MB, Pröbstl D, Nourshargh S. Venular basement membranes ubiquitously express matrix protein low-expression regions: characterization in multiple tissues and remodeling during inflammation. Am J Pathol. 2010;176(1):482-495.
45. Lerman YV, Lim K, Hyun YM, et al. Sepsis lethality via exacerbated tissue infiltration and TLR-induced cytokine production by neutrophils is integrin α3β1-dependent. Blood. 2014;124(24):3515-3523.
46. Dangerfield J, Larbi KY, Huang M-T, Dewar A, Nourshargh S. PECAM-1 (CD31) Homophilic interaction up-regulates α6β1 on transmigrated neutrophils in vivo and plays a functional role in the ability of α6 Integrins to mediate leukocyte migration through the perivascular basement membrane. J Exp Med. 2002;196(9):1201-1212.
47. Munafó DB, Johnson JL, Ellis BA, Rutschmann S, Beutler B, Catz SD. Rab27a is a key component of the secretory machinery of azurophilic granules in granulocytes. Biochem J. 2007;402(2):229-239.
48. Young RE, Thompson RD, Larbi KY, et al. Neutrophil elastase (NE)-deficient mice demonstrate a nonredundant role for NE in neutrophil migration, generation of proinflammatory mediators, and phagocytosis in response to zymosan particles in vivo. J Immunol. 2004;172(7):4493-4502.
49. Sorokin L. The impact of the extracellular matrix on inflammation. Nat Rev Immunol. 2010;10(10):712-723.
50. Delacourt C, Hérigault S, Delclaux C, et al. Protection against acute lung injury by intravenous or intratracheal pretreatment with EPI-HNE-4, a new potent neutrophil elastase inhibitor. Am J Respir Cell Mol Biol. 2002; 26(3):290-297.
51. Hirche TO, Atkinson JJ, Bahr S, Belaaouaj A. Deficiency in neutrophil elastase does not impair neutrophil recruitment to inflamed sites. Am J Respir Cell Mol Biol. 2004; 30(4):576-584.
52. Huber AR, Weiss SJ. Disruption of the subendothelial basement membrane during neutrophil diapedesis in an in vitro construct of a blood vessel wall. J Clin Invest. 1989; 83(4):1122-1136.
53. Reichel CA, Rehberg M, Bihari P, et al. Gelatinases mediate neutrophil recruitment in vivo: evidence for stimulus specificity and a critical role in collagen IV remodeling. J Leukoc Biol. 2008;83(4):864-874.

ARTICLE

Transforming activities of the *NUP98-KMT2A* fusion gene associated with myelodysplasia and acute myeloid leukemia

James N. Fisher,[1,2*] Angeliki Thanasopoulou,[1,2*] Sabine Juge,[1,2] Alexandar Tzankov,[3] Frederik O. Bagger,[1,2] Max A. Mendez,[1,2] Antoine H.F.M. Peters[4,5] and Juerg Schwaller[1,2]

[1]University Children's Hospital Basel (UKBB); [2]Department of Biomedicine, University of Basel; [3]Institute for Pathology, University of Basel; [4]Faculty of Sciences, University of Basel and [5]Friedrich Miescher Institute for Biomedical Research, Basel, Switzerland

**JNF and ATh contributed equally as co-first authors.*

Ferrata Storti Foundation

Haematologica 2020
Volume 105(7):1857-1867

ABSTRACT

Inv(11)(p15q23), found in myelodysplastic syndromes and acute myeloid leukemia, leads to expression of a fusion protein consisting of the N-terminal of nucleoporin 98 (NUP98) and the majority of the lysine methyltransferase 2A (KMT2A). To explore the transforming potential of this fusion we established inducible iNUP98-KMT2A transgenic mice. After a median latency of 80 weeks, over 90% of these mice developed signs of disease, with anemia and reduced bone marrow cellularity, increased white blood cell numbers, extramedullary hematopoiesis, and multilineage dysplasia. Additionally, induction of *iNUP98-KMT2A* led to elevated lineage marker-negative Sca-1$^+$ c-Kit$^+$ cell numbers in the bone marrow, which outcompeted wildtype cells in repopulation assays. Six *iNUP98-KMT2A* mice developed transplantable acute myeloid leukemia with leukemic blasts infiltrating multiple organs. Notably, as reported for patients, iNUP98-KMT2A leukemic blasts did not express increased levels of the *HoxA-B-C* gene cluster, and in contrast to KMT2A-AF9 leukemic cells, the cells were resistant to pharmacological targeting of menin and BET family proteins by MI-2-2 or JQ1, respectively. Expression of *iNUP98-KMT2A* in mouse embryonic fibroblasts led to an accumulation of cells in G1 phase, and abrogated replicative senescence. In bone marrow-derived hematopoietic progenitors, iNUP98-KMT2A expression similarly resulted in increased cell numbers in the G1 phase of the cell cycle, with aberrant gene expression of *Sirt1*, *Tert*, *Rbl2*, *Twist1*, *Vim*, and *Prkcd*, mimicking that seen in mouse embryonic fibroblasts. In summary, we demonstrate that *iNUP98-KMT2A* has *in vivo* transforming activity and interferes with cell cycle progression rather than primarily blocking differentiation.

Introduction

The gene encoding the 98 kDa nuclear pore protein (NUP98) is recurrently involved in chromosomal translocations associated with various hematologic malignancies. Most of these translocations result in the expression of fusion genes comprising the N-terminal phenylalanine-glycine (FG)-repeats of *NUP98* fused to a large group of different partners of which the homeobox family of transcription factors (such as *HOXA9* or *HOXD13*) or non-homeobox epigenetic regulators are a part.[1,2] Like *NUP98*, the lysine methyltransferase *KMT2A*, also referred to as "mixed lineage leukemia" (*MLL*) gene, encoding for a SET-domain histone H3K4 methyltransferase is a recurrent target of leukemia-associated chromosomal rearrangements. These generally lead to expression of fusion transcripts that contain the amino-terminal moiety of *KMT2A* fused to different partners, of which *AF4*, *AF9*, *ENL* and *AF10* are among the most prevalent of the currently more than 70 known.[3,4] Several *KMT2A* fusions have been shown to be hematopoietic oncogenes, which phenocopy the disease *in vivo* when expressed in murine bone mar-

Correspondence:

JUERG SCHWALLER
j.schwaller@unibas.ch

Received: March 1, 2019.

Accepted: September 24, 2019.

Pre-published: September 26, 2019.

doi:10.3324/haematol.2019.219188

Check the online version for the most updated information on this article, online supplements, and information on authorship & disclosures: www.haematologica.org/content/105/7/1857

row (BM).[3-6] In cases in which these fusions do not contain the KMT2A-SET (suppressor of variegation 3–9, enhancer of zeste, and trithorax) domain, they acquire H3K79 or H4R3 histone methyltransferase- or acetyltransferase activity through interactions with several co-factors.[5,6] The interaction between chromatin and KMT2A fusions, mediated by the N-terminal menin- and the LEDGF (lens epithelium-derived growth factor) binding domain, has been shown to be crucial for maintenance of the leukemic phenotype.[7-10] Exploration of the KMT2A-menin-LEDGF interaction triad has led to the development of a series of promising small molecules with potent antileukemic activity.[11,12] More recent studies have proposed physical interactions between NUP98, and NUP98 fusion proteins, with KMT2A and non-specific lethal histone-modifying protein complexes. Parallel genetic studies using mouse models suggested that NUP98-fusion gene driven leukemogenesis might be dependent on KMT2A function.[13-15]

Inv(11)(p15q23) has been reported as the sole chromosomal abnormality in patients with several hematologic malignancies including myelodysplastic syndromes (MDS) and acute myeloid leukemia (AML);[16-20] however, to date NUP98-KMT2A fusion expression has only been reported in two patients with AML.[19] Using fluorescent *in situ* hybridization and reverse transcription quantitative polymerase chain reaction (PCR), Kaltenbach *et al.* found that inv(11)(p15q23) leads to fusion of the *NUP98-FG*-repeats to almost the entire *KMT2A* open reading frame (ORF).[19] In this case, exon 1 encoding for the N-terminal menin-LEDGF interaction domain is lost. In contrast to other KMT2A- or NUP98-fusion associated diseases, NUP98-KMT2A$^+$ leukemic blasts did not express known KMT2A targets such as the *HOXA*-gene cluster (*HOXA5*, *HOXA7*, *HOXA9*, or *HOXA10*) suggesting alternative mechanisms of transformation. As the size of the *NUP98-KMT2A* fusion ORF (>12 kb) limits the ability to test its transforming activity by retroviral expression in BM cells, we generated an inducible transgenic mouse model. We found that *iNUP98-KMT2A* expression led to a symptomatic[21] hematologic disease mimicking human MDS or AML that, as in patients, was not associated with elevated expression of the *Hox-A-B-C* gene cluster.[19] Thus, our work formally proves that a fusion, in which the N-terminus of *KMT2A* is replaced by the FG-repeats of *NUP98*, is a leukemogenic oncogene.

Methods

Primary induction of iNUP98-KMT2A expression

Adult transgenic mice were provided with doxycycline-impregnated chow pellets (400 ppm Doxycycline Diet, Harlan-Teklad) *ad libitum* from 6-8 weeks of age until analysis. All experiments were conducted in compliance with Swiss animal welfare laws and were approved by the Swiss Cantonal Veterinary Office of Basel Stadt.

Flow cytometry, colony-forming assays and cell culture

Total BM cells were isolated from wildtype (WT) C57BL/6 and *iNUP98-KMT2A* mice and processed with the Direct Lineage Cell Depletion kit (Miltenyi Biotec, Bergisch Gladbach, Germany). For immunophenotypic analysis, cells were incubated with antibodies recognizing the mouse lineage markers: CD11b (Mac-1), Ly-6G (Gr-1), CD117 (c-Kit), FcγRII/III, Ter119, CD71, B220, CD3, and CD34. For lineage marker-negative Sca-1$^+$ c-Kit$^+$ (LSK) characterization, lineage marker negative (Lin$^-$) BM cells were stained with Ly-6A/E (Sca-1), c-Kit, CD150 (SLAM1) and CD48, as well as CD45.1 and CD45.2 antibodies.

For proliferation experiments, 1x10^5 Lin$^-$ BM cells were cultured in liquid media containing murine stem cell factor (100 ng/mL), murine interleukin 3 (6 ng/mL), human interleukin 6 (10 ng/mL) and doxycycline (1 μg/mL). For colony-forming assays, 5x10^3 Lin$^-$ cells were plated in 2 mL of methylcellulose (MethoCult M3434, StemCell Technologies, Vancouver, Canada) and counted after 8-10 days. For cell cycle analysis, cells were fixed for 16 h at 4°C in a 4% paraformaldehyde solution (Thermo Scientific, Monza, Italy) then stained with Hoechst 33342 (Invitrogen, Waltham, USA) and pyronin Y (Sigma, St. Louis, USA) for 40 min at room temperature, flowed for 15 min on ice, before washing in FACS buffer and analysis. For *in vitro* experiments, unless indicated otherwise, doxycycline was used at a concentration of 1 μg/mL.

PO-PRO-1 and 7-aminoactinomycin D staining of apoptotic cells

Apoptotic cells were quantified using the PO-PRO-1 and 7-aminoactinomycin D staining kit (Invitrogen, Waltham, USA) in accordance with the kit protocol.

Expression analysis of senescence-related genes in *iNUP98-KMT2A* mouse embryonic fibroblasts

Mouse embryonic fibroblasts (MEF) were generated by isolation of E14.5 embryos from *iNUP98-KMT2A* mice and the genotype was checked by PCR. To investigate senescence, WT and iNUP98-KMT2A MEF were grown in Dulbecco modified Eagle medium with doxycycline and serially passaged into 100 mm plates when 90% confluence was reached. β-Galactosidase staining was performed using the Senescence β-Galactosidase Staining kit (Cell Signaling, Leiden, the Netherlands) when WT MEF started showing signs of senescence. RNA was extracted from MEF cell pellets at early and late passages and senescence-related gene expression was analyzed by quantitative real-time PCR using a commercially available kit (RT2 Profiler PCR Array, QIAGEN AG, Hombrechtikon, Switzerland) (*Online Supplementary Table S2*) as well as by manual quantitative PCR using specific primers. Gene expression levels on the RT^2 Profiler PCR Array were normalized to an internal panel of housekeeping genes, whereas individual quantitative PCR data were normalized to *Gapdh*.

Exposure of leukemic blasts to menin and BET inhibitors

iNUP98-KMT2A and KMT2A-AF9 leukemic blasts were isolated and treated for 48 h *in vitro* with 0-500 nM of the BRD4 inhibitor JQ1/vehicle (dimethylsulfoxide, DMSO) or 0-12 μM of the menin-interaction inhibitor MI-2-2/vehicle (DMSO). Cell cycle analysis was performed at the 48 h time-point after staining with Hoechst 33342 and pyronin Y as described above.

Results

Establishing *iNUP98-KMT2A* transgenic mice

To address the transforming potential of *NUP98-KMT2A*, we cloned a full-length human fusion ORF into the *p2LOX* targeting-vector to integrate it into the *Hprt* gene locus on the X-chromosome under the control of a doxycycline-responsive element in embryonic stem cells. A reverse Tet transactivator (*rtTA*) stably integrated in the

Rosa26 locus allows doxycycline-regulated transgene expression (Figure 1A).[19,22,23] We used primarily female mice to mitigate the effects of any potential sex-related differences in transgene expression.

Induction of *iNUP98-KMT2A* results in an myelodysplastic syndrome-like disease *in vivo*

Primary-induced iNUP98-KMT2A mice developed signs of distress after a variable latency of 13-106 weeks (median latency=80 weeks, n=22) (Figure 1B). Blood values from non-induced iNUP98-KMT2A mice did not differ significantly from those of WT mice (*Online Supplementary Figure S1A*). We also explored disease induction by transplanting total BM from naïve (off doxycycline) iNUP98-KMT2A mice into lethally irradiated syngenic WT mice. In comparison to primary-induced mice, BM transplant recipient animals developed the symptoms earlier (median latency=32 weeks, *P*=0.0007, log-rank test, n=5) (Figure 1B, *Online Supplementary Table S3*).

Most symptomatic primary-induced iNUP98-KMT2A mice had peripheral blood counts in the normal range with slightly increased numbers of white blood cells, and reticulocytes. Decreases were seen in hemoglobin levels and red blood cell numbers (*P*=0.049, unpaired *t*-test, n=15) (Figure 1C). Blood values from iNUP98-KMT2A BM transplant recipients revealed a similar trend to those of primary-induced samples in all parameters analyzed with significantly increased numbers of white blood cells (*P*=0.0006, unpaired *t*-test, n=5) and reduced cellular hemoglobin levels (*P*=0.03, unpaired *t*-test, n=5). Notably, the overall cellularity of the BM of primary-induced mice was reduced (*P*=0.0099, unpaired *t*-test, n=9) relative to controls. Further analysis of different BM subpopulations revealed decreased numbers of myeloid cells (Mac-1$^+$/Gr-1$^+$), B cells (B220$^+$), and T cells (CD3$^+$) (*Online Supplementary Figure S1B*). Signs of intramedullary apoptotic cell death was found in some but not all mice as measured by combined PO-PRO-1 and 7-aminoactinomycin D staining (Figure 1C) with non-significant increased apoptosis of CD71$^+$Ter119$^+$, but not of myeloid (Mac-1$^+$, Gr-1$^+$) or lymphoid (CD3$^+$/CD8$^+$/B220$^+$) cells from primary-induced animals relative to WT controls (*Online Supplementary Figure S1C*). In primary induced mice we occasionally observed signs of dysplasia on blood smears, with the appearance of bi-lobed myeloid cells and polychromatophilic reticulocytes (Figure 1D) as well as signs of extramedullary hematopoiesis in the spleen and the liver (Figure 1E).

The BM of iNUP98-KMT2A mice that had been on doxycycline for several months displayed rather heterogeneous immunophenotypes: some showed an increase in Mac-1$^+$/Gr-1$^+$ cells, whereas others showed a marked decrease in mature myeloid cells with concomitant increases in FcγRII/III$^+$ and c-Kit$^-$ populations (Figure 1F, G).

To address potential reversibility, we transplanted iNUP98-KMT2A BM cells into lethally-irradiated WT recipients on doxycycline: upon development of symptoms in the first mouse, we reverted to non-doxycycline chow and followed the remaining mice for several months. Disease-free survival was significantly increased by the removal of doxycycline food (median latency=49 weeks, *P*=0.002, log-rank test, n=6) (Figure 1B) although analysis of peripheral blood at death revealed that many parameters remained similar to those of BM transplant recipients on doxycycline until death (Figure 1C).

Collectively, these data show that transgenic expression of *iNUP98-KMT2A* alters the hematopoietic system *in vivo*: there were increases in the numbers of white blood cells and apoptotic cells, and decreases in hemoglobin and the numbers of red blood cells and cells in the BM with signs of extramedullary hematopoiesis and morphological signs of dysplasia with some interindividual differences.

Expression of *iNUP98-KMT2A* leads to expansion and competitive advantage of hematopoietic stem and progenitor cells

We next studied the impact of *iNUP98-KMT2A* expression on the cellular hierarchy of the BM. We found that prior to developing symptoms (mean time on doxycycline: 36 weeks), iNUP98-KMT2A mice displayed an expansion of Lin$^-$ Sca-1$^+$ c-Kit$^+$ (LSK) hematopoietic stem and progenitor cells (HSPC) (*P*=0.04, unpaired *t*-test, n=4) (Figure 2A, *Online Supplementary Figure S1D*). Further breakdown of the LSK compartment revealed no significant changes in the relative distribution of CD34$^-$ long-term hematopoietic stem cells, and CD34$^+$, CD48$^+$, CD150$^-$ multipotent progenitors (Figure 2B). Interestingly, we found that iNUP98-KMT2A LSK, but not mature cells, from asymptomatic mice (mean time on doxycycline: 55 weeks) were cycling more than control cells as shown by a reduced fraction of quiescent cells in G_0 phase (*P*=0.0098, unpaired *t*-test, n=3) and an increase in the G_1 fraction (Figure 2C, *Online Supplementary Figure S1E*).

To address the functional consequence of the increased LSK number in iNUP98-KMT2A mice on doxycycline, we performed competitive repopulation assays. Naïve CD45.2$^+$ iNUP98-KMT2A or WT (CTRL) total BM cells were transplanted 1:1 with CD45.1$^+$ WT total BM cells into lethally-irradiated CD45.1$^+$ WT recipients (on doxycycline) and the cellular chimerism in the peripheral blood was determined 4, 8, 12, 18, and 25 weeks after transplantation. We observed that the proportion of CD45.2$^+$ iNUP98-KMT2A cells in the peripheral blood steadily increased over time (Figure 2D) whereas the chimerism in mice that received CD45.2$^+$ WT BM cells did not change significantly, remaining near to 50%. The percentage of iNUP98-KMT2A CD45.2$^+$ cells was initially lower than that of CTRL (WT) (*P*=0.0153, *t*-test, n=5). After 18 weeks, CD45.2$^+$ iNUP98-KMT2A cell numbers had increased by 1.6-fold compared to week 4 (*P*=0.034, *t*-test, n=5) and by 25 weeks CD45.2$^+$ iNUP98-KMT2A cell numbers had further increased relative to initial measurements (*P*=0.004, *t*-test, n=5) and were 20% greater than CD45.2$^+$ WT cells at the same time-point [*P*=0.019, 2-way analysis of variance (ANOVA), n=4]. Interestingly, iNUP98-KMT2A CD45.2$^+$ cells contributed to a greater extent to the myeloid lineage (Gr-1$^+$) and the B lineage (B220$^+$) but equally to the T lineage (CD3$^+$), compared to WT controls (Figure 2E). Transplantation of total BM from primary recipients into lethally-irradiated CD45.1$^+$ secondary recipients resulted in a heterogeneous outcome: in two mice ("M1" & "M2") the BM was dominated by CD45.2$^+$ cells, while two other mice ("M4" & "M5") showed predominantly CD45.1$^+$ cells. One mouse ("M3") developed a CD45.2$^+$ AML 23 weeks after transplantation (Figure 2F).

Some iNUP98-KMT2A mice develop transplantable acute myeloid leukemia

After a median latency of 62 weeks, six out of 22 iNUP98-KMT2A mice on doxycycline developed a

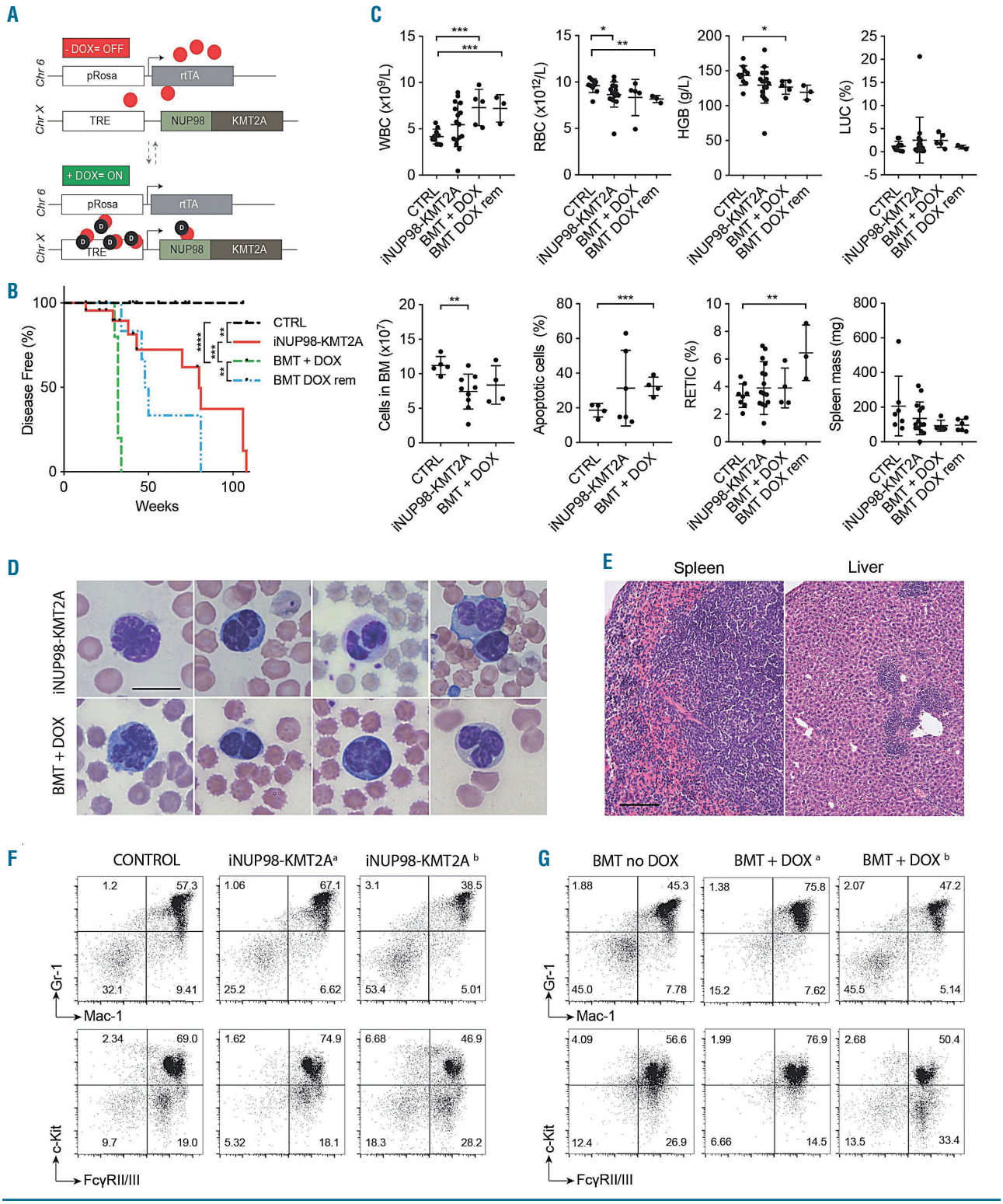

Figure 1. Expression of *iNUP98-KMT2A* leads to development of a myelodysplastic syndrome-like disease in transgenic mice. (A) iNUP98-KMT2A mice contain a reverse Tet transactivator (*rtTA*) element in the *Rosa26* gene locus on chromosome 6 (Chr 6), and a human *NUP98-KMT2A* open reading frame after a TET-responsive element (TRE) in the *Hprt* locus on the X-chromosome (Chr X). Administration of the tetracycline analog, doxycycline (DOX) leads to expression of the *NUP98-KMT2A* fusion construct. (B) Kaplan-Meier curves for DOX-exposed primary-induced adult (6-10 weeks) iNUP98-KMT2A mice and wildtype (WT) littermates (CTRL), as well as adult WT irradiated recipients of iNUP98-KMT2A total bone marrow transplants (BMT) exposed to DOX (BMT + DOX) and BMT recipients taken off DOX (BMT DOX rem) after 31 weeks. **P*<0.05, ***P*<0.01, ****P*<0.001, *****P*<0.0001, log-rank test. (C) Blood values from DOX-exposed adult iNUP98-KMT2A mice and WT littermates (CTRL), as well as adult WT irradiated recipients of iNUP98-KMT2A total BMT exposed to DOX (BMT + DOX) and BMT recipients taken off DOX (BMT DOX rem) after 31 weeks. **P*<0.05, ***P*<0.01, ****P*<0.001, unpaired *t*-tests. WBC: white blood cells; RBC: red blood cells; HGB: hemoglobin; LUC: abnormal leukocytes. (D) Dysplastic immature myeloid cells on peripheral blood smears of pre-leukemic DOX-induced iNUP98-KMT2A mice as well as WT recipients of iNUP98-KMT2A total BMT on DOX. Scale bar: 10 μm. (E) Histopathology sections of DOX-exposed iNUP98-KMT2A mice show extramedullary hematopoiesis in the spleen and liver. Scale bar: 100 μm. (F) Immunophenotype (Mac-1, Gr-1, FcγRII/III and c-Kit, given in %) of total bone marrow cells from pre-leukemic iNUP98-KMT2A mice. The flow plots are representative of three mice/group. (G) Immunophenotype (Mac-1, Gr-1, FcγRII/III and c-Kit, given in %) of total bone marrow cells from WT mice transplanted with iNUP98-KMT2A bone marrow on DOX. Mice exhibited two diverse phenotypes; denoted *a* and *b*. Transplanted mice off DOX were used as the negative control.

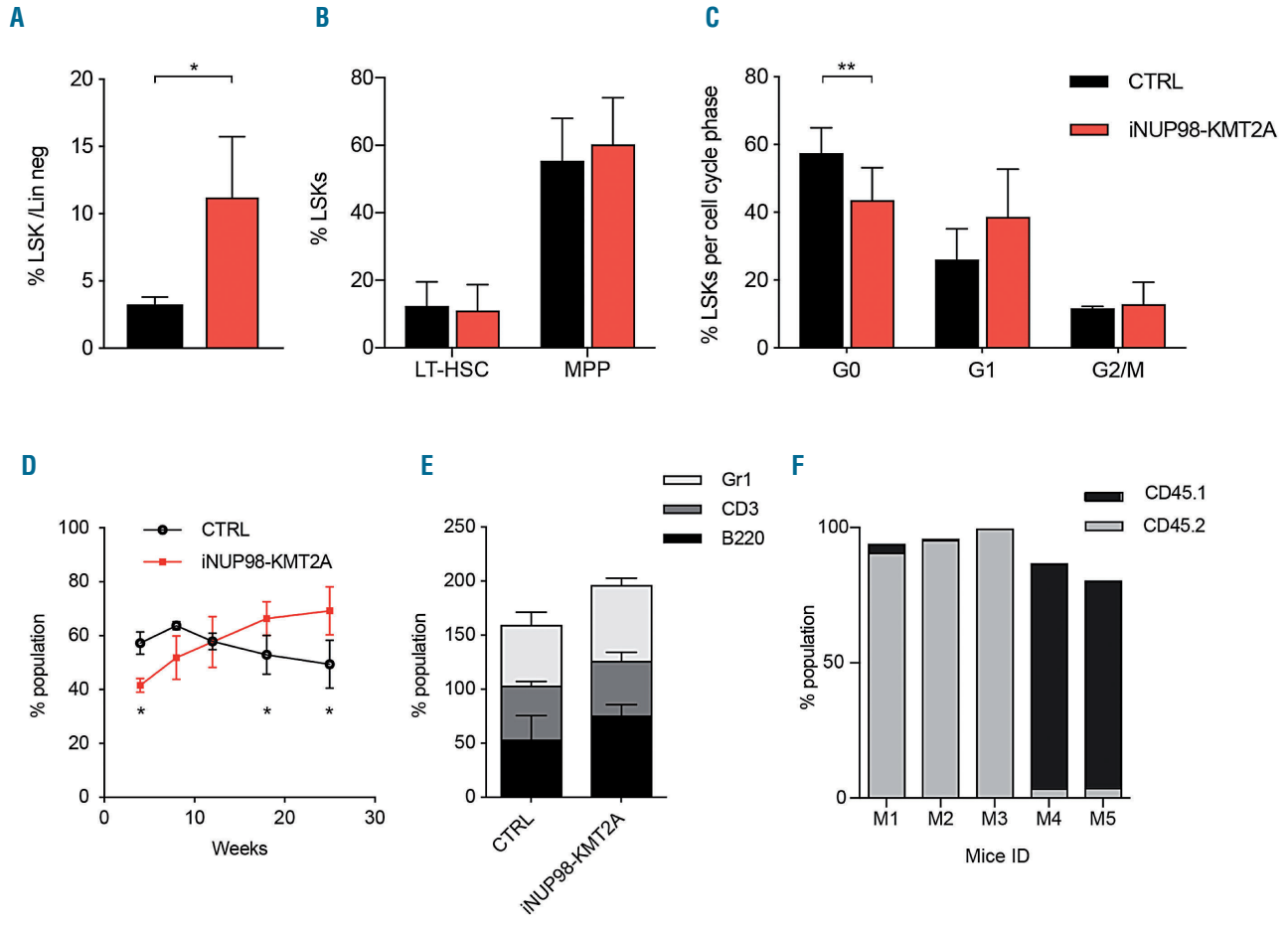

Figure 2. Expression of *iNUP98-KMT2A* results in LSK cell expansion with a competitive repopulation advantage. (A) Lineage negative (Lin^-) bone marrow (BM) cells from pre-leukemic iNUP98-KMT2A mice and wildtype (WT) littermate controls (CTRL) were stained for c-Kit and Sca-1 and analyzed by flow cytometry. *P<0.05, unpaired t-test. (B) Lin^- BM from pre-leukemic iNUP98-KMT2A mice and WT littermate controls were stained for markers of long-term hematopoietic stem cells (LT-HSC) (LSK, $CD150^+$, $CD48^-$) and multipotent progenitors (MPP) (LSK, $CD34^+$, $CD48^+$, $CD150^-$) and analyzed by flow cytometry. The percentages of LSK identified as LT-HSC and MPP are shown. (C) Cell cycle analysis of LSK from pre-leukemic iNUP98-KMT2A mice and WT littermate controls. **P<0.01, unpaired t-test. (D) Competitive repopulation assay: lethally-irradiated CD45.1 WT recipients were transplanted with a 1:1 mixture of total BM cells from CD45.2 iNUP98-KMT2A and CD45.1 WT mice in the presence of doxycycline (DOX). The percentage of CD45.2 cells present in the peripheral blood was measured by flow cytometry over a period of 25 weeks. *P<0.05, unpaired t-test. (E) At week 25 of the competitive repopulation assay, the $CD45.2^+$ cells were analyzed for percentages of Gr-1, CD3, and B220 markers. (F) Cellular BM chimerism of WT $CD45.1^+$ mice 25 weeks after competitive transplantation with $CD45.2^+$ iNUP98-KMT2A BM. All mice were exposed to DOX throughout the experiment.

leukemic phenotype characterized by the presence of leukemic blasts on peripheral blood smears, and extensive leukemic infiltration in the BM, spleen, liver and lungs (Figure 3A, *Online Supplementary Figure S2A*). This was accompanied by significantly increased white blood cell counts (P=0.0018, unpaired t-test, n=5) and abnormal leukocytes ("LUC") (P=0.0468, unpaired t-test, n=5) counts in the periphery and splenomegaly (Figure 3B, *Online Supplementary Table S4*). Immunophenotypic analysis of highly-infiltrated BM revealed intermediate to high expression levels of myeloid markers Mac-1, Gr-1, and FcγRII/III in five out of six mice, with baseline expression of B220 and CD3 lymphoid markers characterizing the disease as AML (Figure 3C, *Online Supplementary Figure S2B-D*).

Transplantation of total BM from diseased mice into sublethally-irradiated WT mice induced disease in 100% of recipients. Whereas disease development was fully doxycycline-dependent upon transplantation of AML cells from one donor ("M1") (median latency 28 weeks, P=0.025, log-rank test, n=4), leukemic cells from another donor ("M2") resulted in disease in all recipients regardless of doxycycline administration, with a similar latency (26-37 weeks) to that of recipients of "M1" cells on doxycycline (Figure 3D). Flow cytometric analysis of BM samples from transplanted leukemic mice revealed heterogeneity in M1 ("M1a" & "M1b") BM recipients, including a marked doxycycline-dependent increase in $CD3^+$ cells, but a consistent myeloid phenotype in recipients of M2 (Figure 3E).

Given the long latency to develop primary disease, we explored whether additional genotoxic insults might accelerate disease induction. Indeed, sublethal γ-irradiation (1x 600 cGy) of asymptomatic 3- to 4-week old iNUP98-KMT2A mice on doxycycline resulted in earlier onset of disease symptoms than that observed in sublethally-irradiated WT mice (median latency 26 weeks *vs.* undefined; P=0.032, log-rank test, n=5) (Figure 3F, *Online*

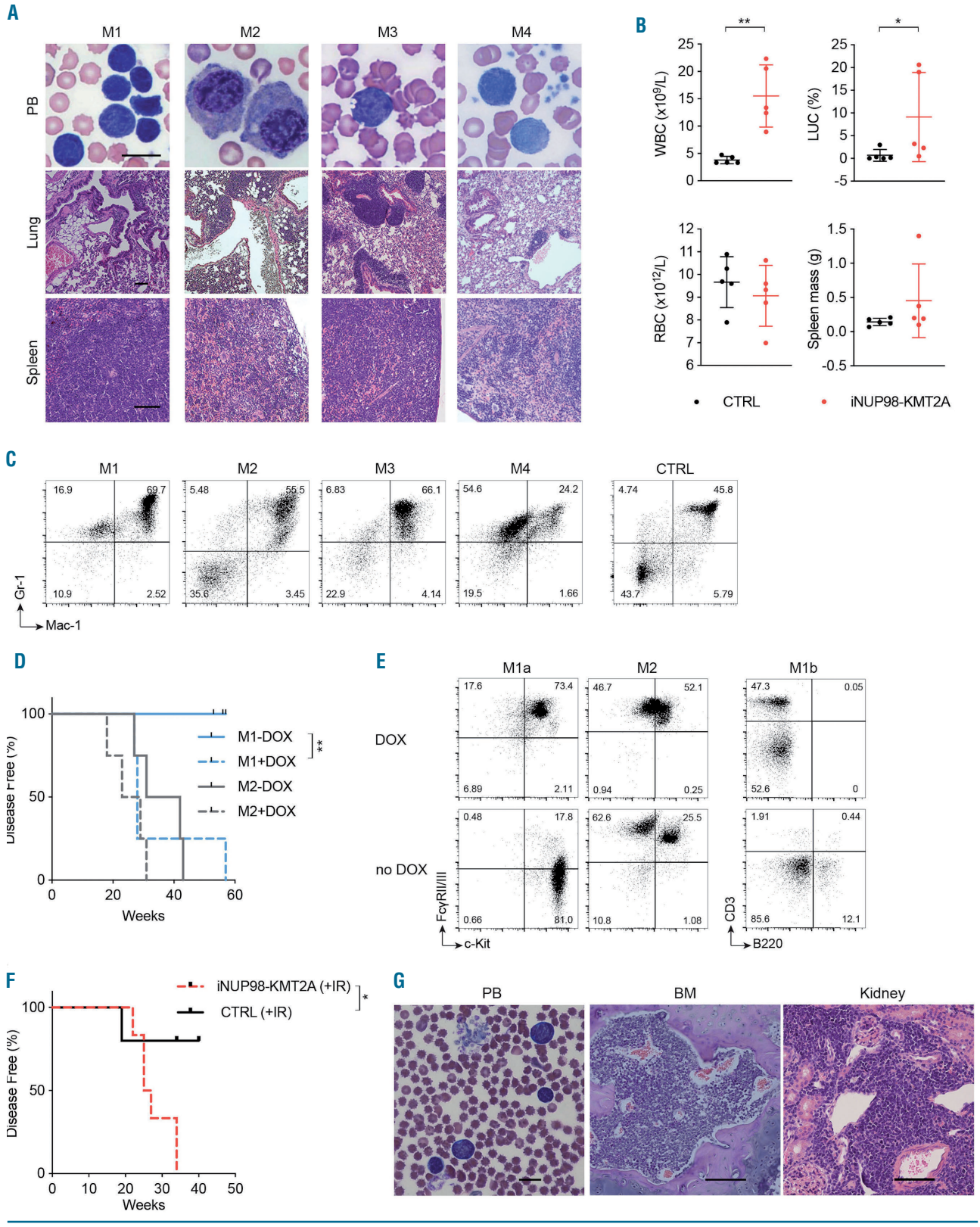

Figure 3. Expression of *iNUP98-KMT2A* induces a transplantable acute myeloid leukemia in some mice. (A) Histological sections and peripheral blood (PB) smears from four leukemic iNUP98-KMT2A mice. Scale bar: 10 μm. (A) Blood values from doxycycline (DOX)-treated iNUP98-KMT2A mice which developed symptoms of leukemia as well as wildtype (WT) littermate controls (CTRL). **P*<0.05, ***P*<0.01, unpaired *t*-test, n=5. WBC: white blood cells; LUC: abnormal leukocytes; RBC: red blood cells. (C) Gr-1 and Mac-1 expression on total BM cells from leukemic iNUP98-KMT2A mice and a representative control mouse. (D) Total BM from leukemic mice M1 and M2 was transplanted into WT recipients in the presence or absence of DOX. Kaplan-Meier curves show disease-free survival of transplanted animals. ***P*<0.01, log-rank test. (E) Representative immunophenotypes of total BM of recipients (on DOX) (from Figure 3D) either transplanted with iNUP98-KMT2A acute myeloid leukemia from mouse M1: M1a and M1b; or from mouse M2. (F) iNUP98-KMT2A mice were exposed to DOX 48 h prior to sublethal irradiation (600 cGy). Irradiated (IR) WT mice were used as controls. Kaplan-Meier curves illustrate disease-free survival. **P*<0.05, log-rank test. (G) Representative histopathology section of a symptomatic irradiated iNUP98-KMT2A mouse. The BM is infiltrated with blasts which are also visible in the peripheral blood (PB) and kidney. Scale bars: PB: 10 μm; BM & kidney: 100 μm.

Supplementary Table S5) and that seen in our cohort of primary-induced, non-irradiated iNUP98-KMT2A mice on doxycycline (median latency 26 *vs.* 80 weeks; *P*=0.0003, log-rank test, n=6) (*Online Supplementary Figure 3A*). All symptomatic mice had extensive multi-organ infiltration by leukemic blasts, which were visible on peripheral blood smears as well as in the BM and kidneys (Figure 3G). Collectively, these data show that expression of *iNUP98-KMT2A* leads to an MDS-like disease and in some cases to transplantable AML in mice.

Expression of *iNUP98-KMT2A* results in aberrant cell cycle progression and escape from senescence

In the presence of doxycycline (1 μg/mL), *ex vivo* proliferation of Lin$^-$ iNUP98-KMT2A BM cells was significantly impaired in liquid culture containing cytokines (murine stem cell factor, interleukin-6, and interleukin-3 (*Online Supplementary Figure S3B*). Expression of *iNUP98-KMT2A* was verified on day 6 of the culture (*Online Supplementary Figure S3C*). However, *iNUP98-KMT2A* expression did not significantly alter the clonogenic growth of BM cells in methylcellulose containing doxycycline (*Online Supplementary Figure S3D*). Cell cycle analysis of Lin$^-$ iNUP98-KMT2A BM cells challenged with doxycycline *in vitro* revealed an increase in the number of cells in G_1 phase (*P*=0.033, unpaired *t*-test, n=3) at the expense of G_0 and G_2/M phases (*P*=0.049, unpaired *t*-test, n=3) (*Online Supplementary Figure S3E*), similar to what was observed in LSK from iNUP98-KMT2A mice on doxycycline (Figure 2C).

To further explore the impact of *iNUP98-KMT2A* expression on cell cycle regulation we established MEF. We first verified *iNUP98-KMT2A* expression in the MEF (Figure 4A). We then determined cell cycle progression of iNUP98-KMT2A MEF on doxycycline and found accumulation of the cells in the G_1 phase (*P*=0.081, unpaired *t*-test, n=3) with a significant reduction of the percentage of cells in the G_2/M phase (*P*=0.029, unpaired *t*-test, n=3) (Figure 4B). Initially, both iNUP98-KMT2A and WT MEF grew at similar rates; however, upon serial propagation of the cells we observed reduced growth of WT MEF with signs of senescence (visualized by X-gal staining for senescence-associated β-galactosidase activity) after 10-13 passages (Figure 4C, *Online Supplementary Figure S3F, G*). In contrast, iNUP98-KMT2A MEF continued to grow at an increased rate (*P*=0.0156, Wilcoxon matched-pairs signed rank test, n=2) up to, and beyond, passage 40. To understand how iNUP98-KMT2A MEF escape senescence, we compared the expression of 84 genes related to cell cycle regulation and senescence using a commercial array-based reverse transcription PCR assay. Combining two independent experiments revealed no significant changes in gene expression at an early time-point (passage 1) (Figure 4D) while the levels of expression of eight genes were significantly reduced in iNUP98-KMT2A MEF relative to WT MEF at later passages (passage 10-13) (Figure 4E).

Genes that were found to be dysregulated in late-passage iNUP98-KMT2A MEF samples were further analyzed in iNUP98-KMT2A HSPC, which had been exposed to doxycycline *in vitro* for 48 h. Expression patterns observed in MEF for *Sirt1*, *Rbl2*, *Twist1*, *Prkcd*, *Vim*, and *Tert* were found to be similar in iNUP98-KMT2A HSPC, demonstrating common patterns of gene regulation in MEF and primary iNUP98-KMT2A cells (Figure 4F).

iNUP98-KMT2A$^+$ acute myeloid leukemia cells do not express the *HoxA-B-C* gene cluster and are resistant to compounds targeting the KMT2A-menin interaction

In contrast to other NUP98 fusions, primary patients' NUP98-KMT2A AML cells were shown to express reduced levels of the *HOXA-B-C* gene cluster.[19] Likewise, leukemic blasts from diseased *iNUP98-KMT2A* mice generally expressed very low levels of *HoxA5*, *HoxA9*, *HoxA10*, *HoxB4*, *HoxB6*, *HoxC6* and *HoxC9* mRNA compared to normal BM cells or to leukemic blasts transformed by retroviral *KMT2A-ENL* (*rKMT2A-ENL*) or the *rKMT2A-AF9* fusion genes (Figure 5A).[24]

The lack of *KMT2A* exon 1 encoding for the very N-terminus, which mediates the menin/LEDGF interaction, predicts that cells carrying the NUP98-KMT2A fusion protein would be resistant to small molecule menin inhibitors. However, if leukemic transformation by NUP98 fusions depends on KMT2A, as suggested by recent studies,[14,25] NUP98-KMT2A leukemic blasts might be susceptible to inhibition by small molecules targeting critical KMT2A functional interactions. To address this question, we exposed cells from two leukemic iNUP98-KMT2A mice ("M1" & "M3") to different doses of the small molecule menin inhibitor (MI-2-2) and to a bromodomain inhibitor blocking BET-family proteins including BRD4 (JQ1) previously shown to efficiently block KMT2A and KMT2A-fusion controlled transcription.[26] As shown in Figure 5B, MI-2-2 (3-12 μM) did not impair growth of iNUP98-KMT2A leukemic blasts but at 6 μM and 12 μM induced a G_1 cycle arrest in leukemic cells expressing the rKMT2A-AF9 fusion (*P*<0.0001, two-way ANOVA, n=2), with a concomitant decrease in the proportion of cells in the S-phase (*P*<0.0001, two-way ANOVA, n=2) and in the G_2/M-phase (6 μM: *P*=0.0246; 12 μM: *P*=0.0144, two-way ANOVA, n=2). Exposure of iNUP98-KMT2A cells to low (0.05-0.5 μM) doses of JQ1 did not induce cell cycle arrest or significant cytotoxicity as seen in rKMT2A-AF9 cells (Figure 5C), but increased the fraction of cells in the G_1 phase of the cycle, suggesting alternative transforming mechanisms of NUP98-KMT2A compatible with a defective cell cycle checkpoint control.

Discussion

Inv(11)(p15q23) has been reported in a heterogeneous group of human hematologic malignancies including MDS, AML, peripheral T-cell lymphoma, childhood acute lymphoblastic acute leukemia, myeloma and hairy cell leukemia.[20] In the majority of the myeloid cases, inv(11)(p15q23) was the sole cytogenetic abnormality, suggesting a role as a leukemogenic driver. Expression of a *NUP98-KMT2A* fusion gene has so far been reported in two AML patients with inv(11)(p15q23).[19] Detailed molecular work-up of additional patients is needed to delineate the epidemiology of this rare entity. Notably, inv(11)(p15q23) was also found in some solid cancers but never analyzed in more detail.[20] To determine the transforming potential of the *NUP98-KMT2A* fusion gene we developed inducible transgenic mice. This approach avoids some of the drawbacks of retroviral gene transfer such as cooperating integration events or transduction bias of early myeloid progenitor cells. In addition, the large size of the *NUP98-KMT2A* fusion ORF would clear-

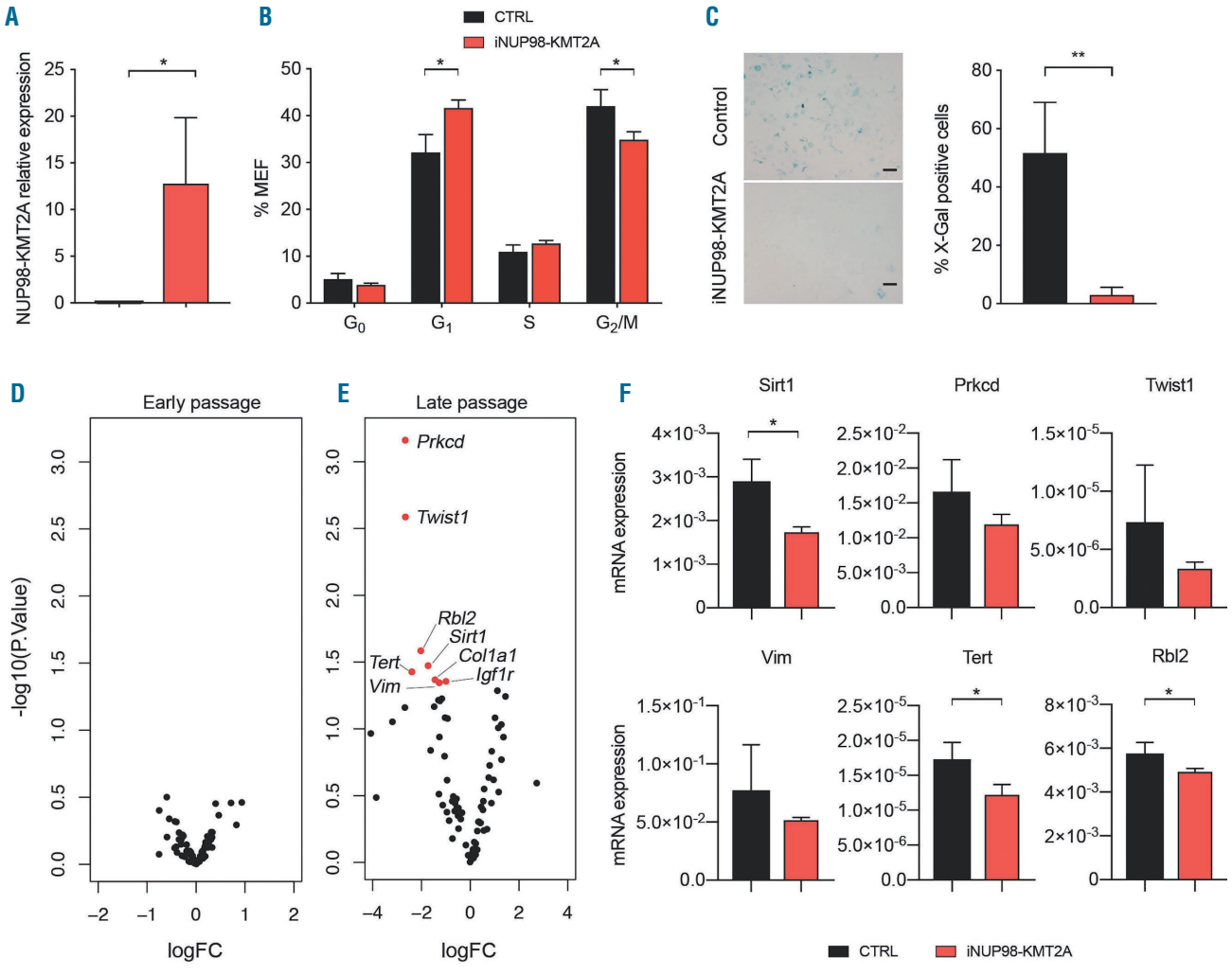

Figure 4. *iNUP98-KMT2A* expression impairs cell cycle progression of murine embryonic fibroblasts and bone marrow-derived hematopoietic stem and progenitor cells. (A) Murine embryonic fibroblasts (MEF), derived from iNUP98-KMT2A and wildtype (WT) control (CTRL) littermate mice were cultured in vitro in the presence of doxycycline (DOX) (1 μg/mL). *iNUP98-KMT2A* expression is shown relative to the level of *GAPDH* expression. **P*<0.05, unpaired *t*-test, n=3. (B) Flow cytometry-based cell cycle analysis showed increased G_1 and decreased G_2/M fractions of *in vitro*-cultured iNUP98-KMT2A+ MEF compared to WT controls. **P*<0.05, unpaired *t*-test, n=3. (C) iNUP98-KMT2A and WT MEF cultured for eight passages in the presence of DOX (1 μg/mL) were stained for senescence-associated B-galactosidase activity with X-Gal (left panel). The number of X-Gal$^+$ cells in the culture was quantified (right panel). Images and counts are representative of three biological replicates. Scale bars: 100 μm. ***P*<0.01, unpaired t-test, n=3. (D) Differential mRNA expression from early (passages 1-2) and late (passages 8-10) passaged WT and iNUP98-KMT2A MEF analyzed by a RT2 PCR array. Significant (*P*<0.05) changes are highlighted in red. (E) Validation of differentially expressed genes in MEF (Figure 4D) by quantitative polymerase chain reaction analysis in WT and iNUP98-KMT2A hematopoietic stem and progenitor cells after exposure to DOX (1 μg/mL) *in vitro* for 48 h. *<0.05, unpaired *t*-test, n=3.

ly limit the generation of high-titer retroviral particles. We used a doxycycline-regulated transgenic expression system in which the *rtTA* is integrated into the ubiquitously expressed *Rosa26* locus and the *NUP98-KMT2A* fusion is in the *Hprt* locus under control of a tet-responsive minimal promoter, previously used to model the impact of cellular origin in *KMT2A-AF9* and *KMT2A-ENL*-driven leukemia.[22,23,27]

Secondary transplantation of iNUP98-KMT2A leukemic cells revealed that the inherent leakiness of the system might be sufficient to drive the phenotype in the absence of doxycycline after cellular selection in the mouse (Figure 3D) suggesting that, in contrast to *KMT2A-AF9* or *KMT2A-ENL*, low level *NUP98-KMT2A* transgene expression is sufficient to exert its oncogenic activity or that expression of the transgene might be required for initial transformation but not for maintenance of neoplastic cells in all cases.

Retroviral expression, as well as constitutive or conditional activation, of many AML-associated fusions [involving the retinoic acid receptor alpha (RARA), core binding factor (CBF) or KMT2A] in the hematopoietic system of the mouse often closely phenocopies human disease.[28,29] In most of these models, AML develops after a long latency without evidence of a symptomatic pre-leukemic MDS phase, with few exceptions such as the *Vav1*-promoter driven *NUP98-HOXD13* fusion.[30] NUP98-HOXD13 mice developed T-cell leukemia, undifferentiated leukemia, megakaryocytic and erythroid leukemia or symptomatic MDS. In contrast, iNUP98-KMT2A mice (5 out of 22) only developed Gr-1$^+$/Mac-1$^+$/c-Kit$^+$ AML. Leukemic transformation of NUP98-HOXD13 mice was

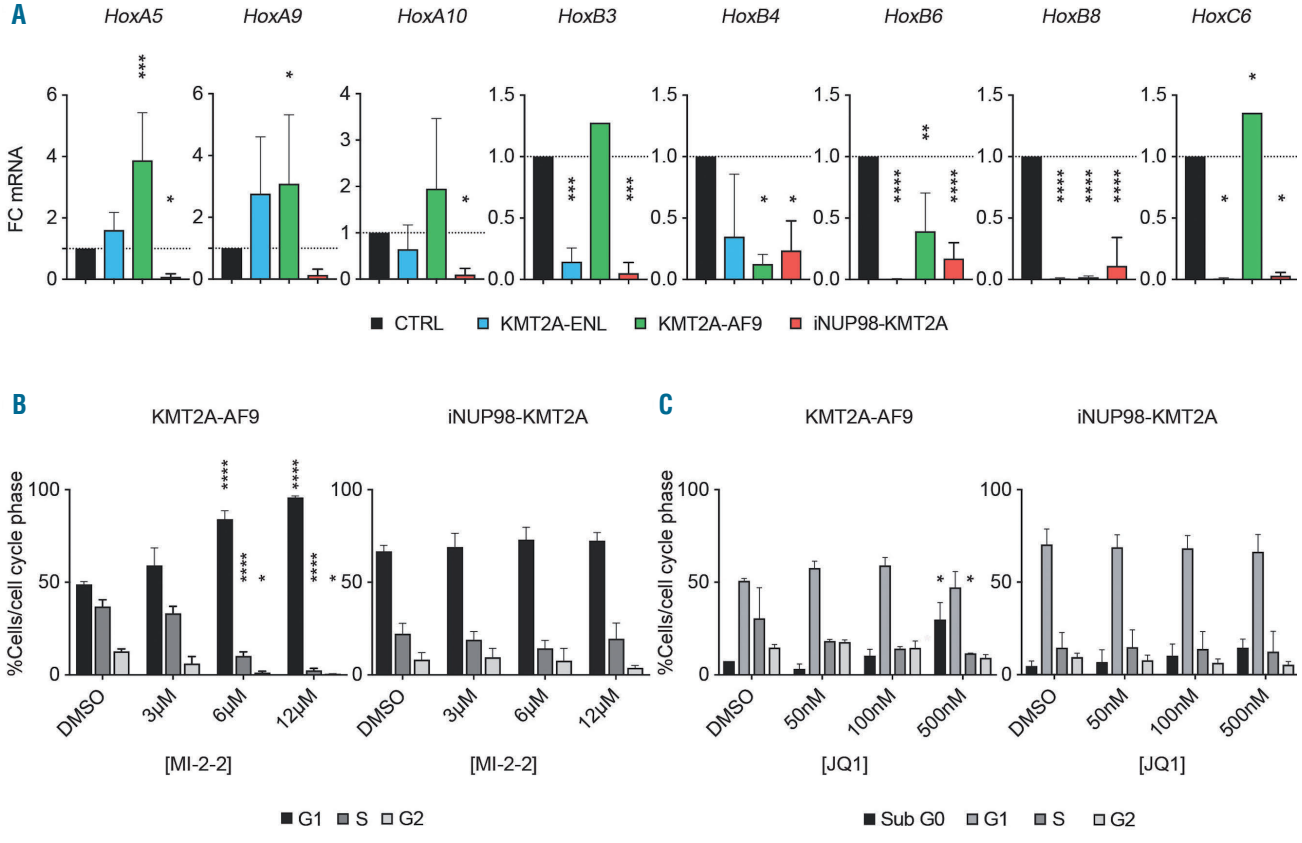

Figure 5. iNUP98-KMT2A acute myeloid leukemia cells express low levels of *Hox* genes and are resistant to small molecule menin and Brd4 inhibitors. (A) Expression of *HoxA*, *-B*, and *-C* genes was quantified by quantitative polymerase chain reaction (qPCR) analysis in total bone marrow from wildtype (WT) control (CTRL) cells, leukemic cells from iNUP98-KMT2A mice as well as from mice transplanted with retrovirally-transduced KMT2A-ENL (rKMT2A-ENL) and rKMT2A-AF9 cells. Expression relative to that of WT cells is shown. **P*<0.05, ***P*<0.01, ****P*<0.001, *****P*<0.0001, one-way analysis of variance (ANOVA) relative to control, n=3. (B) rKMT2A-AF9 and iNUP98-KMT2A leukemic blasts were treated with the menin inhibitor, MI-2-2, for 48 h at the indicated concentrations and the cell cycle phase was analyzed by flow cytometry. The figure shows the percentage of cells in each phase of the cell cycle. **P*<0.05, ***P*<0.01, ****P*<0.001, *****P*<0.0001, two-way ANOVA relative to cells treated with dimethylsulfoxide (DMSO), n=2. (C) rKMT2A-AF9 and iNUP98-KMT2A leukemic blasts were treated with the BRD4 inhibitor, JQ1, for 48 h at the indicated concentrations. Cell cycle phase was analyzed by flow cytometry. The figure shows the percentage of cells in each phase of the cell cycle. **P*<0.05, two-way ANOVA relative to DMSO-treated cells, n=2.

accompanied by spontaneous mutations in *Nras*, *Kras* and *Cbl*; however, no such mutations were found in three iNUP98-KMT2A mice that developed AML[31] *(data not shown)*. Several studies also demonstrated leukemogenic cooperation of NUP98-HOXD13 with overexpression of *Meis1*, *MN1*, or loss of *p53* or *p15*^{INK4B}.[32-35] Intercrossing of transgenic NUP98-HOXD13 mice with *Flt3*-internal tandem duplication (ITD) knock-in mice resulted in acceleration to a fully-penetrant AML phenotype.[36] In contrast to NUP98-HOXD13, we observed that transplantation of iNUP98-KMT2A BM cells retrovirally overexpressing *FLT3*-ITD did not accelerate the disease (*data not shown*).[36]

In the presence or absence of *FLT3*-ITD, pre-leukemic NUP98-HOXD13 cells expressed significantly increased levels of *HoxA7*, *HoxA9*, *HoxB4*, *HoxB6*, *HoxB7*, *HoxC4* and *HoxC6* mRNA.[30,36] In sharp contrast, BM cells from diseased iNUP98-KMT2A mice expressed significantly reduced levels of the *HoxA-B-C* gene cluster compared to normal BM cells, recapitulating what was shown in primary NUP98-KMT2A$^+$ AML cells.[19] Expression levels of *HoxA-B-C* genes below those observed in normal HSPC suggest that the iNUP98-KMT2A fusion may affect the function of normal KMT2A in a dominant-negative manner.

Previous work showed that KMT2A plays a critical role in cell cycle progression.[37] Interestingly, under baseline conditions, we found a higher proportion of iNUP98-KMT2A Lin$^-$ cells in S-phase when compared to WT cells supporting previous studies indicating that ablation of normal KMT2A function results in defective S-phase cell cycle entry. The percentage of both WT and iNUP98-KMT2A cells in S-phase decreased following exposure to ionizing radiation (*data not shown*) as has been demonstrated previously.[38] Interestingly, compared to control cells, *in vitro* doxycycline treatment of both iNUP98-KMT2A BM-derived HSPC and MEF led to the accumulation of cells in the G_1-phase, mirroring what was seen in LSK cells taken from iNUP98-KMT2A mice that had been on doxycycline food for several months. Further experiments with MEF showed that expression of *iNUP98-KMT2A* abrogated cellular senescence: compared to WT cells, iNUP98-KMT2A MEF on doxycycline never showed any signs of crisis and could easily be propagated for >45 passages. In contrast, iNUP98-KMT2A cells off doxycycline showed signs of a crisis at passages 10-12 but were able to escape and could also be propagated for over 40 passages (*data not shown*), suggesting that very low expression of *iNUP98-KMT2A* is suffi-

cient to provide the cells the signals to escape apoptosis after crisis.

Among the genes downregulated in late passage iNUP98-KMT2A relative to control MEF, many have been implicated in cell cycle- or senescence-regulatory capacities. Previously, *sirtuin1* (*sirt1*)-deficient MEF were shown to be resistant to replicative senescence through a p53-dependent mechanism;[39] there is also evidence to suggest that Sirt1 plays a crucial role in Foxo3-activated cell cycle arrest.[40] It has been shown that the insulin-like growth factor 1 receptor (IGF1R) ligand, insulin-like growth factor (IGF1), is involved in cellular senescence control through the Sirt1-p53 axis,[41] in line with a proposed model whereby p53-dependent cellular senescence is counteracted by inhibition of IGF1R signaling.[42] In a lung fibroblast cell model, Rbl2 (p130) expression was increased along with E2F-4 and markers of cellular senescence following heat shock protein-27 (HSP27) knock-down. Inhibition of Rbl2 counteracted the effects of HSP27 knock-down and significantly reduced senescence-associated β-galactosidase staining in a p53-independent manner.[43] Additionally, the ribonuclease polymerase Tert (telomerase reverse transcriptase), which maintains telomeric ends, has a well-demonstrated role in resisting senescence; however, some primary tumor samples have tested negative for telomerase activity[44] and alternative mechanisms to overcome replication-associated telomeric shortening have been proposed with evidence for alternative lengthening of telomeres in 10-15% of cancers.[45] Finally, the role of protein kinase C delta (Prkcd) in senescence is currently poorly understood, but studies have suggested that Prkcd is an important mediator of transforming growth factor-β-induced senescence.[46]

Peptides and small molecule antagonists of KMT2A-menin/LEDGF interactions have been shown to reduce the transforming activity of KMT2A fusions by interfering with binding to targets, including the *HOX-A* gene cluster.[5-10] It has been shown that leukemic transformation by NUP98 fusions is KMT2A-dependent;[14] this would support the idea that iNUP98-KMT2A AML cells are susceptible to small molecules targeting the N-terminus of WT KMT2A. Conversely, the lack of the menin/LEDGF interaction site would predict poor sensitivity of iNUP98-KMT2A AML cells to these compounds. Indeed, compared to KMT2A-AF9-driven cells, iNUP98-KMT2A leukemic cells were resistant to blockade of the KMT2A-menin interaction by the small molecule MI-2-2 at concentrations previously demonstrated to inhibit growth of human KMT2A-AF4 and murine KMT2A-AF9 transformed cells.[12,47] iNUP98-KMT2A AML cells also showed a reduced sensitivity to the BET-bromodomain inhibitor JQ1, which interferes with active transcription and elongation through displacement of BRD4 from chromatin,[48] while challenge of KMT2A-AF9 cells recapitulated published growth inhibition.[26] This suggests that targeting KMT2A might not be suitable for efficient therapeutic interference with NUP98-KMT2A AML.

Acknowledgments

The authors thank Danny Labes, Telma Lopes, Emmanuel Traunecker, and Lorenzo Raeli from the University of Basel Flow Cytometry Facility; Nicole Meier and the members of the Animal Care Facility at the University of Basel; Masao Seto for the full-length human KMT2A mRNA; Michael Kyba for providing the A2Lox-Cre ES cells; and Patrick Kopp and Jean-Françoise Spetz for their assistance generating the iNUP98-KMT2A mice.

Funding

JS's laboratory was supported by: grants from Swiss Cancer Research (KFS-4258-08-2017, KFS-3487-08-2014) and the Swiss National Science Foundation (SNF, 31003_A_173224/1). AP was supported by the Novartis Research Foundation. Basel, Switzerland.

References

1. Gough SM, Slape CI, Aplan PD. NUP98 gene fusions and hematopoietic malignancies: common themes and new biologic insights. Blood. 2011;118(24):6247-6257.
2. Takeda A, Yaseen NR. Nucleoporins and nucleocytoplasmic transport in hematologic malignancies. Semi Cancer Biol. 2014;27:3-10.
3. Muntean AG, Hess JL. The pathogenesis of mixed-lineage leukemia. Annu Rev Pathol. 2012;7:283-301.
4. de Boer J, Walf-Vorderwulbecke V, Williams O. In focus: MLL-rearranged leukemia. Leukemia. 2013;27(6):1224-1228.
5. Yokoyama A. Transcriptional activation by MLL fusion proteins in leukemogenesis. Exp Hematol. 2016;46:21-30.
6. Slany RK. The molecular mechanics of mixed lineage leukemia. Oncogene. 2016; 35:5215-5223.
7. Murai MJ, Chruszcz M, Reddy G, Grembecka J, Cierpicki T. Crystal structure of menin reveals binding site for mixed lineage leukemia (MLL) protein. J Biol Chem. 2011;286(36):31742-31748.
8. Huang J, Gurung B, Wan B, et al. The same pocket in menin binds both MLL and JUND but has opposite effects on transcription. Nature. 2012;482(7386):542-546.
9. Yokoyama A, Somervaille TC, Smith KS, Rozenblatt-Rosen O, Meyerson M, Cleary ML. The menin tumor suppressor protein is an essential oncogenic cofactor for MLL-associated leukemogenesis. Cell. 2005;123 (2):207-218.
10. Yokoyama A, Cleary ML. Menin critically links MLL proteins with LEDGF on cancer-associated target genes. Cancer Cell. 2008;14(1):36-46.
11. Grembecka J, He S, Shi A, et al. Menin-MLL inhibitors reverse oncogenic activity of MLL fusion proteins in leukemia. Nat Chem Biol. 2012;8(3):277-284.
12. Borkin D, Pollock J, Kempinska K, et al. Property focused structure-based optimization of small molecule inhibitors of the protein-protein interaction between menin and mixed lineage leukemia (MLL). J Med Chem. 2016;59(3):892-913.
13. Pascual-Garcia P, Jeong J, Capelson M. Nucleoporin Nup98 associates with Trx/MLL and NSL histone-modifying complexes and regulates Hox gene expression. Cell Rep. 2014;9(2):433-442.
14. Xu H, Valerio DG, Eisold ME, et al. NUP98 fusion proteins interact with the NSL and MLL1 complexes to drive leukemogenesis. Cancer Cell. 2016;30(6):863-878.
15. Shima Y, Yumoto M, Katsumoto T, Kitabayashi I. MLL is essential for NUP98-HOXA9-induced leukemia. Leukemia. 2017;31(10):2200-2210.
16. Mitani K, Sato Y, Hayashi Y, et al. Two myelodysplastic syndrome cases with the inv(11)(p15q23) as a sole chromosomal abnormality. Br J Haematol. 1992;81(4):512-515.
17. Inaba T, Hayashi Y, Hanada R, Nakashima M, Yamamoto K, Nishida T. Childhood myelodysplastic syndromes with 11p15 translocation. Cancer Genet Cytogenet. 1988;34(1):41-46.
18. Calabrese G, Fantasia D, Spadano A, Morizio E, Di Bartolomeo P, Palka G. Karyotype refinement in five patients with acute myeloid leukemia using spectral karyotyping. Haematologica. 2000;85(11):1219-1221.
19. Kaltenbach S, Soler G, Barin C, et al. NUP98-MLL fusion in human acute myeloblastic leukemia. Blood. 2010;116(13):2332-2335.
20. Huret JL. t(17;20)(q21;q11). Atlas Genet Cytogenet Oncol Haematol. 2018;2:51.
21. Joh T, Kagami Y, Yamamoto K, et al. Identification of MLL and chimeric MLL

gene products involved in 11q23 translocation and possible mechanisms of leukemogenesis by MLL truncation. Oncogene. 1996;13(9):1945-1953.
22. Iacovino M, Hernandez C, Xu Z, Bajwa G, Prather M, Kyba M. A conserved role for Hox paralog group 4 in regulation of hematopoietic progenitors. Stem Cells Dev. 2009;18(5):783-792.
23. Stavropoulou V, Kaspar S, Brault L, et al. MLL-AF9 expression in hematopoietic stem cells drives a highly invasive AML expressing EMT-related genes linked to poor outcome. Cancer Cell. 2016;30(1):43-58.
24. Thanasopoulou A, Tzankov A, Schwaller J. Potent co-operation between the NUP98-NSD1 fusion and the FLT3-ITD mutation in acute myeloid leukemia induction. Haematologica. 2014;99(9):1465-1471.
25. Franks TM, McCloskey A, Shokirev MN, Benner C, Rathore A, Hetzer MW. Nup98 recruits the Wdr82-Set1A/COMPASS complex to promoters to regulate H3K4 trimethylation in hematopoietic progenitor cells. Genes Dev. 2017;31(22):2222-2234.
26. Zuber J, Shi J, Wang E, et al. RNAi screen identifies Brd4 as a therapeutic target in acute myeloid leukaemia. Nature. 2011;478(7370):524-528.
27. Stavropoulou V, Almosailleakh M, Royo H, et al. A novel inducible mouse model of MLL-ENL-driven mixed-lineage acute leukemia. HemaSphere. 2018;2(4):e51.
28. Milne TA. Mouse models of MLL leukemia: recapitulating the human disease. Blood. 2017;129(16):2217-2223.
29. Fisher JN, Stavropoulou V, Kalleda N, Schwaller J. The impact of the cellular origin in acute myeloid leukemia: learning from mouse models. Hemasphere. 2019;3(1):e152.
30. Lin YW, Slape C, Zhang Z, Aplan PD. NUP98-HOXD13 transgenic mice develop a highly penetrant, severe myelodysplastic syndrome that progresses to acute leukemia. Blood. 2005;106(1):287-295.
31. Slape C, Liu LY, Beachy S, Aplan PD. Leukemic transformation in mice expressing a NUP98-HOXD13 transgene is accompanied by spontaneous mutations in Nras, Kras, and Cbl. Blood. 2008;112(5):2017-2019.
32. Pineault N, Buske C, Feuring-Buske M, et al. Induction of acute myeloid leukemia in mice by the human leukemia-specific fusion gene NUP98-HOXD13 in concert with Meis1. Blood. 2003;101(11):4529-4538.
33. Slape C, Hartung H, Lin YW, Bies J, Wolff L, Aplan PD. Retroviral insertional mutagenesis identifies genes that collaborate with NUP98-HOXD13 during leukemic transformation. Cancer Res. 2007;67(11):5148-5155.
34. Humeniuk R, Koller R, Bies J, Aplan P, Wolff L. Brief report: loss of p15Ink4b accelerates development of myeloid neoplasms in Nup98-HoxD13 transgenic mice. Stem Cells. 2014;32(5):1361-1366.
35. Imren S, Heuser M, Gasparetto M, et al. Modeling de novo leukemogenesis from human cord blood with MN1 and NUP98HOXD13. Blood. 2014;124(24):3608-3612.
36. Greenblatt S, Li L, Slape C, et al. Knock-in of a FLT3/ITD mutation cooperates with a NUP98-HOXD13 fusion to generate acute myeloid leukemia in a mouse model. Blood. 2012;119(12):2883-2894.
37. Liu H, Cheng EH, Hsieh JJ. Bimodal degradation of MLL by SCFSkp2 and APCCdc20 assures cell cycle execution: a critical regulatory circuit lost in leukemogenic MLL fusions. Genes Dev. 2007;21(19):2385-2398.
38. Liu H, Takeda S, Kumar R, et al. Phosphorylation of MLL by ATR is required for execution of mammalian S-phase checkpoint. Nature. 2010;467(7313):343-346.
39. Chua KF, Mostoslavsky R, Lombard DB, et al. Mammalian SIRT1 limits replicative life span in response to chronic genotoxic stress. Cell Metab. 2005;2(1):67-76.
40. Brunet A, Sweeney LB, Sturgill JF, et al. Stress-dependent regulation of FOXO transcription factors by the SIRT1 deacetylase. Science. 2004;303(5666):2011-2015.
41. Tran D, Bergholz J, Zhang H, et al. Insulin-like growth factor-1 regulates the SIRT1-p53 pathway in cellular senescence. Aging Cell. 2014;13(4):669-678.
42. Duan L, Maki CG. The IGF-1R/AKT pathway determines cell fate in response to p53. Transl Cancer Res. 2016;5(6):664-675.
43. Park AM, Tsunoda I, Yoshie O. Heat shock protein 27 promotes cell cycle progression by down-regulating E2F transcription factor 4 and retinoblastoma family protein p130. J Biol Chem. 2018;293(41):15815-15826.
44. Kim NW, Piatyszek MA, Prowse KR, et al. Specific association of human telomerase activity with immortal cells and cancer. Science. 1994;266(5193):2011-2015.
45. Cesare AJ, Reddel RR. Alternative lengthening of telomeres: models, mechanisms and implications. Nat Rev Genet. 2010;11(5):319-330.
46. Katakura Y, Udono M, Katsuki K, et al. Protein kinase C delta plays a key role in cellular senescence programs of human normal diploid cells. J Biochem. 2009;146(1):87-93.
47. Shi A, Murai MJ, He S, et al. Structural insights into inhibition of the bivalent menin-MLL interaction by small molecules in leukemia. Blood. 2012;120(23):4461-4469.
48. Filippakopoulos P, Qi J, Picaud S, et al. Selective inhibition of BET bromodomains. Nature. 2010;468(7327):1067-1073.

Ferrata Storti Foundation

Haematologica 2020
Volume 105(7):1868-1878

Calreticulin exposure on malignant blasts correlates with improved natural killer cell-mediated cytotoxicity in acute myeloid leukemia patients

Iva Truxova,[1] Lenka Kasikova,[1,2] Cyril Salek,[3,4] Michal Hensler,[1] Daniel Lysak,[5] Peter Holicek,[1,2] Pavla Bilkova,[1] Monika Holubova,[6] Xiufen Chen,[7] Romana Mikyskova,[8] Milan Reinis,[8] Marek Kovar,[9] Barbora Tomalova,[9] Justin P. Kline,[7,10,11] Lorenzo Galluzzi,[12,13,14,15,16] Radek Spisek[1,2] and Jitka Fucikova[1,2]

[1]Sotio, Prague, Czech Republic; [2]Department of Immunology, Charles University, 2nd Faculty of Medicine and University Hospital Motol, Prague, Czech Republic; [3]Institute of Hematology and Blood Transfusion, Prague, Czech Republic; [4]Institute of Clinical and Experimental Hematology, 1st Faculty of Medicine, Charles University, Prague, Czech Republic; [5]Department of Hematology and Oncology, University Hospital in Pilsen, Czech Republic; [6]Laboratory of Tumor Biology and Immunotherapy, Biomedical Center, Faculty of Medicine in Pilsen, Charles University, Pilsen, Czech Republic; [7]Department of Medicine, University of Chicago, Chicago, IL, USA; [8]Laboratory of Immunological and Tumour models, Institute of Molecular Genetics of the Czech Academy of Sciences, Prague, Czech Republic; [9]Laboratory of Tumor Immunology, Institute of Microbiology of the Czech Academy of Sciences, Prague, Czech Republic; [10]Committee on Immunology, University of Chicago, Chicago, IL, USA; [11]University of Chicago Comprehensive Cancer Center, Chicago, IL, USA; [12]Department of Radiation Oncology, Weill Cornell Medical College, New York, NY, USA; [13]Sandra and Edward Meyer Cancer Center, New York, NY, USA; [14]Caryl and Israel Englander Institute for Precision Medicine, New York, NY, USA; [15]Department of Dermatology, Yale School of Medicine, New Haven, CT, USA and [16]Universite de Paris, Paris, France

Correspondence:

JITKA FUCIKOVA
fucikova@sotio.com

Received: April 8, 2019.

Accepted: September 26, 2019.

Pre-published: October 3, 2019.

doi:10.3324/haematol.2019.223933

Check the online version for the most updated information on this article, online supplements, and information on authorship & disclosures: www.haematologica.org/content/105/7/1868

ABSTRACT

In some settings, cancer cells responding to treatment undergo an immunogenic form of cell death that is associated with the abundant emission of danger signals in the form of damage-associated molecular patterns. Accumulating preclinical and clinical evidence indicates that danger signals play a crucial role in the (re-)activation of antitumor immune responses *in vivo*, thus having a major impact on patient prognosis. We have previously demonstrated that the presence of calreticulin on the surface of malignant blasts is a positive prognostic biomarker for patients with acute myeloid leukemia (AML). Calreticulin exposure not only correlated with enhanced T-cell-dependent antitumor immunity in this setting but also affected the number of circulating natural killer (NK) cells upon restoration of normal hematopoiesis. Here, we report that calreticulin exposure on malignant blasts is associated with enhanced NK cell cytotoxic and secretory functions, both in AML patients and *in vivo* in mice. The ability of calreticulin to stimulate NK-cells relies on $CD11c^{+}CD14^{high}$ cells that, upon exposure to CRT, express higher levels of IL-15Rα, maturation markers (CD86 and HLA-DR) and CCR7. CRT exposure on malignant blasts also correlates with the upregulation of genes coding for type I interferon. This suggests that $CD11c^{+}CD14^{high}$ cells have increased capacity to migrate to secondary lymphoid organs, where can efficiently deliver stimulatory signals (IL-15Rα/IL-15) to NK cells. These findings delineate a multipronged, clinically relevant mechanism whereby surface-exposed calreticulin favors NK-cell activation in AML patients.

Introduction

In response to some treatments including anthracycline-based chemotherapy, high hydrostatic pressure or radiation therapy, cancer cells mount unsuccessful adaptive responses to stress that are accompanied by the release of endogenous

molecules that convey danger signals, which are cumulatively known as damage-associated molecular patterns (DAMPs).[1-4] The spatiotemporally regulated emission of DAMPs by cells undergoing immunogenic cell death (ICD) generates a pronounced immunostimulatory milieu that, in the presence of adequate antigenicity (such as that conferred to cancer cells by somatic mutations), supports the initiation of tumor-targeting immunity.[2,5] ICD-relevant DAMPs encompass endoplasmic reticulum (ER) chaperones such as calreticulin (CALR, best known as CRT) and heat-shock proteins (HSPs), nuclear components such as high mobility group box 1 (HMGB1), nucleic acids, as well as small metabolites like ATP.[6,7] In physiological scenarios, DAMPs are mostly intracellular, which prevents their detection by the immune system. Conversely, DAMPs that are secreted into the extracellular space or exposed on the plasma membrane of dying cancer cells can be recognized by the immune system via pattern recognition receptors (PRRs), and hence can drive the activation of therapeutically relevant innate and cognate immune responses.[2,8] In line with this notion, DAMP accumulation in the tumor microenvironment has been correlated with increased infiltration by multiple immune cell subsets, including mature dendritic cells (DCs) and effector memory T cells.[9-12] Moreover, factors linked to danger signaling – including (but not limited to) DAMPs expression levels, PRR expression levels, genetic polymorphisms in DAMP- or PRR-coding genes, and activation of relevant stress responses in cancer cells – have been attributed prognostic values in several cohorts of patients with cancer.[13]

Considerable work has been dedicated to elucidate the mechanisms whereby DAMPs affect the phenotype and function of myeloid cells that operate as antigen-presenting cells (APCs).[2,8] On the contrary, little attention has been given to the effects of DAMPs on cells of the innate lymphoid system, such as natural killer (NK) cells, despite the fact that NK cells are emerging as potent players in the control of metastases.[14] Indeed, surface-exposed HSP family A member 1A (HSPA1A, best known as HSP70) promotes NK-cell-dependent cytotoxicity *in vitro*[15,16] and *in vivo*,[17] while exosome-associated HSP70 can stimulate NK-cell migration and effector functions.[18,19] Similarly, extracellular HMGB1 can stimulate NK-cell activity upon binding to Toll-like receptor 2 (TLR2) and TLR4.[20] Here, we report that CRT exposure on the surface of malignant blasts from acute myeloid leukemia (AML) patients is associated with improved NK-cell secretory and cytotoxic functions. Mechanistic studies revealed that surface-exposed CRT stimulates NK-cell activity indirectly, through the upregulation of IL-15Rα on myeloid $CD11c^{+}CD14^{high}$ cells. Moreover, CRT exposure on AML malignant blasts also correlates with the upregulated expression of genes coding for type I interferon (IFN), which are also involved in the capacity of DCs to enhance NK-cell effector functions.

Table 1. Clinical and biological characteristics of acute myeloid leukemia patients.

Variable	Cohort (n=50)
Age at diagnosis	
< 50 years	23 (46%)
≥ 50 years	27 (54%)
Median (years)	52
Range (years)	21-73
Sex	
Male	23 (46%)
Female	27 (54%)
White blood cell count at diagnosis	
< 30.000/mm^3	42 (84%)
≥ 30.000/mm^3	8 (16%)
Median (10^9 cells/L)	6.9
Range (10^9 cells/L)	0-402.8
Blasts in peripheral blood	
Median (%)	25
Range (%)	0-91
De novo AML	41 (82%)
Secondary AML	9 (18%)
FAB classification	
M0	1 (2%)
M1	10 (20%)
M2	12 (26%)
M4	7 (14%)
M5	10 (20%)
M6	1 (2%)
MDS	8 (16%)
Cytogenetic profile	
Favorable	6 (12%)
Intermediate	29 (58%)
Unfavorable	8 (16%)
Missing data	7 (14%)
Molecular characteristics	
FLT3-ITD	7 (14%)
NPM1 mutated	12 (24%)
CEBPA mutated	2 (4%)
Induction chemotherapy	
Daunorubicin + Ara-C (3+7)	38 (76%)
Idarubicin + Ara-C (3+7)	10 (20%)
FLAG + Idarubicin	1 (2%)
Palliative treatment	1 (2%)
CR	40 (80%)
Consolidation	
Chemotherapy only	14 (28%)
HSCT	30 (60%)
No consolidation	6 (12%)

AML: acute myeloid leukemia; AM1-ETO: acute myeloid leukemia 1-ETO fusion protein; CEBPA: CCAAT/enhancer-binding protein alpha; CR: complete remission; FLAG: fludarabine + high-dose cytarabine + granulocyte colony-stimulating factor (G-CSF); FLT3-ITD: fms-like tyrosine kinase 3-internal tandem duplication; HSCT: hematopoietic stem cell transplantation; MDS: myelodysplastic syndrome; NPM1: nucleophosmin 1. FAB: French-American-British.

Methods

Patients

44 patients diagnosed with AML and treated at the Institute of Hematology and Blood Transfusion in Prague between December 2015 and March 2018 plus six AML patients diagnosed and treated at the Department of Hemato-oncology of the Pilsen Hospital between January 2017 and January 2018 were enrolled in this study. Informed consent was obtained according to the Declaration of Helsinki, and the study was approved by the local ethics committee. The main clinical and biological characteristics of the patients are summarized in Table 1. Induction chemotherapy consisted mainly (96%) of seven days cytarabine plus idarubicin or daunorubicin for the first three days (standard "7+3" regimen).

Flow cytometry

Peripheral blood mononuclear cell (PBMCs) isolated from AML patients or C57BL/6 (B6) mice, as well as mouse splenocytes,

bone-marrow derived DCs and tumor cells were stained with panels of fluorescent antibodies to evaluate the abundance, phenotype and function of immune cell subsets (*Online Supplementary Table S1-2*). Briefly, cells were incubated with primary antibodies or appropriate isotype controls for 20 min at 4 °C. For the analysis of CRT levels on AML blasts, PBMCs were labeled with anti-CD45 PerCP (Exbio) and anti-CD33 PE monoclonal antibodies (BioLegend). Malignant blasts from AML patients were defined as $CD45^+$ cells expressing high levels of CD33 ($CD33^{high}$). Surface CRT staining was performed by a three-step procedure: (1) incubation with primary CRT-specific antibody (Enzo Life Sciences), (2) incubation with an APC-conjugated secondary antibody (Jackson Immunoresearch Laboratories) and (3) incubation with Annexin V-FITC (Exbio) and 4′,6-diamidino-2-phenylindole (DAPI, from Molecular Probes) to assess the cell viability. Surface-exposed CRT levels were analyzed only on live ($AnnV^-DAPI^-$) and dying ($AnnV^+/DAPI^-$) but not dead ($DAPI^+$) cells. Flow cytometry data were acquired on the LSRFortessa analyzer (BD Biosciences) and analyzed with the FlowJo software package (Tree Star, Inc.).

Statistical analysis

Survival analyses were performed by using log-rank tests upon patient stratification into two groups based on the median cutoff of continuous variables. Univariate and multivariate Cox proportional hazard analysis was performed to assess the association of clinicopathological or immunological parameters with relapse-free survival (RFS). Variables that were intrinsically correlated were not included in multivariate Cox regressions. Fisher's exact tests, Student's *t*-tests, and the Wilcoxon and Mann-Whitney tests were used to test for association between variables, *P*-values are reported (considered not significant when >0.05).

Results

CRT exposure on malignant blasts is associated with increased NK-cell frequency and upregulation of ligands for activating NK-cell receptors

We previously demonstrated a link between CRT exposure on malignant blasts and clinically-relevant anticancer immunity in AML patients.[10] To extend these findings, we examined the potential impact of CRT on the plasma membrane (ecto-CRT) of $CD45^+CD33^+$ malignant blasts on the frequency and phenotype of NK cells from AML patients prior to the initiation of anthracycline-based chemotherapy and at the recovery of normal hematopoiesis. Patients were stratified based on the median percentage of $DAPI^-$ecto-CRT^+ blasts at diagnosis into a CRT^{Hi} and CRT^{Lo} group. In baseline conditions (prior to induction chemotherapy), we were unable to identify statistically significant differences in the frequency and absolute numbers of circulating $CD45^+CD3^-CD56^+$ NK cells between these two groups of patients (Figure 1A-B). Conversely, upon complete remission and recovery of nonmalignant hematopoiesis, CRT^{Hi} AML patients had significantly higher frequency and absolute numbers of $CD45^+CD3^-CD56^+$ NK cells in the circulation as compared to their CRT^{Lo} counterparts (Figure 1A-B). These results are in line with previously published data from our group.[10] Of note, CRT^{Hi} AML patients did not display increased frequency of $CD45^+CD3^-CD56^+$ NK cells in the bone marrow as compared to their CRT^{Lo} counterparts (*Online Supplementary Figure S1A*).

As NK-cell activation is modulated by the balance between stimulatory and inhibitory signals delivered by multiple ligand/receptor interactions,[14] we next analyzed the levels of common activating (NKp30, NKp46, NKp80, NKG2D, DNAM-1 and CD16) and inhibitory (CD158e1, CD158bj, CD158ah, NKG2A, ILT2) NK-cell receptors by flow cytometry. With the exception of $ILT2^+$ cells (which were less represented in the circulation of CRT^{Hi} AML patients upon remission), we failed to detect significant differences in the percentage of NK cells staining positively for these receptors between CRT^{Hi} and CRT^{Lo} AML patients, neither prior to induction chemotherapy nor upon complete remission (Figure 1C and *Online Supplementary Figure S1B*). Because CRT exposure relies on ER stress responses,[21] and different stress response pathways may also modulate the expression of ligands for NK-cell receptors,[22] we decided to evaluate the potential connection between CRT exposure and the levels of multiple NK-cell ligands on the surface of $CD45^+CD33^+$ blasts, namely major histocompatibility complex (MHC) class I polypeptide-related sequence A (MICA), MICB, UL16 binding protein 2 (ULBP2), ULBP5, ULBP6, poliovirus receptor (PVR, also known as CD155), nectin cell adhesion molecule 2 (NECTIN2, also known as CD112 and PVRL2), and B7-H6, by flow cytometry. We found that the percentage of $DAPI^-$ecto-CRT^+ blasts positively correlates with the percentage of AML blasts staining positively for MICA, MICB, CD155 and CD112 (Figure 1D). In the attempt to identify a potential connection between the exposure of NK-cell-activating ligands (NKALs) and ER stress, we retrieved normalized *MICA, ULBP2, PVR* and *NECTIN2* expression levels for 173 AML patients from The Cancer Genome Atlas (TCGA) public database and analyzed their correlation with the expression levels of genes involved in the ER stress response, namely activating transcription factor 4 (*ATF4*), DNA damage inducible transcript 3 (*DDIT3*) and HSP family A (Hsp70) member 5 (*HSPA5*). However, linear regression analysis showed limited degrees of correlation (*Online Supplementary Figure S1C*), suggesting the involvement of other stress response mechanisms in the exposure of NKALs by malignant blasts. Altogether, these findings indicate that malignant blasts from AML patients display different danger signals on their surface, and this influences the abundance of circulating NK cells.

CRT exposure on malignant blasts correlates with improved NK-cell effector functions in AML patients in remission

Since the ability of surface-exposed CRT to deliver activatory signals to NK cells had not been previously investigated, we set out to address this possibility. To this aim, we evaluated degranulation and IFN-γ production by NK cells from CRT^{Hi} and CRT^{Lo} AML patients upon non-specific stimulation with phorbol 12-myristate 13-acetate (PMA) and ionomycin by flow cytometry (*Online Supplementary Figure S1D*). We failed to detect statistically significant differences in the frequency of NK cells responding to stimulation with IFN-γ production ($IFN\text{-}\gamma^+CD45^+CD3\text{-}CD56^+$ cells) and degranulation ($CD107a^+GZMB^+CD45^+CD3^-CD56^+$ cells) between CRT^{Hi} and CRT^{Lo} AML patients prior to induction chemotherapy (Figure 2A). On the contrary, upon remission and recovery of non-malignant hematopoiesis, CRT^{Hi} patients exhibited significantly improved NK-cell secretory and cytotoxic effector functions compared to

their CRT^{Lo} counterparts (Figure 2B). To evaluate NK-cell effector functions in a more direct manner, we also performed NK-cell cytotoxicity assays using NK cell-sensitive human chronic myelogenous leukemia K562 cells as targets. In general, NK cells isolated from AML patients at recovery had slightly higher cytotoxic functions than NK cells isolated from AML patients prior to induction chemotherapy (Figure 2C). Importantly, while surface-exposed CRT failed to affect the ability of NK cells isolated from AML patients prior to the initiation of treatment

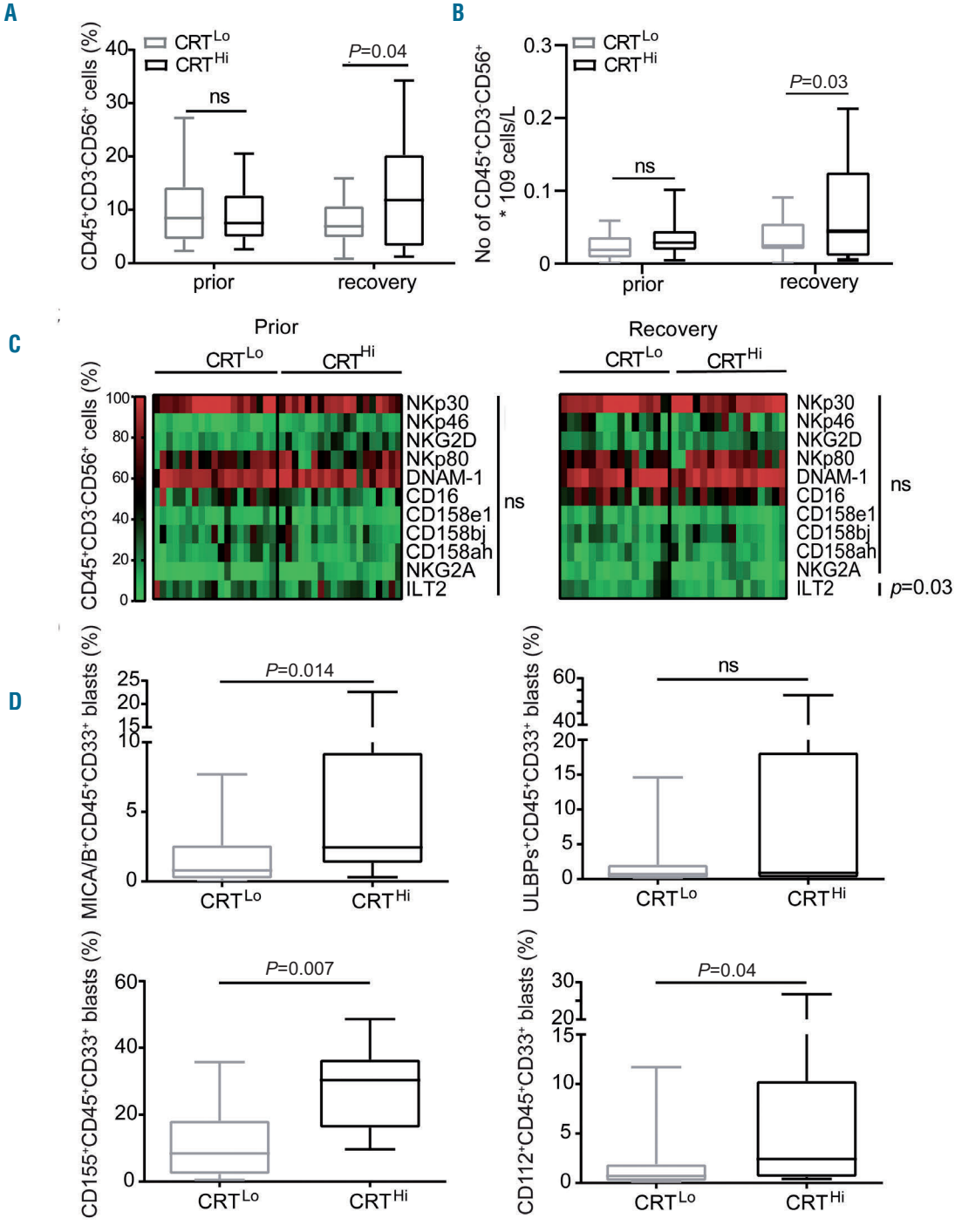

Figure 1. The impact of ecto-CRT on natural killer (NK) cells and the levels of NK-cell ligands present on acute myeloid leukemia blasts. (A) The percentage and (B) absolute numbers of circulating CD45$^+$CD3$^-$CD56$^+$ NK cells in CRT^{Hi} *versus* CRT^{Lo} acute myeloid leukemia (AML) patients before the induction chemotherapy (Prior, n=45) and at re-establishment of normal hematopoiesis (recovery, n=37) determined by flow cytometry. Boxplots: lower quartile, median, upper quartile; whiskers, minimum, maximum; ns: not significant. (C) The frequency of CD45$^+$CD3$^-$CD56$^+$ NK cells staining positively for different NK cell receptors (namely NKp30, NKp46, NKG2D, NKp80, DNAM-1, CD16, CD158e1, CD158bj, CD158ah, NKG2A and ILT2) in CRT^{Hi} and CRT^{Lo} AML patients before the induction chemotherapy (prior, n=38) and at re-establishment of normal hematopoiesis (recovery, n=31) determined by flow cytometry. ns: not significant. (D) The percentage of CD45$^+$CD33$^+$ blasts staining positively for NK cell ligands (MICA/B, ULBP, CD155 and CD112) in CRT^{Hi} *versus* CRT^{Lo} AML patients prior to the induction chemotherapy (n=21) determined by flow cytometry. Boxplots: lower quartile, median, upper quartile; whiskers, minimum, maximum; ns: not significant. CRT: calreticulin.

to efficiently kill K562 cells (Figure 2D), CRT^{Hi} patients in remission possessed NK cells with superior cytotoxic functions compared to their CRT^{Lo} counterparts (Figure 2E). These data are consistent with the results reported above (Figure 2A-B).

Surface-exposed CRT influences NK-cell effector functions indirectly, by affecting the phenotype of CD11c^{+}CD14^{high} cells

To further evaluate the impact of surface-exposed CRT on NK cells and the mechanisms underlying its NK cell-stimulatory effects, we performed a set of *in vitro* experiments with recombinant CRT (rCRT). Pre-incubation of purified NK cells with rCRT did not affect the capacity of NK cells to release cytotoxic granules containing perforin 1 (PRF1) or secrete IFN-γ in response to either nonspecific stimulation with PMA and ionomycin or exposure to K562 cells (Figure 3A and *Online Supplementary Figure 2A*). Conversely, adding rCRT to whole PBMCs led to significant increase in the percentage of CD45^{+}CD3^{-}CD56^{+} NK cells degranulating in response to PMA plus ionomycin or exposure to K562 cells (Figure 3B), with no effects on IFN-γ secretion (Online Supplementary Figure S2B). We confirmed these results with NK-cell cytotoxicity assays, as

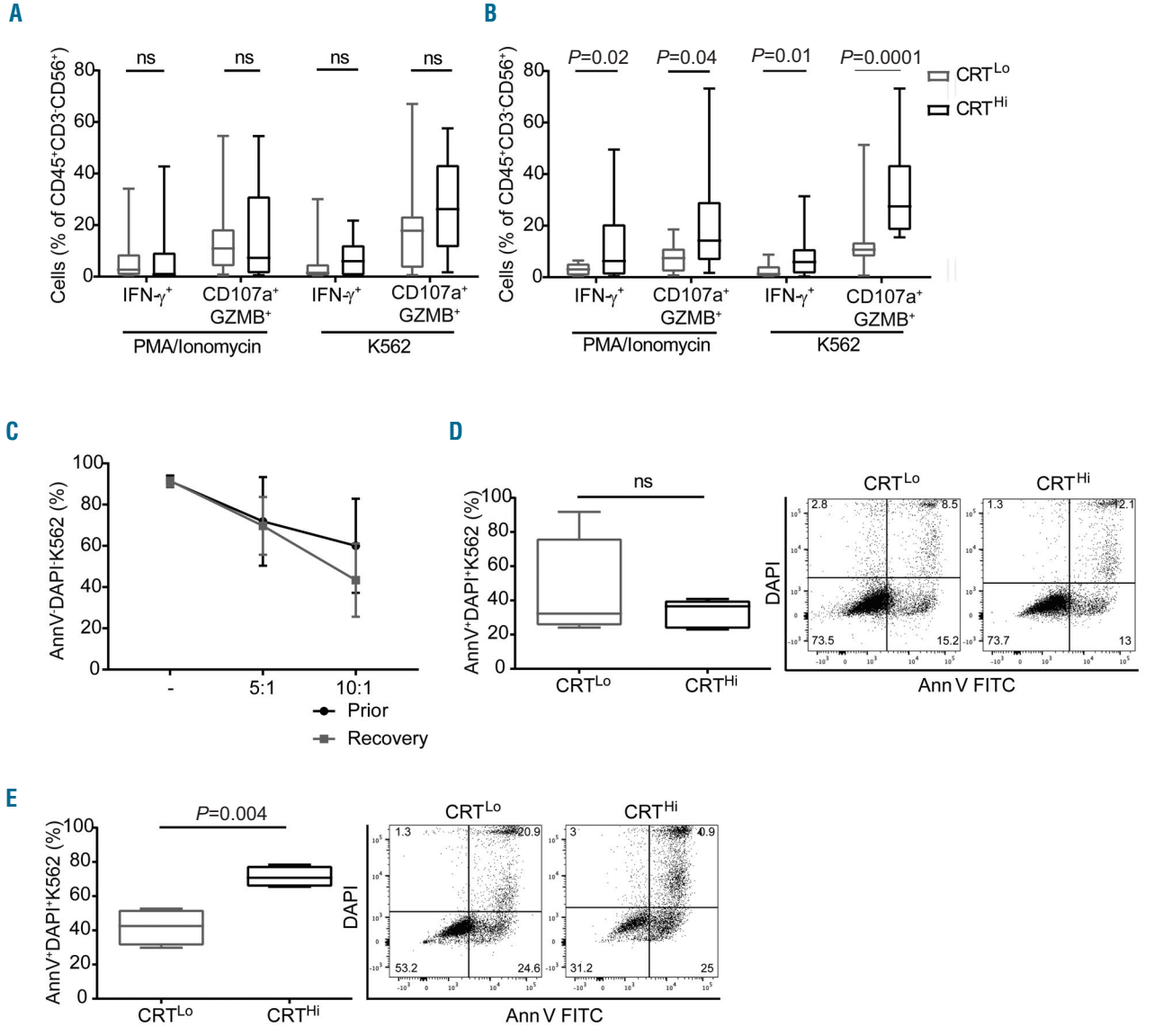

Figure 2. The impact of ecto-CRT on the activation and cytotoxic potential of natural killer cells in acute myeloid leukemia patients. (A, B) The percentage of IFN-γ and degranulating (CD107a^{+}/GZMB^{+}) CD45^{+}CD3^{-}CD56^{+} natural killer (NK) cells upon PMA + Ionomycin or K562 cell line stimulation in 17 CRT^{Lo} and 18 CRT^{Hi} acute myeloid leukemia (AML) patients prior to the induction chemotherapy (A) or in 12 CRT^{Lo} and 12 CRT^{Hi} AML patiens after the restoration of normal hematopoiesis (B). Patient samples were analyzed by flow cytometry. Box plots: lower quartile, median, upper quartile; whiskers, minimum, maximum; ns: not significant. (C) Cytotoxic potential of NK cells isolated from AML patients before the initiation of chemotherapy (Prior, n=10) versus upon the restoration of normal hematopoiesis (Recovery, n=10). Purified NK cells were tested for their ability to kill target K562 cell line at two different effector:target cell ratios (5:1 and 10:1) and the viability of K562 cells was determined by flow cytometry after 4 hours (h). (D, E) Cytotoxic potential of NK cells isolated from five CRT^{Hi} and 5 CRT^{Lo} AML patients before the initiation of chemotherapy (D) or upon the restoration of normal hematopoiesis (E). Purified NK cells were tested for their ability to kill target K562 cell line at effector:target cell ratio 5:1 and the percentage of dead (AnnV^{+}DAPI^{+}) K562 cells was determined by flow cytometry after 4 h. The representative dot plots of NK cell cytotoxicity assay showing the viability of target K562 cells in CRT^{Hi} *versus* CRT^{Lo} AML patients before the initiation of chemotherapy (D) or upon the restoration of normal hematopoiesis (E) are shown. Box plots: lower quartile, median, upper quartile; whiskers, minimum, maximum; ns: not significant. CRT: calreticulin.

NK cells isolated from PBMCs pre-incubated with rCRT were able to kill an increased amount of K562 cells compared to NK cells isolated from control PBMC (Figure 3B). These results suggest that CRT stimulate NK cells indirectly, via mechanisms that involve other cellular components of the PBMC mixture.

Previous *in vitro* studies support a role for APCs, mainly DCs, in NK-cell activation.[23] We therefore decided to focus on the phenotype of APCs exposed to rCRT. We found that incubating PBMCs from healthy donors (HD) with rCRT induced the upregulation of the chemotaxis-associated receptor C-C motif chemokine receptor 7 (CCR7) and the maturation-associated molecules CD86 and HLA-DR on $CD11c^{+}CD14^{high}$ cells and increased the frequency of $CD11c^{+}CD14^{high}$ expressing interleukin 15 receptor subunit alpha (IL15RA, best known as IL-15Rα) (Figure 3C),which is crucial for the activatory trans-presentation of IL-15 to NK cells.[24] Inspired by these data, we investigated the relationship between CRT exposed on malignant blasts and the phenotype of APCs in AML patients in remission. We found that CRT^{Hi} patients harbor a significantly higher percentage of $CD11c^{+}CD14^{high}$ cells expressing CCR7 and IL-15Rα compared to their CRT^{Lo} counterparts (Figure 3D), suggesting that these cells have an increased capacity to migrate to secondary lymphoid organs, where they can efficiently activate NK cells. In vitro assays suggested a prominent role for human myeloid over plasmocytoid DCs in NK-cell activation upon exposure to rCRT (*Online Supplementary Figure S3A*). Of note, also mouse PBMCs or bone marrow-derived DCs exposed to rCRT upregulated activation markers including CD54, CD86, and MHC class II molecules, and secreted increased amounts of IL-12 (*Online Supplementary Figure S3B-D*).

We have previously shown that the PMBCs of CRT^{Hi} AML patients who are in complete remission and have

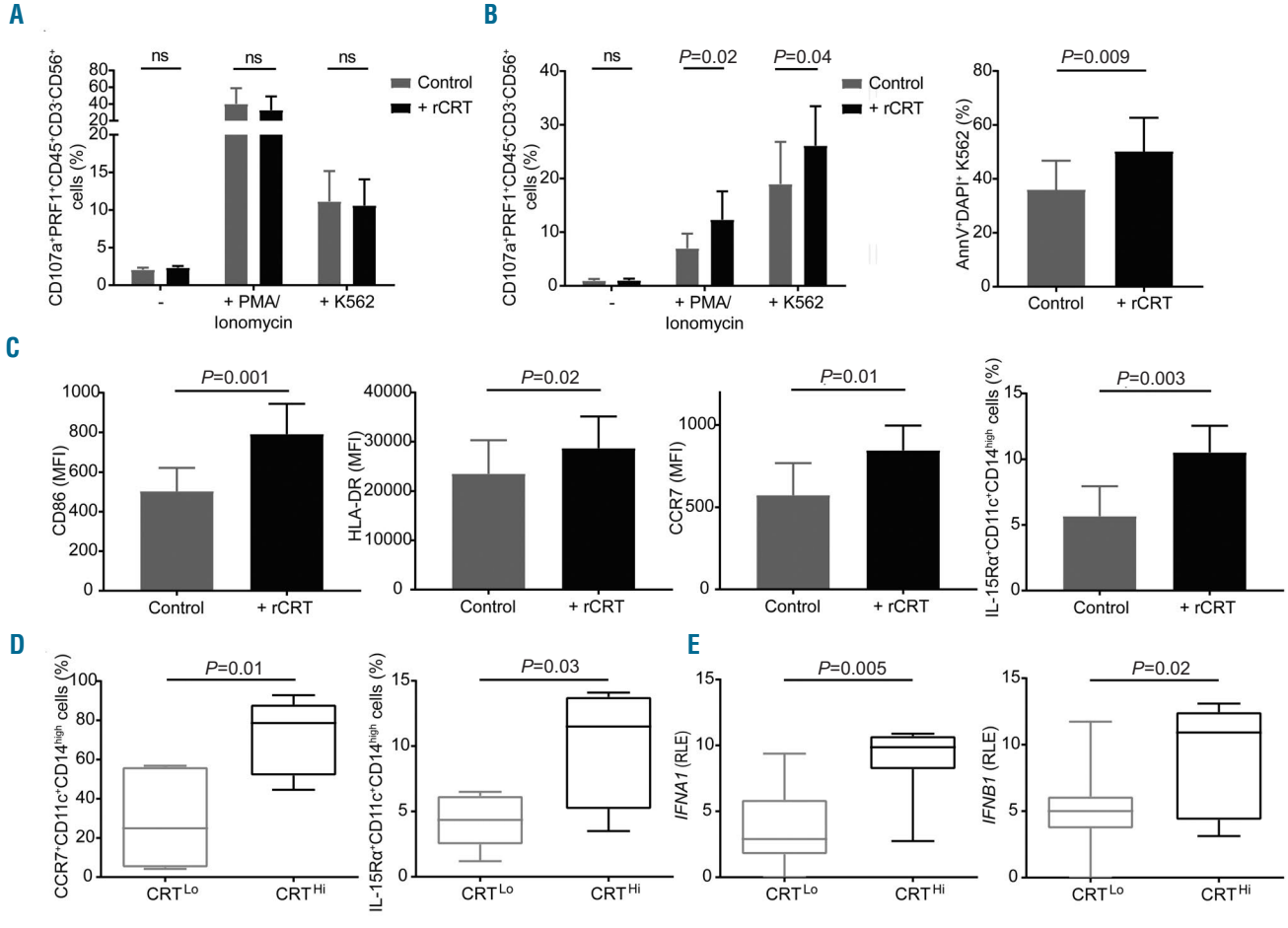

Figure 3. The mechanism of natural killer cell-stimulatory effects of calreticulin and its impact on $CD11c^{+}CD14^{high}$ cell phenotype. (A, B) The effect of recombinant human calreticulin (rCRT, Sino Biological Inc.) on effector functions of natural killer (NK) cells isolated from healthy donors (HDs) (n=8) or NK cells in HD peripheral blood mononuclear cells (PBMC) mixture (n=8). Purified NK cells (A) or whole PBMC (B) were pre-incubated with 5 μg/mL of rCRT overnight and subsequently stimulated by PMA + Ionomycin or K562 cell line for 4 hours (h). The percentage of responding ($CD107a^{+}PRF1^{+}CD45^{+}CD3^{-}CD56^{+}$) NK cells was determined by flow cytometry. Alternatively, NK cells were purified from rCRT-pre-incubated PBMC and their capacity to kill K562 cell line was tested in cytotoxicity assay. The percentage of dead ($AnnV^{+}DAPI^{+}$) K562 cells was determined by flow cytometry after 4 h (B). NK cells/PBMCs without rCRT and unstimulated NK cells/PBMC were used as a negative controls; ns: not significant. (C) The expression of maturation-associated molecules (CD86 and HLA-DR) and CCR7 on $CD11c^{+}CD14^{high}$ cells in HD PBMCs (n=8) incubated with rCRT (5 μg/mL) overnight *versus* control PBMCs without rCRT as determined by flow cytometry. The expression of individual markers is shown as mean fluorescence intensity (MFI). Flow cytometry was also used for the detection of $IL\text{-}15R\alpha^{+}CD11c^{+}CD14^{high}$ cells in rCRT-pre-incubated *versus* control PBMCs. (D) The frequency of CCR7+ and $IL\text{-}15R\alpha^{+}CD11c^{+}CD14^{high}$ cells in CRT^{Hi} *versus* CRT^{Lo} AML patients upon the restoration of normal hematopoiesis (n=16) determined by flow cytometry. Boxplots: lower quartile, median, upper quartile; whiskers, minimum, maximum. (E) Quantitative RT-PCR-assisted quantification of IFNA1 and IFNB1 expression levels in PBMCs from 20 CRT^{Hi} *versus* 21 CRT^{Lo} acute myeloid leukemia (AML) patients at recovery of normal hematopoiesis. Boxplots: lower quartile, median, upper quartile; whiskers, minimum, maximum.

recovered normal, non-malignant hematopoiesis exhibit a remarkable upregulation of genes linked to T_H1 polarization, T-cell activation and cytotoxic immune responses.[10] To confirm and extend these findings, we assessed the expression levels of 46 genes linked to immune function, with particular focus on NK-cell activity, in the PBMCs of 37 AML patients in remission (*Online Supplementary Table S3*). We identified five genes that were differentially expressed in CRT^{Hi} *versus* CRT^{Lo} patients, namely, *IFNA1, IFNB1, CD3E, CD8A* and *CD28* (Figure 3E and *Online Supplementary Figure S4A*). Importantly, type I IFN including the products of *IFNA1* and *IFNB1* are also involved in the capacity of DCs to enhance NK-cell effector functions (23).

Taken together, our results suggest that CRT exposure on the surface of malignant blasts stimulates NK-cell effector functions indirectly, by altering the migratory capacity, surface phenotype, and secretory profile of $CD11c^{+}CD14^{high}$ APCs.

CRT exposure is associated with increased NK- and T-cell responses in mice

To examine the impact of surface-exposed CRT on anticancer immunity *in vivo*, we generated subcutaneous tumors in B6 mice with mouse wild-type (WT) AML C1498 cells (C1498.WT) or C1498 cells constitutively exposing CRT on the plasma membrane (C1498.CRT), and monitored disease progression (*data not shown*) and immune responses. T-cell response was analyzed both in the tumor and spleen (19 days after tumor cell injection) and NK-cell response only in spleen (three days after tumor cell injection) (Figure 4A). Importantly, developing C1498.CRT tumors resulted in an enrichment of activated $CD107a^{+}$ NK cells (defined as $CD45^{+}CD3^{-}NK1.1^{+}$ cells) in the spleen, and enhanced the capacity of NK cells to respond to PMA plus ionomycin stimulation (Figure 4B). In addition, we observed that C1498.CRT tumors are infiltrated by $CD4^{+}$and $CD8^{+}$ T cells with improved effector functions in response to non-specific stimulation with

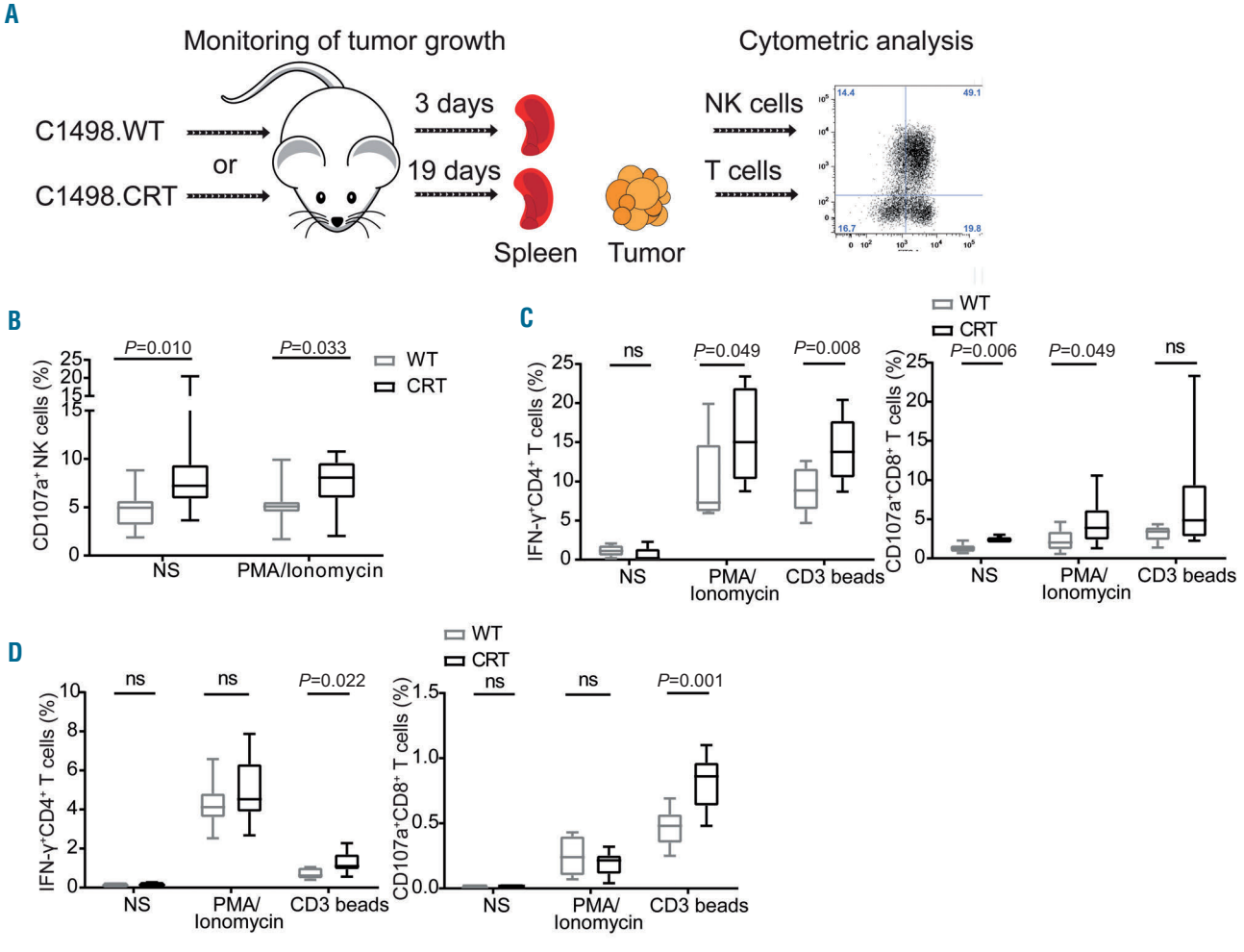

Figure 4. The role of calreticulin in natural killer-cell- and T-cell-based immune response *in vivo* in mice. (A) Schematic representation showing the process of C1498.WT/CRT tumor generation and monitoring the immune responses. To generate tumors *in vivo*, $1x10^6$ C1498.WT or C1498.CRT cells were inoculated sub cutaneoulsy into the lower right flank of B6 mice on day 0 (D0). Tumor size was measured every two days by standard laboratory caliper. Mice were sacrificed on D3 or D19 and spleen and tumors were harvested for analysis of functional status of natural killer (NK) cells (spleen on D3) and T cells (both spleen and tumors on D19) by flow cytometry. The experiment was performed three times. (B) The frequency of $CD107a^{+}$ NK cells (defined as $CD45^{+}CD3^{-}NK1.1^{+}$ cells) in spleen harvested from mice injected with C1498.CRT *versus* C1498.WT without further *in vitro* stimulation or upon stimulation with PMA + Ionomycin determined by flow cytometry. Box plots: lower quartile, median, upper quartile; whiskers, minimum, maximum. (C, D) The frequency of activated IFN-$\gamma^{+}CD4^{+}$ T cells and $CD107a^{+}$ $CD8^{+}$ T cells upon *in vitro* PMA + Ionomycin or anti-CD3 bead stimulation in C1498.CRT *versus* C1498.WT tumors (C) or spleen (D) determined by flow cytometry. Unstimulated cells were used as a controls. Box plots: lower quartile, median, upper quartile; whiskers, minimum, maximum; ns: not significant. WT: wild-type.

PMA plus ionomycin and/or anti-CD3 beads (Figure 4C). Similarly, splenocytes isolated from C1498.CRT-bearing mice contained $CD4^+$ and $CD8^+$ T cells that were more responsive to stimulation than their counterparts from C1498.WT-bearing mice (Figure 4D).

In line with this notion, PBMCs from CRT^{Hi} AML patients in complete remission contained significantly higher frequencies of both $CD8^+$ and $CD4^+$ T cells responding by IFN-γ secretion to PMA plus ionomycin (*Online Supplementary Figure S4B-C*), with a slightly subsignificant trend towards increased numbers of $CD107a^+GZMB^+CD8^+$ T cells (*Online Supplementary Figure S4D*), compared with their CRT^{Lo} counterparts, comforting previously published data from our group.[10] Quantification of several cytokines essential for NK-cell homeostasis and functions (IL-21, IL-15, IFN-γ and IFN-α2) and for hematopoietic stem cell (HSC) differentiation (IL-3 and IL-7) in the sera of AML patients in remission also revealed higher IFN-γ levels in CRT^{Hi} *versus* CRT^{Lo} patients (*Online Supplementary Figure S4E*).

CRT exposure on malignant blasts and the frequency of NKG2D$^+$ cells correlate with RFS in AML patients

To evaluate the prognostic impact of CRT exposure on malignant blasts and verify our previous results on a larger subgroup of our patients,[10] we investigated RFS upon stratifying AML patients based on the median percentage of $DAPI^-$ blasts staining positively for surface CRT. In line with our previous observations,[10] CRT^{Hi} patients exhibited a significantly improved RFS compared with CRT^{Lo} patients (median: >60 *vs.* 14 months, P=0.027) (Figure 5A). Using a similar cutoff approach based on the median value, we also examined whether the mRNA levels of *KLRK1*, encoding the key NK-cell activating receptor NKG2D, would convey prognostic information in AML patients. We found that patients expressing high levels of *KLRK1* ($KLRK1^{Hi}$) had a significantly lower risk of relapse compared to their $KLRK1^{Lo}$ counterparts (median: 39 *vs.* 10 months, P=0.039) (Figure 5B). We validated these findings at the protein level by stratifying a larger group of patients based on the median frequency of $CD45^+CD3^-CD56^+NKG2D^+$ NK cells. Patients with a high frequency of NK cells expressing NKG2D ($NKG2D^{Hi}$) exhibited significantly improved RFS, compared with their $NKG2D^{Lo}$ counterparts (median: >35 *vs.* 24 months, P=0.035) (Figure 5C). However, neither univariate nor multivariate Cox proportional hazard analysis confirmed these findings, potentially reflecting a limited follow-up of this prospectively collected patient cohort, or other confounding factors including disease subtype and inter-individual heterogeneity (Table 2-3). Since both CRT exposure on malignant blasts and NKG2D levels influenced RFS in our cohort of AML patients, we evaluated the combined prognostic value of ecto-CRT^+ blasts and the *KLRK1* mRNA levels or $CD45^+CD3^-CD56^+NKG2D^+$ NK-cell frequency by stratifying the cohort in three groups: CRT^{Hi}/$KLRK1^{Hi}$ or CRT^{Hi}/$NKG2D^{Hi}$ patients, CRT^{Lo}/$KLRK1^{Lo}$ or CRT^{Lo}/$NKG2D^{Lo}$ patients and patients in which the percentage of CRT^+ blasts was discordant with the *KLRK1* mRNA levels or the frequency of $CD45^+CD3^-CD56^+NKG2D^+$ NK cells (CRT/$KLRK1^{Mix}$ or CRT/$NKG2D^{Mix}$). We found that CRT^{Hi}/$KLRK1^{Hi}$ or CRT^{Hi}/$NKG2D^{Hi}$ patients had superior RFS as compared with their CRT^{Lo}/$KLRK1^{Lo}$ or CRT^{Lo}/$NKG2D^{Lo}$ counterparts (CRT^{Hi}/$KLRK1^{Hi}$ *vs.* CRT^{Lo}/$KLRK1^{Lo}$, P=0.050; CRT^{Hi}/$NKG2D^{Hi}$ *vs.* CRT^{Lo}/$NKG2D^{Lo}$, P=0.037) (Figure 5D-E).

Discussion

CRT exposure on cancer cells conveys robust prognostic information in patients with a variety of malignancies, generally reflecting the activation of clinically-relevant tumor-targeting immune responses.[13] Previous work from our group demonstrated that the presence of CRT on the surface of malignant blasts from AML patients correlates not only with an increased frequency of effector memory $CD4^+$ and $CD8^+$ T cells but also with an increased proportion of circulating NK cells, suggesting that CRT exposure is linked to both adaptive and innate immunity.[10] Inspired by accumulating evidence on the key role of NK cells in natural and therapy-driven immunosurveillance,[25-29] we decided to extend these initial observations and characterize the link between surface-exposed CRT and NK-cell activity in AML patients. Indeed, NK cells from patients with high CRT exposure on malignant blasts exhibited improved secretory and cytotoxic effector functions (Figure 2B and E).

As we excluded the possibility that CRT would mediate direct immunostimulatory effects on NK cells (Figure 3A and *Online Supplementary Figure S2A*), we thought that CRT exposure would be linked to increased levels of NKALs on the surface of malignant blasts, because both these processes have been linked to intracellular ER stress signaling.[30] Indeed, the percentage of $CD45^+CD33^+$ malignant blasts staining positively for ecto-CRT^+ correlated with the frequency of blasts staining positively for various NKALs (Figure 1D). However, we were unable to document any correlation between the NKAL expression levels and mRNA abundance of genes involved in the ER stress response (which we and others previously demonstrated to constitutively occur in AML blasts independent of therapy)[10,12] (*Online Supplementary Figure S1C*). These findings suggest that NKALs and CRT are exposed on the surface of AML blasts *via* mechanistically distinct stress response pathways. Replication stress and the consequent DNA damage response stand out as a promising candidate for NKAL exposure in this setting.[30]

We also found that NK-cell activation by CRT involves a population of $CD11c^+CD14^{high}$ cells that, upon exposure to CRT, express maturation markers (CD86 and HLA-DR), acquires improved migratory capacity as a consequence of CCR7 expression, and delivers stimulatory signals to NK cells via IL-15Rα/IL-15 trans-presentation[24] and type I IFN. Consistent observations in peripheral blood of HDs and AML patients, suggest that $CD11c^+CD14^{high}$ cells exposed to CRT have a superior capacity to migrate to secondary lymphoid organs where they can efficiently activate NK cells (Figure 3C-E). Thus, surface-exposed CRT appears to trigger the phenotypic and functional maturation of $CD11c^+CD14^{high}$ cells leading to (i) cell contact-dependent NK-cell activation via trans-presented IL-15, as well as (ii) cell contact-independent NK-cell activation via type I IFNs. Importantly, type I IFN signaling in DCs results not only in a superior ability to drive antigen-specific T-cell priming,[31] but also in IL-15 production,[32] potentially supporting a robust adaptive and innate immune response of therapeutic relevance. Our findings and elegant preclinical data from Chen and colleagues[10,33] lend robust support to

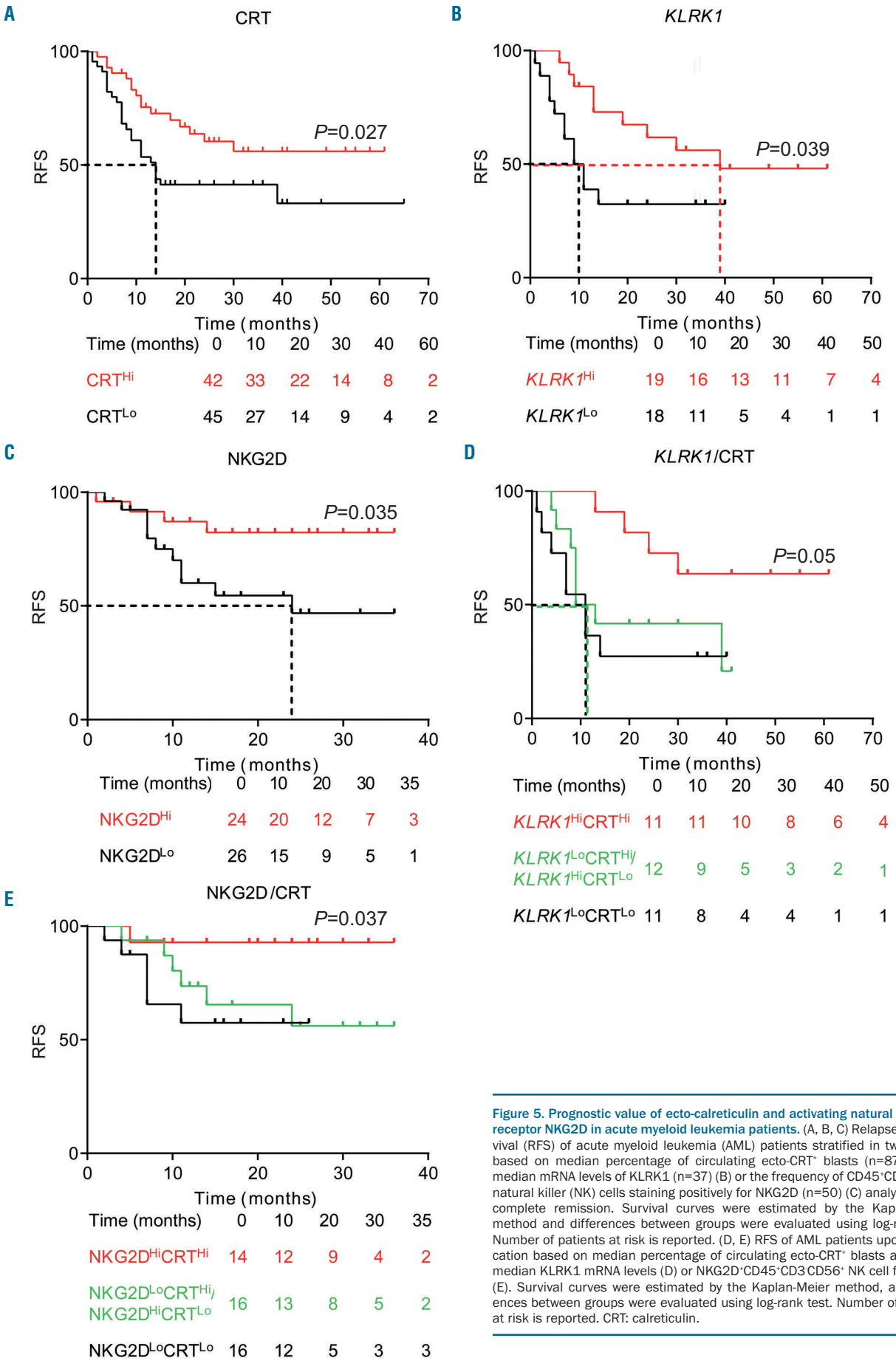

Figure 5. Prognostic value of ecto-calreticulin and activating natural killer cell receptor NKG2D in acute myeloid leukemia patients. (A, B, C) Relapse-free survival (RFS) of acute myeloid leukemia (AML) patients stratified in two groups based on median percentage of circulating ecto-CRT$^+$ blasts (n=87) (A), on median mRNA levels of KLRK1 (n=37) (B) or the frequency of CD45$^+$CD3$^-$CD56$^+$ natural killer (NK) cells staining positively for NKG2D (n=50) (C) analyzed upon complete remission. Survival curves were estimated by the Kaplan-Meier method and differences between groups were evaluated using log-rank test. Number of patients at risk is reported. (D, E) RFS of AML patients upon stratification based on median percentage of circulating ecto-CRT$^+$ blasts along with median KLRK1 mRNA levels (D) or NKG2D$^+$CD45$^+$CD3$^-$CD56$^+$ NK cell frequency (E). Survival curves were estimated by the Kaplan-Meier method, and differences between groups were evaluated using log-rank test. Number of patients at risk is reported. CRT: calreticulin.

Table 2. Univariate Cox proportional hazard analysis.

Variable	RFS HR (95% CI)	RFS P
Age	1.02 (0.99-1.04)	0.19
Sex	0.79 (0.44-1.43)	0.45
Peripheral blast counts	1.00 (0.99-1.01)	0.26
HSCT	0.76 (0.40-1.44)	0.40
Ecto-CRT^{+} blasts (%)	0.99 (0.98-1.00)	0.22
KLRK1 expression	0.80 (0.53-1.19)	0.27
NKG2D^{+} NK cells (%)	0.96 (0.92-1.01)	0.13

CI, 95% confidence interval; HR, hazard ratio; *p< 0.05; RFS, relapse-free survival.

Table 3. Multivariate Cox proportional hazard analysis.

Variable	RFS HR (95% CI)	RFS P
Age	1.07 (1.01-1.13)	0.007*
Sex	1.34 (0.50-3.60)	0.55
Peripheral blast counts	1.00 (0.98-1.02)	0.71
HSCT	0.62 (0.21-1.83)	0.39
Ecto-CRT^{+} blasts (%)	0.98 (0.96-1.00)	0.10
KLRK1 expression	0.69 (0.44-1.07)	0.10
NKG2D^{+} NK cells (%)	0.95 (0.90-1.01)	0.11

CI, 95% confidence interval; HR, hazard ratio; *p< 0.05; RFS, relapse-free survival.

this possibility. Indeed, *in vivo* application of C1498 AML cells engineered to constitutively expose CRT on their surface elicited an accumulation of highly functional NK cells and CD4^{+} and CD8^{+} T cells in mouse tumors and/or spleen (Figure 4B-D).

Finally, both CRT exposure on malignant blasts and NK cell-related marker NKG2D were associated with improved RFS amongst AML patients (Figure 5A-C), corroborating previously published data.[10,34] Combinatorial assessment of the prognostic value of these parameters identified significantly prolonged RFS in KLRK1^{Hi}CRT^{Hi} and NKG2D^{Hi}CRT^{Hi} subgroup of patients (Figure 5D-E). However, these findings could not be confirmed using univariate and multivariate Cox proportional hazard analysis, potentially reflecting a limited follow-up period, the small size of the patient cohort, disease subset and/or inter-patient heterogeneity. Thus, the precise prognostic value of CRT exposure on AML blasts and NKGD2 levels on NK cells remains to be validated in independent patient series.

Taken together, our results support the association of CRT with enhanced activation of the innate and adaptive anticancer immunity. Parallel assessment of CRT exposure on malignant blasts and immune cell parameters, such as NK-cell markers, may provide prognostic information and have therapeutic relevance for AML patients in the future.

Funding

This study was exclusively sponsored by Sotio, Prague, Czech Republic.

Acknowledgments

The authors thank Anna Fialova for her valuable help with statistical analysis and to Jana Bieblova for help with FACS and ELISA analysis. LG is supported by a Breakthrough Level 2 grant from the US Department of Defense (DoD), Breast Cancer Research Program (BRCP) (#BC180476P1), by the 2019 Laura Ziskin Prize in Translational Research (#ZP-6177, PI: Formenti) from the Stand Up to Cancer (SU2C), by a Mantle Cell Lymphoma Research Initiative (MCL-RI, PI: Chen-Kiang) grant from the Leukemia and Lymphoma Society (LLS), by a startup grant from the Dept. of Radiation Oncology at Weill Cornell Medicine (New York, NY, USA), by a Rapid Response Grant from the Functional Genomics Initiative (York, NY, USA), by industrial collaborations with Lytix (Oslo, Norway) and Phosplatin (York, NY, USA), and by donations from Phosplatin (York, NY, USA), the Luke Heller TECPR2 Foundation (Boston, USA) and Sotio a.s. (Prague, Czech Republic).

References

1. Fucikova J, Moserova I, Truxova I, et al. High hydrostatic pressure induces immunogenic cell death in human tumor cells. Int J Cancer. 2014;135(5):1165-1177.
2. Galluzzi L, Buque A, Kepp O, Zitvogel L, Kroemer G. Immunogenic cell death in cancer and infectious disease. Nat Rev Immunol. 2017;17(2):97-111.
3. Spisek R, Charalambous A, Mazumder A, Vesole DH, Jagannath S, Dhodapkar MV. Bortezomib enhances dendritic cell (DC)-mediated induction of immunity to human myeloma via exposure of cell surface heat shock protein 90 on dying tumor cells: therapeutic implications. Blood. 2007;109(11):4839-4845.
4. Vanpouille-Box C, Demaria S, Formenti SC, Galluzzi L. Cytosolic DNA sensing in organismal tumor control. Cancer Cell. 2018;34(3):361-378.
5. Galluzzi L, Chan TA, Kroemer G, Wolchok JD, Lopez-Soto A. The hallmarks of successful anticancer immunotherapy. Sci Transl Med. 2018;10(459).
6. Garg AD, Vandenberk L, Fang S, et al. Pathogen response-like recruitment and activation of neutrophils by sterile immunogenic dying cells drives neutrophil-mediated residual cell killing. Cell Death Differ. 2017;24(5):832-843.
7. Mehta MM, Weinberg SE, Chandel NS. Mitochondrial control of immunity: beyond ATP. Nat Rev Immunol. 2017;17(10):608-620.
8. Krysko DV, Garg AD, Kaczmarek A, Krysko O, Agostinis P, Vandenabeele P. Immunogenic cell death and DAMPs in cancer therapy. Nat Rev Cancer. 2012;12(12):860-875.
9. Fucikova J, Becht E, Iribarren K, et al. Calreticulin Expression in human non-small cell lung cancers correlates with Increased accumulation of antitumor immune cells and favorable prognosis. Cancer Res. 2016;76(7):1746-1756.
10. Fucikova J, Truxova I, Hensler M, et al. Calreticulin exposure by malignant blasts correlates with robust anticancer immunity and improved clinical outcome in AML patients. Blood. 2016;128(26):3113-3124.
11. Peng RQ, Chen YB, Ding Y, et al. Expression of calreticulin is associated with infiltration of T-cells in stage IIIB colon cancer. World J Gastroenterol. 2010;16(19):2428-2434.
12. Wemeau M, Kepp O, Tesniere A, et al. Calreticulin exposure on malignant blasts predicts a cellular anticancer immune response in patients with acute myeloid leukemia. Cell Death Dis. 2010;1:e104.
13. Fucikova J, Moserova I, Urbanova L, et al. Prognostic and predictive value of DAMPs and DAMP-associated processes in cancer. Front Immunol. 2015;6:402.
14. Lopez-Soto A, Gonzalez S, Smyth MJ, Galluzzi L. Control of metastasis by NK cells. Cancer Cell. 2017;32(2):135-154.
15. Gehrmann M, Schonberger J, Zilch T, et al. Retinoid- and sodium-butyrate-induced

decrease in heat shock protein 70 membrane-positive tumor cells is associated with reduced sensitivity to natural killer cell lysis, growth delay, and altered growth morphology. Cell Stress Chaperones. 2005;10(2):136-146.
16. Gross C, Holler E, Stangl S, et al. An Hsp70 peptide initiates NK cell killing of leukemic blasts after stem cell transplantation. Leuk Res. 2008;32(4):527-534.
17. Multhoff G, Pfister K, Botzler C, et al. Adoptive transfer of human natural killer cells in mice with severe combined immunodeficiency inhibits growth of Hsp70-expressing tumors. Int J Cancer. 2000; 88(5):791-797.
18. Gastpar R, Gehrmann M, Bausero MA, et al. Heat shock protein 70 surface-positive tumor exosomes stimulate migratory and cytolytic activity of natural killer cells. Cancer Res. 2005;65(12):5238-5247.
19. Vulpis E, Cecere F, Molfetta R, et al. Genotoxic stress modulates the release of exosomes from multiple myeloma cells capable of activating NK cell cytokine production: Role of HSP70/TLR2/NF-kB axis. Oncoimmunology. 2017;6(3):e1279372.
20. Qiu Y, Yang J, Wang W, et al. HMGB1-promoted and TLR2/4-dependent NK cell maturation and activation take part in rotavirus-induced murine biliary atresia. PLoS Pathog. 2014;10(3):e1004011.
21. Panaretakis T, Kepp O, Brockmeier U, Tesniere A, Bjorklund AC, Chapman DC, et al. Mechanisms of pre-apoptotic calreticulin exposure in immunogenic cell death. EMBO J. 2009;28(5):578-590.
22. Zingoni A, Fionda C, Borrelli C, Cippitelli M, Santoni A, Soriani A. Natural killer cell response to shemotherapy-stressed cancer cells: role in tumor immunosurveillance. Front Immunol. 2017; 8:1194.
23. Degli-Esposti MA, Smyth MJ. Close encounters of different kinds: dendritic cells and NK cells take centre stage. Nat Rev Immunol. 2005;5(2):112-124.
24. Van den Bergh JM, Lion E, Van Tendeloo VF, Smits EL. IL-15 receptor alpha as the magic wand to boost the success of IL-15 antitumor therapies: The upswing of IL-15 transpresentation. Pharmacol Ther. 2017;170:73-79.
25. Costello RT, Fauriat C, Sivori S, Marcenaro E, Olive D. NK cells: innate immunity against hematological malignancies? Trends Immunol. 2004;25(6):328-333.
26. Delahaye NF, Rusakiewicz S, Martins I, et al. Alternatively spliced NKp30 isoforms affect the prognosis of gastrointestinal stromal tumors. Nat Med. 2011;17(6):700-707.
27. Khaznadar Z, Boissel N, Agaugue S, et al. Defective NK Cells in Acute myeloid leukemia patients at diagnosis are associated with blast transcriptional signatures of immune evasion. J Immunol. 2015;195(6): 2580-2590.
28. Kroemer G, Senovilla L, Galluzzi L, Andre F, Zitvogel L. Natural and therapy-induced immunosurveillance in breast cancer. Nat Med. 2015;21(10):1128-1138.
29. Pasero C, Gravis G, Granjeaud S, et al. Highly effective NK cells are associated with good prognosis in patients with metastatic prostate cancer. Oncotarget. 2015;6(16): 14360-14373.
30. Galluzzi L, Yamazaki T, Kroemer G. Linking cellular stress responses to systemic homeostasis. Nat Rev Mol Cell Biol. 2018;19 (11):731-745.
31. Fuertes MB, Woo SR, Burnett B, Fu YX, Gajewski TF. Type I interferon response and innate immune sensing of cancer. Trends Immunol. 2013;34(2):67-73.
32. Mattei F, Schiavoni G, Belardelli F, Tough DF. IL-15 is expressed by dendritic cells in response to type I IFN, double-stranded RNA, or lipopolysaccharide and promotes dendritic cell activation. J Immunol. 2001; 167(3):1179-1187.
33. Chen X, Fosco D, Kline DE, Kline J. Calreticulin promotes immunity and type I interferon-dependent survival in mice with acute myeloid leukemia. Oncoimmunology. 2017;6(4):e1278332.
34. Han B, Mao FY, Zhao YL, et al. Altered NKp30, NKp46, NKG2D, and DNAM-1 expression on circulating NK cells is associated with tumor progression in human gastric cancer. J Immunol Res. 2018;2018: 6248590.

ARTICLE

Bortezomib with standard chemotherapy for children with acute myeloid leukemia does not improve treatment outcomes: a report from the Children's Oncology Group

Richard Aplenc,[1] Soheil Meshinchi,[2*] Lillian Sung,[3*] Todd Alonzo,[4] John Choi,[5] Brian Fisher,[6] Robert Gerbing,[7] Betsy Hirsch,[8] Terzah Horton,[9] Samir Kahwash,[10] John Levine,[11] Michael Loken,[12] Lisa Brodersen,[12] Jessica Pollard,[13] Susana Raimondi,[5] Edward Anders Kolb[14] and Alan Gamis[15]

RA and SM contributed equally to this work.

[1]The Children's Hospital of Philadelphia, Division of Oncology, Philadelphia, PA, USA; [2]Fred Hutchinson Cancer Research Center, Seattle, WA, USA; [3]The Hospital for Sick Children, Toronto, ON, Canada; [4]University of Southern California, Los Angeles, CA, USA; [5]St. Jude Children's Research Hospital, Memphis, TN, USA; [6]The Children's Hospital of Philadelphia, Division of Infectious Disease, Philadelphia, PA, USA; [7]Children's Oncology Group, Monrovia, CA, USA; [8]University of Minnesota, Minneapolis, MN, USA; [9]Texas Children's Hospital, Houston, TX, USA; [10]Nationwide Children's Hospital, Columbus, OH, USA; [11]Mount Sinai Medical Center, New York, NY, USA; [12]Hemaologics Inc., Seattle, WA, USA; [13]Dana Farber Cancer Center, Boston, MA, USA; [14]Alfred I. duPont Hospital for Children, Wilmington, DE, USA and [15]Children's Mercy Hospital and Clinics, Kansas City, MO, USA

Ferrata Storti Foundation

Haematologica 2020
Volume 105(7):1879-1886

ABSTRACT

New therapeutic strategies are needed for pediatric acute myeloid leukemia (AML) to reduce disease recurrence and treatment-related morbidity. The Children's Oncology Group Phase III AAML1031 trial tested whether the addition of bortezomib to standard chemotherapy improves survival in pediatric patients with newly diagnosed AML. AAML1031 randomized patients younger than 30 years of age with *de novo* AML to standard treatment with or without bortezomib. All patients received the identical chemotherapy backbone with either four intensive chemotherapy courses or three courses followed by allogeneic hematopoietic stem cell transplantation for high-risk patients. For those randomized to the intervention arm, bortezomib 1.3 mg/m^2 was given on days 1, 4 and 8 of each chemotherapy course. For those randomized to the control arm, bortezomib was not administered. In total, 1,097 patients were randomized to standard chemotherapy (n=542) or standard chemotherapy with bortezomib (n=555). There was no difference in remission induction rate between the bortezomib and control treatment arms (89% *vs.* 91%, *P*=0.531). Bortezomib failed to improve 3-year event-free survival (44.8±4.5% *vs.* 47.0±4.5%, *P*=0.236) or overall survival (63.6±4.5 *vs.* 67.2±4.3, *P*=0.356) compared with the control arm. However, bortezomib was associated with significantly more peripheral neuropathy (*P*=0.006) and intensive care unit admissions (*P*=0.025) during the first course. The addition of bortezomib to standard chemotherapy increased toxicity but did not improve survival. These data do not support the addition of bortezomib to standard chemotherapy in children with *de novo* AML. (Trial registered at *clinicaltrials.govNCT01371981; https://www.cancer.gov/clinicaltrials/ NCT01371981*).

Introduction

Pediatric acute myeloid leukemia (AML) is the second most common pediatric leukemia and requires intensive therapy for cure.[1,2] Despite the intensity of AML chemotherapy, which includes a very high cumulative lifetime anthracycline exposure in patients treated with chemotherapy alone or allogeneic donor stem cell transplantation (SCT) in first remission, approximately 50% of patients will experi-

Correspondence:

RICHARD APLENC
aplenc@email.chop.edu

Received: March 7, 2019.

Accepted: February 5, 2020.

Pre-published: February 6, 2020.

doi:10.3324/haematol.2019.220962

Check the online version for the most updated information on this article, online supplements, and information on authorship & disclosures: www.haematologica.org/content/105/7/1879

ence disease recurrence.[3,4] Moreover, treatment-related mortality limits the ability to further intensify therapy.[5] Thus, new therapies are needed to improve the outcomes of children with AML.

The development and evaluation of targeted therapies for children with AML is the highest clinical research priority for the Myeloid Committee in the Children's Oncology Group (COG).[6] After successfully demonstrating an improvement in event-free survival (EFS) in children treated with gemtuzumab,[3,4] COG sought to evaluate the efficacy of bortezomib, a first-generation proteasome inhibitor approved for multiple myeloma and non-Hodgkin lymphoma. Bortezomib was selected based on preliminary data demonstrating that AML blasts have increased proteasomes and are more sensitive to proteasome inhibitor-mediated apoptosis,[7] AML stem cells have increased NF-κB that is selectively targeted with proteasome inhibitors,[8-11] preclinical data from the pediatric preclinical testing program showing activity against leukemia cell lines,[12,13] and studies in adults with AML demonstrating clinical benefit.[14-16] At the time of the opening of the AAML1031 study, a COG pediatric phase I single agent bortezomib trial had determined the single agent maximum tolerated dose,[17] and a phase II trial (AAML07P1), combining bortezomib with AML chemotherapy for patients with relapsed AML, was nearing completion.[18]

Since the available safety and efficacy data for combining bortezomib with standard AML chemotherapy was limited, COG, in collaboration with the Cancer Therapy Evaluation Program (CTEP), designed AAML1031 as a definitive efficacy phase III trial with an interim toxicity analysis to ensure that combining bortezomib with standard AML chemotherapy was safe. The primary objective of AAML1031 was to definitively assess the impact of bortezomib in combination with standard AML chemotherapy on EFS for children with newly diagnosed AML without high allelic ratio (HAR) FLT3 ITD. A second objective was to evaluate the impact of bortezomib on overall survival (OS). Based on the available preliminary data at the time of study initiation, bortezomib was hypothesized to improve both EFS and OS. Multiple secondary objectives included an expanded safety assessment, multiple biology correlative studies, and secondary clinical data analyses.

Methods

The AAML1031 study was an open-label multi-center randomized trial including patients aged 0 to 29.5 years with previously untreated primary AML. Exclusion criteria were: prior chemotherapy, acute promyelocytic leukemia [t(15;17)], juvenile myelomonocytic leukemia, bone marrow failure syndromes, or secondary AML. The National Cancer Institute's central institutional review board (IRB) and IRB at each enrolling center approved the study; patients and families provided informed consent or assent as appropriate. The trial was conducted in accordance with the Declaration of Helsinki. The trial was registered at *clinicaltrials.gov identifier: NCT01371981.*

Patients were randomly assigned at enrollment to either standard AML treatment or standard treatment with bortezomib. Randomization was conducted in blocks of four. Bortezomib was administered at a dose of 1.3 mg/m^2 once on days 1, 4, and 8 of each chemotherapy course.

Patients with high allelic ratio FLT3 ITD were offered enrollment on a phase I sorafenib treatment arm if that arm was open. Patients with HAR FLT3 ITD who declined enrollment in the sorafenib arm, or who enrolled while the arm was suspended, continued to receive treatment according to their initial randomization. These patients were included in safety analyses but were excluded from all efficacy analyses.

Patients were classified as low- or high-risk after Induction I. Low-risk patients received four courses of chemotherapy and high-risk patients received three courses of chemotherapy followed by allogeneic SCT. High-risk patients without an appropriate donor received four courses of chemotherapy.

The primary end point was EFS from study entry. EFS was defined as the time from study entry until death, refractory disease, or relapse of any type, whichever occurred first. The secondary end points were OS, remission rates, relapse risk, post induction disease-free survival (DFS), and treatment-related mortality (TRM). OS was defined as time from study entry until death. Relapse risk was defined as the time from the end of Induction II for patients in complete remission (CR) to relapse, where deaths without a relapse were considered competing events. DFS was defined as the time from end of Induction II for patients in CR until relapse or death. Refractory disease was defined as the persistence of central nervous system (CNS) disease after Induction I, or the presence of morphologic bone marrow blasts ≥5% or any extramedullary disease at the end of Induction II. Patients with refractory disease were removed from protocol therapy. TRM was defined as the time from either study entry, or from end of Induction II for patients in CR, to deaths without a relapse, with relapses considered as competing events. Patients without an event were censored at their date of last known contact. However, for TRM analyses, patients were censored 30 days post end of therapy or 200 days post SCT.

Statistical analysis

The study was designed with 1-sided testing and 2.5% type I error rate and 80% power to detect a 9% difference in EFS plateaus (52% *vs.* 61%, hazard ratio = 0.78) between patients without HAR FLT3 ITD randomized to standard therapy *versus* bortezomib/standard combination therapy. All *P*-values are two-sided. Please see the *Online Supplementary Appendix* for additional details of the methods used.

Results

Between February 2011 and January 2016, 1,231 patients were enrolled on the AAML1031 study; patients were aged 0 to 29.5 years and had previously untreated primary AML at 184 institutions. Data for this analysis were frozen at December 31, 2017, with a median follow-up period of 3.0 years (range, 0-6.0 years) for patients alive at last contact. A total of 132 patients were excluded: 32 patients not meeting eligibility criteria, 102 patients with HAR FLT3 ITD who either enrolled (n=60) or did not enroll (n=42) on the phase I sorafenib treatment arm that concluded enrollment on July 31, 2017; this left 1,097 patients eligible for analysis. Figure 1 illustrates the reasons for exclusion and shows that 555 participants were randomized to the bortezomib arm and 542 to the control arm.

Accrual to the main randomization was completed on January 15, 2016. As of March 14, 2016, the projected relapse event horizon was reached and outcome analyses indicated that the addition of bortezomib did not improve EFS, DFS or OS, but did demonstrate a higher incidence of

non-fatal treatment-related toxicities. Therefore, institutions were notified on this date that patients receiving protocol therapy on the bortezomib arm should switch to the standard chemotherapy arm immediately. There were 22 patients who were receiving protocol therapy on the bortezomib arm at this time.

Table 1 and *Online Supplementary Table S1* summarizes the demographic characteristics of patients by study arm; no significant differences were observed in these demographic characteristics. Of note, 33% and 13% of patients had favorable cytogenetic or molecular features, respectively, and <5% had unfavorable cytogenetic features.

Table 1. Patient demographics and clinical characteristics by treatment arm.

Characteristic	Overall		Arm A		Arm B		*P*
	N	%	N	%	N	%	
Gender							
Male	572	52%	285	53%	287	52%	0.773
Female	525	48%	257	47%	268	48%	
Age at diagnosis, years							
Median	9.2		9.5		9.1		0.511
Range	0 - 29.5		0.03 - 29.5		0 - 29.2		
0-1 [0-730 day old]	237	22%	107	20%	130	23%	0.139
2-10	372	34%	189	35%	183	33%	0.507
11-15	273	25%	139	26%	134	24%	0.565
16-20	188	17%	91	17%	97	17%	0.763
≥21	27	2%	16	3%	11	2%	0.300
Race							
American Indian or Alaskan Native	9	1%	3	1%	6	1%	0.506
Asian	51	5%	24	5%	27	6%	0.699
Native Hawaiian or other Pacific Islander	8	1%	3	1%	5	1%	0.726
Black or African American	136	14%	69	14%	67	14%	0.793
White	767	79%	384	80%	383	78%	0.652
Multiple Races	1	0%	0	0%	1	0%	1.000
Unknown	125		59		66		
Ethnicity							
Hispanic or Latino	199	19%	99	19%	100	19%	0.945
Not Hispanic or Latino	863	81%	427	81%	436	81%	
Unknown	35		16		19		
Leukemic burden, WBC, x $10^9/\mu L$							
Median	17.7		17		19.2		0.185
Range	0.6 - 2730		0.6 - 2730		0.6 - 2600		
N. of patients with >100 x $10^9/\mu L$	178	16%	85	16%	93	17%	0.620
CNS disease classification at study entry							
CNS1	730	69%	358	70%	372	69%	0.617
CNS2	215	20%	100	20%	115	21%	0.507
CNS3	108	10%	53	10%	55	10%	0.905
Unknown	44		31		13		
Non-CNS extramedullary disease	170	15%	82	15%	88	16%	0.720
Risk factors and classification							
Cytogenetics affecting risk classification							
t(8;21)	166	20%	84	16%	82	15%	0.725
Inv(16), t(16;16)	114	13%	57	11%	57	11%	0.883
-7	21	3%	9	2%	12	2%	0.545
-5/5q-	13	1%	6	1%	7	1%	0.814
Institution mutation results							
Low FLT3-ITD allelic ratio (≤0.4)	77	7%	37	7%	40	7%	0.805
NPM	80	7%	37	7%	43	8%	0.558
CEBPα	66	6%	29	5%	37	7%	0.364
MRD at end of induction I							
Negative	782	75%	386	75%	396	75%	0.929
Positive	261	25%	128	25%	133	25%	
MRD positive %, median	2.3		2.8		1.9		0.247
MRD positive %, range	0.1 - 93		0.1 - 93		0.1 - 92		
Unknown	54		28		26		
Risk group assignment							
Low	836	78%	417	79%	419	78%	0.664
High	230	22%	111	21%	119	22%	

AML: acute myeloid leukemia; CNS: central nervous system; ITD high AR: internal tandem duplication with high allelic ratio; MRD: minimum residual disease; WBC: white blood cell count.

Minimal residual disease (MRD) assessment at the end of Induction I was available in 95% of patients, and was negative in 75%. Thus, approximately 78% of all patients were classified as low-risk based on cytogenetic, molecular, and disease response features, while 22% were classified as high-risk.

Of the 1,097 patients enrolled on AAML1031, approximately 84% survived and achieved a remission at the end of two courses of induction. For the 1,024 patients who initiated the second course of induction therapy and were evaluable at the end of Induction II, the remission rate was 90% and there was no difference between study arms. No differences in EFS and OS were observed by study arm (Table 2 and Figure 2). Specifically, the 3-year EFS from study entry for the no bortezomib and bortezomib arms were 44.8%±4.5% *versus* 47.0%±4.5% (P=0.236) and the

Table 2. Event-free survival, overall survival, and treatment-related mortality by study arm.

	Overall		Arm A		Arm B		*P*
	N	% ± 2 SE%	N	% ± 2 SE%	N	% ± 2 SE%	
3-year EFS from study entry	1097	45.9 ± 3.2	542	44.8 ± 4.5	555	47.0 ± 4.5	0.236
3-year OS from study entry	1097	65.4 ± 3.1	542	63.6 ± 4.5	555	67.2 ± 4.3	0.356
3-year CI of relapse from study entry	1097	47.2 ± 3.2	542	48.0 ± 4.5	555	46.4 ± 4.4	0.378
1-year TRM from study entry	1097	11.8 ± 5.2	542	13.3 ± 8.2	555	10.5 ± 6.6	0.577
3-year DFS from end of Induction I	1015	47.8 ± 3.3	506	46.9 ± 4.6	509	48.7 ± 4.6	0.261
3-year OS from end of Induction I	1015	66.6 ± 3.2	506	65.2 ± 4.6	509	68.0 ± 4.5	0.451
3-year DFS from end of Induction II	910	52.4 ± 3.5	453	51.8 ± 4.9	457	53.0 ± 4.9	0.444
3-year OS from end of Induction II	910	70.5 ± 3.3	453	69.3 ± 4.8	457	71.7 ± 4.7	0.453
1-year TRM from end of Induction II	910	9.7 ± 5.2	453	10.4 ± 7.6	457	9.0 ± 7.2	0.331

EFS: event-free survival; OS: overall survival; CI: cumulative incidence; TRM: treatment-related mortality; DFS: disease-free survival; SE: standard error.

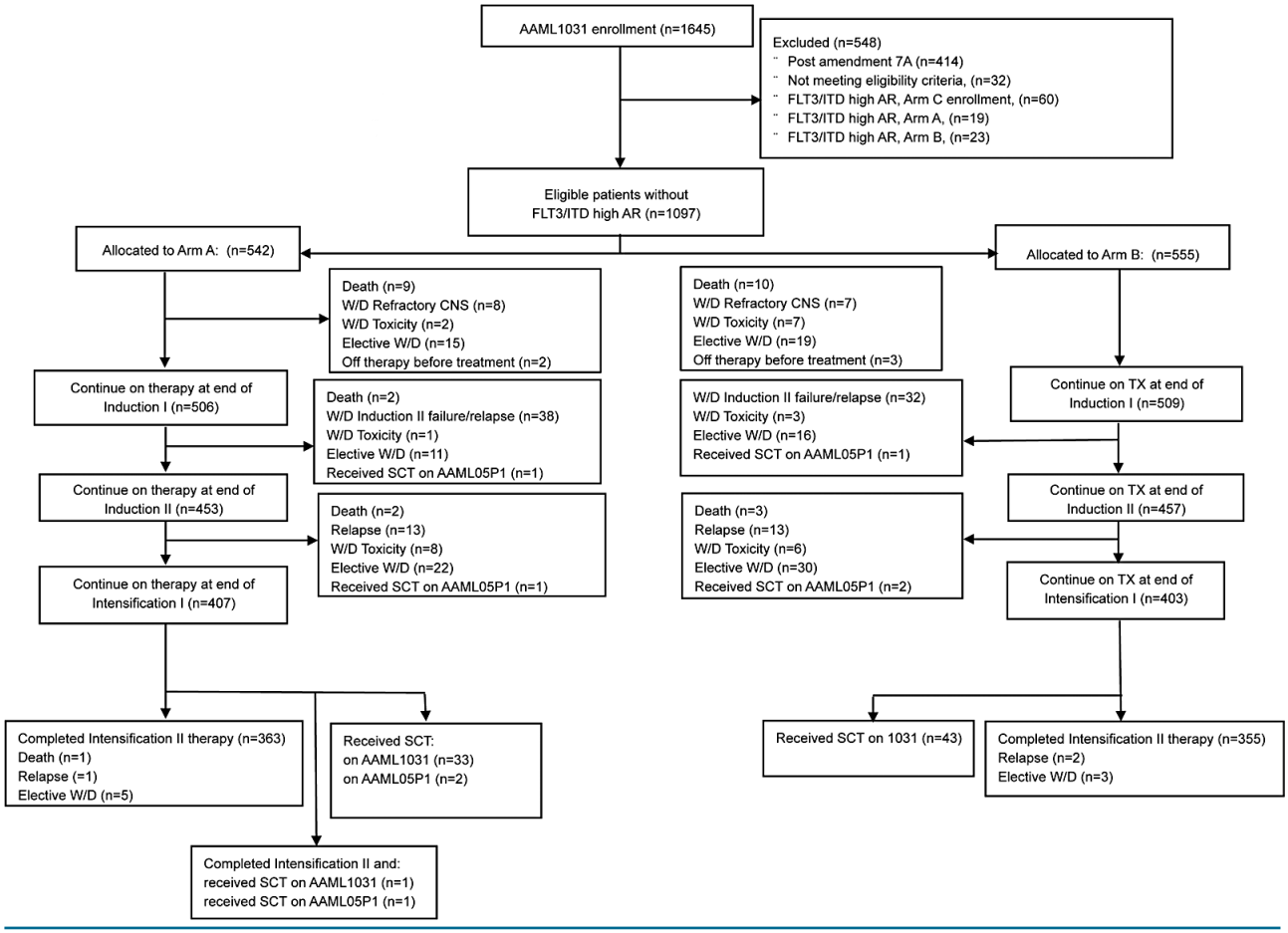

Figure 1. Consort diagram – AAML1031, as of December 31, 2017. High AR: W/D: Elective withdrawal. Reasons include terminating therapy to due to physician's choice or patient's refusal of further protocol therapy. SCT: stem cell transplantation; TX: therapy; n: number.

3-year OS from study entry were 63.6%±4.5% *versus* 67.2%±4.3% (*P*=0.356). Similar outcomes by randomization arm were observed for the cumulative incidence of relapse, 1-year TRM, and DFS/OS from the end of Induction II (Table 2).

Subgroup analyses by risk group (*Online Supplementary Table S2*) showed similar outcomes between treatment arms for both low- and high-risk patients. Combining the two arms, 3-year DFS and OS for low-risk patients was 52.9%±3.7% and 74.1%±3.4%, respectively while 3-year DFS and OS for high-risk patients was 27.8%±6.6% and 36.9%±7.6%. Subgroup analyses by NPM, CEBPA, CBF, and KMT2A molecular subtypes (*Online Supplementary Table S3*) and by age category (*Online Supplementary Table S4*) did not show any evidence of subtype- or age-specific bortezomib responses.

Univariable and multivariable Cox analyses from study entry and end of Induction II are shown in Table 3 and *Online Supplementary Table S5*. Initial white blood cell count (WBC) >100x10^9/L was significantly associated with an increased risk of relapse, treatment-related mortality, and decreased survival from study entry. Age greater or equal to 11 years old was associated with a decreased risk of relapse and increased survival. Black race, a previously observed risk factor,[3,19] was no longer a significant risk factor for relapse or death. The magnitude and significance of these associations remained stable between univariate and multivariable analyses.

Interim analyses of TRM and acute respiratory distress syndrome (ARDS) after 100 patients were randomized to bortezomib did not cross predefined toxicity thresholds. Overall TRM and targeted toxicity data are shown in Table 4 and *Online Supplementary Table S6*. No differences were observed in overall or course-specific TRM. While most toxicity rates did not differ by treatment arm, peripheral neuropathy, dose reductions, and pediatric Intensive Care Unit (PICU) admissions were consistently increased in patients receiving bortezomib in combination with standard chemotherapy. Course-specific increased rates of ARDS and hypoxia were observed in the patients treated with bortezomib together with standard chemotherapy. However, the reported rates of these toxicities was relatively low and did not differ from rates in patients treated with standard chemotherapy alone. No differences in infectious complications, renal toxicities, or decline in shortening fraction/ejection fraction were observed between treatment arms (*Online Supplementary Table S7*). Subgroup toxicity analyses by patient age demonstrated increased toxicities in Arm B patients with increasing age (*Online Supplementary Table S8*) amongst patients who completed all four courses of chemotherapy.

Discussion

The AAML1031 trial data demonstrate that the addition of bortezomib to standard chemotherapy does not improve EFS or OS. However, bortezomib caused additional treatment-related toxicity, specifically peripheral neuropathy, dose reductions, and PICU admissions. Given the lack of clinical benefit and increased toxicity observed in the bortezomib treatment arm, bortezomib was discontinued in all patients who remained on protocol mandated therapy. While the preliminary data regarding bortezomib efficacy in adults with AML was promising,[14-16] and pediatric preclinical models demonstrated a potential biological rationale for combining bortezomib with pediatric AML chemotherapy,[12,13] the results of AAML1031 do not support the addition of bortezomib to current pediatric AML chemotherapy. This trial result illustrates the need for specific pediatric clinical trials in AML, even in the context of a promising efficacy signal in adult AML.

Several important additional conclusions may be drawn from these data. First, the outcomes seen on the AAML1031 trial are generally similar to those seen on the standard arm of the immediately antecedent phase III trial, AAML0531, and are slightly inferior to outcomes reported in other pediatric co-operative oncology groups.[3,20-22] The observed differences in outcomes between other pediatric co-operative oncology group clinical trials and AAML1031 are still not completely understood but stem, in part, from the elimination of chemotherapy cycle 5 (Capizzi AraC) for low-risk patients with uninformative molecular features.[23] Further investigations will evaluate differences in

Table 3. Multivariable analyses.

		OS from study entry			EFS from study entry			TRM from study entry		
	N	HzR	95% CI	*P*	HzR	95% CI	*P*	HzR	95% CI	*P*
Treatment arm										
Arm A	482	1			1			1		
Arm B	487	0.91	0.73 - 1.13	0.383	0.95	0.80 - 1.13	0.567	0.87	0.49 - 1.57	0.652
Age at diagnosis, years										
2-10	318	1			1			1		
0-1	209	1.26	0.94 - 1.68	0.118	1.21	0.96 - 1.53	0.100	0.80	0.32 - 1.99	0.638
≥11	442	0.86	0.66 - 1.11	0.231	0.78	0.64 - 0.96	0.017	1.25	0.65 - 2.40	0.498
WBC at diagnosis, x10^9/L										
≤ 100	805	1			1			1		
> 100	164	1.42	1.08 - 1.86	0.013	1.64	1.32 - 2.03	<0.001	1.79	0.92 - 3.48	0.089
Race										
Non-black	832	1			1			1		
Black	137	1.30	0.97 - 1.75	0.084	1.02	0.79 - 1.31	0.884	1.86	0.95 - 3.62	0.068

OS: overall survival; EFS: event-free survival; TRM: treatment-related mortality; HzR: hazard ratio; CI: confidence interval; WBC: white blood cell count.

Table 4. Targeted toxicity by phase of therapy.

	Phase of therapy	Induction I			Induction II			Intensification I			Intensification II		
	Treatment arm	Arm A	Arm B	A vs. B P	Arm A	Arm B	A vs. B P	Arm A	Arm B	A vs. B P	Arm A	Arm B	A vs. B P
Toxicity	N	574	580		518	529		460	469		373	361	
Cardiac	Heart failure	4	4		3	6		5	10		10	13	
		0.7%	0.7%	1.000	0.6%	1.1%	0.506	1.1%	2.1%	0.206	2.7%	3.6%	0.474
	EF decreased	4	6		1	5		8	19		4	11	
		0.7%	1.0%	0.753	0.2%	0.9%	0.218	1.7%	4.1%	0.036	1.1%	3.0%	0.059
	Cardiac LVSD	5	8		4	4		13	15		9	16	
		0.9%	1.4%	0.413	0.8%	0.8%	1.000	2.8%	3.2%	0.740	2.4%	4.4%	0.132
Neurologic	Peripheral neuropathy/	6	20		4	17		8	14		5	10	
	Paresthesia/neuralgia	1.0%	3.4%	0.006	0.8%	3.2%	0.005	1.7%	3.0%	0.212	1.3%	2.8%	0.171
	Seizure	2	1		1	0		0	0		0	3	
		0.3%	0.2%	0.623	0.2%	0.0%	0.495	0.0%	0.0%	1.000	0.0%	0.8%	0.119
Pulmonary	ARDS	2	12		2	3		6	3		3	1	
		0.3%	2.1%	0.008	0.4%	0.6%	1.000	1.3%	0.6%	0.337	0.8%	0.3%	0.624
	Hypoxia	21	35		7	10		7	24		15	17	
		3.7%	6.0%	0.060	1.4%	1.9%	0.490	1.5%	5.1%	0.002	4.0%	4.7%	0.648
	Respiratory failure	10	18		2	3		4	5		8	5	
		1.7%	3.1%	0.133	0.4%	0.6%	1.000	0.9%	1.1%	1.000	2.1%	1.4%	0.435
Renal	Acute kidney injury	9	10		0	4		1	6		2	1	
		1.6%	1.7%	0.835	0.0%	0.8%	0.124	0.2%	1.3%	0.124	0.5%	0.3%	1.000
	Creatinine increased	0	5		1	2		0	2		0	1	
		0.0%	0.9%	0.062	0.2%	0.4%	1.000	0.0%	0.4%	0.500	0.0%	0.3%	0.492
Microbiologically documented sterile site infections (at least 1 occurrence)	Viridans group Streptococcus	21	25		55	53		70	78		83	75	
		3.7%	4.3%	0.572	10.6%	10.0%	0.750	15.2%	16.6%	0.556	22.3%	20.8%	0.627
	Gram Negative Bacilli	9	16		23	31		41	49		53	43	
		1.6%	2.8%	0.165	4.4%	5.9%	0.299	8.9%	10.4%	0.429	14.2%	11.9%	0.356
	Fungi	16	7		3	7		0	2		6	6	
		2.8%	1.2%	0.055	0.6%	1.3%	0.342	0.0%	0.4%	0.500	1.6%	1.7%	0.955
Dose reductions		8	31		8	33		4	37		9	47	
		1.4%	5.3%	<0.001	1.5%	6.2%	<0.001	0.9%	7.9%	<0.001	2.4%	13.0%	<0.001
PICU admissions		121	155		43	66		53	84		72	71	
		21.1%	26.7%	0.025	8.3%	12.5%	0.027	11.5%	17.9%	0.006	19.3%	19.7%	0.901

ARDS: adult respiratory distress syndrome; EF: ejection fraction; LVSD: left ventricular cystolic dysfunction; PICU: pediatric intensive care unit.

study populations, including characteristics such as obesity, molecularly-defined risk differences between study populations, efficacy of the backbone treatment regimen, variations in supportive care practices, and the potential impact of structural differences in the provision of health services. Additional analyses including comparisons focusing on the efficacy of dexrazoxane as a cardioprotectant,[24] specific cytogenetic abnormalities (MLL translocation subgroups), the use of MRD testing for outcome prediction, optimizing risk classification, the intensification of Induction II therapy with cytarabine and mitoxantrone, and the role of allogeneic donor SCT, are ongoing.

Second, COG, in partnership with the Cancer Therapy Evaluation Program (CTEP) can conduct complex clinical trials that contain phase I, phase II, and phase III components. The sorafenib study arm, which will be reported separately, served as a phase I trial of the feasibility and initial efficacy assessment of incorporating sorafenib into pediatric AML. Moreover, at the initiation of AAML1031, the only published data for bortezomib in pediatric AML was as a single agent.[17] While limited safety data were available during the 2-year planning process prior to the opening of the AAML1031 trial in June, 2011, full safety and efficacy data were not available until the subsequent closure of the AAML07P1 trial in December, 2011.[18] Given these limited toxicity data, the AAML1031 trial included a planned targeted toxicity (ARDS and TRM) analyses after the randomization of 100 patients to the bortezomib treatment arm. The successful monitoring of bortezomib-associated toxicities on the AAML1031 trial highlights the ability of COG, in partnership with the CTEP, to conduct complex clinical trials that provide definitive efficacy testing of a novel agent in the setting of limited preliminary toxicity data.

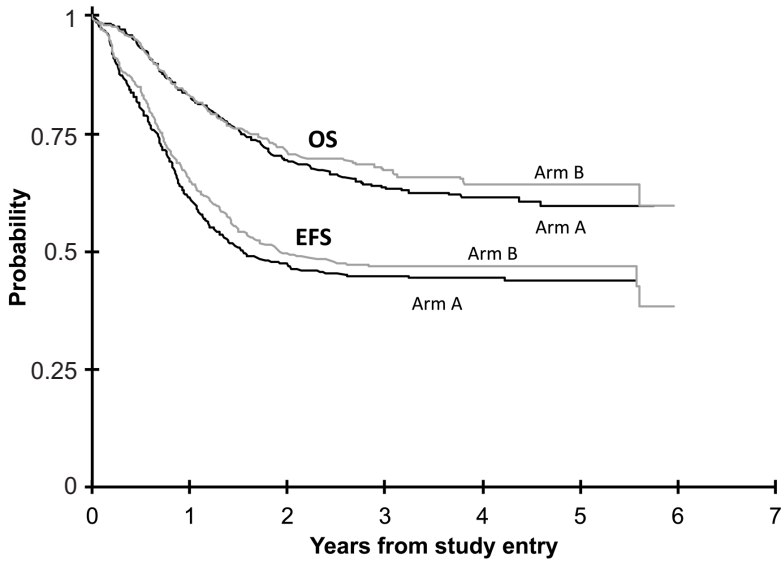

Figure 2. Event-free survival (EFS) and overall survival (OS) by treatment arm.

Several limitations of this clinical trial require acknowledgment. First, correlative biology data on the unfolded protein response and other biomarkers of bortezomib efficacy are currently ongoing and thus could not be included in this report. These ongoing studies may define subgroup populations who may benefit from bortezomib.[25] Second, comprehensive molecular profiling of each individual AML case is ongoing but is still not complete.[26] The completion of this work will likely enable the next generation of risk prediction and therapy individualization. Finally, the ongoing analyses of changes in chemotherapy course sequence and use of allogeneic donor SCT will face the well documented challenges of limitations in chemotherapy toxicity reporting,[27,28] and the challenges faced by all cooperative oncology groups to collect and account for variable supportive care practices and particular factors at the level of each individual center that may impact treatment outcomes.

In conclusion, the AAML1031 trial demonstrates that bortezomib can be combined safely with standard pediatric AML chemotherapy but that this combination does not improve EFS or OS and is associated with increased toxicity. Thus, these data do not support the use of bortezomib in pediatric AML therapy at this time. Despite this, the successful conduct of this very complex trial highlights the clinical trial capabilities of COG in partnership with the CTEP, and may serve as a paradigm for definitive efficacy clinical trials initiated in the setting of limited preliminary data. Finally, the AAML1031 clinical trial data set, in conjunction with ongoing biology studies, will serve as an invaluable data platform for future clinical and translational investigations.

Acknowledgments

The AAML1031 study team would like to acknowledge the patients and families who participated in the AAML1031 clinical trial.

Funding

This research was supported by NCTN Operations Center Grant (U10CA180886) and NCTN Statistics & Data Center Grant (U10CA180899).

References

1. Zwaan CM, Kolb EA, Reinhardt D, et al. Collaborative Efforts Driving Progress in Pediatric Acute Myeloid Leukemia. J Clin Oncol. 2015;33(27):2949-2962.
2. Tarlock K, Meshinchi S. Pediatric acute myeloid leukemia: biology and therapeutic implications of genomic variants. Pediatr Clin North Am. 2015;62(1):75-93.
3. Gamis AS, Alonzo TA, Meshinchi S, et al. Gemtuzumab ozogamicin in children and adolescents with de novo acute myeloid leukemia improves event-free survival by reducing relapse risk: results from the randomized phase III Children's Oncology Group trial AAML0531. J Clin Oncol. 2014; 32(27):3021-3032.
4. Cooper TM, Franklin J, Gerbing RB, et al. AAML03P1, a pilot study of the safety of gemtuzumab ozogamicin in combination with chemotherapy for newly diagnosed childhood acute myeloid leukemia: A report from the children's oncology group. Cancer. 2011;118(3):761-769.
5. Lange BJ, Smith FO, Feusner J, et al. Outcomes in CCG-2961, a children's oncology group phase 3 trial for untreated pediatric acute myeloid leukemia: a report from the children's oncology group. Blood. 2008;111(3):1044-1053.
6. Gamis AS, Alonzo TA, Perentesis JP, Meshinchi S, Committee COGAML. Children's Oncology Group's 2013 blueprint for research: acute myeloid leukemia. Pediat Blood Cancer. 2013;60(6):964-971.
7. Matondo M, Bousquet-Dubouch MP, Gallay N, et al. Proteasome inhibitor-induced apoptosis in acute myeloid leukemia: a correlation with the proteasome status. Leuk Res. 2010;34(4):498-506.
8. Colado E, Alvarez-Fernandez S, Maiso P, et al. The effect of the proteasome inhibitor bortezomib on acute myeloid leukemia cells and drug resistance associated with the CD34+ immature phenotype. Haematologica. 2008;93(1):57-66.
9. Guzman ML, Neering SJ, Upchurch D, et al. Nuclear factor-kappaB is constitutively activated in primitive human acute myelogenous leukemia cells. Blood. 2001; 98(8):2301-2307.
10. Guzman ML, Swiderski CF, Howard DS, et al. Preferential induction of apoptosis for primary human leukemic stem cells. Proc Natl Acad Sci U S A. 2002;99(25):16220-16225.
11. Jordan CT, Guzman ML, Noble M. Cancer stem cells. N Engl J Med. 2006;355(12): 1253-1261.
12. Horton TM, Gannavarapu A, Blaney SM, et al. Bortezomib interactions with chemotherapy agents in acute leukemia in vitro. Cancer Chemother Pharmacol. 2006;

58(1):13-23.
13. Niewerth D, Franke NE, Jansen G, et al. Higher ratio immune versus constitutive proteasome level as novel indicator of sensitivity of pediatric acute leukemia cells to proteasome inhibitors. Haematologica. 2013;98(12):1896-1904.
14. Attar EC, De Angelo DJ, Supko JG, et al. Phase I and pharmacokinetic study of bortezomib in combination with idarubicin and cytarabine in patients with acute myelogenous leukemia. Clin Cancer Res. 2008; 14(5):1446-1454.
15. Blum W, Schwind S, Tarighat SS, et al. Clinical and pharmacodynamic activity of bortezomib and decitabine in acute myeloid leukemia. Blood. 2012;119(25): 6025-6031.
16. Orlowski RZ, Voorhees PM, Garcia RA, et al. Phase 1 trial of the proteasome inhibitor bortezomib and pegylated liposomal doxorubicin in patients with advanced hematologic malignancies. Blood. 2005; 105(8):3058-3065.
17. Horton TM, Pati D, Plon SE, et al. A phase 1 study of the proteasome inhibitor bortezomib in pediatric patients with refractory leukemia: a Children's Oncology Group study. Clin Cancer Res. 2007;13(5):1516-1522.
18. Horton TM, Perentesis JP, Gamis AS, et al. A Phase 2 study of bortezomib combined with either idarubicin/cytarabine or cytarabine/etoposide in children with relapsed, refractory or secondary acute myeloid leukemia: a report from the Children's Oncology Group. Pediatric Blood Cancer. 2014;61(10):1754-1760.
19. Aplenc R, Alonzo TA, Gerbing RB, et al. Ethnicity and survival in childhood acute myeloid leukemia: a report from the Children's Oncology Group. Blood. 2006; 108(1):74-80.
20. Hasle H, Abrahamsson J, Forestier E, et al. Gemtuzumab ozogamicin as postconsolidation therapy does not prevent relapse in children with AML: results from NOPHO-AML 2004. Blood. 2012;120(5):978-984.
21. Creutzig U, Zimmermann M, Bourquin JP, et al. Randomized trial comparing liposomal daunorubicin with idarubicin as induction for pediatric acute myeloid leukemia: results from Study AML-BFM 2004. Blood. 2013;122(1):37-43.
22. Tsukimoto I, Tawa A, Horibe K, et al. Risk-stratified therapy and the intensive use of cytarabine improves the outcome in childhood acute myeloid leukemia: the AML99 trial from the Japanese Childhood AML Cooperative Study Group. J Clin Oncol. 2009;27(24):4007-4013.
23. Getz KD, Alonzo TA, Sung L, et al. Four versus five chemotherapy courses in patients with low risk acute myeloid leukemia: a Children's Oncology Group report. J Clin Oncol. 2017; 35(15_suppl): 10515-10515.
24. Getz KD, Sung L, Leger K, et al. Effect of dexrazoxane on left ventricular function and treatment outcomes in patients with acute myeloid leukemia: A Children's Oncology Group report. J Clin Oncol. 2018; 36(15_suppl):10501-10501.
25. Hoff FW, Qiu Y, Hu W, et al. Abstract 451: Proteomic profiling of the unfolded protein response identifies patients benefiting from bortezomib in pediatric acute myeloid leukemia. Cancer Res. 2018;78(Suppl 13):451.
26. Bolouri H, Farrar JE, Triche T Jr, et al. The molecular landscape of pediatric acute myeloid leukemia reveals recurrent structural alterations and age-specific mutational interactions. Nat Med. 2018;24(1):103-112.
27. Miller TP, Li Y, Getz KD, et al. Using electronic medical record data to report laboratory adverse events. Br J Haematol. 2017; 177(2):283-286.
28. Miller TP, Troxel AB, Li Y, et al. Comparison of administrative/billing data to expected protocol-mandated chemotherapy exposure in children with acute myeloid leukemia: A report from the Children's Oncology Group. Pediatric Blood Cancer. 2015;62(7):1184-1189.

ARTICLE

# Relapses and treatment-related events contributed equally to poor prognosis in children with ABL-class fusion positive B-cell acute lymphoblastic leukemia treated according to AIEOP-BFM protocols

Gunnar Cario,[1*] Veronica Leoni,[2*] Valentino Conter,[2*] Andishe Attarbaschi,[3] Marketa Zaliova,[4] Lucie Sramkova,[4] Gianni Cazzaniga,[2] Grazia Fazio,[2] Rosemary Sutton,[5] Sarah Elitzur,[6] Shai Izraeli,[6] Melchior Lauten,[7] Franco Locatelli,[8] Giuseppe Basso,[9] Barbara Buldini,[9] Anke K. Bergmann,[10] Jana Lentes,[10] Doris Steinemann,[10] Gudrun Göhring,[10] Brigitte Schlegelberger,[10] Oskar A. Haas,[3] Denis Schewe,[1] Swantje Buchmann,[1] Anja Moericke,[1] Deborah White,[11] Tamas Revesz,[12] Martin Stanulla,[13] Georg Mann,[3] Nicole Bodmer,[14] Nira Arad-Cohen,[15] Jan Zuna,[4] Maria Grazia Valsecchi,[2] Martin Zimmermann,[13] Martin Schrappe[1#] and Andrea Biondi[2#]

[1]Pediatrics, University Hospital Schleswig-Holstein, Campus Kiel, Kiel, Germany; [2]Clinica Pediatrica and Centro Ricerca Tettamanti, Università di Milano-Bicocca, Fondazione MBBM/ S.Gerardo Hospital, Monza, Italy; [3]St. Anna Kinderspital and Children's Cancer Research Institute, Vienna, Austria; [4]CLIP, Department of Pediatric Hematology and Oncology, 2nd Faculty of Medicine, Charles University and University Hospital Motol, Prague, Czech Republic; [5]Molecular Diagnostics, Children's Cancer Institute, University of NSW, Sydney, NSW, Australia; [6]Pediatric Hematology-Oncology, Schneider Children's Medical Center, Petah Tikva, and Sackler Faculty of Medicine, Tel Aviv University, Israel; [7]Pediatrics, University Hospital Schleswig-Holstein, Campus Lübeck, Lübeck, Germany; [8]Department of Pediatric Hematology and Oncology, Scientific Institute for Research and Healthcare (IRCCS) Childrens' Hospital Bambino Gesù, Sapienza, University of Rome, Rome, Italy; [9]IIGM Torino and Pediatric Hemato-Oncology, SDB Departiment, University of Padova, Padova, Italy; [10]Department of Human Genetics, Medical School Hannover, Hannover, Germany; [11]Cancer Theme, South Australian Health and Medical Research Institute, Adelaide, Australia; [12]Women's and Children's Hospital, SA Pathology, University of Adelaide, Adelaide, Australia; [13]Department of Pediatric Hematology/Oncology, Hannover Medical School, Hannover, Germany; [14]University Children's Hospital Zurich, Zurich, Switzerland and [15]Pediatric Hematology-Oncology Department, Ruth Rappaport Children's Hospital, Rambam Health Care Campus, Rappaport Faculty of Medicine, Technion-Israel Institute of Technology, Haifa, Israel

*GC, VL and VC contributed equally as co-first authors.

#MS and AB contributed equally as co-senior authors.

Ferrata Storti Foundation

Haematologica 2020
Volume 105(7):1887-1894

Correspondence:

GUNNAR CARIO
gunnar.cario@uksh.de

Received: July 8, 2019.

Accepted: October 10, 2019.

Pre-published: October 10, 2019.

doi:10.3324/haematol.2019.231720

Check the online version for the most updated information on this article, online supplements, and information on authorship & disclosures: www.haematologica.org/content/105/7/1887

ABSTRACT

ABL-class fusions other than *BCR-ABL1* characterize around 2-3% of precursor B-cell acute lymphoblastic leukemia. Case series indicated that patients suffering from these subtypes have a dismal outcome and may benefit from the introduction of tyrosine kinase inhibitors. We analyzed clinical characteristics and outcome of 46 ABL-class fusion positive cases other than *BCR-ABL1* treated according to AIEOP-BFM (Associazione Italiana di Ematologia-Oncologia Pediatrica-Berlin-Frankfurt-Münster) ALL 2000 and 2009 protocols; 13 of them received a tyrosine kinase inhibitor (TKI) during different phases of treatment. ABL-class fusion positive cases had a poor early treatment response: minimal residual disease levels of ≥$5x10^{-4}$ were observed in 71.4% of patients after induction treatment and in 51.2% after consolidation phase. For the entire cohort of 46 cases, the 5-year probability of event-free survival was 49.1+8.9% and that of overall survival 69.6+7.8%; the cumulative incidence of relapse was 25.6+8.2% and treatment-related mortality (TRM) 20.8+6.8%. One out of 13 cases with TKI added to chemotherapy relapsed while eight of 33 cases

without TKI treatment suffered from relapse, including six in 17 patients who had not received hematopoietic stem cell transplantation. Stem cell transplantation seems to be effective in preventing relapses (only three relapses in 25 patients), but was associated with a very high TRM (6 patients). These data indicate a major need for an early identification of ABL-class fusion positive acute lymphoblastic leukemia cases and to establish a properly designed, controlled study aimed at investigating the use of TKI, the appropriate chemotherapy backbone and the role of hematopoietic stem cell transplantation. (Registered at: *clinicaltrials.gov identifier: NTC00430118, NCT00613457, NCT01117441).*

Introduction

Continuous optimization of risk-adapted multi-agent treatment has led to excellent curative rates in the majority of children and adolescents suffering from acute lymphoblastic leukemia (ALL).[1-9] However, the progress in ALL subtype classification according to the nature of specific sentinel genetic aberrations identified molecular ALL subgroups like low-hypodiploid, *KMT2A*-rearranged or *BCR-ABL1* positive precursor-B-ALL (B-ALL) with distinct biological and clinical characteristics associated with poor outcome. Intensive chemotherapy, including allogeneic hematopoietic stem cell transplantation (HSCT) for some of these patients, is associated with severe toxicity and long-term sequelae.

In this context, one of the first ALL genetic aberrations identified was the gene fusion *BCR-ABL1* resulting from the chromosomal translocation t(9;22) (generating the so-called Philadelphia chromosome), translated into the BCR-ABL1 fusion protein, a constitutively active tyrosine kinase, which can be inhibited by tyrosine kinase inhibitors (TKI). This is an excellent example for a successful molecular treatment target: the addition of the first-generation TKI imatinib to intensive chemotherapy backbone has led, in fact, to a significant improvement of outcome in children with Philadelphia chromosome positive ALL (Ph^+ ALL) with cure rates of 60-70%.[10-18] The Children's Oncology Group (COG) studies showed a clear advantage in Ph^+ ALL from continuous protracted exposure to TKI combined with chemotherapy, challenging the indications to transplant for all patients with Ph^+ ALL.[16-18] COG results were confirmed by the European intergroup study group for treatment of Ph^+ ALL (EsPhALL) in the EsPhALL2004 and the subsequent EsPhALL2010 studies, showing that intensive chemotherapy combined with imatinib given continuously from induction phase allows a remarkable reduction in the rate of HSCT, without affecting outcome.[13-15] However, these trials also demonstrated that the combination of chemotherapy and imatinib is associated with a high rate of treatment-related toxicity and mortality.

In the last decade, different tyrosine kinase gene fusions other than *BCR-ABL1* have been identified which are sensitive to TKI similar as *BCR-ABL1*. These so called ABL-class fusions typically comprise rearrangements of the *ABL1, ABL2, PDGFRB* and *CSF1R* genes, each of which can have different fusion partner genes. ABL-class fusion positive B-ALL subtypes other than BCR-ABL1 have been identified showing a gene expression profile largely similar to that of Ph^+ ALL. Therefore, they are included in the *BCR-ABL1*-/Ph-like-ALL group recognized as a provisional entity in the 2016 World Health Organization classification of myeloid neoplasms and acute leukemia although they only make up a minor proportion of patients in this new category. Whereas BCR-ABL1-/Ph-like-ALL accounts for 15-20% of all pediatric B-ALL, the frequency of ABL-class fusion positive B-ALL is estimated to be about 2-3% which is similar to the frequency of *BCR-ABL1* pos. ALL.[19-21] *BCR-ABL1*-/Ph-like ALL is associated with other high-risk clinical features, such as older age, elevated white blood cell (WBC) count at diagnosis, high rates of end-induction minimal residual disease (MRD), as well as increased risk of induction failure and of leukemia relapse.[22-28]

Data on the ABL-class fusion positive ALL other than Ph^+ ALL are rare and are limited to anecdotal case reports. In this study, we retrospectively analyzed clinical characteristics and outcome of ABL-class fusion positive cases treated based on contemporary MRD-based protocols of the Associazione Italiana di Ematologia-Oncologia Pediatrica-Berlin-Frankfurt-Münster (AIEOP-BFM ALL study group. The aim was to provide a comprehensive picture of current outcome of these cases without the addition of a TKI to chemotherapy, and to get first data on those cases in which a TKI was added to chemotherapy. It should serve as a basis on which to decide whether the addition of a TKI to chemotherapy may be beneficial, when taking into account the risk of a relevant increase of toxicity and treatment-related mortality (TRM).

Methods

Patients and diagnostics

This retrospective survey of ABL-class fusion positive B-ALL other than Ph^+ ALL was performed in patients aged 1-17 years, treated from October 2000 to August 2018 according to the AIEOP-BFM ALL 2000 and 2009 protocols in Centers in Austria, Australia, Czech Republic, Germany, Israel, Italy, and Switzerland.

Routine diagnostics was performed according to national standards based on protocol requirements.[8,9,29-31] Diagnosis of ALL was made when 25% or more lymphoblastic cells were present cytomorphologically in the bone marrow. Flow-cytometry immunophenotyping was performed based on the AIEOP-BFM consensus guidelines.[29] Complete remission (CR) was defined as the absence of physical signs of leukemia or detectable leukemia cells on blood smears, a bone marrow with active hematopoiesis and <5% blasts, and morphologically normal cerebrospinal fluid. Presence of *ETV6-RUNX1, BCR-ABL1* and *KMT2A-AFF1* fusion transcripts was screened as previously described.[8,9]

ABL-class fusions screening, not required by protocols, was performed in a minority of patients according to the policy of individual centers or due to poor response to treatment. Methods used included fluorescence *in situ* hybridization (FISH, e.g. using probes by Cytocell®, Cambridge, UK), multiplex or singleplex reverse-transcription polymerase chain reaction (PCR),[32] array comparative genomic hybridization (CGH) (Agilent Technologies, Waldbronn, Germany) with subsequent confirmation by panel-

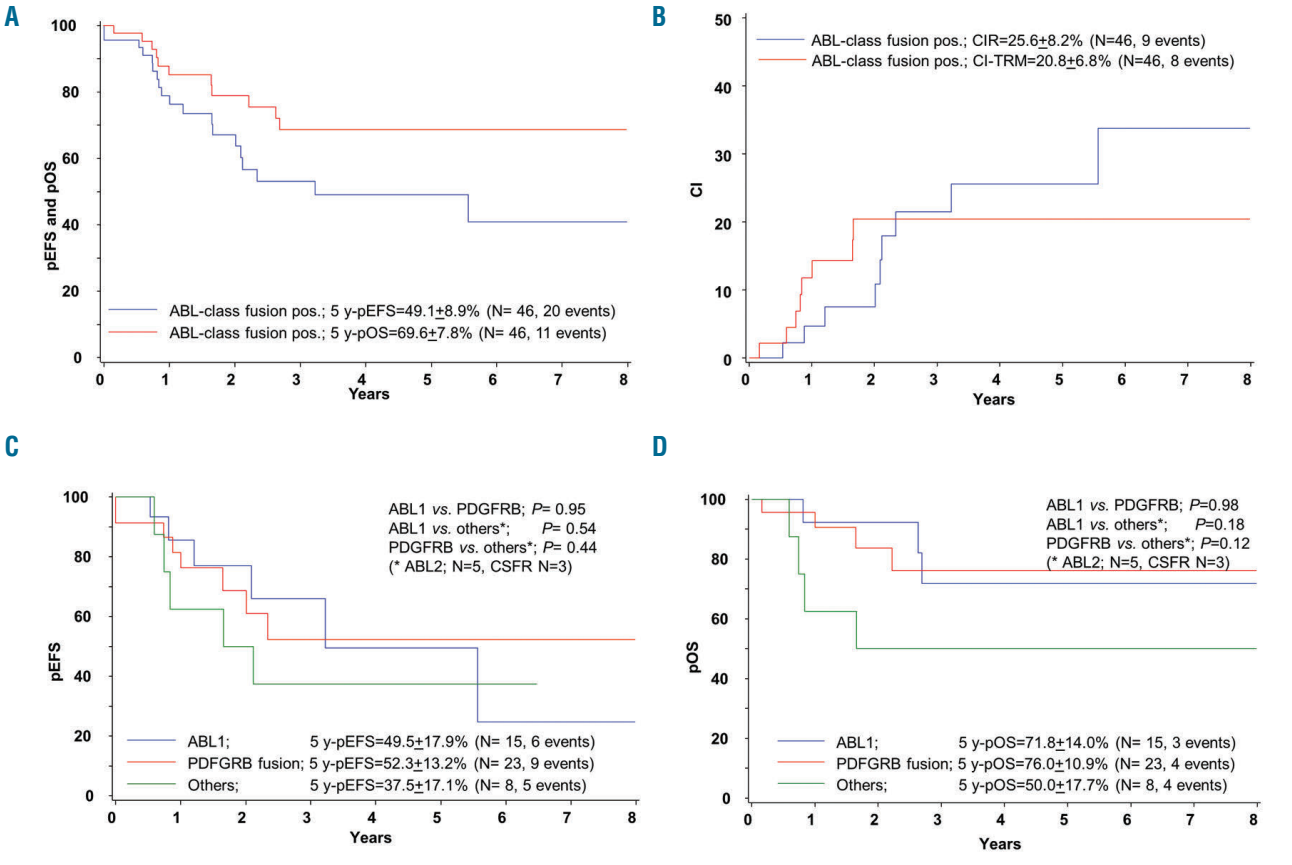

Figure 1. Treatment outcome of patients with pediatric ABL-class fusion positive acute lymphoblastic leukemia (ALL). Kaplan-Meier estimates for the whole cohort of 46 cases. (A) Event-free survival (pEFS) and overall survival (pOS) at 5 years (y). (B) Cumulative incidence of relapses (CIR) and of treatment-related mortality (CI-TRM) at 5 years. According to ABL-class fusion subtype, *ABL1, PDGFRB,* others (*ABL2* n=5, *CSFR* n=2): (C) EFS. (D) OS.

based RNA-sequencing (e.g. TruSight RNA Pan-Cancer Panel; Illumina, San Diego, CA, USA), whole transcriptome or direct panel-based RNA-sequencing.

In both protocols, patient stratification was mainly based on quantitative assessment of minimal residual disease (MRD) using clone-specific immunoglobulin- and T-cell receptor-gene rearrangements by PCR (PCR-MRD) after induction (treatment day 33) and consolidation (day 78) therapy. In AIEOP-BFM ALL 2009, MRD was additionally measured by flow cytometry on treatment day 15 (FCM-MRD).[33] The logistics of the AIEOP-BFM ALL studies, cell sample isolation, and MRD marker identification, as well as MRD-based risk stratification of the AIEOP-BFM ALL 2000 study, have been previously reported.[8,9] In the AIEOP-BFM ALL 2009 trial, patients were additionally allocated to the high-risk (HR) group, when PCR-MRD was ≥$5x10^{-4}$ on day 33 and still measurable on day 78 and/or if FCM-MRD at day 15 was ≥10%.

Details on chemotherapy regimens and randomized treatment interventions, as well as HSCT indication, were reported elsewhere.[8,9,34] The study AIEOP-BFM ALL 2000 is registered at *www.clinicaltrials.gov* by BFM as NCT00430118 and by AIEOP as NCT00613457; the study AIEOP-BFM ALL 2009 is registered as NCT01117441. The analyses were approved by local Institutional Review Boards and informed consent was obtained from the patients and/or guardians in accordance with the Declaration of Helsinki.

Statistical analysis

Event-free survival (EFS) was calculated from diagnosis to first failure, which was defined as death during induction therapy, resistance, relapse, death in CR, or development of a second malignant neoplasm (SMN). Rates were calculated according to Kaplan-Meier and compared by log-rank test.[35,36] Kaplan-Meier plots that compared HSCT with chemotherapy were adjusted to account for the waiting time to transplantation (with a landmark at median time to HSCT). Cumulative incidence of relapse and TRM functions were constructed by the method of Kalbfleisch and Prentice and compared with Gray test.[37,38] Proportional differences between patient groups were analyzed by χ^2 or Fisher's exact tests.

Results

We identified 46 ABL-class fusion positive cases diagnosed between October 2000 and August 2018 treated according to AIEOP-BFM ALL 2000 and 2009 protocols.

ABL1 fusions were identified in 15 cases, *ABL2* fusions in five cases, *CSF1R* fusions in three cases, and *PDGFRB* rearrangements in 23 cases (*Online Supplementary Table S1*).

Overall, 33 patients received chemotherapy without the addition of any TKI (no-TKI group); a TKI was added on an individual basis and not according to protocol during treatment in 13 cases (TKI group; imatinib in 8 and dasatinib in 5 cases) diagnosed between February 2011 and April 2018. In eight of these 13 cases, TKI was introduced at the end of induction or during consolidation therapy, in four during post-consolidation HR-blocks and in one case

after HSCT (for details see *Online Supplementary Figure S1*).

Altogether, 36 of 46 (78.3%) patients were treated in the HR group [(no-TKI 24 of 33 (72.7%)], TKI 12 of 13 (92.3%)), and HSCT in first CR was performed in 25 of 46 (54.3%) patients: in 16 of 33 (48.5%) of no-TKI and in 9 of 13 (69.3%) of TKI-treated patients (Table 1). Compared to the entire group of B-ALL patients of the AIEOP-BFM ALL 2000 study, ABL-class fusion positive cases were older and

Table 1. Patients' and clinical characteristics and response to treatment according to ABL-class fusion and tyrosine kinase inhibitor (TKI) treatment in comparison with the entire AIEOP-BFM 2000 B-ALL cohort.

	ABL-class fusion pos cases Total n (%)	Treatment without additional TKI[1]				Treatment with additional TKI				ALL-BFM 2000 B-ALL	P[2]
		All n (%)	PDGFRB fusion n (%)	ABL1 fusion n (%)	Others[3] n (%)	All n (%)	PDGFRB fusion n (%)	ABL1 fusion n (%)	Others n (%)	Total n (%)	
N. of patients	46 (100.0)	33 (100.0)	17 (100.0)	10 (100.0)	6 (100.0)	13 (100.0)	6 (100.0)	5 (100.0)	2 (100.0)	3854 (100.0)	
Sex											n.s.
Male	29 (63.0)	22 (66.7)	12 (70.6)	7 (70.0)	3 (50.0)	7 (53.8)	3 (50.0)	3 (60.0)	1 (50.0)	2062 (53.5)	
Female	17 (37.0)	11 (33.3)	5 (29.4)	3 (30.0)	3 (50.0)	6 (46.2)	3 50.0)	2 (40.0)	1 (50.0)	1792 (46.5)	
Age at diagnosis (years)											<.0001
0 – 9	22 (47.8)	15 (45.5)	7 (41.2)	7 (70.0)	1 (16.7)	6 (46.2)	1 (16.7)	4 (80.0)	1 (50.0)	2999 (77.8)	
>10	24 (52.2)	18 (54.5)	10 (58.8)	3 (30.0)	5 (83.3)	7 (53.8))	5 (83.3)	1 (20.0)	1 (50.0)	855 (22.2)	
WBC count[4] (x10^9/L)											<.0001
Lower than 50	16 (34.8)	14 (42.4)	8 (47.1)	4 (40.0)	2 (33.3)	2 (15.4)	2 (33.3)	0	0	3288 (85.3)	
50-<100	9 (19.6)	7 (21.2)	4 (23.5)	2 (20.0)	1 (16.7)	2 (15.4)	1 (16.7)	1 (20.0)	0	325 (8.4)	
100 or higher	19 (41.3)	12 (36.4)	5 (29.4)	4 (40.0)	3 (50.0)	7 (53.8)	3 (50.0)	3 (60.0)	1 (50.0)	241 (6.3)	
No information	2 (4.3)	0	0	0	0	2 (15.4)	0	1 (20.0)	1 (50.0)	0	
NCI Risk group[5]											<.0001
SR	7 (15.2)	7 (21.2)	3 (17.6)	3 (30.0)	1 (16.7)	0	0	0		2574 (66.8)	
HR	37 (80.4)	26 (78.8)	14 (82.4)	7 (70.0)	5 (83.3)	11 (84.6)	6 (100.0)	4 (80.0)	1 (50.0)	1280 (33.2)	
No information	2 (4.3)	0	0	0	0	2 (15.4)	0	1 (20.0)	1 (50.0)	0	
Pred. response[6]											<.0001
Good	22 (47.8)	17 (51.5)	5 (29.4)	9 (90.0)	3 (50.0)	5 (38.5)	1 (16.7)	3 (60.0)	1 (50.0)	3619 (93.9)	
Poor	23 (50.0)	16 (48.5)	12 (70.6)	1 (10.0)	3 (50.0)	7 (53.8)	5 (83.3))	1 (20.0)	1 (50.0)	214 (5.6)	
No information	1 (2.2)	0		0	0	1 (7.7)	0	1 (20.0)	0	21 (0.5)	
MRD[7] at End of induction											<.0001
≥5x10^{-2}	22 (47.8)	17 (51.5)	13 (76.5)	1 (10.0)	3 (50.0)	5 (38.5)	4 (66.6)	1 (20.0)		86 (2.2)	
5x10^{-4}-<5x10^{-2}	8 (17.4)	5 (15.2)	2 (11.8)	3 (30.0)	0	3 (23.1)	1(16.7)	1 (20.0)	1 (50.0)	610 (15.8)	
<5x10^{-4}	12 (26.1)	9 (27.3)	1 (5.9)	6 (60.0)	2 (33.3)	3 (23.1)	0	3 (60.0)	0	2925 (75.9)	
No information	4 (8.7)	2 (6.1)	1 (5.9)	0	1 (16.7)	2 (15.4)	1 (16.7)	0	1 (50.0)	233 (6.0)	
MRD after consolidation											<.0001
≥5x10^{-2}	9 (19.6)	8 (24.2)	5 (29.4)	1 (10.0)	2 ()	1 (7.7)	0	1 (20.0)	0	34 (0.9)	
5x10^{-4}-<5x10^{-2}	12 (26.1)	9 (27.3)	8 (47.1)	0	1 (16.7)	3 (23.1)	2 (33.3)	0	1 (50.0)	151 (3.9)	
<5x10^{-4}	20 (43.5)	15 (45.5)	3 (17.6)	9 (90.0)	3 (33.3)	5 (38.5)	2 (33.3)	3 (60.0)		3452 (89.6)	
No information	5 (10.9)	1 (3.0)	1 (5.9)	0	0	4 (30.8)	2 (33.3)	1 (20.0)	1 (50.0)	217 (5.6)	
Treatment group											<.0001
SR	3 (6.5)	3 (9.1)	0	2 (20.0)	1 (16.7)	0	0	0	0	1337 (34.7)	
IR	5 (10.9)	4 (12.1)	0	3 (30.0)	1 (16.7)	1 (7.7)	0	1 (20.0)	0	2088 (54.2)	
HR	36 (78.3)	24 (72.7)	17 (100.0)	3 (30.0)	4 (66.7)	12 (92.3)	6 (100.0)	4 (80.0)	2 (100.0)	429 (11.1)	
No information	2 (4.3)	2 (6.1)	0	2 (20.0)	0	0	0	0		0	
HSCT[8]											<.0001
No	21 (45.7)	17 (51.5)	5 (29.9)	10 (100.0)	2 (33.3)	4 (30.7)	1 (16.7)	3 (60.0)	0	3684 (95.1)	
Yes	25 (54.3)	16 (48.5)	12 (70.1)	0	4 (66.7)	9 (69.3)	5 (83.3)	2 (40.0)	2 (100.0)	216 (4.9)	

ALL: acute lymphoblastic leukemia. [1]TKI: tyrosine kinase inhibitor. [2]Fisher test comparing all ABL-class positive cases to the B-ALL AIEOP-BFM 2000 cohort, patients with no information excluded from test. [3]Others: ABL2 n=5, CSFR1 n=3. [4]WBC: white blood cell count. [5]NCI-SR, WBC <50x10^9/L and age <10 years; NCI-HR, WBC >50x10^9/L and/or age >10 years. [6]Good: <1,000 leukemic blood blasts / µL on treatment day 8, poor: more than 1000 /µL. [7]MRD: minimal residual disease. [8]HSCT: hematopoietic stem cell transplantation.

had higher white blood cell counts at diagnosis (WBC), with a statistically significant difference for NCI-HR features (P<0.0001 each) (Table 1). ABL-class fusion positive cases had a significantly worse response to treatment compared to the entire B-ALL 2000 cohort: prednisone poor response (PPR) was observed in 50% *versus* 5.6% of patients with data available, high MRD level (≥5x10^{-4}) after induction treatment (EoI) in 71.4% *versus* 19.2% and after consolidation (EoC) in 51.2% *versus* 5.1% of cases with data available. There are, however, differences by type of ABL-class fusion: the majority of PDGFRB-fusion positive cases with data available showed a PPR (17 of 23, 73.9%), high EoI-MRD (20 of 21, 95.2% with data available) as well as high EoC-MRD (15 of 20, 75% with data available). In contrast, in ABL1-class positive cases, PPR (2 of 14, 14.3%), high EoI-MRD (6 of 15, 40.0%), and high EoC-MRD (2 of 14, 14.3%) were observed much less frequently (Table 1). Of note, we observed a favorable MRD response (MRD negative or low-positive) at EoC in 5 of 6 ABL-class positive cases with MRD data available in whom a TKI was added to chemotherapy before EoC (three had an ABL1-fusion and two had a *PDGFRB*-fusion).

For the entire cohort of 46 cases, 5-year EFS was 49.1+8.9% and 5-year OS 69.6+7.8%; CIR was 25.6+8.2% (9 events) and TRM 20.8+6.8% (8 events) (Figure 1A and B). Six of the nine patients with leukemia relapse in first CR were successfully treated subsequently and are in long-term CR. One case was resistant to treatment (resistance defined as blast persistence after three HR blocks) and two presented with SMN after HSCT (one thyroid cancer and one lymphoma), both patients with SMN were treated successfully. Details of the events are shown in Table 2.

No significant differences in 5-year EFS and 5-year OS were observed comparing the ABL-class subgroups *ABL1*-fusions, *PDGFRB*-fusions and other fusions (5 *ABL2* and 3 *CSFR1* fusions) (Figure 1C and D). Interestingly, the ABL1-fusion positive group, which showed a better treatment sensitivity as compared to the *PDGFRB*-fusion positive group, had a higher frequency of relapses (5 of 15 patients vs. 3 of 23); of note HSCT was performed only in 2 of 15 ABL1-fusion positive cases *versus* 17 of 23 *PDGFRB*-fusion positive cases (*Online Supplementary Figure S2A-C*).

Patients treated with TKI had worse features (12 of 13

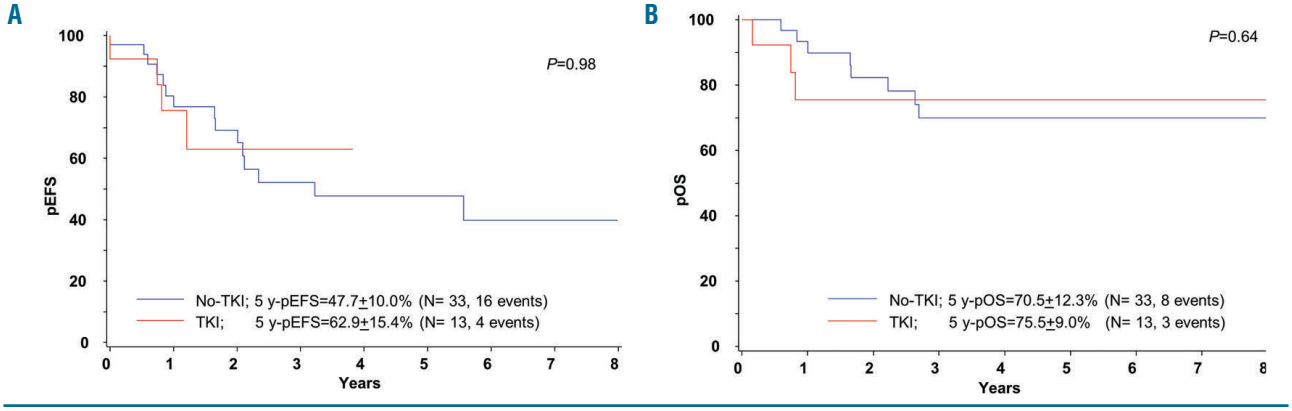

Figure 2. Treatment outcome of patients with pediatric ABL-class fusion positive acute lymphoblastic leukemia (ALL) according to treatment without or with tyrosine kinase inhibitor (TKI). Kaplan-Meier estimates comparing patients treated without TKI (no-TKI) and with TKI (TKI) are shown. (A) Event-free survival (EFS) at 5 years (y). (B) Overall survival (OS) at 5 years.

Table 2. Distribution of events according to tyrosine kinase inhibitor (TKI) treatment.

	Total n (%)	No TKI[1] n (%)	TKI n (%)
All cases	46 (100.0)	33 (100.0)	13 (100.0)
Resistant[2]	1 (2.2)	1 (3.0)	0
Relapses[3]	9 (19.6)	8 (24.2)[4]	1 (7.7)[5]
After chemotherapy	6 (13.0)	6 (18.1)	0
After HSCT[6]	3 (6.5)	2 (6.1)	1 (7.7)
Death in induction	1 (2.2)	0	1 (7.7)
Death in CR[7]	7 (15.2)	5 (15.2)	2 (15.4)
After chemotherapy	1 (2.2)	0	1 (7.7)
After HSCT	6 (13.0)	5 (15.2)	1 (7.7)
SMN[8]	2 (4.4)	2 (6.1)	0

ALL: acute lymphoblastic leukemia. [1]TKI: tyrosine kinase inhibitor. [2]Resistant patients are those who did not achieve complete remission (CR) by end of the third high-risk (HR) block of chemotherapy. [3]Relapses: 5 cases ABL1 fusion positive (pos.), 3 cases PDGFRB fusion pos., 1 case CSF1R fusion pos. [4]No-TKI relapses: after chemotherapy: 1 very early, 3 early, 2 very late (both RCSD11-ABL1 pos.), after hematopoietic stem cell transplantation (HSCT): 4 months and 17 months after HSCT. [5]TKI relapse: 1 case 9 months post HSCT. [6]HSCT. [7]CR: complete remission. [8]SMN: second malignant neoplasms: 1 case with post-transplant lymphoma, 1 case with thyroid cancer after HSCT.

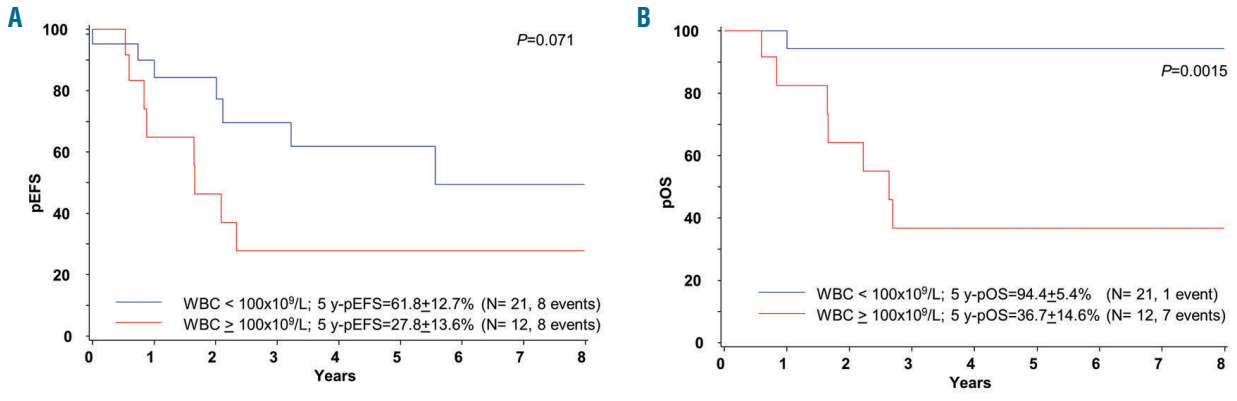

Figure 3. Treatment outcome of patients with pediatric ABL-class fusion positive acute lymphoblastic leukemia (ALL) according to white blood cell count at diagnosis (WBC). Kaplan-Meier estimates comparing patients with WBC <100x10⁹/L and patients with WBC equal or >100x10⁹/L are shown. (A) Event-free survival (pEFS) at 5 years. (B) Overall survival (pOS) at 5 years.

were HR *vs.* 24 of 33 in no-TKI treated patients) and the majority of them underwent HSCT (9 of 13 *vs.* 16 of 33); their 5-year EFS and 5-year-OS did not differ significantly compared with the no-TKI group: EFS no-TKI 47.7+10.0%, TKI 62.9+5.4%, *P*=0.98; OS no-TKI 70.9+9.0%, TKI 75.5+12.3%, *P*=0.64 (Figure 2A and B). Whereas TRM was similar in both groups, only one out of 13 cases of the TKI patients relapsed *versus* 8 of 33 of no-TKI cases (*Online Supplementary Figure S3A and B*). Of note, there were four late occurring events in the no-TKI group: two SMN after HSCT and two late relapses in *ZMIZ1-ABL1* positive patients not transplanted.

No significant difference in outcome between patients treated with or without HSCT were seen: 5-year EFS was 47.9+11.4% *versus* 55.0+15.5%, *P*=0.35; 5-year OS 66.7+10.5% *versus* 84.0+10.6%, *P*=0.22) (*Online Supplementary Figure S4A and B*). However, analyzing the events in more detail, it is remarkable that the majority of events in HSCT-treated patients (n=25) were non-relapse events (TRM=6, SMN=2, relapses=3) whereas in patients not transplanted (n= 21) relapses predominated (TRM=1, relapses=6) (Table 2). In those patients who were not treated with TKI, the CIR and TRM rate in transplanted *versus* not transplanted cases were 13.2+9.3% *versus* 43.8+17.8%, *P*=0.06 (CIR) and 32.3+12.4% *versus* 0.0%, *P*=0.034 (TRM) *(Online Supplementary Figure S4C and D*).

Analysis by MRD showed a 5-year EFS of 40.4±11.4% in EoI-MRD≥5x10^{-4} *versus* 76.2±14.8% in EoI MRD<5x10^{-4}, *P*=0.11) (*Online Supplementary Figure S5A*); CIR was similar in both MRD groups (27.3+11.2% *vs.* 23.8+15.9%, *P*=0.74), while TRM in patients with EoI-MRD≥5x10^{-4} was 25.4+9.4% *versus* 0.0% in EoI MRD<5x10^{-4} (*P*=0.1) (*Online Supplementary Figure S5B*). By EoC-MRD, 5-year EFS in cases with an MRD≥5x10^{-4} was 46.2+12.1% *versus* 56.7+15.4% in those with MRD<5x10^{-4}, *P*=0.31. However, it should be considered that 19 of 21 patients with EoC-MRD≥5x10^{-4} received HSCT *versus* only three of 20 patients with MRD<5x10^{-4} (*Online Supplementary Figure S6*).

We also analyzed the outcome of patients with a WBC higher or less than 100x10^{9}/L: 5-year EFS was 36.8+12.7% *versus* 59.9+11.6%, respectively, *P*=0.21, while 5-year OS was significantly lower in patients with a WBC >100x10^{9}/L (48.8+12.9% *vs.* 87.4+6.8%, *P*=0.036). This difference was more pronounced in the no-TKI group with a 5-year EFS 27.8+13.6% *versus* 61.8+12.7%, *P*=0.07 and an OS of 36.7+14.6% *versus* 94.4+5.4%, respectively, *P*=0.0015) (Figure 3A and B).

Discussion

The improvement in genetic diagnostics has allowed the identification of rare ALL subgroups with specific clinical characteristics and target lesions. In this context, ABL-class fusion positive B-ALL other than Ph^{+} ALL constitutes a challenging entity, which is estimated to represent about 2-3% of childhood ALL. The frequency is reported in the context of the *BCR-ABL1*-/Ph-like ALL, which is higher in adolescents and associated with higher risk features and a worse outcome as compared to the non-*BCR-ABL1*-/Ph-like ALL patients.[20,21,23,26] First protocols based on "precision medicine" have been designed to identify and treat ALL patients with drugs specific for targetable lesions given in addition to standard chemotherapy (e.g. St Jude Total XVII (NCT03117751) and AALL1131(NCT02883049)). Within the *BCR-ABL1*-/Ph-like ALL group, it is suggested that patients with ABL-class fusion positive ALL might benefit from the addition of TKI to chemotherapy. However, besides the above mentioned on-going trials, no controlled studies have been conducted in this field so far, and the published data on the role of TKI for this subgroup is restricted to case reports.[21,39,40]

We report here the largest series of ABL-class fusion positive cases, treated according to two consecutive AIEOP-BFM ALL protocols with a stratification mostly based on MRD response. Screening for ABL-class rearrangements was not required by the protocols and was often done retrospectively in the frame of research projects, thus, no conclusions on incidence can be drawn from this retrospective study. Likewise, due to the selection in screening policy, the outcome data need to be interpreted with great caution. Nevertheless, the cohort described here provides interesting information and clearly shows the urgent need for prospective co-operative clinical studies.

When compared with other B-ALL patients recruited in the AIEOP-BFM ALL protocols, the ABL-class fusion pos-

itive cases identified in this study included higher proportions of patients aged ten years or older and presenting with hyperleukocytosis (WBC ≥100x10^9/L). Interestingly, the distribution by age and WBC counts is similar to that of patients with Ph$^+$ ALL included in the EsPhALL studies.[15] Poor MRD response at the end of consolidation phase IB (≥5x10^{-4}) was detected in a high proportion of patients with available data (21 of 41, 51%); similar to that of Ph$^+$ ALL patients treated without TKI in the AIEOP-BFM ALL 2000 study, where 22 of 54 (41%) patients had high MRD (≥5x10^{-4}) after consolidation phase.[8] Interestingly, in patients who had already been treated with a TKI during consolidation, the majority (6 of 8) had either a low positive or negative EoC-MRD, suggesting a beneficial role of the addition of TKI; however, the low number of TKI-treated patients with EoC-MRD data available does not allow any definitive conclusion to be drawn.

The EFS of the entire cohort was poor, particularly for patients not receiving TKI: <50% at 5 years, very similar to the outcome of Ph$^+$ ALL patients treated in AIEOP-BFM ALL 2000 without TKI.[8] This poor outcome was observed even though most patients were treated according to the high-risk schedule and more than half of them underwent HSCT in first CR, a strategy similar to that applied for the cohort of Ph$^+$ ALL patients of the AIEOP-BFM ALL 2000 study.[8] Interestingly, the outcome was dismal in patients with WBC ≥100x10^9/L, as reported also for Ph$^+$ ALL patients treated in the EsPhALL studies.[14,15]

The impact of HSCT in the cohort reported here is not clear since transplanted patients had an outcome similar to that of patients who were not transplanted. However, patients who received HSCT had worse features, thus, per protocol, an indication for HSCT (and considering the fact that HSCT was associated with a very low rate of relapses), one may infer that HSCT might be effective in disease control. HSCT was, however, also associated with high TRM: six out of 25 patients died of TRM.

Only a minority of our patients (13 of 46) received a TKI (either imatinib or dasatinib). It was not given by protocol; it was used in different schedules, basically decided by treating physicians, and generally due to poor response to chemotherapy. Obviously, the identification of the target lesion had already been achieved during treatment. Of note, most of these patients (9 of 13) also received HSCT, two of them not based on an indication provided by the protocol but on the knowledge of an ABL-class fusion. Although the rate of relapses was low in this small group, their overall outcome was similar to those patients not treated with TKI. Due to the low number of TKI-treated patients, the potentially confounding influence of HSCT and the very short follow up, no conclusions on the benefit of the use of TKI can be drawn from this study. However, given also the biological and clinical similarities with the Ph$^+$ ALL, it is plausible that the early and protracted administration of TKI on top of chemotherapy might improve treatment response and outcome while reducing the need for HSCT in CR1, as shown for Ph$^+$ ALL.[14-18]

This study, despite being the largest in this field, is limited by its retrospective nature. The complex interaction of confounding factors, such as case selection bias, stratification criteria, chemotherapy intensity, HSCT, and different timing/modalities of delivering targeted therapies, do not allow the benefit of a precision medicine approach to be appropriately assessed. There is, therefore, an urgent need for a prospective controlled clinical trial.

To this purpose, it will be crucial to include the early identification of ABL-class fusion ALL cases in the initial diagnostic work-up of patients and to treat them in a properly designed study to investigate the role of TKI and to identify the appropriate chemotherapy backbone. Given the rarity of this clinical entity, this goal can only be pursued by an international collaborative network, like in pediatric Ph$^+$ ALL.

Funding

The project was supported by Grants of Deutsche Krebshilfe, the Madeleine-Schickedanz-Stiftung für Leukämieforschung, the Deutsche Forschungsgemeinschaft (DFG, BE 6555/1-1 and BE 6555/2-1 (GC and AKB)), the Stiftung MHHplus (DSt), the Italian Association for Cancer Research (AIRC) (IG grants to GiC and AB), the Czech Health Research Council - NV15-30626A (MZ) and the Cancer Australia PdCCRs APP1128727 (for RS and DLW). SI and SE were supported by TRANSCALL2 from the Israeli Health Ministry and by the Israeli cancer association.

References

1. Hunger SP, Mullighan CG. Redefining ALL classification: toward detecting high-risk ALL and implementing precision medicine. Blood. 2015;125(26):3977-3987.
2. Conter V, Aricò M, Valsecchi MG, et al. Long-term results of the Italian Association of Pediatric Hematology and Oncology (AIEOP) Acute Lymphoblastic Leukemia Studies, 1982-1995. Leukemia. 2000; 14(12):2196-2204.
3. Schrappe M, Reiter A, Zimmermann M, et al. Long-term results of four consecutive trials in childhood ALL performed by the ALL-BFM study group from 1981 to 1995. Leukemia. 2000;14(12):2205-2222.
4. Möricke A, Reiter A, Zimmermann M, et al. Risk-adjusted therapy of acute lymphoblastic leukemia can decrease treatment burden and improve survival: treatment results of 2169 unselected pediatric and adolescent patients enrolled in the trial ALL-BFM 95. Blood. 2008;111(9):4477-4489.
5. Pui CH, Evans WE. Treatment of acute lymphoblastic leukaemia. N Engl J Med. 2006;354(2):166-178.
6. Moghrabi A, Levy DE, Asselin B, et al. Results of the Dana-Farber Cancer Institute ALL Consortium Protocol 95-01 for children with acute lymphoblastic leukemia. Blood. 2007;109(3):896-904.
7. Carroll WL, Bhojwani D, Min DJ, et al. Pediatric acute lymphoblastic leukemia. Hematology Am Soc Hematol Educ Program. 2003:102-113.
8. Conter V, Bartram CR, Valsecchi MG, et al. Molecular response to treatment redefines all prognostic factors in children and adolescents with B-cell precursor acute lymphoblastic leukemia: results in 3184 patients of the AIEOP-BFM ALL 2000 study. Blood. 2010;115(16):3206-3214.
9. Schrappe M, Valsecchi MG, Bartram CR, et al. Late MRD response determines relapse risk overall and in subsets of childhood T-cell ALL: results of the AIEOP-BFM-ALL 2000 study. Blood. 2011;118(8):2077-2084.
10. Bernt KM, Hunger SP. Current concepts in pediatric Philadelphia chromosome-positive acute lymphoblastic leukemia. Front Oncol. 2014;4:54.
11. Fielding AK. Treatment of Philadelphia chromosome-positive acute lymphoblastic leukemia in adults: a broader range of options, improved outcomes, and more therapeutic dilemmas. Am Soc Clin Oncol Educ Book. 2015:e352-359.
12. Aricò M, Schrappe M, Hunger SP, et al. Clinical outcome of children with newly diagnosed Philadelphia chromosome-positive acute lymphoblastic leukemia treated between 1995 and 2005. J Clin Oncol. 2010;28(31):4755-4761.
13. Biondi A, Schrappe M, De Lorenzo P, et al.

Imatinib after induction for treatment of children and adolescents with Philadelphia-chromosome positive acute lymphoblastic leukaemia (EsPhALL): a randomised, open-label, intergroup study. Lancet Oncol. 2012; 13(9):936-945.
14. Biondi A, Cario G, De Lorenzo P, et al. Long-term follow up of pediatric Philadelphia positive acute lymphoblastic leukemia treated with the EsPhALL2004 study: high white blood cell count at diagnosis is the strongest prognostic factor. Haematologica. 2019;104(1):13-16.
15. Biondi A, Gandemer V, De Lorenzo P, et al. Imatinib treatment of paediatric Philadelphia chromosome-positive acute lymphoblastic leukaemia (EsPhALL2010): a prospective, intergroup, open-label, single-arm clinical trial. Lancet Haematol. 2018; 5(12):641-652.
16. Schultz KR, Bowman WP, Aledo A, et al. Improved early event-free survival with imatinib in Philadelphia chromosome-positive acute lymphoblastic leukemia: a children's oncology group study. J Clin Oncol. 2009;27(31):5175-5181.
17. Schultz KR, Carroll A, Heerema NA, et al. Long-term follow-up of imatinib in pediatric Philadelphia chromosome-positive acute lymphoblastic leukemia: Children's Oncology Group Study AALL0031. Leukemia. 2014;28(7):1467-1471.
18. Slayton WB, Schultz KR, Kairalla JA, et al. Dasatinib plus intensive chemotherapy in children, adolescents, and young adults with philadelphia chromosome-positive acute lymphoblastic leukemia: results of Children's Oncology Group Trial AALL0622. J Clin Oncol. 2018;36(22):2306-2314.
19. Roberts KG, Yang Y, Turner DP, et al. Oncogenic role and therapeutic targeting of ABL-class and JAK-STAT activating kinase alterations in Ph-like ALL. Blood Adv. 2017;1(20):1657-1671.
20. Den Boer ML, van Slegtenhorst M, De Menezes RX, et al. A subtype of childhood acute lymphoblastic leukaemia with poor treatment outcome: a genome-wide classification study. Lancet Oncol. 2009;10(2):125-134.
21. Roberts KG, Li Y, Payne-Turner D, et al. Targetable kinase-activating lesions in Ph-like acute lymphoblastic leukemia. N Engl J Med. 2014;371(11):1005-1015.
22. Arber DA, Orazi A, Hasserjian R, et al. The 2016 revision to the World Health Organization classification of myeloid neoplasms and acute leukemia. Blood. 2016; 127(20):2391-2405.
23. Boer JM, Koenders JE, van der Holt B, et al. Expression profiling of adult acute lymphoblastic leukemia identifies a BCR-ABL1-like subgroup characterized by high non-response and relapse rates. Haematologica. 2015;100(7):261-264.
24. Harvey RC, Mullighan CG, Wang X, et al. Identification of novel cluster groups in pediatric high-risk B-precursor acute lymphoblastic leukemia with gene expression profiling: correlation with genome-wide DNA copy number alterations, clinical characteristics, and outcome. Blood. 2010; 116(23):4874-4884.
25. van der Veer A, Waanders E, Pieters R, et al. Independent prognostic value of BCR-ABL1-like signature and IKZF1 deletion, but not high CRLF2 expression, in children with B-cell precursor ALL. Blood. 2013;122(15):2622-2629.
26. Roberts KG, Pei D, Campana D, et al. Outcomes of children with BCR-ABL1–like acute lymphoblastic leukemia treated with risk-directed therapy based on the levels of minimal residual disease. J Clin Oncol. 2014;32(27):3012-3020.
27. Boer JM, Steeghs EM, Marchante JR, et al. Tyrosine kinase fusion genes in pediatric BCRABL1-like acute lymphoblastic leukemia. Oncotarget. 2017;8(3):4618-4628.
28. Reshmi SC, Harvey RC, Roberts KG, et al. Targetable kinase gene fusions in high-risk B-ALL: a study from the Children's Oncology Group. Blood. 2017; 129(25):3352-3361.
29. Dworzak MN, Buldini B, Gaipa G, et al. AIEOP-BFM consensus guidelines 2016 for flow cytometric immunophenotyping of Pediatric acute lymphoblastic leukemia. Cytometry B Clin Cytom. 2018;94(1):82-93.
30. van der Velden VH, Cazzaniga G, Schrauder A, et al. European Study Group on MRD detection in ALL (ESG-MRD-ALL). Analysis of minimal residual disease by Ig/TCR gene rearrangements: guidelines for interpretation of real-time quantitative PCR data. Leukemia. 2007;21(4):604-611.
31. van der Does-van den Berg A, Bartram CR, Basso G, et al. Minimal requirements for the diagnosis, classification, and evaluation of the treatment of childhood acute lymphoblastic leukemia (ALL) in the "BFM Family" Cooperative Group. Med Pediatr Oncol. 1992;20(6):497-505.
32. Reshmi SC, Harvey RC, Roberts KG, et al. Targetable kinase gene fusions in high-risk B-ALL: a study from the Children's Oncology Group. Blood. 2017; 129(25):3352-3361.
33. Basso G, Veltroni M, Valsecchi MG, et al. Risk of relapse of childhood acute lymphoblastic leukemia is predicted by flow cytometric measurement of residual disease on day 15 bone marrow. J Clin Oncol. 2009;27(31):5168-5174.
34. Möricke A, Zimmermann M, Valsecchi MG, et al. Dexamethasone vs prednisone in induction treatment of pediatric ALL: results of the randomized trial AIEOP-BFM ALL 2000. Blood. 2016;127(17):2101-2112.
35. Kaplan EL, Meier P. Nonparametric estimation from incomplete observations. J Am Stat Assoc. 1958;53(282):457-481.
36. Mantel N. Evaluation of survival data and two new rank order statistics arising in its consideration. Cancer Chemother Rep. 1966;50(3):163-170.
37. Kalbfleisch JD, Prentice RL. The statistical analysis of failure time data (ed 1). New York: John Wiley and sons. 1980:163-188.
38. Gray RJ. A class of K-sample tests for comparing the cumulative incidence of a competing risk. Ann Stat. 1988;16(3):1141-1154.
39. Weston BW, Hayden MA, Roberts KG, et al. Tyrosine kinase inhibitor therapy induces remission in a patient with refractory EBF1PDGFRB-positive acute lymphoblastic leukemia. J Clin Oncol. 2013;31(25):413-416.
40 Lengline E1, Beldjord K, Dombret H, Soulier J, Boissel N, Clappier E. Successful tyrosine kinase inhibitor therapy in a refractory B-cell precursor acute lymphoblastic leukemia with EBF1-PDGFRB fusion. Haematologica. 2013;98(11):146-148.

ARTICLE

Genetic and phenotypic characterization of indolent T-cell lymphoproliferative disorders of the gastrointestinal tract

Craig R. Soderquist,[1] Nupam Patel,[1] Vundavalli V. Murty,[1] Shane Betman,[1] Nidhi Aggarwal,[2] Ken H. Young,[3] Luc Xerri,[4] Rebecca Leeman-Neill,[1] Suzanne K. Lewis,[5] Peter H. Green,[5] Susan Hsiao,[1] Mahesh M. Mansukhani,[1] Eric D. Hsi,[6] Laurence de Leval,[7] Bachir Alobeid[1] and Govind Bhagat[1]

[1]Department of Pathology and Cell Biology, Columbia University Irving Medical Center, New York Presbyterian Hospital, New York, NY, USA; [2]Department of Pathology, University of Pittsburgh Medical Center, Pittsburgh, PA, USA; [3]Department of Hematopathology, MD Anderson Cancer Center, Houston, TX, USA; [4]Department of Bio-Pathology, Institut Paoli-Calmettes, Aix-Marseille University, Marseille, France; [5]Department of Medicine, Celiac Disease Center, Columbia University Irving Medical Center, New York Presbyterian Hospital, New York, NY, USA; [6]Pathology and Laboratory Medicine Institute, Cleveland Clinic, Cleveland, OH, USA and [7]Institute of Pathology, Lausanne University Hospital (CHUV), Lausanne, Switzerland.

Ferrata Storti Foundation

Haematologica 2020
Volume 105(7):1895-1906

ABSTRACT

Indolent T-cell lymphoproliferative disorders of the gastrointestinal tract are rare clonal T-cell diseases that more commonly occur in the intestines and have a protracted clinical course. Different immunophenotypic subsets have been described, but the molecular pathogenesis and cell of origin of these lymphocytic proliferations is poorly understood. Hence, we performed targeted next-generation sequencing and comprehensive immunophenotypic analysis of ten indolent T-cell lymphoproliferative disorders of the gastrointestinal tract, which comprised $CD4^+$ (n=4), $CD8^+$ (n=4), $CD4^+/CD8^+$ (n=1) and $CD4^-/CD8^-$ (n=1) cases. Genetic alterations, including recurrent mutations and novel rearrangements, were identified in 8/10 (80%) of these lymphoproliferative disorders. The $CD4^+$, $CD4^+/CD8^+$, and $CD4^-/CD8^-$ cases harbored frequent alterations of JAK-STAT pathway genes (5/6, 82%); *STAT3* mutations (n=3), *SOCS1* deletion (n=1) and *STAT3-JAK2* rearrangement (n=1), and 4/6 (67%) had concomitant mutations in epigenetic modifier genes (*TET2*, *DNMT3A*, *KMT2D*). Conversely, 2/4 (50%) of the $CD8^+$ cases exhibited structural alterations involving the 3' untranslated region of the *IL2* gene. Longitudinal genetic analysis revealed stable mutational profiles in 4/5 (80%) cases and acquisition of mutations in one case was a harbinger of disease transformation. The $CD4^+$ and $CD4^+/CD8^+$ lymphoproliferative disorders displayed heterogeneous Th1 ($T\text{-bet}^+$), Th2 ($GATA3^+$) or hybrid Th1/Th2 ($T\text{-bet}^+/GATA3^+$) profiles, while the majority of $CD8^+$ disorders and the $CD4^-/CD8^-$ disease showed a type-2 polarized ($GATA3^+$) effector T-cell (Tc2) phenotype. Additionally, CD103 expression was noted in 2/4 $CD8^+$ cases. Our findings provide insights into the pathogenetic bases of indolent T-cell lymphoproliferative disorders of the gastrointestinal tract and confirm the heterogeneous nature of these diseases. Detection of shared and distinct genetic alterations of the JAK-STAT pathway in certain immunophenotypic subsets warrants further mechanistic studies to determine whether therapeutic targeting of this signaling cascade is efficacious for a proportion of patients with these recalcitrant diseases.

Introduction

Non-Hodgkin lymphomas frequently occur in the gastrointestinal (GI) tract, with the majority representing B-cell neoplasms.[1–3] T-cell lymphomas account for 10-20% of all primary GI lymphomas.[1–3] Aggressive lymphomas, including

Correspondence:

CRAIG SODERQUIST
crs2130@cumc.columbia.edu

GOVIND BHAGAT
gb96@cumc.columbia.edu

Received: July 8, 2019.

Accepted: September 25, 2019.

Pre-published: September 26, 2019.

doi:10.3324/haematol.2019.230961

Check the online version for the most updated information on this article, online supplements, and information on authorship & disclosures: www.haematologica.org/content/105/7/1895

enteropathy-associated T-cell lymphoma (EATL) and monomorphic epitheliotropic intestinal T-cell lymphoma (MEITL), are among the more common types of primary GI T-cell lymphomas, which are associated with high morbidity and mortality.[1,4,5] In recent years, there has been a growing awareness of indolent T- and natural killer (NK)-cell lymphoproliferative disorders, which can also arise within the GI tract and involve a variety of GI organs.[6,7] The pathogenesis of indolent NK-cell disorders is unclear and it is not yet known if they constitute neoplastic proliferations of NK cells.[7] Indolent T-cell lymphoproliferative disorders (ITLPD) of the GI tract, which constitute an immunophenotypically diverse group of clonal T-cell diseases, have been better characterized and hence included as provisional entities in the revised 4th edition of the World Health Organization (WHO) classification of lymphoid neoplasms.[1] The clinical, morphological, and immunophenotypic features of ITLPD of the GI tract differ from those of other types of primary GI T-cell lymphomas[6,8–16] and their cellular derivation, although not well established, is also considered to be distinct.[9,11] Overlapping genomic and genetic alterations have been reported in EATL and MEITL.[17–21] Limited data suggest a different spectrum of genomic aberrations in ITLPD of the GI tract,[11,13] and until recently, no recurrent genetic abnormality had been identified in these disorders.[15] However, the mutational landscape and molecular pathways underlying the initiation and progression of ITLPD of the GI tract are unknown and the cell of origin of the different immunophenotypic subsets has not been defined. To gain further insights into the biology of these rare diseases, we performed comprehensive immunohistochemical, molecular and targeted next-generation sequencing analyses of a series of ten cases.

Methods

Case selection

The pathology department databases of multiple institutions were searched for primary GI T-cell lymphomas, over a 23-year period (1996-2018), to identify cases fulfilling histopathological and clinical criteria of ITLPD as defined in the revised WHO classification.[1] Clinical data, including therapy and outcomes, were obtained from the treating physicians or electronic medical records. The study was performed in accordance with the principles of the Declaration of Helsinki and protocols approved by the Institutional Review Boards of the participating institutions.

Morphology and immunophenotypic analysis

Hematoxylin and eosin-stained formalin-fixed, paraffin-embedded (FFPE) biopsy sections were reviewed to assess cyto-architectural features. Immunohistochemical staining was performed using a comprehensive panel of antibodies, including those directed against T-cell antigens, lineage-associated transcription factors, immune checkpoint molecules, histone modifications and cytokine signaling molecules (*Online Supplementary Methods*). The percentage of cells expressing nuclear T-bet and GATA3 was assessed in areas of dense lymphocytic infiltration determined by CD4 and CD8 staining. Cases with >50% cellular staining by both markers were deemed to co-express T-bet and GATA3. For pSTAT3 and pSTAT5, >10% nuclear staining was considered positive. Flow cytometry was performed on cell suspensions prepared from tissue samples (*Online Supplementary Methods*).

T-cell receptor gene rearrangement analysis

Polymerase chain reaction (PCR) analysis to determine clonal T-cell receptor beta (*TRB*) and/or gamma (*TRG*) gene rearrangement was performed using the 'Biomed-2' primers on DNA extracted from fresh or FFPE GI biopsies, lymph nodes, peripheral blood, and bone marrow mononuclear cells, as previously described.[22]

Next-generation sequencing

Targeted next-generation sequencing of lesional and matched normal (control) tissue samples was performed using a custom panel of 465 cancer-associated genes, as previously described.[23] Variant calling required a variant allelic fraction of at least 5% and at least ten variant reads. Variants with an allele prevalence >0.01% in gnomAD, those reported as benign or likely benign in ClinVar, and germline variants present in the normal samples or inferred from variant allelic fractions were excluded from the analysis. Non-synonymous variants that were not known driver mutations were analyzed by PolyPhen-2, SIFT, REVEL, and MetaSVM algorithms. Copy number changes were determined based on read depths using fragments per kilobase per million mapped reads[24] normalized to a pool of sex-matched control samples. The Fusion and Chromosomal Translocation Enumeration and Recovery Algorithm (FACTERA)[25] was used to detect structural chromosomal alterations, which were confirmed by PCR using breakpoint-specific primers and Sanger sequencing of the PCR products (*Online Supplementary Methods*).

Fluorescent *in-situ* hybridization analysis

Fluorescent *in-situ* hybridization (FISH) analysis was performed to assess for *SETD2* and *JAK2* alterations on FFPE tissue sections using custom designed hybridization probes and dual-color break-apart probes (Oxford Gene Technologies Inc, Tarrytown, NY, USA), respectively, as previously described.[17,26] Hybridization patterns of at least 100 tumor nuclei were reviewed for each probe. Cases were considered to have *SETD2* deletion if the percentage of nuclei with *SETD2* locus deletion exceeded the cut-off value of 11.2%, and *JAK2* rearrangement if the frequency of split-signals exceeded the cut-off value of 5.0%.

Results

Clinical characteristics and patients' outcomes

Ten patients (male:female = 8:2) with ITLPD of the GI tract were identified at the contributing centers (cases 1, 2, and 4 were reported previously).[11] The clinical features are summarized in Table 1. The median age at diagnosis was 45 years (range, 37-64 years). The ethnicity of eight patients for whom this information was available was: White (n=5), Hispanic (n=2), and Asian (n=1). The most common signs and symptoms were diarrhea (70%), weight loss (60%), and abdominal pain (50%), with durations ranging from 2 to 16 years prior to diagnosis. Two patients lacked GI symptoms, with disease detected incidentally during routine colonoscopy and workup for inguinal lymphadenopathy. One patient had peptic ulcer disease, *H. pylori* infection and was serologically positive for hepatitis B and C viruses (case 9) and one patient (case 10) had a history of Crohn disease. Eight patients had been previously misdiagnosed as having celiac disease, seronegative and refractory to a gluten-free diet, and/or other types of lymphomas. The endoscopic findings included mucosal nodularity (70%), scalloping (40%), erythema (40%), decreased duodenal folds (30%), and polyps (20%). Common radiographic findings included abdomi-

nal lymphadenopathy (55%), bowel wall thickening (33%), and dilated bowel loops (33%). Biopsy-proven sites of disease included the small intestine (90%), colon (60%), stomach (40%), bone marrow (30%, one case only had cytogenetic evidence of disease), and inguinal lymph nodes (20%). Seven of nine (77%) patients received therapeutic interventions consisting of steroids and/or chemotherapy; two were monitored expectantly. Six of

Table 1. Clinical characteristics of patients with gastrointestinal indolent T-cell lymphoproliferative disorders.

Case	Age	Sex	Eth	Presenting signs & symptoms	Duration of symptoms prior to diagnosis (years)	Other conditions	Prior diagnosis	Endoscopic findings	Radiographic findings	Sites of involvement†	Ann Arbor stage (at diagnosis)	Treatment	Outcome (cause of death)
1*	53	M	W	Diarrhea, weight loss, night sweats	16	None	Celiac disease	Mucosal nodularity, scalloping, decreased duodenal folds, erythema	Mild mesenteric LAD, mild FDG activity	Duodenum, jejunum, ileum	IEB	Bud	AWD, 9 years
2*	50	F	W	Diarrhea, weight loss, abd pain, fatigue	3	None	Celiac disease	Mucosal nodularity, scalloping	SB wall thickening and dilation	Duodenum, ileum, appendix, colon, stomach, BM‡	IEB	Pral, Romi, Bud	AWD, 7 years
3	64	F	NA	No GI symptoms	0	NA	None	Sessile polyp in colon	NA	Colon	NA	NA	NA
4*†	37	M	W	Diarrhea, weight loss	2	None	Celiac disease	Mucosal nodularity, scalloping	Normal	Duodenum, ileum, colon, stomach	IEB	Bud, Pred, Aza	D, 11 years (Large cell trans)
5	62	M	H	Diarrhea, weight loss	NA	NA	Celiac disease, EATL	Mucosal nodularity, scalloping, mosaic pattern, increased vascularity, ulcer	SB and LB dilation	Duodenum, jejunum, inguinal LN	IEB	CP, Dox, VCR, Pred	D, 1 year (SB perf)
6	41	M	NA	No GI symptoms	0	MG	None	Polypoid ileal lesions	Mesenteric and iliac LAD	Ileum, colon, stomach, inguinal LN, BM	IVE	None	AWD, 1 year
7	38	M	W	Diarrhea, abd pain, vomiting	5	Lyme disease	EATL	Mucosal nodularity, decreased duodenal folds, gastric erythema	SB wall thickening, intuss, mesenteric LAD	Duodenum, jejunum, ileum, colon	IE	None	AWD, 21 years
8	38	M	H	Diarrhea, weight loss, abd pain	5	CHD	MEITL	Mucosal nodularity, erythema, friability	Mesenteric and retroperitoneal LAD, incr FDG activity	Duodenum, ileum, colon	IEB	CP, Dox, VCR, Bud, Pred, Etop, AGS67E	AWD, 7 years
9†	41	M	A	Abd pain	3	PUD, *H. pylori*, viral hep (B & C)	Atyp lymphoid infiltrate, favor MZL	Mucosal nodularity, decreased duodenal folds	Abd LAD, mild FDG activity, splenomegaly	Duodenum, stomach, BM	IE	IFN, CP, Dox, VCR, Pred, Gem	D, 27 years (Large cell trans)
10	49	M	W	Diarrhea, weight loss, abd pain	5	Crohn disease§	Celiac disease, EATL	Flattened SB mucosa, gastric erythema	Mild SB wall thickening and dilation, partial SB obstruction	Duodenum, jejunum	IEB	CP, Dox, VCR, Pred, Mes, Aza	AWD, 19 years

A: Asian; abd: abdominal; AGS67E: anti-CD37 monoclonal antibody AGS67E; AWD: alive with disease; Aza: azathioprine; BM: bone marrow; Bud: budesonide; CHD: congenital heart disease; CP: cyclophosphamide; D: dead; Dox: doxorubicin; EATL: enteropathy associated T-cell lymphoma; Eth: ethnicity; Etop: etoposide; F: female; FDG: fluorodeoxyglucose; Gem: gemcitabine; GI: gastrointestinal; H: Hispanic; hep: hepatitis; IFN: interferon; incr: increased; intuss: intussusception; LAD: lymphadenopathy; LB: large bowel; LN: lymph node; M: male; MEITL: monomorphic epitheliotropic intestinal T-cell lymphoma; Mes: mesalamine; MG: monoclonal gammopathy; MZL: marginal zone lymphoma; NA: not available; perf: perforation; PUD: peptic ulcer disease; Pral: pralatrexate; Pred: prednisone; Romi: romidepsin; SB: small bowel; trans: transformation; VCR: vincristine; W: White. *Previously published cases. †Findings prior to large cell transformation. ‡Bone marrow involvement was detected by cytogenetic analysis; there was no morphological or immunophenotypic evidence of disease and TCRβ polyclonal chain reaction showed polyclonal products. §Biopsies diagnosed as Crohn disease were not reviewed by authors.

nine (66%) patients are alive with persistent disease and three (33%) have died; one (case 5) due to septicemia and multiorgan failure following chemotherapy-induced intestinal perforation 1 year after diagnosis and two (cases 4 and 9) due to disease transformation 11 and 27 years after diagnosis.

Morphological features

All cases with involvement of the small intestines displayed a dense diffuse or nodular infiltrate of small-sized lymphocytes in the lamina propria (Figures 1A and 2A), with extension into the submucosa noted in a subset. Villous atrophy was observed in three of the nine cases of ITLPD (cases 2, 4, 9) (Figure 1B), however the villi were expanded (blunted appearance) (Figure 2B) in many cases, and all except one (case 10) showed crypt hyperplasia. The lymphocytes had round, ovoid or mildly irregular nuclei, variable fine or coarse chromatin, indistinct or small nucleoli, and scant or moderate cytoplasm (Figures 1C and 2C). No significant increase in intraepithelial lymphocytes was identified (Figures 1B and 2B), although focal lymphocytic infiltration of the epithelium was present in four of nine cases of ITLPD (cases 1, 2, 4, and 7). Scattered lymphoid aggregates were seen in all except one ITLPD (case 5). Sparse, patchy mucosal infiltrates were noted in the seven cases with gastric and/or colonic involvement. Mitotic figures and apoptotic cells were inconspicuous. No angiocentricity, angiodestruction, ulceration, or necrosis was observed. The histopathological findings of the small intestinal biopsy from one patient with large cell transformation, available for review (case 4), were reported previously.[11]

Immunophenotypic features

The immunophenotypic profiles of all cases are summarized in Table 2. Four of ten (40%) ITLPD were $CD4^+$ (Figure 1D), four (40%) were $CD8^+$ (Figure 2D) and one each (10%) was $CD4^+/CD8^+$ ("double-positive") and $CD4^-/CD8^-$ ("double-negative"). All cases analyzed expressed CD2 (Figure 1E) and CD3 (Figures 1F and 2E). Other T-cell antigens were expressed by the majority (Figure 1G, H); variable downregulation or loss of CD5 and/or CD7 was seen in four of ten cases (2/4 $CD4^+$, 1/4 $CD8^+$, and 1/1 double-negative). All except one $CD8^+$ case and the $CD4^-/CD8^-$ case displayed a cytotoxic immunophenotype, with TIA-1 expression (Figure 2F) noted in three of four cases and variable granzyme B expression (Figure 2G) observed in two of four $CD8^+$

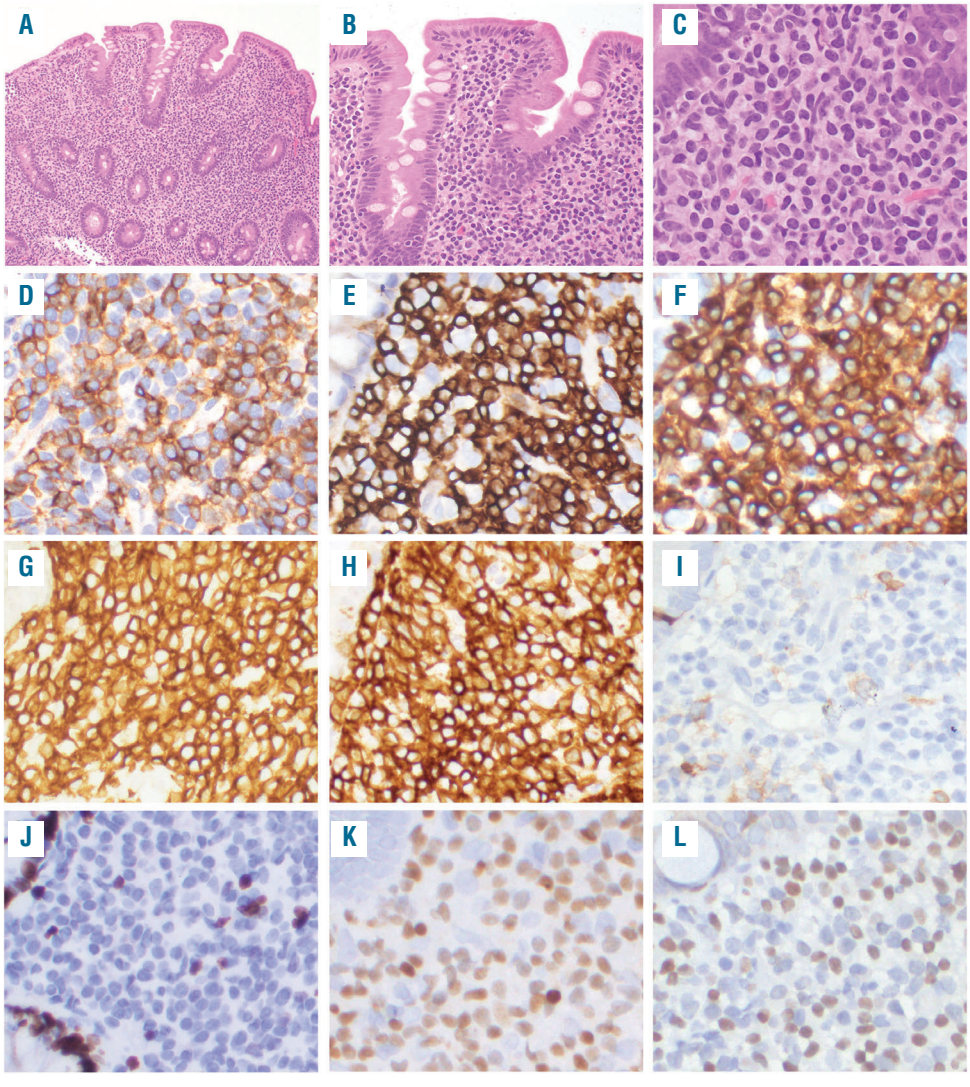

Figure 1. Morphological and immunophenotypic features of $CD4^+$ indolent T-cell lymphoproliferative disorders of the gastrointestinal tract. (A) A duodenal biopsy (case 2) shows a dense lymphocytic infiltrate within the lamina propria, as well as villous atrophy and crypt hyperplasia. (B) There is no increase in intraepithelial lymphocytes. (C) The lymphocytes are small and have round to ovoid nuclei, fine chromatin, indistinct or small nucleoli, and moderate pale pink cytoplasm. The lymphocytes express (D) CD4, (E) CD2, (F) CD3, (G) CD5, and (H) CD7. (I) The neoplastic cells do not express CD103. (J) The Ki-67 proliferation index is low (<5%). The majority of cells are (K) T-bet$^+$, however, 50% also express (L) GATA3.

cases and in the CD4$^-$/CD8$^-$ case. CD103 expression was detected in two of four CD8$^+$ cases (Figure 2H), with one also showing partial CD56 expression (case 8) (Figure 2I). The CD4$^+$/CD8$^+$ and the CD4$^-$/CD8$^-$ cases expressed PD-1. CD20 highlighted mucosal lymphoid follicles, but the neoplastic cells were CD20$^-$ in all ITLPD. Surface TCRαβ expression was observed in all cases evaluated by flow cytometry and none expressed TCRγδ. All analyzed cases were negative for BCL6, CD10, FoxP3, MATK, PD-L1 or CD30, however CD30 expression (and acquisition of cytotoxic proteins) was observed, and previously reported, upon large cell transformation (case 4).[11] The Ki-67 proliferation index was low (<5%) in all ITLPD evaluated (Figures 1J and 2J).

Determination of the cell of origin

Since a good correlation between the transcriptional profiles and immunohistochemistry for T-bet and GATA3 has been reported in T-cell lymphomas,[27] we assessed T-bet and GATA3 expression by immunohistochemistry to determine the cell of origin of ITLPD (Table 2, *Online Supplementary Table S1*, *Online Supplementary Figure S1*). The CD4$^+$ cases showed heterogeneity with regards to T-bet and GATA3 expression: one case each was T-bet$^+$ and GATA3$^+$, suggesting T-helper type 1 (Th1) and type 2 (Th2) lineage, respectively and two cases showed T-bet and GATA3 co-expression - hybrid Th1/Th2 profile (Figure 1K, L). The CD4$^+$/CD8$^+$ ITLPD also co-expressed T-bet and GATA3. The CD4$^-$/CD8$^-$ case and three of the four (75%) CD8$^+$ cases were GATA3$^+$, implying a type-2-polarized effector T-cell (Tc2) phenotype and one CD8$^+$ case showed T-bet and GATA3 co-expression (Figure 2K, L). Sequential analysis of one CD4$^+$ ITLPD (case 2) showed a shift from a Th1/Th2 (T-bet and GATA3 co-expression) to Th2 (GATA3) phenotype over the course of disease. Double staining for T-bet and GATA3, performed in a subset (cases 2, 7, and 8), confirmed distinct T-bet and GATA3$^+$ as well as T-bet and GATA3 co-expressing lymphocytes (*data not shown*).

T-cell receptor gene rearrangement analysis

Clonal *TRB* and/or *TRG* rearrangement products were detected in all ITLPD. In patients in whom longitudinal testing was performed, similar sized peaks were observed in all samples, confirming persistence of the same lymphocytic clone.

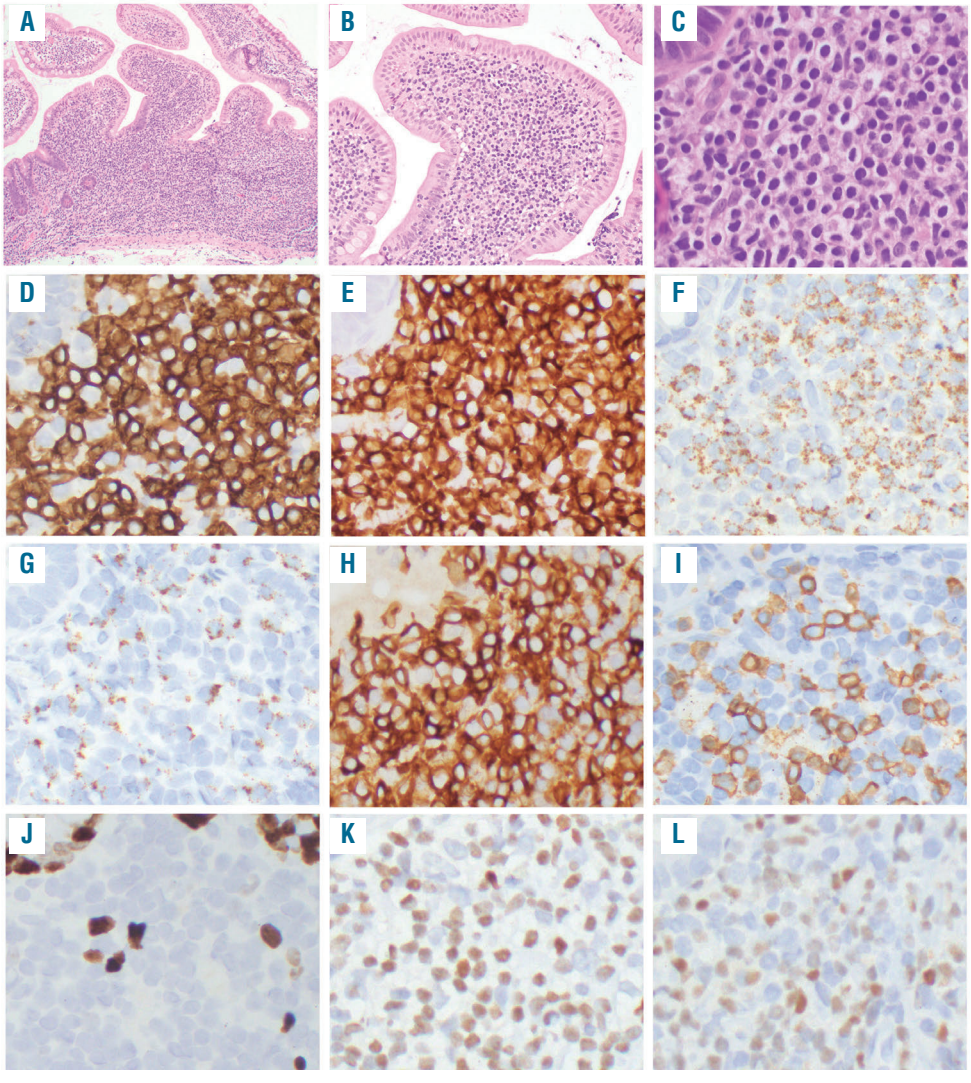

Figure 2. Morphological and immunophenotypic features of CD8$^+$ indolent T-cell lymphoproliferative disorders of the gastrointestinal tract. (A) An ileal biopsy (case 8) shows a dense mucosal lymphocytic infiltrate expanding the lamina propria and widening the villi; no villous atrophy is present but the crypts are hyperplastic. (B) Small clusters of lymphocytes are seen within the villus epithelium along the lateral edges. There is no increase in intraepithelial lymphocytes. (C) The lymphocytes are small and have round or oval nuclei, condensed chromatin, indistinct nucleoli, and scant to moderate clear or pale pink cytoplasm. The lymphocytes express (D) CD8 and (E) CD3. Most of the cells express the cytotoxic marker (F) TIA1 and (G) granzyme B is expressed by a subset. (H) The lymphocytes are CD103$^+$ and a subset expresses (I) CD56. (J) The Ki-67 proliferation index is low (<5%). The majority of cells express (K) GATA3, but 60% also show (L) T-bet expression.

Table 2. Immunophenotypic characteristics of gastrointestinal indolent T-cell lymphoproliferative disorders.

Case	CD4	CD8	CD2	CD3	CD5	CD7	TIA-1	GrzB	Perf	CD103	CD56	BCL6	CD10	PD-1	PD-L1	FoxP3	MATK	TCRαβ	TCRγδ	CD30	Ki67 (%)	T-bet	GATA3
1*	+	-	+	+	-/+	-	-	-	-	-	-	-	-	-	-	-	-	+	-	-	<5	+	-
2*	+	-	+	+	+	+	-	-	-	-	-	-	-	-	-	-	-	+	-	-	<5	+	+
3	+	-	NA	+	+	+	-	-	-	-	-	NA	NA	NA	-	NA	-	+	-	-	NA	-	+
4*†	+	-	+	+	+/-	-	-	-	-	-	-	-	-	-	-	-	-	+/-	-	-	<5	+	+
5	+	+	+	+	+	+	-	-	-	-	-	-	-	+	-	-	-	+	-	-	<5	+	+
6	-	-	+	+	+	-/+	+	-/+	NA	-	-	-	-	+	NA	-	NA	+	-	-	<5	-	+
7	-	+	+	+	+	+	-	-	-	+	-	-	-	-	-	-	-	+	-	-	<5	-	+
8	-	+	+	+	+	+	+	+/-	-	+	+/-	-	-	-	-	-	-	+	-	-	<5	+	+
9†	-	+	+	+	-	-/+	+	-	-	-	-	-	-	-	-	-	-	+	-	-	<5	-	+
10	-	+	+	+	+	+	+	+	-	-	-	-	-	-	-	-	NA	+	-	-	<5	-	+
TOTAL	5/10 (50%)	5/10 (50%)	9/9 (100%)	10/10 (100%)	8/10 (80%)	6/10 (60%)	4/10 (40%)	2/10 (20%)	0/9 (0%)	2/10 (20%)	1/10 (10%)	0/9 (0%)	0/9 (0%)	2/9 (22%)	0/9 (0%)	0/9 (0%)	0/8 (0%)	10/10 (100%)	0/10 (0%)	0/10 (0%)		5/10 (50%)	9/10 (90%)
CD4+	4/4 (100%)	0/4 (0%)	3/3 (100%)	4/4 (100%)	3/4 (75%)	2/4 (50%)	0/4 (0%)	0/4 (0%)	0/4 (0%)	0/4 (0%)	0/4 (0%)	0/3 (0%)	0/3 (0%)	0/3 (0%)	0/4 (0%)	0/3 (0%)	0/4 (0%)	4/4 (100%)	0/4 (0%)	0/4 (0%)		3/4 (75%)	3/4 (75%)
DP	1/1 (100%)	1/1 (100%)	1/1 (100%)	1/1 (100%)	1/1 (100%)	1/1 (100%)	0/1 (0%)	0/1 (0%)	0/1 (0%)	0/1 (0%)	0/1 (0%)	0/1 (0%)	0/1 (0%)	1/1 (100%)	0/1 (0%)	0/1 (0%)	0/1 (0%)	1/1 (100%)	0/1 (0%)	0/1 (0%)		1/1 (100%)	1/1 (100%)
DN	0/1 (0%)	0/1 (0%)	1/1 (100%)	1/1 (100%)	1/1 (100%)	0/1 (0%)	1/1 (100%)	0/1 (0%)	NA	0/1 (0%)	0/1 (0%)	0/1 (0%)	0/1 (0%)	1/1 (100%)	NA	0/1 (0%)	NA	1/1 (100%)	0/1 (0%)	0/1 (0%)		0/1 (0%)	1/1 (100%)
CD8+	0/4 (0%)	4/4 (100%)	4/4 (100%)	4/4 (100%)	3/4 (75%)	3/4 (75%)	3/4 (75%)	2/4 (50%)	0/4 (0%)	2/4 (50%)	1/4 (25%)	0/4 (0%)	0/4 (0%)	0/4 (0%)	0/4 (0%)	0/4 (0%)	0/3 (0%)	4/4 (100%)	0/4 (0%)	0/4 (0%)		1/4 (25%)	4/4 (100%)

+: positive; -: negative; DN: double-negative; DP: double-positive; GrzB: granzyme B; NA: not available; Perf: perforin; TCRαβ: T-cell receptor alpha-beta; TCRγδ: T-cell receptor gamma-delta. *Previously published cases. †Findings at diagnosis prior to large cell transformation.

Next-generation sequencing analysis

Targeted sequencing of 20 ITLPD biopsies from ten patients and seven matched normal samples (cases 1, 2, 4, 7-10) revealed 36 genetic variants, including 29 nonsynonymous single nucleotide variants, one small indel, and six structural variants. The average on-target coverage was 1059x (range 809x - 1639x). Twenty-three of the 36 alterations were predicted to be pathogenic based on the published literature or prediction algorithms; the remaining 13 mutations were classified as variants of uncertain significance (*Online Supplementary Table S2*).

The genetic alterations and their expected functional consequences are summarized in Table 3. Pathogenic or potentially pathogenic changes were identified in eight of ten (80%) ITLPD. Three of four (75%) $CD4^+$ cases and the $CD4^+/CD8^+$ and $CD4^-/CD8^-$ cases harbored alterations of JAK-STAT signaling pathway genes. *STAT3* SH2 domain hotspot mutations (D661Y and S614R) were noted in three cases and one case each had a *SOCS1* deletion and a *STAT3-JAK2* rearrangement. Of note, conventional cytogenetic analysis had previously revealed a balanced translocation t(9;17)(p24;q21) in the latter case, the breakpoints corresponding to the *JAK2* and *STAT3* loci, and *JAK2* rearrangement was confirmed by FISH analysis. Concomitant mutations in epigenetic modifier genes (*TET2, DNMT3A,* and *KMT2D*) were observed in four

Table 3. Genetic alterations in gastrointestinal indolent T-cell lymphoproliferative disorders.

Case	Phenotype	Time point (years following diagnosis)	Genetic alterations	Predicted functional consequence
1	$CD4^+$	2.5	*STAT3* (c.1981G>T, p. D661Y) *TET2* (c.2457T>G, p. Y819*)	Activation of JAK-STAT pathway Altered DNA methylation
		7.9	*STAT3* (c.1981G>T, p. D661Y) *TET2* (c.2457T>G, p. Y819*)	Activation of JAK-STAT pathway Altered DNA methylation
2	$CD4^+$	0	*STAT3-JAK2* rearrangement *TNFAIP3* (c.857T>G, p.L286*)	Activation of JAK-STAT pathway Activation of NF-κB pathway
		2.2	*STAT3-JAK2* rearrangement *TNFAIP3* (c.857T>G, p.L286*)	Activation of JAK-STAT pathway Activation of NF-κB pathway
		6.4	*STAT3-JAK2* rearrangement *TNFAIP3* (c.857T>G, p.L286*)	Activation of JAK-STAT pathway Activation of NF-κB pathway
3	$CD4^+$	0	*SOCS1* deletion	Activation of JAK-STAT pathway
4	$CD4^+$	0.5	*KMT2D* (c.13105_13108del, p.L4369fs)	Altered histone modification
		7.4	*KMT2D* (c.13105_13108del, p.L4369fs) *DIS3* (c.1115T>C, p.L372P)	Altered histone modification Altered RNA processing and decay
		11.5	*KMT2D* (c.13105_13108del, p.L4369fs) *DIS3* (c.1115T>C, p.L372P) *MAPK1* (c.965A>T, p.E322V) *TP53* (c.743G>A, p.R248Q) *POLE* (c.4090C>T, p.R1364C)	Altered histone modification Altered RNA processing and decay Activation of RAS-RAF-MAPK pathway DNA repair/cell cycle dysregulation Altered DNA repair and replication
		11.7†	*KMT2D* (c.13105_13108del, p.L4369fs) *DIS3* (c.1115T>C, p.L372P) *MAPK1* (c.965A>T, p.E322V) *TP53* (c.743G>A, p.R248Q) *POLE* (c.4090C>T, p.R1364C) *TET2* (c.2725C>T, p.Q909*) *SMAD4* (c.404G>A, p.R135Q) *SF3B1* (c.2584G>A, p.E862K)	Altered histone modification Altered RNA processing and decay Activation of RAS-RAF-MAPK pathway DNA repair/ cell cycle dysregulation Altered DNA repair and replication Altered DNA methylation Activation of TGF-β pathway Altered RNA splicing
5	$CD4^+/CD8^+$	0	*STAT3* (c.1842C>G, p.S614R) *DNMT3A* (c.2116G>T, p.G706W) *CDKN2A* (c.322G>A, p.D108N)	Activation of JAK-STAT pathway Altered DNA methylation Cell cycle checkpoint (G1-to-S) dysregulation
6	$CD4^-/CD8^-$	0	*STAT3* (c.1840A>C, p.S614R) KMT2D (c.9415C>G, p.P3139A)	Activation of JAK-STAT pathway Altered histone modification
7	$CD8^+$	0	*IL2-RHOH* rearrangement‡	Unknown
		3.9	*IL2-RHOH* rearrangement‡	Unknown
		6.1	*IL2-RHOH* rearrangement‡	Unknown
8	$CD8^+$	0	*IL2* 3' UTR deletion‡, *IL2-TNIP3* rearrangement‡ *MCM5* (c.2080A>T, p.I694F)	Unknown Cell cycle dysregulation
		4.3	*IL2* 3' UTR deletion‡, *IL2-TNIP3* rearrangement‡ *MCM5* (c.2080A>T, p.I694F)	Unknown Cell cycle dysregulation
		6.4	*IL2* 3' UTR deletion‡, *IL2-TNIP3* rearrangement‡ *MCM5* (c.2080A>T, p.I694F)	Unknown Cell cycle dysregulation
9	$CD8^+$	14	None identified	NA
10	$CD8^+$	10.8	None identified	NA

NA: not applicable. †Large cell transformation. ‡Confirmed by breakpoint-specific polymerase chain reaction and Sanger sequencing.

cases. A missense mutation in the cell cycle regulatory gene *CDKN2A* and a nonsense mutation in *TNFAIP3* were detected in one case each.

Two of the CD8+ ITLPD exhibited structural chromosome alterations involving the interleukin-2 (*IL2*) gene. One case demonstrated an *IL2-RHOH* (Ras homolog family member H) rearrangement, representing an inversion of chromosome 4, with breakpoints occurring in the 3' untranslated region (3' UTR) of both *IL2* (chr4:123372863, c.*44) (Figure 3A) and *RHOH* (chr4:40246032, c.*449) genes. This rearrangement did not affect the coding sequence, but resulted in the deletion of a portion of the 3' UTR of *IL2*, including five of the six AU-rich regulatory elements (ARE, AUUUA). The "reciprocal" *RHOH-IL2* rearrangement had breakpoints in the 3' UTR of *RHOH* (chr4:40246006, c.*424) and intron 3 of *IL2* (chr4:123373085, c.352-67). Another CD8+ case demonstrated a 1.2 Mb deletion on chromosome 4q, beginning 5 base pairs downstream of the *IL2* stop codon (chr4:123372903, c.*5) (Figure 3D) and ending 6 kilobases upstream of the TNFAIP3 interacting protein 3 (*TNIP3*) gene (chr4:122154953), deleting all regulatory elements from the *IL2* 3' UTR. In addition, an inversion, with breakpoints in exon 4 of *IL2* (chr4:123372912, c.457) and intron 2 of *TNIP3* (chr4:122128556, c.89+9014) was identified (Figure 3D). A missense mutation in the minichromosome maintenance complex component 5 (*MCM5*) gene was also identified in this case. The chromosome breakpoints were confirmed in all ITLPD samples with structural *IL2* alterations via PCR amplification and Sanger sequencing

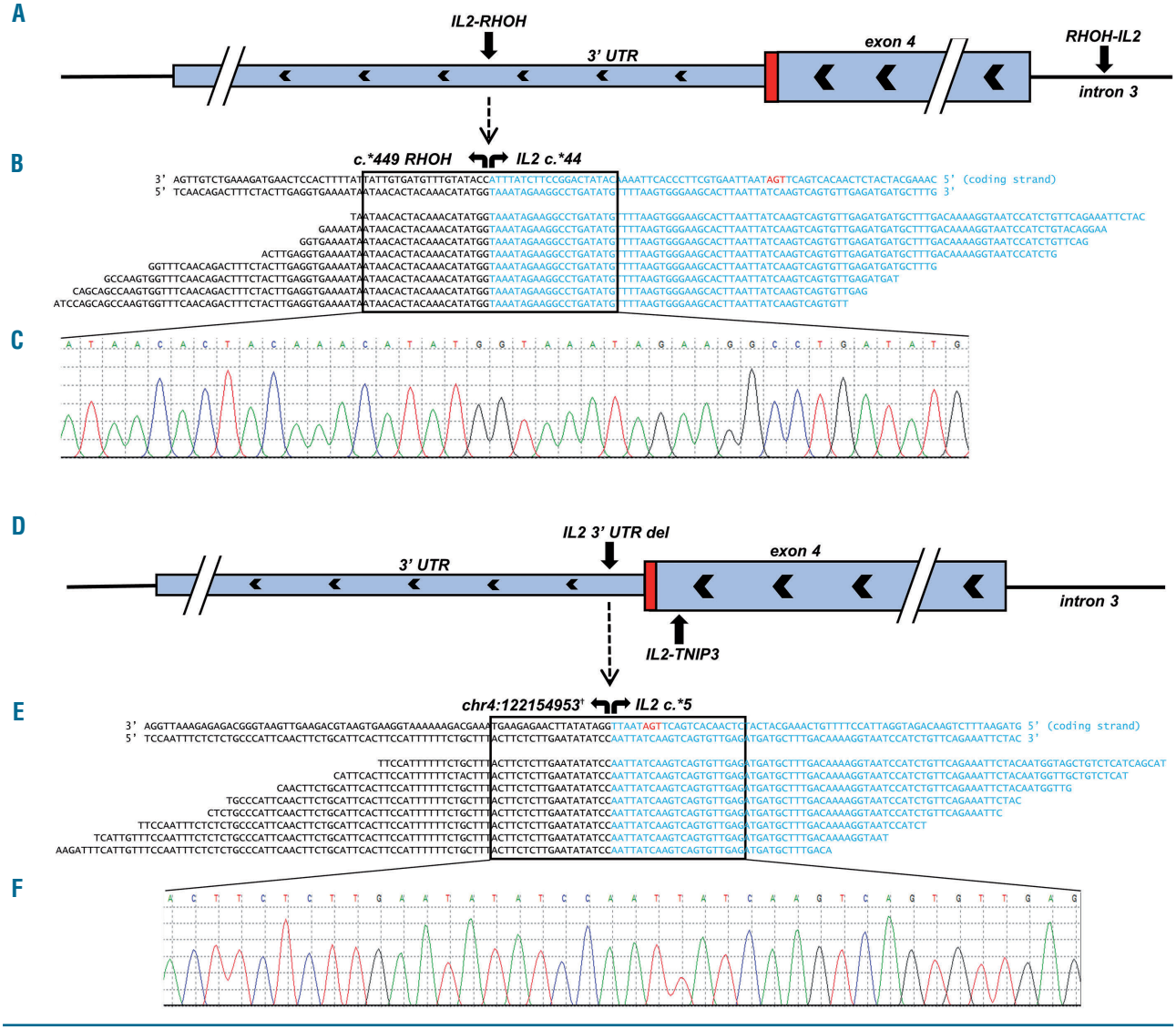

Figure 3. Structural chromosome alterations of the *IL2* gene in CD8+ indolent T-cell lymphoproliferative disorders. In case 7, (A) two chromosome breaks were detected as a consequence of a rearrangement involving the 3' untranslated region (UTR) of *IL2* and 3' UTR of *RHOH* ("*IL2-RHOH*") and a reciprocal rearrangement involving intron 3 of *IL2* and the 3' UTR of *RHOH* ("*RHOH-IL2*"). (B) Pile-up of a subset of reads mapping to the *IL2-RHOH* rearrangement. (C) Sanger sequencing validation of the fusion breakpoints. In case 8, (D) two chromosome breaks were observed due to a 1.2 Mb deletion spanning the majority of the 3' UTR of *IL2* and a portion of the intergenic region between *IL2* and *TNIP3* ("*IL2 3' UTR del*") and an inversion involving exon 4 of *IL2* and intron 2 of *TNIP3* ("*IL2-TNIP3*"). (E) Pile-up of a subset of reads mapping to the *IL2* 3' UTR deletion. (F) Sanger sequencing validation of the deletion breakpoints. †Chromosome position based on assembly GRCh37.p13.

(Figure 3B, C, E, F). No pathogenic mutations or structural abnormalities were observed in two CD8+ ITLPD (cases 9 and 10), although a variant of uncertain significance was observed in one case (*Online Supplementary Table S2*).

Longitudinal analysis of five ITLPD (cases 1, 2, 4, 7, 8) revealed stable mutational profiles in four ITLPD. Accrual of mutations over time was noted in one CD4+ ITLPD (case 4). Only a *KMT2D* frameshift mutation was detected in the first biopsy, obtained shortly after diagnosis. Additional mutations were identified at later time points, including a missense *TP53* mutation prior to disease transformation. Of interest, biopsies at the first, second, and fourth time-points had shown different chromosome copy number changes (reported previously),[11] but none of the altered regions corresponded to the loci of mutated genes.

Evaluation of the SETD2-H3K36me3 axis

No *SETD2* mutations were observed by next-generation sequencing analysis and FISH did not detect any *SETD2* deletions in the cases analyzed. Additionally, no loss of SETD2 protein or H3K36me3 was detected by immunohistochemistry and H3K36me2 expression was observed in all analyzed cases (Figure 4A-C, *Online Supplementary Table S3*).

Evaluation of JAK-STAT pathway activation

Due to the presence of frequent and recurrent genetic alterations targeting the JAK-STAT pathway and *IL2* genes, we evaluated pSTAT3-Y705 and pSTAT5-Y694 expression by immunohistochemistry to assess activation of the JAK-STAT signaling pathway. All nine tested cases only showed single scattered or small clusters of nuclear pSTAT3-Y705 and pSTAT5-Y694 positive cells (<10%) in all biopsies (Figure 4E, F, *Online Supplementary Table S3*).

Discussion

Despite an increasing awareness of ITLPD of the GI tract, deciphering their molecular pathogenesis and cellular origins has been challenging, in part due to the rarity of these disorders. In this study, comprising one of the largest series of cases evaluated, we delineate novel genetic alterations, including recurrent mutations and rearrangements, suggest cellular origins, and expand the immunophenotypic spectrum of these diseases.

The clinical presentations and disease course of our patients were largely congruent with previous descriptions.[6,8-16] Of interest, the ITLPD were detected incidentally in two asymptomatic patients, which has rarely been documented.[10] A history of Crohn disease has been reported in some patients with CD8+ ITLPD,[12,13] which was also the case for one patient in our series. Prior erroneous diagnoses of seronegative, refractory celiac disease in a high proportion (50%) of patients were deemed to be the consequence of misinterpretation of the histopathological changes and incomplete laboratory testing. Due to the relatively recent recognition of these disorders, it is not surprising that 40% of the ITLPD in the current study had been previously misdiagnosed as aggressive intestinal T-cell lymphomas (EATL and MEITL). Extra-GI disease was observed more frequently (40%) in our series than in previously reported series, and transformation to aggressive lymphoma, which is considered rare,[8,11,15,28] occurred in two patients, including one with a CD8+ ITLPD. These findings emphasize the need for comprehensive clinical and laboratory evaluation and long-term follow-up of individuals with these disorders.

Next-generation sequencing of the ITLPD revealed genetic alterations in 80% of the cases, including mutations in JAK-STAT signaling pathway genes, observed in

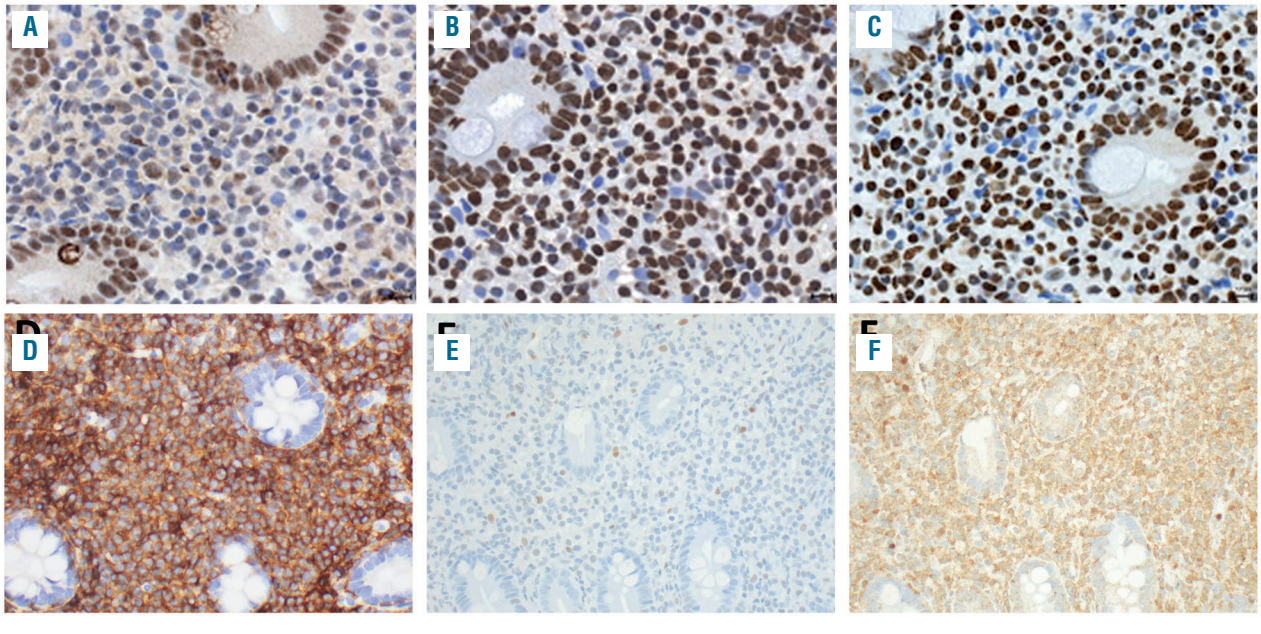

Figure 4. Analysis of the SETD2-H3K36me3 axis and JAK-STAT pathway activation. Immunohistochemical analysis of a CD4+ indolent T-cell lymphoproliferative disorder with *STAT3-JAK2* rearrangement (case 2) shows preserved (A) SETD2, (B) H3K36me2, and (C) H3K36me3 protein expression. The lymphocytes express (D) CD4. Only a few scattered (E) pSTAT3-Y705+ and (F) pSTAT5-Y694+ cells are noted (comprising <10% of the neoplastic lymphocytes).

75% of the CD4+ cases and in the CD4+/CD8+ and CD4-/CD8- cases. The *STAT3* D661Y and S614R mutations are well-characterized hotspot mutations that impart greater hydrophobicity to the SH2 dimerization surface and promote STAT3 nuclear localization and activation.[29] These mutations have been described in a myriad of lymphoid neoplasms and are quite frequent in T-large granular lymphocytic leukemia.[29] Perry *et al.* did not detect *STAT3* SH2 domain hotspot mutations in five cases analyzed by Sanger sequencing, although all tested cases were CD8+.[12] Deletion of *SOCS1*, a negative regulator of the JAK family proteins,[30] which was seen in a colonic CD4+ ITLPD, is a recurrent abnormality in a variety of T-cell lymphomas and more commonly reported in mycosis fungoides.[31] We confirm that *STAT3-JAK2* rearrangement is a recurrent event in CD4+ ITLPD although this alteration was only observed in one (25%) of our cases compared to four of five (80%) cases in the series reported by Sharma *et al.*[15]

Loss-of-function mutations in epigenetic modifier genes (*TET2*, *DNMT3A*, *KMT2D*) represented the next most commonly altered gene class, identified in 40% of cases and restricted to CD4+, CD4+/CD8+, and CD4-/CD8- cases. Mutations in epigenetic modifiers, which are believed to be early events in lymphomagenesis[32,33] and known to cooperate with other mutations in fostering neoplastic transformation,[33,34] have also been reported in diverse T-cell malignancies.[33,35] However, in contrast to other T-cell lymphomas,[36] *IDH1/2* mutations were not observed in any ITLPD. Although not recurrent, mutations in *CDKN2A* and *TNFAIP3* suggest roles of cell cycle deregulation[37] and NF-κB activation[38] in the pathogenesis of at least some ITLPD.

Structural chromosome alterations recurrently targeting the 3' UTR of the *IL2* gene, which were identified in 50% of the CD8+ ITLPD, have not been described before. The rearrangements and deletions led to the loss of most or all of the regulatory ARE involved in mRNA stability. Studies in mitogen-stimulated Jurkat cells have shown that deletion of these regulatory elements, which act as binding sites for components of the mRNA degradation machinery,[39] results in a longer half-life of *IL2* mRNA.[40] Whether these alterations lead to changes in the cellular localization of the *IL2* transcript or affect the assembly or composition of protein complexes that modulate activities beyond its 3' UTR-independent functions has not been investigated. An *IL2-TNFRSF17* rearrangement,[41] resulting from t(4;16)(q26;p13),[41] was previously reported in a CD4+ ITLPD.[9] However, in contrast to our cases, the breakpoints in that case mapped to intron 3 of *IL2* and exon 1 of the B-cell maturation antigen (*BCMA*) gene, also known as tumor necrosis factor receptor superfamily member 17 (*TNFRSF17*).[41] The authors detected chimeric *IL2-TNFRSF17* mRNA, but no fusion protein was identified. The functional significance of the prior and current *IL2* genetic alterations remains unknown.

Despite the frequent JAK-STAT pathway gene mutations and structural alteration of the *IL2* gene, which encodes a key T-cell cytokine that signals via the JAK-STAT pathway,[42] none of the ITLPD analyzed showed high-level pSTAT3 or pSTAT5 expression. Our findings are similar to those of Perry *et al.* who also did not observe significant pSTAT3 expression,[12] but contrast with those of Sharma *et al.* who reported pSTAT5 expression in three of four cases with *STAT3-JAK2* rearrangements.[15] The reasons for these discrepant findings are unclear. It is plausible that the mutations simply augment the sensitivity of ITLPD to cytokine stimulation, enhancing ligand-mediated signaling as described in other T-cell lymphomas,[43] and aberrant proliferations of intraepithelial lymphocytes in refractory celiac disease type 2[44] that harbor *STAT3* mutations.

On analysis of serial samples, acquisition of additional mutations, including those targeting genes involved in the DNA damage response (*TP53*, *POLE*) were only identified in an ITLPD that transformed to aggressive lymphoma. It is possible that ineffective DNA repair mechanisms fueled acquisition of additional mutations and complex chromosome changes in this case.[11] It is unclear if prolonged azathioprine therapy played a role in genomic evolution. Nonetheless, this and other cases in our series as well as those published previously highlight the futility of genotoxic chemotherapeutic agents for treating ITLPD of the GI tract. The prognostic relevance of periodic genetic analysis needs to be assessed in future larger studies.

Our findings indicate that ITLPD of the GI tract share certain pathogenic mechanisms with other intestinal T-cell lymphomas. As in our cohort, mutations in JAK-STAT pathway genes represent the most frequent alterations in EATL, MEITL, and intestinal T-cell lymphoma, not otherwise specified.[17-21] Similarly, loss-of-function mutations in epigenetic modifier genes and DNA damage repair genes have also been reported in aggressive intestinal T-cell lymphomas.[17,18] In contrast to EATL and MEITL, however, *SETD2* mutations or deletions were not seen in any ITLPD and the burden of pathogenic alterations in ITLPD appears lower.[17,18]

ITLPD of the GI tract are immunophenotypically heterogeneous diseases. Our study revealed a few unique features that are worth highlighting. In addition to CD4+, CD8+, and CD4-/CD8- ITLPD, we describe a CD4+/CD8+ (double-positive) case. Two ITLPD with a similar phenotype were recently reported from the USA and China.[15,45] Two of our CD8+ ITLPD expressed CD103, which has not been documented before. Prior sporadic cases of CD103+ ITLPD have all been of CD4 T-cell lineage.[10,13] These ITLPD could arise from αE integrin-expressing lamina propria T cells,[46] but the possibility of activation-induced upregulation of CD103 cannot be excluded.[47,48] Of note, one CD103+ CD8+ ITLPD also showed focal CD56 expression. Distinguishing such cases from MEITL can be challenging; however, in addition to the clinical presentation and course, the presence of small lymphocytes with bland cytomorphology confined to the lamina propria, absent MATK expression, and a low Ki-67 index, can help establish a diagnosis of ITLPD. Evaluation of SETD2 and H3K36me3 expression can also aid in differentiating ITLPD from MEITL, which frequently show loss of SETD2 and H3K36 trimethylation.[17]

ITLPD of the GI tract are thought to originate from mucosal T cells, but the cell of origin of different disease subsets has not been clarified. Absence of FoxP3 and T-follicular helper (TFH) cell markers in the current and previously reported CD4+ ITLPD[11,16] argues against their derivation from regulatory T cells or TFH cells. Based on expression of T-bet and GATA3, which are transcription factors regulating CD4+ Th1 *vs.* Th2 cell fate decisions, the CD4+ and CD4+/CD8+ ITLPD in our series displayed Th1, Th2, or hybrid Th1/2 profiles. It is not known whether ITLPD with the latter profile develop directly

from naïve T cells into bifunctional mucosal Th1/2 cells, similar to those described in primary immune responses against parasites, which help dampen inflammation,[49] or derive from Th1 or Th2 cells that have undergone cytokine-mediated reprogramming to acquire a Th1/Th2 phenotype, with concomitant production of Th1 and Th2 cytokines.[50] The phenotypic shift from a Th1/Th2 to Th2 profile over time, observed in one $CD4^+$ case, suggests lineage (and possibly functional) plasticity of at least a subset of ITLPD. The majority of the $CD8^+$ cases and the $CD4^-/CD8^-$ ITLPD displayed a Tc2 phenotype.[51] Besides orchestrating diverse functions in $CD4^+$ T-helper cells, GATA3 also regulates the activation, homeostasis, and cytolytic activity of $CD8^+$ T cells.[52] The significance of T-bet/GATA3 co-expression in $CD8^+$ ITLPD is unknown. It must be pointed out that despite the reported concordance between the transcriptional and protein expression profiles of T-bet and GATA3 in certain T-cell lymphomas,[27] the definitive lineage (and function) of neoplastic T cells cannot be ascertained based on the expression of single lineage-associated transcription factors. Cytokine profiling and *in vitro* functional studies are awaited for confirmation of our observations. Contrary to observations in peripheral T-cell lymphoma, not otherwise specified,[27,53,54] however, an inferior prognostic impact of GATA3 expression was not apparent in our series of ITLPD.

In conclusion, our study reveals considerable immunophenotypic and genetic heterogeneity of GI ITLPD. We describe recurrent and novel genetic abnormalities in different immunophenotypic subtypes of GI ITLPD which implicate deregulated cytokine signaling and epigenetic alterations in disease pathogenesis. It is hoped that future unbiased interrogation of ITLPD genomes and transcriptomes as well as mechanistic studies will help to clarify the cell of origin and the functional consequences of the underlying genetic aberrations in these rare disorders, opening the door for targeted, less toxic and more effective therapies.

Acknowledgments

We would like to thank Raymond Yeh, PhD, for designing the primers, analyzing Sanger sequencing results, and generating electropherogram images of the IL2 rearrangements.

References

1. Swerdlow S, Campo E, Harris N, et al., editors. World Health Organization Classification of Tumours of Haematopoietic and Lymphoid Tissues. Lyon, France: IARC; 2016.
2. Foukas PG, de Leval L. Recent advances in intestinal lymphomas. Histopathology. 2015;66(1):112-136.
3. Wu XC, Andrews P, Chen VW, Groves FD. Incidence of extranodal non-Hodgkin lymphomas among whites, blacks, and Asians/Pacific Islanders in the United States: anatomic site and histology differences. Cancer Epidemiol. 2009;33(5):337-346.
4. Delabie J, Holte H, Vose JM, et al. Enteropathy-associated T-cell lymphoma: clinical and histological findings from the International Peripheral T-Cell Lymphoma Project. Blood. 2011;118(1):148-156.
5. Tan SY, Chuang SS, Tang T, et al. Type II EATL (epitheliotropic intestinal T-cell lymphoma): a neoplasm of intra-epithelial T-cells with predominant CD8αα phenotype. Leukemia. 2013;27(8):1688-1696.
6. Matnani R, Ganapathi KA, Lewis SK, Green PH, Alobeid B, Bhagat G. Indolent T- and NK-cell lymphoproliferative disorders of the gastrointestinal tract: a review and update. Hematol Oncol. 2017;35(1):3-16.
7. Xia D, Morgan EA, Berger D, Pinkus GS, Ferry JA, Zukerberg LR. NK-cell enteropathy and similar indolent lymphoproliferative disorders. Am J Clin Pathol. 2018; 151(1):75-85.
8. Carbonnel F, D'Almagne H, Lavergne A, et al. The clinicopathological features of extensive small intestinal CD4 T cell infiltration. Gut. 1999;45(5):662-667.
9. Carbonnel F, Lavergne A, Messing B, et al. Extensive small intestinal T-cell lymphoma of low-grade malignancy associated with a new chromosomal translocation. Cancer. 1994;73(4):1286-1291.
10. Hirakawa K, Fuchigami T, Nakamura S, et al. Primary gastrointestinal T-cell lymphoma resembling multiple lymphomatous polyposis. Gastroenterology. 1996;111(3): 778-782.
11. Margolskee E, Jobanputra V, Lewis SK, Alobeid B, Green PH, Bhagat G. Indolent small intestinal CD4+ T-cell lymphoma is a distinct entity with unique biologic and clinical features. PLoS One. 2013;8(7): e68343.
12. Perry AM, Warnke RA, Hu Q, et al. Indolent T-cell lymphoproliferative disease of the gastrointestinal tract. Blood. 2013;122(22):3599-3606.
13. Malamut G, Meresse B, Kaltenbach S, et al. Small intestinal CD4+ T-cell lymphoma is a heterogenous entity with common pathology features. Clin Gastroenterol Hepatol. 2014;12(4):599-608.
14. Edison N, Belhanes-Peled H, Eitan Y, et al. Indolent T-cell lymphoproliferative disease of the gastrointestinal tract after treatment with adalimumab in resistant Crohn's colitis. Hum Pathol. 2016;57:45-50
15. Sharma A, Oishi N, Boddicker RL, et al. Recurrent STAT3-JAK2 fusions in indolent T-cell lymphoproliferative disorder of the gastrointestinal tract. Blood. 2018;131(20): 2262-2266.
16. Sena Teixeira Mendes L, Attygalle AD, Cunningham D, et al. CD4-positive small T-cell lymphoma of the intestine presenting with severe bile-acid malabsorption: a supportive symptom control approach. Br J Haematol. 2014;167(2):265-269.
17. Roberti A, Dobay MP, Bisig B, et al. Type II enteropathy-associated T-cell lymphoma features a unique genomic profile with highly recurrent SETD2 alterations. Nat Commun. 2016;(7):12602.
18. Moffitt AB, Ondrejka SL, McKinney M, et al. Enteropathy-associated T cell lymphoma subtypes are characterized by loss of function of SETD2. J Exp Med. 2017;214(5):1371-1386.
19. Nairismägi ML, Tan J, Lim JQ, et al. JAK-STAT and G-protein-coupled receptor signaling pathways are frequently altered in epitheliotropic intestinal T-cell lymphoma. Leukemia. 2016;30(6):1311-1319.
20. Küçük C, Jiang B, Hu X, et al. Activating mutations of STAT5B and STAT3 in lymphomas derived from γδ-T or NK cells. Nat Commun. 2015;(6):6025.
21. Nicolae A, Xi L, Pham TH, et al. Mutations in the JAK/STAT and RAS signaling pathways are common in intestinal T-cell lymphomas. Leukemia. 2016;30(11):2245-2247.
22. van Dongen JJM, Langerak AW, Brüggemann M, et al. Design and standardization of PCR primers and protocols for detection of clonal immunoglobulin and T-cell receptor gene recombinations in suspect lymphoproliferations: report of the BIOMED-2 Concerted Action BMH4-CT98-3936. Leukemia. 2003;17(12):2257-2317.
23. Margolskee E, Jobanputra V, Jain P, et al. Genetic landscape of T- and NK-cell post-transplant lymphoproliferative disorders. Oncotarget. 2016;7(25):37636-37648.
24. Trapnell C, Williams BA, Pertea G, et al. Transcript assembly and quantification by RNA-Seq reveals unannotated transcripts and isoform switching during cell differentiation. Nat Biotechnol. 2010;28(5):511-515.
25. Newman AM, Bratman S V., Stehr H, et al. FACTERA: a practical method for the discovery of genomic rearrangements at breakpoint resolution. Bioinformatics. 2014;30(23):3390-3393.
26. Tang G, Sydney Sir Philip JK, Weinberg O, et al. Hematopoietic neoplasms with 9p24/JAK2 rearrangement: a multicenter study. Mod Pathol 2019;32(4):490-498.
27. Iqbal J, Wright G, Wang C, et al. Gene expression signatures delineate biologic and prognostic subgroups in peripheral T-cell lymphoma. Blood. 2014;123(19):2915-2924.
28. Perry AM, Bailey NG, Bonnett M, Jaffe ES, Chan WC. Disease progression in a patient with indolent T-cell lymphoproliferative

disease of the gastrointestinal tract. Int J Surg Pathol. 2019;27(1):102-107.
29. Koskela HLM, Eldfors S, Ellonen P, et al. Somatic STAT3 mutations in large granular lymphocytic leukemia. N Engl J Med. 2012;366(20):1905-1913.
30. Liau NPD, Laktyushin A, Lucet IS, et al. The molecular basis of JAK/STAT inhibition by SOCS1. Nat Commun. 2018;9 (1):1558.
31. Bastidas Torres AN, Cats D, Mei H, et al. Genomic analysis reveals recurrent deletion of JAK-STAT signaling inhibitors HNRNPK and SOCS1 in mycosis fungoides. Genes Chromosom Cancer. 2018;57(12):653-664.
32. Schwartz FH, Cai Q, Fellmann E, et al. TET2 mutations in B cells of patients affected by angioimmunoblastic T-cell lymphoma. J Pathol. 2017;242(2):129-133.
33. Van Arnam JS, Lim MS, Elenitoba-Johnson KSJ. Novel insights into the pathogenesis of T-cell lymphomas. Blood. 2018;131(21): 2320-2330.
34. Zang S, Li J, Yang H, et al. Mutations in 5-methylcytosine oxidase TET2 and RhoA cooperatively disrupt T cell homeostasis. J Clin Invest. 2017;127(8):2998-3012.
35. Watatani Y, Sato Y, Miyoshi H, et al. Molecular heterogeneity in peripheral T-cell lymphoma, not otherwise specified revealed by comprehensive genetic profiling. Leukemia. 2019;33(12):2867-2883.
36. Cairns RA, Iqbal J, Lemonnier F, et al. IDH2 mutations are frequent in angioimmunoblastic T-cell lymphoma. Blood. 2012;119(8):1901-1903.
37. Foulkes WD, Flanders TY, Pollock PM, Hayward NK. The CDKN2A (p16) gene and human cancer. Mol Med. 1997;3(1):5-20.
38. Wenzl K, Manske MK, Sarangi V, et al. Loss of TNFAIP3 enhances MYD88L265P-driven signaling in non-Hodgkin lymphoma. Blood Cancer J. 2018;8(10):97.
39. Myer VE, Fan XC, Steitz JA. Identification of HuR as a protein implicated in AUUUA-mediated mRNA decay. EMBO J. 1997;16(8):2130-2139.
40. Chen CY, Del Gatto-Konczak F, Wu Z, Karin M. Stabilization of interleukin-2 mRNA by the c-Jun NH2-terminal kinase pathway. Science. 1998;280(5371):1945-1949.
41. Laâbi Y, Gras MP, Carbonnel F, et al. A new gene, BCM, on chromosome 16 is fused to the interleukin 2 gene by a t(4;16)(q26;p13) translocation in a malignant T cell lymphoma. EMBO J. 1992;11(11):3897-3904.
42. Ross SH, Cantrell DA. Signaling and function of interleukin-2 in T lymphocytes. Annu Rev Immunol. 2018;36(1):411-433.
43. Chen J, Zhang Y, Petrus MN, et al. Cytokine receptor signaling is required for the survival of ALK- anaplastic large cell lymphoma, even in the presence of JAK1/STAT3 mutations. Proc Natl Acad Sci U S A. 2017;114(15):3975-3980.
44. Ettersperger J, Montcuquet N, Malamut G, et al. Interleukin-15-dependent T-cell-like innate intraepithelial lymphocytes develop in the intestine and transform into lymphomas in celiac disease. Immunity. 2016;45(3):610-625.
45. Guo L, Wen Z, Su X, Xiao S, Wang Y. Indolent T-cell lymphoproliferative disease with synchronous diffuse large B-cell lymphoma. Medicine (Baltimore). 2019;98(17): e15323.
46. Farstad IN, Halstensen TS, Lien B, Kilshaw PJ, Lazarovitz AI, Brandtzaeg P. Distribution of β7 integrins in human intestinal mucosa and organized gut-associated lymphoid tissue. Immunology. 1996;89(2): 227-237.
47. Micklem KJ, Dong Y, Willis A, et al. HML-1 antigen on mucosa-associated T cells, activated cells, and hairy leukemic cells is a new integrin containing the beta 7 subunit. Am J Pathol. 1991;139(6):1297-301.
48. Shaw SK, Brenner MB. The beta 7 integrins in mucosal homing and retention. Semin Immunol. 1995;7(5):335-342.
49. Peine M, Rausch S, Helmstetter C, et al. Stable T-bet+GATA-3+ Th1/Th2 hybrid cells arise in vivo, can develop directly from naive precursors, and limit immunopathologic inflammation. PLoS Biol. 2013;11 (8):e1001633.
50. Hegazy AN, Peine M, Helmstetter C, et al. Interferons direct Th2 cell reprogramming to generate a stable GATA-3+T-bet+ cell subset with combined Th2 and Th1 cell functions. Immunity. 2010;32(1):116-128.
51. Fox A, Harland KL, Kedzierska K, Kelso A. Exposure of human CD8+ T cells to type-2 cytokines impairs division and differentiation and induces limited polarization. Front Immunol. 2018;9:1141.
52. Tai TS, Pai SY, Ho IC. GATA-3 Regulates the homeostasis and activation of CD8+ T cells. J Immunol. 2013;190(1):428-437.
53. Wang T, Feldman AL, Wada DA, et al. GATA-3 expression identifies a high-risk subset of PTCL, NOS with distinct molecular and clinical features. Blood. 2014;123 (19):3007-3015.
54. Manso R, Bellas C, Martín-Acosta P, et al. C-MYC is related to GATA3 expression and associated with poor prognosis in nodal peripheral T-cell lymphomas. Haematologica. 2016;101(8):e336-338.

ARTICLE

Pre-treatment maximum standardized uptake value predicts outcome after frontline therapy in patients with advanced stage follicular lymphoma

Paolo Strati,[1] Mohamed Amin Ahmed,[1] Nathan H. Fowler,[1] Loretta J. Nastoupil,[1] Felipe Samaniego,[1] Luis E. Fayad,[1] Fredrick B. Hagemeister,[1] Jorge E. Romaguera,[1] Alma Rodriguez,[1] Michael Wang,[1] Jason R. Westin,[1] Chan Cheah,[1] Mansoor Noorani,[1] Lei Feng,[2] Richard E. Davis[1] and Sattva S. Neelapu[1]

[1]Department of Lymphoma and Myeloma, The University of Texas MD Anderson Cancer Center and [2]Department of Biostatistics, The University of Texas MD Anderson Cancer Center, Houston, TX, USA

Ferrata Storti Foundation

Haematologica 2020
Volume 105(7):1907-1913

ABSTRACT

The impact of pre-treatment maximum standardized uptake value (SUV_{max}) on the outcome of follicular lymphoma (FL) following specific frontline regimens has not been explored. We performed a retrospective analysis of 346 patients with advanced stage follicular lymphoma (FL) without histological evidence of transformation, and analyzed the impact of SUV_{max} on outcome after frontline therapy. Fifty-two (15%) patients had a SUV_{max} >18, and a large lymph node ≥6 cm was the only factor associating with SUV_{max} >18 on multivariate analysis (odds ratio 2.7, 95% confidence interval [CI]: 1.3-5.3, *P*=0.006). The complete response rate was significantly lower among patients treated with non-anthracycline-based regimens if SUV_{max} was >18 (45% *vs.* 92%, *P*<0.001), but not among patients treated with R-CHOP (*P*=1). SUV_{max} >18 was associated with significantly shorter progression-free survival among patients treated with non-anthracycline-based regimens (77 months vs. not reached, *P*=0.02), but not among patients treated with R-CHOP (*P*=0.73). SUV_{max} >18 associated with shorter overall survival (OS) both in patients treated with R-CHOP (8-year OS 70% vs. 90%, *P*=0.02) and non-anthracycline-based frontline regimens (8-year OS 50% *vs.* 85%, *P*=0.001). In conclusion, pre-treatment PET scan has prognostic and predictive value in patients with advanced stage FL receiving frontline treatment.

Introduction

Despite its indolent biology, follicular lymphoma (FL) can be fluorodeoxyglucose (FDG) avid on positron emission tomography (PET). A wide range of inter- and intra-patient degree of FDG avidity has been reported, with a maximum standardized uptake (SUV_{max}) value ranging between 3 and 40.[1-4] PET scan is more sensitive and specific than standard computed tomography (CT) scan in identifying nodal and extra-nodal disease, altering stage assignation in 10-31% of patients with FL, and determining a treatment plan revision based on upstaging (I-II to III-IV) in 34-45% of cases.[5-10] PET-based imaging is also an effective tool for early detection of FL transformation, incremental threshold of SUV_{max} values associating with increasing test specificity.[11-14] False positivity is still possible, though, and histological confirmation through tissue biopsy is recommended.[15,16]

Despite its beneficial effect on staging reassignment and histological classification, the prognostic role of PET-based imaging at time of diagnosis remains unclear, with conflicting data published in the literature with regards to its impact on the Follicular Lymphoma International Prognostic Index (FLIPI) determination.[6,8,17] In addition, while multiple studies have investigated the association between a post-treatment PET scan and the risk of relapse, limited data are available regarding the predictive role of pre-treatment PET data in the frontline setting.[18-22] We provide a

Correspondence:

SATTVA S. NEELAPU
sneelapu@mdanderson.org

Received: June 28, 2019.

Accepted: October 4, 2019.

Pre-published: October 10, 2019.

doi:10.3324/haematol.2019.230649

Check the online version for the most updated information on this article, online supplements, and information on authorship & disclosures: www.haematologica.org/content/105/7/1907

retrospective analysis of 346 patients with advanced stage FL, in whom a PET-CT scan was performed prior to initiation of therapy, and analyze the impact of SUV_{max} on the quality of response and outcomes after frontline therapy.

Methods

Patient selection

This is a retrospective analysis of patients with stage III or IV FL, grades I, II, or IIIA, receiving frontline treatment at the MD Anderson Cancer Center (MDACC) between August, 2001 and April, 2014, and who had a pre-treatment PET-CT scan performed. Patients with histological diagnosis of FL grade IIIB or concurrent diffuse large B-cell lymphoma (DLBCL) were excluded.

The clinical and laboratory features were confirmed by review of the medical records. Frontline therapy was administered according to the previously described schedule.[23-27] The FLIPI and FLIPI-2 scores were calculated as previously described.[28,29] Lugano classification was used to define complete response.[30,31] The study was approved by the Institutional Review Board of the MDACC and conducted in accordance with our institutional guidelines and the principles of the Declaration of Helsinki.

PET scan and SUV_{max} threshold selection

Baseline PET-CT scans were obtained at MDACC before initiation of frontline therapy. After patients had fasted for at least 4-6 hours, blood glucose was measured and confirmed to be <140 mg/dL (<200 mg/dL for patients with diabetes) before injection of 333-407 MBq (9-11 mCi) of [^{18}F]FDG. Emission scans were acquired at 2-3 minutes per field of view in the three-dimensional mode after a 60-minute uptake time (±10 minutes). CT non-contrast images were acquired in helical mode with 3.75-mm slices from the skull base through the midthigh. Commercially available iterative algorithms were used for image reconstruction. PET images were collected and transferred to commercially available software (MIMVista version 6.4.9; MIMVista Corporation, Cleveland, OH). SUV_{max} was calculated as previously described.[32] All reports of pre-treatment scans and of scans performed to assess response to frontline therapy were reviewed by an oncologist with expertise in lymphoma.

Analyzing multiple single unit increments of SUV_{max} among all 346 patients included in the study, 18 showed the strongest association with progression-free survival (PFS) (hazard ratio [HR] 1.5, 95% confidence interval [CI]: 0.95-2.3, P=0.08), and was selected as cut-off for further analysis (*Online Supplementary Table S1*).

Statistical methods

Association with categorical variables was evaluated using χ^2 or Fisher exact tests, or the Mann-Whitney test, as appropriate, and logistic regression was used for multivariate analysis. Only factors significant (P-value <0.05) on univariate analysis were included in multivariate models. PFS was defined as the time from the start of therapy to progression of disease, death, or last follow-up (whichever occurred first). Overall survival (OS) was defined as the time from the start of therapy to death or last follow-up. PFS and OS were calculated for all patients in the study and for subgroups of patients using Kaplan-Meier estimates and were compared between subgroups using the log-rank test. Multivariable Cox regression analysis was performed to assess the associations between patient characteristics and PFS or OS. A P-value of <0.05 (two-tailed) was considered statistically significant. Statistical analyses were completed using SPSS 21.

Results

Patient baseline characteristics

Three-hundred and forty-six patients were included in the study, median SUV_{max} was 11 (range: 1.5-42), and 52 (15%) patients had a SUV_{max} >18. All 52 patients with SUV_{max} >18 had a biopsy of the most FDG-avid lymph node, and no histological evidence of transformation was observed. Baseline characteristics are shown in Table 1. On univariate analysis, factors associated with SUV_{max} >18 were male sex (67% *vs.* 52%, P=0.05), elevated β2-microglobulin (65% *vs.* 47%, P=0.02), elevated lactate dehydrogenase (LDH)(37% *vs.* 13%, P<0.001), presence of B symptoms (35% *vs.* 14%, P=0.01), and a large lymph node >6 cm (64% *vs.* 30%, P<0.001)(Table 1). On multivariate analysis, a large lymph node ≥6 cm was the only factor maintaining its association with SUV_{max} >18 (odds ratio [OR] 2.7, 95% CI: 1.3-5.3, P=0.006)(Table 2).

Response to frontline therapy: complete response (CR)

One-hundred and fifty-one (44%) patients were treated with frontline rituximab, cyclophosphamide, doxorubicin, vincristine and prednisone (R-CHOP), and 195 (56%) with other therapies, including rituximab and bendamustine (BR) in 55 (16%) patients, rituximab and lenalidomide (R^2) in 63 (18%), rituximab, fludarabine, mitoxantrone, and dexamethasone (R-FND) in 24 (7%), and single agent rituximab in 53 (15%) patients. Two-hundred and thirty-two (65%) patients received maintenance rituximab and 114 (33%) were observed after completion of frontline therapy. While no differences in the use of maintenance therapy were observed between the two groups (75% *vs.* 67%, P=0.20), a significantly higher proportion of patients with baseline pre-treatment SUV_{max} >18 were treated with R-CHOP *versus* non-anthracycline-based regimens (75% *vs.* 38%, P<0.001), so subsequent results were stratified by treatment arm.

Among 342 patients evaluable for response, 305 (89%) achieved CR; the CR rate was 91% for patients with SUV_{max} <18 and 80% for patients with SUV_{max} >18 (P=0.03). No association between SUV_{max} and CR rate was observed among patients treated with R-CHOP (89% for SUV_{max} > 18 vs. 88% for SUV_{max} < 18, P=1). However, SUV_{max} >18 significantly associated with a lower CR rate among patients treated with other frontline regimens (45% for SUV_{max} >18 vs. 92% for SUV_{max} <18) (P<0.001) (Figure 1). After excluding patients treated with single agent rituximab a trend for a lower CR rate among patients treated with other frontline regimens and SUV_{max} >18 was observed (80% *vs.* 94%, P=0.17); of interest, in this group, only five patients with SUV_{max} >18 were evaluable for response, likely limiting achievement of statistical significance.

Progression-free survival (PFS) and PFS24

After a median follow-up of 94 months (95% CI: 88-100 months), median PFS was not reached, and a trend for decreased PFS was observed in patients with baseline SUV_{max} >18 compared to patients with baseline <18 (114 months *vs.* not reached, P=0.08). Baseline ≥18 did not associate with shorter median PFS among patients treated with frontline R-CHOP (114 months *vs.* 144 months, P=0.73), but it did associate with significantly shorter PFS among patients treated with other frontline regimens (77 months vs. not reached, P=0.02)(Figure 2). After excluding

patients treated with single agent rituximab, a trend for shorter PFS among patients treated with other frontline regimens and baseline SUV_{max} >18 was observed (77 months *vs.* not reached, *P*=0.17); of interest, in this group, only seven patients with baseline SUV_{max}>18 were evaluable for survival, likely limiting achievement of statistical significance.

Use of maintenance rituximab associated with a significantly longer PFS (not reached *vs.* 84 months, *P*<0.001); the association between use of maintenance rituximab

Table 1. Patient baseline characteristics and association with pre-treatment maximum standardized uptake value (SUV_{max}) >18.

	Number (percentage)			
	All patients (N=346)	SUV_{max} < 18 (N=294)	SUV_{max} > 18 (N=52)	*P*
Age				
< 60 years	199 (57)	168 (57)	31 (60)	0.76
≥ 60 years	147 (43)	126 (43)	21 (40)	
Female	157 (45)	140 (48)	17 (33)	0.05
Male	189 (55)	154 (52)	35 (67)	
Hemoglobin				
≥ 12 g/dL	286 (83)	245 (83)	41 (79)	0.43
< 12 g/dL	60 (17)	49 (17)	11 (21)	
β2-microglobulin				
≤ ULN	165 (51)	148 (53)	17 (35)	0.02
> ULN	161 (49)	129 (47)	32 (65)	
LDH				
≤ ULN	288 (84)	255 (87)	33 (63)	<0.001
> ULN	56 (16)	37 (13)	19 (37)	
Grade				
1-2	339 (99.5)	288 (99)	51 (100)	1
3A	3 (0.5)	3 (1)	0 (0)	
Ki-67				
< 40%	173 (86)	147 (87)	26 (79)	0.28
≥ 40%	29 (14)	22 (13)	7 (21)	
Bone marrow				
not involved	159 (47)	134 (46)	25 (50)	0.65
involved	182 (53)	157 (54)	25 (50)	
B-symptoms				
absent	286 (83)	252 (86)	34 (65)	0.001
present	60 (17)	42 (14)	18 (35)	
Ann Arbor Stage				
III	102 (29)	87 (30)	15 (29)	1
IV	244 (71)	207 (70)	37 (71)	
Involved nodal areas				
< 5	139 (42)	114 (40)	25 (50)	0.22
≥ 5	193 (58)	168 (60)	25 (50)	
Largest lymph node				
< 6 cm	179 (64)	163 (70)	16 (36)	<0.001
≥ 6 cm	99 (36)	71 (30)	28 (64)	
Extra-nodal disease				
absent	203 (59)	175 (60)	28 (54)	0.27
present	143 (41)	119 (40)	24 (46)	
FLIPI score				
low	67 (19)	56 (19)	11 (21)	0.11
Intermediate	137 (40)	123 (42)	14 (27)	
high	142 (41)	115 (39)	27 (52)	
FLIPI-2 score				
low	29 (8)	26 (9)	3 (6)	0.16
Intermediate	186 (54)	163 (55)	23 (44)	
high	131 (38)	105 (36)	26 (50)	

LDH: lactate dehydrogenase; ULN: upper limit of normal; FLIPI: follicular lymphoma international prognostic index; SUV_{max}: maximum standardized uptake value.

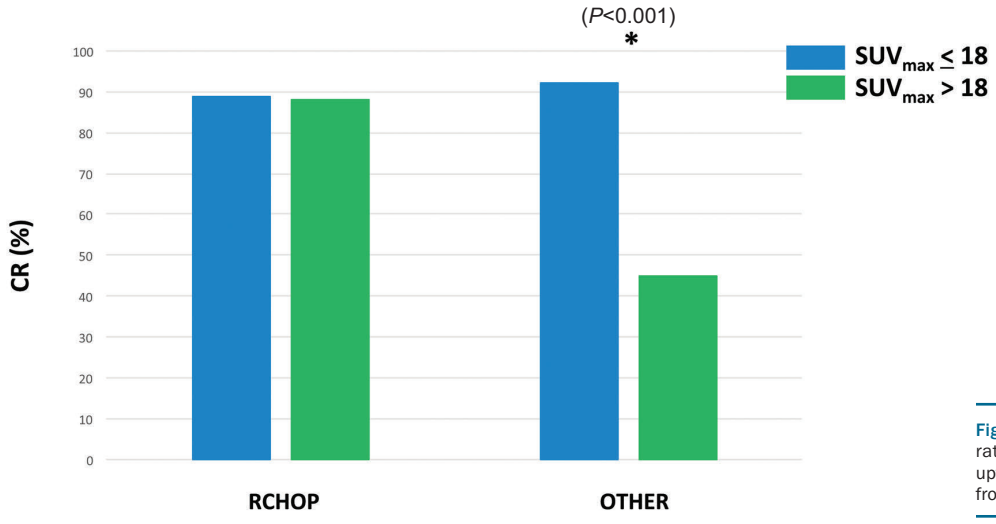

Figure 1. Complete response (CR) rates by maximum standardized uptake (SUV_{max}) values according to frontline regimen.

and prolonged PFS was maintained also after adjusting for pre-treatment SUV_{max} >18 (HR 2, 95% CI: 1.3-2.9, *P*<0.001). Further subgroup analysis, to assess the effect of maintenance rituximab after specific regimens according to pre-treatment SUV_{max} >18 could not be performed, because of small population samples.

Excluding 11 patients who did not progress and were lost to follow-up within 24 months, 67 (20%) patients had a PFS of less than 24 months: PFS <24 months was observed in 51 (18%) patients with baseline SUV_{max} <18, and 16 (34%) of patients with baseline SUV_{max} >18 (*P*=0.02). SUV_{max} >18 did not associate with a significantly higher rate of PFS <24 months among patients treated with R-CHOP (32% *vs.* 24%, *P*=0.39), but it did associate with a higher rate of PFS <24 months among patients treated with other regimens (40% *vs.* 14%, *P*=0.05). After excluding patients treated with single agent rituximab, a trend for higher PFS24 rate among patients treated with other frontline regimens and SUV_{max} >18 was observed (20% *vs.* 11%, *P*=0.45); of interest, only five patients with SUV_{max} >18 were evaluable for PFS24, likely limiting achievement of statistical significance.

Overall survival (OS) and risk of transformation

After a median follow-up of 94 months (95% CI: 88-100 months), median OS has not been reached, and it was significantly shorter among patients with SUV_{max} >18 (8-year OS 65% *vs.* 89%, *P*=0.001). SUV_{max} >18 associated with shorter OS both in patients treated with frontline R-CHOP (8-year OS 70% *vs.* 90%, *P*=0.02) and in patients treated with other frontline regimens (8-year OS 50% vs. 85%, *P*=0.001)(Figure 3). A trend for longer OS was observed among patients with SUV_{max} >18 when comparing treatment with frontline R-CHOP to other frontline treatments (8-year OS 70% *vs.* 50%, *P*=0.15). The association between SUV_{max} >18 and OS was maintained also on multivariate analysis including either FLIPI score (HR 2.6, 95% CI: 1.5-4.6, *P*=0.001) or FLIPI-2 score (HR 2.2, 95% CI: 1.3-3.9, *P*=0.006).

At the most recent follow-up, 18 (5%) patients have progressed with histological evidence of transformation to large B-cell lymphoma, after a median time of 23 months (range: 5-139 months). Twelve transformations (4%) occurred among patients with baseline SUV_{max} <18, and six (11%) among patients with baseline SUV_{max} >18 (*P*=0.04). Of these 18 patients, 11 had received frontline R-CHOP (of whom six had baseline SUV_{max} >18) and seven other frontline regimens (none of whom had baseline SUV_{max} >18). After excluding patients treated with single agent rituximab, a statistically significant shorter OS among patients treated with other frontline regimens and SUV_{max} >18 was observed (86 months *vs.* not reached, *P*=0.05).

Discussion

Recent guidelines recommend the use of PET-CT in FL for initial staging, evaluation of potential transformation, and at time of response assessment.[31,33] However, the impact of baseline PET-based imaging on the outcome following specific frontline treatment has not been previously explored.

In our analysis, an SUV_{max} cut-off of 18 was identified as clinically significant, showing the strongest association with PFS. SUV_{max} cut-offs of 10, 14 and 17 have been proposed in previous retrospective studies to identify patients with FL at higher risk of transformation to DLBCL,[11,12,14] with OR for transformation of 1.25 for each increase in unit of SUV_{max}.[10] To this regard, patients with histological evidence of FL grade IIIB or DLBCL were excluded from this study. Although tumor heterogeneity may have caused a false-negative result, elevated SUV_{max} in the absence of histological evidence of transformation may reflect a more aggressive biology, associating with a worse outcome, as already shown in other forms of low grade B-cell lymphomas.[34] It is interesting to note that in our study the only factor significantly associated with SUV_{max} >18 was the lymph node size ≥6 cm and that more transformations occurred in patients with pre-treatment SUV_{max} >18 (11% *vs.* 4%, *P*=0.04). While a core needle biopsy of a large lymph node may miss a diagnosis of DLBCL, the large tumor size may also simply be a surrogate marker of accelerated biology in the absence of transformation. Prospective studies, employing excisional biopsy, as opposed to core biopsy, may shed light on this question.

In our study, patients with SUV_{max} >18 were more frequently treated with R-CHOP, compared to other thera-

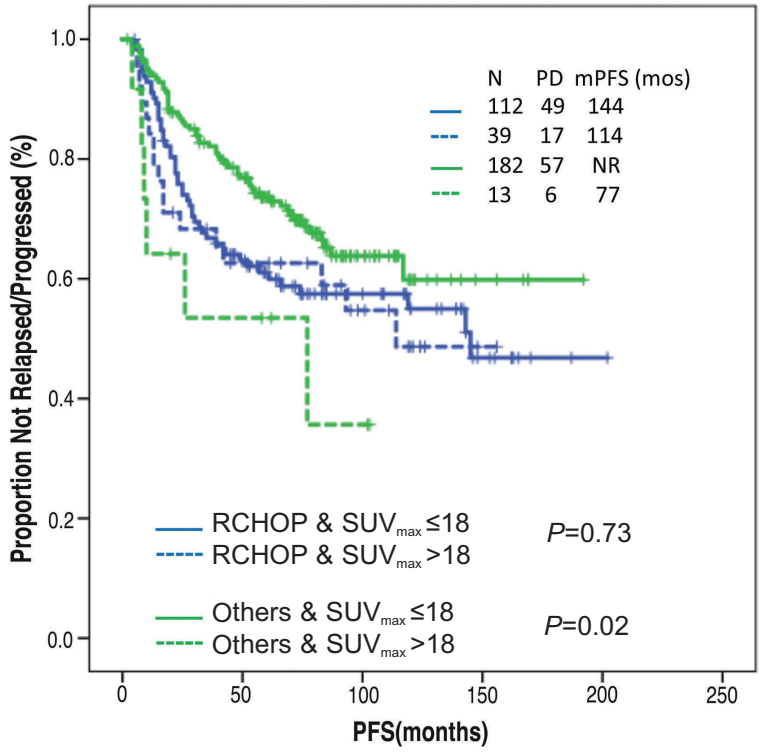

Figure 2. Association between progression-free survival (PFS) and maximum standardized uptake (SUV_{max}) separated by frontline treatment arm.

Table 2. Multivariate analysis of baseline characteristics associated with pre-treatment maximum standardized uptake value (SUV_{max}) >18

	Total (N=263)	Number (percentage) OR [95% CI]	*P*-multi
Female	123	1.9 [0.9-3.8]	0.08
Male	140		
β2-microglobulin			
≤ ULN	135	1.3 [0.6-2.7]	0.56
> ULN	128		
LDH			
≤ ULN	218	2 [0.9-4.1]	0.08
> ULN	45		
B-symptoms			
absent	214		
present	49	1.5 [0.7-3.1]	0.26
Largest lymph node			
< 6 cm	169	2.7 [1.3-5.3]	0.006
≥ 6 cm	94		

Overall, 263 of 346 patients had no missing values for all five variables, and were included in the model: 42 with SUV_{max} >18 and 221 with SUVmax ≤18. LDH: lactate dehydrogenase; ULN: upper limit of normal; SUV_{max}: maximum standardized uptake value.

pies (including BR, R-FND, R[2] and single agent rituximab). Abou-Nassar et al. had previously reported similar findings, likely reflecting the treating physician's concern for occult transformation, and subsequent need for anthracycline-based therapy.[17] We acknowledge as a potential bias of our study that patients with SUV_{max} >18 treated with other therapies may have not been fit for R-CHOP, based on variables not analyzed in this study, such as comorbidities, reflecting a clinician's therapeutic bias, and therefore more likely to experience a dismal outcome.

Of interest, in our study, the association between SUV_{max} >18 and lower CR rate, observed for the whole population, was lost among patients treated with R-CHOP. In the rituximab era, the use of anthracycline-based regimens, such as R-CHOP, has significantly improved the outcome of patients with previously untreated transformed FL, resulting in response rates and survival similar to what has been observed in de novo DLBCL.[35-38] Our results indicate that patients with more aggressive forms of FL, as suggested by pre-treatment SUV_{max} >18, may benefit from anthracycline-based therapies as the CR rates were significantly lower with alternative regimens. This is further supported by the fact that in our analysis the lower PFS associated with SUV_{max} >18 (including high rates of progressions

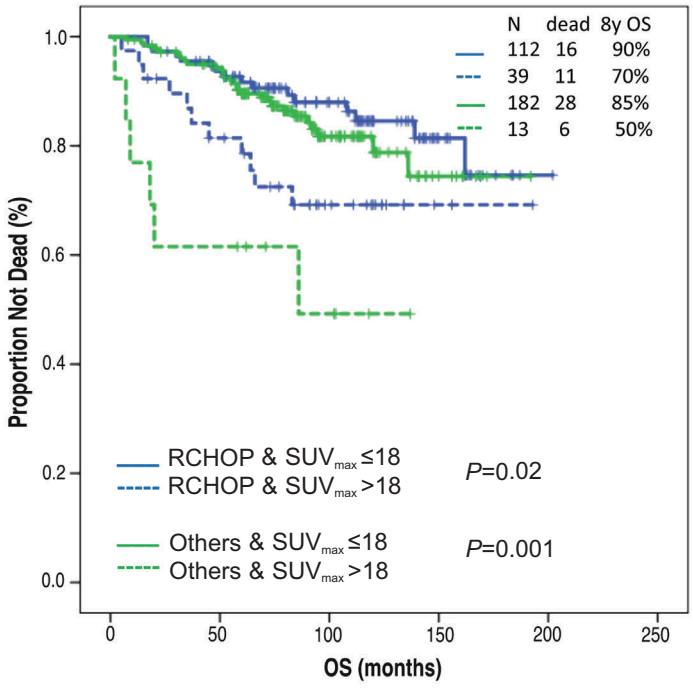

Figure 3. Association between overall survival (OS) and maximum standardized uptake (SUV_{max}) separated by frontline treatment arm.

within 24 months from treatment initiation) was overcome by the use of frontline R-CHOP. These novel and clinically relevant findings highlight the need to examine the impact of pre-treatment SUV_{max} on outcomes in recently completed randomized phase 3 trials in FL comparing different frontline regimens such as R-CHOP, BR, and/or R^2.[24,25,39] It is important to note that, as only three patients with FL grade IIIA were included in this study, these results can apply only to patients with grades I-II FL.

Finally, despite the beneficial effect of R-CHOP on CR rate and PFS of patients with SUV_{max} >18, subsequent transformations were still observed among patients treated with this regimen. However, this was not unexpected as not all patients with occult or histologically proven transformed FL achieve durable remissions with R-CHOP. Recurrent disease with transformation after R-CHOP can be salvaged with high-dose chemotherapy with autologous stem cell transplantation and/or chimeric antigen receptor T-cell therapy.[40-44] While patients with transformation at the time of relapse who are anthracycline-naïve can be salvaged with R-CHOP, the superior OS observed in patients treated with frontline R-CHOP compared with other regimens within the sub-group of patients with SUV_{max} >18 (8- year OS 70% *vs.* 50%, *P*=0.15) raises the possibility that upfront treatment with anthracycline-based regimen may lead to better outcomes in such patients. On the other hand, relapses occurring in patients with high SUV_{max} after frontline R-CHOP may have a more aggressive biology, including transformation, explaining the difference in OS according to SUV_{max} observed in patients treated with this regimen.

We acknowledge that there are some limitations due to the retrospective nature of this study and the well-known variability and limited reproducibility of SUV measurements.[45] For example, consistent criteria may not have been used to select patients in whom to perform a tissue biopsy for exclusion of transformation, and therefore patients with concurrent undiagnosed FL grade IIIB and/or DLBCL may have been included in the study. There was also likely variability in dose-intensity of the chemotherapy between patients. The total metabolic tumor volume (TMTV) was not calculated in this analysis, and the latter has been shown to predict the outcome after frontline therapy in patients with high-burden FL.[46] Upon further validation, TMTV and other PET-based functional parameters, such as total lesion glycolysis, may in the future provide a more standardized approach to assess the prognostic value of pre-treatment PET in patients with FL.

Nevertheless, the significant decrease in the CR rate, PFS, and OS observed in patients with SUV_{max} >18 in our study suggest that a pre-treatment PET scan has a prognostic and predictive value in patients with advanced stage FL receiving frontline treatment and prospective randomized trials are warranted to investigate this further.

Funding

This research is supported in part by the MD Anderson Cancer Center Support Grant P30 CA016672.

References

1. Jerusalem G, Beguin Y, Najjar F, Hustinx R, Fassotte MF, Rigo P, et al. Positron emission tomography (PET) with 18F-fluorodeoxyglucose (18F-FDG) for the staging of low-grade non-Hodgkin's lymphoma (NHL). Ann Oncol. 2001;12(6):825-830.
2. Karam M, Novak L, Cyriac J, Ali A, Nazeer T, Nugent F. Role of fluorine-18 fluorodeoxyglucose positron emission tomography scan in the evaluation and follow-up of patients with low-grade lymphomas. Cancer. 2006;107(1):175-183.
3. Wohrer S, Jaeger U, Kletter K, et al. 18F-fluoro-deoxy-glucose positron emission tomography (18F-FDG-PET) visualizes follicular lymphoma irrespective of grading. Ann Oncol. 2006;17(5):780-784.
4. Elstrom R, Guan L, Baker G, et al. Utility of FDG-PET scanning in lymphoma by WHO classification. Blood. 2003;101(10):3875-3876.
5. Wirth A, Foo M, Seymour JF, Macmanus MP,

Hicks RJ. Impact of [18f] fluorodeoxyglucose positron emission tomography on staging and management of early-stage follicular non-hodgkin lymphoma. Int J Radiat Oncol Biol Phys. 2008;71(1):213-219.
6. Luminari S, Biasoli I, Arcaini L, et al. The use of FDG-PET in the initial staging of 142 patients with follicular lymphoma: a retrospective study from the FOLL05 randomized trial of the Fondazione Italiana Linfomi. Ann Oncol. 2013;24(8):2108-2112.
7. Janikova A, Bolcak K, Pavlik T, Mayer J, Kral Z. Value of [18F]fluorodeoxyglucose positron emission tomography in the management of follicular lymphoma: the end of a dilemma? Clin Lymphoma Myeloma. 2008;8(5):287-293.
8. Le Dortz L, De Guibert S, Bayat S, et al. Diagnostic and prognostic impact of 18F-FDG PET/CT in follicular lymphoma. Eur J Nucl Med Mol Imaging. 2010;37(12):2307-2314.
9. Chen YK, Yeh CL, Tsui CC, Liang JA, Chen JH, Kao CH. F-18 FDG PET for evaluation of bone marrow involvement in non-Hodgkin lymphoma: a meta-analysis. Clin Nucl Med. 2011 Jul;36(7):553-559.
10. Smith SD, Redman M, Dunleavy K. FDG PET-CT in follicular lymphoma: a case-based evidence review. Blood. 2015; 125(7):1078-1082.
11. Schoder H, Noy A, Gonen M, et al. Intensity of 18fluorodeoxyglucose uptake in positron emission tomography distinguishes between indolent and aggressive non-Hodgkin's lymphoma. J Clin Oncol. 2005;23(21):4643-4651.
12. Bodet-Milin C, Kraeber-Bodere F, Moreau P, Campion L, Dupas B, Le Gouill S. Investigation of FDG-PET/CT imaging to guide biopsies in the detection of histological transformation of indolent lymphoma. Haematologica. 2008;93(3):471-472.
13. Noy A, Schoder H, Gonen M, et al. The majority of transformed lymphomas have high standardized uptake values (SUVs) on positron emission tomography (PET) scanning similar to diffuse large B-cell lymphoma (DLBCL). Ann Oncol. 2009; 20(3):508-512.
14. Karam M, Feustel PJ, Vera CD, Nazeer T. Features of large cell transformation of indolent lymphomas as observed on sequential PET/CT. Nucl Med Commun. 2011;32(3): 177-185.
15. Cook GJ, Fogelman I, Maisey MN. Normal physiological and benign pathological variants of 18-fluoro-2-deoxyglucose positron-emission tomography scanning: potential for error in interpretation. Semin Nucl Med. 1996;26(4):308-314.
16. Hofman MS, Hicks RJ. Imaging in follicular NHL. Best Pract Res Clin Haematol. 2011;24(2):165-177.
17. Abou-Nassar KE, Vanderplas A, Friedberg JW, et al. Patterns of use of 18-fluoro-2-deoxy-D-glucose positron emission tomography for initial staging of grade 1-2 follicular lymphoma and its impact on initial treatment strategy in the National Comprehensive Cancer Network Non-Hodgkin Lymphoma Outcomes database. Leuk Lymphoma. 2013;54(10):2155-2162.
18. Salles G, Seymour JF, Offner F, et al. Rituximab maintenance for 2 years in patients with high tumour burden follicular lymphoma responding to rituximab plus chemotherapy (PRIMA): a phase 3, randomised controlled trial. Lancet. 2011; 377(9759):42-51.
19. Luminari S, Biasoli I, Versari A, et al. The prognostic role of post-induction FDG-PET in patients with follicular lymphoma: a subset analysis from the FOLL05 trial of the Fondazione Italiana Linfomi (FIL). Ann Oncol. 2014;25(2):442-447.
20. Trotman J, Fournier M, Lamy T, et al. Positron emission tomography-computed tomography (PET-CT) after induction therapy is highly predictive of patient outcome in follicular lymphoma: analysis of PET-CT in a subset of PRIMA trial participants. J Clin Oncol. 2011;29(23):3194-3200.
21. Dupuis J, Berriolo-Riedinger A, Julian A, et al. Impact of [(18)F]fluorodeoxyglucose positron emission tomography response evaluation in patients with high-tumor burden follicular lymphoma treated with immunochemotherapy: a prospective study from the Groupe d'Etudes des Lymphomes de l'Adulte and GOELAMS. J Clin Oncol. 2012;30(35):4317-4322.
22. Trotman J, Barrington SF, Belada D, et al. Prognostic value of end-of-induction PET response after first-line immunochemotherapy for follicular lymphoma (GALLIUM): secondary analysis of a randomised, phase 3 trial. Lancet Oncol. 2018;19(11):1530-1542.
23. Flinn IW, van der Jagt R, Kahl BS, et al. Randomized trial of bendamustine-rituximab or R-CHOP/R-CVP in first-line treatment of indolent NHL or MCL: the BRIGHT study. Blood. 2014;123(19):2944-2952.
24. Rummel MJ, Niederle N, Maschmeyer G, et al. Bendamustine plus rituximab versus CHOP plus rituximab as first-line treatment for patients with indolent and mantle-cell lymphomas: an open-label, multicentre, randomised, phase 3 non-inferiority trial. Lancet. 2013;381(9873):1203-1210.
25. Morschhauser F, Fowler NH, Feugier P, et al. Rituximab plus Lenalidomide in Advanced Untreated Follicular Lymphoma. N Engl J Med. 2018;379(10):934-947.
26. Nastoupil LJ, McLaughlin P, Feng L, et al. High ten-year remission rates following rituximab, fludarabine, mitoxantrone and dexamethasone (R-FND) with interferon maintenance in indolent lymphoma: Results of a randomized Study. Br J Haematol. 2017;177 (2):263-270.
27. Martinelli G, Schmitz SF, Utiger U, t al. Long-term follow-up of patients with follicular lymphoma receiving single-agent rituximab at two different schedules in trial SAKK 35/98. J Clin Oncol. 2010;28(29): 4480-4484.
28. Solal-Celigny P, Roy P, Colombat P, et al. Follicular lymphoma international prognostic index. Blood. 2004;104(5):1258-1265.
29. Federico M, Bellei M, Marcheselli L, et al. Follicular lymphoma international prognostic index 2: a new prognostic index for follicular lymphoma developed by the international follicular lymphoma prognostic factor project. J Clin Oncol. 2009; 27(27):4555-4562.
30. Brice P, Bastion Y, Lepage E, et al. Comparison in low-tumor-burden follicular lymphomas between an initial no-treatment policy, prednimustine, or interferon alfa: a randomized study from the Groupe d'Etude des Lymphomes Folliculaires. Groupe d'Etude des Lymphomes de l'Adulte. J Clin Oncol. 1997;15(3):1110-1117.
31. Cheson BD, Fisher RI, Barrington SF, et al. Recommendations for initial evaluation, staging, and response assessment of Hodgkin and non-Hodgkin lymphoma: the Lugano classification. J Clin Oncol. 2014; 32(27):3059-3068.
32. Pinnix CC, Ng AK, Dabaja BS, et al. Positron emission tomography-computed tomography predictors of progression after DA-R-EPOCH for PMBCL. Blood Adv. 2018;2(11): 1334-1343.
33. Barrington SF, Mikhaeel NG, Kostakoglu L, et al. Role of imaging in the staging and response assessment of lymphoma: consensus of the International Conference on Malignant Lymphomas Imaging Working Group. J Clin Oncol. 2014;32(27):3048-3058.
34. Falchi L, Keating MJ, Marom EM, et al. Correlation between FDG/PET, histology, characteristics, and survival in 332 patients with chronic lymphoid leukemia. Blood. 2014;123(18):2783-2790.
35. Link BK, Maurer MJ, Nowakowski GS, et al. Rates and outcomes of follicular lymphoma transformation in the immunochemotherapy era: a report from the University of Iowa/MayoClinic Specialized Program of Research Excellence Molecular Epidemiology Resource. J Clin Oncol. 2013;31(26):3272-3278.
36. Wagner-Johnston ND, Link BK, Byrtek M, et al. Outcomes of transformed follicular lymphoma in the modern era: a report from the National LymphoCare Study (NLCS). Blood. 2015;126(7):851-857.
37. Alonso-Alvarez S, Magnano L, Alcoceba M, et al. Risk of, and survival following, histological transformation in follicular lymphoma in the rituximab era. A retrospective multicentre study by the Spanish GELTAMO group. Br J Haematol. 2017; 178(5):699-708.
38. Gleeson M, Hawkes EA, Peckitt C, et al. Outcomes for transformed follicular lymphoma in the rituximab era: the Royal Marsden experience 2003-2013. Leuk Lymphoma. 2017;58(8):1805-1813.
39. Flinn IW, van der Jagt R, Kahl B, et al. First-line treatment of patients with indolent non-Hodgkin lymphoma or mantle-cell lymphoma with bendamustine plus rituximab versus R-CHOP or R-CVP: results of the BRIGHT 5-Year follow-up Study. J Clin Oncol. 2019;37(12):984-991.
40. Casulo C, Burack WR, Friedberg JW. Transformed follicular non-Hodgkin lymphoma. Blood. 2015;125(1):40-47.
41. Nair R, Neelapu SS. The promise of CAR T-cell therapy in aggressive B-cell lymphoma. Best Pract Res Clin Haematol. 2018; 31(3):293-298.
42. Locke FL, Ghobadi A, Jacobson CA, et al. Long-term safety and activity of axicabtagene ciloleucel in refractory large B-cell lymphoma (ZUMA-1): a single-arm, multicentre, phase 1-2 trial. Lancet Oncol. 2019;20(1):31-42.
43. Neelapu SS, Locke FL, Bartlett NL, et al. Axicabtagene ciloleucel CAR T-Cell therapy in refractory large B-cell lymphoma. N Engl J Med. 2017;377(26):2531-2544.
44. Schuster SJ, Bishop MR, Tam CS, et al. Tisagenlecleucel in adult relapsed or refractory diffuse large B-Cell lymphoma. N Engl J Med. 2019;380(1):45-56.
45. Kinahan PE, Fletcher JW. Positron emission tomography-computed tomography standardized uptake values in clinical practice and assessing response to therapy. Semin Ultrasound CT MR. 2010;31(6): 496-505.
46. Meignan M, Cottereau AS, Versari A, et al. Baseline metabolic tumor volume predicts outcome in high-tumor-burden follicular lymphoma: a pooled analysis of three multicenter studies. J Clin Oncol. 2016; 34(30): 3618-3626.

Ferrata Storti Foundation

Haematologica 2020
Volume 105(7):1914-1924

Efficacy of central nervous system prophylaxis with stand-alone intrathecal chemotherapy in diffuse large B-cell lymphoma patients treated with anthracycline-based chemotherapy in the rituximab era: a systematic review

Toby A. Eyre,[1] Faouzi Djebbari,[2] Amy A. Kirkwood[3] and Graham P. Collins[1]

[1]Department of Clinical Haematology, Oxford University Hospitals NHS Foundation Trust, Oxford; [2]Department of Pharmacy, Oxford University Hospitals NHS Foundation Trust, Oxford and [3]Cancer Research UK & UCL Cancer Trials Centre, UCL Cancer Institute, London, UK

ABSTRACT

Central nervous system (CNS) relapse of diffuse large B-cell lymphoma remains uncommon but catastrophic. The benefit of stand-alone intrathecal prophylaxis in reducing CNS recurrence is unclear and remains controversial. No systematic review analysing the evidence for stand-alone intrathecal prophylaxis has been performed in the era of anti-CD20 monoclonal antibody therapy. A comprehensive search (01/2002-01/2019) was systematically performed using Ovid MEDLINE®, Ovid EMBASE® and Cochrane. Studies were selected from a total of 804, screened based on predefined inclusion/exclusion criteria, and were critically appraised. Three post hoc analyses (RICOVER-60, RCHOP-14/21, GOYA), one prospective database and 10 retrospective series were included. 7,357 rituximab/obinutuzumab-exposed patients were analysed. The median percentage receiving intrathecal prophylaxis was 11.9%. Cumulative CNS relapse incidence ranged from 1.9% at 6.5 years to 8.4% at 5 years. Median time (of medians) to CNS relapse was 10 months. 73% developed isolated CNS relapses, 24% concurrent CNS/systemic relapse, and 3% post-systemic relapse. Reported CNS relapse sites were: parenchymal (58%), leptomeningeal (27%), and both (12%). Event rates were low resulting in limited power within each study to provide robust univariable/multivariable analysis. Intrathecal prophylaxis was not a univariable or multivariable factor associated with a reduction in CNS relapse in any study. We found no strong evidence for the benefit, or indeed genuine lack of benefit, of stand-alone intrathecal prophylaxis in preventing CNS relapse in diffuse large B-cell lymphoma-treated patients using anthracycline-based immunochemotherapy. Current published study designs limit the strength of such conclusions.

Correspondence:

TOBY A. EYRE
toby.eyre@ouh.nhs.uk

Received: June 20, 2019.

Accepted: September 2, 2019.

Pre-published: September 5, 2019.

doi:10.3324/haematol.2019.229948

Check the online version for the most updated information on this article, online supplements, and information on authorship & disclosures: www.haematologica.org/content/105/7/1914

Introduction

Relapse of diffuse large B-cell lymphoma (DLBCL) within the central nervous system (CNS) following front line anthracycline-based immunochemotherapy is relatively uncommon (typically 2-5%).[1–4] It typically occurs within the first year of follow up post-treatment and has devastating consequences. The median overall survival following recurrence within the CNS is approximately 2-5 months[5,6] with few patients achieving long term survival. As a result, attempts over many years have been made to reduce the risk of this complication of DLBCL. Although risk factors[1,4] for CNS relapse have been clearly described over recent years and the CNS international prognostic index (CNS-IPI) has been established and validated, the optimal and widely applicable CNS prophylactic strategy remains somewhat controversial.

High dose, systemic anti-metabolite therapy, typically in the form of high dose methotrexate (HDMTX), is the most commonly employed systemic prophylactic

therapy. The evidence base for the efficacy of HDMTX in the rituximab era is relatively weak but has been demonstrated in retrospective single or multicentre series.[7–9] No randomised prospective studies have been performed. HDMTX is given either following[10] or in an intercalated fashion alongside rituximab-based immunochemotherapy.[7] HDMTX prophylaxis is widely administered for this purpose; however its toxicity profile typically limits its use to patients under 70 years of age, without serous effusions and with adequate renal function.

Intrathecal (IT) anti-metabolites, typically methotrexate (MTX) and/or cytarabine (ara-c), have also been employed either as stand-alone therapy in patients deemed at high risk of CNS relapse, or as adjunctive therapy to high dose intravenous anti-metabolites. The theoretical basis for IT prophylaxis has historically been extrapolated from the management of other lymphoid cancers such as Burkitt lymphoma[11] and acute lymphoblastic leukemia.[12] Although not a universally applied practice, many centres continue to employ stand-alone IT prophylaxis in DLBCL patients at higher risk of CNS relapse who are otherwise being treated with curative intent but who are considered unsuitable candidates for HDMTX due to, for example, age, inadequate renal function, or patient/physician preference. Historical studies have demonstrated that IT methotrexate does not achieve therapeutic concentrations within the brain parenchyma[13] and IT chemotherapy administration has the potential for well described morbidity[14] as well as resource and administrative burden.

Although it is clear that rituximab reduces systemic relapse and improves survival in DLBCL,[15] summarised data within a systematic review published in 2015 are conflicting as to whether rituximab reduces CNS relapse.[5] There is some evidence that leptomeningeal recurrence may have become less common since the introduction of rituximab, with the majority of CNS relapses being parenchymal in origin.[10–12] There are few data suggesting that IT prophylaxis may reduce CNS relapse, although this is based on relatively small single or multicentre retrospective studies in heterogenous cohorts primarily from the pre-rituximab era.[19,20]

To date, there is no international consensus regarding which patients should receive stand-alone IT prophylaxis alongside rituximab and anthracycline-based frontline immunochemotherapy and no systematic reviews have been specifically performed to help answer this important question. An initial scoping review found a relatively small number of publications directly related to this question, and as such a comprehensive systematic review was deemed necessary. The purpose of this systematic review was, therefore, to identify evidence of effectiveness of stand-alone IT prophylaxis in patients treated in the front-line setting for DLBCL with anthracycline-based curative chemotherapy in the anti-CD20 monoclonal antibody era. Our systematic review was not designed to assess the relative value of combined IT and high dose intravenous anti-metabolite prophylaxis or high dose intravenous anti-metabolite prophylaxis alone as strategies to reduce CNS relapse risk.

Method

Search strategy

The review was conducted systematically in accordance with the Preferred Reporting Items for Systematic Review and Meta-Analysis Protocols (PRISMA-P) guidelines[21,22] and was registered on the PROSPERO database (CRD42019121174). A comprehensive search was conducted following a systematic search strategy using the electronic databases: Ovid MEDLINE®, Ovid EMBASE® and Cochrane Central Register of Controlled Trials. Boolean operators 'AND' and 'OR' were employed, as well as truncation (*).

Searches included the title and abstract where possible and were restricted to English language only. The search strategy was date restricted from 2002 until January 2019 as the pivotal trial establishing the benefit of rituximab in combination with CHOP was published in January of the year 2002.[15] Search strategy comprised three main components, using relevant Medical Subject Headings (MESH) terms where possible. Disease component(s) were searched for using the following search terms: diffuse large B-cell lymphoma, DLBCL, central nervous system relapse, CNS relapse, central nervous system recurrence, CNS recurrence, central nervous system progression, CNS progression. Prior therapies component(s) were searched for using the following search terms: rituximab, doxorubicin, anthracycline, R-CHOP, EPOCH and R-CHOEP. Intervention component(s) were searched for using the following search terms: central nervous system prophylaxis, CNS prophylaxis, intrathecal, intrathecal prophylaxis, intrathecal chemotherapy, intrathecal methotrexate, intrathecal cytarabine.

Full search strategies are summarised in the *Online Supplementary Tables S1-3*. The search was expanded using retrospective snowballing from the reference lists of initial studies included to ensure a sensitive and comprehensive search.

Screening search results

Search results were independently double-screened by the research team both at abstract and full text screening stages using eligibility criteria displayed in Table 1. Disagreements between any two researchers were referred to a third researcher to reach a consensus.

Quality appraisal and data extraction

Standardised Critical Appraisal Skills Programme (CASP) tools (*https://casp-uk.net/casp-tools-checklists*) were utilised to appraise the quality of study design, methodology and data reporting. CASP tools used were specific to each study type reviewed (*e.g.* clinical trial, cohort study). Studies were assigned a quality rating score as follows: 5 (high), 4 (moderate to high), 3 (moderate), 2 (moderate to low), or 1 (low). Limitations identified from reported data in individual studies were reported including low quality rating papers, which were also transparently reported in the review.

Data extraction and analysis

Extracted data were reviewed by all the research team (FD, TAE, GPC) and tabulated to summarise key findings. Key data extracted from each study were: author and year of publication, design, sample characteristics (type of rituximab-containing immunochemotherapy, key inclusion criteria), and reported outcomes (cumulative incidence of CNS relapse, site of CNS relapse, concurrence of systemic relapse and a documented analysis of the effectiveness of IT prophylaxis in preventing CNS relapse). For studies including patients treated both with and without rituximab, presented data for rituximab-exposed patients where available (superscript 'R', Table 2). The research design(s) and study characteristics, clarity of reporting, and statistical significance of reported data were assessed to determine the strengths and limitations of the evidence. All included studies underwent full statistical analysis (AAK).

Table 1. Key eligibility criteria.

Key Eligibility Criteria	
Inclusion	**Exclusion**
•Studies of DLBCL as the dominant lymphoma subtype assessing the risk of CNS relapse	• Case series with <100 patients treated with rituximab-chemotherapy
•Studies of DLBCL in the rituximab era: rituximab or obinutuzumab exposed patients represented ≥100 patients and the majority of the patients within the individual study.	•CNS involvement at diagnosis
•Studies of DLBCL treated with anthracycline-based chemotherapy	•Non-rituximab or non-obinutuzumab exposed cohorts
•Studies analysing the relative influence of stand-alone IT prophylaxis on outcome	•Cohorts where no patients received CNS prophylaxis
•Meta-analysis	•Early phase clinical trials
•Late phase clinical trials	•Pharmacokinetic studies
•Cohort studies	•Narrative reviews
•Cross-sectional studies	•Opinion papers
•Retrospective studies	•Education papers
•Observational studies	•Commentaries
•Case-control studies	•Editorials
	•Conference abstracts
	•Case-reports
	•Animal studies

DLBCL: diffuse large B cell lymphoma; CNS: central nervous system; IT: intrathecal.

Results

Search results

Of 804 search results, 12 studies were eligible for inclusion. One study was later excluded because of the authors concerns over quality of the reported study.[23] Following the search expansion phase, three additional studies were included.[6,24,25] In total, 14 studies met eligibility criteria for this review. Full details of the PRISMA inclusion/exclusion process are presented in Figure 1. Three studies were *post hoc* analyses from prospective randomised controlled clinical trials, one was an analysis of a multicentre, national, prospective database and all others were retrospective data series (seven single centre; three multicentre). Three studies were conducted in Japan, two in the USA and Canada, and one each in Germany, the UK, China, Singapore, South Korea and Thailand respectively.

A cumulative total of 7,357 (74.7%) anti-CD20 monoclonal antibody-exposed patients were assessed across the 14 series which included a cumulative total of 9,842 patients overall. All studies used rituximab or obinutuzumab[24] plus CHOP (cyclophosphamide, doxorubicin, vincristine and prednisolone) or CHOP-like regimens as the chemotherapy backbone given at between 14-28 day intervals apart from a single study which analysed a cohort treated with DA-EPOCH (dose adjusted etoposide, prednisolone, vincristine, cyclophosphamide and doxorubicin).[26] Five studies included patients ≥18 years, two studies included patients ≥16 years, one study included patients ≥15 years and one included patients 60-80 years. Five studies did not define age criteria. Three studies included patients with transformed indolent B-cell non-Hodgkin lymphoma (iNHL), and four studies included a relatively small number of patients with primary mediastinal B-cell lymphoma (PMBCL). The median percentage of patients receiving some form of IT prophylaxis across each individual study was 11.9% (range: 4.0-38.9%). The dosing frequency, total number of IT injections administered and chemotherapy agent used varied (Table 2). The IT chemotherapy agent was not defined in all studies, although methotrexate and ara-C were the only employed agents used when described.

CNS relapse outcomes

The cumulative incidence rate of CNS relapse was reported in 10 studies and a crude rate of CNS relapse (number of CNS events/total number of patients) was reported in four studies. The cumulative incidence CNS relapse rate from eight studies reporting rates in anti-CD20 monoclonal antibody-specific cohorts ranged between 1.9% at a median of 6.5 years follow-up[27] and 8.4% at 5 years.[28] Across the nine studies specifically reporting a median time to CNS relapse in anti-CD20 monoclonal antibody-exposed (sub)populations, the median of those median times reported was 10 months.

In 10 studies reporting details regarding the nature of the CNS relapses in rituximab or obinutuzumab exposed patients, there were 73% (128 of 175) isolated CNS relapses, 24% (42 of 175) CNS relapses concurrent at the time of systemic relapse, and 3% (5 of 175) cases of CNS relapse occurring at a later time point following documented systemic relapse.

Ten studies provided a detailed breakdown of the anatomical site of CNS relapse in rituximab or obinutuzumab-exposed patients. In total there were 191 CNS relapses, of which 111 (58%) were parenchymal, 52 (27%) were leptomeningeal, 23 (12%) were both parenchymal and leptomeningeal, one was intraocular (1%) and four (2%) were either not known or not specifically defined. Therefore, a total of 70% (134 of 191) of patients had demonstrable parenchymal involvement at CNS relapse.

Intrathecal prophylaxis efficacy

Efficacy analyses were performed in all 14 studies and these are presented Tables 3A-C. Patients receiving IT prophylaxis typically had demonstrable risk factors for CNS relapse, although the recommendations for IT prophylaxis varied considerably across studies (Table 4). As such, these

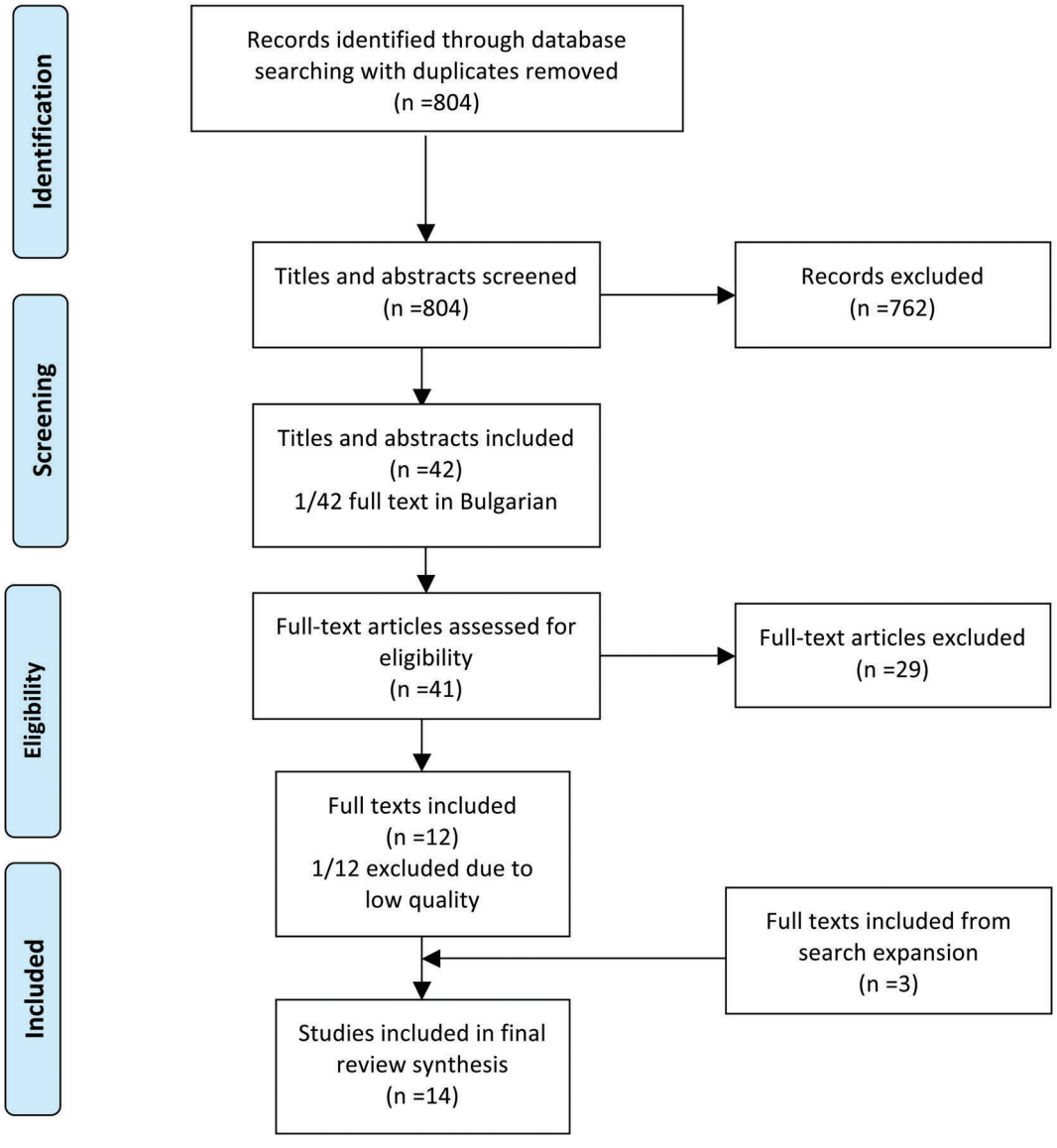

Figure 1. PRISMA Flow diagram of search strategy and inclusion/exclusion.

patients often were at higher risk of relapse than patients not receiving IT prophylaxis. Univariable analysis was performed in all studies and no study demonstrated clear evidence of a reduction in the risk of CNS relapse when IT prophylaxis was used. Multivariable analyses were performed and described in nine studies (Tables 3A-C). IT prophylaxis was not found to be a univariable or multivariable factor associated with a statistically significant reduction in the risk of CNS relapse in any of the studies examined.

No adjusted analyses were described in one study.[28] Adjusted analyses were reported in the remaining four studies in a variety of forms 1. Adjustment for CNS-IPI (n=2);[24,27] 2. Propensity matching to analyse survival (progression-free and overall survival) but not CNS relapse (n=1);[29] 3. Proportional hazard ratio to assess interaction between rituximab and IT prophylaxis with a univariable/multivariable analysis looking at clinical risk factors associated with CNS relapse and not IT prophylaxis (n=1).[30] None of these adjusted analyses showed that IT prophylaxis provided any benefit in reducing the risk of CNS relapse in the anti-CD20 antibody era.

Of note, no individual analysis reported the morbidity associated with IT prophylaxis in terms of the risk of adverse events, for example, risk of systemic infection, post lumbar puncture headache or dural leak.

Quality and statistical appraisal

We identified a range of study types including *post hoc* analyses of randomised clinical trials, prospective and retrospective cohort studies. None of the studies prospectively asked whether CNS IT stand-alone prophylaxis reduces the rate of CNS relapse. Although the absolute number of patients included within each study was relatively large, the absolute event number across studies was low. As a result, the statistical power within each study to provide

Table 2. Data extraction table.

Data to be extracted	Item
Publication ID	• Author • Publication date
Study aim	• Title/Purpose/Aim
Study design	• Study type and design: meta-analysis, late phase clinical trial, *post hoc* analysis of late phase clinical trials, cohort study, cross-sectional study, retrospective study, observational study, case-control study • Key study inclusion criteria for cohort studied if specified in manuscript
Sample characteristics	• Number of participants • Years of data collection • DLBCL subtypes • Proportion and total number of cohort receiving rituximab-containing anthracycline-based regimen • Rituximab or obinutuzumab-containing immunochemotherapy regimen(s) used for DLBCL treatment • Proportion of patients (total +/- rituximab or obinutuzumab exposed patients depending on what is reported) receiving IT prophylaxis • Type of IT prophylaxis received
Findings	• Number of CNS relapses and whether concurrent with systemic relapse or isolated CNS relapse: either of total population or rituximab population. This will be specified in analysis. • Cumulative incidence of CNS relapse at time point described in manuscript: either of total population or rituximab population. This will be specified in analysis. • Site of CNS relapse: parenchymal, leptomeningeal, both, unknown: either of total population or rituximab population. This will be specified in analysis. • Documentation of the analysis of the effectiveness of IT prophylaxis in assessing the CNS relapse risk.
Strengths and limitations	• CASP tool scores and comment on the nature and quality of the statistician analysis performed

DLBCL: diffuse large B cell lymphoma; CNS: central nervous system; IT: intrathecal; CASP: Critical Appraisal Skills Programme.

clear, robust univariable and multivariable analysis was limited. A number of studies[28,35] within the analysis simply report the hazard ratio or absolute percentage relapse rate comparison between patients receiving IT prophylaxis *versus* those not in receipt of prophylaxis.

The studies included often show that the rate of CNS relapse is increased in patients receiving prophylaxis. This finding primarily relates to the confounding effects of patient selection *i.e.* those at higher risk of CNS relapse are those who receive prophylaxis, however, no attempt was made to adjust for these risk factors in a number of the studies. As such, it is difficult to formally discern the value of IT prophylaxis from univariable, unadjusted analysis. A negative or null result *i.e.* hazard ratio ≥ 1 (or more events in the IT-prophylaxis group) as seen in 8 of 11 studies, or small, non-significant protective effect as seen in 3 of 11 studies does not imply that CNS prophylaxis is harmful or ineffective, but may show that it is simply not enough to overcome the increased baseline risk in the population which were treated.

A single study[23] was excluded from the analysis because of concerns regarding the integrity of the data and the quality of the analysis performed. A comparison across the 14 studies was also limited by the variable indications for IT prophylaxis and the different histologies and regimens included.

Multivariable analyses could help to reduce the effects of (known) confounding factors but, in this case, there are multiple factors of interest (median 16, range: 11-26) in the 13 papers which quote univariable analysis results) and, given the small number of events (median 20, range: 8-61), all of the cohorts studied would fail the ten-events-per-factor rule,[36] which is generally suggested to ensure the stability of a statistical model.

A number of papers[2,17,25,32,34,35,37] (Villa *et al.*, Tai *et al.*, Guirguis *et al.*, Tomita *et al.*, Cai *et al.*, Wudhikarn *et al.* and possibly Song *et al.*). reduced the number of factors in multivariable analyses by only including those factors with $P>/\geq 0.1$ in the univariable analysis. In some cases this meant CNS IT prophylaxis was not included in multivariable models at all[17,25,32] (Villa *et al.*, Guirguis *et al.*, possibly Song *et al.*), and in others it may have excluded factors which were not significant but did have a confounding effect on the benefit of CNS prophylaxis. Two studies (*post hoc* analysis of the R-CHOP 14 *vs.* 21 and GOYA randomised controlled trials) presented results adjusted for the CNS-IPI only[27] (Gleeson *et al.*) or within the different CNS-IPI risk levels[24] (Klanova *et al.*), neither found any benefit to IT prophylaxis but, as with reduced the models mentioned above, both could also have suffered from the exclusion of confounders. Kumar and colleagues used a propensity score to match patients with and without CNS

Table 3A. Studies reporting an efficacy analysis of stand-alone intrathecal prophylaxis in front line diffuse large B-cell lymphoma in rituximab era

Reference: author, journal, year	N	Data set: type and years	Study inclusion	1st line R-chemotherapy	CNS Relapse	% receiving IT prophylaxis	Median time to CNS relapse (range/95% CI given as available)	Cumulative incidence of CNS relapse (95% CI provided where reported)	Site of CNS relapse	Evidence of IT CNS prophylaxis effectiveness?	CASP Score
Boehme *et al.*, Blood 2009[30]***	1217	*Post hoc* analysis of RICOVER-60 trial	60-80 years with untreated 'aggressive B-cell lymphoma'. 944 (81.6%) DLBCL. 1% PMBCL.	R-CHOP-14: 608 CHOP-14: 609.**	Total: 58/22[R] Isolated: 34/16[R] Concurrent: 24/6[R]	22.4% (273/1222) ≥1 IT MTX. 16.6% (202/1222) 4 IT MTX	All patients: 8 months (range 1-39)	2-year: 4.1% (95% CI 2.3-5.9%)[R]	11[R] parenchymal, 2[R] both; 9[R] leptomeningeal	Overall percentage of CNS events: IT MTX 2.5% *vs.* nil 4.4%; whole cohort. A subgroup analysis of high risk patients adjusted for IPI found a significant interaction between IT MTX exposure and Rituximab exposure (RR = 6.1), with the risk of CNS relapse significantlyreduced if IT MTX was given in CHOP group but no difference in R-CHOP group. Effect of rituximab significant regardless of IT MTX.	3
Shimazu *et al.*, Int J of Hematol 2009[31]	403	Retrospective single center; 1996-2007	No age limit defined; untreated *de novo* DLBCL or transformed indolent NHL	CHOP/ CHOP-like: 165 R-CHOP/ R-CHOP-like: 338	Total: 42/22[R] Isolated: 28/14[R] Concurrent: 14/8[R]	4.7% (18/385) IT prophylaxis	21.5 months[R]	All patients: 1-year: 6.5% (95% CI: 6.0-7.14)	32 parenchymal; 10 leptomeningeal	Overall % of CNS events 1/18 (5.6%) IT prophylaxis *vs.* 40/367 (10.9%) for nil. Use of IT prophylaxis did not appear significantly decrease CNS relapse in logistic regression UVA (P=0.478) or MVA (P=0.571).	2
Villa *et al.* Ann Oncol 2009[25]***	435	Retrospective, single center; 1999-2005	≥16 years with advanced stage or any stage DLBCL or PMBCL with testicular involvement	CHOP: 126 R-CHOP: 309	Total: 31/19 [R] Isolated: 18/15[R] Concurrent: 13/4[R] (including 4/3[R]) post- systemic	4% (12) IT prophylaxis[R] alternating IT MTX and ara-C	6.7 months[R]	3-year: 6.4%[R]	12[R] parenchymal; 4[R] both; 3[R] leptomeningeal	Overall % of CNS events: CHOP cohort, 3/8 (37.5%) IT prophylaxis *vs.* 9/118 (7.6%) for nil. R-CHOP cohort, 0/12 (0%) IT prophylaxis *vs.* 19/297 (6.5%) (7.6%) for nil. Use of IT prophylaxis did not appear to decrease CNS relapse on UVA (P=0.364, R-CHOP cohort) not included in MVA (P>0.1 in UVA)	2
Tai *et al.*, Ann Hematol 2011[2]	499	Retrospective, single center; 2000-2008	No age limit defined; untreated DLBCL	CHOP: 179 R-CHOP: 320	Total: 30/20[R] Isolated: N/R Concurrent: N/R	18% (59/320) IT prophylaxis[R]	All patients: 6.7 months (range 1.9-45.2) 2-year: 6.0% (95% CI: 3.8-9.4)[R]	N/R		Overall % of CNS events (all patients): 9/82 (11.0%) IT prophylaxis *vs.* 21/417(5.0%) for nil. Use of IT prophylaxis did not appear to decrease CNS relapse on UVA (P=0.032; higher in those receiving IT prophylaxis, or P=0.98, high risk only). For all patients, MVA non-significant (P-value not reported), unclear if IT prophylaxis was included in R-CHOP only MVA. Only factors with P<0.1 in UVA included in MVA. No IPI-adjusted analysis.	2

*two patients received high dose methotrexate. **five CNS involvement at diagnosis excluded. R = in RCHOP subgroup. ***studies added after initial and post-systematic review scoping. NCCN: National Comprehensive Cancer Network; CNS: central nervous system; R-CHOP: rituximab, cyclophosphamide, doxorubicin, vincristine, prednisolone; RDA-EPOCH: rituximab plus dose adjusted etoposide, prednisolone, vincristine, cyclophosphamide, doxorubicin; O-CHOP: obinutuzumab, cyclophosphamide, doxorubicin, vincristine, prednisolone DLBCL: diffuse large B-cell lymphoma; NHL: non-Hodgkin lymphoma; ASCT: autologous stem cell transplantation; HGT: high grade transformation; CLL: chronic lymphocytic leukaemia; FL: follicular lymphoma; GZ: gray zone; CR1: first complete remission; PMBCL: primary mediastinal B-cell lymphoma; IPI: international prognostic index; IT: intrathecal; MTX: methotrexate; HD: high dose; ara-C: cytarabine; HC: hydrocortisone; HR: hazard ratio; CI: confidence interval; UVA: univariable analysis; MVA: multivariable; N/R: not reported; IQR: interquartile range; RR: risk ratio; OS: overall survival; PFS: progression-free survival.

prophylaxis allowing for a univariable analysis comparing these groups. They also found no difference in CNS relapse risk, but again this would rely on how well matched the groups were and whether this was enough to overcome the issues with confounding.

Analyses, including which factors were or were not included in multivariable analyses, were often poorly described with some papers using inappropriate methods which did not allow for time[31] (Shimazu *et al.*) when comparing risk factors, and with a lack of consistency in dealing with competing risks (systemic only relapse or death from other causes). This means the cumulative incidences

Table 3B. Studies reporting an efficacy analysis of stand-alone intrathecal prophylaxis in front line diffuse large B-cell lymphoma in rituximab era

Reference: author, journal, year	N	Data set: type and years	Study inclusion	1st line R-chemotherapy	CNS Relapse	% receiving IT prophylaxis	Median time to CNS relapse (range/95% CI given as available)	Cumulative incidence of CNS relapse (95% CI provided where reported)	Site of CNS relapse	Evidence of IT CNS prophylaxis effectiveness?	CASP Score
Guirguis *et al.* Br J Haematol 2012[17]	214	Retrospective, single center; 1999-2005	≥16 years with DLBCL ≥1 cycle of R-CHOP; including transformed indolent NHL	R-CHOP (100%)	Total: 8 Isolated: 6 Concurrent: 2 (post systemic)	4.7% IT MTX prophylaxis	17 months (range 6–35)	Not reported; Overall rate: 3.7%	5 parenchymal; 1 both; 2 leptomeningeal	Use of IT prophylaxis did not appear to decrease CNS relapse on UVA (P=0·994). Only factors with P<0.1 in UVA included in MVA.	2
Kumar *et al.* Cancer 2012[29]	989	Prospective NCCN NHL database, multi- center; 2001-2008	No age limit defined; untreated DLBCL	R-CHOP-21 (100%)	Total: 20 Isolated: 14 Concurrent: 6	11.8% (117/989 CNS prophylaxis), most IT (71.8%)	12.8 months	Not reported; overall rate: 2.5 year 2% (95 CI: 1.1-2.9%)	13 parenchymal only. 7 'not parenchymal only'.	Overall rates: prophylaxis (10.9%) *vs.* nil (2.1%), P=0.007. In ≥2 predefined high-risk features, CNS relapse not differ significantly: prophylaxis (5.4%) *vs.* nil (1.4%; P=0.08). Propensity matched population (n=230) "No difference in OS or PFS" according to receipt of CNS prophylaxis. Discussion says "not associated with a reduction in CNS relapse or OS".	2
Song *et al.* Medicine (Baltimore) 2015[32]	180	Retrospective, single center; 2009-2015	No age limit defined; untreated DLBCL	R-CHOP (100%)	Total: 12 Isolated: 12 Concurrent: 0	25.6% (46/180) IT MTX	Not reported	Not reported; overall rate: 6.7%	6 parenchymal; 6 leptomeningeal	IT prophylaxis showed no protective effect on UVA (HR 2.31, range 0.73-7.25 P=0.15: higher in those receiving IT CNS prophylaxis). Unclear if IT prophylaxis was included in MVA analyses but not reported to be significant in MVA.	2
Tomita *et al.* Leuk Lymphoma 2015[33]	322	Retrospective, multi-center; 2003-2009	18-80 years with untreated DLBCL achieving CR1	R-CHOP (100%)	Total: 11 Isolated: 11 Concurrent: 0	12% (40/322): 4 IT MTX and HC after CR was achieved	8.2 months (range 3.5–34.0)	3-year: 3.6%	7 parenchymal; 3 both; 1 leptomeningeal	3-year risk 8.7% in IT prophylaxis *vs.* 2.9% nil (P=0.14). IT MTX not associated with CNS relapse on MVA (HR 0.78, 95% CI: 0.18-3.42; P=0.74) Subgroup analysis for high risk patients only showed "no significant difference"	3

*two patients received high dose methotrexate. **five CNS involvement at diagnosis excluded. R = in RCHOP subgroup. ***studies added after initial and post-systematic review scoping. NCCN: National Comprehensive Cancer Network; CNS: central nervous system; R-CHOP: rituximab, cyclophosphamide, doxorubicin, vincristine, prednisolone; RDA-EPOCH: rituximab plus dose adjusted etoposide, prednisolone, vincristine, cyclophosphamide, doxorubicin; O-CHOP: obinutuzumab, cyclophosphamide, doxorubicin, vincristine, prednisolone DLBCL: diffuse large B-cell lymphoma; NHL: non-Hodgkin lymphoma; ASCT: autologous stem cell transplantation; HGT: high grade transformation; CLL: chronic lymphocytic leukaemia; FL: follicular lymphoma; GZ: gray zone; CR1: first complete remission; PMBCL: primary mediastinal B-cell lymphoma; IPI: international prognostic index; IT: intrathecal; MTX: methotrexate; HD: high dose; ara-C: cytarabine; HC: hydrocortisone; HR: hazard ratio; CI: confidence interval; UVA: univariable analysis; MVA: multivariable; N/R: not reported; IQR: interquartile range; RR: risk ratio; OS: overall survival; PFS: progression-free survival.

Table 3C. Studies reporting an efficacy analysis of stand-alone intrathecal prophylaxis in front line diffuse large B-cell lymphoma in rituximab era

Reference: author, journal, year	N	Data set: type and years	Study inclusion	1st line R-chemotherapy	CNS Relapse	% receiving IT prophylaxis	Median time to CNS relapse (range/95% CI given as available)	Cumulative incidence of CNS relapse (95% CI provided where reported)	Site of CNS relapse	Evidence of IT CNS prophylaxis effectiveness?	CASP Score
Cai et al Chin j Cancer 2016[34]	511	Retrospective, single center; 2003-2012	≥18 years with newly diagnosed DLBCL	CHOP: 135 R-CHOP: 376	Total: 25/14[R] Isolated: N/R Concurrent: N/R	11.8%R (44/373 (3 unknown)): IT MTX and ara-C for each cycle of R-CHOP	6.5 months R	3-year: 4.9%. 3-year: 2.7%[R]	Not reported	3-year risk in IT prophylaxis *vs.* nil: 6.5% *vs.* 1.8% (P=0.083)[R]. IT prophylaxis not associated with CNS relapse on MVA (P-value not reported).	2
Kanemasa *et al.* Ann Hematol 2016[28]	413	Retrospective, single center; 2004-2015	No age limit defined; untreated *de novo* DLBCL	≥1 cycle R-CHOP R-CHOP-like or (100%)	Total: 27 Isolated: 16 Concurrent: 11	15.0% ≥1 IT MTX +/-ara-C prophylaxis	15 months	5-year: 8.4% (95% CI: 5.6-12.4%)	9 parenchymal; 2 both; 16 leptomeningeal	IT prophylaxis no protective effect on UVA (HR 0.85, range (0.29–2.45) P=0.76). No IPI-adjusted analysis or MVA performed.	2
Gleeson *et al.* Ann Oncol 2017[27]	984	*Post hoc* analysis of R-CHOP-14 *vs.* 21 trial; 2005-2008	≥18 years with untreated bulky stage I or stage II–IV DLBCL	R-CHOP-14 or 21 (100%)	Total: 21 Isolated: 11 Concurrent: 10	175 (17.8%) overall: *163 IT MTX (16.6%); 11 unknown; 1 IT ara-C and MTX	8.1 months (95% CI: 1.0-15.1)	6.5 year: 1.9%	17 parenchymal; 4 leptomeningeal	Adjusting for CNS-IPI, no demonstrated benefit (HR=1.12; 95% CI, 0.40-3.14; p=0.83)	2
Malecek *et al.* Am J Hematol 2017[26]	223	Retrospective, multi-center; 2004-2014	≥18 years, untreated *de novo* DLBCL or transformed (CLL or FL), GZ NHL, PMBCL.	≥2 cycles R-DA-EPOCH. No ASCT consolidation (100%)	Total: 13 Isolated: 13 Concurrent: 0	38.6% (86/223) (IT MTX 83; IT ara-C 2; IT MTX and ara-C 1)	10 months (range 2.1–27.0)	Not reported; overall rate: 5.8%	4 parenchymal; 1 both; 5 leptomeningeal; 3 unknown	In all patients; 5.8% rate of CNS relapse in both IT prophylaxis and no prophylaxis groups (P>0.99). Subgroup (n=139) non-HIV DLBCL: 7 (5%) CNS relapse; no difference in risk for prophylaxis *vs.* nil (P=0.699), no factors significant in MVA (assuming this included IT prophylaxis).	2
Wudhikarn *et al.* Ann Hematol 2017[25]	2034	Retrospective, nationwide multi-center; 2006-2013	≥15 years with untreated DLBCL; ≥1 cycle of CHOP-like	R-CHOP or RCHOP-like: 663 CHOP-like: 1371	Total: 61 Isolated: 47 Concurrent: 14	10.9% IT prophylaxis. 11.8%[R]. 8 HDMTX or ara-C overall.	8.4 months (IQR 5.9–12.2)	2-year: 2.7% (95% CI 2.0-3.5%)	23 parenchymal; 7 both; 25 leptomeningeal; unknown; 6	IT prophylaxis no protective effect on UVA (HR 3.5, range 1.98–6.06, P<0.001) higher in those receiving IT prophylaxis). This remained the case in MVA (P<0.001, no effect size given).	2
Klanova *et al.* Blood 2019[24]****	1418	*Post hoc* analysis of GOYA trial	≥18 years, untreated *de novo* DLBCL; IPI ≥2 or IPI 1 if ≤60 years or IPI 0 if bulk	O-CHOP: 706 R-CHOP: 712	Total: 38 Isolated: N/R Concurrent: N/R	9.9% (140/1418) IT prophylaxis (either MTX, ara-C or both)	8.5 months (range 0.9-43.5)	2-year: 2.8%	27 parenchymal; 3 both; 6 leptomeningeal; 1 intraocular; unknown; 1	2-year CNS relapse rate no different between IT *vs.* no IT prophylaxis: overall (2.8% *vs.* 2.6%) and according to CNS-IPI. No formal MVA including IT prophylaxis performed.	3

*two patients received high dose methotrexate. **five CNS involvement at diagnosis excluded. R = in RCHOP subgroup. ***studies added after initial and post-systematic review scoping. NCCN: National Comprehensive Cancer Network; CNS: central nervous system; R-CHOP: rituximab, cyclophosphamide, doxorubicin, vincristine, prednisolone; RDA-EPOCH: rituximab plus dose adjusted etoposide, prednisolone, vincristine, cyclophosphamide, doxorubicin; O-CHOP: obinutuzumab, cyclophosphamide, doxorubicin, vincristine, prednisolone DLBCL: diffuse large B-cell lymphoma; NHL: non-Hodgkin lymphoma; ASCT: autologous stem cell transplantation; HGT: high grade transformation; CLL: chronic lymphocytic leukaemia; FL: follicular lymphoma; GZ: gray zone; CR1: first complete remission; PMBCL: primary mediastinal B-cell lymphoma; IPI: international prognostic index; IT: intrathecal; MTX: methotrexate; HD: high dose; ara-C: cytarabine; HC: hydrocortisone; HR: hazard ratio; CI: confidence interval; UVA: univariable analysis; MVA: multivariable; N/R: not reported; IQR: interquartile range; RR: risk ratio; OS: overall survival; PFS: progression-free survival.

Table 4. Recommendations for central nervous system prophylaxis within individual studies.

Reference: author, year, journal	Recommendations for CNS intrathecal prophylaxis	High risk disease sites or clinical features for which CNS prophylaxis recommended
Boehme *et al*., Blood, 2009[30]	Mandatory for 'high risk' sites	Bone marrow, testes, upper neck or head including nasal sinuses, orbital, oral cavity, tongue, and salivary glands.
Shimazu *et al*., Int J Hematol 2009[31]	Discretion of treating physician, but recommendations provided	Nasal sinuses, testis or vertebra
Villa *et al*., Ann Oncol 2009[25]	Discretion of treating physician, but recommendations provided	Pre-2002: bone marrow or peripheral blood involvement, epidural, advanced-stage testicular lymphoma, or sinus involvement. After 2002, only sinus involvement.
Tai *et al*., Ann Oncol 2011[2]	Discretion of treating physician.	Not defined
Guirguis *et al*., Br J Haematol 2012[17]	Per 'high-risk' DLBCL according to our locally published haematology site group	Unavailable
Kumar *et al*., Cancer, 2012[29]	Discretion of treating physician.	Not defined
Song *et al*., Medicine (Baltimore), 2015[32]	Discretion of treating physician, but recommendations provided	Given to patients with high intermediate/high IPI or involvement of testis, breast, nasal cavity or orbit.
Tomita *et al*., Leuk Lymphoma, 2015[33]	A written strategy prior to the study, even if it not necessarily followed.	In general, ≥1 risk factor: LDH ≥2 ULN; bulk ≥10 cm; ECOG PS 2; or involvement of the bone marrow, skin, testis, nasal/ paranasal tissue, bone or breast.
Cai *et al*., Chin J Cancer, 2016[34]	Discretion of the local investigator but recommendations provided	High level of Ki-67; and involvement of the testis, breast, or kidney.
Kanemasa *et al*., Ann Oncol 2016[28]	Discretion of treating physician, but recommendations provided	Testis, breast, paranasal sinuses, or bone marrow.
Gleeson *et al*., Ann Oncol2017[27]	Discretion of the local investigator but recommendations provided	Bone marrow, peripheral blood, nasal/paranasal sinuses, orbit and testis.
Malecek *et al*., Am J Hematol 2017[26]	Discretion of treating physician.	Not defined
Wudhikarn *et al*., Ann Hematol 2017[35]	Not reported	Not defined
Klanova *et al*., Blood, 2019[24]	Discretion of treating physician.	Not defined

CNS: central nervous system; ECOG: Eastern co-operative oncology group; PS: performance status, LDH: lactate dehydrogenase; DLBCL: diffuse large B cell lymphoma.

may not be comparable between studies, with just two making it clear that they treated deaths as a competing risk[31,35] (Shimazu *et al*. and Wudhikarn *et al*.) and none of the studies appearing to consider systemic only relapse as a competing risk, even those that did not include CNS relapse post systemic relapse as an event.

Perhaps the most convincing evidence of the lack of efficacy of IT CNS prophylaxis in the rituximab era comes from the RICOVER-60 trial.[30] All patients considered high-risk (infiltration of bone marrow and testes or sites in the upper neck or head), should have been treated with IT MTX. There was significant non-compliance to this rule with only 57.1% receiving CNS prophylaxis. This allowed Boehme and colleagues to perform as subgroup analysis. They found that, in a multivariable Cox model including IPI factors, there was a significant interaction between IT MTX exposure and rituximab exposure (RR=6.1), with risk of CNS relapse significantly reduced with IT MTX in the CHOP group but with no difference seen in the R-CHOP group. The effect of rituximab was significant regardless of IT MTX. This is a non-randomised comparison in a small subset of patients (47-67 per group and only six events in the R-treated cohort) who were all aged over 60 years and not all had DLBCL. However, it is the only paper to provide any evidence of a differential effect of IT MTX in rituximab-treated *versus* non-rituximab treated patients, which is not simply based on lower rates of CNS relapse when compared to data from the pre-rituximab era.

Although none of these papers show any evidence of a benefit in giving CNS IT prophylaxis in either univariable analyses or multivariable analyses, they are also all unable to convincingly rule one out due to small numbers of events and the confounding caused by the indications for CNS prophylaxis.

Subsequent to the completion of the systematic review, we have recently published outcomes of 690 elderly patients (≥70 years) treated with R-CHOP (full or dose attenuated).[38] Our results are consistent with those presented within the systematic review but suffer from similar issues of small event number and the risk of confounding factors. We also showed no clear benefit for stand-alone IT prophylaxis although we found that IT prophylaxis was associated with an increased risk of infection-related hospital admission during R-CHOP (odds ratio *vs.* no prophylaxis) 2.20 (95% CI: 1.31-3.67; *P*=0.01).

The only real method to formally answer this question is with a randomised clinical trial of IT CNS prophylaxis vs no IT CNS prophylaxis in patients deemed unsuitable for high dose MTX. Unfortunately, due to the low event

rate this would need to be a very large study. Even if we assume a relatively high risk patient group (*e.g.* CNS-IPI 4-6) with a 4-6% risk of CNS relapse and aim to detect a large effect size (*i.e.* a halving of this rate), to achieve 80% power we would require 1,432 (6-3%), 1,722 (5-2.5%) or 2,368 (4-2%) patients. Despite the lack of conclusive evidence of its benefit, it may be difficult to persuade many clinicians to randomise patients with multiple baseline risk factors to potentially receive no CNS directed therapy. A trial performed in patients considered unsuitable for high dose methotrexate due to age, renal impairment, performance status or comorbidities would prove particularly challenging to perform.

CASP analysis

For the 14 studies included within the systematic review, a CASP analysis was performed. Cohort studies were scored as moderate in three studies.[24,30,37] These included 2 of the 3 *post hoc* analyses performed from large prospective randomised clinical trials[24,30] and scored moderate to low in the remaining 11 studies. The key reasons for the low quality rating scores included: a) retrospective, single centre data; b) low event numbers with unadjusted analyses; c) variable indications and IT prophylaxis regimens used; d) variable histologies included.

Strengths and limitations

No previous systematic review has explored the potential benefit of stand-alone IT prophylaxis in rituximab or obinutuzumab exposed DLBCL patients. To ensure transparency and to facilitate scrutiny of this review, a systematic protocol was registered and published prior to conducting the review, which was undertaken according to best practice and reporting guidelines. Each stage of the review process was independently double-screened, and any discrepancies discussed among the research team until consensus was reached. One limitation of the search strategy was restricting the search to publications in English; however the search expansion strategy ensured a comprehensive and sensitive review. The quality of evidence reviewed was limited by the small number of CNS relapse events in many of the studies. A number of the studies highlighted were initially powered for other means *i.e.* the primary end point of the specific clinical trial. As such, within trial GOYA and R-CHOP 14 *versus* 21 populations, for example, there was a heterogenous approach to the use of IT prophylaxis with variable criteria for delivery, dosing schedules and chemotherapy used.

Recommendations

On the basis of the evidence analysed within this systematic review, there are no convincing published data, adjusted for well described confounding variables, that clearly suggest that stand-alone IT chemotherapy CNS prophylaxis reduces the risk of CNS relapse in patients treated with anthracycline-based front-line immunochemotherapy using an anti-CD20 antibody. It must also be recognised however that no individual study provides strong evidence for lack of benefit of stand-alone IT prophylaxis. The nature of the evidence analysed is limited by the individual study designs, the low event rate, variable prophylaxis protocols used, the retrospective nature of studies, some evidence for lack of compliance and the absence of control groups. Although the quality of evidence precludes firm recommendations, the authors suggest that the available evidence should lead to judicious use of stand-alone IT chemoprophylaxis. Our conclusions relate primarily to patients receiving R-CHOP immunochemotherapy and intentionally do not reference the evidence for high dose anti-metabolites. There was only a single study that studied DA-EPOCH-R and as such conclusions related to IT usage in that setting are more limited. The focus of this systematic review was DLBCL histology, and as such we intentionally have made no conclusions regarding the role of IT prophylaxis in other histologies such as Burkitt lymphoma or indeed specific subgroups of DLBCL such as double hit lymphoma or HIV-associated DLBCL.

Conclusions

There is no strong evidence to support the use of stand-alone IT chemotherapy prophylaxis for patients treated with anthracycline-based chemotherapy in the rituximab era. Conversely, the strength of evidence suggesting a genuine lack of evidence is also weak. The majority (70%) of CNS relapses occurring in anti-CD20 antibody exposed patients treated in our systematic review involved parenchymal tissue. No study within the systematic review reported a toxicity analysis of intrathecal chemotherapy and as such few meaningful conclusions can be made regarding the morbidity of IT prophylaxis from these series. The quality of the data is relatively weak to poor. Although some of the studies included relatively large numbers of patients, the absolute number of CNS relapse events limits the power to perform high quality multivariable analysis or adjusted analysis. As such, we conclude that there is little evidence for the benefit of stand-alone IT CNS prophylaxis in preventing CNS relapse in DLBCL-treated patients using anthracycline-based immunochemotherapy.

Acknowledgments

We thank Nia Roberts and Tatjana Petrinic, librarians at Oxford's Bodleian Healthcare Library for their support with the search strategy for this review. Views expressed are those of the authors and not necessarily those of the NHS or the NIHR or the United Kingdom's Department of Health.

Funding

GPC is supported by the NIHR Biomedical Research Centre, based at Oxford University Hospitals Trust, Oxford. The views expressed are those of the author(s) and not necessarily those of the NHS, Oxford University Hospitals NHS Foundation Trust, the NIHR Biomedical Research Centre or the Department of Health.

References

1. El-Galaly TC, Villa D, Michaelsen TY, et al. The number of extranodal sites assessed by PET/CT scan is a powerful predictor of CNS relapse for patients with diffuse large B-cell lymphoma: An international multicenter study of 1532 patients treated with chemoimmunotherapy. Eur J Cancer. 2017; 75:195-203.
2. Tai WM, Chung J, Tang PL, et al. Central nervous system (CNS) relapse in diffuse large B cell lymphoma (DLBCL): Pre- and post-rituximab. Ann Hematol. 2011; 90(7):809-818.
3. Cabannes-Hamy A, Peyrade F, Jardin F, et al. Central nervous system relapse in patients over 80 years with diffuse large B-cell lymphoma: an analysis of two LYSA studies. Cancer Med. 2018;7(3):539-548.
4. Schmitz N, Zeynalova S, Nickelsen M, et al. CNS International Prognostic Index : A risk model for CNS relapse in patients with diffuse large B-cell lymphoma treated with R-CHOP. J Clin Oncol. 2016;34(26):3150-3156.
5. Ghose A, Elias HK, Guha G, Yellu M, Kundu R, Latif T. Influence of rituximab on central nervous system relapse in diffuse large B-cell lymphoma and role of prophylaxis. A systematic review of prospective studies. Clin Lymphoma, Myeloma Leuk. 2015;15(8):451-457.
6. Boehme V, Zeynalova S, Kloess M, et al. Incidence and risk factors of central nervous system recurrence in aggressive lymphoma - A survey of 1693 patients treated in protocols of the German High-Grade Non-Hodgkin's Lymphoma Study Group (DSHNHL). Ann Oncol. 2007;18(1):149-157.
7. Abramson JS, Hellmann M, Barnes JA, et al. Intravenous methotrexate as central nervous system (CNS) prophylaxis is associated with a low risk of CNS recurrence in high-risk patients with diffuse large B-cell lymphoma. Cancer. 2010;116(18):4283-4290.
8. Ferreri AJM, Bruno-Ventre M, Donadoni G, et al. Risk-tailored CNS prophylaxis in a mono-institutional series of 200 patients with diffuse large B-cell lymphoma treated in the rituximab era. Br J Haematol. 2015; 168 (5):654-662.
9. Cheah CY, Herbert KE, O'Rourke K, et al. A multicentre retrospective comparison of central nervous system prophylaxis strategies among patients with high-risk diffuse large B-cell lymphoma. Br J Cancer. 2014; 111(6):1072-1079.
10. Mcmillan A, Ardeshna KM, Cwynarski K, Lyttelton M, Mckay P, Montoto S. Guideline on the prevention of secondary central nervous system lymphoma: British Committee for Standards in Haematology. Br J Haematol. 2013;163(2):168-181.
11. Dunleavy K, Pittaluga S, Shovlin M, et al. Low-intensity therapy in adults with Burkitt's lymphoma. N Engl J Med. 2013;369(20):1915-1925.
12. Pui C-H, Campana D, Pei D, et al. Treating childhood acute lymphoblastic leukemia without cranial irradiation. N Engl J Med. 2009;360 (26):2730-2741.
13. Blasberg RG, Patlak C, Fenstermacher JD. Intrathecal chemotherapy: brain tissue profiles after ventriculocisternal perfusion. J Pharmacol Exp Ther. 1975;195(1):73-83.
14. De la Riva P, Andres-Marín N, Gonzalo-Yubero N, et al. Headache and other complications following intrathecal chemotherapy administration. Cephalalgia. 2016; 37(11):1109–1110.
15. Coiffier B, Lepage E, Briere J, et al. CHOP chemotherapy plus rituximab compared with CHOP alone in elderly patients with diffuse large-B-cell lymphoma. 2002; 346(4):235-242.
16. Zhang J, Chen B, Xu X. Impact of rituximab on incidence of and risk factors for central nervous system relapse in patients with diffuse large B-cell lymphoma: A systematic review and meta-Analysis. Leuk Lymphoma. 2014;55(3):509-514.
17. Guirguis HR, Cheung MC, Mahrous M, et al. Impact of central nervous system (CNS) prophylaxis on the incidence and risk factors for CNS relapse in patients with diffuse large B-cell lymphoma treated in the rituximab era: A single centre experience and review of the literature. Br J Haematol. 2012;159(1):39-49.
18. Mitrovic Z, Bast M, Bierman PJ, et al. The addition of rituximab reduces the incidence of secondary central nervous system involvement in patients with diffuse large B-cell lymphoma. Br J Haematol 2012;157(3):401-403.
19. Arkenau HT, Chong G, Cunningham D, et al. The role of intrathecal chemotherapy prophylaxis in patients with diffuse large B-cell lymphoma. Ann Oncol. 2007; 18(3):541-545.
20. Tomita N, Kodama F, Kanamori H, Motomura S, Ishigatsubo Y. Prophylactic intrathecal methotrexate and hydrocortisone reduces central nervous system recurrence and improves survival in aggressive non-Hodgkin lymphoma. Cancer. 2002; 95(3):576-580.
21. Grant MJ, Booth A. A typology of reviews: An analysis of 14 review types and associated methodologies. Health Info Libr J. 2009;26(2):91-108.
22. Moher D, Shamseer L, Clarke M, et al. Preferred reporting items for systematic review and meta-analysis protocols (PRISMA-P) 2015 statement. Syst Rev. 2016;4:1.
23. Avilés A, Jesús Nambo M, Neri N. Central nervous system prophylaxis in patients with aggressive diffuse large B cell lymphoma: An analysis of 3,258 patients in a single center. Med Oncol. 2013;30(2):520-526.
24. Klanova M, Sehn LH, Bence-Bruckler I, et al. Integration of COO into the clinical CNS International Prognostic Index could improve CNS relapse prediction in DLBCL. Blood. 2019;133(9):919-926.
25. Villa D, Connors JM, Shenkier TN, Gascoyne RD, Sehn LH, Savage KJ. Incidence and risk factors for central nervous system relapse in patients with diffuse large B-cell lymphoma: The impact of the addition of rituximab to CHOP chemotherapy. Ann Oncol. 2009;21(5):1046-1052.
26. Malecek MK, Petrich AM, Rozell S, et al. Frequency, risk factors, and outcomes of central nervous system relapse in lymphoma patients treated with dose-adjusted EPOCH plus rituximab. Am J Hematol. 2017;92(11):1156-1162.
27. Gleeson M, Counsell N, Cunningham D, et al. Central nervous system relapse of diffuse large B-cell lymphoma in the rituximab era: Results of the UK NCRI R-CHOP-14 versus 21 trial. Ann Oncol. 2017;28(10):2511-2516.
28. Kanemasa Y, Shimoyama T, Sasaki Y, et al. Central nervous system relapse in patients with diffuse large B cell lymphoma: analysis of the risk factors and proposal of a new prognostic model. Ann Hematol. 2016; 95(10):1661-1669.
29. Kumar A, Vanderplas A, Lacasce AS, et al. Lack of benefit of central nervous system prophylaxis for diffuse large B-cell lymphoma in the rituximab era: Findings from a large national database. Cancer. 2012;118(11):2944-2951.
30. Boehme V, Schmitz N, Zeynalova S, Loeffler M, Pfreundschuh M. CNS events in elderly patients with aggressive lymphoma treated with modern chemotherapy (CHOP-14) with or without rituximab: An analysis of patients treated in the RICOVER-60 trial of the German High-Grade Non-Hodgkin Lymphoma Study Group (DSHNHL). Blood. 2009;113(17):3896-3902.
31. Shimazu Y, Notohara K, Ueda Y. Diffuse large B-cell lymphoma with central nervous system relapse: Prognosis and risk factors according to retrospective analysis from a single-center experience. Int J Hematol. 2009;89(5):577-583.
32. Song YS, Lee WW, Lee JS, Kim SE. Prediction of central nervous system relapse of diffuse large B-cell lymphoma using pretherapeutic [18F]2-fluoro-2-deoxyglucose (FDG) positron emission tomography/computed tomography. Medicine (Baltimore). 2015;94(44):e1978.
33. Tomita N, Takasaki H, Ishiyama Y, et al. Intrathecal methotrexate prophylaxis and central nervous system relapse in patients with diffuse large B-cell lymphoma following rituximab plus cyclophosphamide, doxorubicin, vincristine and prednisone. Leuk Lymphoma. 2015;56(3):725-729.
34. Cai QQ, Hu LY, Geng QR, et al. New risk factors and new tendency for central nervous system relapse in patients with diffuse large B-cell lymphoma: a retrospective study. Chin J Cancer. 2016;35(1):87.
35. Wudhikarn K, Bunworasate U, Julamanee J, et al. Secondary central nervous system relapse in diffuse large B cell lymphoma in a resource limited country: result from the Thailand nationwide multi-institutional registry. Ann Hematol. 2017;96(1):57-64.
36. Peduzzi P, Concato J, Feinstein AR, Holford TR. Importance of events per independent variable in proportional hazards regression analysis II. Accuracy and precision of regression estimates. J Clin Epidemiol. 1995;48(12):1503-1510.
37. Tomita N, Yokoyama M, Yamamoto W, et al. Central nervous system event in patients with diffuse large B-cell lymphoma in the rituximab era. Cancer Sci. 2012;103(2):245-251.
38. Eyre TA, Kirkwood AA, Wolf J, et al. Standalone intrathecal central nervous system (CNS) prophylaxis provide unclear benefit in reducing CNS relapse risk in elderly DLBCL patients treated with R-CHOP and is associated increased infection-related toxicity. Br J Haematol. 2019;187(2):185-194.

ARTICLE

Multiple myeloma exploits Jagged1 and Jagged2 to promote intrinsic and bone marrow-dependent drug resistance

Michela Colombo,[1] Silvia Garavelli,[1] Mara Mazzola,[2] Natalia Platonova,[1] Domenica Giannandrea,[1] Raffaella Colella,[1] Luana Apicella,[1] Marialuigia Lancellotti,[1] Elena Lesma,[1] Silvia Ancona,[1] Maria Teresa Palano,[1] Marzia Barbieri,[3,4] Elisa Taiana,[3,4] Elisa Lazzari,[1] Andrea Basile,[3] Mauro Turrini,[5] Anna Pistocchi,[2] Antonino Neri[3,4] and Raffaella Chiaramonte[1]

[1]Department of Health Sciences, Università degli Studi di Milano, Milano; [2]Department of Medical Biotechnology and Translational Medicine, Università degli Studi di Milano, Milano; [3]Department of Oncology and Hemato-Oncology, Università degli Studi di Milano, Milano; [4]Hematology, Fondazione IRCCS Cà Granda, Ospedale Maggiore Policlinico, Milano and [5]Department of Hematology, Division of Medicine, Valduce Hospital, Como, Italy

Ferrata Storti Foundation

Haematologica 2020
Volume 105(7):1925-1936

ABSTRACT

Multiple myeloma is still incurable due to an intrinsic aggressiveness or, more frequently, to the interactions of malignant plasma cells with the bone marrow (BM) microenvironment. Myeloma cells educate BM cells to support neoplastic cell growth, survival, acquisition of drug resistance resulting in disease relapse. Myeloma microenvironment is characterized by Notch signaling hyperactivation due to the increased expression of Notch1 and 2 and the ligands Jagged1 and 2 in tumor cells. Notch activation influences myeloma cell biology and promotes the reprogramming of BM stromal cells. In this work we demonstrate, *in vitro, ex vivo* and by using a zebrafish multiple myeloma model, that Jagged inhibition causes a decrease in both myeloma-intrinsic and stromal cell-induced resistance to currently used drugs, i.e. bortezomib, lenalidomide and melphalan. The molecular mechanism of drug resistance involves the chemokine system CXCR4/SDF1α. Myeloma cell-derived Jagged ligands trigger Notch activity in BM stromal cells. These, in turn, secrete higher levels of SDF1α in the BM microenvironment increasing CXCR4 activation in myeloma cells, which is further potentiated by the concomitant increased expression of this receptor induced by Notch activation. Consistently with the augmented pharmacological resistance, SDF1α boosts the expression of BCL2, Survivin and ABCC1. These results indicate that a Jagged-tailored approach may contribute to disrupting the pharmacological resistance due to intrinsic myeloma cell features or to the pathological interplay with BM stromal cells and, conceivably, improve patients' response to standard-of-care therapies.

Introduction

Multiple myeloma (MM) is the second most common hematologic malignancy. It is still incurable, with a median overall survival that has not been substantially extended since the introduction of anti-myeloma agents such as melphalan, lenalidomide, and bortezomib.[1] The typical clinical course of MM displays a remission-relapse pattern due to the appearance of drug-resistant malignant cells, reducing the numbers of effective salvage regimens.[2] Therefore, a more stable response requires the development of a therapeutic approach that prevents drug resistance.

Multiple myeloma cells accumulate in the bone marrow (BM), where they establish anomalous signaling loops with BM-residing non-tumor cells, resulting in the exchange of anti-apoptotic factors which critically induce drug resistance.[3]

The Notch pathway includes four transmembrane receptors (Notch1-4) activat-

Correspondence:

RAFFAELLA CHIARAMONTE
raffaella.chiaramonte@unimi.it

MICHELA COLOMBO
michela.colombo@ndcls.ox.ac.uk

Received: March 10, 2019.

Accepted: September 26, 2019.

Pre-published: October 3, 2019.

doi:10.3324/haematol.2019.221077

Check the online version for the most updated information on this article, online supplements, and information on authorship & disclosures: www.haematologica.org/content/105/7/1925

ed by the interaction with five ligands (Jagged1-2 and Dll1-3-4) on adjacent cells.[4-6] Notch receptors and ligands have been found to be aberrantly expressed in MM cells.[7-10] We recently demonstrated that Jagged1 and the Notch transcriptional target HES5 are increasingly expressed in MM and in primary plasma cell leukemia.[11] Moreover, Jagged1 and Notch1 are over-expressed during progression from the benign monoclonal gammopathy of uncertain significance (MGUS) to MM,[12] while Jagged2 overexpression is already detected at the MGUS stage[13] and can be ascribed to aberrant acetylation of its promoter[14] or to altered post-translational processing due to aberrant expression of the ubiquitin ligase Skeletrophin.[15] Finally, Notch2 hyperexpression is associated with the high-risk translocations t(14;16)(q32;q23) and t(14;20)(q32;q11).[16]

Recently, we and other groups pointed out the importance of Jagged ligands in providing MM cells with the ability to shape the surrounding microenvironment, interacting with osteoclast progenitors,[17] and promoting a release of BM stromal cell (BMSC) key factors, including IL6, IGF1 and VEGF.[11,13]

Aberrant levels of Notch signaling are associated with pharmacological resistance in different tumor settings[6] and correlate with the expression of anti-apoptotic genes, such as *BCL2*[18] and *Survivin/BIRC5*,[19] or regulates the expression of *ABCC1*,[46] which contributes to multidrug resistance in MM.[20]

Given this, we hypothesized that the aberrant expression of Notch receptors and ligands in MM cells may foresee the development of drug resistance by inducing autonomous activation of Notch in MM cells, and by triggering Notch signaling in the surrounding BMSC and boosting their ability to support MM cell drug resistance.[21,22]

Previous studies investigated how BMSC support the development of drug resistance in MM cells by activating Notch signaling.[23-25] *Vice versa*, here we show that also the overexpression of MM cell-derived Jagged ligands triggers Notch signaling dysregulation in the BM niche and promotes MM cell intrinsic pharmacological resistance as well as BMSC-dependent drug resistance.

Methods

Cell lines and primary cells

The human MM cell lines (HMCL), OPM2 (ACC-50) and U266 (ATCC® TIB-196) were purchased from the DSMZ and ATCC, respectively. Primary cells were isolated from patient BM aspirates and MM cells were purified using the Human Whole Blood CD138$^+$ Selection Kit EasySep (StemCell Technologies). Detailed information is available in *Online Supplementary Table S1*. Primary BMSC were isolated as previously reported.[11] The Ethical Committee of the Università degli Studi di Milano, Italy, approved this study (approval n. 8/15).

Details of all cell treatments are available in the *Online Supplementary Appendix*.

Luciferase reporter assay

HS5 cells were transiently transfected with a Notch reporter plasmid pNL2.1 carrying a 6xCSL Notch responsive element[26] and with the vector constitutively expressing the firefly luciferase upon the thymidine kinase promoter (pGL4.54[luc2/TK]). After 24 hours (h), HS5 cells were cultured alone or placed in co-culture with scrambled (Scr) or Jagged1 and Jagged2 knockdown (J1/2KD) HMCL and incubated for 24 h. Luciferase activity was measured using Nano-Glo® Dual-Luciferase® Reporter assay kit (Promega) on the Glowmax instrument (Promega).

In vivo experiments on xenografted zebrafish embryos

Zebrafish AB strains obtained from the Wilson lab, University College London, UK, were maintained according to the national guidelines (Italian Ministerial Decree of 4/03/2014 2014, n. 26). All experiments were conducted within five days post fertilization.

Dechorionated zebrafish embryos were injected with Scr or J1/2KD U266 cells stained with the CM-Dil dye into the yolk (200 cells in 10 nl, 5-20 nl injection volume/embryo) with a manual microinjector (Eppendorf, Germany) using glass microinjection needles.

Xenograft-positive embryos divided randomly into the following groups: Scr-injected embryos treated with DMSO, Scr-injected embryos treated with 10 nM bortezomib, J1/2KD-injected embryos treated with DMSO, and J1/2KD-injected embryos treated with 10 nM bortezomib. Tumor growth was evaluated 48 h post injection (hpi) by fluorescence microscopy. Further details are available in the *Online Supplementary Appendix*.

Further details and information concerning cell cultures, RNA isolation and quantitative real-time polymerase chain reaction (qRT-PCR), RNAi assay, apoptosis assays, flow cytometry, ELISA, western blot and statistical analysis can be found in the *Online Supplementary Appendix*: experimental procedures.

Results

Jagged1/2 inhibition improves multiple myeloma cell response to standard-of-care drugs by increasing the anti-apoptotic background

To assess if Jagged1 and Jagged2 contribute to MM intrinsic drug resistance, we took advantage of an established knockdown (KD) approach using specific siRNAs for Jagged ligands[11,17] and analyzed MM cell response to three standard-of-care drugs: bortezomib (Bor), melphalan (Melph), and lenalidomide (Len). Two HMCL, OPM2 and U266 cells, were transfected with Jagged1 and Jagged2 (J1/2KD) or the scrambled control (Scr) siRNAs and then were treated with 6 nM Bor or 30 μM Melph or with 15 or 30 μM Len (respectively for U266 and OPM2 cells) (Figure 1A). The efficacy of J1/2KD was assessed by evaluating the expression of Jagged ligands and the active forms of the two Notch receptors expressed in MM cells, Notch intracellular domains 1 and 2 (NICD1 and NICD2), by western blot (Figure 1B).

The apoptosis rate of J1/2KD HMCL treated or not with Bor, Melph and Len was analyzed by flow cytometry. Figure 1C shows the effect of Bor, Melph and Len on HMCL normalized on DMSO-treated cells compared to J1/2KD HMCL treated with the drugs and normalized on untreated J1/2KD HMCL. J1/2KD induced an appreciable increase in HMCL sensitivity to standard-of-care drugs, with statistical significance reached in all cases, with the exception of U266 cells treated with Bor and Melph (P=0.06), that in any case confirmed the trend (Figure 1C). The basal apoptotic effect of J1/2KD is shown in *Online Supplementary Figure S1*. Concerning Len treatment, it is worth mentioning that, although Scr HMCL are resistant to this drug, J1/2KD cells acquire drug sensitivity. The selective inhibition of Jagged1 or Jagged2 is clearly less

effective in comparison with the simultaneous J1/2KD, that maximizes the biological outcome (*Online Supplementary Figure S2*).

These results indicate that the expression of Jagged1 and 2 stimulates autonomous Notch activity in MM cells that, consequently, may be inhibited by Jagged silencing. This evidence prompted us to verify whether the increased pharmacological sensitivity of MM cells induced by J1/2KD was associated to variations in the expression of recognized anti-apoptotic Notch targets, such as BCL2[18] and *Survivin/BIRC5*,[19] or with the levels of *ABCC1* reported to have a significant impact in MM.[19,20,27] J1/2KD, validated by the decrease in Jagged1, 2 and HES1 and 6 gene expression, significantly inhibited the expression of the studied anti-apoptotic genes analyzed by qRT-PCR (Figure 2A and B). The effect of J1/2KD on gene expression was seen not to be due to an increased apoptosis rate in HMCL (approx. 15%) (*Online Supplementary Figure S1*). J1/2KD effect on anti-apoptotic effectors was assessed at protein levels by flow cytometry (Figure 2C and D and *Online Supplementary Figure S3*) and western blot (*Online Supplementary Figure S4*). By contrast, the selective inhibition of Jagged1 or Jagged2 was not sufficient to significantly down-regulate the expression of these genes (*Online Supplementary Figure S5*).

Jagged1 and Jagged2 silencing contributes to multiple myeloma cell ability to promote bone marrow stromal cell-mediated drug resistance

Multiple myeloma cells localize within the BM and interact with several cell types, hijacking their functions to promote tumor progression. BMSC are a crucial target in this process that sustains malignant cell proliferation and survival.[22] Since Jagged-mediated activation of Notch pathway is involved in cell-cell communication,[6] we hypothesized that MM cell-derived Jagged ligands could activate Notch in BMSC, possibly determining BMSC-mediated drug resistance.

To explore this hypothesis, we first verified that HMCL-derived Jagged1 and Jagged2 were able to trigger the activation of Notch signaling in a BMSC line, HS5, using a Notch reporter assay. Scr HMCL are able to activate Notch signaling in co-cultured HS5 cells (Figure 3A), while this ability is lost by J1/2KD HMCL, indicating that MM-derived Jagged may activate Notch signaling in BMSC.

To verify if Jagged-mediated activation of Notch in BMSC affected the ability of these cells to promote drug resistance in MM cells, we used flow cytometry to analyze the apoptotic rate of Scr or J1/2KD HMCL cultured alone or co-cultured with HS5 cells after treatment with standard-of-care drugs. As expected, HS5 cells show a clear

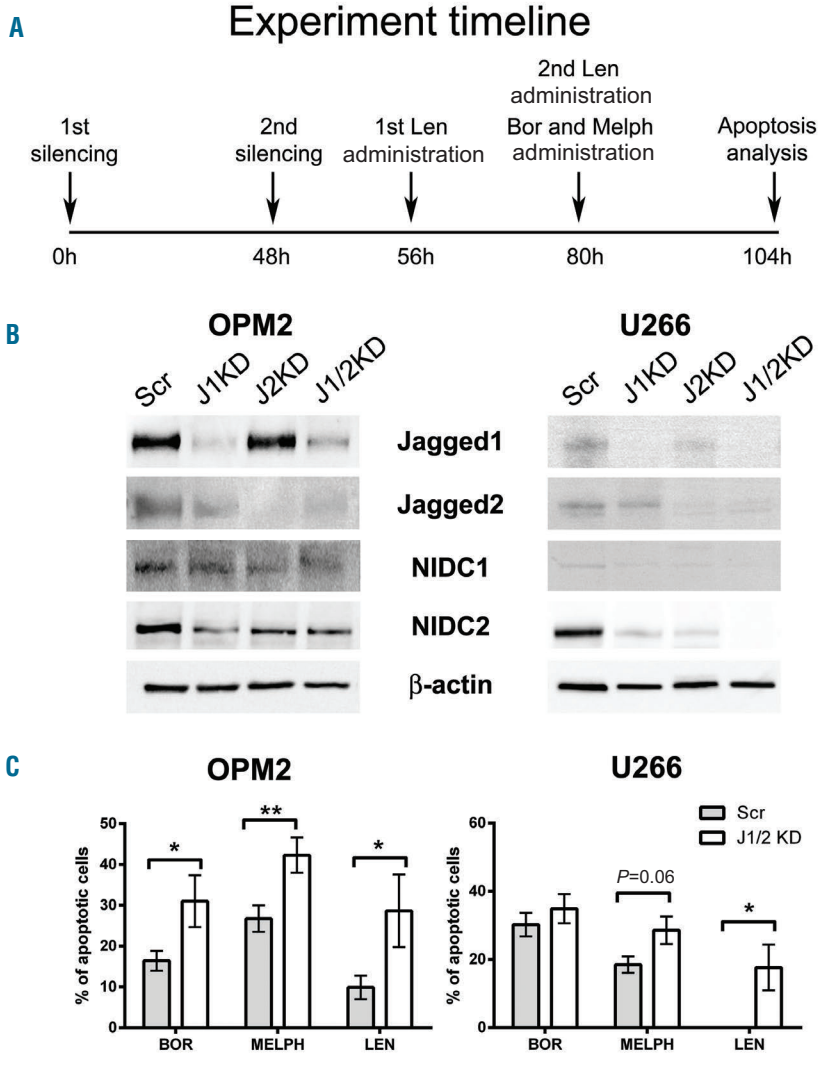

Figure 1. J1/2 silencing increases drug response in multiple myeloma (MM) cells. (A) Timeline of the experiment to study J1/2KD effect drug response in MM cell lines (HMCL). h: hour. (B) Representative western blots showing the expression of Jagged1, Jagged2, NICD1 and NICD2 in OPM2 and U266 cells following single and combined Jagged1 and/or Jagged2 silencing. β-actin was used as loading control. (C) The effect of J1/2KD on OPM2 (left) and U266 (right) cell response to bortezomib (Bor), melphalan (Melph) and lenalidomide (Len) was evaluated by Annexin V staining. MM cells were transfected with two specific siRNAs targeting Jagged1 and Jagged2 (J1/2KD) or the corresponding scrambled control (Scr) and treated with Bor, Melph or Len. Values of apoptosis of Scr HMCL were normalized to the corresponding DMSO-treated controls and values of J1/2KD HMCL treated with drugs were normalized to DMSO-treated J1/2KD HMCL. Results are shown as the mean±standard error of at least three independent experiments, and statistical analysis was performed using Mann-Whitney test (*P<0.05; **P<0.01).

trend of protection of HMCL from apoptosis induced by Bor (15% in OPM2 and 26% in U266), Melph (20% in OPM2 and 11% in U266), and Len (14% in OPM2) (Figure 3B and C), although the statistical significance was reached only in the case of OPM2 treated with Bor. Conversely and more importantly, J1/2KD induced a statistically significant increase in apoptosis, re-establishing HMCL drug sensitivity by hampering BMSC-mediated protection (HS5 cells do not display any significant increase in apoptosis; *data not shown*). Notably, although U266 cells were resistant to Len treatment in culture alone or in the presence of HS5 cells, apoptotic rate increased up to approximately 20% upon J1/2KD. The basal apoptotic effect of J1/2 KD on MM cells cultured with HS5 cells is reported in *Online Supplementary Figure S6*. As before, the selective Jagged1 or Jagged2 silencing was less effective than the simultaneous J1/2KD (*Online Supplementary Figure S7*).

Since HS5 cells could act as a source of paracrine/autocrine Jagged ligands, we wondered why they cannot rescue J1/2KD in MM cells. Western blot analysis indicates that the expression levels of Jagged1 and Jagged2 in HS5 cells are significantly lower than those expressed by OPM2 and U266 cells (*Online Supplementary Figure S8*). This can reasonably explain why, in our co-culture system, Notch signaling activated in HMCL by BMSC is not sufficient to rescue the loss of Jagged1 and Jagged2 in MM cells.

We further explored whether Jagged-mediated Notch activation in BMSC could promote the pharmacological resistance of MM cells by up-regulating the anti-apoptotic effectors previously analyzed, Survivin, BCL2, and ABCC1. To evaluate gene expression changes, we took advantage of a co-culture system including OPM2 or U266 cells with a non-human mimic model of BMSC, the murine cell line of NIH3T3 fibroblasts. This approach enabled us to precisely assess the expression levels of human (HMCL-derived) anti-apoptotic genes in co-culture by using species-specific primers. Results showed that BMSC were able to promote the expression of the anti-apoptotic effectors *Survivin, BCL2,* and *ABCC1* in Scr HMCL, while BMSC co-cultured with J1/2KD HMCL lost this ability (Figure 4A and B). Importantly, using an entire-

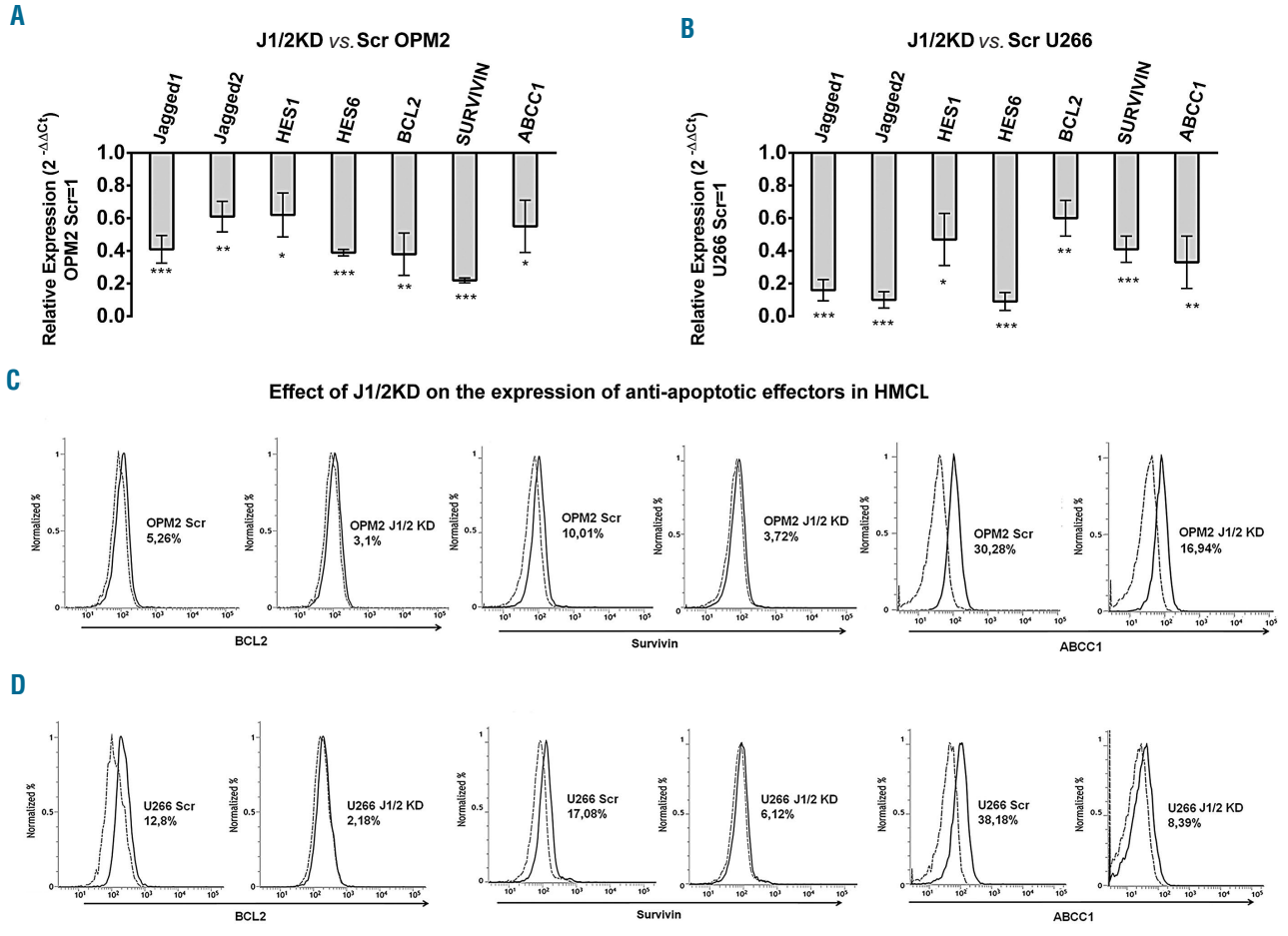

Figure 2. J1/2 withdrawal affects multiple myeloma (MM) cells anti-apoptotic background. We analyzed how J1/2KD affects Notch activation and the expression of anti-apoptotic genes in human multiple myeloma cell lines (HMCL). (A and B) Confirmation of J1/2KD efficacy in OPM2 (A) and U266 (B) cells was obtained by quantitative polymerase chain reaction (qPCR) assay assessing the relative gene expression variation of Jagged1 and Jagged2 and Notch target genes HES1 and HES6 (normalized to GAPDH) in cells transfected with J1/2 siRNA compared to cells transfected with Scr siRNA, calculated by the $2^{-\Delta\Delta Ct}$ formula. The expression levels of the anti-apoptotic effectors BCL2, Survivin, and ABCC1 were also analyzed. Data are expressed as mean± standard deviation of at least three independent experiments. Two-tailed *t*-test confirmed statistically significant downregulation of the tested genes; **P*<0.05; ***P*<0.01; ****P*<0.001. (C and D) Histograms display the levels of BCL2, Survivin and ABCC1 protein (black lines) analyzed by flow cytometry in J1/2KD OPM2 or Scr OPM2 (C) and J1/2KD U266 or Scr U266 (D) and an isotype-matched control (gray line). Histograms are representative of at least three independent experiments.

ly human co-culture system, we observed the same effects when we used flow cytometry to measure the protein expression of Survivin, BCL2, and ABCC1 in Scr or J1/2KD HMCL co-cultured with human GFP+ HS5 (Figure 4C-E and *Online Supplementary Figure S9*).

The CXCR4/SDF1α axis is a mediator of Notch pathway ability to determine drug resistance in multiple myeloma

To further study the molecular mechanisms underlying BMSC-induced drug resistance generated by Notch activation in the MM microenvironment, we explored the possible involvement of the chemokine system CXCR4/SDF1α, a key player in MM development and progression, and a downstream regulator of Notch signaling.[28,29] We hypothesized that Notch ability to promote pharmacological resistance in MM cells might be mediated by SDF1α. We reasoned that the main source of SDF1α in the BM was the stromal cell population. Therefore we explored if Jagged ligands, expressed by MM cells, could trigger the BMSC-mediated production of SDF1α and if J1/2KD might inhibit this effect.

The analysis was performed by taking advantage of co-culture systems of Scr or J1/2KD HMCL grown on a layer murine (NIH3T3) or human (HS5) stromal cells to measure the variations in SDF1α gene or protein expression. Results obtained by qRT-PCR with murine-specific primers (Figure 5A) indicate that HMCL promoted the activation of Notch signaling (HES5) and SDF1α gene expression in NIH3T3 cells, which could be reverted by J1/2KD.

Similar results were observed at protein level as assessed by flow cytometry analysis (Figure 5B and *Online Supplementary Figure S10*) on co-cultures composed of HMCL and the human GFP+ HS5 cells. Of note, the selective inhibition of Jagged1 or Jagged2 is clearly less effective if compared with the simultaneous J1/2KD, that maximizes the outcome on SDF1α inhibition (*Online Supplementary Figure S11*). Flow cytometric results were validated by ELISA on conditioned media (Figure 5C) indicating that MM cell-derived Jagged can increase SDF1α production by BMSC. We further confirmed that the variation in SDF1α expression was the consequence of Jagged-activated Notch signaling in BMSC by an assessment that showed that the stimulation with Jagged1 and/or Jagged2 peptides can increase HS5 cell-mediated secretion of SDF1α, measured by ELISA (Figure 5D). Additionally, we knocked down Notch1 expression in HS5 cells (N1KD HS5) by using a specific siRNA, as previously reported,[11] and observed that SDF1α expression significantly decreased in comparison to control HS5 cells (Figure 5E). Since Notch1 silencing does not significantly affect HS5 cell viability (On*line Supplementary Figure S12*), we could exclude the possibility that reduction of SDF1α expression might be due to HS5 cell apoptosis.

On the other hand, we verified that J1/2KD was associated to a reduced CXCR4 expression in HMCL used in co-culture experiments. J1/2KD HMCL significantly decreased CXCR4 expression in comparison to Scr HMCL (Figure 5F and *Online Supplementary Figure S13*).

We assessed the outcome of SDF1α stimulation on the anti-apoptotic background of HMCL by analyzing the levels of *Survivin, BCL2,* and *ABCC1* in U266 cells treated with 500 ng/mL SDF1α for 48 h. We observed an increase in *Survivin, BCL2*, and *ABCC1* gene expression by qRT-PCR analysis (Figure 5G) confirmed at protein level by western blot (Figure 5H). These results suggest that SDF1α can promote MM cell ability to survive to drug administration, at least in part, by stimulating tumor cell anti-

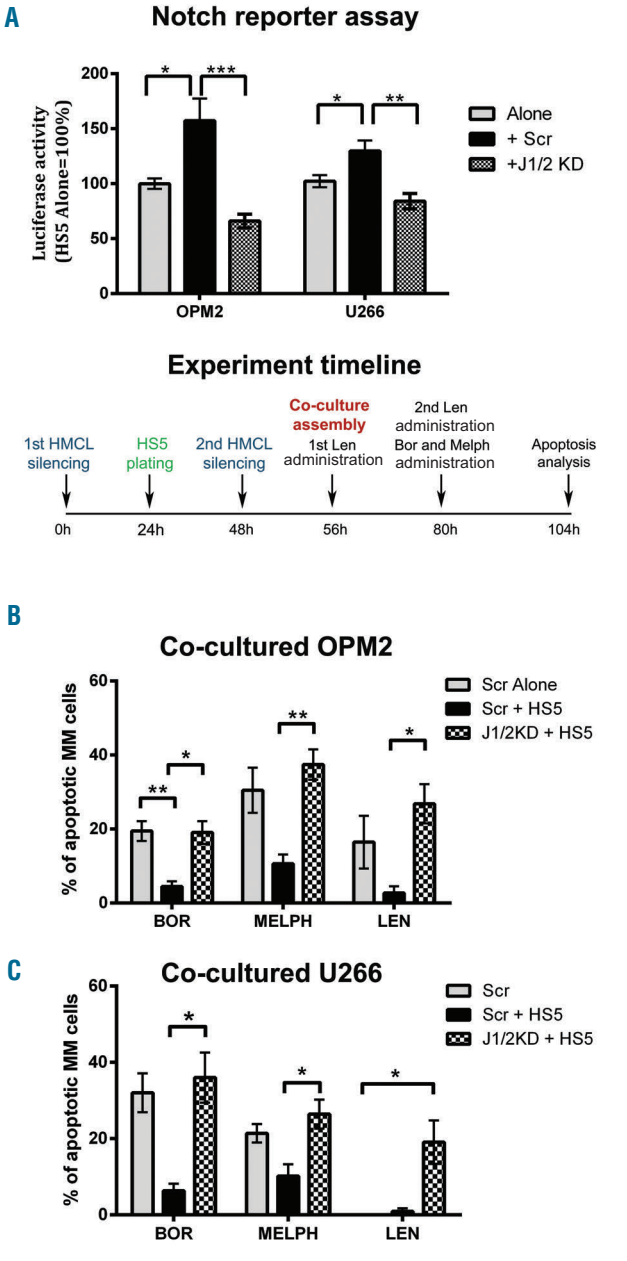

Figure 3. Effect of J1/2 inhibition on multiple myeloma (MM) cells ability to promote bone marrow (BM)-induced drug resistance. (A) A Notch-responsive dual luciferase assay was carried out in HS5 cells cultured alone or in the presence of Scr or J1/2KD human multiple myeloma cell lines (HMCL) for 24 hours (h). Data were normalized on luciferase activity in HS5 cells cultured alone (=100). Mean±standard deviation of three independent experiments are shown. Statistical analysis was performed using one-way ANOVA and Tukey post-test (*P<0.05; **P<0.01; ***P<0.001). (B and C) Co-cultures of J1/2KD or Scr HMCL with the BM stromal cell (BMSC) line HS5 were established to evaluate the effect of J1/2KD on BMSC-induced drug resistance. The experimental timeline is reported. Graphs show the percentage of apoptotic OPM2 (B) or U266 (C) cells (Annexin V+/GFP-). Values of apoptosis of each type of culture (Scr alone, Scr + HS5 and J1/2KD + HS5) treated with drugs are normalized to the corresponding controls treated with DMSO. Results are shown as mean±standard error of at least three independent experiments. Statistical analysis was performed using Kruskal-Wallis and Dunn post-test (*P<0.05; **P<0.01).

apoptotic defenses (Survivin, BCL2) and detoxification ability (ABCC1). Consistently, the treatment of U266-HS5 co-culture system with 50 μM AMD3100 (an antagonist of SDF1 binding to CXCR4), abrogated BMSC-induced resistance to the analyzed drugs (Figure 5I).

Translational potential of approaches inhibiting Jagged-mediated Notch activation in a multiple myeloma microenvironment

We further verified whether the ability of MM cells to promote BMSC-induced drug resistance was dependent on Jagged1 and Jagged2 expression by using primary co-culture systems of highly purified CD138$^+$ MM cells and BMSC isolated from BM aspirates of patients at MM onset (*Online Supplementary Table S1*).

Primary CD138$^+$ cells were transduced with the lentiviral vector pLL3.7 carrying Jagged1/2 shRNAs or Scr shRNAs and the efficiency was assessed by flow cytometry (*Online Supplementary Figure S14*). In order to maintain CD138$^+$ cell viability during *ex vivo* drug administration, after lentiviral transduction, they were co-cultured with primary BMSC stained with PKH26. Co-cultures were maintained for 72 h and treated for the last 24 h with 6 nM Bor (8 patients) or 30 μM Melph (10 patients), or for the last 48 h with 15 μM Len (9 patients) or the corresponding vehicle. The apoptotic rate of MM cells (expressing the GFP codified by the pLL3.7 vector) was detected by flow cytometry analyzing the GFP$^+$/Annexin-V-APC$^+$ subpopulation (Figure 6A). Results showed that J1/2KD significantly increased apoptosis of primary MM cells treated with

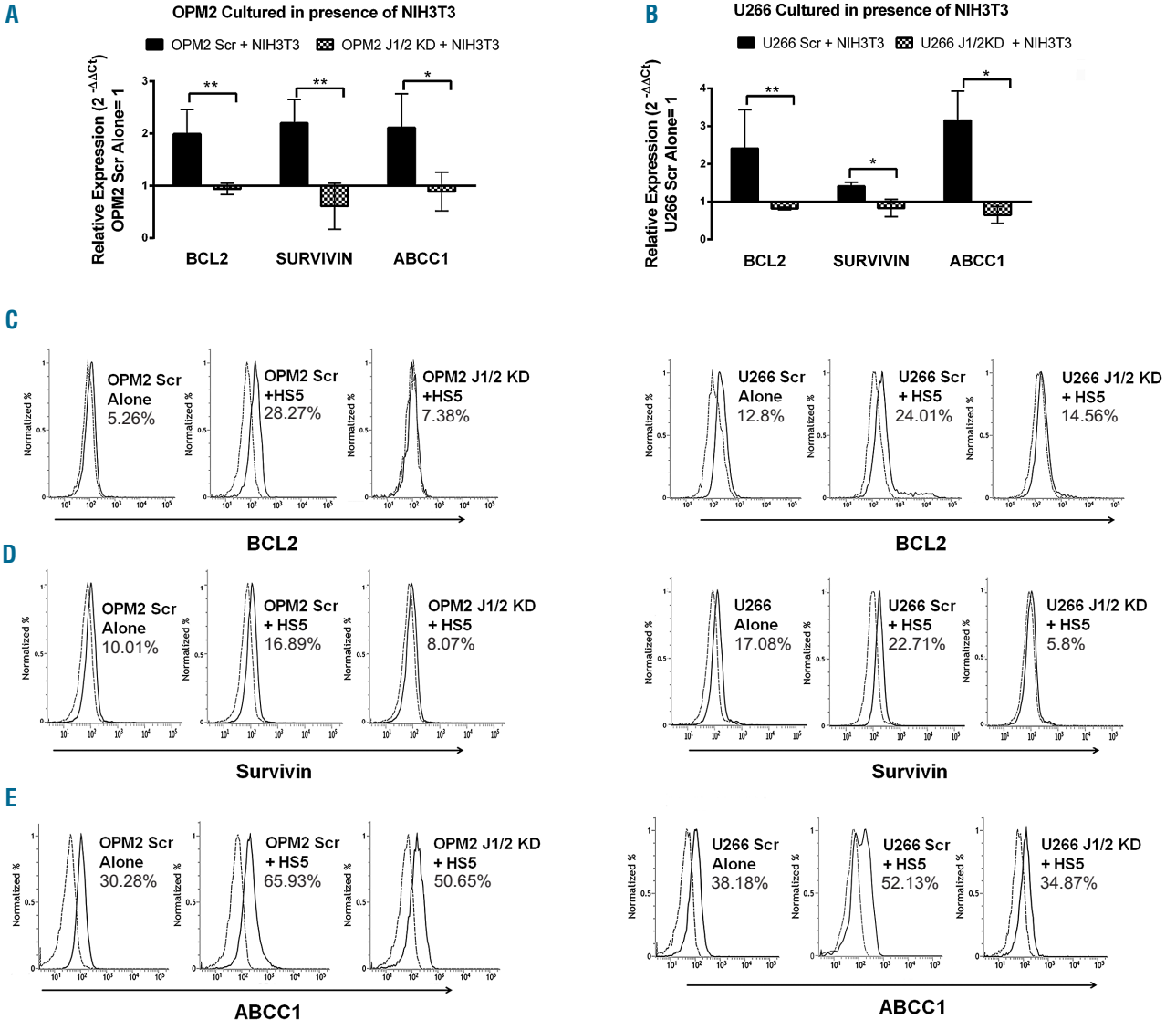

Figure 4. J1/2KD is crucial to determine bone marrow (BM)-induced drug resistance. We investigated how J1/2KD affects the molecular outcome of multiple myeloma (MM) cells crosstalk with BM stromal cells (BMSC). Quantitative real-time polymerase chain reaction (qRT-PCR) for BCL2, Survivin and ABCC1 gene expression in Scr or J1/2KD OPM2 cells (A) and Scr or J1/2KD U266 cells (B) cultured in the presence of the NIH3T3 cell line. Graphs show the relative expression levels normalized to GAPDH and compared with Scr cells cultured alone (=1), calculated by the $2^{-\Delta\Delta Ct}$ formula. Mean±standard deviation are shown. Statistical analysis was performed using two-tailed *t*-test (*P<0.05; **P<0.01). Histograms show the levels of intracellular BCL2 (C), Survivin (D), and ABCC1 (E) (black lines) analyzed by flow cytometry in Scr or J1/2KD OPM2 cells (left panels) and Scr or J1/2KD (right panels) in single culture or co-cultured with GFP$^+$ HS5 cells. The isotype-matched control is shown in gray. Histograms are representative of at least three independent experiments.

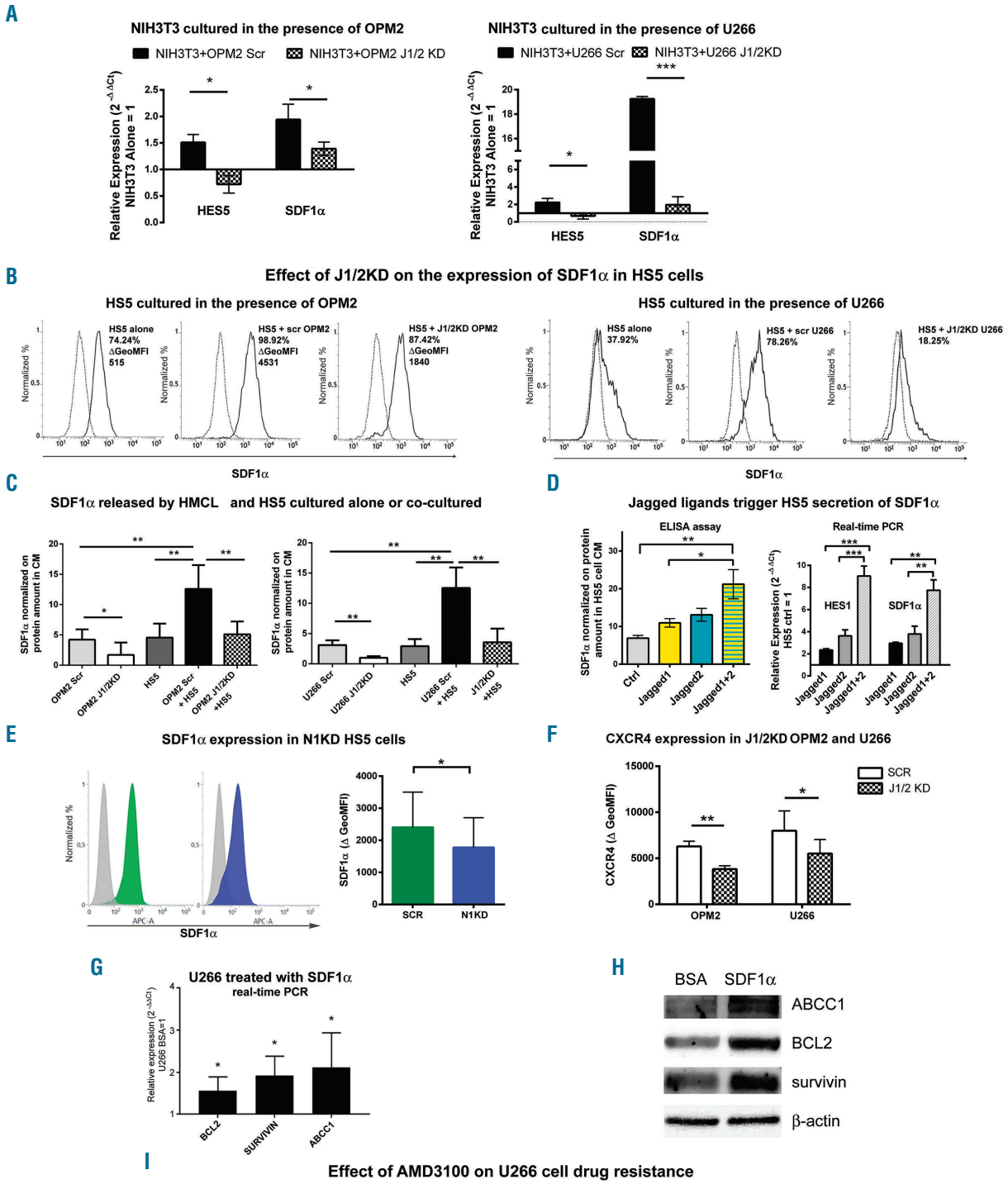

Legend on next page

Figure 5. Multiple myeloma (MM) cell-derived Jagged ligands promote resistance to apoptosis through the modulation of the CXCR4/SDF1α axis in the bone marrow (BM) niche. We evaluated the effect of J1/2KD in human multiple myeloma cell lines (HMCL) on the CXCR4/SDF1α axis in the BM and the consequence on the pharmacological resistance. (A) qRT-PCR for SDF1α and HES5 gene expression in NIH3T3 cells co-cultured with J1/2KD or Scr OPM2 cells (left panel) or J1/2KD or Scr U266 cells (right panel) compared to NIH3T3 cultured alone (=1), calculated by the $2^{-\Delta\Delta Ct}$ formula. HES5 was used as a control for Notch pathway activity. Mean±standard deviation of four experiments are shown. Statistical analysis was performed using two-tailed *t*-test (*P<0.05; ***P<0.001). (B) Intracellular SDF1α level in HS5 cells co-cultured with J1/2KD HMCL. Histograms show the levels of intracellular SDF1α (black lines) analyzed by flow cytometry in GFP$^+$ HS5 cells cultured alone or co-cultured with J1/2KD or Scr OPM2 cells (left panel) and J1/2KD or Scr U266 cells (right panel), and the isotype-matched control (dotted line). Histograms are representative of at least three independent experiments. Due to a high percentage of SDF1α expressing HS5 cells cultured with OPM2, we also show ΔGeoMFI. The apparent discrepancy between the two different basal levels of SDF1α produced by HS5 cells used as control in the co-culture systems with OPM2 or U266 cells is due to the effect of the different HS5 cell concentrations (see *Online Supplementary Methods*). (C) SDF1α levels in conditioned media of Scr or J1/2KD HMCL, HS5 cells or co-culture systems have been assessed by ELISA. Statistical analysis was performed using one-way ANOVA and Tukey post-test (*P<0.05; **P<0.01). (D) Effect of stimulation with Jagged1 and Jagged2 peptides on the secretion of SDF1α by HS5 cells. Statistical analysis was performed using one-way ANOVA and Tukey post-test (*P<0.05; **P<0.01; ***P<0.001). (E) Contribution of the Notch pathway to the ability of stromal cells to produce SDF1α. SDF1α levels were measured in Scr or N1KD HS5 cells. Flow cytometry histograms (left) and graphs (right) display the levels of intracellular SDF1α (ΔGeoMFI) analyzed in HS5 Scr (green) or HS5 N1KD cells (blue) and an isotype-matched control (gray); the graph shows mean±standard error of mean (SEM) of SDF1α expression levels. Statistical analysis was performed by *t*-test (*P<0.05). (F) Status of CXCR4 expression in Scr or J1/2KD HMCL used in co-culture experiments with HS5 cells. Values in the graph represent mean±SEM of CXCR4 expression levels (ΔGeoMFI) measured by flow cytometry. Statistical analysis was performed by *t*-test (*P<0.05; **P<0.01). (G) To evaluate if SDF1α contributes to BCL2, Survivin and ABCC1 expression, U266 cells were cultured in the presence of 500 ng/mL recombinant SDF1α for 48 h and analyzed by qRT-PCR. Graphs show the relative expression levels of the indicated genes compared with the corresponding values in BSA-treated cells (=1), calculated by the $2^{-\Delta\Delta Ct}$ formula. Mean values +/- standard deviations of three independent experiments are shown. Statistical analysis was performed using two-tailed *t*-test (*P<0.05). (H) Results were further confirmed by western blot analysis. Images were acquired using the UV-tech Alliance system and are representative of three independent experiments. (I) To assess if the SDF1α/CXCR4 axis affects MM cell drug resistance, U266 cells cultured alone or with GFP$^+$ HS5 cells were treated with 6 nM bortezomib (Bor), 30 μM melphalan (Melph), 15 μM lenalidomide (Len) or DMSO in the presence or absence of 50 μM AMD3100. Apoptotic MM cells were measured by flow cytometry as Annexin-V$^+$/GFP$^-$ cells. Graph shows mean±SEM of at least three independent experiments. Statistical analysis was performed using one-way ANOVA and Tukey's post-test: *P<0.05; **P<0.01; ****P<0.0001.

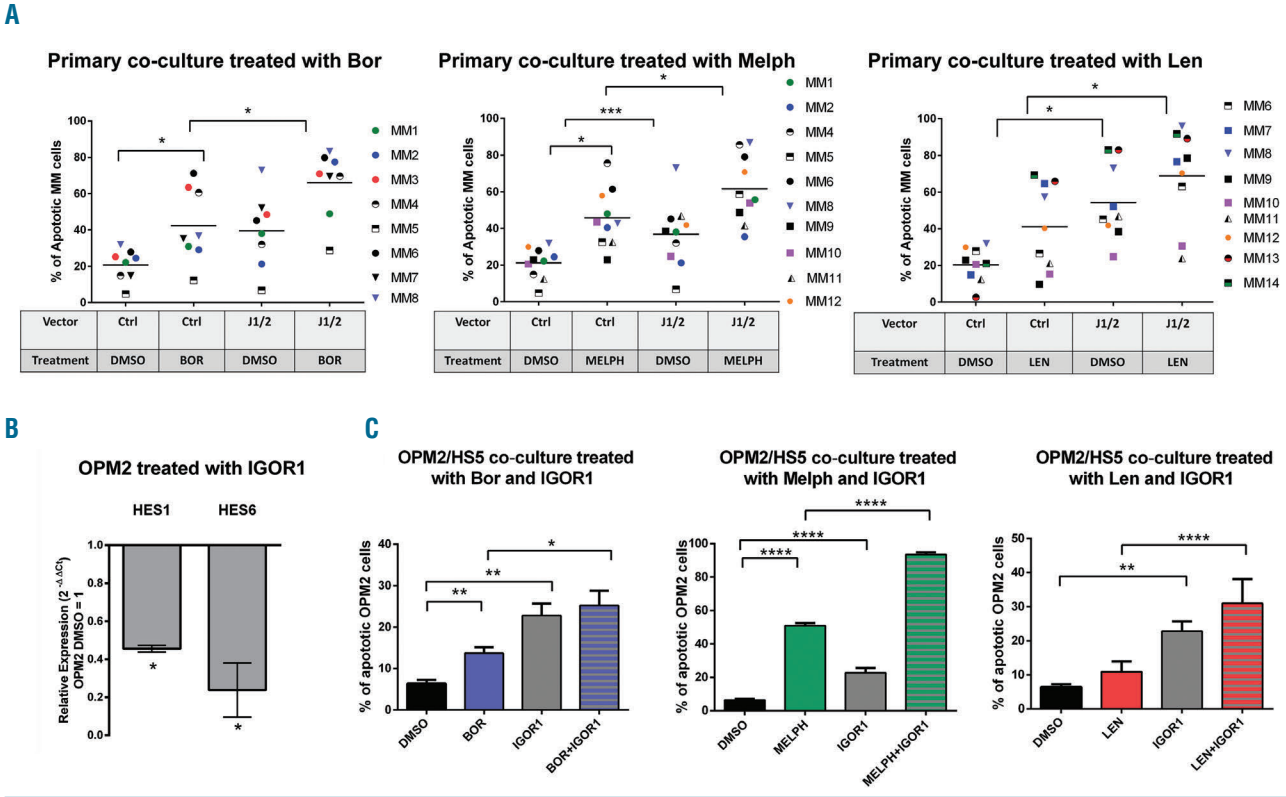

Figure 6. Translational potential of Jagged1/2 inhibition: outcome on *ex vivo* cultures of multiple myeloma (MM) patients' cells and treatment with small molecule affecting Notch-Jagged interaction. (A) Outcome of J1/2KD on primary CD138$^+$ MM cells response to standard-of-care drugs in a primary co-culture system with bone marrow stromal cells (BMSC). Levels of apoptosis were analyzed by flow cytometry on primary MM cells transduced with the lentiviral vector pLL3.7 codifying for the Jagged1 and 2 shRNAs (J1/2) or the corresponding control (Ctrl), and then co-cultured with BMSC from MM patients. Co-cultures were maintained for 72 hours (h) and treated for the last 24 h with 6 nM bortezomib (Bor) (left panel; 8 patients) or 30 μM melphalan (Melph) (central panel; 10 patients) and for 48 h with 15 μM lenalidomide (Len) (right panel; 9 patients) or DMSO. The percentage of infected MM cells that underwent apoptosis (GFP$^+$/AnnexinV$^+$) was detected by flow cytometry. Statistical analysis was performed using one-way ANOVA and Tukey post-test (*P<0.05; **P<0.01; ***P<0.001). (B and C) Effect of the inhibitory small molecule, IGOR1, on MM drug resistance. OPM2 cells treated with 30 μM IGOR1 were cultured on a monolayer of HS5 GFP$^+$ cells in the presence or the absence of different drugs as described in the Methods. (B) Quantitative polymerase chain reaction assay shows that IGOR1 inhibits Notch pathway in OPM2 cells, as demonstrated by the downregulation of Notch target genes, HES1 and HES6. Relative gene expression variation was normalized to GAPDH and calculated by the $2^{-\Delta\Delta Ct}$ formula. Mean values +/- standard deviations of three experiments are shown. Statistical analysis was performed using two-tailed *t*-test (*P<0.05). (C) The levels of apoptosis of OPM2 cells treated with IGOR1 and the indicated drugs were measured by staining with Annexin-V-APC (C). Graph shows mean values +/- standard deviations of at least three independent experiments. Statistical analysis was performed using one-way ANOVA and Tukey's post test (*P<0.05; **P<0.01; ****P<0.0001).

all the analyzed drugs, in agreement with the findings obtained *in vitro*.

To verify if the inhibitory approach based on J1/2KD had a translational potential, we recapitulated the experiments of MM-BMSC interplay by using IGOR1, a novel small molecule recently developed in our laboratory[30] to uncouple Notch-Jagged interaction. IGOR1 is able to inhibit Notch activation in OPM2 cells and significantly increases the efficacy of the administered drugs, with a higher efficiency for Mel and Len (Figure 6B and C).

Jagged1 and Jagged2 blockade promotes sensitivity to bortezomib in a zebrafish xenograft myeloma model

Bortezomib is one of the most commonly used drugs for the treatment of newly-diagnosed and refractory MM patients.[31] In recent years, several studies have supported the hypothesis that the development of resistance to such treatment is strongly dependent upon the BM microenvironment, with a significant contribution of the CXCR4/SDF1α axis.[32-34] Due to the results obtained *in vitro* concerning the role of this chemokine axis in the development of pharmacological resistance to Bor, we validated the effect of J1/2KD on MM cell resistance to Bor by taking advantage of a novel zebrafish xenograft MM model.

Zebrafish embryos were recently validated as a complementary *in vivo* model for MM that allows the rapid screening of MM cells response to chemotherapeutic drugs.[35] Moreover, this model fully recapitulates the cytokine milieu present in the human BM, since zebrafish-secreted growth factors, such as IL6 and SDF1α, support MM cells growth *in vivo*.[33,35] To validate our *in vitro* and *ex vivo* findings, Scr or J1/2KD U266 cells vitally labeled with the fluorescent dye CM-Dil were injected in the yolk area of 48 hpf zebrafish embryos. Xenotransplanted embryos were visualized by fluorescent microscopy to verify the presence of MM cells at the injection site at 2 hpi (Figure 7A-D), treated or not with 10 nM Bor and, visualized at 48 hpi for tumor cell growth (Figure 7A'-D'). Representative images of whole embryos are shown in *Online Supplementary Figure S15*.

As shown, the addition of 10 nM Bor to the embryo medium inhibited tumor growth of approximately 57% compared to controls (Figure 7A' and B'), without affecting embryo viability. A similar effect was induced by J1/2KD (Figure 7A'-C'), while the combination of J1/2KD and Bor significantly reduced tumor growth in comparison to all other experimental groups (-82% in comparison to the control) (Figure 7A'-D').

Discussion

Multiple myeloma progression is characterized by development of drug resistance causing patient relapse

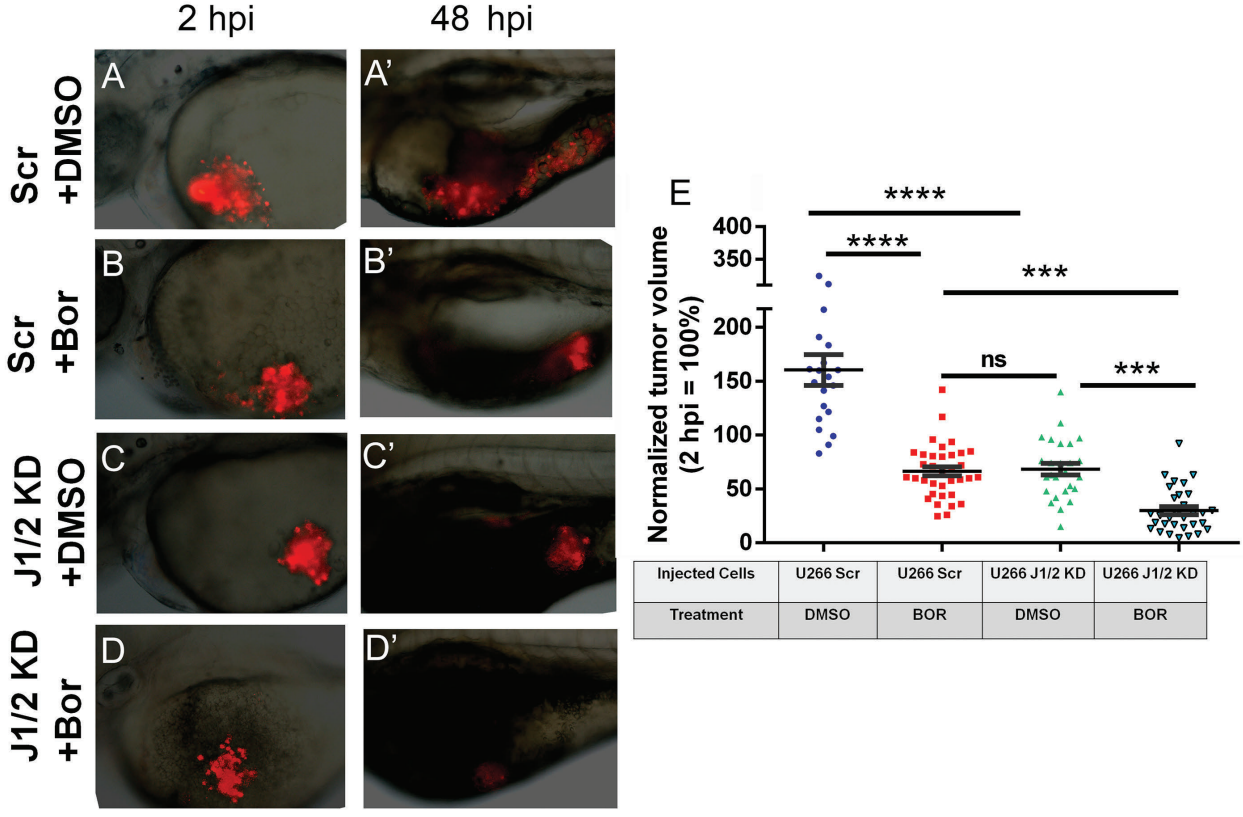

Figure 7. Evaluation of tumor growth inhibition of myeloma cells xenotransplanted in zebrafish embryos. Fluorescent microscopy images of CM-DiI stained multiple myeloma (MM) xenografts at 2 hours (h) post injection (hpi) (A-D) and 48 h post injection (hpi) (A'-D') into the yolk of zebrafish embryos. (A'-D') Tumor growth analyses indicates that MM xenografts are responsive to treatment with bortezomib (Bor) (compare A' and B'). Xenotransplanted J1/2KD cells also show reduced tumor growth (compare A' and C'). These effects are increased combining the injection of J1/2KD cells with Bor treatment (compare A', B', C' and D'). (E) Dot-plot shows the increase in tumor burden at 48 hpi, normalized to tumor area at 2 hpi (Scr+DMSO= 20 embryos; Scr+ Bor= 26 embryos; J1/2KD+ DMSO= 35 embryos; J1/2KD+ Bor=31 embryos). Statistical analysis was performed using one-way ANOVA and Tukey post-test (***P<0.001; ****P<0.0001).

and contributing to the fatal outcome of this disease. The close interaction of MM cells with healthy BM cells represents an important source of factors able to promote malignant cell growth and survival.

The Notch pathway is capable of mediating the cell-cell communication. Current evidence provided by different groups, including ours, highlighted the importance of Jagged ligands in the pathological communication between tumor and healthy cells within the myeloma BM. MM-derived Jagged ligands activate Notch receptors in the nearby BM cells inducing osteoclastogenesis, osteolysis,[17] angiogenesis,[36] and BMSC-mediated release of key cytokines including IL6, IGF1 and VEGF.[11,13] Moreover, the activation of Notch signaling in MM cells, induced by tumor cell-derived[37,38] or BMSC-derived Jagged[1,25] stimulates MM cell proliferation,[38] resistance to apoptosis,[37] and a decrease in drug sensitivity.[25]

This work is specifically focused on the pathological communication of MM cells and BMSC mediated by Notch signaling and on its outcome on MM drug resistance. Notably, the Notch pathway is known to be a key player in BM-induced drug resistance in other hematologic malignancies. Indeed, Krampera's group provided evidence of how the BM-driven activation of Notch3 and Notch4 in B-ALL[39-41] and Notch1, Notch2 and Notch4 in chronic lymphocytic leukemia,[42] results in chemoresistance, while Notch1-Jagged1 crosstalk supports BM-induced drug resistance in AML.[43]

As far as MM is concerned, in spite of the recent advances in the field, we still do not have a complete picture of the bidirectional crosstalk between BMSC and MM cells, which is indicated by the expression of Notch receptors and ligands on both cell types.[11,12,16,23,25,44] This work aims to fill some of those gaps by providing novel information about the effects of the aberrant expression of MM-derived Jagged ligands on the intrinsic tumor cell drug resistance and by investigating a key aspect that has never been previously explored, i.e. the outcome of MM-derived Jagged ligands on BMSC-induced drug resistance.

To address these issues, we interfered with the mRNA expression of MM-derived Jagged ligands and investigated J1/2KD outcomes in tumor cells and in surrounding BMSC. We observed *in vitro* that MM cell-derived Jagged ligands could trigger Notch signaling in the nearby MM cells by homotypic interaction. Notch activation resulted in the increased expression of anti-apoptotic effectors including BCL2, Survivin, and the multidrug resistance transporter ABCC1, along with the increase in MM cell survival to standard-of-care drugs, such as Bor, Len, and Melph. Notably, besides observing homotypic activation of Notch signaling among MM cells, we found that HMCL can trigger Notch signaling in the neighboring BMSC and, in turn, Notch activation boosts the ability of BMSC to increase the pharmacological resistance of MM cells. This effect was clearly dependent on MM-derived Jagged ligands, since J1/2KD completely abrogated BMSC support. At least in part, the pro-tumor effect of Notch-"educated" BMSC was due to their ability to increase SDF1α levels in the BM microenvironment. Indeed, soluble or MM cell-derived Jagged ligands may induce a Notch-dependent increase in SDF1α secretion by BMSC; on the contrary, J1/2KD HMCL lose this ability and N1KD interferes with BMSC to release SDF1α.

The Notch-dependent activation of SDF1α secretion by BMSC is potentially more important than the previously observed secretion induced by Notch activation in MM cells,[29] since BMSC are the most effective producers of this cytokine in the BM.

To complete the picture of a Notch signaling effect on the SDF1α/CXCR4 axis in myeloma BM, we also demonstrated that MM cell-derived Jagged ligands may further enhance the anti-apoptotic signaling of SDF1α by stimulating the expression of its receptor CXCR4 on the MM cell surface.

The contribution of the SDF1α/CXCR4 axis to MM pharmacological resistance was confirmed by the ability of the antagonist molecule AMD3100 to abrogate U266 cell resistance to (Bor), (Melph) and (Len) induced by BMSC, consistent with the findings of Azab *et al*.[32]

Although the downstream molecular mechanisms of Notch-associated drug resistance in MM still need to be fully elucidated, we showed that the secreted SDF1α can stimulate general mechanisms, including tumor cell anti-apoptotic background, by up-regulating BCL2 and Survivin, or drug extrusion mediated by ABCC1. These antiapoptotic proteins are particularly relevant to MM. Indeed, BCL2 and Survivin are over-expressed in MM cells, where they play an important role in cell survival, and significantly correlate with disease stage;[20,27,45] on the other hand, xenobiotic transporters, such as ABCC1, are well known mediators of MM multidrug resistance,[20] modulated by Notch in different cancer settings.[46]

The general validity of these novel findings stems from the observed improvement in drug-response promoted by J1/2KD in *ex vivo* co-culture systems of CD138$^+$ MM cells and BMSC from BM aspirates of newly-diagnosed MM patients.

Additionally, *in vivo* validation of these findings in a zebrafish xenograft MM model engrafted with U266 cells confirmed that J1/2KD promoted an increased sensitivity to Bor *in vivo*, showing a wider decrease in tumor burden compared to the control.

The present results provide novel and important information to help improve the current picture on the effect of Notch-mediated communication in myeloma BM. Indeed, since both BMSC and MM cells carry Notch receptors and ligands, their bidirectional crosstalk needs to be taken into consideration. We sought to fill the gap in the available information on the role of MM cells, such as Notch signaling sending cells in the BM. Here we discuss our findings according to the previous literature data in order to summarize the overall picture (Figure 8). Previous work reported the consequences of Notch activity in MM cells (mainly using γ-secretase inhibitors), identifying the following molecular mechanisms: i) upregulation of p21 induced MM cell growth inhibition and increased survival;[23] ii) Notch/HES1 mediated downregulation of the pro-apoptotic protein Noxa;[24] iii) Notch up-regulated expression of integrin αvβ5 resulting in increased adhesion to vitronectin and consequent protection from pro-apoptotic drugs;[47] iv) upregulation of the enzyme cytochrome P450,[44] implicated in drug metabolism and in the onset of several malignancies.[48] Concerning the contribution of Notch in BMSC-dependent drug resistance, previous investigations were focused on the autonomous contribution of BMSC-derived Notch ligands in MM cell behavior (Figure 8).[23,25,44]

In this work, we found that the alteration induced in the BM by the presence of MM cells aberrantly expressing Jagged ligands is a key step in "educating" the tumor microenvironment to a pro-tumor type of behavior.

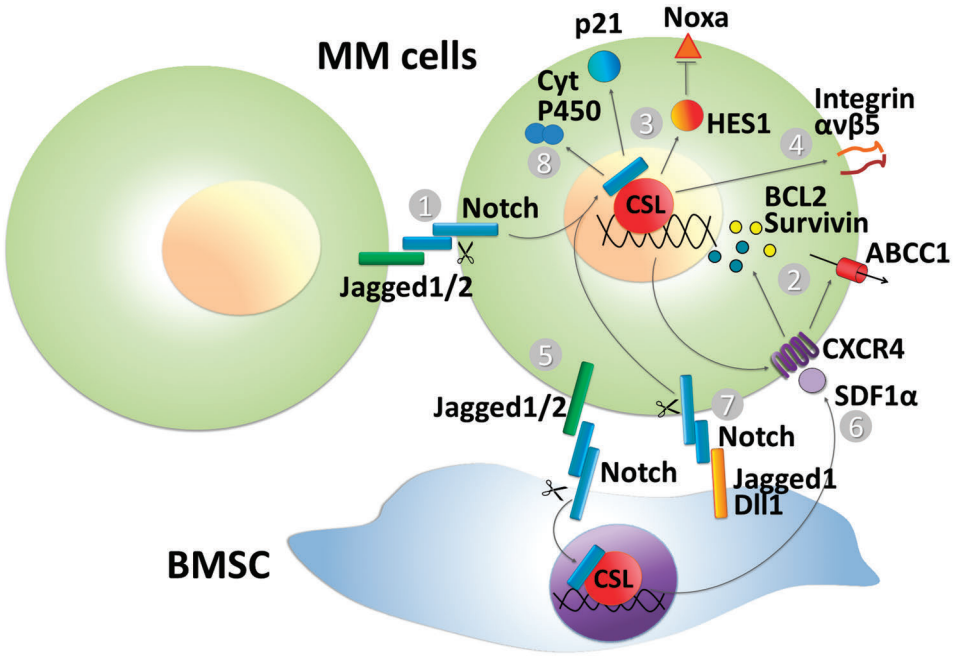

Figure 8. Mechanism underlying Notch ability to promote drug resistance in multiple myeloma (MM) microenvironment. Jagged1/2 overexpression in MM cells causes hyperactivation of Notch signaling in the bone marrow (BM) milieu, which, in turn, promotes drug resistance by modifying both MM cell and BM stromal cell (BMSC) behavior. Indeed, (1) Notch activation in MM cell triggered by Jagged1/2 through homotypic interactions sustains resistance to drug-induced apoptosis in different ways. Notch can (2) promote the expression of the pro-survival factors BCL2, Survivin, and ABCC1 and the chemokine receptor CXCR4; (3) up-regulates HES1, which in turn inhibits the expression of the pro-apoptotic protein Noxa; (4) promotes the expression of integrin αvβ5, thus enhancing MM cell adhesion to vitronectin. (5) MM-derived Jagged1/2 may also activate Notch in BMSC, (6) boosting its ability to produce SDF1α, which in turn, by activating CXCR4 signaling in MM cell, promotes the expression of the anti-apoptotic factors BCL2, Survivin, and ABCC1, improving MM cell pharmacological resistance. On the other hand, (7) BMSC activate the Notch pathway in MM cells through their basal expression of Jagged1 and Dll4, (8) promoting the expression of cytochrome P450 and p21, thereby supporting MM cell resistance to therapy.

Indeed, MM cell-derived Jagged1 and 2 may switch on Notch signaling in tumor and non-tumor BMSC by triggering Notch signaling, activating MM cell anti-apoptotic background, increasing SDF1α level in the BM, and, finally, resulting in supporting MM cell resistance to standard-of-care drugs (Figure 8).

Overall, our findings provide the proof-of-principle that selective targeting of Jagged ligands in MM cells can restore tumor cell sensitivity to therapy, laying the foundation for the development of combined low-toxic therapeutic options to restore drug sensitivity and overcome fatal drug resistance of relapsing MM patients. Recently, inhibitory small molecules[30] or neutralizing antibodies[49] directed to inhibit the activation of Notch signaling mediated by Jagged ligands have been developed. This prompted us to confirm the translational potential of our results by testing the anti-tumor effect of an inhibitory small molecule developed in our laboratory, IGOR1, which was directed to uncouple Notch-Jagged interaction.[30] *In vitro* results showed that IGOR1 had the ability to increase MM cell pharmacological response, with higher efficacy if combined with Melph and Len.

The importance of our results stems from the evidence that a Jagged-tailored therapy might represent a more suitable clinical approach to achieve the inhibition of Notch signaling in the BM of MM patients. Indeed, it lacks the potential adverse effects of pan-Notch blockade obtained with γ-secretase inhibitors (GSI), that provided promising results in an *in vivo* MM model by increasing the chemotherapeutic effect of doxorubicin and melphalan,[24] but that were associated with severe gastrointestinal toxicity due to intestine metaplasia.[50,51]

Funding

This study was supported by grants from Associazione Italiana Ricerca sul Cancro, AIRC Investigator Grant to RC (20614) and AN (16722), My First Grant to AP (18741); Fondazione Italiana per la Ricerca sul Cancro to MC (post-doctoral fellowship 18013) and ET (post-doctoral fellowship 19370); Università degli Studi di Milano to RC (Linea 2B-2017 - Dept. Health Sciences), to NP (post-doctoral fellowship type A), SG, MTP and EL (PhD fellowship in Molecular and Translational Medicine), DG (PhD fellowship in Experimental Medicine).

References

1. Kumar SK, Rajkumar V, Kyle RA, et al. Multiple myeloma. Nat Rev Dis Primers. 2017;3:17046.
2. Nijhof IS, van de Donk N, Zweegman S, Lokhorst HM. Current and New Therapeutic Strategies for Relapsed and Refractory Multiple Myeloma: An Update. Drugs. 2018;78(1):19-37.
3. Manier S, Sacco A, Leleu X, Ghobrial IM, Roccaro AM. Bone marrow microenvironment in multiple myeloma progression. J Biomed Biotechnol. 2012;2012:157496.
4. Chiaramonte R, Basile A, Tassi E, et al. A wide role for NOTCH1 signaling in acute leukemia. Cancer Lett. 2005;219(1):113-120.

5. Colombo M, Mirandola L, Chiriva-Internati M, et al. Cancer Cells Exploit Notch Signaling to Redefine a Supportive Cytokine Milieu. Front Immunol. 2018;9:1823.
6. Platonova N, Lesma E, Basile A, et al. Targeting Notch as a Therapeutic Approach for Human Malignancies. Curr Pharm Des. 2017;23(1):108-134.
7. Colombo M, Mirandola L, Platonova N, et al. Notch-directed microenvironment reprogramming in myeloma: a single path to multiple outcomes. Leukemia. 2013;27(5):1009-1018.
8. Mirandola L, Comi P, Cobos E, Kast WM, Chiriva-Internati M, Chiaramonte R. Notching from T-cell to B-cell lymphoid malignancies. Cancer Lett. 2011;308(1):1-13.
9. Platonova N, Manzo T, Mirandola L, et al. PI3K/AKT signaling inhibits NOTCH1 lysosome-mediated degradation. Genes Chromosomes Cancer. 2015;54(8):516-526.
10. Colombo M, Galletti S, Garavelli S, et al. Notch signaling deregulation in multiple myeloma: A rational molecular target. Oncotarget. 2015;6(29):26826-26840.
11. Colombo M, Galletti S, Bulfamante G, et al. Multiple myeloma-derived Jagged ligands increases autocrine and paracrine interleukin-6 expression in bone marrow niche. Oncotarget. 2016;7(35):56013-56029.
12. Skrtic A, Korac P, Kristo DR, Ajdukovic Stojisavljevic R, Ivankovic D, Dominis M. Immunohistochemical analysis of NOTCH1 and JAGGED1 expression in multiple myeloma and monoclonal gammopathy of undetermined significance. Hum Pathol. 2010;41(12):1702-1710.
13. Houde C, Li Y, Song L, et al. Overexpression of the NOTCH ligand JAG2 in malignant plasma cells from multiple myeloma patients and cell lines. Blood. 2004;104(12):3697-3704.
14. Ghoshal P, Nganga AJ, Moran-Giuati J, et al. Loss of the SMRT/NCoR2 corepressor correlates with JAG2 overexpression in multiple myeloma. Cancer Res. 2009;69(10):4380-4387.
15. Takeuchi T, Adachi Y, Ohtsuki Y. Skeletrophin, a novel ubiquitin ligase to the intracellular region of Jagged-2, is aberrantly expressed in multiple myeloma. Am J Pathol. 2005;166(6):1817-1826.
16. van Stralen E, van de Wetering M, Agnelli L, Neri A, Clevers HC, Bast BJ. Identification of primary MAFB target genes in multiple myeloma. Exp Hematol. 2009;37(1):78-86.
17. Colombo M, Thummler K, Mirandola L, et al. Notch signaling drives multiple myeloma induced osteoclastogenesis. Oncotarget. 2014;5(21):10393-10406.
18. Ye QF, Zhang YC, Peng XQ, Long Z, Ming YZ, He LY. Silencing Notch-1 induces apoptosis and increases the chemosensitivity of prostate cancer cells to docetaxel through Bcl-2 and Bax. Oncol Lett. 2012;3(4):879-884.
19. Ju JH, Yang W, Oh S, et al. HER2 stabilizes survivin while concomitantly down-regulating survivin gene transcription by suppressing Notch cleavage. Biochem J. 2013;451(1):123-134.
20. Buda G, Ricci D, Huang CC, et al. Polymorphisms in the multiple drug resistance protein 1 and in P-glycoprotein 1 are associated with time to event outcomes in patients with advanced multiple myeloma treated with bortezomib and pegylated liposomal doxorubicin. Ann Hematol. 2010;89(11):1133-1140.
21. Kawano Y, Moschetta M, Manier S, et al. Targeting the bone marrow microenvironment in multiple myeloma. Immunol Rev. 2015;263(1):160-172.
22. Colombo M, Platonova N, Giannandrea D, Palano MT, Basile A, Chiaramonte R. Re-establishing Apoptosis Competence in Bone Associated Cancers via Communicative Reprogramming Induced Through Notch Signaling Inhibition. Front Pharmacol. 2019;10:145.
23. Nefedova Y, Cheng P, Alsina M, Dalton WS, Gabrilovich DI. Involvement of Notch-1 signaling in bone marrow stroma-mediated de novo drug resistance of myeloma and other malignant lymphoid cell lines. Blood. 2004;103(9):3503-3510.
24. Nefedova Y, Sullivan DM, Bolick SC, Dalton WS, Gabrilovich DI. Inhibition of Notch signaling induces apoptosis of myeloma cells and enhances sensitivity to chemotherapy. Blood. 2008;111(4):2220-2229.
25. Muguruma Y, Yahata T, Warita T, et al. Jagged1-induced Notch activation contributes to the acquisition of bortezomib resistance in myeloma cells. Blood Cancer J. 2017;7(12):650.
26. Kato H, Taniguchi Y, Kurooka H, et al. Involvement of RBP-J in biological functions of mouse Notch1 and its derivatives. Development. 1997;124(20):4133-4141.
27. Khan N, Kahl B. Targeting BCL-2 in Hematologic Malignancies. Target Oncol. 2018;13(3):257-267.
28. Chiaramonte R, Colombo M, Bulfamante G, et al. Notch pathway promotes ovarian cancer growth and migration via CXCR4/SDF1alpha chemokine system. Int J Biochem Cell Biol. 2015;66:134-140.
29. Mirandola L, Apicella L, Colombo M, et al. Anti-Notch treatment prevents multiple myeloma cells localization to the bone marrow via the chemokine system CXCR4/SDF-1. Leukemia. 2013;27(7):1558-1566.
30. Platonova N, Parravicini C, Sensi C, et al. Identification of small molecules uncoupling the Notch::Jagged interaction through an integrated high-throughput screening. PloS One. 2017;12(11):e0182640.
31. Richardson PG, Sonneveld P, Schuster M, et al. Extended follow-up of a phase 3 trial in relapsed multiple myeloma: final time-to-event results of the APEX trial. Blood. 2007;110(10):3557-3560.
32. Azab AK, Runnels JM, Pitsillides C, et al. CXCR4 inhibitor AMD3100 disrupts the interaction of multiple myeloma cells with the bone marrow microenvironment and enhances their sensitivity to therapy. Blood. 2009;113(18):4341-4351.
33. Sacco A, Roccaro AM, Ma D, et al. Cancer Cell Dissemination and Homing to the Bone Marrow in a Zebrafish Model. Cancer Res. 2016;76(2):463-471.
34. Waldschmidt JM, Simon A, Wider D, et al. CXCL12 and CXCR7 are relevant targets to reverse cell adhesion-mediated drug resistance in multiple myeloma. Br J Haematol. 2017;179(1):36-49.
35. Lin J, Zhang W, Zhao J-J, et al. A clinically relevant in vivo zebrafish model of human multiple myeloma (MM) to study preclinical therapeutic efficacy. Blood. 2016;128(2):249-252.
36. Saltarella I, Frassanito MA, Lamanuzzi A, et al. Homotypic and Heterotypic Activation of the Notch Pathway in Multiple Myeloma–Enhanced Angiogenesis: A Novel Therapeutic Target? Neoplasia. 2019;21(1):93-105.
37. Jia CM, Tian YY, Quan LN, Jiang L, Liu AC. miR-26b-5p suppresses proliferation and promotes apoptosis in multiple myeloma cells by targeting JAG1. Pathol Res Pract. 2018;214(9):1388-1394.
38. Jundt F, Probsting KS, Anagnostopoulos I, et al. Jagged1-induced Notch signaling drives proliferation of multiple myeloma cells. Blood. 2004;103(9):3511-3515.
39. Nwabo Kamdje AH, Krampera M. Notch signaling in acute lymphoblastic leukemia: any role for stromal microenvironment? Blood. 2011;118(25):6506-6514.
40. Nwabo Kamdje AH, Mosna F, Bifari F, et al. Notch-3 and Notch-4 signaling rescue from apoptosis human B-ALL cells in contact with human bone marrow-derived mesenchymal stromal cells. Blood. 2011;118(2):380-389.
41. Takam Kamga P, Dal Collo G, Midolo M, Adamo A, Delfino P. Inhibition of Notch Signaling Enhances Chemosensitivity in B-cell Precursor Acute Lymphoblastic Leukemia. Cancer Res. 2019;79(3):639-649.
42. Nwabo Kamdje AH, Bassi G, Pacelli L, et al. Role of stromal cell-mediated Notch signaling in CLL resistance to chemotherapy. Blood Cancer J. 2012;2(5):e73-e73.
43. Takam Kamga P, Bassi G, Cassaro A, et al. Notch signalling drives bone marrow stromal cell-mediated chemoresistance in acute myeloid leukemia. Oncotarget. 2016;7(16):21713-21727.
44. Xu D, Hu J, De Bruyne E, et al. Dll1/Notch activation contributes to bortezomib resistance by upregulating CYP1A1 in multiple myeloma. Biochem Biophys Res Commun. 2012;428(4):518-524.
45. Romagnoli M, Trichet V, David C, et al. Significant impact of survivin on myeloma cell growth. Leukemia. 2007;21(5):1070-1078.
46. Cho S, Lu M, He X, et al. Notch1 regulates the expression of the multidrug resistance gene ABCC1/MRP1 in cultured cancer cells. Proc Natl Acad Sci U S A. 2011;108(51):20778-20783.
47. Ding Y, Shen Y. Notch increased vitronection adhesion protects myeloma cells from drug induced apoptosis. Biochem Biophys Res Commun. 2015;467(4):717-722.
48. Go R-E, Hwang K-A, Choi K-C. Cytochrome P450 1 family and cancers. J Steroid Biochem Mol Biol. 2015;147:24-30.
49. Li D, Masiero M, Banham AH, Harris AL. The Notch Ligand Jagged1 as a Target for Anti-Tumor Therapy. Front Oncol. 2014;4:254.
50. Milano J, McKay J, Dagenais C, et al. Modulation of notch processing by gamma-secretase inhibitors causes intestinal goblet cell metaplasia and induction of genes known to specify gut secretory lineage differentiation. Toxicol Sci. 2004;82(1):341-358.
51. Wong GT, Manfra D, Poulet FM, et al. Chronic treatment with the gamma-secretase inhibitor LY-411,575 inhibits beta-amyloid peptide production and alters lymphopoiesis and intestinal cell differentiation. J Biol Chem. 2004;279(13):12876-12882.

ARTICLE

Lenalidomide-based induction and maintenance in elderly newly diagnosed multiple myeloma patients: updated results of the EMN01 randomized trial

Sara Bringhen,[1] Mattia D'Agostino,[1] Laura Paris,[2] Stelvio Ballanti,[3] Norbert Pescosta,[4] Stefano Spada,[1] Sara Pezzatti,[5] Mariella Grasso,[6] Delia Rota-Scalabrini,[7] Luca De Rosa,[8] Vincenzo Pavone,[9] Giulia Gazzera,[1] Sara Aquino,[10] Marco Poggiu,[1] Armando Santoro,[11] Massimo Gentile,[12] Luca Baldini,[13] Maria Teresa Petrucci,[14] Patrizia Tosi,[15] Roberto Marasca,[16] Claudia Cellini,[17] Antonio Palumbo,[1]° Patrizia Falco,[18] Roman Hájek,[19,20] Mario Boccadoro[1] and Alessandra Larocca[1]

[1]Myeloma Unit, Division of Hematology, University of Torino, Azienda Ospedaliero-Universitaria Città della Salute e della Scienza di Torino, Torino, Italy; [2]Hematology and Bone Marrow Transplant Unit, Azienda Socio Sanitaria Territoriale Papa Giovanni XXIII, Bergamo, Italy; [3]Sezione di Ematologia e Immunologia Clinica, Ospedale Santa Maria della Misericordia, località Sant'Andrea delle Fratte, Perugia, Italy; [4]Reparto Ematologia e Centro TMO, Ospedale Centrale, Bolzano, Italy; [5]Divisione di Ematologia, Ospedale S. Gerardo, Monza, Italy; [6]Azienda Ospedaliera S. Croce-Carle, Cuneo, Italy; [7]Medical Oncology, Candiolo Cancer Institute FPO-IRCCS, Candiolo, Italy; [8]Hematology and Stem Cell Transplantation Unit, Az. Osp. S. Camillo-Forlanini, Rome, Italy; [9]UOC Ematologia e Trapianto, Az. Osp. C. Panico, Tricase (Lecce), Italy; [10]Ematologia e Centro Trapianti, IRCCS Ospedale Policlinico San Martino, Genova, Italy; [11]Istituto Clinico Humanitas, Humanitas University, Rozzano-Milano, Italy; [12]UOC Ematologia AO Cosenza, Cosenza, Italy; [13]UOC Ematologia, Università degli Studi di Milano, Fondazione IRCCS Cà Granda, Ospedale Maggiore Policlinico, Milano, Italy; [14]Hematology, Azienda Policlinico Umberto I, Roma, Italy; [15]UO Ematologia, Ospedale di Rimini, AUSL della Romagna, Rimini, Italy; [16]Hematology Unit, Department of Medical and Surgical Sciences, University of Modena and Reggio Emilia, Modena, Italy; [17]U.O. Ematologia, Ospedale Santa Maria delle Croci, Ravenna, Italy. [18]SSD Ematologia, ASLTO4, Ospedali di Chivasso Cirié Ivrea, Italy; [19]Department of Hematooncology, University Hospital Ostrava, Ostrava, Czech Republic and [20]Faculty of Medicine, University of Ostrava, Ostrava, Czech Republic

°AP is currently a GlaxoSmithKline AG employee.

Ferrata Storti Foundation

Haematologica 2020
Volume 105(7):1937-1947

Correspondence:

SARA BRINGHEN
sarabringhen@yahoo.com

Received: May 20, 2019.

Accepted: September 26, 2019.

Pre-published: October 3, 2019.

doi:10.3324/haematol.2019.226407

Check the online version for the most updated information on this article, online supplements, and information on authorship & disclosures: www.haematologica.org/content/105/7/1937

ABSTRACT

In the EMN01 trial, the addition of an alkylator (melphalan or cyclophosphamide) to lenalidomide-steroid induction therapy was prospectively evaluated in transplant-ineligible patients with multiple myeloma. After induction, patients were randomly assigned to maintenance treatment with lenalidomide alone or with prednisone continuously. The analysis presented here (median follow-up of 71 months) is focused on maintenance treatment and on subgroup analyses defined according to the International Myeloma Working Group Frailty Score. Of the 654 evaluable patients, 217 were in the lenalidomide-dexamethasone arm, 217 in the melphalan-prednisone-lenalidomide arm and 220 in the cyclophosphamide-prednisone-lenalidomide arm. With regards to the Frailty Score, 284 (43%) patients were fit, 205 (31%) were intermediate-fit and 165 (25%) were frail. After induction, 402 patients were eligible for maintenance therapy (lenalidomide arm, n=204; lenalidomide-prednisone arm, n=198). After a median duration of maintenance of 22.0 months, progression-free survival from the start of maintenance was 22.2 months with lenalidomide-prednisone *vs.* 18.6 months with lenalidomide (hazard ratio 0.85, P=0.14), with no differences across frailty subgroups. The most frequent grade ≥3 toxicity was neutropenia (10% of lenalidomide-prednisone and 21% of lenalidomide patients; P=0.001). Grade ≥3 non-hematologic adverse events were rare (<15%). In fit patients, melphalan-prednisone-lenalidomide significantly prolonged progression-free survival compared to cyclophosphamide-prednisone-

lenalidomide (hazard ratio 0.72, *P*=0.05) and lenalidomide-dexamethasone (hazard ratio 0.72, *P*=0.04). Likewise, a trend towards a better overall survival was noted for patients treated with melphalan-prednisone-lenalidomide or cyclophosphamide-prednisone-lenalidomide, as compared to lenalidomide-dexamethasone. No differences were observed in intermediate-fit and frail patients. This analysis showed positive outcomes of maintenance with lenalidomide-based regimens, with a good safety profile. For the first time, we showed that fit patients benefit from a full-dose triplet regimen, while intermediate-fit and frail patients benefit from gentler regimens. ClinicalTrials.gov registration number: NCT01093196.

Introduction

In the last decade, the increased use of novel agents as initial therapy for multiple myeloma (MM) significantly improved overall survival (OS) in patients ineligible for autologous stem-cell transplantation (ASCT).[1] In Europe, two triplet regimens – bortezomib-melphalan-prednisone and melphalan-prednisone-thalidomide – are considered standards of care for elderly patients ineligible for ASCT.[2,3] Recently, based on the results of the MM020 trial, a new doublet regimen with no alkylating agent was introduced as a new standard for the treatment of transplant-ineligible patients with newly diagnosed MM. That study prospectively compared outcomes of patients treated with melphalan-prednisone-thalidomide *vs*. lenalidomide and low-dose dexamethasone (Rd), and found that Rd until disease progression improved progression-free survival (PFS) and OS, as compared with melphalan-prednisone-thalidomide.[4] The phase III trial MM-015 showed that melphalan-prednisone-lenalidomide (MPR) followed by maintenance with lenalidomide significantly prolonged PFS, as compared with melphalan-prednisone or MPR without maintenance.[5]

Maintenance therapy with lenalidomide improves outcome and its role has been extensively investigated both in ASCT-eligible and -ineligible patients. A recent meta-analysis of three randomized phase III trials confirmed PFS and OS advantages for lenalidomide maintenance after ASCT *vs*. placebo or observation. In the MM-015 trial, elderly patients were treated with lenalidomide as induction and maintenance, which reduced the risk of progression by 51% compared to lenalidomide as induction without maintenance.[5] In the Myeloma XI trial, lenalidomide maintenance reduced the risk of progression by 56% in comparison with observation.[6] Moreover, in this trial both ASCT-eligible and -ineligible patients benefited from lenalidomide maintenance.

The advantage of adding steroids to immunomodulatory drugs during maintenance therapy is unclear. In young patients eligible for ASCT, after a median follow-up of 41 months, median PFS and OS did not differ significantly between patients treated with lenalidomide plus prednisone or lenalidomide alone. No data are available from elderly patients ineligible for ASCT.[7]

The choice of best treatment for each patient is troublesome, especially in elderly patients, since they represent a heterogeneous population in terms of both physical and psycho-social functioning. Furthermore, it is now accepted that chronological and biological ages may not correspond, and that the presence of frailty, comorbidities and disabilities can affect therapy endurance. The OS of frail patients is impaired due to toxic side effects from first-line treatment which may preclude second-line treatment, with third-line therapies in >80-year old MM patients being extremely rare. The "one size fits all" is no longer a suitable approach, and many recommendations suggested that fit patients may benefit from triplet regimens, while intermediate-fit and frail patients may benefit from doublet regimens.[8,9] There are no data from prospective trials supporting these recommendations and a formal comparison between an alkylator-containing triplet regimen *vs*. an alkylator-free doublet regimen, both including lenalidomide, has not yet been performed.

The EMN01 study was designed to compare the PFS of patients treated with triplet *vs*. doublet induction regimens and the PFS following maintenance treatment with lenalidomide-prednisone *vs*. lenalidomide alone. Furthermore, before treatment, a geriatric assessment to assess patients' frailty status according to the International Myeloma Working Group (IMWG) Frailty Score was performed. With this analysis, after more than 5 years of follow-up, we would like to report the safety and efficacy of maintenance treatment in our patients and to perform a post-hoc analysis according to frailty status in both induction and maintenance treatment arms.

Methods

Study design

The study was conducted in 58 Italian and nine Czech centers between August 2009 and September 2012. The details of this multicenter randomized (1:1:1) phase III trial have already been reported and are updated here after a median follow-up of 71 months for survivors.[10] Briefly, 662 newly diagnosed (ND)MM patients ineligible for high-dose therapy plus ASCT because of age (≥65 years) or coexisting comorbidities were enrolled. The study was approved by the institutional review boards at each of the participating centers and registered at ClinicalTrials.gov (NCT01093196). All patients gave written informed consent before entering the study, which was performed in accordance with the Declaration of Helsinki.

Per protocol, patients were stratified by age (≤75 *vs*. >75 years). Based on the recent IMWG geriatric score that stratifies patients according to their frailty status (fit, intermediate-fit, and frail),[11] a post-hoc analysis including age (≤75 *vs*. 76-80 *vs*. >80 years), comorbidities (according to the Charlson score) and cognitive/physical status (according to the Activities of Daily Living and the Instrumental Activities of Daily Living scores) was conducted (*Online Supplementary Table S1*).

Procedures

Six hundred fifty-four patients were randomly assigned to receive induction (*Online Supplementary Figure S1*) with nine 28-day cycles of Rd (n=217) or MPR (n=217) or cyclophosphamide-prednisone-lenalidomide (CPR) (n=220). Rd patients received lenalidomide 25 mg/day for 21 days; dexamethasone 40 mg on days 1, 8, 15, 22 in patients 65-75 years old and 20 mg in those >75 years of age. MPR patients received lenalidomide 10 mg/day for

21 days; oral melphalan 0.18 mg/kg for 4 days in patients 65-75 years old and 0.13 mg/kg in those >75 years of age; prednisone 1.5 mg/kg for 4 days. CPR patients received lenalidomide 10 mg/day for 21 days; oral cyclophosphamide 50 mg every other day for 28 days in patients 65-75 years old and 50 mg every other day for 21 days in those >75 years of age; prednisone 25 mg every other day. After induction, patients were randomized to receive maintenance treatment with lenalidomide alone (R) 10 mg on days 1-21 every 28 days, or in combination with prednisone (RP) 25 mg every other day continuously. After the inclusion of the first 120 patients, the protocol was amended to increment the doses of lenalidomide and cyclophosphamide in patients 65-75 years old in the CPR group, due to negligible toxicities in comparison with those in the two other treatment arms. Therefore, the CPR induction schedule was changed to lenalidomide 25 mg/day for 21 days and oral cyclophosphamide 50 mg/day for 21 days.

Statistical analysis

Updated analyses were performed using data collected on October 31, 2017. All the results were evaluated on an intention-to-treat basis. For univariate analyses, the time-to-event curves were estimated using the Kaplan–Meier method and compared using the log-rank test. Time to event was expressed as median or as 5-year Kaplan–Meier estimate. The Cox proportional hazards model was used to estimate the hazard ratio (HR) values and the 95% confidence intervals (95% CI). Data were analyzed as of May 2018 using R (v3.1.1).

Results

A total of 654 patients were randomly assigned to receive induction with Rd (n=217) or MPR (n=217) or CPR (n=220) (*Online Supplementary Figure S1*). Baseline demographics and disease characteristics were previously reported[10] and were well balanced among the three groups. The median age was 73 years in the Rd and CPR arms, and 74 years in the MPR arm. Twenty-five percent of patients were classified as frail and these patients were evenly distributed among the treatment arms. A total of 402 patients completed the assigned induction treatment and were randomly allocated to receive maintenance with RP (n=198) or R (n=204) (*Online Supplementary Figure S1*, Table 1 for baseline characteristics).

The median follow-up for survivors was 71 months from enrollment. Progression or death occurred in 177 patients (82%) in the Rd arm, 166 (76%) in the MPR arm, and 194 (88%) in the CPR arm. The median PFS was 18.6 months with the doublet and 20.8 months with the triplet combinations (HR 1.05, 95% CI: 0.87-1.25, *P*=0.62) (*Online Supplementary Figure S2*). The median OS was 61.5 months with doublet and 65.7 months with triplet regimens (HR 1.09, 95% CI: 0.87-1.37, *P*=0.47). Comparing the three arms separately, the median PFS was 18.6 months in the Rd arm, 22.2 months in the MPR arm and 18.9 months in the CPR arm (MPR *vs*. CPR: HR 0.78, 95% CI: 0.63-0.96, *P*=0.02; MPR *vs*. Rd: HR 0.84, 95% CI: 0.68-1.04, *P*=0.11) (Figure 1A). The median time to next treatment (TNT) was 23.8 months in the Rd arm, 28.7 months in the MPR arm and 23.8 months in the CPR arm (MPR *vs*. CPR: HR 0.79, 95% CI: 0.64-0.98, *P*=0.03; MPR *vs*. Rd: HR 0.82, 95% CI: 0.66-1.02, *P*=0.07) (Figure 1B). The median progression-free survival 2 (PFS-2) was 41.2 months in the Rd arm, 40.2 months in the MPR arm and 40.8 months in the CPR arm (MPR *vs*. CPR: HR 0.90, 95% CI: 0.72-1.14, *P*=0.40; MPR *vs*. Rd: HR 0.94, 95% CI: 0.74-1.19, *P*=0.63) (Figure 1C). Death occurred in 115 patients (53%) in the Rd arm, 108 (50%) in the MPR arm and 107 (49%) in the CPR arm. The median OS was 61.5 months with Rd, 65.2 months with MPR and 66.4 months with CPR (MPR *vs*. CPR: HR 1.03, 95% CI: 0.79-1.35, *P*=0.83; MPR *vs*. Rd: HR 0.93, 95% CI: 0.72-1.22, *P*=0.61) (Figure 1D). The subgroup analysis of induction treatment in patients with standard- and high-risk cytogenetics showed the same trends observed in the overall population (*Online Supplementary Figure S3*).

A post-hoc analysis according to patients' frailty was performed (Figure 2). In fit patients, an advantage with the triplet regimen MPR was detected: the median PFS was 21.2 months in patients treated with Rd, 25.6 months in the MPR arm and 21.7 months in patients given CPR (MPR *vs*. CPR: HR 0.72, 95% CI: 0.52-1.00, *P*=0.05; MPR *vs*. Rd: HR 0.72, 95% CI: 0.52-0.99, *P*=0.04) (Figure 2A). The median OS was 50.2 months in the Rd group, shorter than in both the MPR (79.9 months) and CPR groups (82.9 months) (MPR *vs*. CPR: HR 1.11, 95% CI: 0.72-1.71, *P*=0.65; MPR *vs*. Rd: HR 0.75, 95% CI: 0.50-1.12, *P*=0.16) (Figure 2B). In intermediate-fit patients, no advantage of one regimen over the others was found: the median PFS was 16.6 months in the Rd arm, 20 months in the MPR arm and 20.9 months in the CPR arm (Figure 2C). The median OS was not reached in the Rd arm, was 60.8 months in the MPR arm and was 66.7 months in the CPR arm (Figure 2D). Not even in frail patients was one regimen found to be superior to another: the median PFS was 18.2 months in the Rd arm, 21.5 months in the MPR arm and 13.8 months in the CPR arm (Figure 2E). The median OS was 48.2 months with Rd, 44.7 months with MPR and 40.5 months with CPR (Figure 2F).

Table 1. Demographics and baseline characteristics of the patients receiving maintenance treatment.

Patients' characteristics	Lenalidomide (R) (n=204)	Lenalidomide-prednisone (RP) (n=198)
Age range, years	50-89	65-87
Median, years	73	73
>75 years, n (%)	61 (30%)	64 (32%)
Sex (male), n (%)	86 (42%)	105 (53%)
Karnofsky score	60-100	60-100
Median	90	90
<80, n (%)	37 (18%)	43 (22%)
Fitness		
Fit, n (%)	101 (50%)	91 (46%)
Intermediate-fit, n (%)	63 (31%)	58 (29%)
Frail, n (%)	40 (20%)	49 (25%)
Creatinine clearance, mL/min	30-168.9	30-150
Median, mL/min	72	70
International Staging System score		
I, n (%)	65 (32%)	65 (33%)
II, n (%)	92 (45%)	88 (44%)
III, n (%)	47 (23%)	45 (23%)
Cytogenetic abnormalities by FISH		
Data available, n (%)	163 (80%)	162 (82%)
Data missing, n (%)	41 (20%)	36 (18%)
High risk*, n (%)	36 (18%)	37 (19%)

* At least one among deletion 17p [del(17p)], translocation (4;14) [t(4;14)] or translocation (14;16) [t(14;16)]. FISH: fluorescence *in situ* hybridization.

During maintenance, 31% of patients in the RP group and 20% of patients in the R group had an improvement in their quality of response. In the RP group, the partial response (PR) rate increased from 87% to 95%, the very good PR (VGPR) rate from 33% to 58%, and the complete response (CR) rate from 5% to 9%. In the R group, the PR rate increased from 83% to 88%, the VGPR rate from 33% to 47%, and the CR rate from 2% to 7%.

After a median follow-up of 62 months from the random assignment to maintenance treatment arms, progression or death occurred in 153 patients (77%) in the RP group and in 164 (80%) in the R group. The median PFS was 22.2 months with RP and 18.6 months with R (HR 0.85, 95% CI: 0.68-1.06, *P*=0.14) (Figure 3A). The median TNT was 32.4 months with RP and 29.8 months with R (HR 0.95, 95% CI: 0.75-1.20, *P*=0.67) (Figure 3B). In both groups, maintenance therapy delayed the median time to next therapy (clinical progression) by approximately 10 months in comparison with the median PFS (biochemical progression). The median PFS-2 was 53.3 months with RP and 42.3 months with R (HR 1.04, 95% CI: 0.80-1.35, *P*=0.79) (Figure 3C). Death occurred in 92 patients (46%) in the RP group and 78 (38%) in the R group. The median OS was 72.3 months with RP and not reached with R therapy (HR 1.21, 95% CI: 0.89-1.64, *P*=0.22) (Figure 3D). Subgroup analysis of maintenance treatment in patients

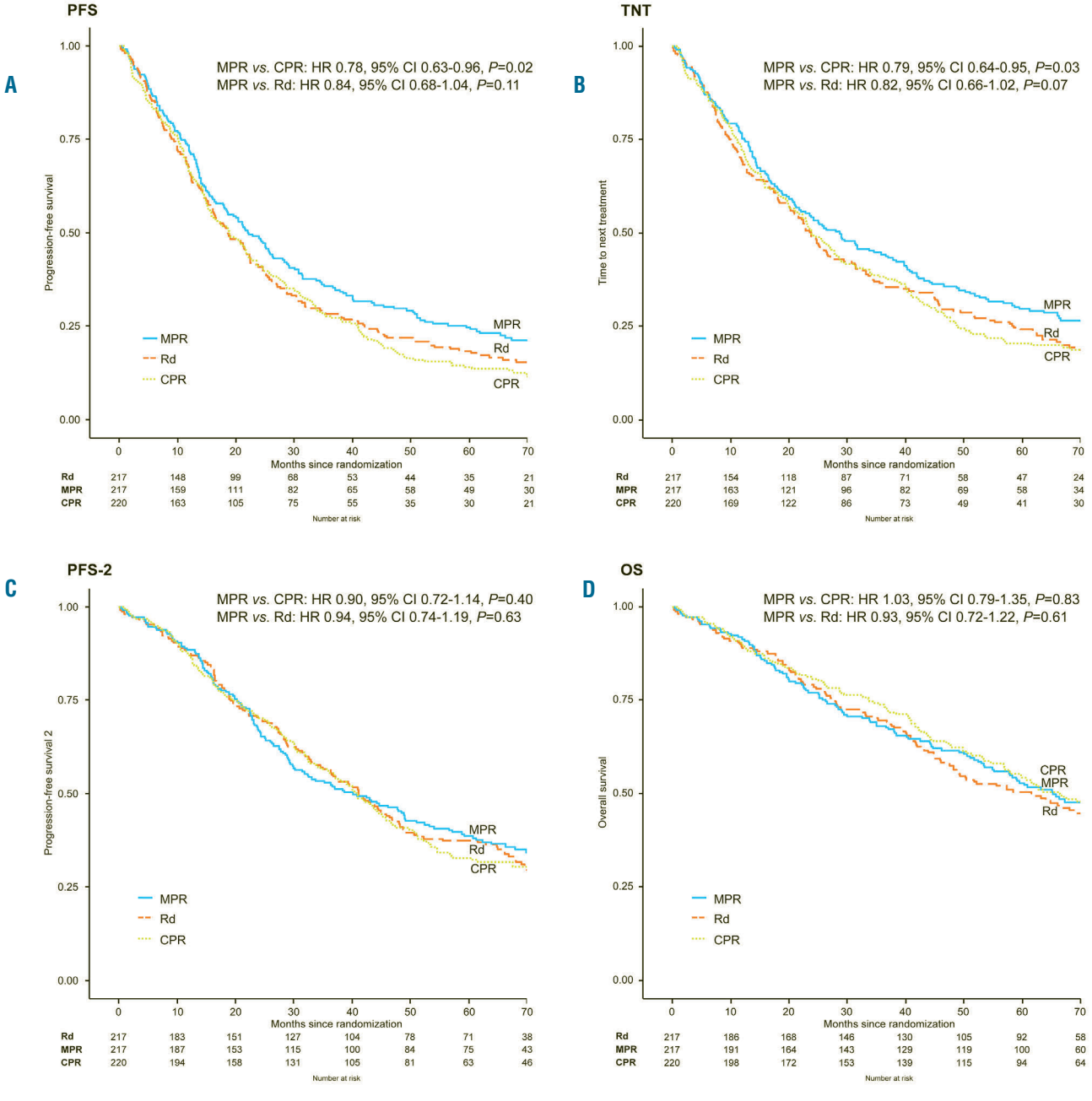

Figure 1. Survival outcomes according to induction treatment arm. (A) Progression-free survival, (B) time to next treatment, (C) progression-free survival 2 and (D) overall survival are shown. All time to events were calculated from the time of random assignment to induction treatment arms. MPR: melphalan-prednisone-lenalidomide; CPR: cyclophosphamide-prednisone-lenalidomide; Rd: lenalidomide-dexamethasone; PFS: progression-free survival; PFS-2: progression-free survival 2; TNT: time to next treatment; OS: overall survival; HR: hazard ratio; CI: confidence interval; *P*: *P* value.

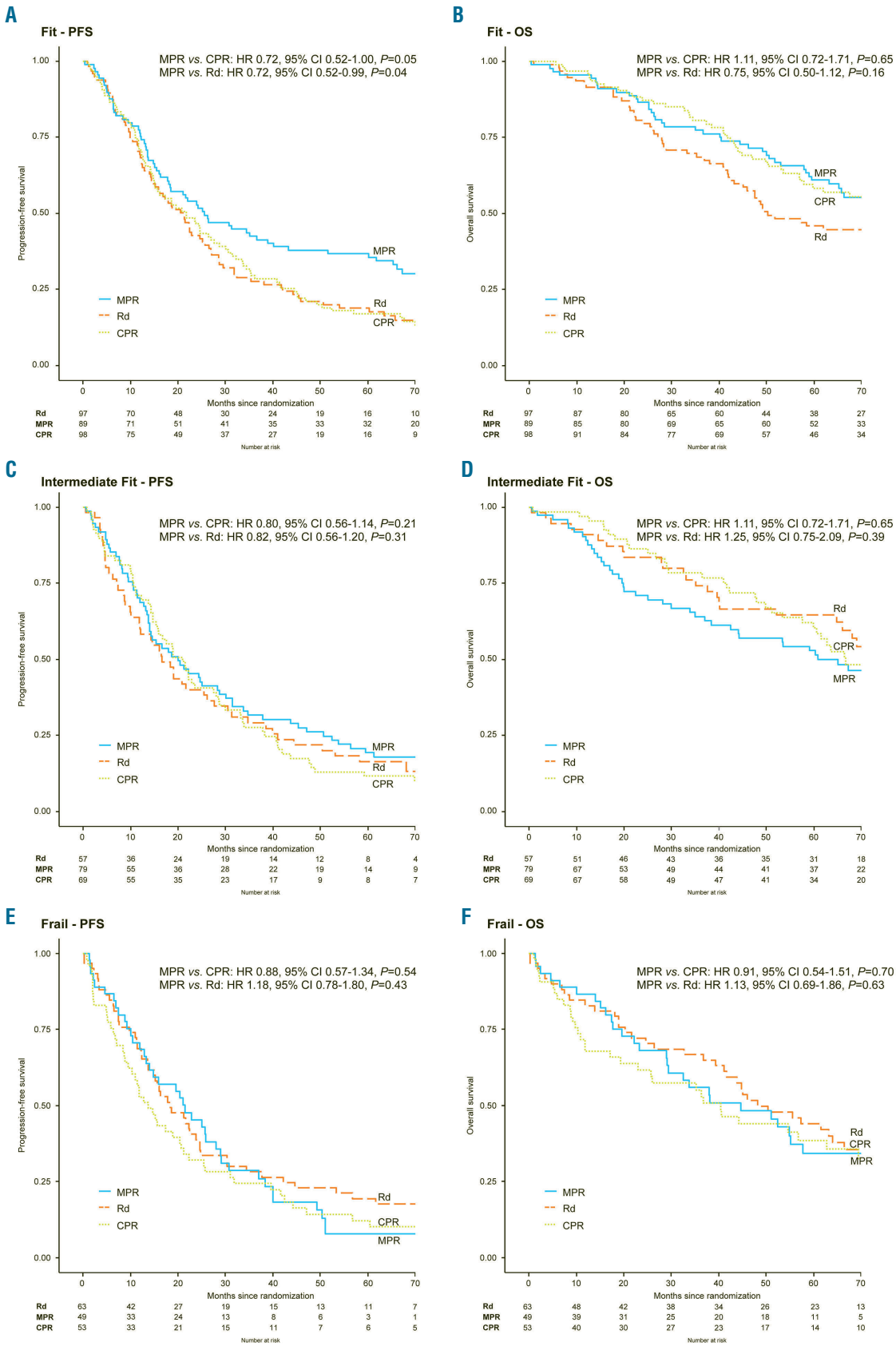

Figure 2. Post-hoc analysis according to frailty status in patients treated with different induction treatments. (A, B) Progression-free survival (PFS) (A) and overall survival (OS) (B) in fit patients according to treatment arm. (C, D) PFS (C) and OS (D) in intermediate-fit patients according to treatment arm. (E; F) PFS (E) and OS (F) in frail patients according to treatment arm. All time to events were calculated from the time of random assignment to induction treatment arms. MPR: melphalan-prednisone-lenalidomide; CPR: cyclophosphamide-prednisone-lenalidomide; Rd: lenalidomide-dexamethasone; HR: hazard ratio; CI: confidence interval; *P*: *P* value.

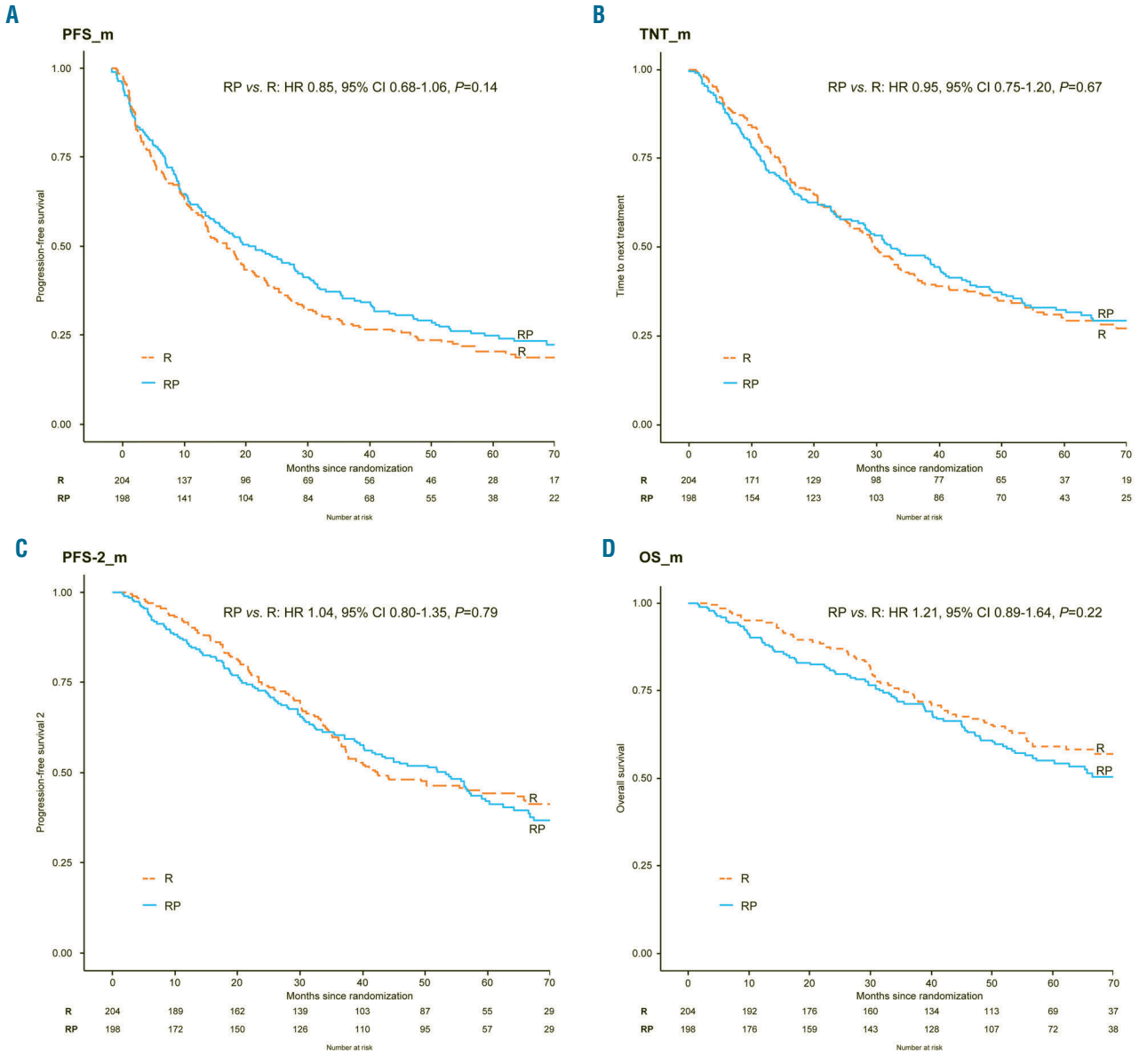

Figure 3. Survival outcomes according to maintenance treatment arm. (A) Progression-free survival, (B) time to next treatment, (C) progression-free survival 2 and (D) overall survival. All time to events were calculated from the time of random assignment to maintenance treatment arms (_m). R: lenalidomide; RP: lenalidomide-prednisone; PFS: progression-free survival; PFS-2: progression-free survival 2; TNT: time to next treatment; OS: overall survival; _m: from the random assignment to maintenance treatment arms; HR: hazard ratio; CI: confidence interval; *P*: *P* value.

with standard- or high-risk cytogenetics showed the same trends observed in the overall population (*Online Supplementary Figure S4*).

A post-hoc analysis according to patients' frailty was also performed for the maintenance phase (Figure 4) and no significant advantage of one regimen over the other was found. In fit patients, the median PFS from start of maintenance was 24.4 months with RP and 19.6 months with R (HR 0.84, 95% CI: 0.60-1.16, *P*=0.29) (Figure 4A). Not even in intermediate-fit and frail patients was one regimen found to be superior to the other (Figure 4C, E). No difference in OS was detected (Figure 4B, D, F).

Safety profiles of induction were reported in the initial analysis.[10] Briefly, the most frequent grade ≥3 toxicities were hematologic. At least one grade ≥3 hematologic adverse event was reported in 29% of patients treated with Rd, 68% of those treated with MPR and 32% of patients treated with CPR (*P*<0.001). The rate of at least one grade ≥3 non-hematologic adverse event did not exceed 31% in any of the three arms. The most frequent grade ≥3 non-hematologic toxicities were infections (9% with Rd, 11% with MPR and 6.5% with CPR), constitutional adverse events (5% with Rd, 9.5% with MPR and 3.5% with CPR) and cardiac toxicities (6% with Rd, 4.5% with MPR and 6% with CPR); no significant differences were detected among the three arms. The rate of discontinuation due to adverse events was similar in the three arms: 14% in the Rd arm, 18% in the MPR arm and 15% in the CPR arm. Lenalidomide was reduced in 16% of patients treated with Rd, 21% of those treated with MPR and 18% of CPR-treated patients, without significant differences among the three arms.

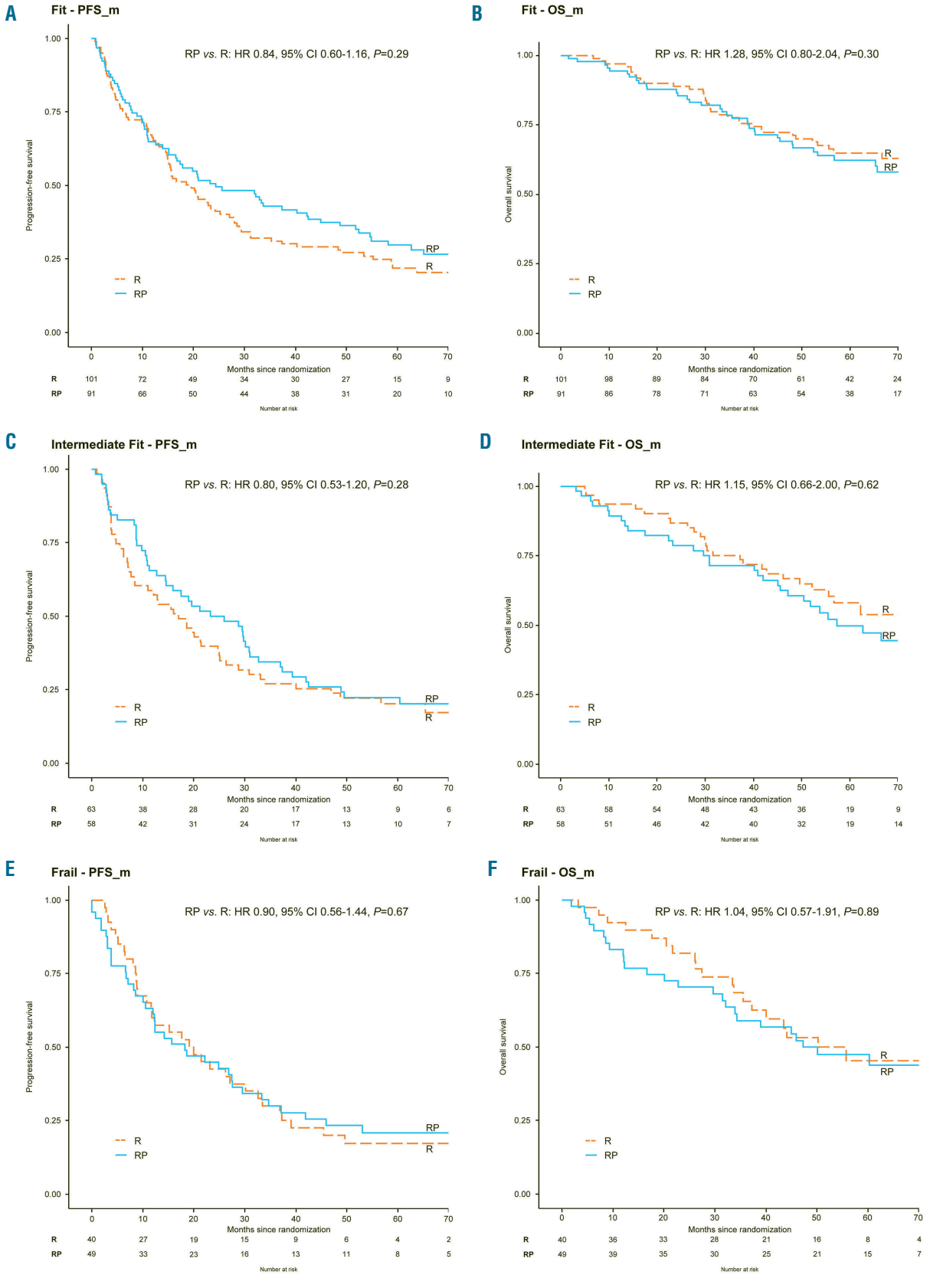

Figure 4. Post-hoc analysis according to frailty status in patients treated with different maintenance treatments. (A, B) Progression-free survival (PFS) (A) and overall survival (OS) (B) in fit patients according to treatment arm. (C, D) PFS (C) and OS (D) in intermediate-fit patients according to treatment arm. (E, F) PFS (E) and OS (F) in frail patients according to treatment arm. All time to events were calculated from the time of random assignment to maintenance treatment arms (_m). R: lenalidomide; RP: lenalidomide-prednisone; PFS_m: progression-free survival from the random assignment to maintenance treatment arms; OS_m: overall survival from the random assignment to maintenance treatment arms; HR: hazard ratio; CI: confidence interval; *P*: *P* value.

The incidence of at least one hematologic adverse event was similar in fit, intermediate-fit and frail patients. The rate of non-hematologic adverse events as well as the rate of discontinuation due to adverse events increased with worsening of fitness status (*Online Supplementary Table S2*). Data from each induction treatment group are presented in Table 3. Frail patients receiving the alkylating-containing regimens had the highest rate of discontinuation due to adverse events.

During maintenance, the most frequent grade ≥3 toxicity was neutropenia, which occurred in 10% of RP and 21% of R patients (P=0.001) (Table 2). Grade ≥3 non-hematologic adverse events were rare and occurred in <15% of patients. The proportion of patients requiring dose discontinuation due to adverse events during maintenance was 18% in the R arm and 21% in the RP arm. The proportion of patients requiring dose reduction during maintenance was 9% in the RP arm and 16% in the R arm (P=0.05). Fifteen cases of second primary malignancies were recorded: six (3%) in the RP group and nine (4%) in the R group. All second primary malignancies were solid tumors.

In the RP group, 133 patients required a second line of therapy: 94 (71%) received bortezomib, 3 (2%) thalidomide or lenalidomide, 17 (13%) other chemotherapy, 16 (12%) died before starting treatment and 3 (2%) were lost to follow-up. In the R group, 138 patients required a second line of therapy: 102 (74%) received bortezomib, 3 (2%) thalidomide or lenalidomide, 21 (15%) other chemotherapy, 7 (5%) died before starting treatment and 5 (4%) were lost to follow-up.

The incidences of at least one hematologic and non-hematologic grade ≥3 adverse events were similar in fit, intermediate-fit and frail patients. Frail patients had the highest rate of discontinuation due to adverse events; a trend towards a higher discontinuation due to adverse events was found in frail *vs.* fit patients (*Online Supplementary Table S2*). Data in each maintenance treatment group are presented in Table 4.

Discussion

One of the aims of this analysis was to compare RP *vs.* R alone as maintenance treatment after induction therapy.

While the use of maintenance therapy is a standard approach in young ASCT-eligible patients with newly diagnosed MM, its use in elderly MM patients after induction treatment is more debated.

In our trial, both maintenance regimens improved the quality of response and produced a time from biochemical to clinical relapse of approximately 10 months. Indeed, as recently described, even when neoplastic plasma cells become lenalidomide-refractory, the immunomodulatory effect of lenalidomide on immune cells may help prolong disease control.[12] A trend toward a slight improvement of PFS in the RP arm was noted as compared to R alone, while OS data were still immature after only 170 deaths (42% of patients).

Regarding safety, maintenance treatment with both regimens was feasible with grade ≥3 non-hematologic adverse event rates of less than 15%. The only difference

Table 2. Grade ≥3 adverse events during maintenance treatment.

Grade ≥3 adverse events	Lenalidomide (R) (n=204)	Lenalidomide-prednisone (RP) (n=198)
Hematologic		
At least one event	46 (23%)	26 (13%)
Anemia	4 (2%)	4 (2%)
Neutropenia	43 (21%)	19 (10%)
Thrombocytopenia	4 (2%)	5 (3%)
Non-hematologic		
At least one event	22 (11%)	28 (14%)
Cardiological	2 (1%)	1
Acute myocardial infarction	1	1
Other	1	0
Vascular	5 (2%)	4 (2%)
Deep vein thrombosis/ thromboembolism	2 (1%)	3 (2%)
Renal	1	2 (1%)
Dermatological	2 (1%)	3 (2%)
Infectious	2 (1%)	4 (2%)
Pneumonia	0	1
Bronchitis	1	1
Sepsis	0	1
Other/not specified	1	1
Nervous	2 (1%)	7 (4%)
Second primary malignancies	9 (4%)	6 (3%)
Hematologic	0	0
Solid	9 (4%)	6 (3%)
Other	9 (4%)	5 (3%)
Discontinuation due to adverse events	36 (18%)	41 (21%)

Table 3. Grade ≥3 hematologic adverse events, non-hematologic adverse events, treatment discontinuation due to adverse events and toxic deaths during induction treatment according to patients' frailty status.

Treatment arm (n)	CPR (n=220)			MPR (n=211)			Rd (n=212)		
Frailty Score class (n)	Fit (98)	Intermediate -fit (69)	Frail (53)	Fit (88)	Intermediate-fit (76)	Frail (47)	Fit (94)	Intermediate-fit (57)	Frail (61)
Hematologic AE G ≥3, n (%)	31 (32)	23 (33)	17 (32)	62 (70)	46 (61)	35 (74)	26 (28)	13 (23)	22 (36)
Non-hematologic AE G ≥3, n (%)	22 (22)	22 (32)	22 (42)	22 (25)	22 (29)	22 (45)	24 (26)	15 (26)	24 (39)
Discontinuation due to AE, n (%)	8 (8)	9 (13)	16 (30)	10 (11)	17 (22)	10 (21)	9 (10)	9 (16)	12 (20)
Death due to AE, n (%)	1 (1)	0	7 (13)	1 (1)	2 (3)	2(4)	1 (1)	1 (2)	4 (7)

CPR: cyclophosphamide-prednisone-lenalidomide; MPR: melphalan-prednisone-lenalidomide; Rd: lenalidomide-dexamethasone; AE: adverse events; G: grade; n: number; %: percentage.

between treatment arms was the most frequent grade ≥3 neutropenia in the R arm compared to RP, which did not translate into a higher infection rate. One of the possible explanations of this finding is based on the effect of prednisone on neutrophils.[13] Glucocorticoid therapy inhibits L-selectin expression on neutrophils that are more prone to enter the bloodstream, delays the migration of circulating neutrophils into tissues, produces a direct antiapoptotic effect on these cells and prompts the release of young neutrophils from the bone marrow leading to an increased peripheral blood neutrophil count.

While dose discontinuation was not different in the RP and R arms, patients treated with R alone more often required dose reductions, which slightly impaired the efficacy of maintenance treatment.

The treatment goal in elderly MM patients is not a trivial issue and international guidelines suggesting personalized treatment according to patients' frailty status are currently based on expert opinions, without the availability of high-quality evidence.[8,9] With all the limitations of a post-hoc analysis, this is the first analysis to show that fit patients benefit from a full-dose triplet regimen while intermediate-fit and frail patients benefit from gentler regimens.

Indeed, fit patients treated with MPR induction showed a statistically significant PFS advantage over those treated with CPR or Rd. Intermediate-fit and frail patients did not show any PFS benefit from one regimen over the others.

A higher hematologic adverse event rate was noted with MPR induction compared to induction with the other regimens.

After the protocol amendment, introduced because of negligible adverse events, the dose of cyclophosphamide was increased. Nevertheless, despite the amendment, cyclophosphamide could still have been underdosed as compared to the dose delivered in other cyclophosphamide-containing regimens used in younger patients.[14,15] This issue could have mitigated the impact on PFS of the addition of cyclophosphamide to lenalidomide-steroid doublets even in fit patients.

Hematologic adverse events were not dependent on patients' frailty status, while the rate of non-hematologic adverse events was correlated to the fitness status but not to the type of induction regimen. Indeed, physicians' limitations to treat frail patients effectively are based on the patients' reduced organ function reserve leading to a higher rate of non-hematologic toxicity, rather than on the hematologic toxicity that is mainly dependent on the treatment itself, as observed with the melphalan-containing regimen in this study.

As expected, frail patients experienced the highest discontinuation rate due to toxicity, and discontinuation was more frequent among patients receiving the alkylator-containing regimens than among those treated with the Rd doublet. It is, therefore, reasonable to support the choice of a full-dose alkylator-containing triplet regimen in fit patients, in order to prioritize the efficacy. Conversely, intermediate-fit and frail patients could benefit from a gentler regimen, since a better safety profile should be pursued in the absence of an advantage in PFS or OS.

In the FIRST trial, a retrospective proxy algorithm (which calculated data from questionnaires on medical history and quality of life) was used to estimate the IMWG Frailty Score.[16] In that post-hoc analysis, continuous Rd was compared to an alkylator-containing triplet regimen; however, differently from our analysis, the novel agent used in the control arm was the first-generation immunomodulatory drug thalidomide. Indeed, in that analysis continuous Rd produced longer PFS and OS compared to melphalan-prednisone-thalidomide across all frailty subgroups, with the greatest benefits observed in fit patients. No lenalidomide-containing triplet regimens were included in that trial.

Despite the limitations of inter-trial comparisons, Rd induction produced a shorter PFS in our study than in the FIRST study (26 months with continuous Rd and 21 months with Rd given for 18 months).[17] Of note, in that trial Rd was given for a fixed duration of 18 months or continuously, while in our trial Rd was given only for 9 months as induction treatment and then both maintenance regimens included lenalidomide given at a lower dose (10 mg instead of 25 mg) and lower steroid doses or no steroids at all, depending on the treatment arm. The same observation, with the same limitations of inter-trial comparisons, can also be applied to the control arm of the more recent MAIA study, in which a median PFS of 31.9 months was obtained with continuous Rd (even longer than the PFS obtained in the FIRST study with an identical regimen).[18]

However, the role of continuous, full-dose treatment *vs.* full-dose induction followed by low-dose maintenance in frailty-defined populations of elderly patients remains an open issue.

Recently, initial results from a randomized phase III trial comparing continuous Rd *vs.* Rd induction followed by lenalidomide maintenance (Rd-R) in intermediate-fit patients were reported.[19] Notably, in this population of patients, continuous Rd did not produce an advantage in PFS compared to Rd-R (15.5 months *vs.* 18.3 months). On the

Table 4. Grade ≥3 hematologic adverse events, non-hematologic adverse events, treatment discontinuation and toxic deaths during maintenance treatment according to patients' frailty status.

Treatment arm (n)	Lenalidomide (R) (n=204)			Lenalidomide-prednisone (RP) (n=198)		
Frailty Score class (n)	Fit (101)	Intermediate-fit (63)	Frail (40)	Fit (91)	Intermediate-fit (58)	Frail (49)
Hematologic AE G ≥3, n (%)	24 (24)	13 (21)	9 (22)	10 (11)	6 (10)	10 (20)
Non-hematologic AE G ≥3, n (%)	12 (12)	5 (8)	5 (12)	12 (13)	9 (16)	7 (14)
Discontinuation due to AE, n (%)	16 (16)	9 (14)	11 (28)	14 (15)	16 (28)	11 (22)
Death due to AE, n (%)	2 (2)	1 (2)	2 (5)	2 (2)	2 (3)	4 (8)

AE: adverse events; G: grade; n: number; %: percentage.

other hand, event-free survival (progression or death from any cause/lenalidomide discontinuation/hematologic grade 4 or non-hematologic grade 3-4 adverse events) was significantly better in the Rd-R arm than in the continuous Rd arm.

These results suggest that at least in intermediate-fit elderly patients with NDMM, treatment intensity during the maintenance phase can be de-escalated with no negative impact on outcome.

The EMN01 trial enrolled patients from 2009 to 2012; thereafter, less toxic and more effective combinations began to be available. For instance, the addition of bortezomib to Rd led to a clinically meaningful improvement in PFS and OS in NDMM patients without intent for immediate ASCT, irrespective of the patients' age.[20] In NDMM patients, the addition of the anti-CD38 monoclonal antibody daratumumab to bortezomib-melphalan-prednisone or Rd doubled PFS, with mild and manageable toxicity.[18,21] Besides, studies exploring the addition of a monoclonal antibody to the bortezomib-Rd combination are ongoing with very promising early results.[22]

Contextualizing our data, quadruplet or triplet regimens containing monoclonal antibodies, immunomodulatory drugs and/or proteasome inhibitors may be the best choices for fit, elderly patients. However, there is still the need for safety and efficacy data on selected intermediate-fit and frail populations receiving new combinations at full or reduced doses. As an example, in the MAIA trial, continuous daratumumab-Rd significantly prolonged PFS compared to continuous Rd, but a higher incidence of infections and a lower lenalidomide cumulative dose due to dose reduction/discontinuation were noted in the daratumumab-Rd arm.[23] Regarding maintenance, data about combinations of monoclonal antibodies plus immunomodulatory drugs outside of the context of continuous therapy are not currently available in elderly patients. In the experimental arm of the ALCYONE trial, daratumumab monotherapy after induction therapy with the daratumumab-bortezomib-melphalan-prednisone quadruplet was well tolerated and improved the duration and depth of response.[24] A longer follow-up of these two studies will inform us about the safety of monoclonal antibody maintenance and the feasibility of long-term treatment with monoclonal antibodies plus immunomodulatory drugs in elderly patients.

Our analysis has some limitations. The trial was designed to show superiority of a three-drug induction regimen over a two-drug induction regimen in the overall population, and thus the study power was not enough to detect a statistically significant difference in the frailty subgroups. However, the outcome differences between treatment arms in fit patients were high enough to reach significant levels.

Moreover, our analysis based on the frailty status was not pre-specified, but the geriatric assessment adopted to calculate the IMWG Frailty Score was obtained from the enrolled patients before the start of therapy. Although patients' allocation to treatment arms was not stratified by IMWG Frailty Score, the stratification by age led to a uniform distribution of fit, intermediate-fit, and frail patients across treatment arms.

In conclusion, this trial showed that the triplet MPR prolonged PFS compared to gentler regimens in elderly fit but not in intermediate-fit and frail MM patients. In intermediate-fit and frail patients, in the absence of differences in terms of efficacy, safety must be prioritized. Maintenance with lenalidomide-based regimens led to good outcomes with a good safety profile.

These data provide the basis for personalized treatment according to a patients' frailty status. Different combinations of new-generation immunomodulatory drugs, proteasome inhibitors and monoclonal antibodies should be evaluated in fit, intermediate-fit and frail patients to confirm these observations. Novel compounds with a good safety profile in combination with a lenalidomide-based maintenance treatment should also be explored in elderly patients.

Role of the funding source

The EMN01 study (NCT01093196) was sponsored by Fondazione Neoplasie Sangue [FO.NE.SA.] ONLUS (Italy) and supported by funding from Celgene, which had no role in the study's design, data collection, data analysis, data interpretation, writing of the report or publication of this contribution. The corresponding author had full access to all the data in the EMN01 study and had final responsibility for the decision to prepare and submit this manuscript for publication, together with the other authors.

Acknowledgments

We thank all the patients who participated in the study, the nurses Silvia Boscolo and Concetta Calicchio and the data managers Antonella Fiorillo and Elena Tigano.

References

1. Palumbo A, Anderson K. Multiple myeloma. N Engl J Med. 2011;364(11):1046-1060.
2. Palumbo A, Bringhen S, Caravita T, et al. Oral melphalan and prednisone chemotherapy plus thalidomide compared with melphalan and prednisone alone in elderly patients with multiple myeloma: randomised controlled trial. Lancet. 2006;367(9513):825-831.
3. San Miguel JF, Schlag R, Khuageva NK, et al. Bortezomib plus melphalan and prednisone for initial treatment of multiple myeloma. N Engl J Med. 2008;359(9):906-917.
4. Benboubker L, Dimopoulos MA, Dispenzieri A, et al. Lenalidomide and dexamethasone in transplant-ineligible patients with myeloma. N Engl J Med. 2014;371(10):906-917.
5. Palumbo A, Hajek R, Delforge M, et al. Continuous lenalidomide treatment for newly diagnosed multiple myeloma. N Engl J Med. 2012;366(19):1759-1769.
6. Jackson GH, Davies FE, Pawlyn C, et al. Lenalidomide maintenance versus observation for patients with newly diagnosed multiple myeloma (Myeloma XI): a multicentre, open-label, randomised, phase 3 trial. Lancet Oncol. 2019;20(1):57-73.
7. Gay F, Oliva S, Petrucci MT, et al. Chemotherapy plus lenalidomide versus autologous transplantation, followed by lenalidomide plus prednisone versus lenalidomide maintenance, in patients with multiple myeloma: a randomised, multicentre, phase 3 trial. Lancet Oncol. 2015;16(16):1617-1629.
8. Larocca A, Dold SM, Zweegman S, et al. Patient-centered practice in elderly myeloma patients: an overview and consensus from the European Myeloma Network (EMN). Leukemia 2018;32(8):1697-1712.
9. Salvini M, D'Agostino M, Bonello F, Boccadoro M, Bringhen S. Determining treatment intensity in elderly patients with multiple myeloma. Expert Rev Anticancer Ther. 2018;18(9):917-930.
10. Magarotto V, Bringhen S, Offidani M, et al. Triplet vs. doublet lenalidomide-containing regimens for the treatment of elderly patients with newly diagnosed multiple myeloma. Blood. 2016;127(9):1102-1108.
11. Palumbo A, Bringhen S, Mateos M-V, et al. Geriatric assessment predicts survival and toxicities in elderly myeloma patients: an International Myeloma Working Group report. Blood. 2015;125(13):2068-2074.

12. Franssen LE, Nijhof IS, Bjorklund CC, et al. Lenalidomide combined with low-dose cyclophosphamide and prednisone modulates Ikaros and Aiolos in lymphocytes, resulting in immunostimulatory effects in lenalidomide-refractory multiple myeloma patients. Oncotarget. 2018;9(74):34009-34021.
13. Nakagawa M, Terashima T, D'yachkova Y, Bondy GP, Hogg JC, van Eeden SF. Glucocorticoid-induced granulocytosis: contribution of marrow release and demargination of intravascular granulocytes. Circulation. 1998;98(21):2307-2313.
14. Stewart AK, Rajkumar SV, Dimopoulos MA, et al. Carfilzomib, lenalidomide, and dexamethasone for relapsed multiple myeloma. N Engl J Med. 2015;372(2):142-152.
15. Jakubowiak AJ, Dytfeld D, Griffith KA, et al. A phase 1/2 study of carfilzomib in combination with lenalidomide and low-dose dexamethasone as a frontline treatment for multiple myeloma. Blood. 2012;120(9):1801-1809.
16. Facon T, Hulin C, Dimopoulos MA, et al. A frailty scale predicts outcomes of patients with newly diagnosed multiple myeloma who are ineligible for transplant treated with continuous lenalidomide plus low-dose dexamethasone on the FIRST trial. Blood. 2015;126(23). Abstract #4239 [ASH 2015 57th Meeting].
17. Facon T, Dimopoulos MA, Dispenzieri A, et al. Final analysis of survival outcomes in the phase 3 FIRST trial of up-front treatment for multiple myeloma. Blood. 2018;131(3):301-310.
18. Facon T, Kumar SK, Plesner T, et al. Phase 3 randomized study of daratumumab plus lenalidomide and dexamethasone (D-Rd) versus lenalidomide and dexamethasone (Rd) in patients with newly diagnosed multiple myeloma (NDMM) ineligible for transplant (MAIA). Blood. 2018;132(Suppl 1). Abstract #LBA-2 [ASH 2018 60th Meeting].
19. Larocca A, Salvini M, De Paoli L, et al. Efficacy and feasibility of dose/schedule-adjusted Rd-R vs. continuous Rd in elderly and intermediate-fit newly diagnosed multiple myeloma (NDMM) patients: RV-MM-PI-0752 phase III randomized study. Blood. 2018;132(Suppl 1). Abstract #305 [ASH 2018 60th Meeting].
20. Durie BG, Hoering A, Sexton R, et al. Longer term follow up of the randomized phase III trial SWOG S0777: bortezomib, lenalidomide and dexamethasone vs. lenalidomide and dexamethasone in patients (pts) with previously untreated multiple myeloma without an intent for immediate autologous stem cell transplant (ASCT). Blood. 2018;132(Suppl 1). Abstract #1992 [ASH 2018 60th Meeting].
21. Mateos M-V, Dimopoulos MA, Cavo M, et al. Daratumumab plus bortezomib, melphalan, and prednisone for untreated myeloma. N Engl J Med. 2018;378(6):518-528.
22. Ocio EM, Otero PR, Bringhen S, et al. Preliminary results from a phase I study of isatuximab (ISA) in combination with bortezomib, lenalidomide, dexamethasone (VRd) in patients with newly diagnosed multiple myeloma (NDMM) non-eligible for transplant. Blood. 2018;132(Suppl 1). Abstract #595 [ASH 2018 60th Meeting].
23. Facon T, Kumar S, Plesner T, et al. Daratumumab plus lenalidomide and dexamethasone for untreated myeloma. N Engl J Med. 2019;380(22):2104-2115.
24. Dimopoulos MA, Mateos M-V, Cavo M, et al. One-year update of a phase 3 randomized study of daratumumab plus bortezomib, melphalan, and prednisone (D-VMP) versus bortezomib, melphalan, and prednisone (VMP) in patients (pts) with transplant-ineligible newly diagnosed multiple myeloma (NDMM): Alcyone. Blood. 2018;132(Suppl 1). Abstract #156 (ASH 2018 60th Meeting].

Ferrata Storti Foundation

Haematologica 2020
Volume 105(7):1948-1956

Antithrombotic prophylaxis for surgery-associated venous thromboembolism risk in patients with inherited platelet disorders. The SPATA-DVT Study

Francesco Paciullo,[1] Loredana Bury,[1] Patrizia Noris,[2] Emanuela Falcinelli,[1] Federica Melazzini,[2] Sara Orsini,[1] Carlo Zaninetti,[2,3] Rezan Abdul-Kadir,[4] Deborah Obeng-Tuudah,[4] Paula G. Heller,[5,6] Ana C. Glembotsky,[5,6] Fabrizio Fabris,[7] Jose Rivera,[8] Maria Luisa Lozano,[8] Nora Butta,[9] Remi Favier,[10] Ana Rosa Cid,[11] Marc Fouassier,[12] Gian Marco Podda,[13] Cristina Santoro,[14] Elvira Grandone,[15,16] Yvonne Henskens,[17] Paquita Nurden,[8] Barbara Zieger,[19] Adam Cuker,[20] Katrien Devreese,[21] Alberto Tosetto,[22] Erica De Candia,[23,24] Arnaud Dupuis,[25] Koji Miyazaki,[26] Maha Othman[27] and Paolo Gresele[1]

[1]Department of Medicine, Section of Internal and Cardiovascular Medicine, University of Perugia, Italy; [2]Department of Internal Medicine, IRCCS Policlinico S. Matteo Foundation, University of Pavia, Pavia, Italy; [3]PhD program in Experimental Medicine, University of Pavia, Pavia, Italy; [4]Haemophilia Centre and Haemostasis Unit, The Royal Free Foundation Hospital and University College London, London, UK; [5]Hematología Investigación, Instituto de Investigaciones Médicas Alfredo Lanari, Universidad de Buenos Aires, CONICET, Buenos Aires, Argentina; [6]Universidad de Buenos Aires, Instituto de Investigaciones Médicas -IDIM-, Buenos Aires, Argentina; [7]Clinica Medica 1 - Medicina Interna CLOPD, Dipartimento Assistenziale Integrato di Medicina, Azienda-Ospedale Università di Padova, Dipartimento di Medicina, Università di Padova, Padova, Italy; [8]Servicio de Hematología y Oncología Médica, Hospital Universitario Morales Meseguery Centro Regional de Hemodonación, IMIB-Arrixaca, Universidad de Murcia, Murcia, Spain; [9]Unidad de Hematología, Hospital Universitario La Paz-IDIPaz, Madrid, Spain; [10]Assistance Publique-Hôpitaux de Paris, Armand Trousseau Children's Hospital, French Reference Centre for Inherited Platelet Disorders, Paris, France; [11]Unidad de Hemostasia y Trombosis, Hospital Universitario y Politecnico La Fe, Valencia, Spain; [12]Consultations d'Hémostase – CRTH, CHU de Nantes, Nantes, France; [13]Medicina III, ASST Santi Paolo e Carlo, Dipartimento di Scienze della Salute, Università degli Studi di Milano, Milan, Italy; [14]Hematology, Department of Translational and Precision Medicine, La Sapienza University of Rome, Rome, Italy; [15]Unità di Ricerca in Aterosclerosi e Trombosi, I.R.C.C.S. "Casa Sollievo della Sofferenza", S. Giovanni Rotondo, Foggia, Italy; [16]Ob/Gyn Department of the First I.M. Sechenov Moscow State Medical University, Moscow, The Russian Federation; [17]Hematological Laboratory, Maastricht University Medical Centre, Maastricht, the Netherlands; [18]Reference Centre for Platelet Disorders, Bordeaux University Hospital Centre, Rythmology and Cardiac Modeling Institute (LIRYC), Xavier Arnozan Hospital, Pessac, France; [19]Division of Pediatric Hematology and Oncology, Faculty of Medicine, Medical Center – University of Freiburg, Freiburg, Germany; [20]Perelman School of Medicine, University of Pennsylvania, Philadelphia, PA, USA; [21]Coagulation Laboratory, Department of Laboratory Medicine, Ghent University Hospital, Department of Diagnostic Sciences, Ghent University, Ghent, Belgium; [22]Hematology Department, S. Bortolo Hospital, Vicenza, Italy; [23]Hemostasis and Thrombosis Unit, Insitute of Internal Medicine, Policlinico Agostino Gemelli Foundation, IRCCS, Rome, Italy; [24]Institute of Internal Medicine and Geriatrics, Università Cattolica del Sacro Cuore, Rome, Italy; [25]Université de Strasbourg, Institut National de la Santé et de la Recherche Médicale, Etablissement Français du Sang Grand Est, Unité Mixte de Recherche-S 1255, Fédération de Médecine Translationnelle de Strasbourg, Strasbourg, France; [26]Department of Transfusion and Cell Transplantation Kitasato University School of Medicine, Sagamihara, Japan and [27]Department of Biomedical and Molecular Sciences, School of Medicine, Queen's University, Kingston, Ontario, Canada

ABSTRACT

Major surgery is associated with an increased risk of venous thromboembolism (VTE), thus the application of mechanical or pharmacologic prophylaxis is recommended. The incidence of VTE in patients with inherited platelet disorders (IPD) undergoing surgical procedures is unknown and no information on the current use and safety of

Correspondence:

PAOLO GRESELE
paolo.gresele@unipg.it

Received: May 28, 2019.

Accepted: September 25, 2019.

Pre-published: September 26, 2019.

doi:10.3324/haematol.2019.227876

Check the online version for the most updated information on this article, online supplements, and information on authorship & disclosures: www.haematologica.org/content/105/7/1948

thromboprophylaxis, particularly of low-molecular-weight-heparin in these patients is available. Here we explored the approach to thromboprophylaxis and thrombotic outcomes in IPD patients undergoing surgery at VTE-risk participating in the multicenter SPATA study. We evaluated 210 surgical procedures carried out in 155 patients with well-defined forms of IPD (VTE-risk: 31% high, 28.6% intermediate, 25.2% low, 15.2% very low). The use of thromboprophylaxis was low (23.3% of procedures), with higher prevalence in orthopedic and gynecological surgeries, and was related to VTE-risk. The most frequently employed thromboprophylaxis was mechanical and appeared to be effective, as no patients developed thrombosis, including patients belonging to the highest VTE-risk classes. Low-molecular-weight-heparin use was low (10.5%) and it did not influence the incidence of post-surgical bleeding or of antihemorrhagic prohemostatic interventions use. Two thromboembolic events were registered, both occurring after high VTE-risk procedures in patients who did not receive thromboprophylaxis (4.7%). Our findings suggest that VTE incidence is low in patients with IPD undergoing surgery at VTE-risk and that it is predicted by the Caprini score. Mechanical thromboprophylaxis may be of benefit in patients with IPD undergoing invasive procedures at VTE-risk and low-molecular-weight-heparin should be considered for major surgery.

Introduction

Venous thromboembolism (VTE) is a severe and sometimes lethal complication of major surgery triggered by the release of pro-thrombotic substances from injured tissues, immobilization, medical comorbidities and favored by thrombophilia. It occurs in 20-25% of patients undergoing general surgery and in up to 60% of patients undergoing orthopedic surgery not receiving antithrombotic prophylaxis.[1-4]

VTE can be largely prevented by the use of mechanical and/or pharmacologic antithrombotic prophylaxis. Mechanical thromboprophylaxis with compressive stockings or intermittent pneumatic compression devices reduces the risk of VTE by 64% and 60%, respectively,[5,6] while pharmacologic thromboprophylaxis with low molecular weight-heparin (LMWH) reduces VTE risk by 75%, although it doubles the risk of major bleeding.[4,7] A meta-analysis of clinical trials comparing mechanical versus pharmacologic thromboprophylaxis in general and orthopedic surgery found a 80% higher risk of deep vein thrombosis (DVT) (including asymptomatic and distal DVT) among patients treated with mechanical thromboprophylaxis but a 57% lower risk of major bleeding.[8] Moreover, a systematic review comparing intermittent pneumatic compression with elastic compressive stockings in surgical patients found a prevalence of DVT of 2.9% in the first group and of 5.9% in the second.[9] Recently, it has been observed that the addition of mechanical to pharmacologic thromboprophylaxis does not provide further benefit.[10]

The risk of VTE associated with surgery changes according to a series of variables. The American College of Chest Physicians (ACCP) evidence-based clinical practice guidelines classify surgical interventions into three VTE-risk categories depending on the type of procedure.[3] Moreover, individual VTE-risk can be estimated more accurately based on patient characteristics and risk factors using appropriate scores, one of the most widely used of which is the "Caprini score" which subdivides patients into four risk categories.[11]

The incidence of VTE in patients with inherited platelet disorders (IPD) undergoing surgical procedures at VTE-risk is unknown, and no clinical trials or large case series have ever been reported, although several reports suggest that these patients may not be protected from thrombosis,[12-15] especially when considering that some prophylactic antihemorrhagic treatments currently used in these patients for the preparation to surgery, like platelet transfusions or recombinant factor VII a (rFVIIa),[16,17] increase VTE-risk.[12,18,19]

Moreover, no systematic studies on the use of thromboprophylaxis in patients with IPD undergoing surgery have been carried out, and no information on the safety of the prophylactic administration of LMWH to IPD patients is available, although isolated reports on the safe administration of anticoagulants to IPD patients have been published.[20-24]

Recently, the large retrospective, multicenter SPATA study evaluated bleeding complications and management of surgery in patients with IPD [17] In the present study we evaluated the approach to thromboprophylaxis adopted for the IPD patients undergoing surgery at VTE-risk participating in the SPATA study. In particular, we aimed to assess current clinical decisions on VTE prevention, to estimate postoperative VTE-risk and to evaluate the association between the use of mechanical or pharmacologic thromboprophylaxis and clinical VTE incidence and surgical bleeding in IPD.

Methods

Study population

In the current sub-study we included all the surgical procedures performed in patients enrolled in the SPATA study according to well-defined laboratory and/or molecular genetic criteria[17,25-27] for whom thromboprophylaxis should have been considered according to current guidelines, including major and minor invasive interventions.[3,11,28] The decision to apply thromboprophylaxis was made by the attending physicians on an individual basis. Patients under 16 years of age were excluded due to the lower intrinsic VTE-risk in younger age.[29,30] Surgery definitions were previously reported.[17] Given the significant *in situ* thrombotic risk of central venous catheter insertion interventions,[31] these were also considered in the analysis as minor procedures with high local thrombotic risk.

A 48-item structured questionnaire on VTE-risk, thrombotic and bleeding events and antithrombotic prophylaxis had to be filled in for each at-risk procedure. The individual bleeding risk was estimated according to the type of IPD and previous individual bleeding history as assessed by the World Health Organisation (WHO)-bleeding score.[17]

The Institutional Review Board of the coordinating center

approved this sub-study (CEAS Umbria, Italy, Approval n. 13138/18).

For further details see the *Online Supplementary Materials and Methods.*

Thromboembolic risk

VTE-risk of surgical patients was estimated using the Caprini Score.[32,33] The enrolled procedures were subdivided into four classes of risk depending on the Caprini score. Surgical procedures were also classified according to procedure-related VTE-risk in three groups as suggested by the 2008 ACCP.[3] Both the Caprini and the procedure-related VTE-risk scores were centrally calculated based on the replies given by the participating investigators to the 48-item questionnaires. Further details are provided in the *Online Supplementary Materials and Methods.*

Thrombotic outcomes

Thrombotic outcomes were defined as any symptomatic thrombosis (deep venous, including distal, and superficial) and/or pulmonary embolism occurring within one month after surgery. For details see the *Online Supplementary Materials and Methods*.

Bleeding outcomes

Previous bleeding history was assessed using the WHO bleeding assessment scale (WHO-BS),[34] while excessive bleeding occurring after surgery and the rate of success of emergency treatment of post-surgical bleeding were classified as previously described.[17] Additionally, data about the need of blood transfusion after surgery were collected. Participating investigators were asked to provide informations about bleeding outcomes occurred both during and immediately after hospitalization for surgery.

The outcome of emergency treatment of excessive post-surgical bleeding was classified as successfully controlled, not responsive to treatment or re-bleeding.[17]

Statistical analysis

As this was a pilot, exploratory study without any *a priori* test hypothesis, we did not perform a formal sample size analysis. Variables not normally distributed were reported as medians and interquartile ranges (IQR), and differences were tested using the Mann–Whitney U test or the Kruskal-Wallis analysis of variance (ANOVA) test. Data are shown as medians and IQR. Categorical variables were analysed using the χ^2 test. A Cochrane-Armitage test of trend was used to evaluate the correlation between dichotomous and ordinal variables. Logistic regression analysis was performed to identify predictors of excessive post-surgical bleeding, of heparin use, of the need for anti-hemorrhagic interventions and of the success of post-surgical bleeding management. All analyses were performed using SPSS version 22.0 (IBM Corporation, Armonk, NY, USA).

Results

Patient characteristics

Out of the 829 surgical procedures included in the SPATA study, 210 carried out in 133 patients met the inclusion criteria, 132 of which were performed in females (63.8%), with 31 patients undergoing more than one procedure. Of these interventions, 110 (52.4%) were carried out in 66 patients with 14 different forms of inherited disorder of platelet function (IPFD), and 100 (47.6%) in 67 patients with seven different forms of inherited disorders of platelet number (IPND) (*Online Supplementary Table S1*). The median age at surgery was 45 years (IQR: 29-56; min 17, max 88). Two patients (0.9%), aged 19 and 26 years undergoing one procedure each, were heterozygous carriers of the FV Leiden mutation, although it should be considered that no systematic search for thrombophilic genetic mutations was made in the enrolled population;[11] procedures (5.2%) were performed in patients with a history of malignancy (median age 55 years; IQR: 52-79), and four (1.9%) in patients with chronic obstructive pulmonary disease (COPD) (median age 51 years; IQR: 42-59). 65 interventions (31%) were performed in patients with a Caprini score ≥5, 60 (28.6%) in patients with a score of 3-4, 53 (25.2%) in patients with a score between 1 and 2, and 32 (15.2%) in patients with a score of 0. The median age was 32 years (IQR: 20-49) for patients with a score of 0, 35 years (IQR: 27-46) for patients with a score of 1-2, 46 (IQR: 32-60) for patients with a score of 3-4, and 52 years (IQR: 41-61) for patients with a score ≥5. Sixty-one interventions (29%) (32 in patients with IPFD and 29 in patients with IPND) were low-risk, 114 (54%) (55 in patients with IPFD and 59 in patients with IPND) were intermediate-risk, and 35 (17%) (23 in patients with IPFD, 12 in patients with IPND) were high-risk.[3] In low-risk procedures, the median age was 49 years (IQR: 33-58), in intermediate-risk 37 years (IQR: 28-53), and in high-risk 53 years (IQR: 33-62).

Type of surgery and antithrombotic prophylaxis

72 procedures were abdominal (34.3%), 55 gynecological (26.2%), 41 orthopedic (19.5%), 14 urological (6.7%), 10 cardiovascular (4.8%), nine thoracic (4.3%), six neurosurgical (2.9%), and three spine surgeries (1.3%). 90 interventions were major surgery (43%) while the other 120 procedures (57%) were minor invasive interventions followed by immobilization for ≥24 hours. The oldest group of patients were those undergoing urological interventions (median age 58 years), while the youngest patients underwent gynecological surgery (median age 36 years). Malignancy was most frequent in patients undergoing thoracic surgery (Table 1). Of the overall 210 surgical procedures, 89% were elective and 11% urgent.

The Caprini score was higher in patients undergoing cardiovascular interventions and lower for abdominal interventions (Table 1).

Out of 210 surgical procedures, 49 (23.3%) were managed with thromboprophylaxis; of these 27 (55.1%) were managed with mechanical thromboprophylaxis alone, using either compression stockings (26 procedures) or intermittent pneumatic compression (one procedure), 19 (38.8%) with LMWH alone, and three (6.1%) with both methods (mechanical and pharmacologic).

Of the 49 interventions managed with thromboprophylaxis, 13 were orthopedic (26.0%), 12 gynecological (24.5%), seven abdominal (14.3%), seven thoracic (14.3 %), seven urological (14.3%) and three neuro-spinal (6%). LMWH prophylaxis was adopted in 22% of the orthopedic procedures, 12.7% of gynecological, 11% of thoracic, 11% of neuro-spinal surgery, 7.1% of urological and 4.2 % of abdominal (Table 1 and Figure 1). The two patients carriers of factor V Leiden mutation were both at intermediate VTE-risk and had a low WHO-BS (0 and 2, respectively). They both underwent gynecological surgery without thromboprophylaxis and did not develop VTE. Patients with a history of malignancy were all classified at an intermediate VTE-risk, and their median WHO-BS was 2. In these patients heparin was used in four procedures,

Table 1. Inherited platelet disorders patient characteristics according to type of surgery.

	Abdominal surgery (N 72)	Gynecological surgery (N 55)	Orthopedic surgery (N 41)	Urological surgery (N 14)	Cardiovascular surgery (N 10)	Thoracic surgery (N 9)	Neuro/spinal surgery (N 9)
Age in years, median (IQR)	47 (29-57)	36 (29-45)	42 (24-58)	58 (45-70)	54 (52-65)	37(28-58)	40 (16-76)
Females, N (%)	38 (54.2)	55 (100)	22 (53.7)	3 (21.4)	6 (60)	2 (22)	3 (30)
Platelet count before surgery (x10^9/L), median (IQR)	120 (65-175)	56 (34-162.5)	139 (103-191.5)	75 (5-90)	60 (425-94)	NA	NA
Malignancy, N (%)	1 (1.4)	2 (3.6)	1 (2.4)	1 (7.1)	2 (20)	3 (33)	1 (11)
WHO bleeding score, median (IQR)	2 (1-4)	2 (1-2)	2 (1-3)	2 (1-3)	3 (1-3)	2 (1-3)	3 (2-4)
Caprini score, median (IQR)	2 (1-4)	3 (2-5)	4 (2-7)	3 (2-4)	7 (3-8)	2(1-5)	2 (0-8)
Caprini class risk, median (IQR)	1 (1-2)	2 (1-3)	2 (1-2)	2 (1-2)	4 (3-4)	2 (1-4)	2 (1-4)
Use of thromboprophylaxis, N (%)	7 (9)	12 (21.8)	13 (31.7)	7 (50)	0	7 (77)	3(30)
Mechanical thromboprophylaxis, N (%)	*5 (6.9)	*7 (12.7)	4 (9.7)	6 (42.9)	0	6 (66)	2(22)
LMWH thromboprophylaxis, N (%)	3 (4.2)	7 (12.7)	9 (22)	1 (7.1)	0	1 (11)	1 (11)
Preoperative antihemorrhagic prophylaxis, N (%)	34 (62.5)	27 (49.1)	25 (62)	9 (64.3)	7 (70)	5 (55)	7 (77)
Any excessive post-surgical bleeding, N (%)	22 (30)	42 (76.5)	5 (12.5)	2 (14.3)	6 (60)	3 (33)	4 (44)

IPD: inherited platelet disorders; IQR: interquartile range; LMWH: low molecular weight heparin; NA: not available; *: in some procedures both mechanical and LMWH thromboprophylaxis was employed.

mechanical thromboprophylaxis in five and no prophylaxis in two. No VTE was recorded in this population (*Online Supplementary Table S2*).

Of the procedures at high VTE-risk according to the Caprini risk stratification (n=65),[33] thromboprophylaxis was adopted in 22 (33.8%) (LWMH in 14, mechanical in six, and both in two) with no VTE events, while in 43 it was not adopted. Regarding procedures at intermediate VTE-risk (n=60), thromboprophylaxis was used in 15 (25%) (mechanical in 11 and pharmacologic in four), while of the procedures at low VTE-risk (n=53) thromboprophylaxis was used in 10 (18.9%) (nine mechanical, one both mechanical and pharmacologic), and of the procedures at very low VTE-risk (n=32), thromboprophylaxis was used in only two patients (6.2%) (one mechanical, one pharmacologic). According to the procedure-related VTE-risk stratification[3,35] high-risk procedures, 114 intermediate-risk and 61 low-risk, were performed. Thromboprophylaxis was adopted in 42% (nine pharmacologic and six mechanical) of the high-risk procedures, in 21% (six pharmacologic, 15 mechanical and three both) of the intermediate-risk and in 16.4% (four pharmacologic and six mechanical) of the low risk procedures. The choice of using LMWH, was significantly associated with the Caprini risk class (P<0.001 and P=0.002 respectively) (*Online Supplementary Table S3*) and with the procedure-related VTE-risk class (P=0.007 and P=0.009, respectively) (Figure 2A). The use of thromboprophylaxis with LMWH was similar between elective and urgent procedures: 10.2% *versus* 13% respectively (P=not significant [n.s.]).

Older age also independently predicted the use of pharmacologic thromboprophylaxis. In fact, LMWH-treated patients were significantly older (median age 67 *vs.* 42 years; P<0.01) and had a higher median Caprini score (8 *vs.* 4; P<0.01) than non-treated patients (Table 2). Additionally, history of cancer was more frequent in heparin users than in non-users (18% *vs.* 3.2%; P=0.018).

On the contrary, neither the WHO-BS nor sex distribution (both in IPFD and IPND) were significantly associated with LMWH use.

Mechanical prophylaxis was applied with graduated compression stockings in 30 procedures (14%) and with intermittent pneumatic compression in one (0.47%), while pharmacologic prophylaxis was undertaken with enoxaparin in 18 procedures (8%), tinzaparin in one (0.47%), dalteparin in one (0.47%), and in two cases (0.95%) type was not specified. Enoxaparin was administered at a median dose of 4,000 IU/day (IQR: 2,000-5,000 IU/day) for a median duration of 15 days (IQR: 7-18), starting on the day of surgery. The use of LMWH, as well as the use of any thromboprophylaxis, increased over time during the observation period covered by the study (LMWH: overall rate [OR] 2.5; 95% confidence interval [CI]: 1.31-4.96; any thromboprophylaxis: OR 1.4; 95% CI: 0.98-2.08) (Figure 3).

Thromboprophylaxis (pharmacologic and/or mechanical) was more common in patients with IPFD compared with those with IPND (34.5% *vs.* 11%; P<0.01) due to the greater use of mechanical thromboprophylaxis in the former (24% *vs.* 3%; P<0.01), even if there was no difference in VTE-risk between the two groups. LMWH was administered in 10% of procedures carried out in patients with IPND (10 procedures), and in 10.9% of those carried out in patients with IPFD (12 procedures).

None of the patients affected by biallelic Bernard Soulier syndrome (bBSS) (n=11) and Glanzmann thrombasthenia (GT) (n=5) received pharmacologic thromboprophylaxis. This finding probably reflects the perception that the VTE-risk of these patients is low, as suggested by previous reports[14] and the fear of bleeding. In IPND, LMWH was neither administered in patients with ACTN1-related thrombocytopenia (n=5) nor in the only patient with X-linked thrombocytopenia (*Online Supplementary Table S1*). Median platelet count of the overall IPD population before surgery was 158x10^9/L (IQR: 120-287) in procedures followed by LMWH *versus* 120x10^9/L (IQR: 8-163) in those where LMWH was not administered (P=n.s.).

Thrombotic outcomes

Two thromboembolic events were recorded (0.95% of all interventions), both occurring in patients who did not receive thromboprophylaxis (3.5% of non-prophylaxed

Table 2. Differences between surgical procedures carried out with or without low molecular weight heparin thromboprophylaxis.

	LMWH use (N=22)	LMWH non use (N=188)	*P*
Age, median (IQR)	67 (79-55)	42 (25-54)	0.01
Females, N (%)	14 (63.6)	120 (63.8)	n.s.
Platelet count before surgery x10^9/L, median (IQR)	158 (120-287)	120 (8-163)	n.s.
IPFD, N (%)	12 (54.5)	98 (52.1)	n.s.
COPD, N (%)	2 (9.1)	2 (1.1)	n.s.
Malignancy, N (%)	4 (18.4)	7 (3.2)	0.018
WHO bleeding score, median (IQR)	2 (0.75-3)	2 (1-3)	n.s.
Caprini score, median (IQR)	8 (5-12)	4 (2-6)	0.02
Caprini class, median (IQR)	4 (3-4)	3(2-4)	0.01
Preoperative antihemorrhagic prophylaxis, N (%)	12 (54.5)	113 (60.1)	n.s.
Any excessive post-surgical bleeding, N (%)	4 (18.2)	46 (25.8)	n.s.
Treatment of post-surgical bleeding, N (%)	6 (28.6)	49 (27.2)	n.s.
Post-surgical bleeding duration, hours, median (IQR)	6 (4-8)	6 (1-6)	n.s.
Failure of post-surgical bleeding control, N (%)	4 (19)	13 (7)	n.s.
Thrombosis, N (%)	0	2 (1)	n.s.

IQR: interquartile range; COPD: chronic obstructive pulmonary disease; IPFD: inherited platelet function disorders; IPND: inherited platelet number disorders; LMWH: low molecular weight heparin; n.s.: not significant.

procedures). One was a pulmonary embolism (PE) in a bBSS patient who underwent mitral valve surgery, the other a femoral DVT in a GT patient occurring after the placement of a central venous femoral catheter for blood transfusions. Both patients were at high VTE-risk[33] (Caprini score 12 and 8, respectively), had received prophylactic platelet transfusions before the invasive procedure, and had suffered excessive post-procedural bleeding prompting red blood cell transfusions. The patient suffering from PE was a 56-year-old obese woman affected by chronic obstructive pulmonary disease. She was then treated with therapeutic dose enoxaparin, but died in hospital from septic shock, disseminated intravascular coagulation and acute respiratory distress syndrome. The patient suffering from DVT was a 60-year-old woman and she was then treated with therapeutic dose enoxaparin for three months, without bleeding complications and with complete resolution of the femoral thrombosis. Both patients had previously undergone major elective surgery without thromboprophylaxis and without thrombotic complications. When dividing the included surgeries according to procedure-related VTE risk, in two of 35 high-risk procedures (0.7%, both IPFD) a VTE event occurred, while in 114 intermediate-risk procedures and 61 low-risk procedures no VTE occurred.

Bleeding outcomes

The percentage of patients who suffered from excessive bleeding after surgery was not significantly different in LMWH users compared with non-users (4 of 22: 18.2% *vs.* 46 of 188: 25.8%; *P*=0.5) and no significant difference in bleeding duration after surgery was found between heparin users and non-users (Table 2). The rate of excessive bleeding was instead significantly higher in urgent (45.5%) than in elective (22.5%) procedures (*P*<0.05).

Also the need of post-surgical blood transfusions did not differ between heparin users and non users (18% *vs.* 19%; *P*=0.51) as well as the use of post-surgical anti-hemorrhagic interventions. In 57 cases emergency treatment of post-surgical bleeding was required (27.1%), with platelet transfusions administered in 38 procedures, anti-fibrinolytic agents in nine, Desmopressin (DDAVP) in one, rFVII in one, other not specified treatment in six, and combination therapy with anti-fybrinolytic and DDAVP in two.

Thromboprophylaxis did not predict the need of post surgical anti-hemorrhagic intervention while the bleeding history did (*Online Supplementary Table S4*). Finally, heparin use was not significantly associated with the rate of success of emergency treatment of excessive post-surgical bleeding, although percentages of cases with treatment failures were numerically higher in LMWH users than in non-users (19% *vs.* 7%; OR 2.05, 95% CI: 0.496-8.536; *P*=0.321) (Table 2 and *Online Supplementary Table S5*). Preoperatory prophylactic prohemostatic treatment was adopted in 125 procedures (59%), in 78 with platelet transfusions, in nine with anti-fibrinolytic agents, in six with DDAVP, in three with activated rFVII and in three with a not-specified agent, in 12 with anti-fibrinolytic agents and DDAVP, in six with platelet transfusions, anti-fibrinolytic and DDAVP in combination, in four with platelet transfusions and anti-fibrinolytics in combination, in two with platelet transfusions and DDAVP in combination, in one with antifibrinolytic agents and a not-specified agent combination, in one with platelet transfusions and not-specified agent combination. Thromboprophylaxis with LMWH was adopted in 10 procedures (11.8%) not managed with preoperatory prohemostatic prophylaxis and in 12 (9.6%) of those managed with preoperatory thromboprohylaxis (*P*=0.651).

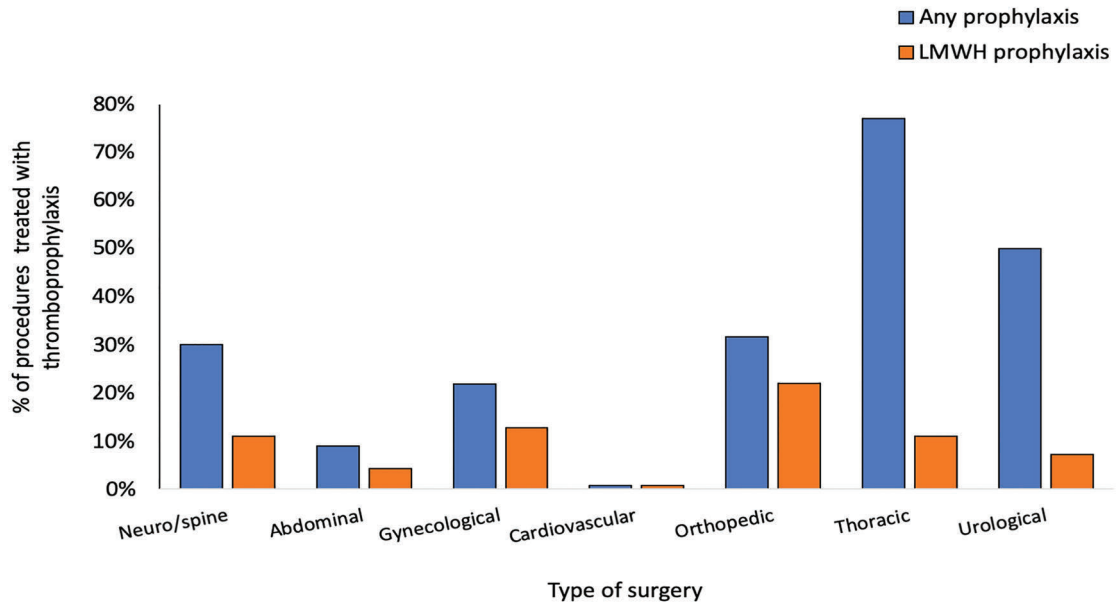

Figure 1. Use of thromboprophylaxis in different types of surgery in the inherited platelet disorder population.

Discussion

Our data show that the current use of thromboprophylaxis in patients with IPD undergoing surgery at VTE-risk is low, probably due to fear of bleeding complications and to the belief that these patients are protected from VTE. In the general population the prevalence of pharmacologic thromboprophylaxis use has been estimated to be 17.7% in neurosurgery, 27% in abdominal surgery, 50% in gynecological surgery, 52% in cardiovascular surgery, 67% in urological surgery, 91% in orthopedic surgery, and 98% in thoracic surgery,[35-38] while in our IPD population it was 0% in cardiovascular surgery, 9% in abdominal surgery, 11% in neuro and spinal surgery, 21.8% in gynecological surgery, 31.7% in orthopedic surgery, 50% in urological surgery, and 77% in thoracic surgery. In IPD patients, as expected, the most frequently employed thromboprophylaxis was mechanical, principally with elastic compression stockings. In otherwise healthy subjects undergoing general and orthopedic surgery the use of compression stockings was shown to exert a significant protective effect against VTE compared with no stockings (9% *vs.* 21%; OR 0.35, 95% CI: 0.28-0.43).[39] In our IPD population this approach seemed to be effective, as no patients using post-surgery elastic compression stockings developed thrombosis, including patients at high risk based on the Caprini score.

In the general population, the risk of surgery-associated VTE in patients not undergoing thromboprophylaxis is strongly dependent on the Caprini score, with an incidence lower than 0.5% when the score is 0, 3% when the score is 1-2, 5% when the score is 3-4, and ≥ 6% when the score is ≥5.[11,33,40] In our IPD population not receiving thromboprophylaxis, no VTE was observed in patients with a Caprini score <5 while in patients with a Caprini score ≥5 symptomatic VTE occurred in 4.7% of the procedures. These data could suggest that the incidence of surgery-associated symptomatic VTE is indeed lower in patients with IPD that in healthy controls, at least when the Caprini score is not high. The ACCP guidelines classify surgical interventions in three groups depending on the risk of developing VTE: low risk (<10%), including minor surgery and interventions not requiring patient immobilization, moderate risk (10-40%), including gynecological and urological open surgery, and high risk (risk up to 80%), including hip or knee arthroplasty, hip fracture surgery, spinal cord injury and procedures associated with high bleeding risk.[3] In our IPD patients, in the high-risk group[3] 58% of the procedures (21 interventions) were performed without prophylaxis and 9.5% of these were followed by VTE, while no VTE events were observed in moderate or low-risk procedures carried out without thromboprophylaxis. Of the two thromboembolic events recorded, one was observed in a GT patient undergoing a femoral vein catheter insertion and the other in a bBSS patient undergoing mitral valve surgery, both with a high individual VTE-risk (Caprini score of 8 and 12, respectively) and not receiving any thromboprophylaxis. Interestingly, the latter is, to our knowledge, the first case of VTE described in a bBSS patient. Pharmacologic thromboprophylaxis with LMWH was adopted in only 10% of all surgical procedures at VTE-risk in our IPD population. The use of thromboprophylaxis with LMWH increased over the observation period covered by the study, reflecting the increased awareness of the thrombotic risk of surgical procedures and of the efficacy of pharmacologic thromboprophylaxis. When heparin thromboprophylaxis was applied, its use did not seem to be guided by the assessment of the individual bleeding risk, but rather by the thromboembolic risk. Indeed, the Caprini score was strongly and independently associated with heparin use in our case series. No VTE was observed in patients undergoing LMWH prophylaxis, including in those belonging to the highest VTE-risk categories according to both the Caprini and procedure-related VTE scores.

LMWH use was neither associated with an increased rate of excessive post-surgical bleeding nor with enhanced need for post-surgical antihemorrhagic intervention. Also the use of preoperative anti-hemorragic prophylaxis was similar in patients treated or not with LMWH. Thus, our results suggest that thromboprophylaxis with LMWH may be safer than anticipated in IPD patients. On the other hand, it should be pointed out that although LMWH did not significantly affect the success rate of emergency treatment of post-surgical bleeding, a numerically higher number of insuccess was observed in patients treated with LMWH. Thus, caution should be used when deciding about LMWH prophylaxis for IPD patients, especially for those at higher bleeding risk (*e.g.* more severe forms and/or patients with higher WHO bleeding scores). The use of post-surgical thromboprophylaxis with LMWH and the rate of VTE were similar between elective and urgent procedures, while the rate of excessive post-surgical bleeding was higher in urgent than in elective procedures, as expected.

Our study has several limitations. First, we only looked for symptomatic VTE, thus the incidence of total VTE may have been significantly underestimated due to the lack of a systematic instrumental diagnostics search of these events during post-surgical follow-up. Indeed, no calf or distal vein thrombosis was reported and the latter could have been overlooked, due to the low clinical expressivity and difficulty of diagnosis. However, the possible underestimation of distal DVT may not significantly diminish the clinical relevance of our observations because untreated distal DVT is associated with a low risk of proximal propagation and PE.[32] Second, the retrospective nature of our study does not allow for definitive conclusions about the impact of heparin use on bleeding in patients with IPD. However, the collection of hemorrhagic post-surgical events was the main aim of our study and great emphasis was given to the careful evaluation of their occurrence. Moreover, the observational multicenter nature of our study, as already observed for other registries of populations with VTE, allowed us to gather a

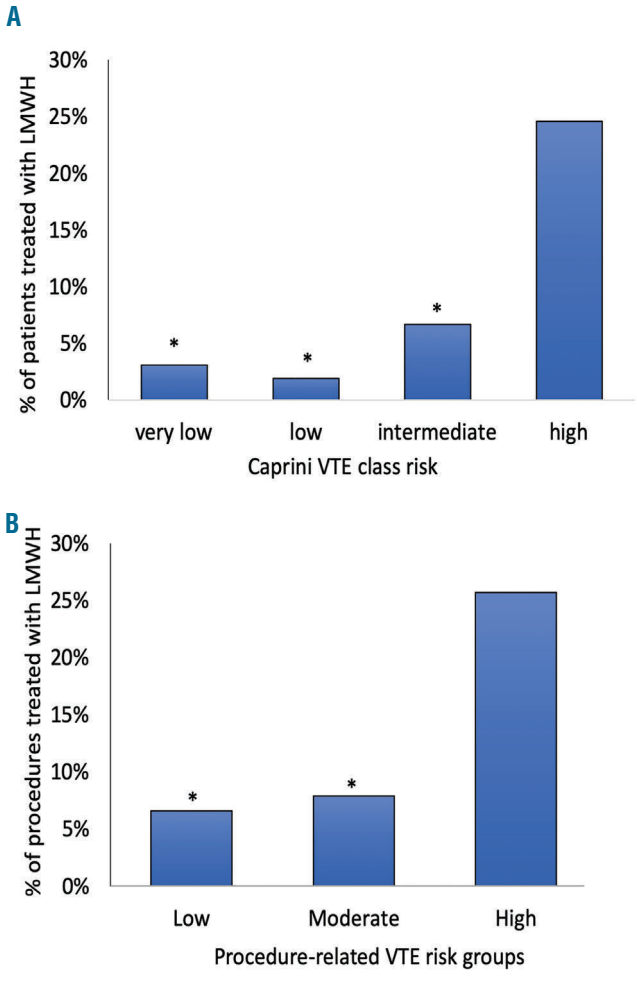

Figure 2. Use of low molecular weight heparin in inherited platelet disorder patients according to venous thromboembolism risk classes. Use of LMWH in IPD patients according to A) Caprini VTE class risk and B) procedure related VTE-risk (*P<0.01 *vs.* high-risk). LMWH: low molecular weight heparin; IPD: inherited platelet disorder; VTE: venous thromboembolism.

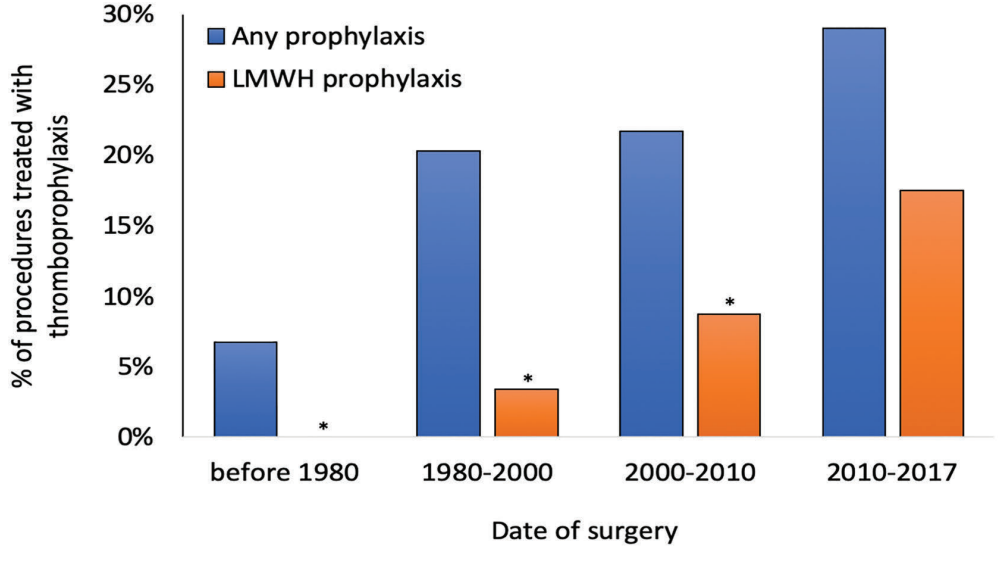

Figure 3. Use of thromboprophylaxis according to date of surgery (*P<0.01 *vs.* 2010-2017). Seven procedures (3.3% of total) were carried out ≤1980.

large patient series in an area difficult to explore with clinical trials, like subjects at high bleeding risk.[41] Indeed, interventional clinical trials generally exclude patients at bleeding risk, limiting the generalizability of the evidence. Registries have been helpful for improving our understanding of the epidemiology, pattern of care and outcomes in such patient subgroups.[41]

Third, our study has a relatively small sample size and it involves a rather heterogeneous population undergoing a wide range of interventions performed over a fairly broad time period, thus limiting the strength of our results compared with studies carried out in the general population, especially when subgroup analyses are concerned. Although this is true, a case series of over 200 procedures carried out in rare-disease patients is not negligible in this clinical context, if one considers that phase 3 studies on LMWH prophylaxis in high-risk surgery and trauma have included between 100 and 440 patients.[42-45]

Despite the above limitations, to the best of our knowledge this is the first study which explored VTE-risk of surgical procedures in a large series of patients with IPD, and our results may represent the starting point for an evidence-based approach to the antithrombotic management of these subjects.

Conclusions

Our findings suggest that VTE incidence is low in patients with IPD undergoing at risk surgery. Moreover, among IPD subjects as well as in the general population, patients at high VTE-risk may be identified by the Caprini score. Our data also suggest that mechanical thromboprophylaxis may be of benefit in patients with IPD undergoing invasive procedures at VTE-risk and that LMWH should be considered for major surgery. Prospective studies are required to further clarify the impact of pharmacologic thromboprophylaxis on VTE and bleeding complications in patients with IPD undergoing surgery.

Funding

This study was promoted by the Scientific Working Group on Thrombocytopenias and Platelet Function Disorders of the European Hematology Association (EHA). LB and EF were supported by a scholarship grant from Fondazione Umberto Veronesi. This study was supported in part by a Telethon grant (GGP15063) to PG. NB holds grants from FIS-FONDOS FEDER (CP14/00024 and PI15/01457).

Acknwoledgments

The authors thank Dr. Giuseppe Guglielmini for help with statistical analysis, Prof. Marco Cattaneo (Università degli Studi di Milano, Italy), Prof. Christian Gachet (University of Strasbourg, France), Dr Alessandro Pecci, Drs Davide Rancitelli, Silvia Ferrari and Irene Bertozzi (University of Padua, Italy) and Dr. Giovanni Favuzzi (IRCCS Casa Sollievo della Sofferenza, San Giovanni Rotondo, Italy) for their contribution to the study.

We thank Dr. Rino Migliacci (Division of Internal Medicine, Ospedale della Valdichiana "S. Margherita", Cortona, Italy) and Prof. Carlo Balduini (Department of Internal Medicine, IRCCS Policlinico S. Matteo Foundation, University of Pavia, Italy) for the critical reading of the manuscript.ì

References

1. Wheeler HB, Anderson FA, Jr. Prophylaxis against venous thromboembolism in surgical patients. Am J Surg. 1991;161(4):507-511.
2. Cohen AT, Tapson VF, Bergmann JF, et al. Venous thromboembolism risk and prophylaxis in the acute hospital care setting (ENDORSE study): a multinational cross-sectional study. Lancet. 2008; 371(9610):387-394.
3. Geerts WH, Bergqvist D, Pineo GF, et al. Prevention of venous thromboembolism: American College of Chest Physicians Evidence-Based Clinical Practice Guidelines (8th Edition). Chest. 2008;133(6 Suppl):381S-453S.
4. Bozzato S, Galli L, Ageno W. Thromboprophylaxis in surgical and medical patients. Semin Respir Crit Care Med. 2012;33(2):163-175.
5. Agu O, Hamilton G, Baker D. Graduated compression stockings in the prevention of venous thromboembolism. Br J Surg. 1999;86(8):992-1004.
6. Urbankova J, Quiroz R, Kucher N, Goldhaber SZ. Intermittent pneumatic compression and deep vein thrombosis prevention. A meta-analysis in postoperative patients. Thromb Haemost. 2005; 94(6):1181-1185.
7. Mismetti P, Laporte S, Darmon JY, Buchmuller A, Decousus H. Meta-analysis of low molecular weight heparin in the prevention of venous thromboembolism in general surgery. Br J Surg. 2001;88(7):913-930.
8. Eppsteiner RW, Shin JJ, Johnson J, van Dam RM. Mechanical compression versus subcutaneous heparin therapy in postoperative and posttrauma patients: a systematic review and meta-analysis. World J Surg. 2010;34(1):10-19.
9. Morris RJ, Woodcock JP. Intermittent pneumatic compression or graduated compression stockings for deep vein thrombosis prophylaxis? A systematic review of direct clinical comparisons. Ann Surg. 2010; 251(3):393-396.
10. Arabi YM, Al-Hameed F, Burns KEA, et al. Adjunctive intermittent pneumatic compression for venous thromboprophylaxis. N Engl J Med. 2019;380(14):1305-1315.
11. Gould MK, Garcia DA, Wren SM, et al. Prevention of VTE in nonorthopedic surgical patients: Antithrombotic Therapy and Prevention of Thrombosis, 9th ed: American College of Chest Physicians Evidence-Based Clinical Practice Guidelines. Chest. 2012;141(2 Suppl): e227S-e277S.
12. d'Oiron R, Menart C, Trzeciak MC, et al. Use of recombinant factor VIIa in 3 patients with inherited type I Glanzmann's thrombasthenia undergoing invasive procedures. Thromb Haemost. 2000;83(5):644-647.
13. Varbella F, Bongioanni S, Gagnor A, et al. Primary angioplasty in a patient with the May-Hegglin anomaly, a rare heredity thrombocytopenia. A case report and review of the literature. Ital Heart J. 2005;6(4):214-217.
14. Girolami A, Sambado L, Bonamigo E, Vettore S, Lombardi AM. Occurrence of thrombosis in congenital thrombocytopenic disorders: a critical annotation of the literature. Blood Coagul Fibrinolysis. 2013;24(1):18-22.
15. Nurden AT. Should studies on Glanzmann thrombasthenia not be telling us more about cardiovascular disease and other major illnesses? Blood Rev. 2017;31(5):287-299.
16. Gresele P, Falcinelli E, Bury L. Inherited platelet function disorders. Diagnostic approach and management. Hamostaseologie. 2016;36(4):265-278.
17. Orsini S, Noris P, Bury L, et al. Bleeding risk of surgery and its prevention in patients with inherited platelet disorders. Haematologica. 2017;102(7):1192-1203.
18. Aledort LM. Comparative thrombotic event incidence after infusion of recombinant factor VIIa versus factor VIII inhibitor bypass activity. J Thromb Haemost. 2004;2(10):1700-1708.
19. Schmidt AE, Henrichs KF, Kirkley SA, Refaai MA, Blumberg N. Prophylactic pre-procedure platelet transfusion is associated with increased risk of thrombosis and mortality. Am J Clin Pathol. 2017;149(1):87-94.
20. Humphries JE, Yirinec BA, Hess CE. Atherosclerosis and unstable angina in Bernard-Soulier syndrome. Am J Clin

Pathol. 1992;97(5):652-655.
21. Gruel Y, Pacouret G, Bellucci S, Caen J. Severe proximal deep vein thrombosis in a Glanzmann thrombasthenia variant successfully treated with a low molecular weight heparin. Blood. 1997;90(2):888-890.
22. Shpilberg O, Rabi I, Schiller K, et al. Patients with Glanzmann thrombasthenia lacking platelet glycoprotein alpha(IIb)beta(3) (GPIIb/IIIa) and alpha(v)beta(3) receptors are not protected from atherosclerosis. Circulation. 2002;105 (9):1044-1048.
23. Seretny M, Senadheera N, Miller E, Keeling D. Pulmonary embolus in Glanzmann's thrombasthenia treated with warfarin. Haemophilia. 2008;14(5):1138-1139.
24. Girolami A, Vettore S, Vianello F, Berti de Marinis G, Fabris F. Myocardial infarction in two cousins heterozygous for ASN41HIS autosomal dominant variant of Bernard-Soulier syndrome. J Thromb Thrombolysis. 2012;34(4):513-517.
25. Noris P, Schlegel N, Klersy C, et al. Analysis of 339 pregnancies in 181 women with 13 different forms of inherited thrombocytopenia. Haematologica. 2014;99(8):1387-1394.
26. Civaschi E, Klersy C, Melazzini F, et al. Analysis of 65 pregnancies in 34 women with five different forms of inherited platelet function disorders. Br J Haematol. 2015;170(4):559-563.
27. Gresele P, Subcommittee on Platelet Physiology of the International Society on T, Hemostasis. Diagnosis of inherited platelet function disorders: guidance from the SSC of the ISTH. J Thromb Haemost. 2015;13(2):314-322.
28. Poon MC, d'Oiron R, Zotz RB, et al. The international, prospective Glanzmann Thrombasthenia Registry: treatment and outcomes in surgical intervention. Haematologica. 2015;100(8):1038-1044.
29. Crous-Bou M, Harrington LB, Kabrhel C. Environmental and genetic risk factors associated with venous thromboembolism. Semin Thromb Hemost. 2016;42(8):808-820.
30. National Institute for Health and Care Excellence. Venous thromboembolism in over 16s: reducing the risk of hospital-acquired deep vein thrombosis or pulmonary embolism. London, 2018. Available from: nice.org.uk/guidance/ng89.
31. Wall C, Moore J, Thachil J. Catheter-related thrombosis: A practical approach. J Intensive Care Soc. 2016;17(2):160-167.
32. Bates SM, Jaeschke R, Stevens SM, et al. Diagnosis of DVT: antithrombotic therapy and prevention of thrombosis, 9th ed: American College of Chest Physicians Evidence-Based Clinical Practice Guidelines. Chest. 2012;141(Suppl 2): e351S-e418S.
33. Caprini JA, Arcelus JI, Hasty JH, Tamhane AC, Fabrega F. Clinical assessment of venous thromboembolic risk in surgical patients. Semin Thromb Hemost. 1991;17 Suppl 3:304-312.
34. Miller AB, Hoogstraten B, Staquet M, Winkler A. Reporting results of cancer treatment. Cancer. 1981;47(1):207-214.
35. Daley MJ, Ali S, Brown CV. Late venous thromboembolism prophylaxis after craniotomy in acute traumatic brain injury. Am Surg. 2015;81(2):207-211.
36. Ho KM, Bham E, Pavey W. Incidence of venous thromboembolism and benefits and risks of thromboprophylaxis after cardiac surgery: a systematic review and meta-analysis. J Am Heart Assoc. 2015; 4(10):e002652.
37. Amin AN, Lin J, Ryan A. Need to improve thromboprophylaxis across the continuum of care for surgical patients. Adv Ther. 2010;27(2):81-93.
38. Dentali F, Malato A, Ageno W, et al. Incidence of venous thromboembolism in patients undergoing thoracotomy for lung cancer. J Thorac Cardiovasc Surg. 2008; 135(3):705-706.
39. Sachdeva A, Dalton M, Lees T. Graduated compression stockings for prevention of deep vein thrombosis. Cochrane Database Syst Rev. 2018;11:CD001484.
40. Caprini JA. Thrombosis risk assessment as a guide to quality patient care. Dis Mon. 2005;51(2-3):70-78.
41. Bikdeli B, Jimenez D, Hawkins M, et al. Rationale, design and methodology of the computerized registry of patients with venous thromboembolism (RIETE). Thromb Haemost. 2018;118(1):214-224.
42. Marassi A, Balzano G, Mari G, et al. Prevention of postoperative deep vein thrombosis in cancer patients. A randomized trial with low molecular weight heparin (CY 216). Int Surg. 1993;78(2):166-170.
43. Bergqvist D, Benoni G, Bjorgell O, et al. Low-molecular-weight heparin (enoxaparin) as prophylaxis against venous thromboembolism after total hip replacement. N Engl J Med. 1996;335(10):696-700.
44. Kock HJ, Schmit-Neuerburg KP, Hanke J, Rudofsky G, Hirche H. Thromboprophylaxis with low-molecular-weight heparin in outpatients with plaster-cast immobilisation of the leg. Lancet. 1995;346(8973):459-461.
45. Lassen MR, Borris LC, Nakov RL. Use of the low-molecular-weight heparin reviparin to prevent deep-vein thrombosis after leg injury requiring immobilization. N Engl J Med. 2002;347(10):726-730.

ARTICLE

Long-term neuropsychological sequelae, emotional wellbeing and quality of life in patients with acquired thrombotic thrombocytopenic purpura

Silvia Riva,[1,2*] Ilaria Mancini,[3*] Alberto Maino,[1,4] Barbara Ferrari,[1] Andrea Artoni,[1] Pasquale Agosti[3] and Flora Peyvandi[1,3]

[1]Fondazione IRCCS Ca' Granda Ospedale Maggiore Policlinico, Angelo Bianchi Bonomi Hemophilia and Thrombosis Center, Milan, Italy; [2]St Mary's University, Twickenham, London, UK; [3]Università degli Studi di Milano, Department of Pathophysiology and Transplantation, and Fondazione Luigi Villa, Milan, Italy and [4]Azienda Provinciale per i Servizi Sanitari, Internal Medicine Unit, Trento, Italy

**SR and IM contributed equally as co-first authors.*

Ferrata Storti Foundation

Haematologica 2020
Volume 105(7):1957-1962

ABSTRACT

Neurological symptoms related to microthrombosis are the hallmark of acute manifestations of acquired thrombotic thrombocytopenic purpura (TTP). Despite the achievement of hematological remission, patients may report persisting neurological impairment that affects their quality of life. To assess the long-term neuropsychological consequences of acute TTP, we recruited 35 acquired TTP patients (77% females, median age at onset 41 years, interquartile range: 35-48) regularly followed at our outpatient clinic of thrombotic microangiopathies in Milan (Italy) from December 2015 to October 2016. Patients underwent a psychological evaluation of memory and attentional functions, emotional wellbeing and health-related quality of life at least three months after their last acute TTP event (median 36 months, interquartile range: 17-54). During the psychological consultation, 17 patients (49%) referred persisting subjective neurological impairment in the frame of a remission phase, with at least one symptom as disorientation, loss of concentration, dizziness, lack of balance, headache and diplopia. Neuropsychological assessment revealed lower scores than the Italian general population pertaining to direct, indirect and deferred memory. A higher degree of impairment of memory domains was found in patients with neurological involvement at the time of presentation of the first acute TTP episode. Anxiety and depression were detected in seven (20%) and 15 (43%) patients, respectively. Health-related quality of life was lower than the Italian general population, with mental domains more impacted than physical domains (mean difference 58.43, 95% confidence interval: 71.49-45.37). Our study demonstrates compromised memory and attention functions, persisting anxiety/depression symptoms and a generally reduced quality of life in patients recovering from acute acquired TTP. New clinical strategies should be considered to improve these symptoms.

Introduction

Thrombotic thrombocytopenic purpura (TTP) is a rare multisystem microangiopathy with fluctuating signs and symptoms. Its mortality rate can reach 90% when patients are left untreated, but it is reduced to 10% if patients are properly treated in the first 24 hours after diagnosis. Recovery is usually complete, but with a risk of relapse and the uncommon occurrence of persistent neurologic, cardiac and renal abnormalities.[1] After recovery, despite normal physical examination and laboratory data, many patients complain of difficulties with memory, headache, loss of concentration and endurance, as expressed at patient support group meetings. Some attempts to quantify those neurological deficits in acquired TTP patients have been made in the context of small observational studies, but without

Correspondence:

FLORA PEYVANDI
flora.peyvandi@unimi.it

Received: May 17, 2019.

Accepted: September 19, 2019.

Pre-published: September 26, 2019.

doi:10.3324/haematol.2019.226423

Check the online version for the most updated information on this article, online supplements, and information on authorship & disclosures: www.haematologica.org/content/105/7/1957

taking into account a whole assessment of cognitive, emotional and health-related quality of life (HrQoL) dimensions.[2-3] Cognitive domains required for complex attention, concentration skills and high level memory functions may be involved in patients with TTP due to diffuse microvascular subcortical lesions, similarly to neurologically normal individuals with untreated hypertension, sickle cell disease and multi-infarct dementia. Two widely accepted measures to evaluate HrQoL are the Short-Form 36 (SF-36)[4] and the EuroQol 5D (EQ-5D).[5] They are self-reported scales providing a numerical score to identify the level of perceived health status. For their generic nature, the SF-36 and the EQ-5D are frequently used in chronic conditions (*e.g.* hemophilia) and are applicable to many diseases.

With this background and gaps of knowledge, we set up a study in order to investigate persistent cognitive abnormalities, emotional wellbeing and quality of life in patients who had recovered from an acute episode of acquired TTP. We also analyzed whether or not the presence of neurological involvement during the acute phase of TTP or severe ADAMTS13 deficiency during disease remission were related to persistent neurocognitive defects. Finally, we investigated whether there was an association between the emotional status of the patients and their quality of life.

Methods

Patients

We performed a cross-sectional study of 35 patients with acquired TTP regularly followed at our out-patient clinic of thrombotic microangiopathies in Milan (Italy). Patients were enrolled at least three months after their last acute TTP event (median time of 36 months, interquartile range [IQR]: 17-54) from December 2015 to October 2016, when they underwent a comprehensive neuropsychological evaluation including memory and attentional functions, emotional wellbeing and HrQoL. Demographic and clinical variables were recorded, including age, sex, ethnicity, job status, level of education, clinical and biochemical data at the time of acute TTP (neurological involvement, platelet count and haemoglobin level at presentation, number of plasma exchange procedures required to attain remission), and plasma ADAMTS13 activity levels at the time of the neuropsychological assessment (± three months). Enrolment criteria are described in the *Online Supplementary Table S1*.

Written informed consent was obtained from all subjects with approval of the Ethics Committee of Fondazione IRCCS Ca' Granda Ospedale Maggiore Policlinico, in accordance with the Declaration of Helsinki.

Neurocognitive, emotional and HrQoL assessments

Neurocognitive and psychological assessments were administered by a board-certified psychologist in the standardized fashion in the frame of a single assessment session, which required approximately 1 hour to be completed, and included a test battery measuring two major cognitive domains, memory and attention,[6-8] the Hamilton Depression (HAM-D)[9] and Anxiety (HAM-A)[10] rating scales for emotional wellbeing, and the Short-Form (SF) 364 form for HrQoL (*Online Supplementary Material and Methods and Online Supplementary Table S2*).

Statistical analysis

Descriptive statistics were used for demographic, clinical and laboratory characteristics. Categorical variables were expressed as counts and percentages, continuous variables as means or medians with standard deviation (SD) or IQR. With regards to neuropsychological and HrQoL analyses, each subject's raw score on each test was converted to a standardized score based on normative data generated from the value of the normal population according to the subject's age and education level, as appropriate.[11-15] Standardized scores of TTP patients were then compared with norm-referenced data from the Italian population[11-15] by calculating the difference of means with 95% confidence intervals (CI) using unpaired and paired t-tests. Similarly, difference of means with 95% CI from unpaired and paired t-tests were used to compare neurocognitive assessment results in acquired TTP patients with and without neurological manifestations during the first acute episode of TTP, and with and without reduced ADAMTS13 activity during disease remission, close to the neuropsychological evaluation. For this analysis, an ADAMTS13 activity cut-off of 45% was used (*i.e.* the lower limit of the normality range in our ADAMTS13 activity assays). With regards to HrQoL, a standardized score of 50 was considered the cut-off for an acceptable quality of life.[15-16] Finally, non-parametric correlation analyses were performed to evaluate the relationship between the results of emotional wellbeing tests and those of neurocognitive assessments or aggregated HrQoL scales.

Statistical analyses were performed by SPSS, release 25.0 (IBM Corp., Armonk, NY, USA), and GraphPad Prism, version 7.03 (GraphPad Software, La Jolla, CA, USA).

Results

Between December 2015 and October 2016, 41 acquired TTP patients were approached for participating in the study during a follow-up visit at our out-patient clinic of thrombotic microangiopathy. Of them, one patient refused to participate and one patient was excluded owing to a pre-existing psychiatric disease. Four were not constantly attended at our center, and therefore they were excluded from the study. Thus, 35 patients were included in the study and underwent psychological tests and neurocognitive examinations (see the *Online Supplementary Material and Methods*). Patient characteristics are reported in Table 1. All but one patient were Caucasian, with a female to male ratio of about 3:1 and a median age at TTP onset of 41 years (IQR: 35-48). At the time of neuropsychological evaluation, 10 (29%) of 35 patients had suffered from recurrent TTP bouts. 22 patients (63%) presented with neurological signs and symptoms at presentation of the first acute TTP episode (including coma [n=2], focal neurological signs [n=12], personality changes [n=2], transient ischemic attack [n=4], seizures [n=1], stroke [n=3]). During the psychological consultation, 17 (49%) patients reported persisting subjective neurological impairment in the remission phase, with at least one symptom as disorientation, loss of concentration, dizziness, lack of balance (unable to control and maintain the body position all the time) headache, and diplopia.

Results of neurocognitive assessment

At the digit span test, 25 (71%) and 23 (66%) patients had a scoring lower than the mean of the general population in direct (mean difference -1.26; 95% CI: -1.64--0.87]) and backward (mean difference -1.49; 95% CI: -

2.02--0.96) memory, respectively (Table 2). Similarly, lower scores in TTP patients were observed in the Rey List tests for both direct (mean difference -5.87; 95% CI: 8.57- -3.17) and deferred memory (mean difference -1.67; 95% CI: -2.32--1.02).

With regards to the attention domain, TTP patients were slower in performing the trail making B test (sustained and divided attention) in comparison with the general population (mean difference 65.09 seconds; 95% CI: 47.23-82.94). Conversely, patients were slightly faster in performing the trail making A test, which measures focused attention (mean difference -10.63 seconds; 95% CI: 15.81--5.44).

When we analyzed scores of neurocognitive assessments in patients with and without neurological signs and symptoms at presentation of the first acute TTP episode, we observed a higher degree of impairment in the memory domains of the first group of patients in 3 of 4 memory tests (digit span [direct]: mean difference -0.78; 95% CI: -1.54--0.02; digit span [backward]: mean difference 0.90; 95% CI: -1.96--0.17]; Rey word list [deferred]: mean difference -1.39; 95% CI: -2.65--0.13) (Table 3).

No differences in neuropsychological assessments were found between patients with ADAMTS13 activity levels during remission below and above 45% (Table 4).

Results of emotional assessment

TTP patients presented a mean level of anxiety with the HAM-A of 9.6 (SD=8.1) and a mean level of depression with the HAM-D of 7.4 (SD=5.7). The presence of clinical anxiety (HAM-A score >13) was detected in seven (20%) of interviewed patients, while the presence of clinical depression (HAM-D score >7) was present in 15 (43%) of them. All seven patients with clinical anxiety presented concomitant clinical depression. Five (14%) patients showed a severe anxiety (HAM-A score >24) and five (14%) a medium level of depression (HAM-D score >18). No patients presented severe levels of depression (HAM-D score >24).

Among the type of disturbances, we found that the most impaired domains in HAM-D were "work activities" (n=10, 77%), "depressed mood" (n=8, 60%) and "early insomnia" (n=4, 27%) while in HAM-A there were "intellectual symptoms" (*i.e.* difficulty in concentration and poor memory) (n=6 82%) and "tension" (n=4, 54%).

At correlation analysis, better wellbeing was associated with better memory function (the sign of the correlation coefficient is negative because of the opposite interpretation scale of the two measurements): HAM-A test *versus*: digit span direct Spearman rho -0.472, P=0.004; digit span backward Spearman rho -0.597, P<0.001; Rey list direct Spearman rho 0.310, P=0.075; Rey list recall: Spearman rho -0.432, P=0.011; HAM-D test *versus*: digit span direct Spearman rho -0.474, P=0.004; digit span backward Spearman rho -0.594, P<0.001; Rey list direct Spearman rho 0.357, P=0.038; Rey list recall: Spearman rho -0.499, P=0.003.

Results of HrQoL assessment

Table 5 displays the mean scores of the SF-36 assessments for each of the eight domains by physical and mental components: physical activity (PA), role physically (RP), bodily pain (BP), general health (GH), vitality (VI), social functioning (SF), role emotional (ER) and mental health (MH). Acquired TTP patients showed lower normalized scores than the Italian reference sample[14] in all scales but physical activity. With regard to the physical components, the most impacted area was the physical role, with a mean score of 57 (median 55; range: 40-85) and 11 patients (31%) with scores below 50. With regard to the mental components, emotional role was the most compromised, with a mean score of 43 (median 43; range: 30-56) and 22 patients (63%) with scores below 50. Overall, the mental dimension was more affected than the physical dimension, with the mental component score MCS-36 (equivalent to the sum of MH, ER, SF and VI scores) lower than the physical component score PCS-36 (equivalent to the sum of PA, RP, BP and GH scores) by almost 60 points (mean difference -58.43; 95% CI: -71.49--45.37) and 15 (43% of patients pertaining to the MCS-36) versus four (11% of patients pertaining to the PCS-36) patients with scores below 50, the commonly accepted cut-off for an acceptable quality of life.[15,16]

Finally, at correlation analysis, the better the mental component score of the HrQoL survey was, the better were the results of emotional wellbeing assessments, especially the anxiety evaluation (MCS-36 *vs.* HAM-A test: Spearman rho -0.358, P=0.035; MCS-36 vs. HAM-D test: Spearman rho -0.316, P=0.064).

Table 1. Demographic and clinical characteristics of 35 thrombotic thrombocytopenic purpura patients included in the study. Clinical and laboratory data pertain the first acute thrombotic thrombocytopenic purpura episode.

Characteristics	TTP patients (n=35)
Demographic data	
Male, n (%)	8 (23)
Caucasian, n (%)	34 (97)
Age at TTP onset, years, median (IQR)	41 (35-48)
Age at neuropsychological evaluation, years, median (IQR)*	45 (39-55)
Mean school level, years	13
Job status – workers, n (%)	30 (77)
Clinical characteristics at the first acute TTP episode	
Neurological involvement, n (%)	22 (63)
Platelet count, x 10^9/L, median (IQR)†	13 (8-27)
Hemoglobin, g/dL, median (IQR)†	7.8 (6.8-10.0)
Number of PEX to attain remission, median (IQR)†	11 (6-20)
Laboratory parameters close to the neuropsychological evaluation†	
Platelet count, x 10^9/L, median (IQR)	251 (212-297)
Hemoglobin, g/dL, median (IQR)	13.4 (12.8-14.3)
ADAMTS13 activity close to neuropsychological evaluation†	
Normal (45-138%), n (%)	16 (47)
Moderately reduced (10-45%), n (%)	12 (35)
Severely reduced (<10%), n (%)	6 (18)

At the time of neuropsychological evaluation, 10 (29%) of 35 patients had suffered from recurrent TTP bouts.*Neuropsychological evaluation was performed at a median time of 36 months (IQR: 17-54) from the last acute TTP event.†Available in 33 (platelet count, hemoglobin and number of PEX to remission at first acute TTP episode),34 (ADAMTS13 activity close to neuropsychological evaluation) and 31 subjects (platelet count and hemoglobin close to the neuropsychological evaluation). IQR: interquartile range; PEX: plasma exchange; TTP: thrombotic thrombocytopenic purpura

Table 2. Descriptive statistics of neuropsychological tests in acquired thrombotic thrombocytopenic purpura patients and mean values of the Italian general population.

Test	TTP patients Mean (SD)	General population Mean	Mean difference (95% CI)
Memory			
Digit span (direct)	5.74 (1.12)	7.00	-1.26 (-1.64, -0.87)
Digit span (backword)	4.51 (1.54)	6.00	-1.49 (-2.02, -0.96)
Rey word list (direct)*	26.37 (7.74)	32.20	-5.87 (-8.57, -3.17)
Rey word list (deferred)*	4.03 (1.86)	5.70	-1.67 (-2.32, -1.02)
Attention			
Trail making A, seconds	34.37 (15.1)	45.00	-10.63 (-15.81, -5.44)
Trail making B, seconds	214.09 (51.99)	149.00	65.09 (47.23, 82.94)

In memory tests a higher score indicates a better performance, in attention tests a lower score indicates a better performance. At the time of neuropsychological evaluation, 10 (29%) of 35 patients had suffered from recurrent TTP bouts. *: Available in 34 TTP patients; CI: confidence interval; SD: standard deviation; TTP: thrombotic thrombocytopenic purpura.

Table 3. Descriptive statistics of neuropsychological tests in acquired thrombotic thrombocytopenic purpura (TTP) patients with and without neurological manifestations at onset of the first acute TTP event.

Test	Neurological involvement at first acute TTP event		Mean difference (95% CI)
	Present (n=22)	Absent (n=13)	
Memory, mean (SD)			
Digit span (direct)	5.45 (1.14)	6.23 (0.93)	-0.78 (-1.54, -0.02)
Digit span (backword)	4.18 (1.59)	5.08 (1.32)	-0.90 (-1.96, 0.17)
Rey word list (direct)*	25.36 (7.73)	27.89 (7.80)	-2.54 (-8.11, 3.04)
Rey word list (deferred)*	3.50 (1.92)	4.89 (1.44)	-1.39 (-2.65, -0.13)
Attention, mean (SD)			
Trail making A, seconds	37.18 (16.26)	29.62 (12.00)	7.57 (-3.01, 18.14)
Trail making B, seconds	207.82 (49.91)	224.69 (55.71)	-16.87 (-53.95, 20.20)

In memory tests a lower score indicates a worse performance, in attention tests a higher score indicates a better performance. At the time of neuropsychological evaluation, 9 of 22 (41%) and 1 of 13 (8%) patients with and without neurological involvement at the first acute TTP event had suffered from recurrent TTP bouts, respectively. *: Available in 34 TTP patients; CI: confidence interval; SD: standard deviation; TTP: thrombotic thrombocytopenic purpura.

Discussion

Neurological signs and symptoms of acute TTP are mainly transient, brief and resolve with remission of the acute phase. Our study demonstrates persisting neurological, neuropsychological, emotional and HrQoL impairments in TTP patients even years after the acute phase.

During the remission phase, TTP patients showed a significant impairment in memory domains (direct, backward and deferred memory) when compared with the general population. This memory impairment was positively associated with the presence of neurological symptoms during the acute phase of the disease, as shown by the comparison between patients with and without neurological involvement during the first acute TTP event. Attention domains were also affected, but they were unrelated to neurological involvement during the acute phase. Our results are in line with previous findings by Kennedy *et al.* in 24 acquired TTP patients from the Oklahoma Registry, who performed significantly worse than the US reference population in both attention and memory functions.[3,17] Conversely, at variance with our results, previous studies did not report an association of neurocognitive impairment with the occurrence of neurological manifestations at the time of the acute TTP event,[3,18] although a trend towards a worse mental performance was detected in German patients with neurological symptoms compared with patients with no neurological symptoms (median of FLei mental performance score: 45 [IQR: 15-65] *vs.* 31 [IQR: 13-40], Mann-Whitney U test P=0.193).[18] It is worth-noticing that the prevalence of relapsing TTP cases were higher in patients with than without neurological symptoms during the first acute event (41% *vs.* 8%). Unfortunately, the low sample size did not allow us to discriminate the effects of these two factors.

Beside cognitive problems, we detected clinical anxiety and depression in 20% and 43% of interviewed patients. An even higher prevalence of depression symptoms in acquired TTP patients was reported in two US and one German cohorts (59%,[17] 81%,19 and 73%,[18] respectively), which included also cases of major depression (29%,18 37%,[19] and 14%).[18] However, a pre-existing diagnosis of depressive disorder was not an exclusion criterion in these studies, which may partly explain the differences in the observed prevalence. In our study, the results of anxiety and depression tests were negatively correlated with scores of neurocognitive assessments, indicating that patients with symptoms of psychologic distress also had more pronounced cognitive defects. This is consistent with the findings of Falter and colleagues,[18] who reported a strong correlation between an impaired mental performance and the severity of depression in 84 TTP patients.

It is interesting to compare our results with other cardio-

Table 4. Descriptive statistics of neuropsychological tests in acquired thrombotic thrombocytopenic purpura patients with and without ADAMTS13 deficiency next to the psychological evaluation.

Test	ADAMTS13 activity during remission		Mean difference (95% CI)
	<45% (n=18)	≥45% (n=16)	
Memory, mean (SD)			
Digit span (direct)	6.06 (1.00)	5.50 (1.16)	0.56 (-0.20, 1.31)
Digit span (backward)	4.61 (1.79)	4.50 (1.27)	0.11 (-0.98, 1.21)
Rey word list (direct)*	27.22 (7.72)	26.09 (7.65)	1.13 (-4.33, 6.59)
Rey word list (deferred)*	4.44 (1.67)	3.73 (2.02)	0.72 (-0.59, 2.02)
Attention, mean (SD)			
Trail making A, seconds	32.06 (13.39)	36.94 (17.32)	-4.88 (-15.62, 5.87)
Trail making B, seconds	209.89 (58.93)	220.94 (45.19)	-11.05 (-48.09, 26.00)

In memory tests a lower score indicates a worse performance, in attention tests a higher score indicates a better performance. At the time of neuropsychological evaluation, 5 of 18 (28%) and 5 of 16 (31%) patients with and without ADAMTS13 deficiency next to the visit had suffered from recurrent TTP bouts, respectively. *: Available in 34 TTP patients; CI: confidence interval; SD: standard deviation.

Table 5. Descriptive statistics of health-related quality of life components in acquired thrombotic thrombocytopenic purpura patients and in Italian reference individuals.

Test	TTP patients (n=35)		General population (n=2031)	Mean difference (95%CI)
	mean (SD)	N with score<50 (%)	mean (SD)	
Physical domain				
Physical activity	81.40 (15.37)	2 (6)	84.46 (23.18)	-3.06 (-8.43 to 2.31)
Limitation physical role	56.77 (13.04)	11 (31)	78.21 (35.93)	-21.44 (-26.17 to -16.72)
Pain	62.20 (13.92)	5 (14)	73.67 (27.65)	-11.47 (-16.39 to -6.55)
General health	59.91 (11.54)	5 (14)	65.22 (22.18)	-5.31 (-9.38 to -1.24)
PCS-36	260.29 (44.63)	4 (11)*	NA	NA
Mental domain				
Vitality	52.46 (12.85)	13 (37)	61.89 (20.69)	-9.43 (-13.93 to -4.93)
Social activity	54.26 (8.60)	7 (20)	77.43 (23.34)	-23.17 (-26.28 to -20.06)
Limitation emotional role	42.69 (8.76)	22 (63)	76.16 (37.25)	-33.47 (-36.86 to -30.08)
Mental health	52.46 (5.45)	4 (11)	66.59 (20.89)	-14.13 (-16.20 to -12.06)
MCS-36	201.86 (23.84)	15 (43)*	NA	NA

At the time of neuropsychological evaluation, 10 (29%) of 35 patients had suffered from recurrent TTP bouts. *Being PCS-36 and MCS-36 the weighted sum of the original scales of the SF-36, this number indicates patients with a score below 200. CI: confidence interval; NA: not available; SD: standard deviation; MCS-36: mental component summary (MCS) of the Short Form (36) Health Status Questionnaire (SF36); PCS-36: physical component summary (PCS) of the Short Form (36) Health Status Questionnaire (SF36); TTP: thrombotic thrombocytopenic purpura.

vascular and neurovascular diseases. High percentage of cognitive impairment were also found in patients after acute coronary syndrome (16% of patients),[20] stroke (one-third of the sample examined),[21] and after a transient ischemic attack (TIA) (more than a third of patients).[22] After TIA, also depressive symptoms were found as prevalent as 34%.[23] However, there are important differences between these studies and ours. First, the evaluation of cognitive decline and depression were generally made during the acute phase and in patients older than ours.[23] Second, the literature mainly highlights a major deterioration at the level of functional abilities in daily life activities, especially in stroke patients. Finally, different tests were performed and different cognitive domains (*e.g.* language) evaluated, making any comparison difficult. We also found an overall impaired quality of life compared with the general population. In the HrQoL domains, mental components were more impaired than physical components, suggesting that the condition determines a considerable emotional burden, probably related to its course of intermittent relapse and remission phases. Indeed, the HrQoL mental domain was negatively affected by the presence of clinical anxiety and depression in our patients. Our findings are consistent with those of Lewis *et al.*[2] and Cataland *et al.*[24] although they reported a greater impact of acquired TTP on the physical component of the HrQoL,2 and on both the mental and the physical component.[24]

We believe that our findings have clinical relevance for the management of TTP patients. Clinicians should be aware of the association between neurological manifestations during the acute TTP episodes and long-term impaired neuropsychological abilities. They should put attention on signs and symptoms of neurological impairment during the remission phase and consider early signs of anxiety and depression in order to improve the quality of life of TTP patients.

Our study has limitations. First, the neurocognitive and emotional status of the patients and their quality of life before their first episode of TTP was not objectively evaluated. However, patients did perceive and referred at the time of the psychological consultation a worsening of their conditions after TTP diagnosis. Second, the evalua-

tion of neurological and cognitive functions abnormalities observed in TTP patients in the remission phase and far from the clinical manifestations of acute TTP were not supported by instrumental neuro-functional analysis such as functional magnetic resonance imaging, which might be needed to assess the aforementioned alterations at the organic level. Third, we included patients with a history of a single acute TTP event but also patients with relapsing TTP, rendering our study population heterogeneous (in order to exclude potential comorbidities only primary TTP patients should be evaluated). However, the occurrence of multiple TTP episodes was never found to be associated with neurocognitive, emotional or HrQoL assessments in any previous study.[3,17,18,24] Fourth, the tests performed to evaluate clinical anxiety and depression, despite being well-validated tools, can only be suggestive of a psychiatric diagnosis, which indeed can only be confirmed by a proper psychiatric interview. Fifth, despite the relatively large sample size for a rare disease, numbers in some analyses are small, leading to statistical uncertainty and wide CI. This is a problem of any study in the field of rare diseases, and stimulate more efforts to promote collaboration between centers. Finally, the design of our study is cross-sectional and, thus cannot provide risk estimates and data about predictive factors. On the other hand, as far as we know, our study is the most comprehensive investigation on TTP patients, including clinical, cognitive, emotional and HrQoL assessment.

In conclusion, we demonstrated that, despite successful treatment with plasma exchange and immunosuppressive therapy in the acute stage of the disease, patients with TTP suffer from long term neurological sequelae even years after the acute phase. TTP patients with neurological involvement at the first acute episode seem to be at higher risk of developing memory dysfunction. Furthermore, TTP patients have increased levels of anxiety and depression, which negatively affect their quality of life. A faster improvement of the acute state of the disease by novel drugs might have a role in this process and further studies are required to solve this question.

References

1. Deford CC, Reese JA, Schwartz LH, et al. Multiple major morbidities and increased mortality during long-term follow-up after recovery from thrombotic thrombocytopenic purpura. Blood. 2013;122(12):2023-2029.
2. Lewis QF, Lanneau MS, Mathias SD, et al. Long-term deficits in health-related quality of life following recovery from thrombotic thrombocytopenic purpura. Transfusion. 2009;49(1):118-124.
3. Kennedy KA, Lewis QF, Scott JG, et al. Cognitive deficits after recovery from thrombotic thrombo- cytopenic purpura. Transfusion. 2009;49(6):1092-1101.
4. Ware Jr, JE, Sherbourne CD. The MOS 36-item short-form health survey (SF-36): I. Conceptual framework and item selection. Med Care. 1992;30(6):473-483.
5. Rabin R, de Charro F. EQ-SD: a measure of health status from the EuroQol Group. Ann Med. 2001;35(5):337-343.
6. Wechsler S. The Semantic Basis of Argument Structure. New York, NY: CSLI Publications (Center for the Study of Language and Information). 1995, Stanford, Cambridge University Press.
7. Rey A. L'Examen clinique en psychologie. (The Clinical Exam in Psychology), 1964, Paris: Presses Universitaires de France.
8. Tombaugh TN. Trail Making Test A and B: normative data stratified by age and education. Arch Clin Neuropsychol. 2004; 19(2):203-214.
9. Hamilton M. A rating scale for depression. J Neurol Neurosurg Psychiatry. 1960;23:56-65.
10. Hamilton M. The assessment of anxiety states by rating. Br J Med Psychol. 1959;32:50-55.
11. Mondini S, Mapelli D, Vestri A, et al. Esame neuropsicologico breve. Milano: Raffaello Cortina Editore. 2003;160.
12. Carlesimo GA, Caltagirone C, Gainotti GU, et al. The mental deterioration battery: normative data, diagnostic reliability and qualitative analyses of cognitive impairment. Eur Neurol. 1996;36(6):378-384.
13. Giovagnoli AR, Del Pesce M, Mascheroni S, et al. Trail making test: normative values from 287 normal adult controls. Ital J Neurol Sci. 1996;17(4):305-309.
14. Apolone G, Mosconi P. The Italian SF-36 Health Survey: translation, validation and norming. J Clin Epidemiol. 1998; 51(11):1025-1036.
15. Ware JE, Kosinski M, Gandek B, et al. The factor structure of the SF-36 Health Survey in 10 countries: Results from the IQOLA Project. J Clinic epidemiol. 1998; 51(11):1159-1165.
16. Obidoa CA, Reisine SL, Cherniack M. How Does the SF-36 Perform in Healthy Populations? A Structured Review of Longitudinal Studies. J Soc Behav Health. 2010;4(1):30-48.
17. Han B, Page EE, Stewart LM, et al. Depression and cognitive impairment following recovery from thrombotic thrombocytopenic purpura. Am J Hematol. 2015; 90(8):709-714.
18. Falter T, Schmitt V, Herold S, et al. Depression and cognitive deficits as long-term consequences of thrombotic thrombocytopenic purpura. Transfusion. 2017; 57(5):1152-1162.
19. Chaturvedi S, Oluwole O, Cataland S, et al. Post-traumatic stress disorder and depression in survivors of thrombotic thrombocytopenic purpura. Thromb Res. 2017;151:51-56.
20. Saczynski JS, McManus DD, Waring ME, et al. Change in cognitive function in the month after hospitalization for acute coronary syndromes: findings From TRACE-CORE (transition, risks, and actions in coronary events–center for outcomes research and education). Circ Cardiovasc Qual Outcomes. 2017;10(12).
21. Lisabeth LD, Sánchez BN, Baek J, et al. Neurological, functional, and cognitive stroke outcomes in Mexican Americans. Stroke. 2014;45(4):1096-1101.
22. van Rooij FG, Kessels RP, Richard E, et al. Cognitive impairment in transient ischemic attack patients: a systematic review. Cerebrovasc Dis. 2016;42(1-2):1-9.
23. Mitchell AJ, Sheth B, Gill J, et al. Prevalence and predictors of post-stroke mood disorders: A meta-analysis and meta-regression of depression, anxiety and adjustment disorder. Gen Hosp Psychiatry. 2017;47:48-60.
24. Cataland SR, Scully MA, Paskavitz J, et al. Evidence of persistent neurologic injury following thrombotic thrombocytopenic purpura. Am J Hematol. 2011;86(1):87-89.

ARTICLE

Fibrinogen gamma gene *rs2066865* and risk of cancer-related venous thromboembolism

Benedikte Paulsen,[1] Hanne Skille,[1] Erin N. Smith,[2] Kristian Hveem,[3,4,5] Maiken E. Gabrielsen,[4,5] Sigrid K. Brækkan,[1,6] Frits R. Rosendaal,[1,7] Kelly A. Frazer,[1,2] Olga V. Gran[1] and John-Bjarne Hansen[1,6]

[1]K.G. Jebsen Thrombosis Research and Expertise Center (TREC), Department of Clinical Medicine, UiT - The Arctic University of Norway, Tromsø, Norway; [2]Department of Pediatrics and Rady's Children's Hospital, University of California, San Diego, La Jolla, CA, USA; [3]St. Olavs Hospital, Trondheim University Hospital, Trondheim, Norway; [4]HUNT Research Centre, Department of Public Health and General Practice, Norwegian University of Science and Technology, Levanger, Norway; [5]K.G. Jebsen Center for Genetic Epidemiology, Department of Public Health, Norwegian University of Science and Technology, Trondheim, Norway; [6]Division of Internal Medicine, University Hospital of North Norway, Tromsø, Norway and [7]Department of Clinical Epidemiology, Leiden University Medical Center, Leiden, the Netherlands

Ferrata Storti Foundation

Haematologica 2020
Volume 105(7):1963-1968

ABSTRACT

Venous thromboembolism (VTE) is a frequent complication in patients with cancer. Homozygous carriers of the fibrinogen gamma gene *(FGG) rs2066865* have a moderately increased risk of VTE, but the effect of the *FGG* variant in cancer is unknown. We aimed to investigate the effect of the *FGG* variant and active cancer on the risk of VTE. Cases with incident VTE (n=640) and a randomly selected age-weighted sub-cohort (n=3,734) were derived from a population-based cohort (the Tromsø study). Cox-regression was used to estimate hazard ratios (HR) with 95% confidence intervals (CI) for VTE according to categories of cancer and *FGG*. In those without cancer, homozygosity at the *FGG* variant was associated with a 70% (HR 1.7, 95% CI: 1.2-2.3) increased risk of VTE compared to non-carriers. Cancer patients homozygous for the *FGG* variant had a two-fold (HR 2.0, 95% CI: 1.1-3.6) higher risk of VTE than cancer patients without the variant. Moreover, the six-months cumulative incidence of VTE among cancer patients was 6.4% (95% CI: 3.5-11.6) in homozygous carriers of *FGG* and 3.1% (95% CI: 2.3-4.7) in those without risk alleles. A synergistic effect was observed between *rs2066865* and active cancer on the risk of VTE (synergy index: 1.81, 95% CI: 1.02-3.21, attributable proportion: 0.43, 95% CI: 0.11-0.74). In conclusion, homozygosity at the *FGG* variant and active cancer yielded a synergistic effect on the risk of VTE.

Introduction

Venous thromboembolism (VTE), a collective term for deep vein thrombosis (DVT) and pulmonary embolism (PE), is a common disease associated with substantial short- and long-term morbidity and mortality.[1,2] The incidence of VTE is 1-2 in 1,000 people/ year, and it increases steeply with age.[3] Malignant disease is associated with a four- to seven-fold increased risk of VTE, and 20-25% of all first lifetime VTE-events are cancer-related.[4,5] VTE, particularly in cancer, leads to prolonged and more frequent hospitalizations, and has a substantial impact on quality of life.[6,7] Complications of VTE, such as recurrence, post-thrombotic syndrome and treatment-related bleeding, occur more frequently in cancer patients,[6,8,9] and the risk of death is higher in cancer patients with than without VTE.[10,11]

Family and twin studies suggest that VTE is highly heritable, and likely results from an interplay between inherited and environmental factors.[12,13] Fibrinogen, the precursor of fibrin, is an essential component in the final stage of the coagulation cascade. The fibrinogen molecule has three subunits called Aα, Bβ and γ, which occur in pairs for a total number of six subunits. The γ chain, transcribed from the

Correspondence:

BENEDIKTE PAULSEN
benedikte.paulsen@uit.no

Received: April 11, 2019.
Accepted: October 3, 2019.
Pre-published: October 3, 2019.

doi:10.3324/haematol.2019.224279

Check the online version for the most updated information on this article, online supplements, and information on authorship & disclosures: www.haematologica.org/content/105/7/1963

fibrinogen gamma gene (*FGG*) located on chromosome 4, has two isoforms, γA and γ'. In the Leiden Thrombophilia Study, the *FGG rs2066865* single nucleotide polymorphism (SNP) was first proposed as a risk factor for VTE by reducing fibrinogen γ' levels.[14] Several later genotyping[15,16] and genome-wide association studies (GWAS)[17,18] confirmed an association between *rs2066865* and VTE risk, whereas two cohort studies found no significant association.[19,20] In a recent meta-analysis including seven studies, *rs2066865* was associated with an increased risk of VTE (OR 1.61, 95% CI: 1.34-1.93).[21]

The majority of the genetic studies have excluded individuals with cancer-related thrombosis. However, as prothrombotic genotypes are fixed, and not influenced by disease, interventions and complications, they may be attractive candidates as biomarkers of VTE risk in cancer patients. Recent studies have suggested that interactions between cancer and other prothrombotic genotypes (factor V variants *rs6025* and *rs4524* and prothrombin *G20210A*) have synergistic effects on the risk of VTE.[22-25] To the best of our knowledge, no study has investigated the impact of *rs2066865* on the risk of VTE in cancer patients. Therefore, we aimed to investigate the joint effect of *rs2066865* and active cancer on the absolute and relative risks of VTE in a population-based case-cohort.

Methods

Study population

The Tromsø Study is a single-center population-based cohort, following residents of the municipality of Tromsø, Norway, with repeated health surveys. The case-cohort was derived from the fourth survey (Tromsø 4), which included 27,158 participants aged 25-97 years. A detailed cohort profile of the Tromsø study has been published previously.[26] The study was approved by the Regional Committee for Medical and Health Research Ethics in Northern Norway, and all participants provided informed written consent to participation. From enrolment in Tromsø 4 (1994/95), subjects were followed until December 31, 2012. Detailed information regarding identification and validation of VTE-events are described in the *Online Supplementary Material and Methods.*

In total, 710 participants developed VTE during follow-up. Of these, 26 did not have blood samples available or of sufficient quality for DNA analyses. The remaining 684 subjects were included as the cases in our study. A subcohort (n=3,931) was composed by randomly sampling individuals from Tromsø 4 weighted for the age distribution of the cases in 5-year age-groups. Due to the nature of the case-cohort design, where each participant has the same probability of sampling, 72 of the cases were also in the subcohort. Subjects with a history of cancer prior to inclusion (n=232) and subjects with missing information on *rs2066865* (n=9) were excluded from the analysis. The final case-cohort consisted of 4,374 subjects, with 640 cases and 3,734 in the subcohort. A flow chart of the case-cohort is displayed in Figure 1.

Baseline measurements and genotyping

Baseline measurements and genotyping methods are described in the *Online Supplementary Materials and Methods.*

Cancer exposure

Cancer assessment is described in the *Online Supplementary Materials and Methods*. Previous studies have shown a strong temporal relation between cancer diagnosis and incident VTE, and up to 50 % of cancer-related VTE events presents within a 2.5-year interval (from six months preceding the cancer diagnosis until 2 years following the cancer diagnosis).[27,28] Therefore, a VTE was defined as related to active cancer if it occurred within this time period.

Subjects who survived the active cancer period without a VTE were censored at the end of the active cancer period (*i.e.* 2 years after cancer was diagnosed). The censoring was performed because information regarding remission and relapse of cancer was unavailable, and extension of the observation period of cancer could result in the dilution of the estimates due to inclusion of VTE cases not necessarily caused by cancer. This approach resulted in censoring of 14 VTE cases that occurred after the active cancer period. Thus, 626 VTE cases were included in the final analyses.

Statistical analysis

Statistical analyses were performed using STATA version 15.0 (Stata Corporation LP, College Station, TX, USA). Cox proportional hazards regression models were used to obtain age- and sex-adjusted HR with 95% CI for VTE across categories of cancer status (no cancer/active cancer) and FGG risk alleles. Cancer was assessed as a time-dependent covariate in the model. Subjects who developed cancer contributed person-time as unexposed from the inclusion date until six months prior a cancer diagnosis, and thereafter contributed person-time in the active cancer group as exposed. Absolute incidence rates (IR) were calculated based on person-time from the original cohort (n=27,128). To calculate joint effects conferred by active cancer and FGG risk alleles, subjects with no cancer and no risk alleles were used as the reference group in the Cox model. Based on the total active cancer person-time at risk derived from the source cohort, 1-Kaplan-Meier curves were used to estimate the cumulative incidence of VTE in subjects with active cancer according to the presence of *FGG* risk alleles. Methods for assessing synergism between *FGG* and active cancer on the risk of VTE are described in detail in the *Online Supplementary Materials and Methods.*

Results

The mean follow-up of the case-cohort was 12.6 years. In total, 854 subjects had active cancer, of which 167 experienced an incident VTE. The baseline characteristics of

Table 1. Baseline characteristics in the entire case-cohort and in the active cancer group.

	Entire case-cohort	Active cancer
Subjects (n)	4374	854
Age (years)	58 ± 13	62 ± 10
Sex (males)	47.0 (2,048)	53.0 (456)
BMI (kg/m^2)	26.0 ± 4	26.0 ± 4
Daily smoking	34.5 (1,464)	43.5 (364)
WBC count (10^9/L)	7.1 ± 1.8	7.2 ± 1.8
Platelet count (10^9/L)	251 ± 60	250 ± 58
*rs2066865**	0.26	0.26
1 risk allele	1,723	334
2 risk alleles	289	51

Values are numbers or percentages with numbers in parenthesis or means ± standard deviation (SD). Active cancer: period from six months before a cancer diagnosis until two years after; BMI: body mass index; Daily smoking indicates smoking at the time of enrollment; WBC: white blood cell; *: allele frequency.

the entire case-cohort and in those with active cancer during follow-up are presented in Table 1. Subjects who developed active cancer were slightly older (61±10 years *vs.* 58±13 years) and reported a higher frequency of daily smoking (46% *vs.* 35%) compared to the entire case-cohort. The minor allele frequency of *rs2066865* was 0.26, which is comparable to reference populations.[14,29] The homozygous variant of the *FGG* was present in 289 (6.6%) subjects, the heterozygous variant in 1,723 (39.4%) subjects, while 2,362 (54.0%) subjects were non-carriers of the *FGG* variant. The allele frequency was essentially similar in subjects who developed cancer. Expected *versus* observed proportions of hetero- and homozygous individuals in the subcohort according to the Hardy-Weinberg equilibrium are presented in *Online Supplementary Table S1*.

The clinical characteristics of the VTE events stratified by the presence of active cancer are shown in Table 2. Compared to the non-cancer-related VTE, cancer-related VTE were more often a DVT (59.2% *vs.* 55.5%) than a PE (40.7% *vs.* 44.4%). The prevalence of provoking factors such as acute medical conditions, immobilization and surgery were essentially similar between the two groups, as were the total proportion of VTE with one or more concurrent provoking factors (44.3% *vs.* 44.7%). Non-cancer related VTE were more likely to be associated with traumas (9.6% *vs.* 2.4%) while other provoking factors *(i.e.* venous catheters) were more frequent in cancer-related VTE (8.4% *vs.* 3.7%).

In participants without cancer, the IR of VTE increased from 1.2 (95% CI: 1.1-1.4) per 1,000 people/year among non-carriers of *FGG rs2066865* to 2.0 (95% CI: 1.5-2.7) per 1,000 people/year among those with two risk alleles. Accordingly, the risk of VTE was 70% (HR 1.7, 95% CI: 1.2-2.3) higher in those with two risk alleles at FGG compared to non-carriers (Table 3). In subjects with active cancer, the risk was 12-fold higher (HR 11.9, 95% CI: 9.3-15.2) in those with no *FGG* risk alleles, and 22-fold higher (HR 22.2, 95% CI: 12.9-38.1) in those with two *FGG* risk alleles, compared to cancer-free subject without risk alleles. Cancer patients with two risk alleles at *FGG* had a two-fold higher (HR 2.0, 95% CI 1.1-3.6) risk of VTE compared to cancer patients without risk alleles. In sub-analyses, the effect of active cancer and homozygosity at FGG yielded higher risk estimates for PE (HR 2.9, 95% CI: 1.3-6.6) than for DVT (HR 1.6, 95% CI: 0.7-3.5).

The cumulative incidence of VTE during the active cancer period is shown in Figure 2. The cumulative incidence of VTE increased particularly during the first six months following a cancer diagnosis, where we found a substantially steeper incline in the incidence curve for subjects with two risk alleles at *FGG rs2066865*. The cumulative incidence of VTE among homozygous carriers was 5.0% (95% CI: 2.4-9.6), 6.4% (95% CI: 3.5-11.6), and 8.0% (95% CI: 4.6-13.9) at three months, six months and 24 months after cancer diagnosis, respectively. The corresponding figures for cancer patients who were non-carriers were 2.1% (95% CI: 1.5-3.0), 3.1% (95% CI: 2.3-4.7), and 4.8% (95% CI: 3.8-6.2), respectively.

A supra-additive effect on the risk of VTE was observed for the combination of homozygosity at the *FGG* variant and active cancer (Table 4). The Relative excess risk by

Table 2. Characteristics of subjects with cancer-related and non-cancer-related first venous thromboembolism.

	Cancer-related VTE	
	Yes (167)	No (459)
Age at VTE diagnosis (years)	69 ±11	68±14
Sex (Males)	44.9 (75)	47.3(217)
VTE type		
Deep vein thrombosis	59.2 (99)	55.5 (255)
Proximal upper limb	5.1 (5)	2.0 (5)
Distal upper limb	1.0 (1)	0 (0)
Proximal lower limb	62.6 (62)	65.9 (168)
Distal lower limb	12.1 (12)	28.2 (72)
Other localizations	19.1 (19)	3.9 (10)
Pulmonary embolism	40.7 (68)	44.4 (204)
Unprovoked event	NA	54.9 (252)
Provoking factors		
Surgery[a]	12.6 (21)	15.3 (70)
Trauma[a]	2.4 (4)	9.6 (44)
Acute medical condition[b]	15.0 (25)	14.2 (65)
Immobilization[c]	20.4 (34)	20.0 (92)
Other provoking factor[d]	8.4 (14)	3.7 (17)
Total provoked[e]	44.3 (74)	44.7 (205)

Values are numbers or percentages with numbers in parenthesis or means ± standard deviation (SD); VTE: venous thromboembolism; NA: not applicable; [a]within eight weeks before the VTE-event; [b]myocardial infarction, ischemic stroke of major infectious disease; [c]bedrest >3 days, wheelchair, long haul travel >4 hours in the past 14 days; [d]presence of other provoking factors noted by the physician (*e.g.* intravenous catheters); [e]one or more provoking factor above

Table 3. Age and sex adjusted hazard ratios for venous thromboembolism according to categories of fibrinogen gamma (FGG) risk alleles and cancer status.

		VTE			PE			DVT		
	Risk Alleles	Events	HR (95% CI)	HR (95% CI)	Events	HR (95% CI)	HR (95% CI)	Events	HR (95% CI)	HR (95% CI)
No cancer	0	242	Ref.	–	112	Ref.	–	130	Ref.	–
	1	170	1.0 (0.8-1.2)	–	70	0.9 (0.6-1.2)	–	100	1.1 (0.8-1.4)	–
	2	47	1.7 (1.2-2.3)	–	22	1.7 (1.1-2.7)	–	25	1.6 (1.1-2.5)	–
Active cancer	0	89	11.9 (9.3-15.2)	Ref.	32	8.3 (5.6-12.5)	Ref.	57	15.3 (11.2-21.1)	Ref.
	1	64	12.2 (9.2-16.1)	1.1 (0.8-1.5)	29	10.6 (7.1-16.3)	1.3 (0.8-2.2)	35	13.4 (9.2-19.6)	1.0 (0.6-1.5)
	2	14	22.2 (12.9-38.1)	2.0 (1.1-3.6)	7	22.8 (10.6-49.1)	2.9 (1.3-6.6)	7	21.6 (10.0-46.4)	1.6 (0.7-3.5)

Active cancer: period from six months before a cancer diagnosis until two years after; CI: confidence interval; DVT: deep vein thrombosis; HR: hazard ratio; PE: pulmonary embolism; VTE: venous thromboembolism.

interaction (RERI) was 9.61 (95% CI: -2.38-21.61) and the Rothmans synergy index (RSI) was 1.81 (95% CI: 1.02-3.21). The proportion attributable to interaction (AP) was 0.43 (95% CI: 0.11-0.74). In sub-group analysis, the estimates of biological interaction were stronger for PE (RSI=2.37, 95% CI: 1.05-5.39) than for DVT (RSI=1.46, 95% CI: 0.65-3.27).

Discussion

In the present study, we aimed to investigate the joint effect of the *rs2066865* SNP at *FGG* and active cancer on the risk of VTE in a case-cohort recruited from the general population. Homozygosity at *rs2066865*, occurring in 6.6% of the study population, was associated with an increased risk of VTE. The combination of an *rs2066865* homozygous risk genotype and active cancer showed a synergistic effect on VTE risk (on an additive scale). The effect was particularly strong for PE. The cumulative incidence of VTE increased substantially during the first six months following a cancer diagnosis, especially among patients with two risk alleles at *FGG rs2066865*. Our findings suggest that homozygosity at *FGG rs2066865* may aid to differentiate patients at high and low risk of cancer-related VTE.

Several observational studies have reported an association between homozygous genotype of *rs2066865* and increased risk of VTE in Caucasians.[14-16,21] In a recent meta-analysis including seven observational studies, the odds ratio of VTE was 1.61 for homozygosity at *rs2066865*.[21] Accordingly, in cancer-free subjects, we found that those with two *rs2066865* risk alleles had a 1.7-fold higher VTE risk than those with 0 risk alleles. The risk estimates for DVT and PE were essentially similar in cancer-free subjects.

Even though the role of prothrombotic genotypes in cancer-related VTE have been scarcely studied, previous studies have found that some prothrombotic genotypes (*e.g.* factor V Leiden and prothrombin G20210A) are associated with increased risk of cancer-related VTE.[22,23,30,31] Further, the combined effect of cancer and factor V variants (factor V Leiden and *rs4524*) exceeded the sum of the individual effects, implicating a biological interaction on VTE risk.[22,24] Accordingly, we found that the combination of *FGG* and active cancer yielded a synergistic effect on VTE risk.

In cancer patients, the cumulative incidence curve of VTE was substantially steeper in individuals homozygous for *FGG* during the first six months following the cancer diagnosis. According to the thrombosis potential model,[32] several risk factors need to be present concurrently to exceed the thrombosis potential and facilitate development of a VTE. In the period following a cancer diagnosis, treatment with surgery and/or chemotherapy is typically initiated, and treatment-related complications such as acute infection and immobilization frequently occur. Thus, the accumulation of several treatment-related risk factors, which adds to the background risk in patients with cancer and risk alleles at FGG, may partly explain the substantial increase in VTE incidence the first half year following a cancer diagnosis.

In contrast to cancer-free subjects, we found that the effect of *rs2066865* was stronger for PE than for DVT in cancer patients. This suggests that the *FGG* variant may play a more essential role in the pathogenesis of PE than DVT in cancer patients. The underlying mechanism(s) for the latter observation is unknown, but may imply that *rs2066865* is associated with fragile thrombi, which are prone to embolization and manifest clinically as PE rather than DVT in cancer patients.

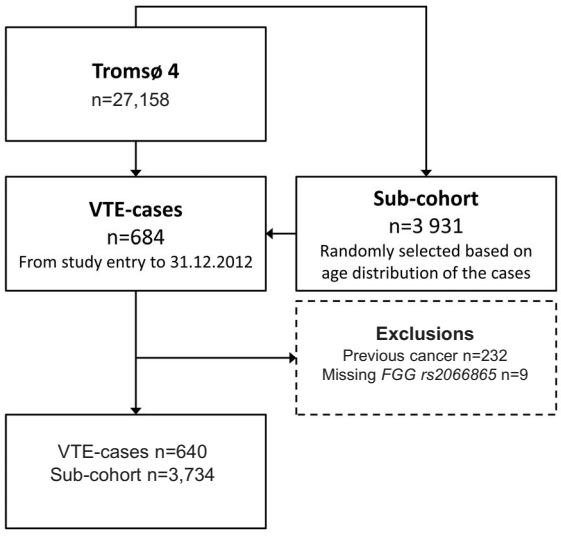

Figure 1. Flow chart for the case-cohort.

The mechanism by which the *rs2066865* affects susceptibility to VTE is not fully elucidated. However, the current hypothesis is that it acts through a phenotype with altered fibrinogen composition and formation. The *rs2066865* SNP tags the *FGG-H2* haplotype. Previous studies have shown that homozygous carriers of the FGG-H2 haplotype had lower levels of γ' fibrinogen and γ' fibrinogen/total fibrinogen concentration[14] without alterations in the total fibrinogen level.[33] The suggested mechanism is that the FGG variant favors formation of the abundant γ-chain isoform (γA) above the minor γ-chain (γ') through alternative splicing of the mRNA of the *FGG*-gene.[14,33] Fibrinogen γ' exhibits an inhibitory activity towards thrombin, due to a high affinity binding site on the γ' chain for thrombin exosite II,[34] which inhibits thrombin-mediated activation of factor VIII,[35] factor V[36] and platelets.[37] Moreover, fibrinogen γ' has been shown to increase the activated protein C (APC) sensitivity.[38] However, studies on the association between low plasma levels of fibrinogen γ' and VTE risk have shown somewhat inconsistent results.[14,20]

Current anticoagulant prophylaxis regimens efficiently prevent first VTE in cancer patients, but at the expense of a substantial risk of major and life-threatening bleedings.[39] Therefore, current international guidelines do not recommend prophylactic anticoagulation to all ambulatory cancer patients.[40,41] Thus, it is vital to recognize patients that are at high risk of cancer associated VTE, in order to identify those who would benefit most from thromboprophylaxis. Prothrombotic genotypes are attractive biomarker candidates, which could be used to distinguish between high and low risk of VTE in cancer patients, since they are fixed and not affected by the clinical status or treatment-related factors. In the present study, 6.4% of cancer

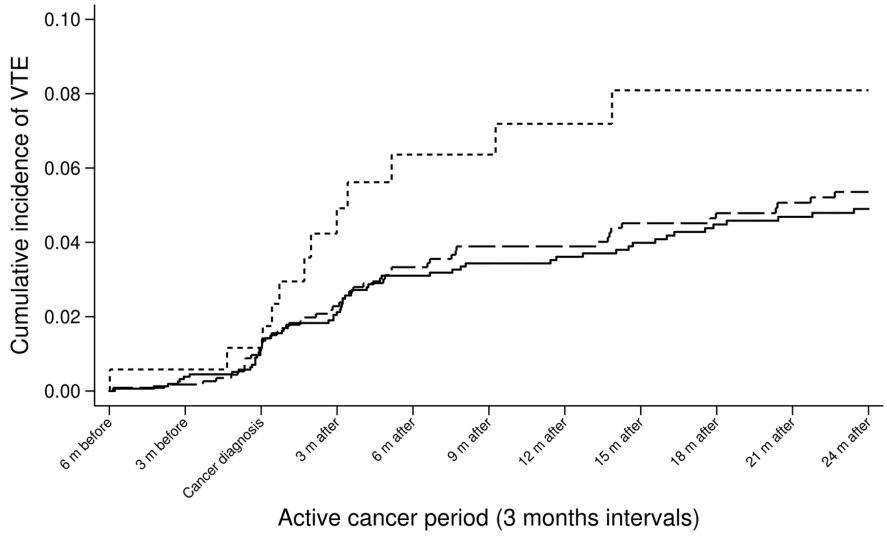

Figure 2. Cumulative incidence of venous thromboembolism in the presence of *FGG rs2066865* risk alleles during the active cancer period. VTE: venous thromboembolism; m: months.

Table 4. Measures of interaction between the homozygous fibrinogen gamma *(FGG)* variant and active cancer on venous thromboembolism.

	Rothmans synergy index (RSI) (95% CI)	Relative excess risk by interaction (RERI) (95% CI)	Proportion due to interaction (AP) (95% CI)
FGG rs2066865			
VTE	1.81 (1.02-3.21)	9.6 (-2.4-21.6)	0.43 (0.11-0.74)
PE	2.37 (1.05-5.39)	13.4 (-4.8-31.7)	0.56 (0.21-0.90)
DVT	1.46 (0.65-3.27)	6.3 (-9.6-22.1)	0.30 (-0.24-0.83)

Rothmans synergy index (RSI) >1 indicates a positive interaction or more than additivity; Relative excess risk by interaction (RERI) >0 indicates a positive interaction or more than additivity; Proportion due to interaction (AP) >0 indicates a positive interaction or more than additivity.VTE: venous thromboembolism; PE: pulmonary embolism; DVT: deep vein thrombosis; CI: confidence interval.

patients with two risk alleles at *FGG rs2066865* developed VTE during the first six months after cancer diagnosis compared to 3.1% of cancer patients without risk alleles. Our findings suggest that FGG may be an attractive gene candidate to pursue in future research on prediction models of VTE risk in cancer patients. We and others have previously reported similar discriminative power of two variants in the *F5* gene (*rs6025* and *rs4524*),[23,24] and a genetic model including nine SNP reported promising predictive capacity on VTE risk in breast cancer.[42] Recently, a new risk prediction model for cancer-related VTE, including clinical characteristics and genetic variants, reported a strong predictive capacity with an area under the curve (AUC) of 0.73 and performed better that the Khorana score (AUC 0.58).[43]

The main strengths of present study are the prospective design, high participation rate and long-term follow-up, making it possible to capture a large quantity of both incident cancer- and VTE-events in the study population. Since all participants live within a single hospital catchment area, the probability of missing outcomes is low. Moreover, both incident VTE-events and cancer diagnoses were systematically validated and objectively confirmed. The study was limited by the lack of statistical power in sub-group analysis (*i.e.* DVT/PE), illustrated by wide CI for our risk estimates. In addition, we did not have access to information on treatment regimens or medical complications among cancer patients. Although there is no reason to believe that the type or intensity of treatment would be influenced by the genetic makeup, such data could have provided further insights into the possible interplay between genes and treatment-related risk factors.

In conclusion, we found that homozygosity at *FGG rs2066865* was associated with an increased risk of VTE, and yielded a synergistic effect on the VTE risk in combination with active cancer, particularly on the risk of PE.

Funding

The K.G. Jebsen Thrombosis Research and Expertise Centre is supported by an independent grant from Stiftelsen Kristian Gerhard Jebsen.

References

1. Heit JA. Venous thromboembolism: disease burden, outcomes and risk factors. J Thromb Haemost. 2005;3(8):1611-1617.
2. White RH. The epidemiology of venous thromboembolism. Circulation. 2003;107(23 Suppl 1):I4-8.
3. Naess IA, Christiansen SC, Romundstad P, Cannegieter SC, Rosendaal FR, Hammerstrom J. Incidence and mortality of venous thrombosis: a population-based study. J Thromb Haemost. 2007;5(4):692-699.
4. Spencer FA, Lessard D, Emery C, Reed G, Goldberg RJ. Venous thromboembolism in the outpatient setting. Arch Intern Med. 2007;167(14):1471-1475.
5. Timp JF, Braekkan SK, Versteeg HH, Cannegieter SC. Epidemiology of cancer-associated venous thrombosis. Blood. 2013;122(10):1712-1723.
6. Prandoni P, Lensing AW, Piccioli A, et al. Recurrent venous thromboembolism and bleeding complications during anticoagulant treatment in patients with cancer and venous thrombosis. Blood. 2002;100(10):

3484-3488.
7. Elting LS, Escalante CP, Cooksley C, et al. Outcomes and cost of deep venous thrombosis among patients with cancer. Arch Intern Med. 2004;164(15):1653-1661.
8. Lee KW, Lip GY. Effects of lifestyle on hemostasis, fibrinolysis, and platelet reactivity: a systematic review. Arch Intern Med. 2003;163(19):2368-2392.
9. Noble S, Pasi J. Epidemiology and pathophysiology of cancer-associated thrombosis. Br J Cancer. 2010;102 Suppl 1:S2-9.
10. Khorana AA, Francis CW, Culakova E, Kuderer NM, Lyman GH. Frequency, risk factors, and trends for venous thromboembolism among hospitalized cancer patients. Cancer. 2007;110(10):2339-2346.
11. Sorensen HT, Mellemkjaer L, Olsen JH, Baron JA. Prognosis of cancers associated with venous thromboembolism. N Engl J Med. 2000;343(25):1846-1850.
12. Larsen TB, Sorensen HT, Skytthe A, Johnsen SP, Vaupel JW, Christensen K. Major genetic susceptibility for venous thromboembolism in men: a study of Danish twins. Epidemiology. 2003;14(3):328-332.
13. Souto JC, Almasy L, Borrell M, et al. Genetic susceptibility to thrombosis and its relationship to physiological risk factors: the GAIT study. Genetic Analysis of Idiopathic Thrombophilia. Am J Hum Genet. 2000;67(6):1452-1459.
14. Uitte de Willige S, de Visser MC, Houwing-Duistermaat JJ, Rosendaal FR, Vos HL, Bertina RM. Genetic variation in the fibrinogen gamma gene increases the risk for deep venous thrombosis by reducing plasma fibrinogen gamma' levels. Blood. 2005;106(13):4176-4183.
15. Uitte de Willige S, Pyle ME, Vos HL, et al. Fibrinogen gamma gene 3'-end polymorphisms and risk of venous thromboembolism in the African-American and Caucasian population. Thromb Haemost. 2009;101(6):1078-1084.
16. Grunbacher G, Weger W, Marx-Neuhold E, et al. The fibrinogen gamma (FGG) 10034C > T polymorphism is associated with venous thrombosis. Thromb Res. 2007;121(1):33-36.
17. Germain M, Saut N, Greliche N, et al. Genetics of venous thrombosis: insights from a new genome wide association study. PLoS One. 2011;6(9):e25581.
18. Germain M, Chasman DI, de Haan H, et al. Meta-analysis of 65,734 individuals identifies TSPAN15 and SLC44A2 as two susceptibility loci for venous thromboembolism. Am J Hum Genet. 2015;96(4):532-542.
19. El-Galaly TC, Severinsen MT, Overvad K, et al. Single nucleotide polymorphisms and the risk of venous thrombosis: results from a Danish case-cohort study. Br J Haematol. 2013;160(6):838-841.
20. Folsom AR, Tang W, George KM, et al. Prospective study of gamma' fibrinogen and incident venous thromboembolism: The Longitudinal Investigation of Thromboembolism Etiology (LITE). Thromb Res. 2016;139:44-49.
21. Jiang J, Liu K, Zou J, et al. Associations between polymorphisms in coagulation-related genes and venous thromboembolism: A meta-analysis with trial sequential analysis. Medicine (Baltimore). 2017;96(13):e6537.
22. Blom JW, Doggen CJ, Osanto S, Rosendaal FR. Malignancies, prothrombotic mutations, and the risk of venous thrombosis. JAMA. 2005;293(6):715-722.
23. Pabinger I, Ay C, Dunkler D, et al. Factor V Leiden mutation increases the risk for venous thromboembolism in cancer patients - results from the Vienna Cancer And Thrombosis Study (CATS). J Thromb Haemost. 2015;13(1):17-22.
24. Gran OV, Smith EN, Braekkan SK, et al. Joint effects of cancer and variants in the Factor 5 gene on the risk of venous thromboembolism. Haematologica. 2016;101(9):1046-1053.
25. Gran OV, Braekkan SK, Hansen JB. Prothrombotic genotypes and risk of venous thromboembolism in cancer. Thromb Res. 2018;164 Suppl 1:S12-S18.
26. Jacobsen BK, Eggen AE, Mathiesen EB, Wilsgaard T, Njolstad I. Cohort profile: the Tromso Study. Int J Epidemiol. 2012;41(4):961-967.
27. Blix K, Severinsen MT, Braekkan S, et al. Cancer-related venous thromboembolism in the general population: results from the Scandinavian Thrombosis and Cancer (STAC) study. J Thromb Haemost. 2015;13:(Suppl 2):549-549.
28. White RH, Chew HK, Zhou H, et al. Incidence of venous thromboembolism in the year before the diagnosis of cancer in 528,693 adults. Arch Intern Med. 2005;165(15):1782-1787.
29. Morange PE, Tregouet DA. Lessons from genome-wide association studies in venous thrombosis. J Thromb Haemost. 2011;9(Suppl 1):258-264.
30. Ramacciotti E, Wolosker N, Puech-Leao P, et al. Prevalence of factor V Leiden, FII G20210A, FXIII Va134Leu and MTHFR C677T polymorphisms in cancer patients with and without venous thrombosis. Thromb Res. 2003;109(4):171-174.
31. Mandala M, Curigliano G, Bucciarelli P, et al. Factor V Leiden and G20210A prothrombin mutation and the risk of subclavian vein thrombosis in patients with breast cancer and a central venous catheter. Ann Oncol. 2004;15(4):590-593.
32. Rosendaal FR. Venous thrombosis: a multicausal disease. Lancet. 1999;353(9159):1167-1173.
33. Willige SU, Rietveld IM, De Visser MCH, Vos HL, Bertina RM. Polymorphism 10034C > T is located in a region regulating polyadenylation of FGG transcripts and influences the fibrinogen gamma'/gamma A mRNA ratio. J Thromb Haemost. 2007;5(6):1243-1249.
34. Farrell DH. gamma' Fibrinogen as a novel marker of thrombotic disease. Clin Chem Lab Med. 2012;50(11):1903-1909.
35. Lovely RS, Boshkov LK, Marzec UM, Hanson SR, Farrell DH. Fibrinogen gamma' chain carboxy terminal peptide selectively inhibits the intrinsic coagulation pathway. Br J Haematol. 2007;139(3):494-503.
36. Omarova F, Uitte De Willige S, Ariens RA, Rosing J, Bertina RM, Castoldi E. Inhibition of thrombin-mediated factor V activation contributes to the anticoagulant activity of fibrinogen gamma'. J Thromb Haemost. 2013;11(9):1669-1678.
37. Lovely RS, Rein CM, White TC, et al. gammaA/gamma' fibrinogen inhibits thrombin-induced platelet aggregation. Thromb Haemost. 2008;100(5):837-846.
38. Omarova F, Uitte de Willige S, Simioni P, et al. Fibrinogen gamma' increases the sensitivity to activated protein C in normal and factor V Leiden plasma. Blood. 2014;124(9):1531-1538.
39. Di Nisio M, Porreca E, Ferrante N, Otten HM, Cuccurullo F, Rutjes AW. Primary prophylaxis for venous thromboembolism in ambulatory cancer patients receiving chemotherapy. Cochrane Database Syst Rev. 2012;(2):CD008500.
40. Kahn SR, Lim W, Dunn AS, et al. Prevention of VTE in nonsurgical patients: Antithrombotic Therapy and Prevention of Thrombosis, 9th ed: American College of Chest Physicians Evidence-Based Clinical Practice Guidelines. Chest. 2012;141(2 Suppl):e195S-e226S.
41. Lyman GH, Bohlke K, Khorana AA, et al. Venous thromboembolism prophylaxis and treatment in patients with cancer: american society of clinical oncology clinical practice guideline update 2014. J Clin Oncol. 2015;33(6):654-656.
42. Brand JS, Hedayati E, Humphreys K, et al. Chemotherapy, genetic susceptibility, and risk of venous thromboembolism in breast cancer patients. Clin Cancer Res. 2016;22(21):5249-5255.
43. Munoz Martin AJ, Ortega I, Font C, et al. Multivariable clinical-genetic risk model for predicting venous thromboembolic events in patients with cancer. Br J Cancer. 2018;118(8):1056-1061.

ARTICLE

Bleeding disorders in adolescents with heavy menstrual bleeding in a multicenter prospective US cohort

Ayesha Zia,[1,2,3,4] Shilpa Jain,[5] Peter Kouides,[6] Song Zhang,[1,7] Ang Gao,[1,7] Niavana Salas,[4] May Lau,[1,3,8] Ellen Wilson,[1,4,9] Nicole DeSimone[1,10] and Ravi Sarode[1,10]

[1]The University of Texas Southwestern Medical Center, Dallas, TX; [2]Department of Pediatrics, Children's Medical Center, Dallas, TX; [3]Division of Hematology/Oncology, Children's Medical Center, Dallas, TX; [4]Children's Medical Center, Dallas, TX; [5]Hemophilia Center of Western New York, John R. Oishei Children's Hospital of Buffalo, Division of Pediatric Hematology-Oncology, Buffalo, NJ; [6]Mary M. Gooley Hemophilia Center, University of Rochester School of Medicine, Rochester, MN; [7]Department of Data and Population Sciences, The University of Texas Southwestern Medical Center, Dallas, TX; [8]Division of Adolescent Medicine, The University of Texas Southwestern Medical Center, Dallas, TX; [9]Department of Obstetrics and Gynecology, The University of Texas Southwestern Medical Center, Dallas, TX and [10]Department of Pathology and Internal Medicine, The University of Texas Southwestern Medical Center, Dallas, TX, USA

Ferrata Storti Foundation

Haematologica 2020
Volume 105(7):1969-1976

ABSTRACT

Heavy menstrual bleeding is common in adolescents. The frequency and predictors of bleeding disorders in adolescents, especially with anovulatory bleeding, are unknown. Adolescents referred for heavy menstrual bleeding underwent an evaluation of menstrual bleeding patterns, and bleeding disorders determined *a priori*. The primary outcome was the diagnosis of a bleeding disorder. Two groups were compared: anovulatory and ovulatory bleeding. Multivariable logistic regression analysis of baseline characteristics and predictors was performed. Kaplan Meier curves were constructed for the time from the first bleed to bleeding disorder diagnosis. In 200 adolescents, a bleeding disorder was diagnosed in 33% (n=67): low von Willebrand factor levels in 16%, von Willebrand disease in 11%, and qualitative platelet dysfunction in 4.5%. The prevalence of bleeding disorder was similar between ovulatory and anovulatory groups (31% *vs.* 36%; *P*=0.45). Predictors of bleeding disorder included: younger age at first bleed (OR: 0.83; 95%CI: 0.73, 0.96), Hispanic ethnicity (OR: 2.48; 95%CI: 1.13, 5.05), non-presentation to emergency department for heavy bleeding (OR: 0.14; 95%CI: 0.05, 0.38), and International Society on Thrombosis and Haemostasis (ISTH) Bleeding Assessment Tool score ≥4 (OR: 8.27; 95%CI: 2.60, 26.44). Time from onset of the first bleed to diagnosis was two years in the anovulatory, and six years in the ovulatory cohort (log-rank test, *P*<0.001). There is a high prevalence of bleeding disorders in adolescents with heavy periods, irrespective of the bleeding pattern. Among bleeding disorders, the prevalence of qualitative platelet dysfunction is lower than previously reported.

Introduction

Heavy menstrual bleeding (HMB) is common in adolescents after menarche.[1] Anovulation is the most common etiology of HMB and is expected to persist for up to five years.[2] Underlying bleeding disorders (BD) are another important etiology of HMB affecting up to 20% of adults and 13-60% of adolescents.[3] A large body of research has focused on the prevalence of BD in adult women and its predictors. In contrast, pediatric literature on BD frequency has only been recently accrued. Most data are retrospective and prevalence studies by and large excluded women with anovulatory bleeding.[4-6] Data on predictors of BD in adolescents with HMB, when anovulation is most prevalent, are scant and it is difficult to determine whom to screen for BD.[3]

Correspondence:

AYESHA ZIA
Ayesha.zia@utsouthwestern.edu

Received: April 29, 2019.

Accepted: October 14, 2019.

Pre-published: October 17, 2019.

doi:10.3324/haematol.2019.225656

Check the online version for the most updated information on this article, online supplements, and information on authorship & disclosures: www.haematologica.org/content/105/7/1969

Our study aimed to describe the frequency, predictors, and time from bleeding onset to BD diagnosis in a prospective cohort of adolescents with HMB, using a well-defined and rigorous protocol of hemostasis testing and platelet function analysis. We hypothesized that the frequency of undiagnosed BD in adolescents with HMB would be similar to adults, and that the menstrual bleeding pattern will not predict a BD.

Methods

Postmenarchal adolescents up to 18 years of age referred for HMB without a diagnosis of BD were eligible to participate (Figure 1). Participants were enrolled prospectively from the Young Women's Blood Disorders Program at The University of Texas Southwestern (UTSW), Dallas, TX (primary site), USA, and the Children's Hospital of Buffalo (CHOB), NY, USA (external site) between July 2014 and December 2017, after informed consent and/or assent.[7] The institutional review board at both UTSW and CHOB (Institutional Review Board numbers: STU 102014-001 and 00003126, respectively) approved the study. Participants were excluded if they did not complete: 1) a minimum of two visits and 2) the minimum BD evaluation, decided *a priori.*

Definitions

Heavy menstrual bleeding was defined by menstrual duration ≥7 days with a sensation of "gushing" or "flooding" or bleeding through a pad or tampon for ≤2 hours.[8,9] Based on the pattern of HMB in the entire cohort, participants were classified and compared among two groups: the anovulatory HMB group was defined as having menstrual duration <21 or >45 days; the ovulatory HMB group was defined when this menstrual pattern was not present.[10]

Laboratory testing

All participants underwent testing that included complete blood count, serum ferritin, prothrombin time (PT), activated partial thromboplastin time (aPTT), fibrinogen, von Willebrand Factor (vWF) analysis (repeated at least twice for every participant), platelet aggregation (repeated if abnormal), Factor (F) XI, FXIII factor assays and systemic hyperfibrinolysis assessment using rotational thromboelastometry (ROTEM).[11] This comprised the minimum BD evaluation for retention into the final analysis.

Iron deficiency/iron deficiency anemia

We defined anemia as hemoglobin <110 g/L and iron deficiency as serum ferritin levels ≤ 20 μg/L.

Bleeding assessment tools

Pictorial Blood Assessment Chart (PBAC) - a PBAC score was computed for all participants, and an average score of three cycles was taken as the final score.[12] Standardized pads and tampons were not provided.

Outcomes

The primary outcome of the study was the diagnosis of BD defined as low von Willebrand disease (vWD), qualitative platelet dysfunction (QPD), clotting factor deficiencies or hyperfibrinolysis.

Statistical analysis

Sample size - based on adult data,[4,5] we assumed that 20% of adolescents with HMB, irrespective of menstrual bleeding pattern, will be diagnosed with BD within six months from study entry; with a total of 180 patients, we estimated the rate of BD in this group with such precision that the 95% confidence interval has a half-length smaller than 8%.[14]

Main outcome

The frequency of BD was compared among groups using χ^2 test.

A multivariable logistic regression model was built following the technique described by Hosmer, Lemeshow, and Sturdivant.[15] Variable selection was performed using the stepwise procedure.

Kaplan-Meier curves were constructed from the first bleed to BD diagnosis for the entire cohort and the main two groups and compared using the log-rank test.

Further information on the methods used is available in the *Online Supplementary Appendix.*

Results

Demographic and clinical characteristics

Two hundred and thirty-five consecutive adolescents were enrolled during the study period, of which 200 participants met eligibility criteria, and had complete outcome data: 185 from UTSW and 15 from CHOB. The median age of participants was 15 years (y) (Table 1), and 28% were Hispanic. Fifty-five percent had normal body mass index (BMI) as determined by Center for Disease Control (CDC) growth charts. The median age at menarche was 12 years, and BD evaluation occurred at a median of three years from menarche. Thirty-three percent presented to the Emergency Department (ED) for evaluation and management of HMB; 25% needed to be hospitalized, of which 19% received packed red blood cells (pRBC). The mean PBAC score was 386 [standard deviation (SD), 243] and the ISTH score was 3.5 (SD 1.3). A

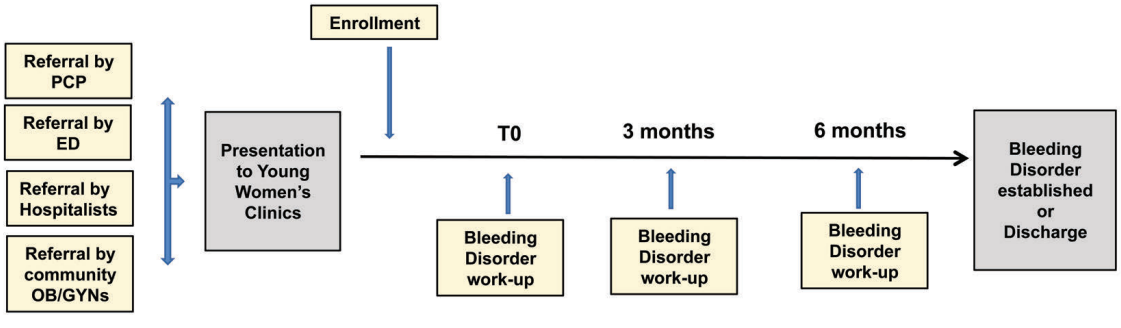

Figure 1. Study design. Prospective, multicenter, observational study of adolescents presenting with heavy menstrual bleeding.

family history of bleeding symptoms or established BD was present in 21% and 6.5%, respectively. Family history of gynecologic or obstetric bleeding was present in 60%: 57% (n=114) with HMB alone; 1.5% (n=3) with HMB and post-partum hemorrhage (PPH) (n=3), and 1.5% (n=3) had only PPH. Of the first-degree relatives with HMB, 38% underwent hysterectomy for HMB (n=44) and 2% underwent endometrial ablation (n=2) to control HMB. Thirty-six percent (n=72) had iron deficiency anemia, 29% (n=57) had iron deficiency alone, and overall iron deficiency was documented in 65% (n=129). Participants with anovulatory HMB had a higher BMI (66.7% *vs.* 36%) and increased frequency of refractory HMB (34% *vs.* 19%), ED visits (42 % *vs.* 25%), hospitalizations (28% *vs.* 17%), and pRBC (24% *vs.* 14%) administration for HMB compared to those with ovulatory pattern bleeding.

Frequency and types of bleeding disorders and additional bleeding symptoms

Overall, 33% (n=67) of adolescents were diagnosed with a BD. Among those with BD, there were no differences in the frequency of BD in the anovulatory and the ovulatory HMB groups (31% *vs.* 36%; *P*=0.45). Low vWF levels were detected in 57% (n=38 of 67); 25% (n=17 of 67) were diagnosed with vWD (type 1=13, type 2=4), 13.5% (n=9 of 67) with QPD, and two participants were found to have coagulation factor deficiencies (one with mild FVIII deficiency (FVIII:C= 29%) and mild FXIII deficiency (FXIII: 40%). One participant, referred for HMB

Table 1. Baseline characteristics of the entire study cohort and according to menstrual bleeding pattern.

	All patients (N=200) n (%)	Anovulatory HMB (N=100) n (%)	Ovulatory HMB (N=100) n (%)
Age, y	15 (10-19)	14 (10-18)	15 (11-19)
Ethnicity			
Hispanic	56 (28)	33 (33)	23 (23)
Non-Hispanic	144 (72)	67 (67)	77(77)
Race			
White	131 (65)	70 (70)	61(61)
Black	41 (20·5)	13 (13)	28 (28)
Other	28 (14)	17 (17)	11 (11)
BMI, kg/m^2	23·3 (14·5-55)	24·4 (17-55)	22·9 (14·5-44)
Normal weight	110 (55)	45 (45)	65 (65)
Overweight/Obese	90 (45)	55 (55)	35 (35)
Age at menarche, y	12 (9-15)	12 (9-15)	12 (9-15)
Years since menarche	3 (1-4)	3 (1-4)	3 (1-4)
Time to HMB, y	0·5 (0-5)	0·5 (0-5)	0·4 (0-5)
Age at first bleed	12 (2-17)	12 (2-16)	12 (2-17)
Refractory HMB$	53 (26·5)	34 (34)	19 (19)
Presentation to ED for HMB@	67 (33.5)	42 (42)	25 (25)
≤ 1 visit	47 (23.5)	26 (26)	21 (21)
≥ 2 visits	19 (9·5)	15 (15)	4 (4)
Hospitalizations for HMB	45 (22·5)	28 (28)	17 (17)
pRBC	38 (84)	24 (86)	14 (82)
Parenteral Iron	76 (38)	36 (36)	40 (40)
PBAC at study entry*#	386 (243)	427 (274)	345 (201)
ISTH-BAT*	3.5 (1·3)	3.4 (1·3)	3.5 (1·3)
FMH of bleeding or BD	55 (27·5)	28 (28)	27 (27)
FMH of gynecologic or obstetric bleeding	120 (60)	55 (55)	65 (65)
Hypermobility	20(20)	9(23)	11(17)
Hemoglobin, g/L	11·8 (3·4-16·4)	11·7 (3·9-15)	11·8 (3·4-16·4)
Ferritin, ng/mL	8 (0·9-78)	10·2 (0·9 – 70)	7·2 (1-98)
TSH, mIU/L	1·5 (1·2-8·4)	1·7 (0·5-8·4)	1·4 (1·2-5·1)
BD diagnosis	67(33)	31(31)	36(36)

Values are medians with interquartile ranges except normally distributed variables marked with an asterisk; mean and standard deviations are reported. BMI: body mass index; ED: emergency department; HMB: heavy menstrual bleeding; ISTH-BAT: International Society of Thrombosis Haemostasis-Bleeding Assessment Tool; pRBC: packed red blood cells; PBAC: pictorial blood assessment chart; TSH: thyroid-stimulating hormone; y: years. Statistically significant differences between the anovulatory and ovulatory groups were found for refractory HMB, presentation to ED and PBAC @ # $*P*=0.01.

Table 2. Types of bleeding disorders in the whole group and according to menstrual bleeding pattern.

	All patients (N=200) n (%)	Anovulatory HMB (N=100) n (%)	Ovulatory HMB (N=100) n (%)
Low	38 (19)	14 (14)	24 (24)
vWF	17 (8.5)	12 (12)	5 (5)
Type 1	13 (6.5)	5(5)	8(8)
Type 2	4 (2)	3(3)	1(1)
Qualitative platelet dysfunction	9 (2)	5 (5)	4(4)
Clotting factor deficiencies	2 (1.5)	2(2)	–
Symptomatic hemophilia carrier	1 (0.5)	1(1)	–

vWF: von Willebrand factor; vWD: von Willebrand disease.

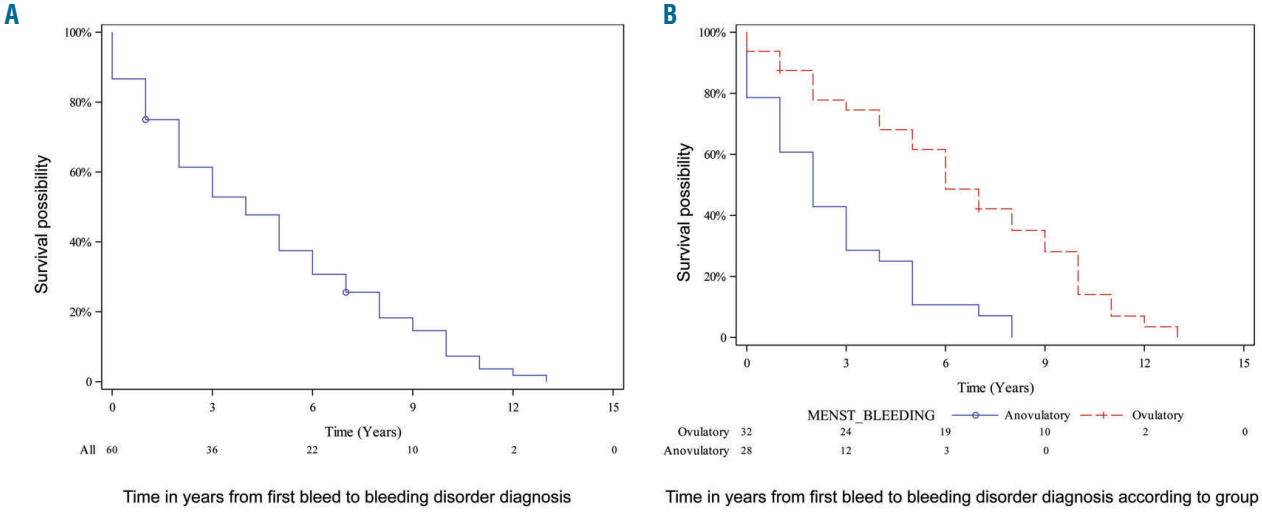

Figure 2. Kaplan-Meier curves showing time from the first bleeding event to bleeding disorder diagnosis. (A) Time until diagnosis for the entire group. (B) Time according to the menstrual bleeding group. The number of patients diagnosed according to the group is shown at the bottom of the graphic, on the x-axis.

four years after menarche because of a brother with FVIII deficiency, was diagnosed to be a symptomatic hemophilia carrier (FVIII: 124%; positive for a pathogenic type 1 intron 22 inversion mutation (F8 c.6429+؟_6430-؟ inv.). None of the participants showed evidence of systemic hyperfibrinolysis based on our testing protocol, though specific testing for plasminogen activator inhibitor or antiplasmin deficiency were not performed (Table 2 and *Online Supplementary Tables S3 and S4*). Of those diagnosed with BD, 29 (43%) had HMB as the sole complaint, 21 (31%) had one additional, 12 (18%) had two, four (6%) had three, and one participant had five additional bleeding symptoms. Of those without BD, 118 (88%) had HMB as the sole complaint; 12 (9%) had one, and 3 (2%) had two additional bleeding symptoms in addition to HMB (*Online Supplementary Table S5*).

Predictors of bleeding disorders

The results of the univariable logistic regression of potential predictors of BD are shown in Table 3. The final model (multivariable, stepwise logistic regression) included four predictors: younger age at first bleeding event, Hispanic ethnicity, non-presentation to ED, and ISTH BAT score of ≥4.

Time to diagnosis

Kaplan-Meier curves showed that the median time from the first bleed to BD diagnosis was four years (range 2-5) in the entire cohort, two years (range 1-3) in the anovulatory group, and six years (range 4-9) in the ovulatory group. There was a significant difference in time to diagnosis across groups (log-rank test, $P<0.0001$) (Figure 2).

Concomitant non-hemostatic disorders

Twenty-three participants with BD were diagnosed with additional disorders: three (1.5%) with polycystic ovarian syndrome, and four with uterine structural abnormalities (three with endometriosis and one with uterine polyps). Four participants without BD were diagnosed with vWF exon 28 polymorphism p.D1472H (suspected based on isolated decreased vWF:RCo) (Table 4). Only 100 participants underwent a joint exam for benign joint hypermobility (BJH); of those, 20 met criteria for BJH.

Discussion

Our study systematically investigated adolescents with HMB and showed that 33% had a BD. Almost 80% of

Table 3. Univariate and multivariate analyses of the association between baseline patient characteristics and bleeding disorder in the entire cohort.

Parameter	OR for BD	95% CI	*P*
		UNIVARIATE ANALYSIS	
Intercept			
Age, y	0·98	0.84, 1.14	0.802
Ethnicity			
Hispanic	1.95	1.03, 3.70	0.038
Non-Hispanic			
Race			
White	1·74	0.45, 6.65	0.416
Black	1·38	0.32, 5.90	0.665
Other			
Age at menarche, y	1.02	0.84, 1.25	0.789
Time to HMB, y	0·84	0.65, 1.09	0.199
Age at first bleed, y	0·74	0.66, 0.84	<0.0001
Refractory HMB			
Yes	1·72	0.90, 3.30	0.099
No			
Surgical bleeding			
Yes	4·57	1.28, 16.31	0.019
No			
Dental bleeding			
Yes	5·42	1.02, 28.78	0.047
No			
Presentation to ED for HMB			
Yes	0·50	0.26, 0.97	0.042
No			
Hospitalization for HMB			
No	2.03	0.93, 4.42	0.072
Yes			
pRBC			
Yes	0·55	0.24, 1.24	0.151
No			
Need for IV iron			
Yes	1·39	0.76, 2.54	0.275
No			
PBAC	1·001	1.0001, 1.002	0.036
ISTH BAT score			
≥3	1·83	0.70, 4.7	0.217
≥4	4·51	1.91, 10.64	0.0006
≤2			
FMH of bleeding or BD			
Positive	3.09	1.61, 6.42	0.0007
Negative			
FMH of GYN/OB bleeding			
Positive	2·23	1.16, 4.29	0.015
Negative			
Hemoglobin, g/L	0.99	0.97, 1.01	0.752
Ferritin, pmol/L	1.00	0.97, 1.02	0.980
		MULTIVARIATE ANALYSIS	
Intercept			
Age at first bleed, y	0·83	0.73, 0.96	0.011
Ethnicity			

Hispanic	2·48	1.13, 5.05	0.021
Non-Hispanic			
ED evaluation for HMB			
Yes	0·14	0.05, 0.38	<0.0001
No			
ISTH BAT score			
≥3	1·57	0.54, 4.13	0.435
≥4	8.27	2.60, 26.44	0.0004
≤2			
	C-statistic:	**0.78**	

BMI: body mass index; ED: emergency department; HMB: heavy menstrual bleeding; ISTH-BAT: International Society of Thrombosis Haemostasis-Bleeding Assessment Tool; pRBC: packed red blood cells; PBAC: pictorial blood assessment chart; TSH: thyroid-stimulating hormone; y: years.

those with BD had a diagnosis of either low vWF or vWD. Our findings suggest that BD are equally prevalent in the anovulatory or ovulatory pattern of menstrual bleeding. Identification of adolescents with BD is the first step in preventing delays in diagnosis and, by extension, long-term untoward complications of BD. HMB soon after menarche is traditionally deemed as "hormonal," and anovulation is the default etiology. These findings have implications for clinicians who routinely manage adolescents with HMB: screening or referral for screening for BD is appropriate, irrespective of the pattern of menstrual bleeding.

Seravalli *et al*. investigated the frequency of BD in adolescents, dividing participants into two groups based on whether abnormal uterine bleeding started in the first two years from menarche or later. Overall, 48% of adolescents were diagnosed with a hemostatic defect (18% with QPD, 14% with vWD, 13% with clotting factor deficiencies, and 7% with an increase in bleeding time), but there were no differences in the prevalence of BD between the groups (44% *vs.* 59%; *P*=0.17).[16] Philipp *et al*. also reported that adolescents and peri-menopausal women were just as likely to have hemostatic defects as were women aged 20-44 years;[17] the former age brackets representing periods of anovulatory menstrual bleeding. Furthermore, Vo *et al*. reported that adolescents with BD were more likely to perceive and report their menstrual cycles as irregular.[18] These studies had certain limitations, such as retrospective data collection, and a lack of uniform and comprehensive laboratory investigation.

In our cohort, younger age at first bleeding event, Hispanic ethnicity, non-presentation to the ED for HMB, and ISTH BAT score of ≥4 were identified as predictors of BD. Younger age at first bleeding event is known to be associated with hemostatic evaluation and BD diagnosis, representing those with an earlier phenotypic expression or more severe bleeding phenotype. Hispanic girls in our cohort were more likely to have a BD, even though non-Hispanics made up the majority. Previous studies have included mostly non-Hispanics; more specifically, women of eastern European ancestry and a lower prevalence of vWD and higher levels of VWF antigen, vWF activity, and FVIII have been reported in black women,[19,20] which can explain these findings. Adolescents who presented to ED for evaluation and management of HMB in our cohort were less likely to have a BD, which is similar to results from another multicenter analysis.[21] This may be further explained by: a) negative family history of HMB (60% of adolescents did not have a first-degree relative with HMB and the caregivers of these adolescents were likely unprepared to manage HMB at home); and b) 55% presenting to the ED had anovulatory bleeding (generally deemed difficult to manage with conventional route and doses of hormones).[22] Moreover, 67% of those with anovulatory bleeding were overweight or obese, the latter being associated with gonadal steroid hormone changes that result in disruption of ovulation and menstrual irregularities including HMB.[23,24] Previous studies show that adolescents who present acute symptoms and require hospitalization are more likely to have an underlying BD that was reported only in descriptive analyses, showing 19% and 33% of patients with abnormal uterine bleeding and coagulation disorders when compared with 74% and 67% without, respectively.[25-27]

When objectively assessing bleeding in patients with BD, consensus guidelines recommend the use of BAT.[28] The ISTH BAT has been shown to optimally identify BD in both adults and children; the pediatric cut-off able to optimally discriminate between no BD and a possible BD is a score of ≥3.[13] Instead, we identified a score of ≥4 to be predictive of BD. Recently, using identical data, ISTH-BAT was shown to be more sensitive for assessment of HMB in women with low vWF levels compared with other BAT, supporting a need to investigate and validate a higher "adolescent" specific cut-off.[29] The ISTH BAT score of ≥4 in those with BD was driven mostly by the presence of additional bleeding symptoms with HMB; 57% of adolescents with BD had other bleeding symptoms compared to 12% in those without BD. Previous data clearly show that the number of hemorrhagic symptoms is higher in the young when a more severe bleeding phenotype or disorder is present.[30,31] The presence of at least three bleeding symptoms, irrespective of severity, result in 99.5% specificity for the most common bleeding disorder, vWD, a finding that has been confirmed in the pediatric age group.[32]

The median time from onset of the first bleeding symptom to BD diagnosis was four years in the entire cohort, two years in the anovulatory, and six years in the ovulatory group. Adolescents with anovulatory HMB had heavier (mean PBAC score 427 *vs.* 345) or difficult to manage menses, resulting in an earlier referral and diagnosis, accounting for an earlier diagnosis. Lavin *et al*., on the other hand, have reported no differences in age at diagnosis for women with low vWF levels who reported HMB to physicians compared to those who did not go to the doctor (age 34.2 *vs.* 33.4 years; *P*=0.7).[29] Even though the time to diagnosis in our cohort is a significant improvement

Table 4. Prevalence of non-hemostatic disorders and concomitant disorders.

	Anovulatory HMB		Ovulatory HMB	
	BD (n=31)	No BD (n=69)	BD (n=36)	No BD (n=64)
PCOS	3	3	0	0
BJH**	3	7	6	4
Uterine structural ab.	1[@]	1[^]	3[@@]	0
Systemic disorders	6*	10[!]	1[#]	4[&]
Exon 28 polym.	0	1	0	3

ab: abnormalities; BD: bleeding disorder; PCOS: polycystic ovarian syndrome; BJH: benign joint hypermobility; polym: polymorphism. **BJH assessment was performed only on 100 participants. Systemic or medical disorders: *depression (n=4), remote history of cancer (n=1), and hypothyroidism (n=1); [!]depression (n=3), asthma requiring medications (n=3), remote history of cancer (n=3), hypothyroidism (n=1); #one had juvenile rheumatoid arthritis; [&]depression (n=1), diabetes mellitus (n=2); celiac disease (n=1). Uterine structural abnormalities; [@]one had endometriosis; [^]one had erosive vaginitis from tampon use; [@@]two were diagnosed with endometriosis, and one was diagnosed with uterine polyps.

from the average delay of 16 years previously reported in women with BD,[33] it highlights the importance of hematologists in the care of adolescents with HMB. For primary care practitioners, the relatively high prevalence of vWD in adolescent HMB is a reminder to test for vWD. A recent retrospective analysis of a large national claims database of 23,888 post-pubertal girls and adolescents with HMB observed a very low rate of screening for vWD of only 8% in those with HMB and 16% in those with severe HMB.[34]

The strengths of our study include the largest powered adolescent cohort ever prospectively examined. Participants underwent a uniform, protocolized evaluation for BD compared to "tiered" testing based on suspicion of a BD. Another finding of interest is an overall lower prevalence of QPD than that previously reported in the literature, where initial abnormal platelet aggregation was not repeated for confirmation. We diagnosed QPD based on reproducible findings, an approach that had been not undertaken in previous studies, leading to the overestimation of QPD (*Online Supplementary Table S4 and Online Supplementary Figure S1*).

Our study has some limitations. Although we consecutively enrolled unselected adolescents with HMB, they had, in effect, already been selected by their referring providers. This referral bias probably led to a higher frequency of BD in our center compared to primary care settings. This bias, however, is inherent to all studies carried out in tertiary care centers. The overall frequency of BD in our cohort is lower than that in previously reported data from other multidisciplinary clinics (33% *vs.* <60%) and is reflective of the stringent criteria used to diagnose BD. We also excluded patients referred for abnormal coagulation profiles, including initial abnormal vWF analysis, which may have under-estimated the prevalence of BD in our cohort.

We did not exclude participants on hormonal suppression for HMB. Even though PBAC scores were calculated for pre-hormonal cycles, it may have impacted PBAC scores and its predictive ability due to recall bias. Moreover, PBAC has not been validated for retrospective use or without using standardized brand pads and tampons. Because our study was conducted in large academic centers with dedicated Young Women's Blood Disorders clinics, our results are unlikely to apply to settings with a low prevalence of BD. Our time to diagnosis is subject to length bias; adolescents with severe bleeding phenotypes were likely referred earlier, leading to differences in time to diagnosis.

Our study will stimulate further research; the pediatric cut-off for an abnormal ISTH BAT score needs to be revisited for the adolescent age group. Even though we showed no difference in the frequency of BD according to HMB pattern, follow-up studies are in order on whether the efficacy of hemostatic-based therapies are equivalent. Finally, future studies are needed to assess the cost-effectiveness of selective testing in multidisciplinary clinics compared with universal screening across the population where the sole bleeding complaint could be HMB. Our predictive model also needs to be validated internally and externally in a larger population.

In summary, a high awareness, irrespective of the type of menstrual bleeding, is paramount to identify adolescents with BD.

Funding

AZ is supported by a grant from the National Institutes of Health (1K23HL132054-01). The funding source was not involved in the study design, analysis and interpretation of data; in the writing of the report or the decision to submit the article for publication.

References

1. Hallberg L, Hogdahl AM, Nilsson L, Rybo G. Menstrual blood loss--a population study. Variation at different ages and attempts to define normality. Acta Obstet Gynecol Scand. 1966;45(3):320-351.
2. Rosenfield RL. Clinical review: Adolescent anovulation: maturational mechanisms and implications. J Clin Endocrinol Metab. 2013;98(9):3572-3583.
3. Zia A, Rajpurkar M. Challenges of diagnosing and managing the adolescent with heavy menstrual bleeding. Thromb Res. 2016;143:91-100.
4. Edlund M, Blomback M, von Schoultz B, Andersson O. On the value of menorrhagia as a predictor for coagulation disorders. Am J Hematol. 1996;53(4):234-238.
5. Kadir RA, Economides DL, Sabin CA, Owens D, Lee CA. Frequency of inherited bleeding disorders in women with menorrhagia. Lancet. 1998;351(9101):485-489.
6. Miller CH, Philipp CS, Stein SF, et al. The spectrum of haemostatic characteristics of women with unexplained menorrhagia. Haemophilia. 2011;17(1):e223-229.
7. Zia A, Lau M, Journeycake J, et al. Developing a multidisciplinary Young Women's Blood Disorders Program: a single-centre approach with guidance for other centres. Haemophilia. 2016; 22(2):199-207.
8. Munro MG, Critchley HOD, Fraser IS,

Committee FMD. The two FIGO systems for normal and abnormal uterine bleeding symptoms and classification of causes of abnormal uterine bleeding in the reproductive years: 2018 revisions. Int J Gynaecol Obstet. 2018;143(3):393-408.
9. Philipp CS, Faiz A, Dowling NF, et al. Development of a screening tool for identifying women with menorrhagia for hemostatic evaluation. Am J Obstet Gynecol. 2008;198(2):163.
10. ACOG Committee on Practice Bulletins--Gynecology. American College of Obstetricians and Gynecologists. ACOG practice bulletin: management of anovulatory bleeding. Int J Gynaecol Obstet. 2001;72(3):263-271.
11. Lang T, Bauters A, Braun SL, et al. Multicentre investigation on reference ranges for ROTEM thromboelastometry. Blood Coagul Fibrinolysis. 2005;16(4):301-310.
12. Higham JM, O'Brien PM, Shaw RW. Assessment of menstrual blood loss using a pictorial chart. Br J Obstet Gynaecol. 1990; 97(8):734-739.
13. Elbatarny M, Mollah S, Grabell J, et al. Normal range of bleeding scores for the ISTH-BAT: adult and pediatric data from the merging project. Haemophilia. 2014; 20(6):831-835.
14. Liu XS. Implications of statistical power for confidence intervals. Br J Math Stat Psychol. 2012;65(3):427-437.
15. David W. Hosmer Jr. SL, Rodney X. Sturdivant. Applied Logistic Regression. 3rd Edition ed: John Wiley & Sons. 2013.
16. Seravalli V, Linari S, Peruzzi E, Dei M, Paladino E, Bruni V. Prevalence of hemostatic disorders in adolescents with abnormal uterine bleeding. J Pediatr Adolesc Gynecol. 2013;26(5):285-289.
17. Philipp CS, Faiz A, Dowling N, et al. Age and the prevalence of bleeding disorders in women with menorrhagia. Obstet Gynecol. 2005;105(1):61-66.
18. Vo KT, Grooms L, Klima J, Holland-Hall C, O'Brien SH. Menstrual bleeding patterns and prevalence of bleeding disorders in a multidisciplinary adolescent haematology clinic. Haemophilia. 2013;19(1):71-75.
19. Kadir RA, Economides DL, Sabin CA, Owens D, Lee CA. Variations in coagulation factors in women: effects of age, ethnicity, menstrual cycle and combined oral contraceptive. Thromb Haemost. 1999; 82(5):1456-1461.
20. Shankar M, Lee CA, Sabin CA, Economides DL, Kadir RA. von Willebrand disease in women with menorrhagia: a systematic review. BJOG. 2004;111(7):734-740.
21. Falcone T, Desjardins C, Bourque J, Granger L, Hemmings R, Quiros E. Dysfunctional uterine bleeding in adolescents. J Reprod Med. 1994;39(10):761-764.
22. Claessens EA, Cowell CA. Dysfunctional uterine bleeding in the adolescent. Pediatr Clin North Am. 1981;28(2):369-378.
23. Seif MW, Diamond K, Nickkho-Amiry M. Obesity and menstrual disorders. Best Pract Res Clin Obstet Gynaecol. 2015;29(4):516-527.
24. Pasquali R, Casimirri F, Plate L, Capelli M. Characterization of obese women with reduced sex hormone-binding globulin concentrations. Horm Metab Res. 1990; 22(5):303-306.
25. Claessens EA, Cowell CA. Acute adolescent menorrhagia. Am J Obstet Gynecol. 1981;139(3):277-280.
26. Smith YR, Quint EH, Hertzberg RB. Menorrhagia in adolescents requiring hospitalization. J Pediatr Adolesc Gynecol. 1998;11(1):13-15.
27. Bevan JA, Maloney KW, Hillery CA, Gill JC, Montgomery RR, Scott JP. Bleeding disorders: A common cause of menorrhagia in adolescents. J Pediatr. 2001;138(6):856-861.
28. O'Brien SH. Bleeding scores: are they really useful? Hematology Am Soc Hematol Educ Program. 2012;2012:152-156.
29. Lavin M, Aguila S, Dalton N, et al. Significant gynecological bleeding in women with low von Willebrand factor levels. Blood Adv. 2018;2(14):1784-1791.
30. Elden L, Reinders M, Witmer C. Predictors of bleeding disorders in children with epistaxis: value of preoperative tests and clinical screening. Int J Pediatr Otorhinolaryngol. 2012;76(6):767-771.
31. van Dijk K, Fischer K, van der Bom JG, Grobbee DE, van den Berg HM. Variability in clinical phenotype of severe haemophilia: the role of the first joint bleed. Haemophilia. 2005;11(5):438-443.
32. Bidlingmaier C, Grote V, Budde U, Olivieri M, Kurnik K. Prospective evaluation of a pediatric bleeding questionnaire and the ISTH bleeding assessment tool in children and parents in routine clinical practice. J Thromb Haemost. 2012;10(7):1335-1341.
33. Kirtava A, Crudder S, Dilley A, Lally C, Evatt B. Trends in clinical management of women with von Willebrand disease: a survey of 75 women enrolled in haemophilia treatment centres in the United States. Haemophilia. 2004;10(2): 158-161.
34. Powers JM, Stanek JR, Srivaths L, Haamid FW, O'Brien SH. Hematologic considerations and Management of adolescent girls with heavy menstrual bleeding and anemia in US Children's Hospitals. J Pediatr Adolesc Gynecol. 2018;31(5):446-450.

ARTICLE

Association of uric acid levels before start of conditioning with mortality after allogeneic hematopoietic stem cell transplantation – a prospective, non-interventional study of the EBMT Transplant Complication Working Party

Olaf Penack,[1] Christophe Peczynski,[2] Steffie van der Werf,[3] Jürgen Finke,[4] Arnold Ganser,[5] Helene Schoemans,[6] Jiri Pavlu,[7] Riitta Niittyvuopio,[8] Wilfried Schroyens,[9] Leylagül Kaynar,[10] Igor W. Blau,[1] Walter van der Velden,[11] Jorge Sierra,[12] Agostino Cortelezzi,[13] Gerald Wulf,[14] Pascal Turlure,[15] Montserat Rovira,[16] Zubeydenur Ozkurt,[17] Maria J. Pascual-Cascon,[18] Maria C. Moreira,[19] Johannes Clausen,[20] Hildegard Greinix,[21] Rafael F. Duarte[22#] and Grzegorz W. Basak[23#]

[1]Charité Universitätsmedizin Berlin, Berlin, Germany; [2]EBMT Statistical Unit, Paris, France; [3]EBMT Data Office, Leiden, the Netherlands; [4]University of Freiburg, Freiburg, Germany; [5]Hannover Medical School, Hannover, Germany; [6]Department of Hematology, University Hospital Leuven and KU Leuven, Leuven, Belgium; [7]Imperial College, London, UK; [8]HUCH Comprehensive Cancer Center, Helsinki, Finland; [9]Antwerp University Hospital, Antwerp, Belgium; [10]Erciyes University Medical Faculty, Kayseri, Turkey; [11]Radboud University – Nijmegen Medical Centre, Nijmegen, the Netherlands; [12]Hospital Santa Creu I Sant Pau, Barcelona, Spain; [13]Fondazione IRCCS – Ca'Granda, Milan, Italy; [14]Universitätsklinikum Göttingen, Göttingen, Germany; [15]CHRU Limoges, Limoges, France; [16]Hospital Clinic, Barcelona, Spain; [17]Gazi University Faculty of Medicine, Ankara, Turkey; [18]Hospital Regional de Málaga, Malaga, Spain; [19]Instituto National do Cancer, Rio de Janeiro, Brazil; [20]Elisabethinen-Hospital, Linz, Austria; [21]LKH – University Hospital Graz, Graz, Austria; [22]Hospital Universitario Puerta de Hierro, Madrid, Spain and [23]Medical University of Warsaw, Warsaw, Poland

[#]RFD and GWB contributed equally as co-senior authors.

Ferrata Storti Foundation

Haematologica 2020
Volume 105(7):1977-1983

ABSTRACT

Uric acid is a danger signal contributing to inflammation. Its relevance to allogeneic stem cell transplantation (alloSCT) derives from preclinical models where the depletion of uric acid led to improved survival and reduced graft-*versus*-host disease (GvHD). In a clinical pilot trial, peri-transplant uric acid depletion reduced acute GvHD incidence. This prospective international multicenter study aimed to investigate the association of uric acid serum levels before start of conditioning with alloSCT outcome. We included patients with acute leukemia, lymphoma or myelodysplastic syndrome receiving a first matched sibling alloSCT from peripheral blood, regardless of conditioning. We compared outcomes between patients with high and low uric acid levels with univariate- and multivariate analysis using a cause-specific Cox model. Twenty centers from 10 countries reported data on 366 alloSCT recipients. There were no significant differences in terms of baseline co-morbidity and disease stage between the high- and low uric acid group. Patients with uric acid levels above median measured before start of conditioning did not significantly differ from the remaining in terms of acute GvHD grades II-IV incidence (Hazard ratio [HR] 1.5, 95% Confidence interval [CI]: 1.0-2.4, *P*=0.08). However, they had significantly shorter overall survival (HR 2.8, 95% CI: 1.7-4.7, *P*<0.0001) and progression free survival (HR 1.6, 95% CI: 1.1-2.4, *P*=0.025). Non-relapse mortality was significantly increased in alloSCT recipients with high uric acid levels (HR 2.7, 95% CI: 1.4-5.0, *P*=0.003). Finally, the incidence of relapse after alloSCT was increased in patients with higher uric acid levels (HR 1.6, 95% CI: 1.0-2.5, *P*=0.04). We conclude that high uric acid levels before the start of conditioning correlate with increased mortality after alloSCT.

Correspondence:

OLAF PENACK
olaf.penack@charite.de

Received: June 4, 2019.

Accepted: October 4, 2019.

Pre-published: October 10, 2019.

doi:10.3324/haematol.2019.228668

Check the online version for the most updated information on this article, online supplements, and information on authorship & disclosures: www.haematologica.org/content/105/7/1977

Introduction

High treatment-associated complication rates remain an important challenge to the success of allogeneic hematopoietic stem cell transplantation (alloSCT). A common mechanism of the major infectious- and non-infectious complications after alloSCT, such as graft-*versus*-host disease (GvHD) and sepsis, is severe inflammation. Critical to excess inflammation after alloSCT are host biomolecules termed 'endogenous danger signals', which can initiate and maintain non-infectious inflammatory responses by acting as pro-inflammatory mediators.[1,2] One such molecule is uric acid. During conditioning for alloSCT, uric acid is released from injured cells and reduced renal clearance may contribute to high uric acid serum levels.[3,4] Uric acid acts as a danger signal by enhancing T-cell responses *via* activation of the NOD-like receptor protein (NLRP) 3 inflammasome.[5,6] A pre-clinical study has provided basic evidence on the regulation of GvHD by uric acid *via* Nlrp3 inflammasome–mediated IL-1 production.[7] The significance of uric acid for alloSCT outcome has been underlined by results from a pilot study reporting reduced incidence of acute GvHD in patients undergoing alloSCT after depletion of uric acid using urate oxidase.[8]

Based on these results, and because uric acid is a routine laboratory parameter assessed in patients undergoing alloSCT, there is a strong rationale to investigate the use of uric acid as a biomarker and possibly as a therapeutic target during alloSCT. To study the role of uric acid levels in alloSCT, the Transplant Complications Working Party (TCWP) of the European Society for Blood and Marrow Transplantation (EBMT) performed a prospective, multicenter, non-interventional study. We hypothesized that a high uric acid level prior to alloSCT is an independent risk factor for increased mortality and for the development of severe acute GvHD.

Methods

Data source, study design and data collection

We asked EBMT centers performing more than 50 alloSCT per year if they were willing to participate in this prospective study. Twenty centers in ten countries agreed to participate. Data collection for the EBMT registry was approved by the institutional review board and/or Ethics Committee in all centers. Data were prospectively collected between August, 2014 and February, 2018. Consecutive alloSCT recipients with acute leukemia, lymphoma or myelodysplastic syndrome (MDS) receiving a first matched sibling alloSCT from peripheral blood, regardless of conditioning, were eligible, provided they had signed an informed consent document that permitted sharing of clinical data according to national rules. Basic data on patient and disease characteristics as well as longer term follow-up was taken from minimal essential data (MED-A) forms, which are submitted from all consecutive patients to the central EBMT registry. In addition, we designed registration and MED-B/C forms that were prospectively collected and specific to this study (see the *Online Supplementary Materials and Methods*). The MED-B/C form contained detailed information on uric acid serum levels prior to alloSCT, patient characteristics, infectious- as well as non-infectious complications, GvHD staging, morbidity and mortality. Uric acid levels were determined at the time of hospital admission for alloSCT directly before the start of conditioning therapy. Treatment teams completed the specific forms at the time of registration and at day +100 after alloSCT.

Endpoints and statistical analyses

Patient, disease, and transplant-related characteristics for the two cohorts (uric acid levels prior to alloSCT above median / uric acid levels below median) were compared by using 2 statistics for categorical variables and the Mann-Whitney test for continuous variables. The primary endpoint was the incidence of acute GvHD. Secondary endpoints were relapse incidence (RI), non-relapse mortality (NRM), overall survival (OS), progression free survival (PFS) and the incidence of chronic GvHD. PFS was defined as survival with no evidence of relapse or progression. RI was defined as the probability of having had a relapse during follow-up time. Death without experiencing a relapse was a competing event. NRM was defined as death without evidence of relapse or progression. OS was defined as the time from alloSCT to death, regardless of the cause. Acute GvHD was graded according to the modified Seattle-Glucksberg criteria[9] and chronic GvHD according to the revised Seattle criteria.[10] Cumulative incidence was used to estimate the endpoints of NRM, RI, acute and chronic GvHD to accommodate for competing risks. To study acute and chronic GvHD, we considered relapse and death to be competing events. Probabilities of OS and PFS were calculated using the Kaplan–Meier method. Univariate analyses were done using the Gray test for cumulative incidence functions and the log rank test for OS and PFS. A Cox proportional hazards model was used for multivariate regression. All variables differing significantly between the two groups or factors associated with one outcome in univariate analysis were included in the Cox model. The following variables entered the multivariate models as possible confounders: age, sex mismatch between recipient and donor, diagnosis, disease status, Karnofsky score, number of CD34 cells given, intensity of conditioning (EBMT definition: myeloablative conditioning (MAC) was defined as total body irradiation (TBI) >6 Grey or oral busulfan >8 mg/kg or intravenous busulfan >6.4 mg/kg), type of GvHD prophylaxis, ATG use, time from diagnosis to transplant, year of transplant and CMV status. As the number of variables was too high regarding the number of events, a stepwise selection using Akaike information criterion (AIC) was run for all the confounding factors. The difference between the two cohorts was then assessed in the final selected model.

Results were expressed as the hazard ratio (HR) with the 95% confidence interval (95% CI). Proportional hazards assumptions were checked systematically for all proposed models using the Grambsch-Therneau residual-based test. All tests were two-sided. The type I error rate was fixed at 0.05 for the determination of factors associated with time-to-event outcomes. Statistical analyses were performed in November 2018 with R 3.4.2 (R Core Team (2017). R: A language and environment for statistical computing. R Foundation for Statistical Computing, Vienna, Austria. URL *https://www.R-project.org/*.)

Results

Patients, transplant characteristics and uric acid measurement

The entry criteria for analysis of primary and secondary endpoints were fulfilled in 386 patients. We used the last uric acid serum level that was masured in the individual patients before start of conditioning. The median time point of measurement was three days before start of conditioning. The range was between 0 days (morning before start of conditioning) to 22 days before conditioning. The main patients and transplant characteristics that were included in the analysis of OS are described in Table 1. Most parameters were balanced between the two cohorts.

Table 1. Patient characteristics.

	Uric acid ≤4.3 mg/dL (n=186)	Uric acid >4.3 mg/dL (n=180)	*P*
Year of transplant median (range) [IQR]	2015 (2014-2018) [2015-2017]	2015 (2014-2018) [2014-2016]	0.10
Patient age (years) median(range)	52 (17-71)	55 (20-71)	0.11
Time from diagnosis to transplant (months) median (range)	4 (1-61)	5 (1-71)	0.09
Sex mismatch			
Female to male	30 (17%)	52 (29%)	0.005
Other combination	148 (83%)	125 (71%)	
Missing	8	3	
Diagnosis			
Acute leukemia	130 (70%)	118 (66%)	0.7
Lymphoma	17 (9%)	19 (10%)	
MDS	39 (21%)	43 (24%)	
Disease status			
CR	120 (66%)	125 (72%)	0.2
Not in CR	61 (34%)	48 (28%)	
Missing	5	7	
DRI			0.7
Low	8 (4%)	7 (4%)	
Intermediate	107 (60%)	105 (63%)	
High	51 (30%)	49 (30%)	
Very high	10 (6%)	5 (3%)	
Missing	10	14	
ATG			
No	100 (54%)	106 (59%)	0.3
Yes	86 (46%)	74 (41%)	
Conditioning intensity			
MAC/Chemo	46 (25%)	37 (21%)	0.2
MAC/TBI	36 (20%)	26 (15%)	
RIC	102 (55%)	115 (64%)	
Missing	2	2	
GvHD prophylaxis			
Calcineurin inhibitor + MMF	85 (48%)	84 (47%)	0.6
Calcineurin inhibitor + MTX	64 (36%)	71 (40%)	
Calcineurin inhibitor mono	27 (15%)	22 (12%)	
Missing	10	3	
Donor/patient CMV			0.2
-/-	28 (16%)	38 (21%)	
Other	146 (83%)	136 (78%)	
Missing	12	6	
Karnofsky score			0.14
10-80	38 (21%)	27 (15%)	
90-100	140 (78%)	149 (84%)	
Missing	8	4	
HT-CI = 0	64 (50%)	56 (40%)	0.19
HT-CI = 1 or 2	20 (15%)	32 (23%)	
HT-CI ≥3	45 (35%)	51 (37%)	
Missing	57	41	

MDS: myelodysplastic syndrome; IQR: interquartile range; CR: complete remission; DRI: disease risk index; ATG: anti-thymocyte globulin; MAC: myeloablative conditioning; RIC: reduced intensity conditioning; TBI: total body irradiation; GvHD: graft-*versus*-host disease; MMF: Mycophenolate mofetil; MTX: Methotrexate; CMV: cytomegalovirus; HT-CI: hematopoietic cell transplantation cumulative incidence.

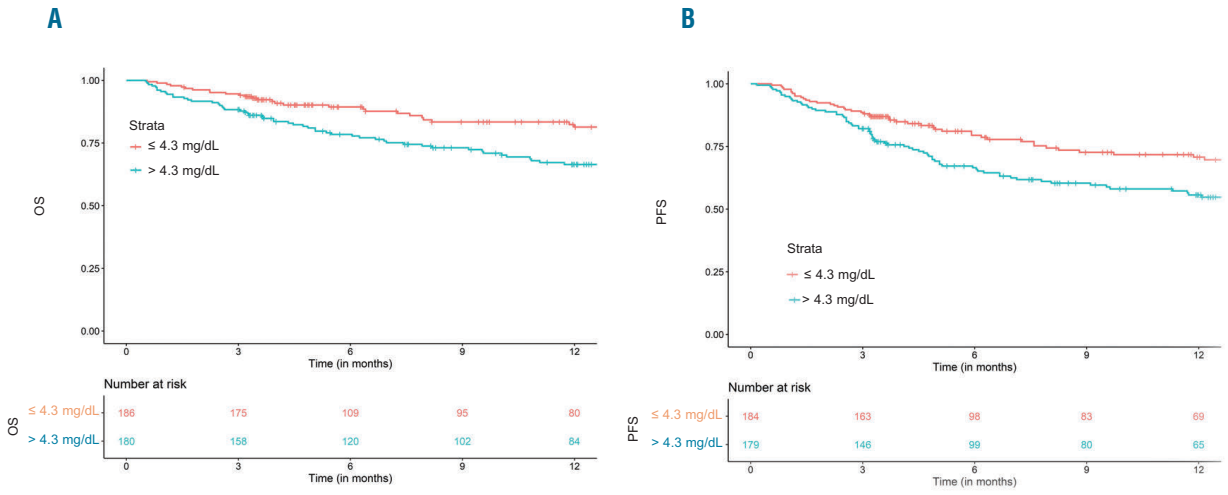

Figure 1. Survival at one year after allogeneic stem cell transplantation. Overall survival (OS) (A) and progression free survival (PFS) (B) after allogeneic stem cell transplantation (alloSCT) in cohorts according to uric acid serum levels prior to alloSCT: with high uric acid serum levels (blue line), patients with low uric acid levels (red line).

However, a higher percentage of sex mismatch transplants in the direction of female donor to male recipient was observed in the group of patients with uric acid above median before alloSCT. The frequency of patients with reduced-intensity conditioning (RIC) *versus* myeloablative conditioning (MAC) did not differ significantly between the high uric acid group and the low uric acid group (P=0.077). When looking exclusively at TBI (P=0.59) or by mixing conditioning intensity and TBI (MAC/Chemo *vs.* MAC/TBI *vs.* RIC: P=0.20), no statistically significant difference could be observed.

Incidence of acute and chronic GvHD

In the present study, the incidence of acute GvHD grades II-IV and grades III-IV in the whole population at 100 days were 25% and 11%, respectively. We observed no significant differences in the frequency of clinically significant acute GvHD grades II-IV in univariate (HR 1.2, 95% CI: 0.8-1.9, P=0.4) and multivariate (HR 1.5, 95% CI: 1.0-2.4, P=0.08) analysis comparing the high- *versus* the low uric acid cohorts. (Table 2 and Table 3). We found no significant differences in the frequency of acute GvHD grades III-IV in univariate (HR=1.8, 95% CI: 0.9-3.4, P=0.08) and multivariate (HR 1.7, 95% CI: 0.9-3.2, P=0.11) analysis in alloSCT recipients with uric acid levels above cut-off before transplantation *versus* those with low uric acid levels (Table 2 and Table 3).

In the whole population, the incidence of chronic GvHD at one year and two years was 27% and 40%, respectively. The incidence of severe chronic GvHD at 1 year and 2 years was 18% and 24%, respectively. We observed no differences in incidence and severity of chronic GvHD between the two cohorts (Table 3 and Table 4). The chronic GvHD incidence was significantly lower in alloSCT recipients receiving anti-T-cell globulin (ATG) as part of the conditioning regimen (ATG, HR 0.25 95% CI: 0.13-0.5, P<0.0001).

Survival endpoints

The median follow-up time was 15.2 months (95% CI: 13.1-17.0) and OS in the whole population at 1 year was 74%. We found, that OS and PFS of alloSCT recipients with uric acid levels above cut-off, measured before start of conditioning, were significantly shorter compared with the low uric acid cohort (Figure 1A, OS univariate HR 2.4, 95% CI: 1.6-3.7, P<0.001; multivariate HR 2.8, 95% CI: 1.7-4.7, P<0.0001) (Figure 1B, PFS univariate HR 2.0, 95% CI: 1.1-3.7, P=0.02; multivariate HR 2.7, 95% CI: 1.4-5.0, P=0.003). Non-relapse mortality was significantly increased in alloSCT recipients with high uric acid levels prior to start of conditioning (Figure 2A, univariate HR 2.0, 95% CI: 1.1-3.7, P=0.02; multivariate HR 2.7, 95% CI: 1.4-5.0, P=0.003). Multivariate as well as univariate analyses are shown in Table 3 and Table 4. We conclude that serum uric acid levels prior to alloSCT are an independent risk factor for mortality.

At the last follow-up 29.3% of the patients were dead (49.6% from relapse, 45.2% alloSCT-related causes and 2.6% from other causes). The causes of death in patients without relapse were mainly due to infection. A descriptive analysis of the causes of death is given in Table 5.

Table 2. Univariate global comparison of acute graft-*versus*-host disease shown at day +100 after allogeneic stem cell transplantation.

Group	Acute GvHD II-IV (95% CI)	Acute GvHD III-IV (95% CI)
Uric acid </=4.3 mg/dL	22% (17-29)	8% (5-13)
Uric acid >4.3 mg/dL	26% (20-33)	14% (9-19)
P-value	0.39	0.08

GvHD: graft-*versus*-host disease; CI: confidence interval.

Incidence of infections

We first looked at the incidence of infections in both cohorts and found no significant differences (multivariate HR 0.8, 95% CI: 0.6-1.1, P=0.4). We than looked at infection-related mortality and found a significant higher number of infection-related deaths in the high uric acid group (Figure 2C, multivariate HR 2.6, 95% CI: 1.2-5.2, P=0.01).

Incidence of relapse

Since uric acid is known to be released from malignant

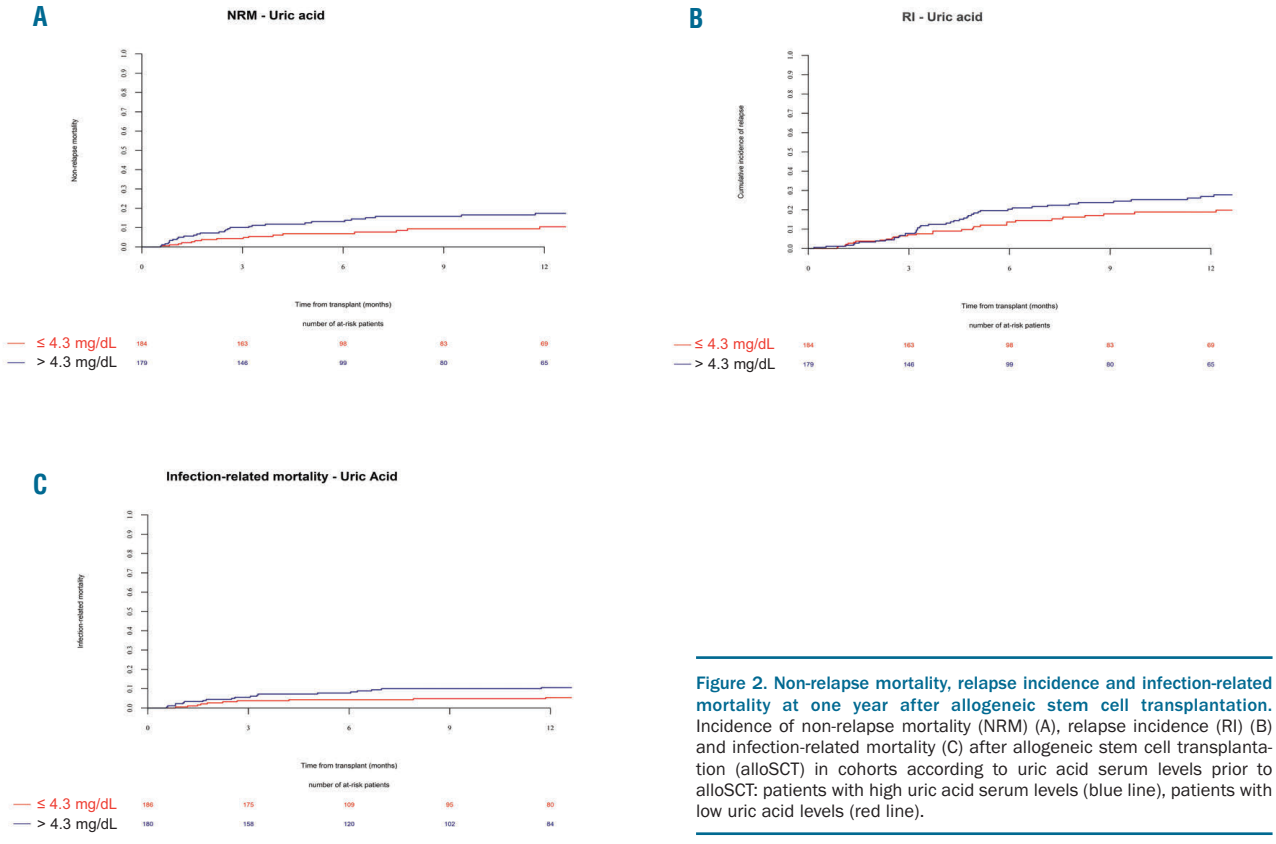

Figure 2. Non-relapse mortality, relapse incidence and infection-related mortality at one year after allogeneic stem cell transplantation. Incidence of non-relapse mortality (NRM) (A), relapse incidence (RI) (B) and infection-related mortality (C) after allogeneic stem cell transplantation (alloSCT) in cohorts according to uric acid serum levels prior to alloSCT: patients with high uric acid serum levels (blue line), patients with low uric acid levels (red line).

Table 3. Multivariate global comparison.

Uric acid >4.3 mg/dL *versus* ≤4,3 mg/dL	HR	95% CI	*P*
Overall Survival	2,83	1,72 - 4,68	<0.0001
Progression Free Survival	1,59	1,06 - 2,39	0.03
Relapse Incidence	1,59	1,02 - 2,49	0.04
Non-Relapse Mortality	2,65	1,41 - 5,01	0.003
Chronic GvHD	0,96	0,63 -1,45	0.84
Extensive Chronic GvHD	1,08	0,62 - 1,88	0.79
Acute GvHD II-IV	1,52	0,95 - 2,43	0.08
Acute GvHD III-IV	1,68	0,88 - 3,19	0.11

GvHD: graft-*versus*-host disease; HR: hazard ratio; CI: confidence interval.

tumours, we were interested in a possible connection of uric acid levels and disease relapse. We found that the relapse incidence in all patients at 1 year was 13%. The relapse incidence was moderately increased in the cohort with higher uric acid levels (Figure 2B, Table 3 and Table 4, univariate HR 1.6, 95% CI: 1.0-2.5; *P*=0.09; multivariate HR 1.6, 95% CI: 1.0-2.5, P=0.04).

Discussion

This prospective study identifies uric acid levels, taken before start of conditioning therapy, as a laboratory biomarker to predict mortality after alloSCT.

In animal experiments and in a clinical pilot study the depletion of uric acid with rasburicase led to a reduced frequency of severe GvHD.[7,8] Therefore, our initial hypothesis was to primarily find an association between uric acid with acute GvHD and then secondarily with NRM. However, we found a strong positive association of uric acid levels with mortality after alloSCT whereas the association between uric acid levels and acute GvHD incidence was not statistically significant. One of the reasons could be the low incidence of GvHD in our cohort due to the patient characteristics of human leukocyte antigen (HLA)-identical sibling transplant with a high proportion of anti-thymocyte globulin (ATG) use. The use of *in vivo* T-cell depletion with ATG in HLA-identical sibling

Table 4. Univariate global comparison of overall survival, non-relapse mortality, relapse incidence as well as chronic graft-*versus*-host disease incidence and severity at one year after allogeneic stem cell transplantation.

Group	OS (95% CI)	PFS (95% CI)	RI (95% CI)	NRM (95% CI)	cGvHD (95% CI)	Extensive cGvHD (95% CI)
Uric acid </=4.3 mg/dL	81% (75-88)	71% (64-79)	19% (13-26)	10% (6-16)	28% (20-36)	16% (10-24)
Uric acid >4.3 mg/dL	66% (59-74)	56% (48-64)	27% (20-34)	17% (12-24)	26% (19-33)	18% (12-25)
P-value	<0.001	0.001	0.09	0.02	0.43	0.85

OS: overall survival; PFS: progression free survival; NRM: non-relapse mortality; RI: relapse incidence: cGvHD: chronic graft-*versus*-host disease; CI: confidence intervall.

alloSCT in European centres increased recently.[11] This trend is reflected by a higher frequency of ATG use in the present study (41-46%) than we had initially expected. Another likely reason is a hyperinflammatory status connected to high uric acid levels not restricted to acute GvHD with a negative impact on different relevant clinical situations after alloSCT, such as sepsis[12] and adult respiratory distress syndrome (ARDS).[13] This view is supported by our observation that death due to both infectious and non-infectious complications after alloSCT was increased in patients with high uric acid levels. Interestingly, an association of uric acid levels with decreased solid organ transplant survival has been described further underlining the significance of uric acid for transplantation biology.[14,15] Our study extends these findings to the setting of alloSCT.

Our study contradicts results from a previous retrospective single centre study, which did not show any significant association of uric acid levels prior to transplantation to mortality after alloSCT.[16] Differences in study designs between the current larger, multicentre and prospective study *versus* the already published smaller, single centre and retrospective study may be the reason for the differing results.

A limitation of this clinical study is the lack of mechanistic insight on the role of uric acid in development of complications after alloSCT. The study design did not allow the investigation of whether the impaired outcome in the high urid acid cohort is due to an active role of uric acid in causing inflammation or whether it is because uric acid primarily is a surrogate biomarker reflecting a hyperinflammatory status and/or activity of the underlying malignancy. However, we found no significant differences regarding the disease status as well as disease risk index (DRI) (complete remission [CR] *vs.* non-CR) in between the two groups (high uric acid *vs.*low uric acid). In addition there were no significant differences in the performance status as well as the alloSCT-CI in between the two groups. This data is no proof, but rather points in the direction that high uric acid values were not merely a reflection of advanced disease or increased co-morbidity in our study.

A further limitation of our results is that our patient population was restricted to alloSCT from HLA-identical sibling donors. We are therefore unable to draw definite conclusions from these results regarding the association of uric acid levels with outcome in matched unrelated donor alloSCT or in haploidentical alloSCT, which are increasingly used. Another limitation is the incomplete understanding of the effects of uric acid on post alloSCT immunity. While previous studies showed that uric acid leads to a inflammatory status in leukocytes and our results demonstrate impaired survival in alloSCT recipients with uric acid levels above median, it may be premature to conclude that uric acid is a negative factor at any time around alloSCT. There are clinical situations where immune activation is necessary and desired – e.g. in anti-infectious and anti-tumor immunity. The impact of depleting uric acid on immune activity in these situations remains to be determined. In addition, it is possible that uric acid is involved in immune reconstitution as it has been suggested recently that changes in uric acid serum levels can indicate incipient or remaining immunological activity after SCT or induction therapy in patients with hematologic malignancies.[17]

In conclusion, this study supports the use of serum uric acid levels as biomarker for alloSCT outcome.

Table 5. Causes of death in both cohorts.

	Uric acid ≤4.3 (n=186) mg/dL	Uric acid >4.3 mg/dL (n=180)
Alive at last follow up	155 (83.3%)	106 (58.9%)
Dead	31 (16.7%)	74 (41.1%)
Dead due to relapse	13 (6.9%)	38 (21.1%)
Dead without relapse	18 (9.7%)	36 (20.0%)
Dead due to infection	5 (3.2%)	20 (11.1%)
Dead due to GvHD	2 (1.0%)	10 (5.6%)
Dead due to infection and GvHD	3 (1.6%)	5 (2.8%)
Dead due to other causes or unknown	8 (4.3%)	1 (0.5%)

GvHD: graft-*versus*-host disease.

Acknowledgments

JP acknowledges the support of the Imperial NIHR-BCR.

References

1. Apostolova P, Zeiser R. The role of purine metabolites as DAMPs in acute graft-versus-host disease. Front Immunol. 2016; 7:439.
2. Zeiser R, Blazar BR. Acute graft-versus-host disease - biologic process, prevention, and therapy. N Engl J Med. 2017;377(22):2167-2179.
3. Cannell PK, Herrmann RP. Urate metabolism during bone marrow transplantation. Bone Marrow Transplant. 1992;10(4):337-339.
4. Joo SH, Park JK, Lee EE, et al. Changes in serum uric acid levels after allogeneic hematologic stem cell transplantation: A retrospective cohort study. Blood Res. 2016;51(3):200-203.

5. Martinon F, Petrilli V, Mayor A, et al. Gout-associated uric acid crystals activate the NALP3 inflammasome. Nature. 2006; 440(7081):237-241.
6. Braga TT, Forni MF, Correa-Costa M, et al. Soluble uric acid activates the NLRP3 inflammasome. Sci Rep. 2017;7:39884.
7. Jankovic D, Ganesan J, Bscheider M, et al. The Nlrp3 inflammasome regulates acute graft-versus-host disease. J Exp Med. 2013;210(10):1899-1910.
8. Yeh AC, Brunner AM, Spitzer TR, et al. Phase I study of urate oxidase in the reduction of acute graft-versus-host disease after myeloablative allogeneic stem cell transplantation. Biol Blood Marrow Transplant. 2014;20(5):730-734.
9. Przepiorka D, Weisdorf D, Martin P, et al. 1994 Consensus conference on acute GVHD grading. Bone Marrow Transplant. 1995;15(6):825-828.
10. Lee SJ, Vogelsang G, Flowers ME. Chronic graft-versus-host disease. Biol Blood Marrow Transplant. 2003;9(4):215-233.
11. Kroger N, Solano C, Wolschke C, Bandini G, et al. Antilymphocyte globulin for prevention of chronic graft-versus-host disease. N Engl J Med. 2016;374(1):43-53.
12. Pehlivanlar-Kucuk M, Kucuk AO, et al. The association between serum uric acid level and prognosis in critically Ill patients, uric acid as a prognosis predictor. Clin Lab. 2018;64(9):1491-1500.
13. Lee HW, Choi SM, Lee J, et al. Serum uric acid level as a prognostic marker in patients with acute respiratory distress syndrome. J Intensive Care Med. 2019;34(5):404-410.
14. Asleh R, Prasad M, Briasoulis A, et al. Uric acid is an independent predictor of cardiac allograft vasculopathy after heart transplantation. J Heart Lung Transplant. 2018; 37(9):1083-1092.
15. Kim DG, Choi HY, Kim HY, et al. Association between post-transplant serum uric acid levels and kidney transplantation outcomes. PloS One. 2018; 13(12):e0209156.
16. Ostendorf BN, Blau O, Uharek L, et al. Association between low uric acid levels and acute graft-versus-host disease. Ann Hematol. 2015;94(1):139-144.
17. Haen SP, Eyb V, Mirza N, et al. Uric acid as a novel biomarker for bone-marrow function and incipient hematopoietic reconstitution after aplasia in patients with hematologic malignancies. J Cancer Res Clin Oncol. 2017;143(5):759-771.

RESEARCH, READ & CONNECT

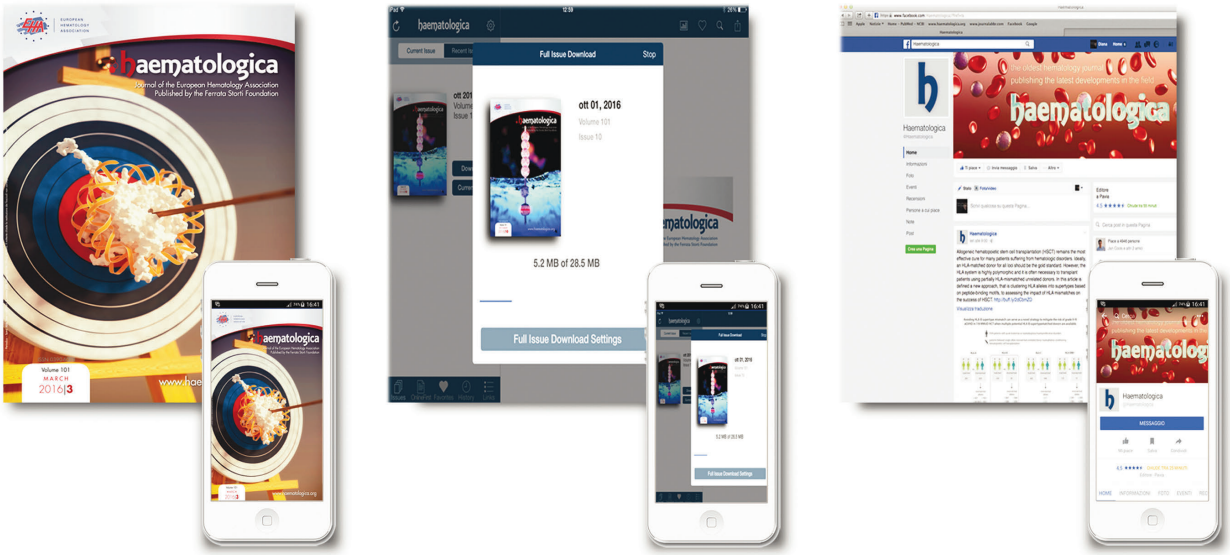

We reach more than
6 hundred thousand readers each year

The first Hematology Journal in Europe

Impressions YTD

9,621,645

Digital Readers

4,431

Total Audience

554,484

Worldwide rank	Impact factor	Total citations
7 th	7.570	16,255

haematologica

Journal of the Ferrata Storti Foundation

Fig. 1.

Fig. 2.

Fig. 3.

haematologica — Vol. 105 n. 7 — July 2020 — 1751-1984